



2

FTD-ID (RS) T-1388-80

# FOREIGN TECHNOLOGY DIVISION



FUNDAMENTALS OF ELECTRICAL PROPULSION  
PLANT DESIGN

by

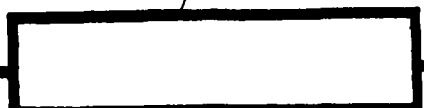
N.A. Kuznetsov, P.V. Kuropatkin, et al



DTIC  
S  
MAY 14 1982  
D

Approved for public release;  
distribution unlimited.

DTIC FILE COPY



88

004

# EDITED TRANSLATION

FTD-ID(RS)T-1388-80

6 April 1982

MICROFICHE NR: FTD-82-C-000451

FUNDAMENTALS OF ELECTRICAL PROPULSION PLANT DESIGN

By: N.A. Kuznetsov, P.V. Kuropatkin, et al

English pages: 761

Source: Osnovy Proyektirovaniya Grebnykh  
Elektricheskikh Ustanovok, Publishing  
House "Sudostroyeniye", Leningrad, 1972,  
pp. 1-656

Country of origin: USSR

Translated by: SCITRAN  
F33657-81-D-0263

Requester: NISC

Approved for public release; distribution unlimited.

SSion For	
GRA&I	<input checked="" type="checkbox"/>
TAB	<input type="checkbox"/>
ounced	<input type="checkbox"/>
ification	

ribution/	
Availability Codes	
Dist	Avail and/or Special
A	



<p>THIS TRANSLATION IS A RENDITION OF THE ORIGINAL FOREIGN TEXT WITHOUT ANY ANALYTICAL OR EDITORIAL COMMENT. STATEMENTS OR THEORIES ADVOCATED OR IMPLIED ARE THOSE OF THE SOURCE AND DO NOT NECESSARILY REFLECT THE POSITION OR OPINION OF THE FOREIGN TECHNOLOGY DIVISION.</p>	<p>PREPARED BY: TRANSLATION DIVISION FOREIGN TECHNOLOGY DIVISION WP.AFB, OHIO.</p>
---	--

U. S. BOARD ON GEOGRAPHIC NAMES TRANSLITERATION SYSTEM

Block	Italic	Transliteration	Block	Italic	Transliteration
А а	<i>А а</i>	A, a	Р р	<i>Р р</i>	R, r
Б б	<i>Б б</i>	B, b	С с	<i>С с</i>	S, s
В в	<i>В в</i>	V, v	Т т	<i>Т т</i>	T, t
Г г	<i>Г г</i>	G, g	У у	<i>У у</i>	U, u
Д д	<i>Д д</i>	D, d	Ф ф	<i>Ф ф</i>	F, f
Е е	<i>Е е</i>	Ye, ye; E, e*	Х х	<i>Х х</i>	Kh, kh
Ж ж	<i>Ж ж</i>	Zh, zh	Ц ц	<i>Ц ц</i>	Ts, ts
З з	<i>З з</i>	Z, z	Ч ч	<i>Ч ч</i>	Ch, ch
И и	<i>И и</i>	I, i	Ш ш	<i>Ш ш</i>	Sh, sh
Й й	<i>Й й</i>	Y, y	Щ щ	<i>Щ щ</i>	Shch, shch
К к	<i>К к</i>	K, k	Ъ ъ	<i>Ъ ъ</i>	"
Л л	<i>Л л</i>	L, l	Ы ы	<i>Ы ы</i>	Y, y
М м	<i>М м</i>	M, m	Ь ь	<i>Ь ь</i>	'
Н н	<i>Н н</i>	N, n	Э э	<i>Э э</i>	E, e
О о	<i>О о</i>	O, o	Ю ю	<i>Ю ю</i>	Yu, yu
П п	<i>П п</i>	P, p	Я я	<i>Я я</i>	Ya, ya

\*ye initially, after vowels, and after ъ, ь; e elsewhere.  
When written as ë in Russian, transliterate as yë or ë.

RUSSIAN AND ENGLISH TRIGONOMETRIC FUNCTIONS

Russian	English	Russian	English	Russian	English
sin	sin	sh	sinh	arc sh	sinh <sup>-1</sup>
cos	cos	ch	cosh	arc ch	cosh <sup>-1</sup>
tg	tan	th	tanh	arc th	tanh <sup>-1</sup>
ctg	cot	cth	coth	arc cth	coth <sup>-1</sup>
sec	sec	sch	sech	arc sch	sech <sup>-1</sup>
cosec	csc	csch	csch	arc csch	csch <sup>-1</sup>

Russian English

rot curl  
lg log

GRAPHICS DISCLAIMER

All figures, graphics, tables, equations, etc.  
merged into this translation were extracted  
from the best quality copy available.

Table of Contents

/649

	Page
Authors' Introduction	13
Listing of Circuit Element Conditional Designations	15
Introduction	21
 Chapter 1	
Electrical Propulsion Plant Equipment Requirements	
§ 1.1 Primary Motor and Main Propulsion Motor Characteristics	30
§ 1.2 Primary Motor Requirements	34
§ 1.3 Main Generator and Main Propulsion Motor Requirements	36
§ 1.4 Main Generator and Main Propulsion Motor Exciter Requirements	39
§ 1.5 Distribution Devices and GEU Control Gear	40
§ 1.6 GEU Auxiliary Mechanism Requirements	45
 Chapter 2	
Direct Current Electrical Propulsion Plant Main Current Circuits	
§ 2.1 Main Current Circuits With Alternate-Series Connection of Generator and Main Propulsion Motor Armatures	49
Generator Series and Parallel Connection. Circuits With One-Armature Main Propulsion Motors. Circuits With Two-Armature Main Propulsion Motors. Circuits With Generators Connected to Electric Motors For Different Propellers.	
§ 2.2 Two-Armature Main Current Circuits	71
§ 2.3 Comparative Evaluation of Different Main Current Circuits	73
 Chapter 3	
Direct Current Electrical Propulsion Plant Field and Regulation Circuits	/650
§ 3.1 Basic Differences in Electrical Propulsion Plant Field Circuits	78
§ 3.2 Excitation Circuits With Separately-Excited Exciters	86
§ 3.3 Excitation Circuits With Three-Winding Exciters	89
Excitation Circuits With Differentially-Compounded Windings Connected to the Main Current Circuit. Excitation Circuits With Differential Connection of the Differentially-Compounded Winding. Circuits for Connection of a Separate Excitation Winding Via a Potentiometer. Excitation Circuit With Generator Switching. Constant Current GEU Excitation Circuits.	

	Page
§ 3.4 Excitation Circuits With Longitudinal Field Amplidynes Ice Navigation Transport Vessel GEU Excitation Circuits. Icebreaker "Lenin" GEU Excitation Circuit.	116
§ 3.5 Excitation Circuits With Transverse Field Amplidynes	123
§ 3.6 Excitation and Control Circuits With Power Magnetic Amplifiers Excitation Circuits With Magnetic Amplifiers As Exciters. Excitation Circuits With Magnetic Amplifiers As Pilot Exciters	128
§ 3.7 Static Excitation Systems With Controlled Rectifiers Experimental GEU Pilot Excitation System On the Icebreaker "Kiev." GEU Pilot Excitation System on the Icebreaker "Murmansk."	150
 Chapter 4	
Direct Current Electrical Propulsion Plant Protection, Indication, and Blocking Circuits	
§ 4.1 GEU Protection Circuits GEU Protection System. GEU Protection Circuits With Single-Winding Exciters. GEU Protection Circuits With Three-Winding Exciters. Ice Navigation Vessel GEU Protection Circuits. GEU Protection Circuits for Single-Shaft Vessels. GEU Protection Circuit Operating From a Constant Current System. GEU Protection Circuit For Dual-Shaft Vessels With Generator Switching to Both Shafts. Icebreaker "Lenin" GEU Protection Circuit. Recommendations on GEU Protection Circuit Selection.	159
§ 4.2 GEU Indication Circuits Indication Types and Elements in GEU Systems. Indication Circuits For GEU With Three-Winding Exciters. Diesel Indication Circuits. Ice Navigation Vessel GEU Indication Circuits. GEU Operating Mode Indication Circuits. Recommendations on GEU Indication Circuit Selection.	183
§ 4.3 GEU Interlock Circuits Interlock Types and Elements in GEU Circuits. Simplest Electromagnetic Interlocks. Electromagnetic Interlock Circuits For GEU With Three- Winding Exciters. Electromagnetic Interlock Circuits For Ice Navi- gation Vessels. Recommendations on Using Electromagnetic Interlocks In GEU Systems.	196
 Chapter 5	
Calculation of the Static Characteristics of Direct Current Electrical Propulsion Plants	/651

	Page
§ 5.1 Basic Equations for GEU Statics	203
Basic Assumptions. Initial Equations For GEU Circuits With Separate Generator Excitation.	
§ 5.2 Analytical Methods For Approximate Static Characteristic Calculations	206
Initial Formulas For Calculation of Static Characteristics. Initial Formulas For Calculation of a GEU With Automated Electrical Machinery and With Regulation of GED Magnetic Flux. Calculation of Additional and Standardizing Resistances in GEU Field Circuits.	
§ 5.3 Graphic-Analytical Method of Calculating Static Characteristics of GEU With Three-Winding Exciters	215
Initial Data for a Graphic-Analytical Construction. A Graphic-Analytical Construction of Generator External Characteristics. A Graphic-Analytical Construction of a GED Mechanical Characteristic. Precise Determination of GED Torque. Calculation of Resistances in Pilot Excitation Circuits. Mechanical Characteristic of Intermediate Mode GED. Special Features of a Construction of the Static Characteristics of GEU With Three-Winding GED Exciters.	
§ 5.4 Graphic-Analytical Method of Calculation of the Static Characteristics of Automated GEU	235
Initial Assumptions. Graphic-Analytical Construction of Generator External Characteristics. Graphic-Analytical Construction of a GED Mechanical Characteristic. Consideration of Armature Reaction. Graphic-Analytical Calculation of a GED Mechanical Characteristic Given Simultaneous Control of Generator and GED Field Fluxes. Analytical Relationships For Elements of GEU With Two-Stage Longitudinal Field EMU. Graphic Construction of a Mechanical Characteristic of a GED With Two-Stage Longitudinal Field EMU.	
§ 5.5 Calculation of the Static Characteristics of GEU With Magnetic Amplifiers	259
Preparatory Calculations and Constructions. Construction of a GED Mechanical Characteristic. Calculation of the Main Propulsion Motor Positive Current Feedback Node. Special Features of Calculating the Static Characteristics of GEU With Magnetic Amplifiers As GED Exciters and Main Generator Pilot Exciters.	

§ 5.6 Static Characteristics of GEU With Controlled Rectifiers  
(Thyristors)

272

Special Features of the Excitation System. Initial Data For Construction of Static Characteristics. Preparatory Calculations and Constructions For GEU Main Operating Modes (Reversing in the GED Field Circuit). Calculation of Generator Control Winding Circuit Parameters. Construction of Power Constancy Hyperboles. Calculation of GED Magnetic Flux. Calculation of GED Exciter Control Winding Circuit Parameters. Construction of a GED Mechanical Characteristic.

§ 5.7 Methodology For Calculation of Icebreaker GEU Static Characteristics

285

Propellor Interaction With Ice Mode. Operation in Sludge (Small Ice Rafts). Operation in Smooth Ice Fields. Operation In Small Packed Floes. Selection of Optimal Form of a GED Mechanical Characteristic.

## Chapter 6

## Electrical Propulsion Plant Stability and Control Quality /652

§ 6.1 Special Features of Analysis of the Stability of Automated GEU

292

§ 6.2 Equations of Standard Automated GEU Links

297

Equation of Motion of the "Primary Motor" Link. Equation of Motion of Primary Motor Velocity Regulator. Equation of Regulation of the Primary Motor With Speed Regulator. Equation of Motion of the "Main Propulsion Motor" Link. Equation of Motion of the "Main Generator" Link. Equation of Motion of the "Generator Exciter" Link. Constraint Equation of EMF and Voltage. Equations of Motion of the "Main Propulsion Motor Exciter" Link. Equation of Motion of the "Transverse Field Amplidyne" Link. Equation of Motion of the "Amplidyne Stabilizing Winding Bridge Circuit" Link. Equations of Motion of the "Three-Stage Longitudinal Field Amplidyne" Link. Equation of Motion of the "Generator--Three- Stage Longitudinal Field Amplidyne Field Winding" Link. Equation of Motion of the "Magnetic Amplifier" Link. Equations of Motion of the "Synchros and Synchro Resolver" Link. Equations of Motion of the "Two-Phase Induction Motor" Link.

	Page
§ 6.3 Equations of Motion and Transfer Functions of Standard Direct Current GEU Systems	337
GEU With Longitudinal Field Amplidynes. GEU With Magnetic Amplifiers in the Excitation and Control System.	
§ 6.4 Analysis of the Stability of Standard GEU Systems	353
GEU With Transverse Field Amplidynes. GEU With Longitudinal Field Amplidynes. GEU With Magnetic Amplifiers.	
 Chapter 7	
Transient Processes in Direct Current Electrical Propulsion Plants (Theory, Analytical, and Graphic-Analytical Calculation Methods)	
§ 7.1 Purpose of the Calculations and Special Features of Transient Processes	373
Determination of Transient Processes in GEU and Their Significance For Insuring the Maneuvering Qualities of Electric Ships. Origin and Nature of the Course of Transient Processes. Requirements Levied on the Nature of Transient Processes When Designing GEU. Purpose of the Calculations and Mathematical Description of the Transient Processes in GEU.	
§ 7.2 The Process of Starting and Reversing a Direct Current Electric Drive	381
Starting the Main Propulsion Motor. Reversing the Main Propulsion Motor.	
§ 7.3 Methodology For Calculation of Transient Processes Based On Frequency Characteristics	385
Formulas Linking Transient Process Characteristics With Frequencies. Frequency Method For Calculating Transient Processes of GEU With A Three-Winding Generator Exciter	
§ 7.4 Analytical Method Of Calculating the Transient Processes of Automated GEU Non-Linear Systems	394
Several Theoretical Assumptions. Calculation of Transient Processes of GEU Systems Given Direct Introduction of the Main Current Circuit Into the Pilot Excitation System. Calculation of GEU Transient Processes Given Differentially-Connected Main Circuit Current Unity Feedback	
§ 7.5 Graphic-Analytical Method of Transient Process Calculation	411

	Page
Assumptions. Calculation of the EMF Increase in a Single-Winding Exciter (of a Conventional DC Generator). Calculation of Exciter EMF Reversal (of a Generator). Calculation of the Transient Processes of an Exciter With Voltage Feedback (from a Self-Excitation Winding). Calculation of Voltage Reversal of an Exciter With Positive Voltage Feedback. Calculation of the EMF Increase of a Generator With a Shunt Winding. Graphic Construction of the Transient Processes of GEU With a Three-Winding Exciter.	
§ 7.6 Reversal Time Calculation Using the Loss Evaluation Method	428
Characteristics of GEU Diesel Primary Motors. Maximum and Critical Diesel Rotational Velocities. Calculation of Reversal Time Using the Loss Evaluation Method for a G--D System.	
 Chapter 8	
Mathematical Modelling For Analysis and Synthesis of Electrical Propulsion Plant Transient Processes	
§ 8.1 General Assumptions	437
Special Features of GEU Transient Processes and Their Calculation Using Modelling Methods. Special Features in Using the Mathematical Modelling Method. Depiction of a Schematic of a Set of Equations for Analog Computers (AVM).	
§ 8.2 Mathematical Modelling of the Dynamic Characteristics of Icebreaker GEU With Magnetic Amplifiers in the Pilot Excitation System in the Propellor-Ice Interaction Mode	442
Initial Data. Calculation of the GEU Static Mode. Main Generator Excitation. Dynamics Equations. Selection of Optimal Characteristics of GEU Dynamics. Some Conclusions on Modelling Icebreaker GEU Dynamics. Effect of Feedback Parameters on Icebreaker GEU Dynamics.	
§ 8.3 Methodology of Analog Computer Analysis and Synthesis of the Dynamic Characteristics of GEU With Magnetic Amplifiers in the GED Excitation System	467
Differential Equations Describing GEU Transient Processes. Calculation of the Parameters and Coefficients of a Differential Equation System. Calculation of the Additional Resistances Included in a Control and Bias Circuit. Calculation of GEU Electromagnetic Circuit Time Constants. Design Formulas for Differential Equation Coefficients. Reduction of the Equation System to Machine Form. Development of the Mathematical Model's Schematic.	

	Page
§ 8.4 Selection of the Optimal Dynamic Characteristics of GEU With Thyristor Excitation Systems	480
Circuit Variant for GEU With Thyristor Pilot Exciters. Circuit Variant for GEU With a Main Generator and Main Propulsion Motor Thyristor Excitation System.	
§ 8.5 Calculation and Study of GEU Transient Processes Using an Analog Computer, Taking Primary Motor Dynamics into Account	490
Special Features of Primary Motor Dynamics and a Method for Their Calculation. System of Equations Describing GEU Transient Processes. Mathematical Modelling of GEU Transient Processes Taking Primary Motor Dynamics Into Account.	
Chapter 9	
Problems of Alternating Current Electrical Propulsion Plant Design and Their Prospective Development	/654
§ 9.1 Basic Characteristics and Selection of Alternating Current Electrical Propulsion Plant Basic Parameters	497
Voltage and Frequency. Main Propulsion Motor Types. Selection of Main Generator Type, Number, and Power. Basic Main Generator and Main Propulsion Motor Requirements. Regulation of Propellor Rotational Speed and Electric Ship Speed.	
§ 9.2 Electrical Propulsion Plant Main Current Circuits	506
Classification. Turboelectric Propulsion Plants (TEGU). Diesel- Electric Propulsion Plants (DEGU).	
§ 9.3 Excitation and Control Systems with Dynamoelectric Automation	513
Basic Assumptions. Automatic Torque Control.	
§ 9.4 Prospective Alternating Current Electric Propulsion Systems	519
Review of Alternating Current GEU Control Systems.	
§ 9.5 Electrical Propulsion Plant Rectifier-Cascade Systems	520
Basic Assumptions. Electrical Cascades. Electromechanical Cascades. Control of a GEU With an Electrical Rectified Cascade.	
§ 9.6 Alternating Current Electrical Propulsion Plants With Static Frequency Converters	532
General Characteristics and Prospective Development. Frequency Converters With a Direct Current Link. Direct Frequency Converters (NPCh). Frequency Converter Circuit Selection. Frequency Converter	

	Page
Control System Operating Principle. Selection of a Frequency Control System With Static Converters. Requirements Levied on Direct Frequency Converter Control Systems. Selection of Direct Frequency Converter Control Systems Given a Resistive Load. Selection of Direct Frequency Converter Control Systems Given a Resistive-Inductive Load.	
Chapter 10	
Transient Processes in an Alternating Current Electric Propellor Drive	
§ 10.1 Special Features of Main Propulsion Motor Starting and Reversal Calculations	567
§ 10.2 Main Propulsion Motor Reversal	571
Reversal Diagrams for Propulsion Plants with Induction GED. Reversal Diagrams for Propulsion Plants with Synchronous and Synchronous-Induction GED. Stages of GED Reversal and Methodology of Their Calculation. Measures to Improve Alternating Current GEU Starting and Braking Characteristics.	
§ 10.3 Calculation of Generator Excitation Characteristics	585
Initial Calculation Data. Calculation Methodology.	
§ 10.4 Calculation of the Starting and Reversal Process for an Electric Propellor Drive With Synchronous Machinery	589
Assumptions Made. Calculation Methodology Given GED Reversal With Plugging.	
§ 10.5 Synchronous Main Propulsion Motor Dynamic Braking	599
Braking Process. Calculation Methodology.	
§ 10.6 Methodology for Transient Process Calculation During Main Propulsion Motor Starting	/655 610
Initial Data. Calculation Sequence.	
§ 10.7 Calculation of Transient Processes During Synchronous Main Propulsion Motor Reversal	616
Initial Data. Reversing Stages Given Absence of Dynamic Braking.	
Chapter 11	
Geometrical and Weight Characteristics of Electrical Propulsion Plant Main Machinery	
§ 11.1 General Considerations	623
Initial Data. Machinery Configuration. Methods of Preliminary Determination of Direct Current Machinery Size Characteristics.	

	Page
§ 11.2 Methodology for Approximate Calculation of Basic Dimensions and Weight of a GEU Salient-Pole Synchronous Machine (Using Volumetric Use Factor $C_A$ )	626
Initial Formulas. Sequence of Calculation of Basic Machinery Dimensions. Weight Calculation of Individual Machinery Parts. Calculation of Fan Drive Motor Power.	
§ 11.3 Methodology for Approximate Calculation of Basic Direct Current GEU Machinery Dimensions and Weight (Using Armature Volumetric Use Factor $C_A$ )	638
Initial Formulas. Sequence of Calculation of Machinery Dimensions. Weight Calculation of Individual Machinery Parts. Calculation of Armature Moment of Gyration.	
Chapter 12 Dual-Current Electrical Propulsion Plants	
§ 12.1 Dual-Current Electrical Propulsion Plant Special Features and Developmental Prospects	647
Overall Advantages. Conversion Systems. Research and Design Tasks.	
§ 12.2 Special Features of Electrical Machinery Operation in a Dual-Current GEU System With Uncontrolled Rectifiers	652
Diagram of the MMF of a Synchronous Generator Running a Rectified Load. Electrical Machinery Operating Modes.	
§ 12.3 Selection of Dual-Current Electrical Propulsion Plant Rectifier Unit Circuits	656
General Assumptions. Calculation of Rectifier Unit Basic Characteristics. Rectifier Unit Comparative Evaluation.	
§ 12.4 Elements of the Theory and Calculation of Characteristics of Dual-Current Electrical Propulsion Plants With Uncontrolled Rectifiers	663
Calculation of Synchronous Generator Current and Voltage Harmonic Components. Numerical Example of Calculation of Higher Harmonics for GED. Calculation of Converter Control Characteristics. Special Features of Calculating Static Characteristics.	
§ 12.5 Elements of the Theory and Calculation of the Characteristics of Dual-Current Electrical Propulsion Plants With Controlled Rectifiers	683
Power Characteristics. Form of the Current and Voltage Curves	

	Page
on the Alternating Current Side. Calculation of Generator Phase Current Harmonics. Calculation of Rectified Voltage Harmonics.	
§ 12.6 Problems Using the Analytical Method in Calculation of Transient Processes in Dual-Current Electrical Propulsion Plants	691
General Assumptions. Analytical Method for an Approximate Calculation. Expression for Undistorted EMF in a Transient Mode.	
§ 12.7 Mathematical Modelling Method of Calculating Transient Processes	/656 702
General Assumptions. Initial Modelling Data. Synchronous Generator Electronic Model. Electronic Model of a GED and its Exciter. Examination of the Special Features of GED Operation from a Rectifier Unit. Electronic Model of the Link Between an SG and GED. Current Converter Electronic Model. Voltage Converter Electronic Model. Examination of a Rectifier Unit. Excitation System Modelling Considering Feedback. Transient Process Electronic Modelling. Transfer Function Modelling.	
§ 12.8 Dual-Current System Main Circuit Circuitry	722
Circuit Selection. Circuits for GEU With VU Consisting of Uncontrolled Rectifiers. Circuits For GEU With Controlled Rectifiers in the Main Circuit.	
§ 12.9 Dual-Current Electrical Propulsion Plant Excitation Systems	730
Excitation System Special Features. Excitation System With Parallel Current Compound Excitation. System of GED Excitation from Controlled Rectifiers. GEU Excitation System During Reversal in the Main Current Circuit.	
§ 12.10 Dual-Current Electrical Propulsion Plant With Single Electrical Power Plant (With Power Take-Off for Shipboard Network Consumers)	740
General Assumptions. Circuit With Power Take-Off From ShED for a Three-Shaft Propulsion Plant. Circuit Variant With Power Take-Off for a Fixed Current System. Special Features of a Power Take-Off and Automatic Control Given a Two-Loop GEU Circuit.	
§ 12.11 Foreign Know-How In Building Dual-Current Electrical Propulsion Plants	751
Bibliography	755

Osnovy proyektirovaniya grebnykh elektricheskikh ustanovok [Fundamentals of Electrical Propulsion Plant Design]

N. A. Kuznetsov, P. V. Kuropatkin, A. B. Khaykin, and N. M. Khomyakov

This book was written to generalize domestic and foreign know-how accumulated in design of electrical propulsion plants (GEU), especially relative to their parameters and characteristics; to examine ways to insure their reliable and economic operation in stable and transient modes, as well as to determine trends in GEU upgrading through use of achievements in electronic technology and automated control equipment.

Different methods were employed to present the material: a set of circuits with descriptions is provided, as are recommendations on their selection; analysis of physical processes (mainly transient) occurring in various GEU systems is supplied; a mathematical description of static and transient processes is provided and ways to compute them are examined.

The authors deemed it necessary to present linear and non-linear analytical and graphic-analytical methods, as well as mathematical modelling methods using analog computers, in the book.

Much of the book has been devoted to engineering methods of computing static and transient processes for typical dc and ac GEU circuits. Methods presented have been proved many times over in GEU design practice and verified in numerous full-scale tests. Materials on future GEU systems, dual-current GEU, and GEU with static frequency converters in particular, have been presented in detail. The authors have generalized know-how accumulated in designing dual-current GEU with uncontrolled rectifiers and they point out ways to use controlled rectifiers and GEU static frequency converters.

The book presents a collection of numerous GEU circuits for propulsion plants in operation and in the planning stages, while pointing out the advantages and

disadvantages of different main field current, control, protection, and monitoring systems and circuits. This allows specialists working in the design area to consider proposed recommendations and correctly to select a circuit in accordance with vessel class and special requirements.

49 tables, 287 illustrations, bibliography of 89 titles.

Reviewer, Doctor of Technical Sciences V. V. Tikhonov

Scientific Editor, Candidate of Technical Sciences S. B. Rukavishnikov

Electrical propulsion plants (GEU) have been developing in recent years. The domestic transport and technical fleet is being augmented mainly by a significant number of special-purpose electrically-powered ships: tugs, ferries, icebreakers, and so on. Under certain operating conditions possessing several advantages over direct propellor drive, electrical propulsion plants provide good operating indicators to transport and technical fleet vessels.

A great deal of know-how has been accumulated in the USSR in design, construction, and operation of GEU and a vast amount of technical literature on these problems has appeared.

Soviet scientists and engineers have participated and are participating in development of GEU theory and their practical use. The works of Doctor of Technical Sciences Professor V. I. Polonskiy, distinguished figure in RSFSR science and technology and founder of GEU theory, Doctor of Technical Sciences V. T. Kas'yanov, the most prominent specialist in the field of electrical machinery design, and other scientists are examples.

The work done by engineer N. A. Agafonov, chief designer of the electrical systems in the nuclear vessel "Lenin," and other specialists facilitated use of these theoretical data in practice, which was manifested in creation of many improved GEU.

The second scientific and technical conference on marine electric propulsion held in 1957 laid the foundation for certain results in operation of ships with electric propulsion and gave the prognosis for further GEU development.

*Technology has made great strides since the conference was held. Excitation systems with static rectifiers and contactless control systems appeared; amplidyne and other elements have occupied a firm place in varied-purpose GEU.*

The goal of this book is to generalize know-how in the design of GEU, [4] especially regarding selection of their parameters and characteristics, to examine ways to insure their reliable and economic operation in fixed and transient modes, as well as to note ways to improve GEU on the basis of modern technological achievements.

This book is the result of collective labor: N. M. Khomyakov wrote the Introduction; N. A. Kuznetsov and N. M. Khomyakov Chapter 1; N. A. Kuznetsov Chapter 2; N. A. Kuznetsov, P. V. Kuropatkin, and A. B. Khaykin Chapter 3; N. A. Kuznetsov Chapter 4; N. A. Kuznetsov, P. V. Kuropatkin, and A. B. Khaykin Chapter 5; A. B. Khaykin Chapter 6; P. V. Kuropatkin, A. B. Khaykin, and N. M. Khomyakov Chapter 7; A. B. Khaykin Chapters 8, 9, and 10; N. M. Khomyakov Chapter 11; and A. B. Khaykin Chapter 12. N. M. Khomyakov provided overall direction to the author collective.

A breakdown of the conditional designators used in the diagrams is provided in a listing at the beginning of the book.

The authors express their sincere gratitude to Doctor of Technical Sciences V. V. Tikhonov and Candidate of Technical Sciences S. B. Rukavishnikov for the valuable comments they made during their review and editing of the book.

The authors will be grateful to the readers for critical comments on this book. We request that comments be sent to: 191065, Leningrad, ul. Gogolya, 8, Izdatel'stvo Sudostroyeniye.

Listing of Circuit Element Conditional Designations

[5]

		<u>Russian</u>
A	automatic switch	A
AVG	generator field circuit breaker	ABГ
AGP	field killing circuit breaker	АГП
AD	induction motor	АД
BBUT	compensation current interblock unit	ББУТ
BD	door interlock	БД
BZ	delay unit	БЗ
BM	diesel fuel supply interblock magnet	БМ
BP	converter unit	БП
BS	comparator	БС
BT	thyristor unit	БТ
BUT	thyristor control unit	БУТ
V	exciter	В
Vst	stabilitron	Вст
VBD	door interlock switch	ВБД
VV	field switch	ВВ
VVG	generator pilot exciter	ВВГ
VG	generator exciter	ВГ
VD	GED exciter	ВД
VDD	additional GED exciter	ВДД
VDK	door contact switch	ВДК
Vk	switch	Вк
VMM	maximum power contact switch	ВММ
VO	main exciter	ВО
VP	feed switch	ВП
VPN	"diesel is ready to receive load" switch	ВПН
Vp	rectifier	Вп
VPU	barring gear starter contacts	ВПУ
VR	stand-by exciter	ВР
VT	auxiliary electropneumatic rectifier	ВТ
VU	rectifier unit	ВУ
G	generator	Г
GB	fire alarm	ГБ
GV	generator switch	ГВ

		<u>Russian</u>	
GVP	generator electric fan starter blocking contact	ГВП	
GPN	constant voltage generator	ГПН	
D	main propulsion motor	Д	
Dz	diesel	Дз	
DV	electric fan starter blocking contacts	ДВ	
DG	diesel generator	ДГ	
DK	door contact	ДК	
Dk	stern motor	Дк	
DL	electric winch motor	ДЛ	
DM	demodulator	ДМ	
DN	voltage sensor	ДН	
Dn	pump motor	Дн	
Dnas	electric pump motor	Днас	
DrN	saturable reactor	ДрН	[6]
DP	commutating pole	ДП	
Dr	choke	Др	
DT	current transducer	ДТ	
Zv	bell	Зв	
I	discrimination switch contact	И	
IV	field switch	ИВ	
K	contactor	К	
KV	field contactor	КВ	
KVV	exciter field contactor	КВВ	
KVD	GED field contactor	КВД	
KVG	generator field contactor	КВГ	
KD	GED armature shunting contactor	КД	
KDD	diesel starting contactor	КДД	
KZ	protection contactor	КЗ	
KMM	maximum power contactor	КММ	
KO	compensating winding	КО	
KP	intermediate contactor	КП	
KRV	"Ahead" reversal contactor	КРВ	
KRN	"Astern" reversal contactor	КРН	
KS	audible signal cancel button	КС	
KT	braking contactor	КТ	
KTG	monitoring tachogenerator	КТГ	

		<u>Russian</u>
KU	control button	КУ
LZh	yellow indicator light	ЛЖ
LK	red indicator light	ЛЗ
LO	scale illumination light	ЛК
LS	indicator light	ЛО
MN	oil pump starter blocking contact	ЛС МН
MP	direct current machine	МП
MT	supervisory telegraph transducer-receiver	МТ
MU	magnetic amplifier	МУ
NVO	separate excitation winding	НВО
NVR	standby exciter separate excitation winding	НВР
OV	field winding	ОВ
OVVG	generator exciter field winding	ОВВГ
OVVD	GED exciter field winding	ОВВД
OVVDD	auxiliary GED exciter field winding	ОВВДД
OVVDD	additional GED exciter field winding	ОВВДД
OVVDO	main GED exciter field winding	ОВВДО
OVG	generator field winding	ОВГ
OVD	GED excitation winding	ОВД
OVDD	GED excitation auxiliary winding	ОВДД
OVDO	GED excitation main winding	ОВДО
OZ	master winding	ОЗ
OZG	generator exciter master winding	ОЗГ
OZD	GED exciter master winding	ОЗД
ON	potential winding	ОН
OMD	GED power control winding	ОМД
OS	stabilized winding	ОС
OSm	bias winding	ОСм
OSN	voltage feedback winding	ОСН
OSS	diesel rotational velocity feedback winding	ОСС
OT	current winding	ОТ
OTG	generator current winding	ОТГ
OTD	motor current winding	ОТД
OU	EMU control winding	ОУ
OUr	compensating winding	ОУр
P	switch	П

Russian

PV	field switch winding	ПВ	
PV0	exciter set starter blocking contacts	ПВ0	
PVR	exciter set starter blocking contacts	ПВР	
PG	generator switch	ПГ	
PGD	diesel control switch	ПГД	
PI	selector switch pedal contact	ПИ	
PIV	field switch pedal contact	ПИВ	[7]
PK	starting button	ПК	
PK-2	supervisory telegraph enunciator	ПК-2	
PK0	differentially-compounded winding	ПК0	
PKR	standby exciter differentially-compounded winding	ПКР	
PO	starting winding	ПО	
POM	power limitation switch	ПОМ	
PP	station switch contact	ПП	
PPP	station switch pedal contact	ППП	
Pr	fuse	Пр	
PR	rotary converter	ПР	
PRV	potentiometrical field regulator	ПРВ	
PS	correlator	ПС	
PSS	network-mode generator switch blocking contacts	ПСС	
PSD	diesel speed switch	ПСД	
PU	control station	ПУ	
PUV	exciter field control station	ПУВ	
PUD	GED field control station	ПУД	
PKh	characteristics indicator	ПХ	
PYaS	scale brightness switch	ПЯС	
R	knife switch	Р	
RB	interlock relay	РБ	
RBD	diesel reversal protection	РБД	
RVb	field regulator	РВб	
RV	time relay	РВ	
RVV	exciter field regulator	РВВ	
RVP	howler	РВП	
RG	cargo relay	РГ	
RD	pressure relay	РД	
RDV	water pressure relay	РДВ	

		<u>Russian</u>
RDM	oil pressure relay	РДМ
RDMD	diesel oil pressure relay	РДМД
Rz	isolator	Рз
RZ	ground relay	РЗ
PZm	delay relay	РЗм
RK	reversal contactor	РК
RM	overvoltage relay	РМ
RMN	undervoltage relay	РМН
RN	voltage relay	РН
RNT	voltage and current regulator	РНТ
RO	bucking winding	РО
ROV	exciter regulating winding	РОВ
RP	overload relay	РП
RPr	intermediate relay	РПр
RS	signal relay	РС
RSD	GED speed limitation relay	РСД
RSDz	diesel operation enunciator relay	РСДз
RSO	rotational speed reduction relay	РСО
RST	turbogenerator speed reduction relay	РСТ
RT	thermal relay	РТ
RTV	coolant temperature relay	РТВ
RTM	diesel oil temperature relay	РТМ
RTS	alarm indicator relay	РТС
RF	field boosting relay	РФ
RTs	centrifugal relay	РЦ
S	capacitor	С
SB	ballast resistance/resistor	СБ
SV	voltage feedback relay	СВ
SVO	self-excitation winding	СВО
SVR	standby exciter field winding	СВР
SG	synchronous generator	СГ
SD	additional resistance/resistor	СД
Sd	engine solenoid	Сд
SL	indicating light	СЛ
SO	series field winding	СО
SP	control station resistance/resistor	СП

		<u>Russian</u>	
SPS	comparison potentiometer resistance/resistor	СПС	
SR	discharge resistance/resistor	СР	
ST	stabilizing transformer	СТ	
SU	standardizing resistance/resistor	СУ	
SUM	synchro	СУМ	
SF	capacitance filter	СФ	[8]
SSh	padding resistor	ССШ	
SE	economic resistance	СЭ	
SYa	connection box	СЯ	
T	diesel regulator electropneumatic rectifiers	Т	
TVG	generator air temperature indicator	ТВГ	
TVD	diesel coolant water temperature indicator	ТВД	
TVDV	main propulsion motor air temperature indicator	ТВДВ	
TG	tachogenerator	ТГ	
TM	oil temperature indicator	ТМ	
TMG	generator oil temperature indicator	ТМГ	
TMD	diesel oil temperature indicator	ТМД	
TN	voltage transformer	ТН	
TP	semiconductor triodes	ТП	
TPT	direct current transformer	ТПТ	
Tr	transformer	Тр	
Trb	turbine	Трб	
TT	current transformer	{ ТТ	
TT	current sensor		
Ur	current balancer	Ур	
FB	functional block	ФБ	
Sh	shunt	Ш	
ShSN	station bus bars	ШСН	
ShED	electric propulsion bus bars	ШЭД	
EI	discriminator switch electromagnetic latch	ЭИ	
EMU	amplidyne	ЭМУ	
EMUG	generator amplidyne-exciter	ЭМУГ	
EMUD	GED amplidyne-exciter	ЭМУД	
EPV	field switch electromagnetic latch	ЭПВ	
EPP	station switch electromagnetic latch	ЭПП	
ER	isolator electromagnetic latch	ЭР	

The birth of marine electric propulsion dates back to 1838, when Russian academician B. S. Yakobi first used it on a boat with a paddle engine, batteries with galvanic elements, and a 3/4 hp electromagnetic motor. The boat carried 12 passengers and traveled upstream on the Neva at speeds of about 4 km/hr.

Marine electric propulsion came into being overseas some two decades after Yakobi's experiment.

The first attempt to create similar devices for submarines dates to 1861 and, by the early 1890's after the appearance of electric storage batteries, electric propulsion plants replaced all other types of motors as the means to propel submerged submarines.

Industrial use of electric propulsion for surface vessels took place for the first time in Russia when in 1903-1904 two oil tankers, "Vandal" and "Sarmat," were built at the Sormova Plant. These vessels were the world's first steamers with electric drive from a primary motor to a propellor shaft. Three non-reversible 120 hp/240 rpm motors (diesels) were installed in "Vandal," while two non-reversible 180 hp/240 rpm motors were installed in "Sarmat." The vessels made about 8 knots.

During movement forward, the primary motors were connected directly via an electromagnetic clutch to propellers. The diesels operated to the propellers via a generator-dc motor electrical drive system during movement backwards and during maneuvering operations. This system was used because no reversible diesels existed at that time. Later on, it did not prove out. We note that both vessels were in service after the Great October Socialist Revolution as well: the [10] former was named "Internatsional" and the latter "Nikolay Ostrovskiy."

Construction of the electric ships in modern use began in 1913. Electric propulsion basically was introduced in combination with steam powerplants both for military surface ships and for vessels in the transport fleet. The first steps in this direction were taken in the USA, where experiments were run with three coalers: "Cyclone," "Neptune," and "Jupiter," with 20,000 tons displacement and cargo capacity of 12,000 tons at 14 knots. The first was equipped with a

triple-expansion steam engine with an indicated capacity of 6700 hp, the second with a turbogear transmission with individual forward and reverse turbines, and the third with a 6300 hp three-phase turboelectric powerplant. The first ship's powerplant weighed 280 tons, while that of the second and especially the third weighed considerably less. Thus, the turboelectric powerplant in "Jupiter" weighed 156 tons.

Following this experiment, the USA used electric propulsion widely for naval vessels. From 1916 through 1927, 118 electric ships (steam turbine and diesel) with a total capacity of about 700,000 hp were built there.

Diesels were used for the first time in electric powerplants in the USA in 1919. By 1927, 17,000 hp was the limit for GEU capacity for the transport fleet (the turboelectric "California" freight and passenger ship) and was 2500 hp for diesel electric ships.

Further electric propulsion development mainly followed the path of construction of turboelectric propulsion plants. The turboelectric ship "Normandy" had the most powerful powerplant (1935). Its main engine consisted of four three-phase current turbogenerators with a capacity of 30,100 kw each at 6000 volts and a rotational velocity of 2400 rpm and four synchronous main propulsion motors with a capacity of 40,000 hp each at a rotational velocity of 243 rpm.

The advantage of alternating current compared to direct current appeared by this time where transport vessels were concerned. This advantage was the high efficiency, simplicity of the electrical machinery, operating reliability, smaller size, and lower cost. Thus, dc machinery has an efficiency of 86%, while that of a three-phase synchronous motor of the same capacity is 95%.

One should establish 1934 as the initiation of electric ship construction in the USSR, when the "El'brus" floating base went into operation. It had a diesel-electric powerplant consisting of two dc diesel generators rated at 1200 hp each (in the diesels) at 300 rpm and two single-armature main propulsion motors rated at 400 kw each at 330 volts and 200 rpm. The electrical propulsion plant's circuit was built using a G--D [generator-diesel) system with differentially-compounded winding system, which provides a power constraint. The main propulsion

motors had rotating frames, which made it possible to replace pole coils [11] without dismantling the machinery.

The passenger vessel "Progress," completed in 1937, was the first river vessel with a diesel-electric propulsion plant in the USSR. The vessel with a displacement of 165 tons had two paddle wheels that rotated at 50 rpm. The diesel rated at 250 hp, 1000 rpm; a 150 kW, 230 V, 1000 rpm generator, propellor motors rated at 66 kW, 220 V, 1070 rpm operated each of its paddles via two-stage reduction gears. This vessel had a draft of 0.52 meters and was operated successfully on small rivers.

Two 12,000 hp diesel-electric icebreakers, "Kirov" and "Kuybyshev," began to be built in 1937 in the USSR. In design, these icebreakers had four 3000 hp diesel generators at 330 volts and 300 rpm.

Diesel generators must operate on three main propulsion motors with a power ratio of 1 : 2 : 1. In 1941 in connection with Fascist Germany's attack on the USSR, construction of these vessels was halted. Between 1937-1937, several passenger and freight and passenger diesel electric ships of the "Wuppertal" and "Patria" (now the "Rossiya") class with the same motor type were built in Germany.

The Second World War brought a halt to construction of vessels with electric propulsion in several countries. Exceptions were the USA and England, where 551 transports were built between 1939 and 1945 -- turboelectric ships with a total capacity of 4.13 million hp, making up about 20% of the powerplant capacities of these countries' fleets.

Several electric maritime vessels were built and placed in operation in the USSR after the Great Patriotic War (see Table B1).

During that period, electric river ships also were built along with the maritime vessels (Table B2).

The nuclear vessel "Lenin" joined the Soviet Arctic Fleet in 1964. Its GEU consists of four turbogenerator aggregates and three dc main propulsion motors with a power ratio of 1 : 2 : 1. The vessel displaces 16,000 tons and has a total

power at the propellers of 40,000 hp. At present, this is the most powerful dc turboelectric propulsion plant.

Overseas, electric propeller drive began to gain prominence in the FRG in 1950 mainly for special-purpose vessels (ferries, tugs, and so forth) with dc diesel-electric powerplants. Some were built with a diesel-electric powerplant, including freight and passenger vessels of the "Falkenstein" class with shaft output of 4650 hp with four diesel generators of 1150 kW each at 300 rpm.

At the same time, the tendency in the FRG was conversion to high-speed diesel aggregates. "Wappen von Hamburg" with shaft output of 2X2675 hp and with diesel generators of 5X325 hp at 1500 rpm is an example.

Table B1

Specifications of USSR Maritime Electric Ships  
(Built 1947-1966)

[12]

Name	Purpose	Year Built	Displacement tons	Shaft Output hp	Speed knots
"Chiaturi"	Dry Cargo	1947	3000	1300	11.5
"General Azi Aslanov and others"	Tanker	1950	12960	2720	11.6
"Nadya" and others	Ferry	1951	3450	3000	12.0
"Neva-1)	Dredger	1951	—	400	—
"Lena," "Ob'," and others	Icebreaker-Transport	1954-1956	11540	7000	15.5
"Kapitan Belousov" and others	Icebreaker	1954-1955	4500	10500	16.5
"Lensovet"	Cargo and Passenger	1956	5775	8000	18.0
"Dneproges" and others	Dry Cargo	1956	10460	6545	16.0
"Aktyubinsk" and others	Refrigerator	1956	10460	6545	16.0
"Mitsy" and others	Whaler	1956	1273	3540	16.5
"Ural"	Tanker	1956	12960	3200	12.2
"Golias"	Tug	1956	1220	1500	12.4
"Moskva" and others	Icebreaker	1960-1966	13300	23000	—

Table B2

Specifications of USSR River Electric Ships  
(Built 1950-1960)

Name	Purpose	Year Built	Displacement tons	Propellor Output, hp	Speed Knots
"Volga" and others	Icebreaker	1955	655	1600	22
"Rossiya" and others	Cargo and Passengers	1952	1000	800	21

We present comparative data on the weight characteristics of powerplants with direct propellor drive and with diesel-electric drive (Table B3) to illustrate the advantages of using high-speed diesels in the Daimler-Benz diesel-electric ship "Tippit." Thanks to placement of the diesel generators in the stern, this vessel's cargo capacity is increased 426 m<sup>3</sup> in bales and 738 m<sup>3</sup> in grain. In spite of less efficiency, ton-mileage turns out to be cheaper. At 12.6 knots and 60,000 miles traversed annually, 7.35 grams of fuel are expended per ton-mile, whereas a vessel with an indirect drive machinery plant uses 8.5 grams of fuel. In addition, the service life of the diesel generators reaches 10,000-14,000 hours.

Table B3

Relative Weight Characteristics of Diesel and Diesel-Electric Powerplants

Propellor Drive Type	Weight, tons		
	Shafting and Propellor Main Motor	Auxiliary Aggregates	Total
Diesel operating directly on the propellor	312	<del>36</del> 32	348
Two medium high-speed diesels with gear transmission rated at 3600 hp, 300 rpm	170	36	206
Five diesel generators, main propulsion motor with gear transmission rated at 4400 hp, 1300 rpm	92	11	103

During the postwar period, construction of steam turboelectric powerplants on vessels in the transport fleet was reduced severely thanks to development of diesel-electric powerplants.

However, the turboelectric powerplant in the English vessel "Canberra" built recently is of considerable interest: its maximum rating is 85,000 hp and its normal rating is 68,000 hp at propellor speeds of 147 and 136.5 rpm, respectively.

Generator data are:

- a) maximum output 32,000 kW at 3087 rpm and frequency of 51.5 Hz,  $\cos \phi = 1$ , voltage 6000 V as one generator operates on one synchronous main propulsion motor;
- b) 30,700 kW at 2400 rpm and a frequency of 40 Hz,  $\cos \phi = 1$ , voltage 4640 V as one generator operates two main propulsion motors.

The main propulsion motors are two-armature motors with an independent cut-in circuit, salient poles, with a damping cage on the poles. The circuit permits feed from one generator for the stators of various main propulsion motors, something required for synchronous operation of the propellers to reduce hull vibrations.

In the USA, vessels in the auxiliary and icebreaker fleets mainly are equipped with electrical propulsion plants. An example is the icebreaker "Glacier" with a dc diesel-electric powerplant rated at 22,000 hp on two propeller shafts. This powerplant has 10 diesel generators operating five aggregates on each propeller.

The following vessels at the present time have the greatest GEU ratings: [14]  
the turboelectric ship "Normandy" with an ac powerplant and shaft output of approximately 160,000 hp;  
the turbonuclear "Lenin" with an ac powerplant and shaft output of about 40,000 hp;  
the diesel-electric ship "Moskva" with a dc powerplant and shaft output of approximately 23,000 hp;  
the diesel-electric ship "Rossiya" with an ac powerplant and shaft output of about 16,000 hp.

These data demonstrate that, based on most qualitative indicators, electrical propulsion plants are the most modern technically in the USSR.

Examining in more detail trends in development of electrical propulsion plants for domestic and foreign fleets, one can make the following conclusions:

1. Basic GEU development follows the line of construction of diesel-electric powerplants mainly for special-purpose vessels (ferries, icebreakers, and so on). Use of high-speed diesels is expanding. Due to the constrained output of these diesels, electric propulsion will become a means of increasing the total shaft output of maritime powerplants.

2. The field of use of diesel-electric propulsion plants (DEGU) on varied-purpose vessels is expanding. The degree of use of the technical possibilities of electric propeller drive is increasing thanks to use of standard diesels on vessels with varied total capacity.

3. Centralized remote control of individual GEU elements from shipboard control stations is occurring.

4. Elements of electrical machinery automation are used to support GEU qualitative characteristics.

5. The field of use of combined electrical propulsion plants (for dredgers, self-propelled cranes, and so forth) is expanding.

Further GEU improvement can be provided through: a) use of high-speed non-reversing diesels and gas turbines; b) use of powerplants with high-speed main propulsion motors; c) improvement in main current and excitation circuitry to provide the maximum increase in vessel survivability; d) automation of control circuitry through use of electrical machinery automation and contact-free control elements; e) improvement in power take-off conditions for auxiliary and other needs.

One should anticipate new trends in GEU development, to include universal use of nuclear power and, in this connection, of steam turbine powerplants, both ac and dc.

An approach new in principle is a dual-current system in which electric power of ac generators using controlled rectifiers is converted to dc transmitted to the main propulsion motors.

The brief review of GEU presented above demonstrates the wide variety of [15] powerplant types differentiated by current type, primary motors, as well as by the parameters of the main circuit and of the control and monitoring circuits. Naturally, in a number of instances, this complicates selection of elements of the powerplant being designed but, at the same time, provides a designer with a chance for creative solution of the problems presented. Thus, in view of the absence in GEU of rigid mechanical connection between primary motors and propellers and thanks to the opportunity to connect several generator aggregates into the feed system for one main propulsion motor, the GEU designer consecutively can develop several circuits with different parameters so that, having selected the preferred variant after careful compilations, he can make further improvements. As a rule, a conventional vessel designer does not have similar opportunities. Being constrained by the limited number of primary motor types at every step, he can provide the required output only through a single set of main generators and, possibly, only through one main current circuit.

Correct selection of the following is of especially great significance as a GEU design is being developed:

- GEU type depending on the purpose of the powerplant;
- current type, current system, amount of voltage, and frequency when ac powerplants are involved;
- parameters of primary motors and main generators; basic parameters of the main propulsion motors (their rating, number, rotational velocity, field system, and so on);
- distribution device circuit, equipment for this circuit;
- field system elements, parameters of electrical machinery and contact-free automation (EMU [amplidynes], magnetic amplifiers, chokes, semiconductor instruments, and so on);
- protection circuits, GEU indicators and interlock.

The latter should be looked upon in a complex with electrical powerplants (EEU) also when selecting the type of maritime powerplant and substantiation of GEU advantages. This is necessary because, for some vessel types, the greatest load on the electric powerplant, based upon which generator number and rating are selected, occurs either when the vessel is at anchor or at slow speeds and can be supplied by GEU generators which, during that time, are not supplying power to the propulsion motor. In this case, there is a requirement to select an EEU generator rating based upon conditions involving full speed and maximum load based upon conditions involving covering it using GEU generators. Dredge pumps, large tugs -- rescue boats, mooring vessels, and the like -- may serve as an example of a similar vessel type.

Joint examination of GEU and EEU exerts an influence on GEU parameters. [16]  
Since three-phase 380 V ac is the basic current type for maritime EEU, GEU generators fed from the shipboard network also must be three-phase 400 V current.

Preference should be given to dual-current GEU in those instances when GEU generators are used to feed the shipboard network.

Analysis of GEU systems is repeated after final determination of GEU main parameters and the characteristics of individual elements. Things checked here include how much the elements enumerated above correspond to the levied requirements

and do they support the stability of the GEU automatic control system. In the event the latter does not meet initial requirements, additional corrective links are introduced. In addition, the quality of GEU transient processes is studied and their correlation with the technical conditions and requirements for reliable, accident-free system operation is evaluated.

It is evident from what has been said that several preliminary approximate calculations must be made in the initial stage of GEU design, with subsequent refinements made by the design bureau and plant suppliers.

## Electrical Propulsion Plant Equipment Requirements

## § 1.1 Primary Motor and Main Propulsion Motor Characteristics

Electric propulsion (electric propellor drive) is used on various ship types. It was used widely in icebreakers (all postwar icebreakers were built with electric propellor drive), tugs, and ferries. Electric propulsion also is used in several dry cargo and refrigerator ships.

When a propellor is provided direct drive from a primary motor, the output of the primary motor is used fully only in the mode for which the propulsion plant is envisioned. For example, if the propulsion plant is envisioned for operation of the vessel on the open sea, then it is necessary to reduce the rotational velocity of the primary motors for every increase in resistance to movement. But, if it is envisioned for towing a load, the primary motors will not be loaded during movement on the open sea since fully loading them requires increasing the propellor rotational velocity and the primary motors do not allow this.

As is known, primary motors with high rotational velocity can be used in GEU. Here, the propellor rotational velocity is selected as an optimum since a main propulsion motor can be envisioned essentially for any rotational velocity.

Possibilities for using high-speed primary motors considerably increased with appearance of dual-current GEU having ac generators and dc main propulsion motors fed via silicon rectifier units.

A rather important advantage of electric propulsion is the capability to feed main propulsion motors from several generators -- so-called power subdivision, whereby electrical propulsion plant survivability is increased.

A GEU makes it possible easily to change, within known limits, the ratio from the primary motor to the propellor, given simultaneous use of the primary [18] motor's full output, as well as to regulate given constant output, i. e., to achieve increased moments on the propellor at a reduced rotational velocity.

Selection of the electric propellor drive requires examination of the entire

complex of shipboard devices servicing its operation: vessel hull, propellor, main propulsion motor, generator, and primary motor and control system, plus examination of a part of this complex in their interaction.

A GEU designer must use individual conclusions from the theory of a vessel's motion and propellor theory. Thus, the power of a main propulsion motor is determined from the expression

$$P_a = \frac{P_0}{1,36\eta_a} \text{ kW} \quad (1.1)$$

where  $P_0$  is the towing power, i. e., the power expended on movement of a given vessel with a given speed, hp;  $\eta$  is the propulsive efficiency of the propellor, equal to 0.6-0.7;  $\eta_a$  is the efficiency of the shafting and support bearing, equal to 0.97-0.98.

Generator power:

$$P_r = \frac{P_a}{m\eta_a} + \Delta P, \quad (1.2)$$

where  $m$  is the number of generators feeding the main propulsion motor;  $\eta_a$  is the efficiency of the main propulsion motor;  $\Delta P$  is losses in the network taken to equal 0.5%.

Primary motor power:

$$N_e = \frac{P_r}{\eta_r}, \quad (1.3)$$

where  $\eta_r$  is generator efficiency.

A further stage in GEU development is calculation and construction of the characteristics of the main propulsion motor, which in turn requires having at one's disposal the characteristics of the propellor  $M = f(n_d)$  for the "movement on the open seas" mode (curve 1 in Fig. 1.1) and for the "moored operation" mode (curve 2). Development of GEU for tugs requires having the characteristics of the propellor  $M = f(n)$  when towing (curve 3). One important special feature of main propulsion plants is use of full primary motor power as the propellor operates

in the entire range of characteristics from movement on the open sea to moored operations, i. e., the main propulsion motor can be assigned characteristics similar to curve 5 in the sector between points A and B.

The use of full motor power in propulsion plants with direct propeller drive from a diesel or turbine is possible only in the propeller operating mode for which the propulsion plant was selected. Examination of the characteristics of primary motors is required to confirm this.

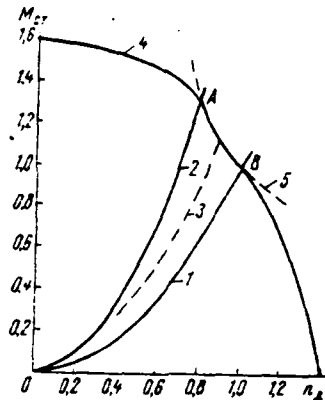


Figure 1.1. Propeller Characteristics. 1--movement in open water; 2--moored operation; 3--movement with a load; 4--idealized primary motor characteristics; 5--constant power curve.

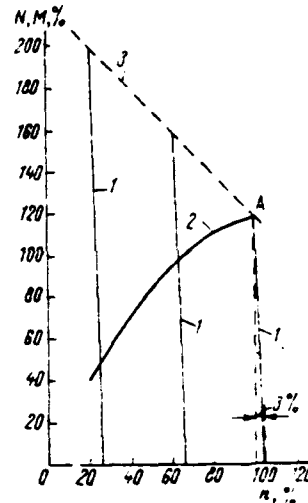


Figure 1.2. Steam Turbine Characteristics. 1--turbine regulatory characteristics; 2--ratio of power  $N$  to rotational velocity  $n$  given full supply of steam. 3--dependence of moment  $M$  on rotating speed  $n$  with complete feed of steam.

Figure 1.2 provides the ratio  $N = f(n)$  and  $M = f(n)$  for a steam turbine. [19]

The steam turbine regulator strives to maintain the rotational velocity unchanged when the load changes. The characteristics of the regulator (line 1) has a 3% slope for propulsion plants. The regulator tunes itself so that speed continuity is provided until reaching a load consisting of 120% of the nominal, after which steam supply will not change (point A). Steam turbine rotational velocity and power drop when the load exceeds 120%.

What has been stated goes for diesels as well. Ratios  $M = f(n)$  and  $N = f(n)$  presented in Figure 1.3 are similar to ratios for turbines except for the one difference that the diesel regulator maintains a constant rotational velocity

during load changes from 0 to 110%. The diesel regulator's characteristics slope also is 3% when the load changes from 0 to 100%.

The following conclusion can be made from examination of the characteristics of primary motors: if a primary motor's full power is used in the moored operation mode, then the motor will be underloaded during movement in open water; if a primary motor is selected for the open water mode of operation, then it will be overloaded during moored operations and its rotational velocity and power will be reduced.

Adjustable-pitch propellers or hydraulic transmissions are used to obtain the full power of primary motors given direct propeller drive and operation in [20] the full range of characteristics from movement in open water to moored operation.

The movement in open water mode is accepted as the nominal mode when designing GEU for liners, dry cargo vessels, and several other special vessel types; for tugs, the movement with a load mode is used, and the moored operation mode is used for icebreakers and vessels used in ice navigation.

Main propulsion motor characteristics also must support a restriction in propeller rotational velocity when it is exposed or is lost, i. e., a restriction on idle rotational velocity to values  $n_{x,x} = (1.2 - 1.4) n_{nom}$ , and, in addition, a restriction on the propeller shaft moment when the propeller seizes (stoppage under current) to value  $M_{cr} = 1.5 - 1.9$  from nominal moment (see Fig. 1.1) for a period of 1-2 minutes. This duration of stoppage under current for a main propulsion motor almost is not reflected in its dimensions, but they require an increase for a more prolonged stoppage.

One also needs to know the reversing characteristics of a propeller (Fig. 1.4), used when computing maneuvering characteristics, along with the propeller characteristics enumerated above in order to design GEU.

Such are the basic special features of electrical propulsion plants.

Serious attention must be paid to selection of primary motors, main generators, and main propulsion motors and on establishment of the proper requirements for

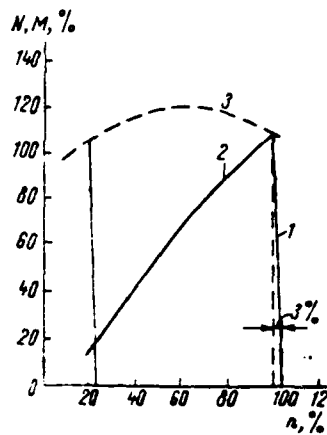


Figure 1.3. Diesel Characteristics.  
 1--Diesel regulating characteristics;  
 2--Relationship of power change  $N$  to the shaft to rotational velocity  $n$ , given full fuel supply; 3--Relationship of moment  $M$  to rotational velocity  $n$ , given full fuel supply.

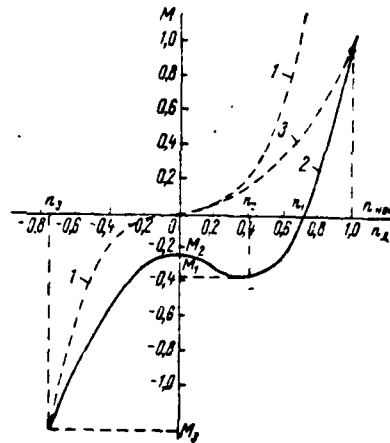


Figure 1.4. Propellor Reversing performance characteristics.  
 1--Moored; 2--Full ahead; 3--Screw

them when designing GEU since propulsion plant quality, reliability, maneuverability, dimensions, and weight depend greatly upon selection of this equipment. [21]

Basic requirements levied on this equipment are enumerated below.

### § 1.2 Primary Motor Requirements

Diesels mainly are used as primary motors in electrical propulsion plants, with turbines used rarely and gas turbines even more rarely. The requirements listed below are levied on primary motors (except for gas turbines).

Primary motors must allow the following temporary overloads: diesels 10% for 1 hour; turbines 20% for 5 minutes.

It is necessary to equip primary motors with universal-mode rpm regulators

with a remote control system for regulation of engine rpm in the entire operating range, 35 to 100% for diesels and 20 to 100% for turbines.

Regulation must be accomplished through action on the fuel supply system for diesels or steam for turbines.

There is a requirement for a grouped remote rotational velocity regulation system for all generators operating in parallel, along with an individual control system, for ac GEU made up of several generators intended for parallel operation. One lever must accomplish this regulation.

Rotational velocity regulation should be accomplished with the aid of a continuous action system. Regulators must provide continuity of the assigned rotational velocity. The maximum average deviation of rotational velocity given a fixed load must not exceed 0.5% of the installed amount. This requirement is important especially for GEU with ac generators and with a power takeoff.

Regulators for ac GEU must provide essentially linear regulatory characteristics. Envisioned in them are devices accomplishing precise subregulation of rotational velocity in the entire range of regulation. Regulators must permit a change in the degree of variation to a running motor of 5% and less.

Maximum deviation of rotational velocity from the previously-set value must not exceed 5% during the discharge and load surge of a 100% load. Establishment of the new rotational velocity must occur in no more than 15 seconds.

Primary motors should be equipped with governors, which cut off the supply of fuel or steam when rotational velocity exceeds the nominal by 15%.

It is desirable that forced lubrication gear mounted on diesels have a productivity reserve for simultaneous lubrication of generator bearings. [22]

The level of primary motor automation must be sufficient to provide for remote starting, rotational velocity regulation, stopping, protection, and indication (visible and audible) of the status of the motor's lubrication and coolant systems. One also must envisage protection acting either to cut out the propulsion plant,

cut off the fuel supply, cut off steam supply if there is emergency engine overheat, or cut off lubricant supply. Remote control and indication should be done from at least two locations.

Primary motors must not create local increased generator overheating and cause local vibrations.

### § 1.3 Main Generator and Main Propulsion Motor Requirements

Generators and main propulsion motors must be calculated for the following current overloads given nominal voltage to insure normal GEU operation as waves strike, in stormy conditions, and when underway in broken ice: 10% for a period of 2 hours, 25% for a period of 5 minutes.

Temporary current overloads at reduced voltage will occur in maneuvering modes. Analysis of several oscillograms from electric ship tests demonstrate that inrushes of current in dc GEU reach  $(1.3 - 2)I_{NOM}$ , and  $(3 - 4)I_{NOM}$  in an ac GEU. Consequently, dc machinery must without damage sustain currents of at least  $2I_{NOM}$  for a period of 5 seconds and main propulsion motor stoppage current of  $I_{ST} \geq 1.6I_{NOM}$  for a period of 1 minute. AC machinery must sustain currents of up to  $4I_{NOM}$  for a period of 3 seconds after extended operation in the nominal mode.

DC main generators rated at more than 500-600 kW as a rule must have a compensating winding, have a field reserve, and allow field current boosting necessary for tuning the circuit and a 20-25% adjustment of characteristics.

AC main generators -- synchronous generators -- must allow a temporary (up to 30 seconds) field boosting of the nominal by a factor of 2.5-3.5 at a frequency 20-30% lower than the nominal and extended field boosting to 110-115% of the nominal when the vessel is underway in stormy conditions and acceleration of transient processes in maneuvering modes.

A synchronous generator's voltage fluctuation during discharge and surge [23] of a 100% load given a nominal power factor must not exceed 10% of the nominal given a 5% change in rotational velocity.

Field systems with compounding are recommended for use for synchronous generators in dual-current GEU with dc main propulsion motors and rectifiers.

It is desirable that the value of the short-circuit ratio (OKZ) be at least 1.2-1.4, but not cause a significant increase in generator size, weight, and cost.

Efficiency, given a normal load without taking the loss for ventilation and excitation into account, must be at least (%):

For dc generators rated, kW:

up to 300	91
up to 600	92
600-1500	94
above 2500	95

For ac generators rated, kW:

1000	95
1000-2000	96
3000-5000	97
above 5000	97.5

The form of the efficiency curve must insure a maximum value at loads 3/4 to 4/4 of nominal.

There is a requirement for the main generators to be waterproof and have a closed- and open-cycle forced ventilation system. Closed-cycle ventilation is preferable since here nothing blows on the machinery and drops of oil and water do not settle in the windings. Forced ventilation can be provided both from individual electric fans and from machinery ventilation systems.

A closed ventilation system should be accompanied by air coolers with the air cooled by outboard water. Also, it is better to locate everything below. Measures must be taken to protect the generators from any leaks that may occur in air cooler pipes.

Main generators must be able to operate without forced ventilation with an approximate 50% load for a period of 2 hours.

Electric heaters which maintain the temperature inside the machinery 2-3° C above the temperature of the environment should be built in to avoid formation of condensates inside generators and main propulsion motors when they are not running.

Bakelite, cloth-based laminate, or other insulation must be used around [24] one of the bearings of the main generators and main propulsion motors to restrict spurious (stray) currents.

DC main propulsion motors must allow field boosting to 20-25% for the period of 1 hour to reduce current in the main circuit in the moored mode, while ac main propulsion motors must allow extended field boosting to 10-15% for increased system stability as the vessel is underway in stormy conditions.

AC main propulsion motors are envisioned for a static overload  $M_{max}/M_{nom} = 1.6 - 1.9$ , while the windings of ac synchronous motors are envisaged for operation in an asynchronous mode for a period of 1-2 minutes after overheating. Main propulsion motor efficiency, without taking the loss for excitation and ventilation into account, must be at least (%):

For dc main propulsion motors rated, kW:

600-1000	92
1000-1500	93
2000-5000	94

For ac main propulsion motors rated, kW:

1000-1500	95
1500-4000	96
above 4000	97

The form of the efficiency change curve in the load function must have maximum value at loads of 3/4-4/4 of nominal.

There is a requirement that the lower part of main propulsion motors, to the shaft line or to the frame parting line, be waterproof and that the upper portion be splashproof.

Ventilation for main propulsion motors is identical to that for generators.

#### § 1.4 Main Generator and Main Propulsion Plant Exciter Requirements

Exciters for dc main generators should have a prolonged power of not less than 1.2 of the power required by the generators' field windings and their discharge resistors in the propulsion plant's nominal operating mode. They also must have at least a 50% voltage reserve for adjustment of the characteristics of individual generators feeding their field windings from a common exciter and to boost the field current.

Direct current main propulsion motor exciters are planned for the prolonged [25] capacity required in the moored mode by the main propulsion plant's field windings and by their discharge resistors.

Three-winding exciters must support a current overload of 1.5-1.75 of nominal for 5 minutes, given a proportional voltage increase, when the differentially-compounded winding circuit is cut.

Magnetization force (n. s.) ratio  $F_c$  of the separate excitation and self-excitation windings in a three-winding exciter should fall in the  $F_s F_c = 2 - 1.25$  range. An increase in self-excitation winding n. s. compared to that of the separate excitation winding should not exceed the aforementioned values, since, at slow speeds, there will be a rapid rise in field voltage and a great variation in propellor rpm values during regulation from greater to smaller and vice versa. An extraordinarily high self-excitation winding n. s. can cause exciter self-excitation.

In a three-winding exciter, inclusion of a differentially-compounded winding directly in the main current circuit or parallel to the windings of auxiliary poles and in the compensation winding of main propulsion plants is permitted.

The design of three-winding exciters with a high-voltage differentially-compounded winding connected with the main current circuit must prevent contact with high-voltage current-carrying parts. A differentially-compounded winding's clamps are placed in a separate housing.

Generators with separate excitation or self-excitation possessing rigid

internal characteristics should be used as exciters for synchronous generators and motors.

Amplidynes used as exciters for main generators and main propulsion plants must have at least three control windings and, in the nominal mode, operate in the unsaturated portion of the magnetization curve.

There is a need in control generator exciters to take measures to reduce residual magnetization emf.

Rectifier units with controlled and uncontrolled silicon rectifiers can be used as exciters for main generators and main propulsion plants. Rectifier units must have a control system that insures the requisite GEU characteristics are obtained.

From the design standpoint, rectifier units should be made in the form of autonomous aggregates with the requisite protection and autonomous cooling system.

The capacity of exciters and their drive motors in ac propulsion plants should be selected with consideration for the requirement to have temporary (to a value greater by a factor of 3.5) boosting of main generator excitation during start-up and reversing of the propulsion motor and prolonged (up to 115%) boosting of [26] generator and main propulsion plant excitation as the ship is under way in stormy conditions.

Generator and motor field boosting can occur both through cutting additional resistors, which shunt during the boosting, into the field winding circuit or through use of volt-adding circuits.

#### § 1.5 Distribution Devices and Electrical Propulsion Plant Control Gear

Electric propulsion boards, panels, and control posts are designed to connect main generators with main propulsion motors, to control the propulsion plant, and to monitor its operation and that of auxiliary mechanisms and devices. Electric propulsion boards and panels can be connected to the electrical powerplant GRShch [main distribution board] and form one common design consisting of individual

panels on which commutating, protective monitoring and indication equipment, and measurement instruments are mounted.

Access must be provided to electric propulsion boards and panels for repair and servicing purposes. All current-carrying board, panel, and station elements retract into or beyond the faceplate. The only thing on the faceplate are levers and knobs for equipment control, monitoring and measurement instrument dials, and indicator lights.

Boards and panels are removable to facilitate loading aboard ship and assembly and disassembly operations. Access to all cables leading into boards and panels and for their disconnection, and to bus bars for connection to panels or parts convenient for transportation.

Cables must be fed to boards, panels, and stations from below to special terminals and assemblies that have markings. Assembly within boards, panels, and stations involves only single-core wire without metal braiding. Wires are gathered into bundles inside boards and clamped to the chassis. Small doors are permitted on the board and panel faceplate and provide access to measurement instrument fuses, indicator lights, and other equipment. Fuse connection diagrams and fuse markings must be placed on the inside of the doors. Pliers for replacing fuses and spare fuses also are located here.

Equipping electric propulsion boards and panels with mnemonic diagrams [27] indicating status of the propulsion plant and generator operation to main propulsion motors is recommended.

It is desirable to position board, panel, and control station operating equipment wheels and levers in the sequence corresponding to that of their manipulation during start, stop, and maneuvering modes. They must have clear and consistent inscriptions: "ahead," "astern," and so on.

Dimensions of knobs and levers used as reversing, line, and cam switches, equipment, and devices must be such that they do not require extraordinary force for manual operation. Maximum force must not exceed 15 kg.

Pneumatic switches need to be used in board and panel main and auxiliary circuits, as a rule. Switches whose contacts arc when tripped must have detachable contacts. In addition, they should be equipped with arc extinction chambers.

Electric propulsion boards and their faceplates must be of rectangular design no more than 2000 mm by 1800 mm, with at least 1000 mm clearance in front of the board. Movable doors for access in behind the board from the face are envisioned. Presence of a clear passage behind the board and installation of two doors, which must have an electromagnetic interlock preventing access behind the board when its bus bars and current-carrying elements are under voltage (prior to cancelling the door interlock using a special key), are mandatory.

Hardwood handrails are installed on electric propulsion boards vertically on the front and horizontally on the rear of the board. Vertical handrails at least 600 mm long must be placed on each board along the vertical and be at a height not exceeding 800 mm from the level of the handrail, while the horizontal handrails must extend along the entire board from the rear and be at a height of at least 1200 mm from the board plating.

Board design envisions a panel portion, which opens from the board face for access to those measurement instruments and other equipment attached to the rear of the board.

Board design also provides easy access to shunts, measurement instruments, and equipment requiring tuning, adjustment, and replacement during operation.

Equipment controlling auxiliary electromechanical equipment serving the propulsion plant should be located on separate electric propulsion board panels.

Indicator lights with corresponding placards must be located near levers [28] and handwheels and indicate their state. Where possible, common indicators should be in the center of the board in a visible location or above the board on a small separate panel. Disrupters and separate audible indicators are recommended for this function.

Rectifier units feeding dc main propulsion plants from ac generators should

permit temporary current overloads: up to  $(2-2,5) I_{HOM}$  for 10 seconds and  $1,5 I_{HOM}$  for 1 minute and must have a  $1,5 U_{HOM}$  voltage reserve.

We recommend building rectifier units as autonomous aggregates with built-in protection preventing an emergency when 5% of the rectifiers break down, during overloads; and when voltage increases to  $1,5 U_{HOM}$ . They must have an autonomous cooling system.

Control stations take the form of individual pedestals with levers, scales, and pointer. The lever must have a fixed position for every scale delineation.

Stations installed in a compartment should have splash protection, while those on open bridges should be waterproof.

Control stations for dc GEU must have at least 11 fixed "ahead" positions, at least 11 "astern" positions, and 1 "stop" position.

Control stations are equipped with a scale containing an arrow -- control station position indicator -- mechanically-linked with the corresponding control station lever. The control station scale must have five detents for the "ahead" position, five for "astern," and one for "stop." The "ahead" and "astern" detents must be designated "dead slow," "slow," "half," "full," and "flank."

There is a lever at the control station for each propellor (we recommend that the control station lever be linked mechanically with sensors in the telegraph circuit). Control station levers must not move more than  $180^\circ$  ( $90^\circ$  in each direction from the zero position) and must have stops to make them easy to operate.

Signal lights (green indicating that a circuit is ready and red indicating an emergency drop in a circuit) and an adjustable resistor, which must be cut in via the potentiometer circuit, need to be installed at a control station.

Control stations in ac plants which regulate GED [main propulsion motor] rpm by changing frequency are not intended for direct propulsion plant control. They serve only to transmit orders to the control panel or electric propulsion

board. Therefore, only tachometer scales, which indicate screw rpm, and indicator lights can be installed at control stations.

An indicator light comes on and a bell sounds when an ac propulsion plant [29] control post lever is moved. These indications continue until the instruction has been implemented, i. e., until the response telegraph pointer coincides with the issuing telegraph pointer.

Control station design envisions easy lever movement, so no more than 5 kg of force is required to move one.

Control stations must consist of prefabricated rigid frames and vertical or horizontal metal panels. Equipment, instruments, and devices used for direct plant control are assembled in them in accordance with the electric propulsion circuit.

There is a requirement for control stations to be rectangular no more than 1800 mm and no less than 1200 mm high, with slanted or vertical panels. At least 1000 mm clearance is left in front of the station. There must be panel areas that open from the front for access to measurement instruments and individual equipment.

As a rule, pneumatic switches and reversers are used. However, special gas and oil switches approved by the USSR Registry also can be used. In this event, all special requirements involving use of this equipment must be met.

Along with main contacts, switches and reversers must have auxiliary contacts and blocking contacts for simultaneous closing and opening excitation circuits, auxiliary circuits, and indication and control circuits.

Switches and reversers can be installed both inside boards and stations and on them. The recommendation when they are installed in boards is to set aside separate panels for them, envisioning in so doing easy access to current-carrying portions and running of cables to main and auxiliary contacts and blocking contacts.

Along with two operating positions, reversers must have a zero position in which all contacts are closed.

Switch and reverser main contacts must sustain instantaneous short circuit currents greater by a factor of 12-15 than the nominal without breaking the circuit, temporary current increases that are greater by a factor of 3, and voltage increases up to 120% of nominal. In addition, contacts are intended for a prolonged operating mode at a current load consisting of 110% of nominal.

Switch and reverser auxiliary contacts intended for cutting generator circuits in and out should be envisioned for a prolonged nominal field current, as well as for temporary (for 30 seconds) field boosting by a factor of 3.5. Switch [30] and reverser auxiliary contacts to electric motor field circuits should be intended for a prolonged nominal field current.

Switch and reverser blocking contacts intended for indication, control, and protection must be intended for prolonged 10 A current.

Generator switches are equipped with a free-tripping mechanism with cut-off electromagnets fed from an independent power source for remote cut-off. The electromagnet coil voltage must not exceed 220 V dc or 380 V ac.

#### § 1.6 Electrical Propulsion Plant Auxiliary Mechanism Requirements

Quality GEU operation depends not only on main generators, main propulsion motors, and primary motors, but on auxiliary (service) mechanisms as well.

A closed ventilation cycle is preferable for GEU electrical machinery, which stipulates the necessity for air cooling. It is advisable to install individual electric fans for main generators and main propulsion motors.

Two electric fans should be used to circulate cool air for main propulsion motors. This increases GEU viability since a main propulsion motor can operate at reduced capacity until damage is repaired if there is an emergency involving one of the fans. This is not mandatory for main generators since several generators work with each main propulsion motor and, in the event of damage to one generator

fan, it can be cut out of the circuit for the time required to repair damage without the main propulsion motor being shut down for an extended period. Main propulsion motor electric fans are installed in the electric motor chassis, while generator fans generally are installed separately, caused by requirements of configuration with primary motors.

Aquatic air coolers are used to cool the air circulating in electrical machinery. Electric coolant pumps move outboard water through the air cooler.

In the event of a leak in the air cooler pipes, water falling inside is carried to the electrical machinery by the circulating air and puts it out of action. Therefore, the condition of the air coolers must be monitored closely and indicators installed to warn of this condition.

Powerful generators and main propulsion motors require forced lubrication of bearings and this is done with the aid of special oil pumps.

GEU primary motors (turbines and diesels) are served by a number of [31] auxiliary mechanisms, which have special requirements levied on them. The following mechanisms must be included in turboelectric propulsion plants within the GEU complex: steam boiler fuel pumps, electric feed pumps, electric boiler fans, turbine condenser circulating pumps, and condensate and oil pumps.

Diesel electric propulsion plants [DEGU] have fewer auxiliary mechanisms since some of them are driven directly from the diesel shaft. DEGU auxiliary mechanisms include: air and oil cooler coolant pumps and those pumping fuel and oil into daily supply tanks.

In addition, GEU auxiliary mechanisms include main generator and main propulsion motor field aggregates, as well as propellor and generator aggregate shaft-rotating devices.

All auxiliary mechanisms must have back-up, which most of all should be considered in this group of mechanisms.

GEU circuits require dc for protection, blocking, and indicator circuits, along with main generator and main propulsion plant excitation.

Feed for the aforementioned circuits is supplied from the shipboard auxiliary network in GEU on ships with a dc auxiliary network. There is a special dc voltage generator for this purpose on ships with an ac network. Semiconductor rectifiers can be used successfully to replace these generators due to development of semiconductor technology. Auxiliary circuits in a GEU with a circuit with unregulated main propulsion motor excitation or a circuit in which excitation is regulated through cutting resistors in and out of the main propulsion motor field winding circuit. Given fixed voltage, exciters can be fed from this exciter.

If main propulsion motor excitation is regulated by a change in field voltage, then a special constant voltage generator or a rectifier is used to feed auxiliary circuits. Main generator, main propulsion motor, and constant voltage generator exciters also can be configured as one aggregate, as is the case on the diesel electric "Lena" and atomic ship "Lenin." This configuration somewhat facilitates maintenance and servicing, but reduces plant viability, which should be considered during project design. This circumstance is very important in the event that main propulsion plants are installed in separate compartments.

It is advisable to place main generator and main propulsion plant excitation aggregates near electric propulsion boards since cables from them must run to [32] the electric propulsion board to commutating and protection gear. This approach considerably reduces cable connection line length and facilitates increased GEU viability.

Considering that diesel electric propulsion plants are the most widely used at the present time, below we provide recommendations applying mainly to these plants.

As already noted, the following groups of mechanisms must be included in the GEU complex: 1--main motor oil pumps; 2--generator oil pumps; 3--main propulsion plant oil pumps; 4--main motor coolant pumps; 5--generator coolant pumps; 6--main propulsion motor coolant pumps; 7--generator electric fans; 8--main propulsion

motor electric fans; 9--main generator exciter sets; 10--main propulsion motor exciter sets; 11--diesel generator barring gear; 12--shaft-turning device for diesel generators.

It is advisable to combine mechanism groups 1 and 2 (just like 4 and 5), i. e., to service generators and motors with one pump. Common pumps should be installed for a group of diesel generators located in one engine room and provide a second (back-up) set of mechanisms for each engine room. There is no back-up for auxiliary mechanism groups 7, 8, 11, and 12.

As is known, the main propulsion motor is controlled by separate control organs for each propellor. Therefore, auxiliary mechanisms linked with main propulsion motors or control units, i. e., groups 3, 6, 9, and 10, should be redundant so they provide one back-up mechanism for two shafts. One back-up set of mechanisms also is installed for single-shaft GEU.

The following requirements are levied on the electric drives of the aforementioned auxiliary mechanisms: electric drives for the mechanisms in groups 1-10 obtain dual feed directly from the GRShch or from the bus bars of the auxiliary mechanisms of the electrical propulsion board, which also is fed by two feeders from the GRShch. All these mechanisms must have local and remote start-up from the electrical propulsion board. Indication of how these mechanisms are operating, covered in detail in Chapter 4, is envisioned on the electrical propulsion board.

Group 11 and 12 mechanisms (barring gear) does not place the ship under way, so do not require dual feed and remote start-up. But, they do require mandatory blocking or indication of the mechanical combination of barring units with propellers or diesel generators.

It is advisable, where possible, to house the aforementioned mechanisms closer together and to the GRShch or to electrical propulsion boards to reduce cable line lengths.

A ship sometimes is required to operate at slow speed. In this event, the [33] rotational velocity of main propulsion motor and main generator electric fans must be controlled since the capacities of this equipment in the slow mode are coincident with the capacities of the electric fans and air cooler coolant pumps themselves.

## Direct Current Electrical Propulsion Plant Main Current Circuits

§ 2.1 Main Current Circuits With Alternate-Series Connection  
of Generator and Main Propulsion Motor Armatures

Generator Series and Parallel Connection. Circuits connecting main generator armatures to main propulsion motor armatures are called electrical propulsion plant [GEU] main current circuits.

In most instances, the main propulsion motors in dc GEU are fed from several generators. This increases plant reliability since, in case a generator breaks down, it is cut out of the circuit, while remaining generators continue to feed the main propulsion motor. A designer must place special attention on careful development of main current circuits because the reliability, servicing ease, and flexibility of the entire GEU depends on them.

Generators feeding a main propulsion motor can be connected in series or in parallel.

In parallel connection, the voltages of the generators and main propulsion motor almost are equal:  $U_x = U_r - \Delta U$ , where  $\Delta U$  are voltage losses in connecting cables. Current in the main propulsion motor armature circuit:  $I_x = \sum I_r$ . The voltage of the generators in this type of connection can be taken as equal to the maximum permitted by the Rules of the USSR Registry (1200 V). Cable sections in generator armature circuits will be as small as possible.

Insuring stable parallel generator operation under variable loads requires primary motors with precision governors, which maintain constancy in generator rotational speed in case of load fluctuations and the load among them is distributed proportionally to their power. The generators must have steeply-drooping external characteristics. [34]

In series connection of generators and main propulsion motors, main propulsion motor armature voltage equals the sum of the voltages of the generators feeding

it:  $U_{\Delta} = \sum U_r - \Delta U$ , where  $\Delta U$  - is the voltage drop in connecting wires.

Identical current flows in a series circuit, i. e.,  $I_{\Delta} = I_r$ . Therefore, generator cable sections must be larger than is the case for a parallel connection.

If  $m-k$  designates the number of operating series-connected generators and  $m$  is their total number, propulsion motor voltage will equal  $U_{\Delta} = U_{\Delta, \text{NOM}} \frac{m-k}{m}$ , where  $U_{\Delta, \text{NOM}}$  - nominal propulsion motor voltage.

Nominal current must flow in the main circuit in order to use the full power of the primary motors. Power being supplied by all operating generators to the main propulsion motor equals

$$\sum P_r = U_{\Delta} I_{\text{NOM}} = U_{r, \text{NOM}} I_{\text{NOM}} \frac{m-k}{m} = \sum P_{rm} \frac{m-k}{m},$$

while the power being supplied by one generator equals its nominal power

$$P_r = \frac{\sum P_r}{m-k} = \frac{\sum P_{rm} \frac{m-k}{m}}{m-k} = \frac{\sum P_{rm}}{m} = P_{r, \text{NOM}},$$

where  $\sum P_{rm}$  - total power of all  $m$  generators.

Main propulsion motor magnetic flux needs to be reduced so that the current in the main circuit, given that  $k$  generators are cut out, will have the nominal value. This is because the main propulsion motor's rotational speed will change in proportion to the voltage change, but its power changes in proportion to the cube of the rotational speed change based on screw characteristic. This situation will be examined in detail in § 5.2.

Given parallel generator connection and several of them being cut out from the main propulsion motor, the current fed by the generators will decrease in proportion to relationship

$$I_{\Delta} = I_{\Delta, \text{NOM}} \frac{m-k}{m},$$

where  $I_{\Delta, \text{NOM}} = m I_{r, \text{NOM}}$ ;  $I_{\Delta, \text{NOM}}$  и  $I_{r, \text{NOM}}$  - nominal current of the propulsion motor and of one generator.

It also is necessary to reduce generator voltage since, given constant nominal voltage, the propulsion motor and propellor will rotate with the previous velocity and overload connected generators and their primary motors. Disregarding the voltage drop in the main circuit and considering, as mentioned above, [35] that the power of the main propulsion motor is proportional to the cube of the rotational speed, one can write

$$\frac{P_{\Delta}}{P_{\Delta, \text{НОМ}}} = \left(\frac{n}{n_{\text{НОМ}}}\right)^3 = \left(\frac{U_{\Delta}}{U_{\Delta, \text{НОМ}}}\right)^3 = \frac{U_{\Delta} I_{\Delta}}{U_{\Delta, \text{НОМ}} I_{\Delta, \text{НОМ}}} = \frac{U_{\Delta} I_{\Delta, \text{НОМ}} \frac{m-k}{m}}{U_{\Delta, \text{НОМ}} I_{\Delta, \text{НОМ}}},$$

from which follows

$$\left(\frac{U_{\Delta}}{U_{\Delta, \text{НОМ}}}\right)^3 = \frac{m-k}{m}; \quad U_{\Delta} = U_{\Delta, \text{НОМ}} \sqrt[3]{\frac{m-k}{m}}.$$

Here, the power of all generators connected in parallel is of

$$\begin{aligned} \sum P_{\Gamma} = P_{\Delta} &= U_{\Delta} I_{\Delta} = U_{\Delta, \text{НОМ}} I_{\Delta, \text{НОМ}} \sqrt[3]{\frac{m-k}{m}} = \\ &= \sum P_{\Gamma m} \sqrt[3]{\frac{m-k}{m}}, \end{aligned}$$

while the power of one generator

$$\begin{aligned} P_{\Gamma} &= \frac{\sum P_{\Gamma}}{m-k} = \frac{\sum P_{\Gamma m}}{m-k} \sqrt[3]{\frac{m-k}{m}} = \\ &= \frac{P_{\Gamma, \text{НОМ}} m}{m-k} \sqrt[3]{\frac{m-k}{m}} = P_{\Gamma m} \sqrt[3]{\frac{m-k}{m}}. \end{aligned}$$

As can be seen, the generator is underloaded in this case. Full loading of the generator and its primary motor requires amplification of the main propulsion motor field magnetic flux, i. e., it must have an excitation reserve, meaning increased main propulsion motor dimensions.

GEU generators are not connected in parallel in domestic shipbuilding due to the aforementioned reasons. Series connection of generators or alternate-series connection of generators and main propulsion motors only is used.

The term alternate-series connection demonstrates that the armatures of

generators and main propulsion motors alternate in series connection. Thus, the greatest voltage between any two points of the main circuit or between any point in the main circuit and the hull is less than the sum of the voltages of the series-connected generators.

Circuits with one-armature main propulsion motors. One main propulsion motor is cut into one generator in the simplest main current circuit. A similar circuit (Figure 2.1) was used on river icebreakers "Volga" and "Don," which have dual-shaft GEU. If one disregards the voltage drop in the circuit, then equality  $U_r = U_n$ , holds for this circuit, where  $U_r$  - is generator voltage and  $U_n$  - is main propulsion motor voltage. Generators and main propulsion [36] motors in circuits can be used with the greatest permissible voltage. A circuit drawback is the inability of any generator to run both main propulsion motors. If one diesel generator breaks down, the vessel must operate on one screw with rudder blade transposed hard over, which reduces vessel speed.

The circuit shown in Figure 2.2 is very flexible. In this circuit as in the previous one, generator and main propulsion motor armature voltages are equal, if one disregards network voltage drop. The circuit permits each generator to run its own main propulsion motor or any generator to run both series-connected main propulsion motors, which provides vessel movement by two screws with any number of generators operating. In this event, each main propulsion motor's armature voltage equals  $U_n = U_r/2$ . Consequently, main propulsion motor rotational speed also equals  $\frac{1}{2}$  of nominal.

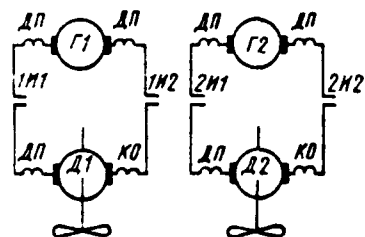


Figure 2.1. Two-Shaft GEU Main Current Circuit.

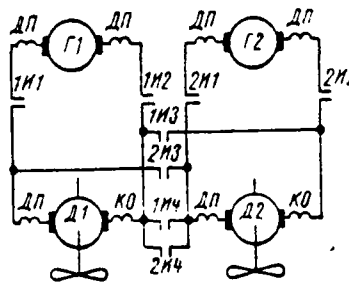


Figure 2.2. Main Current Circuit For GEU With Generators Cut In To Any Main Propulsion Motor.

Switch closing contact sequence is shown in Table 2.1.

A main current circuit with one main propulsion motor, which is fed from two generators, is depicted in Figure 2.3. The voltage of each generator is 460 V, while that of the main propulsion motor is 920 V. This circuit was [37] used on the tug "Atlant," which has a single-shaft electrical propulsion plant. The circuit can be used for one shaft of a two-shaft GEU. Two operating modes can be used in this circuit: 1--two series-connected generators run one main propulsion motor; 2--one (any one) generator runs the main propulsion motor. In the second mode, main propulsion motor armature voltage equals  $\frac{1}{2}$  of the nominal and, consequently, rotational speed will be less [50].

Table 2.1

Selector Switch 1I and 2I Contact Closure  
(See Circuit in Figure 2.2)

Operating Modes	1I1	1I2	1I3	1I4	2I1	2I2	2I3	2I4
G1 to D1	X	X						
G1 to D1 and D2	X	X	X	X				
G1 Cut Out								
G2 to D2					X	X		
G2 Cut Out								
G2 to D1 and D2					X	X	X	X

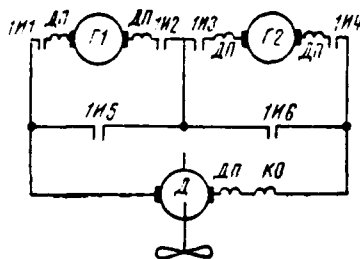


Figure 2.3. Main Current Circuit For The Single-Shaft GEU On The Tug "Atlant".

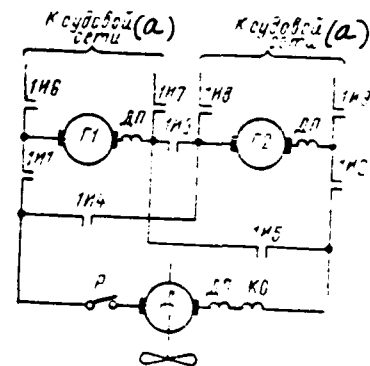


Figure 2.4. Main Current Circuit Of A GEU With Generators Operating To A Single-Armature Main Propulsion Motor. a--To the ship-board network.

Switch contact closure sequence is shown in Table 2.2. As already noted, switching of a circuit from one mode to another is done by means of selector switches. Large currents, which must be commutated by switch contacts, flow in main current circuits. In spite of the fact that switchings of the propulsion plant from one mode to another occur in the dead state, these contacts are huge and complex. Therefore, great efforts must be made when designing main current circuits to reduce the number of contacts in the main circuit to the minimum.

Table 2.2

Selector Switch Contact Closure (See Circuit in Figure 2.3)						
Operating Modes	II1	II2	II3	II4	II5	II6
Cut Off						
G1 and G2 to D	X	X	X	X		
G1 to D	X	X				X
G2 to D			X	X	X	

A main current circuit providing identical operating modes, but with one [38] less contact in the main current circuit (without considering contacts II6--II9 intended for shipboard network feed) is shown in Figure 2.4 to illustrate what has been presented above. The switch contact closure sequence for this circuit is shown in Table 2.3.

<i>a</i> Режим работы	<i>b</i> II1	II2	II3	II4	II5	II6	II7	II8	II9
<i>c</i> Отключено									
<i>d</i> Г1 и Г2 на Д	X	X	X						
<i>e</i> Г1 на Д, Г2 на сеть	X				X			X	X
<i>f</i> Г2 на Д, Г1 на сеть		X		X		X	X		

Table 2.3. Selector Switch Closure Sequence (See Circuit in Figure 2.4). a--Operating modes; b--II1 through II9; c--Cut off; d--G1 and G2 to D; e--G1 to D, G2 to network; f--G2 to D, G1 to network.

In the Figure 2.3 and 2.4 circuits, main propulsion motor armature voltage equals  $U_1 = 2U_r$ , while the generator voltage does not exceed 600 V in accordance with Registry Rules.

The rotational speed of a dc propulsion motor is proportional to the voltage at its terminals. Consequently, in the event one generator is operating the main propulsion motor, the voltage in the aforementioned circuits will be  $U'_a = U_r = \frac{U_a}{2}$  instead of  $U_a = 2U_r$ . Rotational speed will decrease by a factor of 2:  $n_1 = \frac{n}{2}$ . Screw resisting moment is proportional  $M \propto n^2$  and, in this case, will be  $M_1 \propto \left(\frac{n}{2}\right)^2 = \frac{M}{4}$ . Power required by the main propulsion motor equals  $P_1 = \frac{M}{4} \cdot \frac{n}{2} = M_1 n_1 = \frac{P}{8}$  where, n, M, P -- are, respectively, rotational speed, torque, and power of the main propulsion motor in a nominal mode, when two generators operate it.

The magnetic flux of this main propulsion motor in this instance is decreased to insure a full load for the generator and primary motor, thus increasing its rotational speed and load.

Circuits with two-armature main propulsion motors. A circuit with a two-armature main propulsion motor is shown in Figure 2.5. The main propulsion motor and generator armature voltages in this circuit are equal. Therefore, the maximum voltage of 1200 V can be used for the generator and main propulsion motor armatures. [39]

Phenomena identical to those in the circuit shown in Figure 2.4 are observed as one generator runs two main propulsion motors.

One should consider that a two-armature electric motor will be large, heavy, and costly compared to a motor with one armature.

Essentially, this type circuit was used on the tug "Goliath" and the tanker "General Azi Aslanov." This circuit provides the following operating modes: 1--two generators run two main propulsion motor armatures; 2--any generator runs both main propulsion motor armatures [50].

In the second mode, voltage at each main propulsion motor armature will equal  $U_r/2$ , at which time the main propulsion motor demand, using the analogy with the previous circuit, will decrease by a factor of 8. This is seen from Figure 2.6, which provides the curve of the relationship of shaft power to its rotational speed in relative units. Main propulsion motor rotational speed

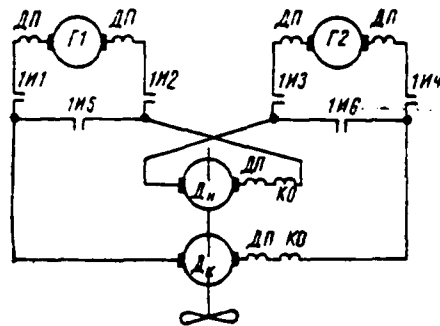


Figure 2.5. GEU Main Current Circuit on the Tanker "General Azi Aslanov".

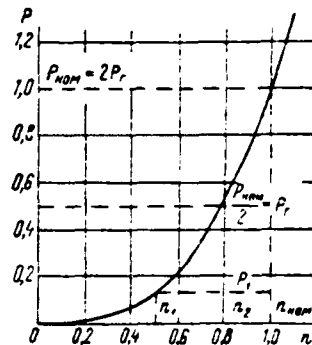


Figure 2.6. Relationship of Shaft Power to Main Propulsion Motor Rotational Speed.

in the second mode will decrease from  $n_{НОМ}$  to  $n_1$ , and demand will decrease to  $P_1$ . In order to load the generator and primary motor, the main propulsion motor magnetic flux is decreased to that amount at which its rotational speed increases to  $n_2$ , demand will rise to  $P_{НОМ} \cdot 2 = P_r$ , and the generator will be loaded fully.

A main current circuit similar to this one is shown in Figure 2.7. It is used on railroad ferries of the "Yuzhnyy" class. In the event one main propulsion motor armature breaks down, it can be cut out of the circuit by means of detachable jumpers I-VII. A differentially-compounded winding PKO of a main generator three-winding exciter, which in this circuit is cut directly into [40] the main current circuit (discussed in detail in § 3.3), also is shown in Figure 2.7. This circuit also envisages electric propulsion generators running the shipboard network at a reduced voltage of 230 V. The selector switch contact closure sequence is presented in Table 2.4.

A selector switch for each propellor's circuit does all switchings when a handwheel is turned.

Increased GEU power and limited number of available diesel generators mean using two-armature electric motors and feeding each armature from two generators, connecting all armatures in a common sequential loop.

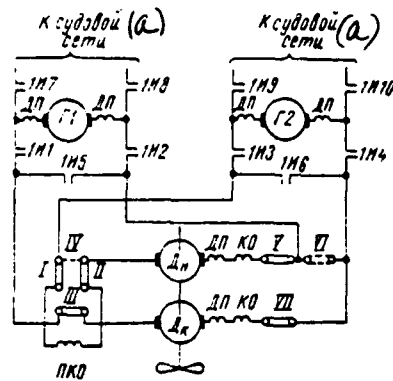


Figure 2.7. Main Current Circuit for "Yuzhnyy" Class Ferries (Circuit for One Shaft). a--To shipboard network.

A similar main current circuit is shown in Figure 2.8. It allows one to provide seven operating modes, with selector switch contact closure shown in Table 2.5.

The inability of one generator to run the main propulsion motor is a drawback of this circuit. Each generator's armature voltage is 500 V, while main propulsion motor armature voltage is 1000 V.

The electric propulsion circuit was redone for newer electric ships based on know-how accumulated from operating the prototype vessel. One selector switch in the new circuit (Figure 2.9) has been replaced by two: 1I switches gen- [42] erators G1 and G1, while 2I switches generators G3 and G4. This circuit makes it possible to connect generator and main propulsion motor armatures in a large number of combinations compared to the circuit shown in Figure 2.8.

Along with separation of the selector switches, knife switches R intended to break the main current circuit prior to setting selector switches have been introduced into this circuit. This is to insure switching of the latter in the absence of current in the circuit and protects their contacts against overheating. Coils of overvoltage relays RM, to be described in Chapter 3, were introduced into the main current circuit.

<i>a</i> Режим работы	<i>b</i> И1	И2	И3	И4	И5	И6	И7	И8	И9	И10
<i>c</i> Отключено										
<i>d</i> Г1 и Г2 на Д	×	×	✓	×						
<i>e</i> Г1 на Д, Г2 на сеть	×	×				×			×	×
<i>f</i> Г2 на Д, Г1 на сеть			×	×	×		×	×		
<i>g</i> Примечание. Контакты И7 и И10 на рис. 2.5 отсутствуют.										

Table 2.4. Selector Switch Contact Closure (See Circuits in Figures 2.5 and 2.7). a--Operating modes; b--Switches И1 through И10; c--Cut off; d--G1 and G2 to D; e--G1 to D, G2 to network; f--G2 to D, G1 to network; g--Note: Contacts И7 and И10 are absent from Figure 2.5.

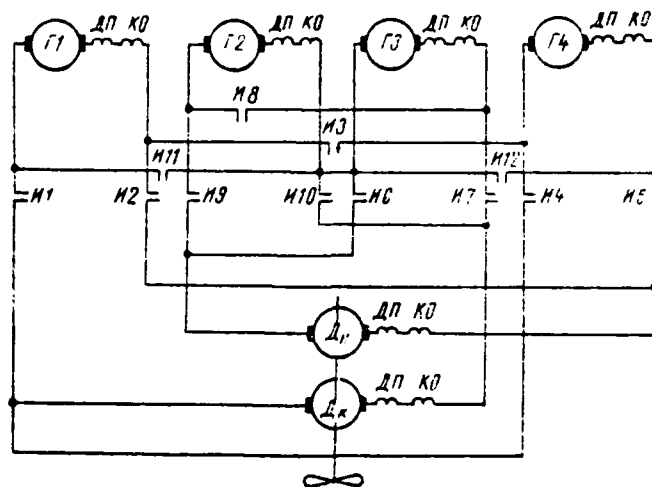


Figure 2.8. GEU Main Current Circuit for "Aktyubinsk" Class Refrigerator Ships.

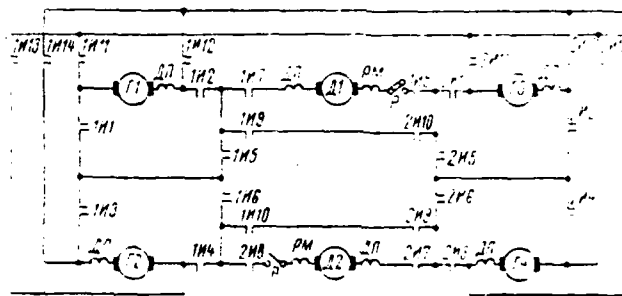


Figure 2.9. Refrigerated Ship Modernized GEU Main Current Circuit.

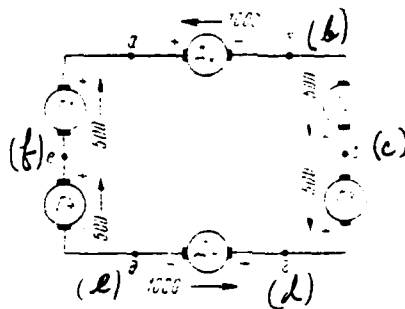


Figure 2.10. Voltage Distribution Circuits in a Loop with Four Generators and One Two-Armature Main Propulsion Motor. Between points a and d, c and f, and b and e, voltage equals zero; Between b and c, c and d, e and f, and f and a, voltage is 500 V; Between a and b, b and d, and a and e, it is 1000 V.

a

Номер режима	Режим работы	c											
		И1	И2	И3	И4	И5	И6	И7	И8	И9	И10	И11	И12
1	Г1-Г4 на Д <sub>н</sub> и Д <sub>к</sub>	×		×		×	×		×		×		
2	Г1, Г3, Г4 на Д <sub>н</sub> и Д <sub>к</sub>	×		×		×	×	×					
3	Г1, Г2, Г3 на Д <sub>н</sub> и Д <sub>к</sub>	×	×					×		×		×	
4	Г2, Г3, Г4 на Д <sub>н</sub> и Д <sub>к</sub>				×	×	×		×		×		
5	Г1, Г2, Г4 на Д <sub>н</sub> и Д <sub>к</sub>	×		×		×				×		×	
6	Г1, Г2 на Д <sub>н</sub>		×							×		×	
7	Г3, Г4 на Д <sub>к</sub>				×			×					×

Table 2.5. Selector Switch Contact Closure (See Circuit in Figure 2.8). a--Mode number; b--Operating modes; c--I1 through I12; 1--G1-G4 to D<sub>n</sub> and D<sub>k</sub>; 2--G1, G3, G4 to D<sub>n</sub> and D<sub>k</sub>; 3--G1, G2, G3 to D<sub>n</sub> and D<sub>k</sub>; 4--G2, G3, G4 to D<sub>n</sub> and D<sub>k</sub>; 5--G1, G2, G4 to D<sub>n</sub> and D<sub>k</sub>; 6--G1, G2 to D<sub>n</sub>; 7--G3, G4 to D<sub>k</sub>.

Selector switch 1I and 2I contact closure sequence is presented in Table 2.6, while several of this circuit's possible operating modes are shown in Table 2.7.

Distribution of voltages in the loop when all generators are operating is depicted in Figure 2.10. As can be seen from this figure, voltages between any points do not exceed 1000 V.

The GEU main current circuit for "Mirnyy" class whalers is shown in Figure 2.11. This envisions four diesel generators running one two-armature main propulsion motor. Each pair of generators in the circuit has a separate selector switch, which makes the following operating modes possible for four positions of each selector switch: 1--four generators running both main propulsion [43]

motor armatures; 2--any three generators running both main propulsion motor armatures; 3--any two generators running both main propulsion motor armatures; 4--any generator running both main propulsion motor armatures. Any armature [44] that breaks down can be cut out of the circuit by means of detachable jumpers I-IV. The switch contact closure sequence is shown in Table 2.8.

a    b

Положение переключателя	111-2111	112-2112	113-2113	114-2114	115-2115	116-2116	117-2117	118-2118	119-2119	1110-2110	1111-2111	1112-2112	1113-2113	1114-2114
6					×	×			×					
5			×	×	×				×					
4	×	×				×			×					
3			×	×	×		×	×		×				
2	×	×				×	×	×						
1	×	×	×	×			×	×						
0					×	×	×	×						
7					×	×	×	×		×	×	×		
8					×	×	×	×				×		

Table 2.6. Selector Switch 1I and 2I Contact Closure (See Circuit in Figure 2.9). a--Switch position; b--Switches 111-1114 and 211-2114.

In all the main current circuits examined above, with the exception of the one depicted in Figure 2.2, generators running different main propulsion motors in multishaft GEU are not envisaged. Each shaft's circuits are autonomous.

Circuits with generators connected to electric motors for different propellers.

The main current circuit for an electrical propulsion plant in which generators can run the main propulsion motors of different propellers is shown in Figure 2.12. Each main propulsion motor has its own 6-position switch for switching the circuit from one mode to another. The following operating modes

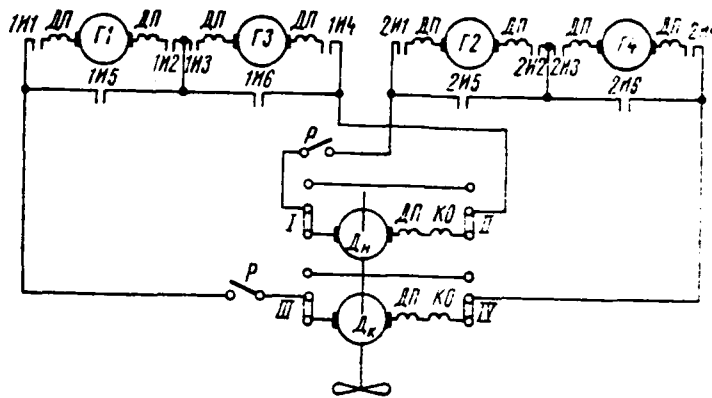


Figure 2.11. GEU Main Current Circuit for "Mirnyy" Class Whalers.

are provided: 1--two generators (G1, G2) run single-armature main propulsion motor D1; 2--generator G1 runs main propulsion motor D2, generator G2 runs the shipboard network; 3--generator G2 runs main propulsion motor D1, generator G1 runs the shipboard network; 4--generator G2 runs the main propulsion motors D1 and D2 of both shafts, generator G1 runs the shipboard network, with the selector switch for the second shaft in this mode being in the zero position; 5--generator G1 runs main propulsion motor D1, generator G2 runs D2, with the motor D2 selector switch having to be in the zero position. Selector switch contact closure sequence is presented in Table 2.9 [29].

The GEU main current circuit for a three-screw port icebreaker is shown in Figure 2.13. This circuit envisions the following operating modes: 1--three diesel generators run the aft main propulsion motors, the first armatures of two-armature generators are connected in series and connected to the starboard main propulsion motor, while the second armatures of these generators are connected to the port motor. The main propulsion motor armature voltage equals 1200 V, while that of each generator is 400 V; 2--two diesel generators run the aft main propulsion motors and one runs the bow motor. Two armatures each from different generators connected in series run each aft main propulsion motor. Armature voltage is 800 V. Both armatures of one diesel generator connected in series run the forward main propulsion motor. Armature voltage is 800 V. [47]

а Номер режима	б Режим работы	в Положения переключателей	
		д 1И	е 2И
0	Отключено	0	0
1	$G1 + G2 + G3 + G4$ на Д1 + Д2	1	1
2	$G1 + G2 + G3$ на Д1 + Д2	1	2
3	$G1 + G2 + G4$ на Д1 + Д2	1	3
4	$G1 + G3 + G4$ на Д1 + Д2	2	1
5	$G2 + G3 + G4$ на Д1 + Д2	3	1
6	$G1 + G2$ на Д1 + Д2	1	0
8	$G1 + G4$ на Д1 + Д2	2	3
10	$G2 + G4$ на Д1 + Д2	3	3
12	$G1$ на Д1 + Д2	2	0
14	$G3$ на Д1 + Д2	0	2
16	$G1 + G2$ на Д1	1	6
19	$G2 + G3$ на Д1	3	4
21	$G1$ на Д1	2	6
23	$G3$ на Д1	0	4
25	$G1 + G3$ на Д2	4	2
27	$G2 + G3$ на Д2	5	2
32	$G3$ на Д2	6	2

Table 2.7. Electrical Propulsion Plant Operating Modes (See Circuit in Figure 2.9). a--Mode number; b--Operating modes; c--Switch position; d--1I; e--2I; 0--Cut out; 1-32 designate generators running motors. (1) - to

The circuit envisages the capability for diesel generator 1G or 2G to run the bow main propulsion motor; 3--any diesel generator runs the aft main propulsion motors (main propulsion motor armature voltage is 400 V each) and one diesel generator runs the forward main propulsion motor (its armature voltage is 800 V).

Избирательный переключатель 1И *я*

<i>а</i> Режим работы	<i>б</i> 1И1	1И2	1И3	1И4	1И5	1И6
<i>с</i> Отключено						
Г1, Г3 <sup>(1)</sup> на Д	×	×	×	×		
Г1 <sup>(1)</sup> на Д	×	×				×
Г2 <sup>(1)</sup> на Д			×	×		

Избирательный переключатель 2И *ф*

<i>а</i> Режим работы	<i>д</i> 2И1	2И2	2И3	2И4	2И5	2И6
<i>с</i> Отключено					×	×
Г2, Г4 <sup>(1)</sup> на Д	×	×	×	×		
Г2 <sup>(1)</sup> на Д	×	×				×
Г4 <sup>(1)</sup> на Д			×	×	×	

Table 2.8. Selector Switch 1I and 2I Contact Closure Sequence (See Circuit in Figure 2.11). a--Operating modes; b--1I1-1I6; c--Cut out; d--2I1-2I6; e--Selector switch 1I; f--Selector switch 2I. Designates generators running motors. (1) - to

Three selector switches 1I, 2I, 3I are used to select the operating mode. Contact closure sequence is depicted in Table 2.10.

In all the main current circuits presented above, except that portrayed in Figure 2.1, switching from one mode to another is done with the aid of selector switches by a turn of a handwheel to the position corresponding to the given [48] operating mode. Usually, one selector switch commutates one main propulsion motor's circuit. Two selector switches are used for mode selection in the circuit depicted in Figure 2.11.

The main current circuit for Finnish-built icebreakers of the "Moskva" and "Leningrad" class is shown in Figure 2.14.

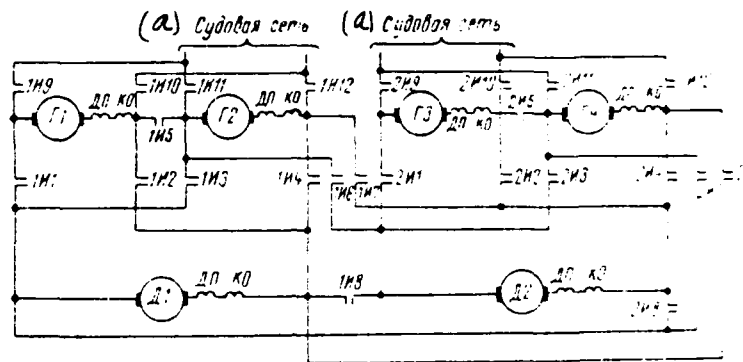


Figure 2.12. Main Current Circuit for a Two-Shaft GEU Providing the Capability for One Generator (G2 or G4) to Run Both Main Propulsion Motors Simultaneously. a--Shipboard network.

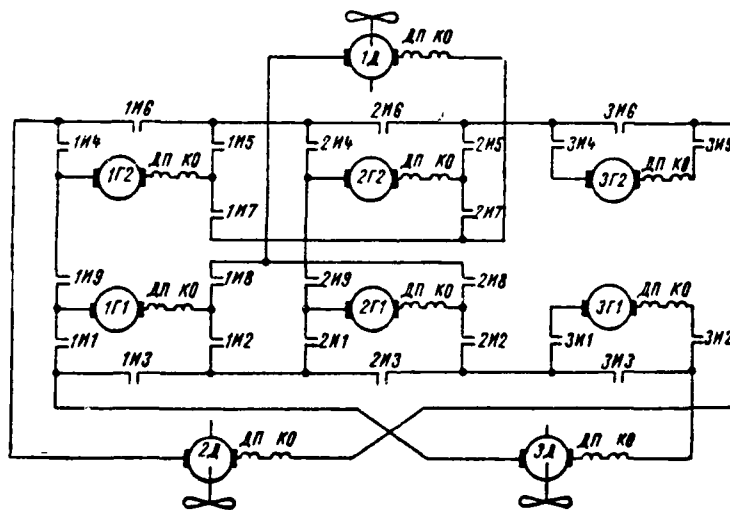


Figure 2.13. Port Icebreaker Main Current Circuit.

а Переключатель 1И

в Режим работы	с												
	1И1	1И2	1И3	1И4	1И5	1И6	1И7	1И8	1И9	1И10	1И11	1И12	
Г1, Г2 <sup>(1)</sup> на Д1	×												
Г1 <sup>(1)</sup> на Д1, Г2 <sup>(2)</sup> на сеть	×	×											
Г1 <sup>(2)</sup> на сеть, Г2 <sup>(1)</sup> на Д1			×	×									
Г1 <sup>(2)</sup> на сеть, Г2 <sup>(1)</sup> на Д1, Д2			×							×			
Г1 <sup>(1)</sup> на Д1, Г2 <sup>(1)</sup> на Д2	×	×					×	×					
д Отключено													

е Переключатель 2И

в Режим работы	ф												
	2И1	2И2	2И3	2И4	2И5	2И6	2И7	2И8	2И9	2И10	2И11	2И12	
Г3, Г4 <sup>(1)</sup> на Д2	×			×	×								
Г3 <sup>(1)</sup> на Д2, Г4 <sup>(2)</sup> на сеть	×	×											
Г3 <sup>(2)</sup> на сеть, Г4 <sup>(1)</sup> на Д2			×	×									
Г3 <sup>(2)</sup> на сеть, Г4 <sup>(1)</sup> на Д1, Д2			×					×	×	×			
Г3 <sup>(1)</sup> на Д2, Г4 <sup>(1)</sup> на Д1	×	×							×				
д Отключено													

Table 2.9. Selector Switch 1I and 2I Contact Closure (See Circuit in Figure 2.12). а--Switch 1I; б--Operating modes; с--Switches 1И1-1И12; д--Cut out; е--Switch 2I; ф--Switches 2И1-2И12. Designates generators running motors or the shipboard network. (1) - to; (2) - to network

The circuit allows each outboard main propulsion motor to be fed by two or one generator, while allowing the amidships main propulsion motor to be fed by four, two, or one generator.

*a* Переключатель 1И

<i>b</i> Режим работы	<i>c</i>								
	1И1	1И2	1И3	1И4	1И5	1И6	1И7	1И8	1И9
<i>e</i> ) 1Г1 <sup>(1)</sup> на ЗД, 1Г2 на 2Д	×	×		×	×				
<i>e</i> ) 1Г1 <sup>(1)</sup> на ЗД, 1Г2 на 2Д	×	×		×	×				
1Г1 и 1Г2 <sup>(1)</sup> на 1Д			×			×	×	×	×

*d* Переключатель 2И

<i>b</i> Режим работы	<i>e</i>								
	2И1	2И2	2И3	2И4	2И5	2И6	2И7	2И8	2И9
<i>e</i> ) 2Г1 <sup>(1)</sup> на ЗД, 2Г2 на 2Д	×	×		×	×				
2Г1 и 2Г2 <sup>(1)</sup> на 1Д			×			×	×	×	×
<i>e</i> ) 2Г1 <sup>(1)</sup> на ЗД, 2Г2 на 2Д	×	×		×	×				

*f* Переключатель 3И

<i>b</i> Режим работы	<i>g</i>					
	3И1	3И2	3И3	3И4	3И5	3И6
<i>e</i> ) 3Г1 <sup>(1)</sup> на ЗД, 3Г2 на 2Д	×	×		×	×	
<i>e</i> ) 3Г1 <sup>(1)</sup> на ЗД, 3Г2 на 2Д	×	×		×	×	
3Г1 и 3Г2 выключены			×			×

Table 2.10. Selector Switch 1I, 2I, 3I Closure (See Circuit in Figure 2.13). a--Switch 1I; b--Operating modes; c--1I1-1I9; d--Switch 2I; e--2I1-2I9; f--Switch 3I; g--3I1-3I9; h--3G1 and 3G2 Cut In. Designates generators running motors. (1) - to

Usually, outboard main propulsion motors are fed from generators in the [49] forward engine room, while the amidships main propulsion motor is fed by those in the aft engine room. A mode in which each main propulsion motor is fed from generators in the forward and aft engine rooms also is possible (Figure 2.15).

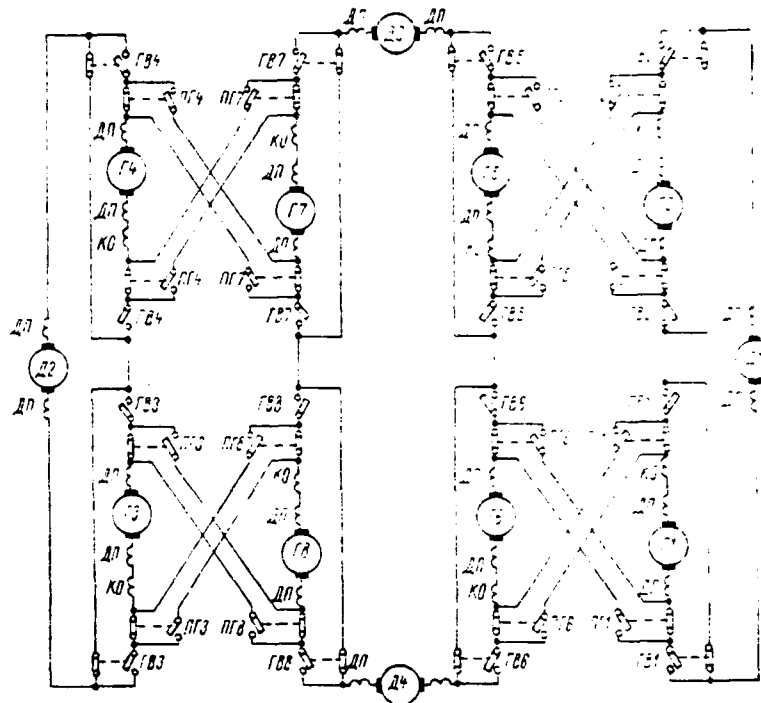


Figure 2.14. Icebreaker "Moskva" GEU Main Current Circuit.

Cutting in any of the GEU operating modes is done with generator switches PG1-PG8 and GV1-GV8 (see Figure 2.14). Generator switches PG are intended for switching each generator to the amidships or outboard main propulsion motors, while switches PV are used to switch main propulsion motor circuits.

The circuit envisions the 11 basic operating modes enumerated below (figures denote the number of operating generators running outboard and amidships main propulsion motors):

Mode I 2-4-2, Mode II 1-4-1, Mode III 2-2-2, Mode IV 0-4-0, Mode V 2-0-2,  
 Mode VI 1-2-1, Mode VII 1-1-1, Mode VII 1-0-1, Mode IX 0-3-0, Mode X 0-2-0,  
 Mode XI 0-1-0.

Operating the generators from one engine room is preferred in Modes IV-XI. [50]

The GEU main current circuit, also selected by means of switches, has been installed on a car paddle ferry in use in New Zealand (Figure 2.16). The circuit envisions three, two, and one diesel generator running one main propulsion motor.

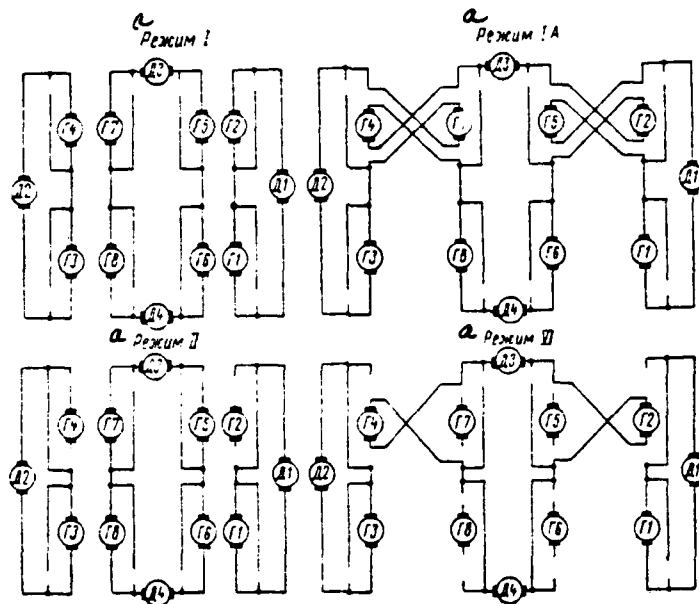


Figure 2.15. Icebreaker "Moskva" GEU Operating Modes. a--Mode.

In some cases, there is a requirement to change GEU operating mode without cutting generators out. This can occur, for example, when two main propulsion plants operating individually are fed from one diesel generator or when there is a need to connect generators or main propulsion motors without cutting off the system.

So-called constant current circuits are used in this instance. Main circuit current in these circuits remains constant at all times, while the speed of the main propulsion motor changes by means of simultaneous regulation of generator and main propulsion motor excitation.

Regulation of these circuits will be covered in detail later. We only are examining the main current circuit in this chapter.

A constant current circuit has been used in a Volga shuttle car ferry with one D50 diesel generator and two main propulsion motors (fore and aft). The [51] circuit is depicted in Figure 2.17 and provides the following operating modes: 1--a diesel generator runs two series-connected main propulsion motors; 2--a diesel generator runs main propulsion motor D1, while the armature of main

propulsion motor D2 is shunted by contactor 2KD; 3--a diesel generator runs main propulsion motor D2, while the armature of main propulsion motor D1 is shunted by contactor 1KD. If main propulsion motors D1 or D2 is damaged, it is cut out by means of jumpers I, II, or III, IV and their circuits are shunted by jumpers V or VI.

We can conclude our review of circuits with alternate-series generator and main propulsion motor connection with this.

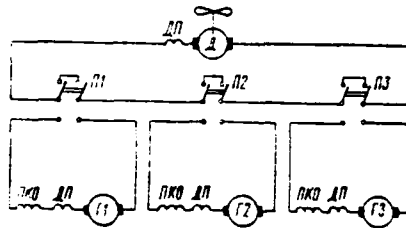


Figure 2.16. Paddlewheel Car Ferry GEU Main Current Circuit.

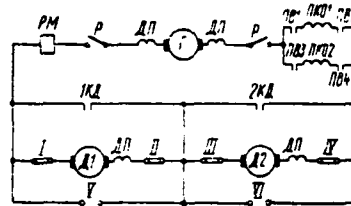


Figure 2.17. Shuttle Car Ferry GEU Main Current Circuit.

There is the concept of using a constant current circuit, in addition to what has been described in maritime ac powerplants, where consumers are not loaded simultaneously to full capacity and where rapid distribution of capacities to any combination of consumers is required. As stated above, they use generators and electric power consumers located in a common series circuit allowing separate distribution of generator capacities among individual consumers. Another advantage of this circuit is that, if all consumers are not cut into full power at the same time, the sum of the generator installed capacity can be less than that of the installed capacity of the consumers, whereby higher systems economy is achieved. In a conventional generator-motor system, generator capacities must equal the capacities of installed consumers.

A self-dumping dredger electrical propulsion plant is a typical example of such a system. All generator power is fed to the propulsion plant as the vessel moves to the work area. During the operation, most of the power goes to the hydraulic dredge pumps, while the propulsion plant uses only a small portion of the electric power (Figure 2.18).

An analogous circuit used on the trawler "Burgomister Schmidt" is shown in Figure 2.19. Three 600 kW, 500 rpm dc generators placed in rotation by [52] diesels feed two main propulsion motors rotating, via the propellor reduction gear, one converter running the three-phase 240 kW current shipboard network and two 103 kW trawl winch electric motors.

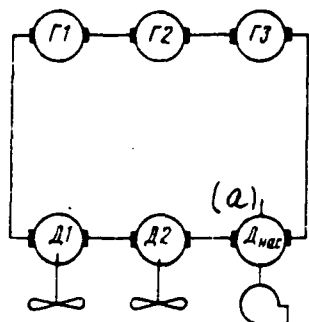


Figure 2.18. Self-Dumping Dredge GEU Main Current Circuit. a--pump motor.  
 $\Delta_{nac}$  - electric pump motor

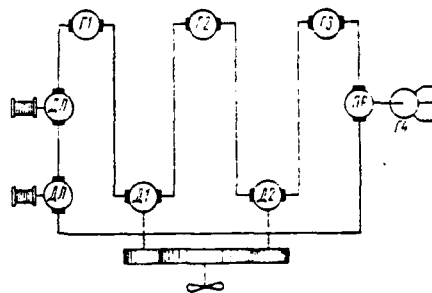


Figure 2.19. Trawler "Burgomister Schmidt" GEU Main Current Circuit.

### § 2.2 Two-Armature Main Current Circuits

During the postwar period, GEU with separately-operating generators running main propulsion motor armatures, so-called two-armature circuits, appeared and began to be used. Each armature in this circuit's two-armature main propulsion motors is fed by its own generators, even though the circuits of both armatures are not connected electrically.

These main current circuits are used when there is a need to change propulsion plant operating mode without removing torque from the main propulsion motor shaft, i. e., mainly for ice navigation vessels and icebreakers. In this case, GEU operating mode changes are made in the following manner: at first, the number of generators in the circuit of the first main propulsion motor armature is changed while the second armature is running, then the same is done for the second armature while the first armature is running.

Drawbacks of these circuits include difficulty in tuning the control system because different generator and exciter characteristics, as well as of the main

propulsion motor armatures themselves, can lead to unequal load distribution between armatures and cause fluctuating transfer of power from one armature to the other.

Practice and theoretical research demonstrated that this circuit can operate stably, but only if electrical machinery or other automation in the generator [53] and main propulsion motor field system is used.

The main current circuit on "Lena" class diesel-electric ships can serve as an example of a two-armature main current system (Figure 2.20). The circuit permits the following operating modes: 1--four diesel generators run two main propulsion motor armatures, two series-connected generators per armature; 2--any three diesel generators run two main propulsion motor armatures, two generators for one armature, the third for the second armature; 3--two generators, one per loop, run the armatures of their own main propulsion motors; 4--two generators in one loop run their own main propulsion motor armature, with the second loop cut out; 5--one generator runs its own main propulsion plant armature, the second loop being cut out.

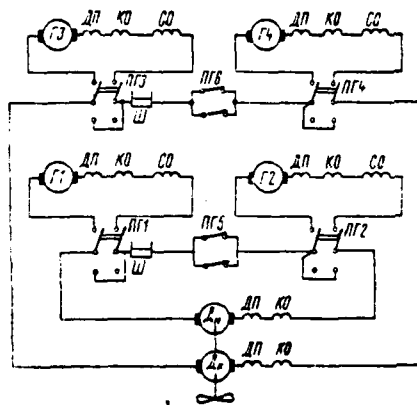


Figure 2.20. "Lena" Class Diesel-Electric Ship GEU Main Current Circuit.

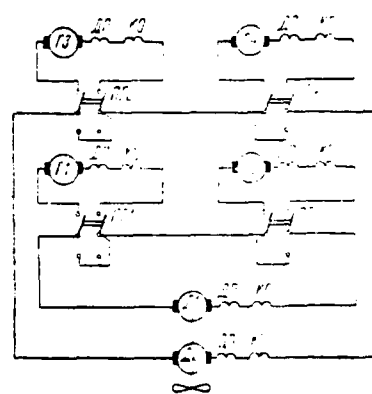


Figure 2.21. "Amguema" Class Active Ice Navigation Vessel GEU Main Current Circuit.

Transfer from one mode to another in the circuit depicted in Figure 2.20 occurs by means of selector switches. Each generator has its own selector switch. Selector switches PG5 and PG6 are intended to protect the main propulsion motor armature circuit against a short circuit when both generators are cut out, even though this precaution also seems excessive since the main propulsion motor field windings also cut out when generators cut out.

The GEU main current circuit for an active ice navigation vessel of the "Amguema" class is depicted in Figure 2.21. This circuit provides the same operating modes as the circuit in Figure 2.20.

A two-armature circuit was used for the electrical propulsion plant on the nuclear icebreaker "Lenin." The main current circuit was built in such a way that each of four turbogenerators run both outboard and the amidships [55] main propulsion motors [11].

Two two-armature dc generators are connected to each icebreaker turbine. One of the armatures on one generator is connected to the starboard main propulsion motor and a second to the port motor. Both armatures of the second generator are connected in parallel and connected to the amidships main propulsion motor.

The amidships main propulsion motor main current circuit is shown in Figure 2.22 and that of an outboard motor in Figure 2.23. These circuits are identical as far as possible operating modes are concerned and differ only in generator armature connection.

The circuits provide the following operating modes: 1--four generators run both main propulsion motor armatures, with two generators per armature; 2--two generators run one armature and one the second main propulsion motor armature; 3--one generator runs each main propulsion plant armature; 4--one generator runs one main propulsion motor armature, the second armature is cut out.

### § 2.3 Comparative Evaluation of Different Main Current Circuits

The variety of main current circuits is stipulated by the specificity of

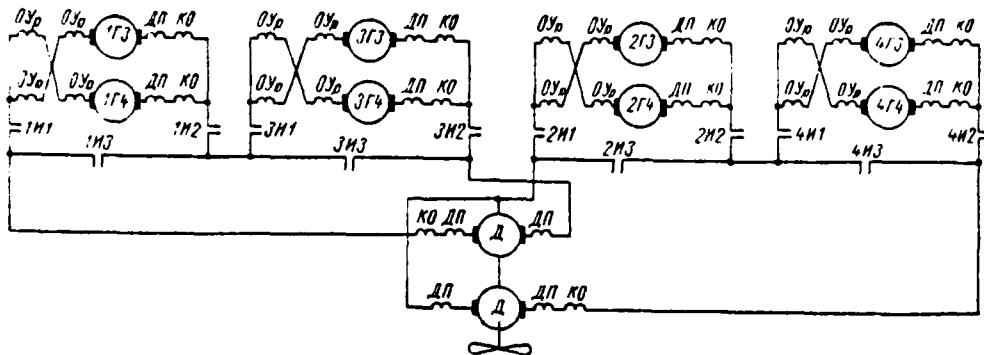


Figure 2.22. Nuclear Icebreaker "Lenin" GEU Amidships Shaft Main Current Circuit.

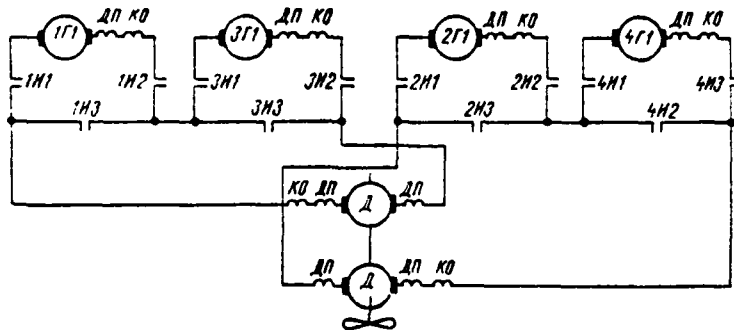


Figure 2.23. Nuclear Icebreaker "Lenin" GEU Starboard Shaft Main Current Circuit.

electrical propulsion plant operation, industrially-assimilated main propulsion motor and diesel generator set power, generator voltage, and requirements for individual GEU types.

Main current circuits with alternate-series armature connection are used the most. Such circuits have been accepted for the majority of domestic and foreign electric ships (England, FRG, Finland, and others). Two-armature circuits are used more rarely. These circuits were used on domestic and Dutch ice navigation vessels and on the nuclear icebreaker "Lenin."

As already noted, electrical propulsion plant quality greatly depends on main current circuit selection. Factors exerting considerable influence on circuit selection include:

number of generators feeding one main propulsion motor;

generator and main propulsion motor armature voltage;  
number of main propulsion motor armatures;  
number of GEU shafts;  
requirement for slow economic speeds;  
requirement that generators feed other consumers of comparable power, as well as main propulsion motors.

One should strive when designing GEU to insure that a main propulsion [56] motor is fed from at least two, but no more than four, generators. In this case, all advantages of electrical propulsion plants can be considered fully: operation of fewer generators at prolonged economic speeds and better primary motor use, great GEU economy at slow speeds, and an increase in operating life overall.

Generator and main propulsion motor voltage exerts significant influence on the amount of copper used in electric propulsion networks: the higher the voltage, the lower the cable section and the less copper used. Main propulsion motor armature voltage, as a rule, should be taken as equal to the maximum permissible voltage. The exception can be circuits in which more than one main propulsion motor is fed from one generator (see Figure 2.17).

The number of main propulsion motor armatures is determined by design considerations based on conditions under which the main propulsion motor is housed, as well as by the voltage and number of generators feeding the main propulsion motor. For example, given restricted width in the main propulsion motor compartment, it is advisable to use a two-armature main propulsion motor of less diameter and greater length. If there is a length restriction involved, a single-armature main propulsion motor should be used.

Selection of the number of main propulsion motor armatures also involves voltage and the number of feeding generators. If there are two generators feeding the main propulsion motor, the voltage of each equals the maximum permissible. If the generators are connected in series and their total voltage exceeds the maximum permissible, a two-armature main propulsion motor should be used and its armatures should be connected to the generators in the series-alternate manner (see Figure 2.7, for instance). Selection of two-armature electric motors

in the circuits shown in Figures 2.8, 2.9, and 2.11 was stipulated by these considerations.

We will make a comparative evaluation of the main current circuits from the point of view of the factors noted above.

Circuits shown in Figures 2.1 and 2.2 can be used for dual-shaft GEU in which one generator feeds one main propulsion motor. However, preference should go to the circuit in Figure 2.2, which provides the capability to operate both main propulsion motors with one generator.

Circuits depicted in Figure 2.3 and 2.4 are useful for those GEU in which two generators run each main propulsion motor. The latter circuit is better since it has one less main contact.

Circuits presented in Figures 2.5 and 2.7 are useful in those instances when generator voltage equals propulsion motor armature voltage. Two-armature main propulsion motors are used in those circuits. The current in the main circuit of the circuits shown in Figures 2.3 and 2.4 is greater by a factor of 2 than in the circuits shown in Figures 2.5 and 2.7. Consequently, the cable section also is greater by a factor of 2.

The circuit depicted in Figure 2.7 also makes it possible to disconnect [57] any main propulsion motor armature from the circuit in the event of breakdown. Detachable jumpers make the disconnect.

Thus, the circuit in Figure 2.4 is recommended for single-armature main propulsion motors and that in Figure 2.5 for two-armature motors.

Circuits shown in Figures 2.9 and 2.11 can be used in powerful GEU in which four generators run each main propulsion motor. The voltage of each generator in these circuits equals  $\frac{1}{2}$  that of one main propulsion motor armature. They are more flexible than the circuit depicted in Figure 2.8.

Circuits shown in Figures 2.4 and 2.5 can be used for each shaft in dual-shaft electrical propulsion plants having two generators per main propulsion motor.

If the need arises in the dual-shaft plant for one generator to run both main propulsion motors, then the circuit in Figure 2.12 can be recommended. This circuit is especially efficient for GEU operating for prolonged periods at slow speeds.

The circuit in Figure 2.13 has been used successfully in icebreakers with three-shaft propulsion plants.

The circuit shown in Figure 2.23, recommended for electrical propulsion plants in ice navigation vessels and icebreakers, is the simplest and most reliable of the two-armature circuits.

The circuit on the icebreaker "Lenin" provides good results for powerful icebreaker GEU. The circuit shown in Figure 2.17 is best for electrical propulsion plants in which one generator feeds two main propulsion motors and requires separate control of each main propulsion motor.

A constant current circuit (see Figure 2.19), which makes it possible to provide separate control of each main propulsion motor cut into the main current loop, is recommended in those instances where generators are required to feed several consumers of comparable power along with main propulsion motors.

The recent tendency is to use GEU generators in modes not requiring supply of full power to main propulsion motors to feed the common shipboard network and special powerful electric power consumers. In this event, circuits shown in Figures 2.7 and 2.12 can be recommended for feeding special dc consumers. Dual-current GEU with ac generators, rectifier units, and dc main propulsion motors should be used to feed special ac consumers.

Selector switch main contacts are not intended for breaking a circuit carrying current. Therefore, if the danger exists of large currents appearing in the main current loop when excitation is removed, knife switches are introduced into the main current circuit (see Figures 2.9 and 2.11).

## Direct Current Electrical Propulsion Plant Field and Regulation Circuits

## § 3.1 Basic Differences in Electrical Propulsion Plant Field Circuits

Electrical propulsion plant excitation systems can be differentiated by the type of exciter used for main generators and main propulsion motors.

Main generator field windings in small electrical propulsion plants [GEU] can be fed directly from the shipboard dc network. These systems are applicable to electrical propulsion plants with generator field currents not exceeding 5 a. Dimensions and weight of control gear (control stations) radically increase if there are large field currents. Therefore, at currents exceeding 5 a, machinery field windings are fed from generator-excitors.

A low-power dc GEU field circuit, in which the generator and main propulsion motor field windings are fed from the shipboard network, is depicted in Figure 3.1.

Several excitation system varieties exist.

A generator field winding is fed from an exciter (separately-excited generator) in excitation systems with separately-excited fields. <sup>(Fig. 3.2)</sup> The exciter field winding is fed via a potentiometric regulator from the dc network. The main propulsion motor winding is fed from the shipboard dc network.

Circuits shown in Figures 3.1 and 3.2 provide the main propulsion motor characteristics depicted in Figure 3.3 (curves 4 and 5). As can be seen in this figure, the primary motor will be underloaded during operation of the screw based on the mooring characteristic at point B since the moment and main circuit current it creates must remain constant so as not to overheat electrical propulsion plant electrical machinery.

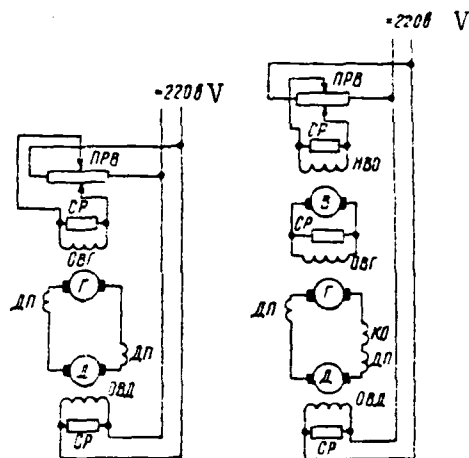
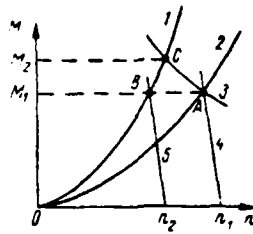


Figure 3.1. GEU Separate Field Circuit Directly from the Network.

Figure 3.2. GEU Field Circuit with Separate Pilot Exciter.

Under a normal primary motor load, the main propulsion motor must run at point C of the mooring characteristic, developing moment  $M_2$ , at which time main circuit current increases and the generator and GED [main propulsion motor] will overheat.

Field systems with three-winding exciters (Figure 3.4) differ from those described above in that the generator field winding is fed from an exciter [59] having three field windings instead of a separate pilot exciter: 1) separate field winding fed via a potentiometric regulator from the shipboard dc network; 2) current, or so-called differentially-compounded, winding fed from the voltage drop at the commutating poles and at the main propulsion motor compensating winding (or cut in series directly into the main current circuit); and 3) self-excitation winding connected to the exciter armature terminals. The separate field winding's magnetization force [n. s.] is counteropposed to the differentially-compounded winding n. s. and matches that of the self-excitation winding. GEU control by such a circuit occurs by means of the field current change according to the amount and direction in the separate field winding.



1 - mooring characteristic of screw; 2 - screw characteristic in open water; 3-hyperbola of equal power; 4 and 5 - characteristics of screw engine

Figure 3.3. Characteristics of GEU with Generator Separate Excitation.

A three-winding exciter provides a main propulsion motor the mechanical characteristic shown in Figure 3.5. This characteristic provides the opportunity to obtain an identical primary motor load as the screw operates in pure water and when moored (points A and B). The primary motor will be overloaded somewhat as the screw runs at intermediate characteristics. Also, the generator and main propulsion motor will experience a current overload during operation at point B. Similar circuits insure normal operation when the screw locks and is exposed since the mechanical characteristic restricts the main propulsion motor moment by the mooring moment  $M_{cr}$ , while the rotational speed at idle by the value  $n_{x.}$ .

A variety of the circuit examined above is one shown in Figure 3.6, [60] used in GEU operating in a constant current circuit. Generator and main propulsion motor excitation in this circuit is controlled simultaneously so that main circuit current remains constant. This circuit provides characteristics identical to those shown in Figure 3.4.

Excitation systems with amplidynes (EMU) insure that primary motors are loaded more fully than do circuits with three-winding exciters.

A circuit for GEU with three-winding exciters for generator excitation and with amplidynes EMU for main propulsion motor excitation is shown in Figure 3.7. The main propulsion motor field winding receives feed from its own exciter, which has two field windings: separate field winding fed from a constant voltage dc network and a bucking [starting] winding fed from an amplidyne with four field windings.

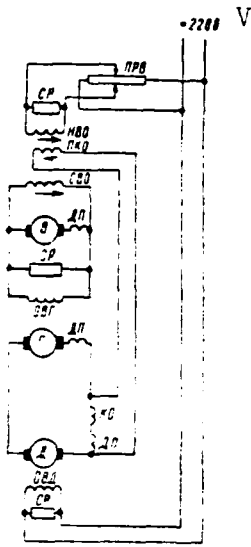


Figure 3.4. Three-Winding Exciter GEU Field Circuit

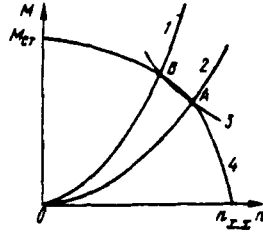


Figure 3.5. Main Propulsion Motor and Screw Characteristics. 1--Screw mooring characteristics; 2--Screw characteristics when moving in pure water; 3--Constant power hyperbole; 4--GED propulsion motor mechanical characteristic;  $M_{cr}$  - mooring moment;  $n_{x, n}$  - rotational speed for idling GED.

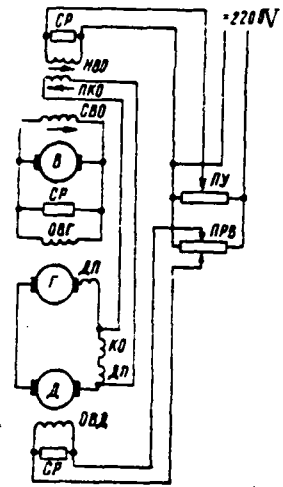


Figure 3.6. Field Circuit for GEU with Three-Winding Exciter Operating from a constant Current Circuit.

An exciter bucking winding with additional resistors SD connected in series and in parallel with it is the EMU load. The EMU master winding is connected in parallel to the separate excitation winding NV0 via a rectifying bridge; the current winding is cut into the voltage drop at the commutating poles and to the main propulsion plant compensating winding and is fed via the rectifying bridge, while the voltage feedback winding is cut into the EMU armature terminals. The magnetization force of the EMU separate excitation winding is counter- [61] opposed to the current winding and voltage feedback winding n. s.

This circuit insures a constant primary motor load as the screw operates in all characteristics from running in open water to moored operations, i. e., the main propulsion motor's mechanical characteristic in this section will follow the constant power hyperbole (Figure 3.8).

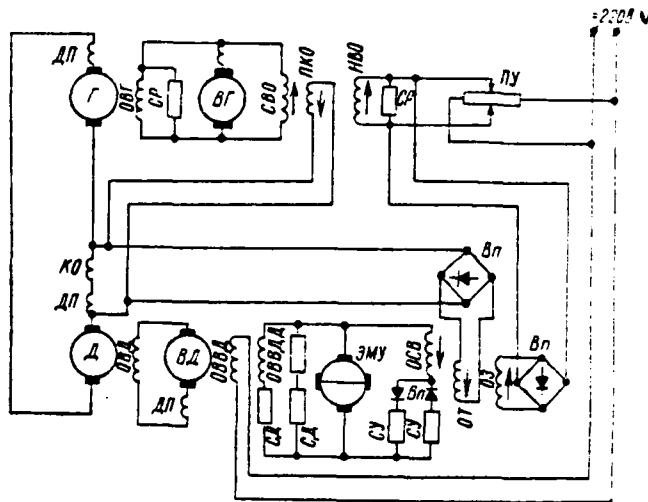


Figure 3.7. Excitation Circuit of GEU with a Three-Winding Generator Exciter and Main Propulsion Motor EMU Exciter.

The excitation circuit shown in Figure 3.9 provides an analogous main propulsion motor mechanical characteristic. An amplidyne with three field windings is used in this circuit for generator excitation: 1) master winding fed from a constant voltage dc network via control station adjusting resistance; 2) current winding cut in in parallel to the main propulsion motor commutating field winding and compensating winding; 3) stabilizing winding. The magnetization force of the master and current windings are counteropposed.

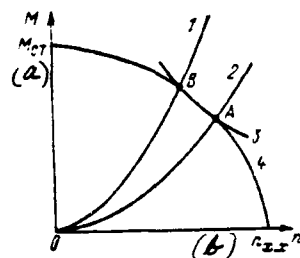


Figure 3.8. GEU Characteristics. 1--Screw mooring characteristic; 2--Screw characteristic when running in open water; 3--Constant power hyperbole; 4--GED mechanical characteristic; a--  $M_{GT}$  mooring moment; b--  $n_{GED}$  GED rotational speed while idling.

The main propulsion motor field winding is fed by an amplidyne with four [62] field windings: 1) master winding fed by a constant voltage dc network; 2) regulating winding cut in to the difference between the reference oscillator voltages and EMU generator voltage; 3) voltage feedback winding cut in to the main propulsion motor exciter EMU armature; 4) stabilizing winding. The master winding's magnetization force is counteropposed to that of the regulating and voltage feedback windings.

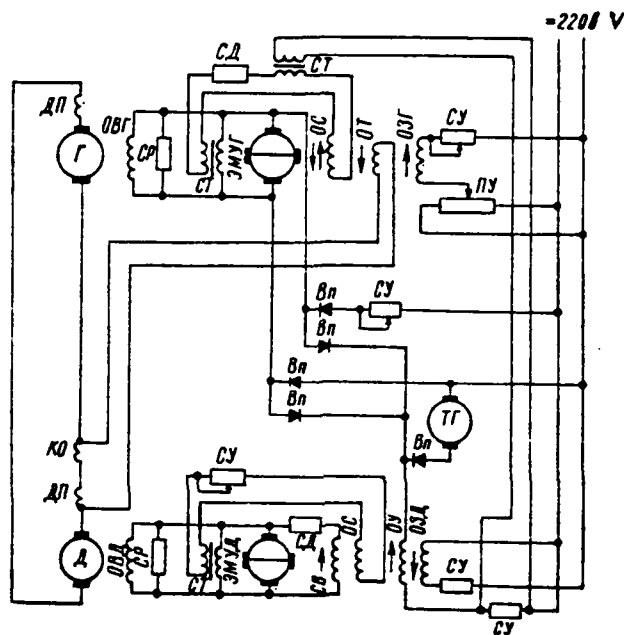


Figure 3.9. Excitation Circuit of a GEU with EMU -- with Generator and GED Exciters.

Besides EMU, magnetic amplifiers and silicon controlled rectifiers, which are becoming more and more widely used, can be used for generator and main propulsion motor excitation.

Exciters intended for main generator excitation either are attached on the same shaft with them or have separate drive. The former method has several drawbacks: field voltage depends on main generator rotational speed, which hinders and complicates main generator voltage regulation by changing primary motor rotational speed; in addition, connection of exciters and main generators via a common shaft also can be the source of fluctuations (oscillations) in the GEU circuit and complicate the excitation system.



under load or moored operations. Boosting relay RF1 trips when there is a significant increase in the current in the main circuit and, with its normally-closed (n. z.) contacts, shunts resistor ~~R<sub>В</sub>~~<sup>VB</sup>, main propulsion motor field current increases, and main circuit current decreases. [64]

An analogous excitation circuit was used for the GEU aboard the tug "Goliaf" and for "Yuzhnyy" class ferries, with the only difference being that each armature's field winding has its own discharging resistor and can be cut out of the circuit by means of handwheels.

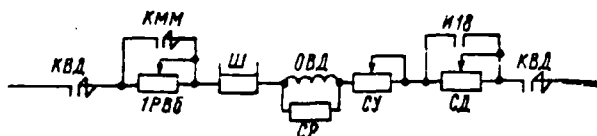


Figure 3.11. Maritime Tug One-Armature Main Propulsion Motor Excitation Circuit.

A maritime tug one-armature main propulsion motor excitation circuit is shown in Figure 3.11. The field winding is connected to the shipboard dc network via main propulsion motor field contactor KVD. Cut in with the field winding in series are: standardizing resistor SU, for characteristics adjustment as the circuit is tuned; resistor 1RVb for boosting the main propulsion motor field current, accomplished by closing contactor KMM contact when there is an increase in propellor moment or an increase in load on the auxiliary generator installed on the same shaft with the main generator; additional resistor SD cut into the field winding circuit by means of the selector switch I18 contactor when one generator runs the main propulsion motor.

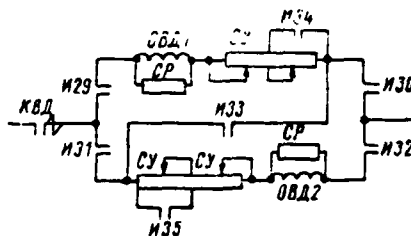


Figure 3.12. Excitation Circuit for an "Aktyubinsk" Class Diesel Electric Ship Two-Armature Main Propulsion Motor Excitation Circuit.

The excitation circuit for a two-armature main propulsion motor on an "Aktyubinsk" class diesel electric ship is presented in Figure 3.12. Main propulsion motor field windings are cut into the constant voltage generator circuit via contactor KVD contacts, selector switch contacts I29-I32, I34, and I35, and standardizing resistor SU. Discharging resistors SD in parallel are cut into each armature's field winding.

The circuit provides the following field winding closings in various GEU modes: parallel field winding closing when all four diesel generators run both main propulsion motor armatures (contacts I29-I32 are closed); series field winding closing when three diesel generators run both main propulsion motor armatures (contacts I29, I32, and I33 are closed); only one field winding is [65] closed (the second is cut out) when two diesel generators run one main propulsion motor armature (contacts I29, I30, I34, or I31, I32, and I35 are closed). In the latter case, part of standardizing resistor SU also is shunted by the contacts of selector switches I34 or I35 for amplification of main propulsion motor current. Contact closure is shown in Table 4.1.

### § 3.2 Excitation Circuits With Separately-Excited Exciters

Separately-excited exciters were not used widely in dc electrical propulsion plants as generator exciters because they do not provide the requisite characteristics. Circuits for GEU with these main generator exciters cannot maintain the approximate constant primary motor power as the screw operates at various characteristics from movement in open water to moored operations. Electric motor moment is proportional to its current and magnetic flux:  $M_a = C/\Phi_a$ . Consequently, current in the main circuit will increase with an increase in moment, given constant current. Therefore, an overload relay, a current relay which at a given current value exceeding the nominal trips and introduces resistance into the exciter separate excitation winding circuit, is cut into the main current circuit to prevent primary motor overload. Generator voltage drops, while main propulsion motor rotational speed and demand drop.

One drawback of this circuit is that it includes a relay reducing circuit reliability and power control occurs in stages.

Restriction of power taken from a primary motor can be achieved also by boosting main propulsion motor excitation. Current in the main circuit drops in proportion to the increase in main propulsion motor magnetic flux and rotational speed decreases. Consequently, its demand drops.

This power restriction method is accompanied by an increase in main propulsion motor dimensions. Therefore, it is used sparingly and for short-term main propulsion motor excitation boosting.

Both of the aforementioned power restriction methods usually are used simultaneously in circuits for GEU with separately-excited exciters.

A circuit for an electrical propulsion plant with separately-excited exciters was used on a diesel-electric ship of postwar domestic production, the tanker "General Azi Aslanov." The GEU excitation circuit is shown in Figure 3.13. [66] One main exciter VO is envisaged for each pair of generators feeding a main propulsion motor and there is one stand-by exciter VR for each generator pair. A stand-by exciter can run only one generator pair simultaneously.

Main generator field windings OVG1 and OVG2 are connected to an exciter via selector switch contacts I9-I14, exciter switch contacts IV5-IV8, field contactor KVG contacts, and shunt Sh. Selector switch I is for cutting the field windings of non-operating generators out of the circuit, while field switch IV is for switching generator field winding feed from the main to the stand-by exciter. Generator field winding OVG2 can be connected directly to the 220 V dc shipboard network by means of selector switch contacts I13 and I14 via a special field regulator when the generator is running the tanker's loading pumps.

Exciter VO and VR separately-excited windings NVO and NVR are connected [67] to a potentiometric regulator via selector switch contacts IV1-IV4, additional resistor SD, standardizing regulator SU, and station switch contacts PP13-PP16. Discharge resistor SR is connected in parallel to each separately-excited winding.

Potentiometric regulator 2PU is connected to the electrical propulsion plant feed network via station switch contacts PP9 and PP10 and voltage relay RN contacts.

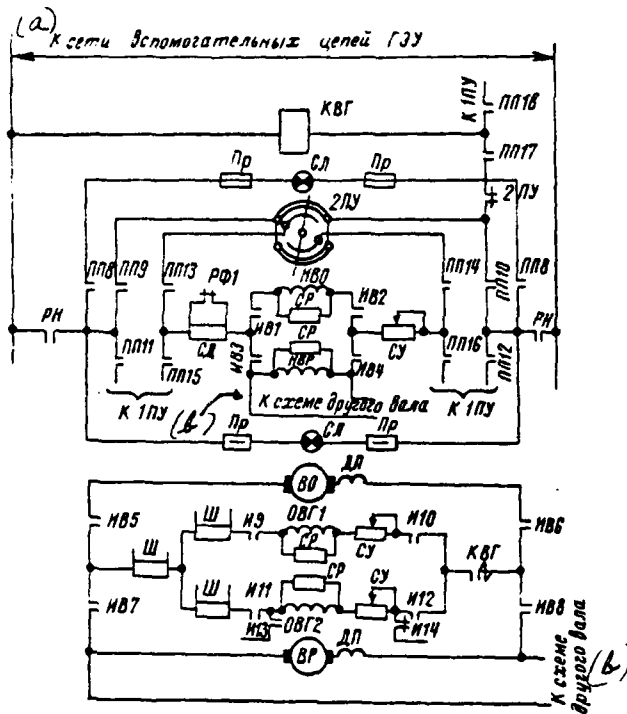


Figure 3.13. Diesel-Electric Ship "General Azi Aslanov" Excitation Circuit. a--To the network of GEU auxiliary circuits; b--To another shaft's circuit.

Resistor SD is shunted by a booster relay RF1 contact, which closes this contact during an overload and introduces resistance into the separately-excited winding circuit. Resistor SU is intended for adjustment of the characteristics as the circuit is tuned. The control station switch serves to switch propulsion plant control from one control station to another.

Main propulsion motor rotational direction regulation and change in this circuit is accomplished through a change in the amount and direction of current in the exciter separate field winding by means of a potentiometric regulator at control stations IPU and 2PU. Generator field current, generator voltage, and main propulsion motor rotational speed will change in accordance with a change in exciter field current.

### § 3.3 Excitation Circuits With Three-Winding Exciters

GEU excitation circuits with three-winding exciters began to be introduced into electrical ships in 1949 and found wide use. Generator field windings on most domestic electric ships built after the war (refrigerator ships, dry cargo ships, whalers, tugs, ferries) are fed by three-winding exciters.

An increase in main circuit current causes a differentially-compounded winding to demagnetize a generator, reducing the voltage at its terminals and, consequently, main propulsion motor rotational speed as well. As the circuit is tuned, a winding n. s. ratio is selected so that primary motor shaft power remains approximately constant as the screw runs at different characteristics from movement in open water to moored operations, given the corresponding screw moment changes.

The three-winding exciter winding closing examined occurs as it operates as a main generator exciter. If a three-winding exciter runs main propulsion motor field windings, then winding closing must be different, to wit: the current winding and self-excitation winding are cut in matched, while the separately- [68] excited winding is cut in unmatched.

This three-winding exciter field winding closing is stipulated by the requirement to reduce main propulsion motor current when it increases by amplifying field current. Great moment will be provided at the same current here.

We will examine several characteristic three-winding exciter generator field circuits in this section.

Excitation circuits with differentially-compounded windings connected to the main current circuit. An excitation circuit with a three-winding exciter on a "Yuzhnyy" class ferry is depicted in Figure 3.14. A special feature of this circuit is that the differentially-compounded winding is cut directly into the main current circuit in series with main generator and main propulsion motor armatures. Advantages are that it is a high-speed circuit, there is a capability to obtain high differentially-compounded winding n. s., and it is safe, since essentially it is impossible to disrupt the differentially-compounded winding.

This circuit's disadvantages include a requirement to pass all main current through the exciter field winding and to have powerful contacts in the field switch, which complicates the design and increases size and weight.

Generator field windings OVG1 and OVG3 are connected to the armature of the main VO or stand-by VR exciters via its own standardizing resistors SU, selector switch contacts I11-I14, and field selector switch contacts IV5-IV8. Discharging resistors SR are connected in parallel to each generator field winding. This circuit has greater flexibility where generator field winding connection is concerned compared to the circuit shown in Figure 3.13, since standardizing resistors are connected to each winding, allowing individual adjustment of each generator's characteristics during tuning.

Self-excitation windings SVO and SVR are connected in parallel to the armatures of the main and stand-by exciters, while standardizing resistor SU is connected in series with each winding for exciter characteristics adjustment as the circuit is tuned. The selector switch serves to cut out the field windings of non-operating generators, while the field switch is used to switch from the main VO to the stand-by VR exciter.

The self-excitation windings of the main NVO and stand-by NVR exciter are connected to potentiometric regulators located at control stations 1PU and 2PU via standardizing resistors SU, field switch contacts IV9-IV12, selector switch contacts I24-I27, and station switch contacts PP5, PP6, PP9, and PP10. Two indicator lights are built into each control station: LZ comes on when the control station is cut in and the circuit is ready to operate; LK comes on [69] when the control station is cut out as a result of a fuse tripping and station switch PP is cut into the assigned station.

A three-winding exciter's differentially-compounded winding directly is cut into the main current circuit via field switch contacts IV1-IV4.

Detachable jumpers make it possible to cut differentially-compounded windings into the main propulsion motor D1 armature circuit or D2 armature circuit.

In this circuit, main propulsion motor rotational speed is regulated by [70]

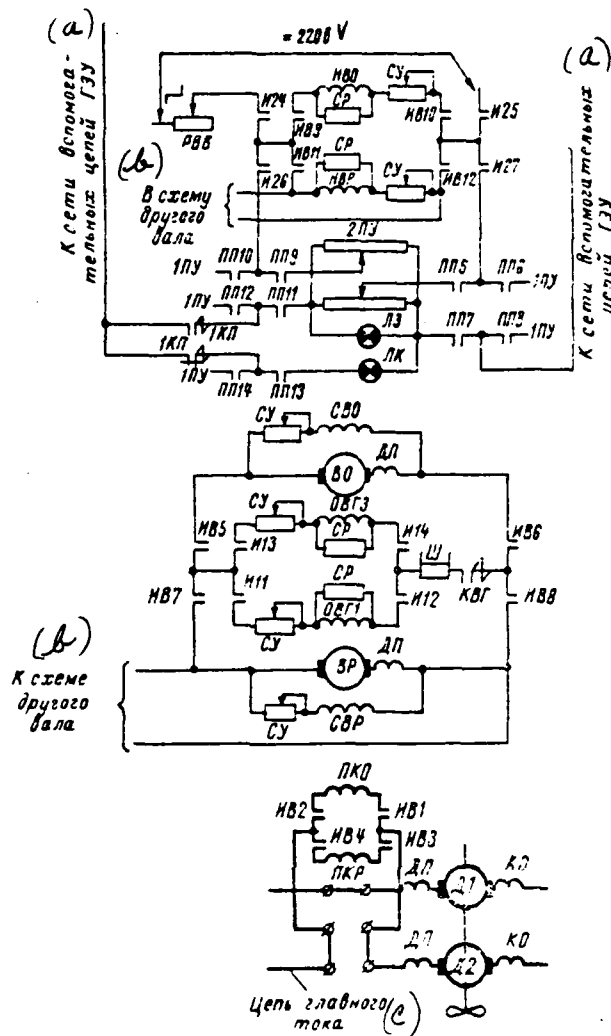


Figure 3.14. "Yuzhnyy" Class Ferry Excitation Circuit.  
 a--To GEU auxiliary circuit network; b--To another shaft's circuit; c--Main current circuit.

changing the amount and direction of the current in the exciter separately-excited winding using the potentiometric regulator at control station 1PU or 2PU, as well as by a change in primary motor rotational speed.

Generator field current, given a constant 550 rpm primary motor rotational speed, is changed at the control station's first positions initially, with primary motor rotational speed changing from 550 to 720 rpm in the final position.

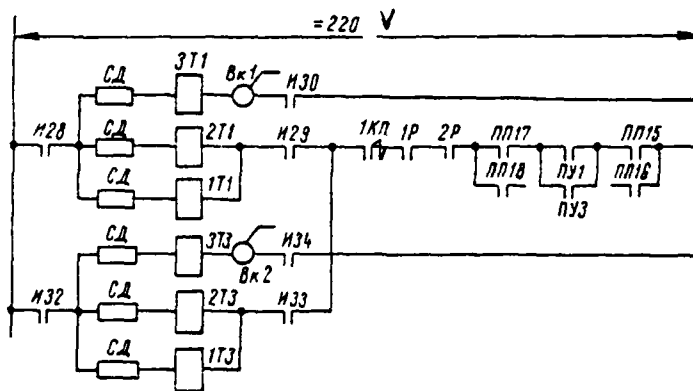


Figure 3.15. Diesel Rotational Speed Regulating Circuit.

A primary motor rotational speed regulation circuit activated by closing, in a certain sequence, electropneumatic rectifiers of diesel governor 1T-3T is depicted in Figure 3.15. When rectifier 3T is closed, the diesel develops 550 rpm; in the final control station position, its contact PU1 for movement ahead or PU3 for movement astern is closed. When these contacts close, electropneumatic rectifiers 1T, 2T receive feed and, acting upon the diesel governor, they increase its rotational speed from 550 to 720 rpm.

Excitation circuits with differential connection of the differentially-compounded winding. A maritime tug GEU excitation circuit is shown in Figure 3.16. This tug's electrical propulsion plant has one shaft with a single-armature main propulsion motor fed by two generators. Both generators' field windings are fed by one three-winding exciter V1. The circuit also envisages stand-by exciter set V2.

Exciter V1 and V2 self-excitation windings SV01 and SV02 are connected to the terminals of the corresponding exciters' armatures via standardizing resistors SU. Field switch contacts PV1-PV4 insure switching the feed of generators OVG1-OVG2 field windings from exciter V1 to V2, while contacts PV5 and PV6 [71] provide the generator OVG1 or OVG2 field winding connection to exciter V2 when either of these two generators runs the shipboard network. Selector switch contacts I10, I13, I14, and I17 connect generator field windings to the exciter armature when the generators run the electric propulsion, while contacts I11, I12, I15, and I16 connect the field winding of any generator running the shipboard network.



AD-A114 423

FOREIGN TECHNOLOGY DIV WRIGHT-PATTERSON AFB OH  
FUNDAMENTALS OF ELECTRICAL PROPULSION PLANT DESIGN, (U)  
APR 82 N A KUZNETSOV, P V KUROPATKIN  
FTD-ID(RS)T-1388-80

F/G 21/3

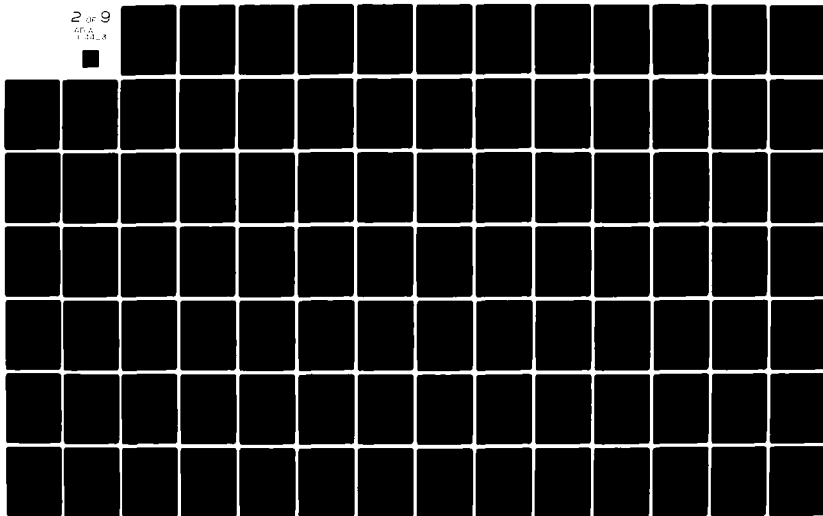
UNCLASSIFIED

NL

2 of 9

44-A

1133-1



Consequently, standardizing resistor SU is connected in series to each differentially-compounded winding.

Three-winding exciter V1 and V2 self-excitation windings NV01 and NV02 are connected to the dc network via station switch contacts PP7-PP19, field switch contacts PV13-PV16, additional resistors 2SD-4SD, and a control station adjusting resistor, for example 2PU.

In this circuit, separately-excited winding NV01 or NV02 is connected to the GEU auxiliary network, rather than to a potentiometric regulator as in previous circuits. This regulation circuit is worse for many reasons, particularly because currents in separately-excited windings will change, given identical control station positions, as the separately-excited windings are cut in and out. This means additional circuit tuning every time switching occurs. This is done in this circuit by connecting additional resistor 3SD to the separately-excited winding NV01 and NV02 circuit by means of selector switch contact I23 when one of the windings is cut out of the circuit.

Main propulsion motor rotational speed regulation in this circuit occurs by means of a current change in the three-winding exciter separately-excited winding by cutting a regulating resistor in and out in stages to a control station, for example 2PU. In addition, screw rotational speed is regulated by a change in diesel generator rotational speed by means of a separate governor.

The switch contact I and PV closure sequence is shown in Table 3.1.

A diesel generator rotational speed regulation circuit is depicted in Figure 3.17. In this circuit, indicator light 2LZh indicates the presence of voltage in the circuit's feed circuits. Diesel generator rotational speed regulation circuits are connected to the feed network by switches 1VP for DG1 and 2VP for DG2. We will examine only one generator's regulation circuits since those of the second generator are analogous. Indicator light 5LZh indicates connection of diesel regulation and protection circuits. Diesel protection is provided [74] by a circuit consisting of oil pressure relay contacts connected in series in the diesel lubrication system, additional resistor 22SD connected in parallel with resistor 23SD and diesel fuel supply interblock magnet IBM. Relay contacts

(b)

(a) Переключатель И

№ режима	(c) Режим работы ГЭУ	(d)																			
		I10	I11	I12	I13	I14	I15	I16	I17	I18	I19	I20	I21	I22	I23	I24	I25	I26	I27	I28	I29
0																					
1	G1, G2 на Д <sup>(1)</sup>	×			×	×			×	×	×	×	×		×	×	×	×		×	×
2	G1 на Д, G2 на сеть <sup>(1) (2)</sup>	×			×		×	×			×				×	×			×		×
3	G1 на сеть, G2 на Д <sup>(2) (1)</sup>		×	×		×			×				×	×		×				×	

(1) - to; (2) to network

(b)

(e) Переключатель ПВ

№ режима	(c) Режим работы	(f)																			
		PV1	PV2	PV3	PV4	PV5	PV6	PV7	PV8	PV9	PV10	PV11	PV12	PV13	PV14	PV15	PV16	PV17	PV18		
1	V1 на ГЭУ																				
2	V2 на ГЭУ																				
3	V1 на ГЭУ, V2 на сеть																				

Table 3.1. Switch Contact I and PV Closure (See Circuit in Figure 3.16).  
 a--Switch I; b--Mode number; c--GEU operating modes; d--I10-I29; Designates generators running motors, network, and GEU; e--Switch PV; f--PV1-PV8;  
 1--V1 to GEU; 2--V2 to GEU; 3--V1 to GEU, V2 to network.

1RDMD close if there is a pressure drop in the diesel lubrication system and [75] electromagnet IBM, which cuts off the supply of fuel, is cut in.

Electropneumatic rectifiers 1T1-3T1 directly regulate diesel generator rotational speed. They are connected to the dc network via additional resistors 13SD-15SD, diesel control switch 1PGD, and diesel speed switches 1PSD-PSD. Switch contact PSD and 1PSD closure sequence is shown in Table 3.2.

After the starting of the diesel, its rotational speed is increased by switch 1PSD (located near the diesel) from 300 to 560 rpm (fifth switch 1PSD position) due to heating up with switch 1PGD set in the first position. Here, electropneumatic rectifier 3T1 is cut in. After the diesel warms up, the switch

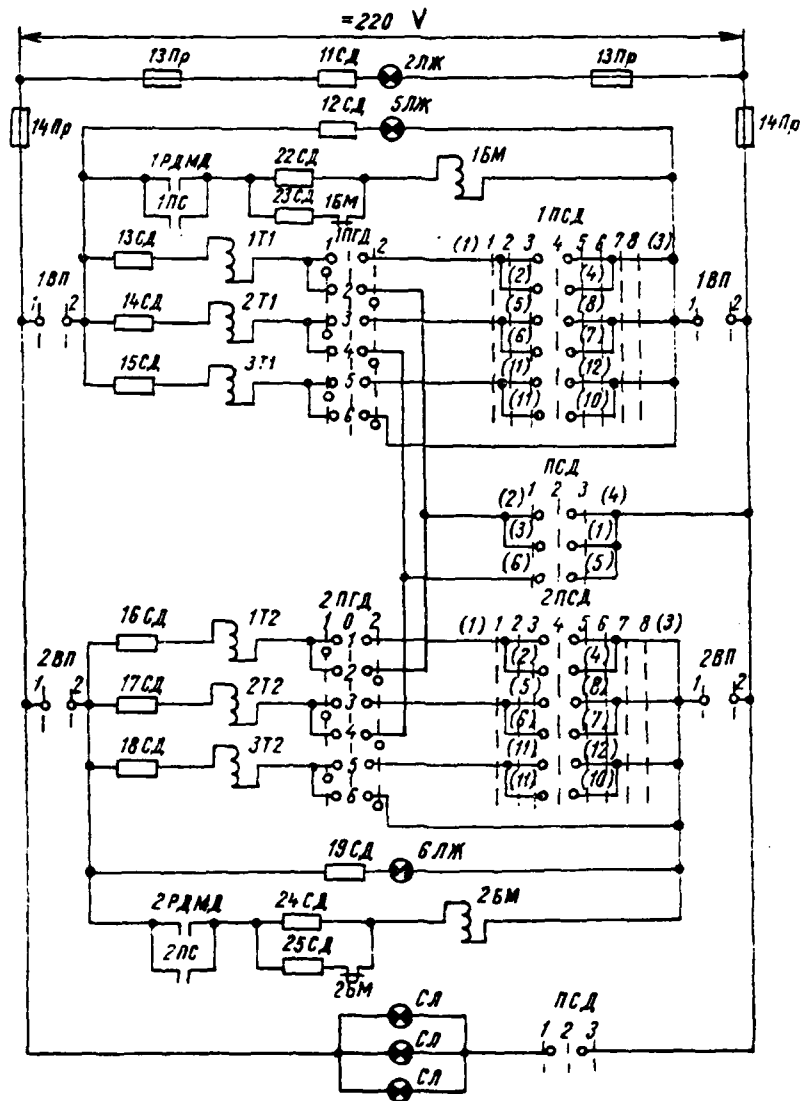


Figure 3.17. Diesel Generator Speed Regulation Circuit.

1PGD lever is moved from first to second position. Rectifier 3T1 remains cut in, but control is transferred to switch PSD installed on the electrical propulsion board by closing electro-pneumatic rectifiers 1T1 and 2T1.

Switch PSD has three lever positions: in the first, rectifier 1T1 is cut in and diesel speed increases to 615 rpm; in the second, with 1T1 cut out, 2T1 is cut in and diesel speed increases to 675 rpm; in the third position, both rectifiers are cut in and diesel speed reaches 740 rpm.

This circuit, with individual control levers for diesel generator speed and generator excitation, is more complex to operate than those in which control is combined into one lever, as was the case for "Yuzhnyy" class ferries, "Aktyubinsk" class refrigerator ships, "Mirnyy" class whalers, and so on.

When separately-excited windings and resistor regulation windings are connected in series, the field current of these windings can not be reduced to zero since regulating resistance would have to equal infinity to do so. Regulating resistance must be high in order to reduce the field current in separately-excited windings to that value which would cause the main propulsion motor to stop.

Wires with a small section are used to restrict the size of control station resistors for their initial stages, which reduces control station mechanical stability. In addition, reversal contacts (contacts 2PU2-2PU3 and 2PU4-2PU5 in the circuit shown in Figure 3.16) are envisioned at a control station in this circuit to change the field current.

We will examine two methods of current regulation in a separately-excited winding:

- 1) connection of a separately-excited winding to a feed network in series with a regulating resistor;
- 2) connection of a separately-excited winding to the feed network via a potentiometric regulator.

A circuit for the first connection method is depicted in Figure 3.18. [77]  
Here,  $U$  -- network voltage;  $i$  -- current in the field winding circuit;  $r_{\text{н}}$  -- separate excitation winding resistance;  $r_{\text{р}}$  -- adjusting resistance.

To derive the formula for the relationship of winding and adjusting resistances, we introduce the designation:  $a = \frac{r_{\text{р. ном}}}{r_{\text{н}}}$  -- ratio of adjusting resistance given nominal field current  $i_{\text{ном}}$  to the amount of separate excitation winding resistance;  $k = \frac{i_{\text{ном}}}{i_{\text{мин}}}$  -- ratio of nominal current to minimal.

(a) Контакты	(b) Положения рукоятки							
	1	2	3	4	5	6	7	8
1-3				×				×
2-4		×				×		
5-8			×	×				
6-7							×	^
11-12					×	×		
11-10							×	×
Скорость вращения дизеля, об/мин (c)	410	460	510	560	610	660	710	760

(d) Замыкание контактов переключателя ПСД

(a) Контакты	(b) Положения рукоятки		
	1	2	3
2-4	×		
1-3			×
6-5	×	×	
(e) Запасные контакты 8-5			×
Запасные контакты 9-11			×
Запасные контакты 10-12	×		
Запасные контакты 13-15			×
Запасные контакты 14-16	×		
Запасные контакты 18-20		×	
Запасные контакты 22-24		×	
(c) Скорость вращения дизеля, об/мин	615	675	740

Table 3.2. Switch Contact 1PSD-2PSD Closure (See Circuit in Figure 3.17). a--Contacts; b--Lever position; c--Diesel rotational speed, rpm; d--Switch Contact PSD Closure; e--Reserve contacts.

Considering that nominal field current equals

$$i_{\text{НОМ}} = \frac{U}{r_{\text{н}} + r_{\text{р. ном}}},$$

while minimal field current must be less by a factor of  $k$ , we get the following expression for the ratio of field regulator maximum resistance to nominal resistance:

$$\frac{r_{\text{р. макс}}}{r_{\text{р. ном}}} = \frac{k - ku - 1}{a}. \quad (3.1)$$

The curves of the dependence of current on resistance for different values  $a$  have been constructed in Figure 3.19 from expression (3.1). It can be seen from these curves, a reduction in field current  $i_{\text{НОМ}}$  by a factor of 10 at  $a$ , equal to 1, requires an increase in resistance at the control station by a factor of 19. But, a ratio like  $\frac{r_{\text{р. макс}}}{r_{\text{р. ном}}}$  is disadvantageous since, first, in the given instance, the field winding must be counted on to provide nominal field current at half voltage and, second, field current here increases by a factor of 2 as well. Given  $a = 0.25$  for an identical field current decrease, it would be best to increase sequentially connected resistance by a factor of 46.

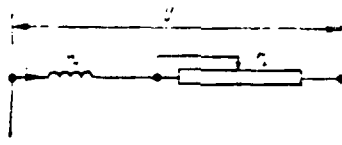


Figure 3.18. Circuit for Connection of a Field Winding in Series with Adjusting Resistance.

Circuits for connection of a separate excitation winding via a potentiometer.

A circuit for connection of a separate excitation winding to the feed net- [78]  
work via a potentiometric regulator is shown in Figure 3.20. The following designations are used in the circuit:  $U$  -- network voltage;  $i$  -- total current in the potentiometer circuit;  $r_p$  --- potentiometer adjusting resistance;

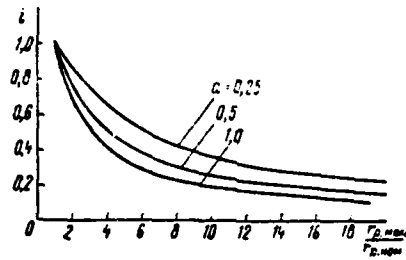


Figure 3.19. Curves of the Relationship of the Current in a Separately-Excited Winding to the Amount of Series-Connected Resistance.

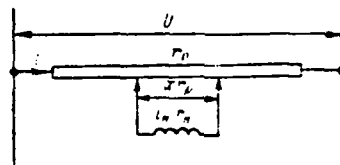


Figure 3.20. Circuit for Connection of a Field Winding Via a Potentiometric Regulator.

$r_n$  -- separate field winding resistance;  $i_n$  -- current in the separate field winding;  $x r_p$  -- resistance between points from which voltage is picked off to the separate excitation winding.

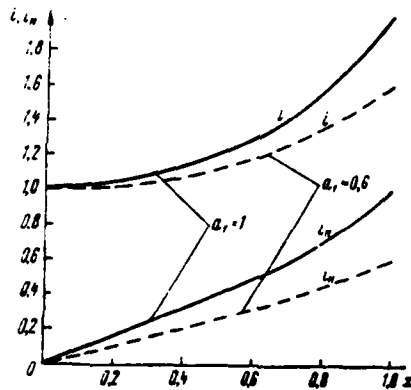


Figure 3.21. Curves of the Relationship of Total and Field Winding Current to the Amount of Potentiometer Resistance Introduced in Parallel to this Winding.

Derivation of the relationships of currents to resistance amounts requires us to take  $a_1 = r_p / r_u$  as the ratio of potentiometer resistance to separate excitation winding resistance.

Using these designations, one can derive the following relationships, in relative units, for the current in the potentiometer circuit and for current in the separate excitation winding:

$$\left. \begin{aligned} \bar{i} &= \frac{1 + a_1 x}{1 + a_1 x - a_1 x^2}; \\ \bar{i}_u &= \frac{a_1 x}{1 + a_1 x - a_1 x^2}. \end{aligned} \right\} \quad (3.2)$$

Curves constructed from the expressions in (3.2) are shown in Figure 3.21. As can be seen from the curves, a decrease in value  $a$  means an increase in the linearity of field current change. In other words, the less the potentiometer resistance compared to the field winding resistance, the more linear the relationship of field current to potentiometer resistance introduced in parallel to the separate excitation winding, i. e., the more stable the regulation.

Controller-type control stations, where resistance is changed in stages given closure of the corresponding command controller contacts, have come into use recently. A controller-type station circuit for staged connection of resistance for the circuit shown in Figure 3.16 is depicted in Figure 3.22. Control station contact closure sequence is shown in Table 3.3.

A circuit for a control station with potentiometric resistance connection, which can be used for the circuit in Figure 3.16 in place of the circuit shown in Figure 3.22, is presented in Figure 3.23.

A regulation circuit for GEU with series-connected adjusting resistance [79] has become quite widespread and is used, for instance, on "Akmolinsk" and "Dneproges" class diesel electric ships and "Mirnyy" class whalers, but newly-developed GEU should use potentiometric regulators connected by means of circuits shown in Figure 3.23.

Excitation circuits with generator switching. Dual-shaft electrical propulsion plant field circuits are complicated greatly when one main propulsion motor's generators can run another main propulsion motor. A similar circuit is shown in Figure 3.24.

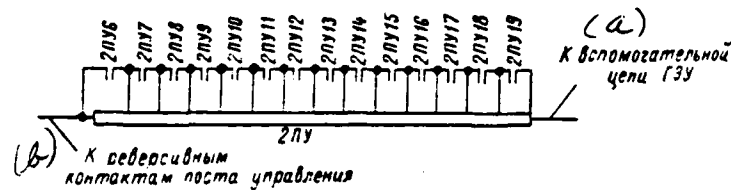


Figure 3.22. Circuit for Connection of Adjusting Resistance in the Excitation System in Figure 3.16. a--To GEU auxiliary circuit; b--To control station reversal contacts.

This is a circuit for a dual-shaft GEU with single-armature main propulsion motors, each fed by two diesel generators. In addition, the starboard main propulsion motor's diesel generator G2 can run the port main propulsion motor, while the port main propulsion motor's diesel generator D4 can run the starboard main propulsion motor. Both of these generators at different times can also run both series-connected main propulsion motors and, by the same token, each diesel generator can run the shipboard network.

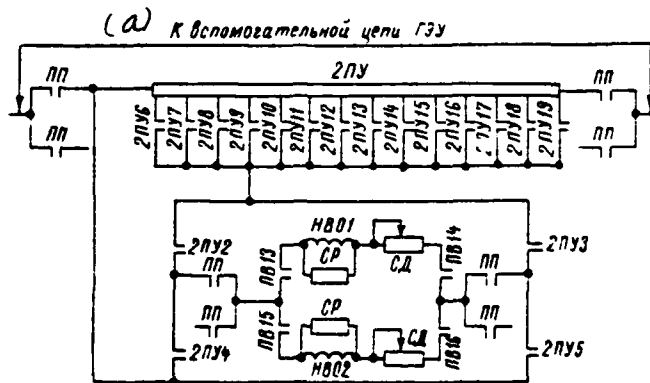


Figure 3.23. Control Station Circuit with Potentiometric Regulator and Staged Resistance Change. a--To GEU auxiliary circuit.

One three-winding exciter V1 and V2 is installed to feed each generator [83] field winding. The field windings of two or one generator are connected to the armature of each exciter depending on how many generators are feeding the starboard or port main propulsion motor. A stand-by exciter, which can be connected instead of any main exciter, is envisaged, but it cannot simultaneously run generators feeding different propulsion motors.

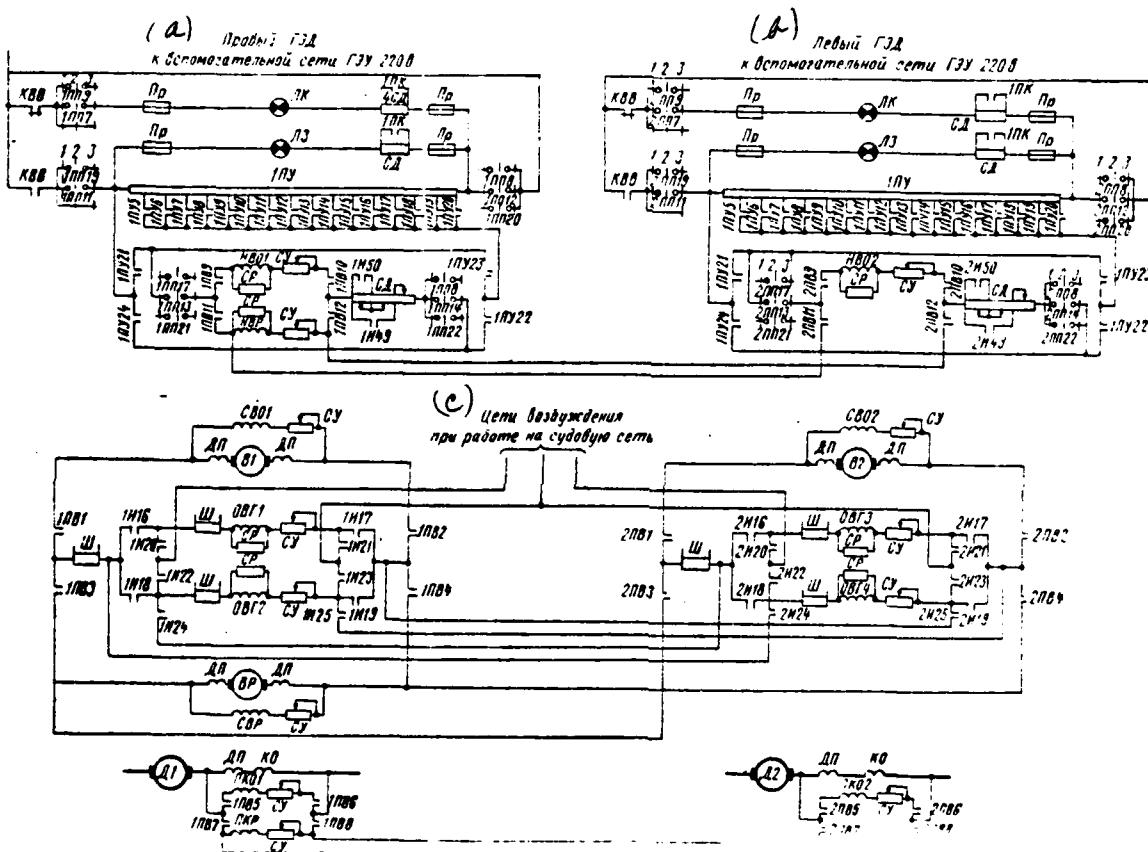


Figure 3.24. Dual-Shaft GEU Field Circuit. a--Starboard GED to GEU auxiliary 220 V network; b--Port GED to GEU 220 V auxiliary network; c--Field circuits when running the shipboard network.

Generator field windings are connected to exciter V1 and V2 armatures via standardizing resistors SU, selector switch contacts, shunts Sh, and field switch contacts. Self-excitation windings SV01 and SV02 are connected in parallel



to the exciter armatures. Selector switch contacts 1I16-1I19, and analogously 2I16-2I19, connect generator field windings to the exciters, while selector switch contacts 1I20-1I24, and analogously 2I20-2I23, connect them to the excitation system when running the shipboard network. Contacts 1I24 and 1I25 connect the generator G2 field winding to the exciter V2 armature when this generator runs the port main propulsion motor. In a similar manner, selector switch contacts 2I24 and 2I25 connect the generator G4 field winding. The three-winding exciter separate field windings are connected to controller-type potentiometric stations.

Each winding's circuit has standardizing resistors SU. Additional resistors SD, which are shunted by selector switch contacts 1I49 and 2I49 when two generators are connected to a main propulsion motor, are connected in series to the separate excitation windings. If the main propulsion motor is fed by one generator, then contact 1I49 opens and a part of resistor SD is introduced in series, since its residual resistance remains shunted by selector switch contact 1I50 or 2I50. Resistor SD is introduced completely into the separate excitation circuit when two main propulsion motors are fed by one generator. Contact 1I50 or 2I50 opens in this case.

Separate excitation windings are connected to the control station via station switch 1PP or 2PP.

A control station has two indicator lights: red LK, which lights up when the control station is cut out by contactor KVV when a protection trips, and green LZ, which comes on when the control station is ready for normal operation.

Three-winding exciter differentially-compounded windings are connected in parallel to the windings of main propulsion motor commutating poles DP and compensating winding KO via field switch contacts 1PV5-1PV8. Selector switch contact 1I and 2I closure sequence is shown in Table 3.4, that of switches 1PV and 2PV in Table 3.5, and that of control station PU contacts in Table 3.6.

Main propulsion motor rotational speed regulation in the circuit being examined occurs through a change in generator excitation by switching, in [87] stages, potentiometric station resistance at diesel generator rotational speed of 660 rpm. Two control station contacts must be closed simultaneously at the

control station, given a field current regulation potentiometric circuit, i. e., one stage of the potentiometer resistance always remains closed. This is done as a safeguard so no circuit will be broken as contacts are switched, which can occur if the previous contact opens before the subsequent one closes.

(a) № режима	(b) Режим работы	(c) К схеме на рис. 3.24										(d) К схеме на рис. 3.25													
		1116	1117	1118	1119	1120	1121	1122	1123	1124	1125	1152	1153	1154	1155	1156	1157	1158	1159	1160	1161	1162	1163	1164	1165
0																									
1	G1 и G2 на Д1	×	×	×	×							×	×		×	×	×		×	×	×	×			
2	G1 на Д1, G2 на сеть	×	×					×	×			×	×		×	×					×	×			
3	G1 на сеть, G2 на Д1			×	×	×	×					×		×		×		×	×	×	×				
4	G1 на сеть, G2 на Д1 и Д2			×	×	×	×					×		×		×		×	×	×	×				
5	G1 на Д1, G2 на Д2	×	×							×	×	×	×	×	×	×					×	×	×	×	×

Table 3.4. Selector Switch Contact 1I (2I Analogously) Closure. a--Mode number; b--Operating mode; c--For the Figure 3.24 circuit; d--For the Figure 3.25 circuit; e--1116-1125, 1152-1165. Designates generators running motors or the shipboard network. (1) - to; (2) - to network

(a) Положение переключателей	(b) Подключаемый возбудитель	(c) 11PV1	11PV2	11PV3	11PV4	11PV5	11PV6	11PV7	11PV8	11PV9	11PV10	11PV11	11PV12
0	(1) Отключено												
1	(2) Основной	×	×			×	×			×	×		
2	(3) Резервный			×	×			×	×			×	

Table 3.5. Field Switch Contact 1PV (Analogously 2PV) Closure (See Figure 3.24 Circuit). a--Switch position; b--Connected exciter; c--1PV1-1PV12; 1--Cut out; 2--Main; 3--Stand-by.

(a) Контакт поста управления	(b) Положения рукоятки поста управления																														
	(c) назад										(d) стоп	(e) вперед																			
	15	14	13	12	11	10	9	8	7	6		5	4	3	2	1	1	2	3	4	5	6	7	8	9	10	11	12	13	14	15
(f) 1ПУ1	x														x																
1ПУ2	x	x	x	x	x	x	x	x	x	x	x	x	x	x	x	x	x	x	x	x	x	x	x	x	x	x	x	x	x		
1ПУ3	x		x																								x		x		
1ПУ4	x	x																										x	x		
1ПУ5															x		x														
1ПУ6															x	x															
1ПУ7															x	x															
1ПУ8															x	x															
1ПУ9															x	x															
1ПУ10															x	x															
1ПУ11															x	x															
1ПУ12															x																
1ПУ13															x																
1ПУ14															x																
1ПУ15															x																
1ПУ16															x																
1ПУ17															x																
1ПУ18															x																
1ПУ19	x	x													x																
1ПУ20	x														x																
1ПУ21	x	x	x	x	x	x	x	x	x	x	x	x	x	x	x	x	x	x	x	x	x	x	x	x	x	x	x	x	x		
1ПУ22	x	x	x	x	x	x	x	x	x	x	x	x	x	x	x	x	x	x	x	x	x	x	x	x	x	x	x	x	x		
1ПУ23															x	x	x	x	x	x	x	x	x	x	x	x	x	x	x		
1ПУ24															x	x	x	x	x	x	x	x	x	x	x	x	x	x	x		
1ПУ25															x																
1ПУ26															x																
(g) Скорость вращения дизеля, об/мин	810	760	710												660														710	760	810

Table 3.6. Control Station Contact Closure (See Figure 3.24 Circuit). a--Control station contact; b--Control station lever position; c--Astern; d--Ahead; e--Stop; f--1PU1-1PU26; g--Diesel rotational speed, rpm.

After separate excitation windings have been connected directly to the network, i. e., all potentiometric resistance has been introduced, main propulsion motor rotational speed regulation will be accomplished through changing diesel generator rotational speed.

A circuit for this type of regulation is shown in Figure 3.25. A special feature of this circuit is that diesel generators DG1 and DG4 can run the starboard and port main propulsion motors. Each diesel has four diesel regulator electro-pneumatic rectifiers, as can be seen from the circuit: VT, 1T-3T. Electropneumatic rectifier VT is cut in in the control station zero position and cuts out one row of diesel fuel injectors. Solenoids 1T-3T regulate diesel generator rotational speed.

Electropneumatic rectifiers VT, 1T-3T are connected to the shipboard 220 V dc network via additional resistors SD, diesel speed switches 1PSD-4PSD, and selector switch contacts 1I52, 1I62, 1I65 or 2I52, 2I62, 2I65, while electro-pneumatic rectifiers 1T, 2T, in addition, via station switches and contacts are connected to the same 220 V dc network.

The diesel generator rotational speed regulation circuit has yellow indicator light LZh indicating the presence of voltage in the feed network. Non-operating diesel generators DG1 or DG2 are cut out of the regulation circuit by selector switches (contacts 1I58-1I56; 2I58-2I56 and contacts 1I57-1I60; 2I57-2I60 correspondingly). Regulation circuit feed is cut out by contacts 1I52 and 1I61, while feed to the regulation circuit elements located at control stations are cut out by contact 1I62.

Diesel rotational speed switches 1PSD-4PSD regulate diesel generator speed from the engine room as the motor is started and warmed up. Switch contact 1PSD-4PSD closure sequence is presented in Table 3.7.

During starting, the engineman warms up the diesel generators and brings their rotational speed up to 660 rpm (electropneumatic rectifiers VT1-VT4 are cut in), followed by diesel generator control being transferred to remote control stations.

Electropneumatic rectifiers 1T1, 1T2 and 2T1, 2T2 are cut in and out in particular sequence at remote control stations by the first station's con- [89] tacts 1PU3 and 1PU4. Here, diesel generator rotational speed changes in three stages: 710, 760, and 810 rpm, given generator constant field current. Control stations are connected to the diesel generator rotational speed regulation circuit via control station switch contacts 1PP-2PP.

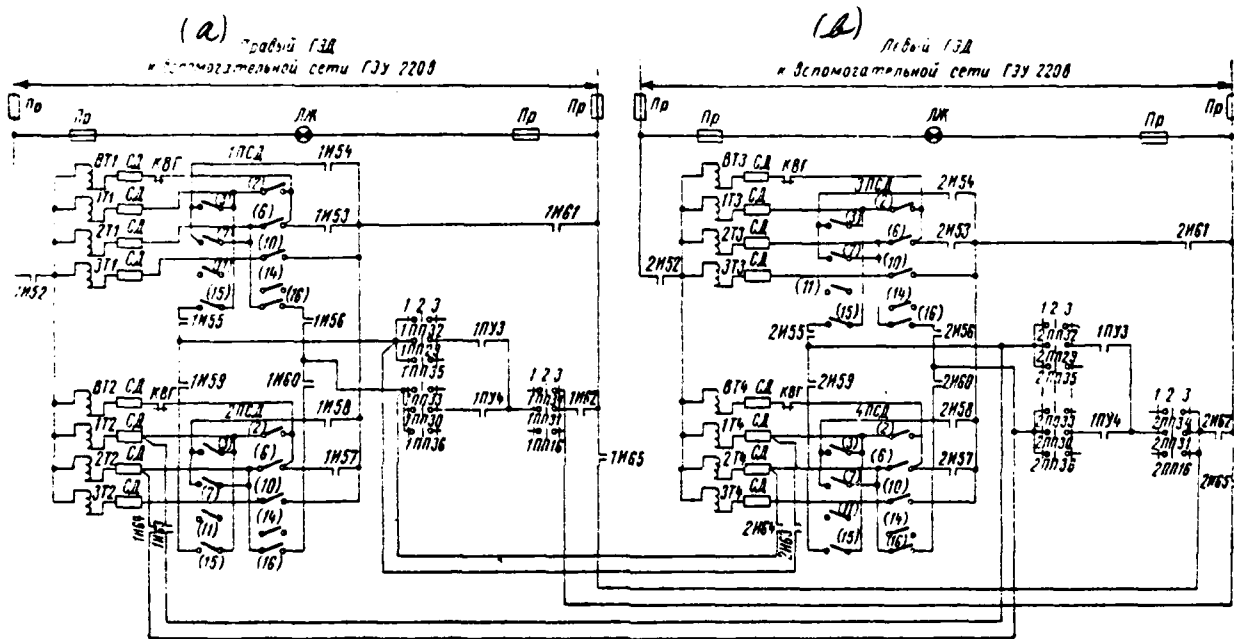


Figure 3.25. Diesel Generator Rotational Speed Regulation Circuit for GEU (See Figure 3.24). a--Starboard GED to GEU 220 V auxiliary network; b--Port GED to GEU 220 V auxiliary network.

The circuit depicted in Figure 3.25 is complicated compared to conventional circuits due to presence of additional contacts between main propulsion motor control circuits caused by the capability of diesel generators DG2 and DG4 to run the starboard and port main propulsion motors.

For example, when diesel generator DG2 is connected to the port main propulsion motor (selector switch 2I in the port main propulsion motor circuit must be

(a) Номера контактов		(d) Положения рукоятки													
(b) левая стороны	(c) правая стороны	1		2		3		4		5		6		7	
		л.	п.	л.	п.	л.	п.	л.	п.	л.	п.	л.	п.	л.	п.
	2														
3															
	6														
7															
	10														
11															
	14														
15	16														
(e) Скорость вращения дизеля, об/мин		460	510	560	610	660	710	760							
(f) Примечание: л. — левая, п. — правая сторона.															

Table 3.7. Switch Contact 1PSD-4PSD Closure (See Figure 3.25 Circuit). a--Contact numbers; b--Port; c--Starboard; d--Lever position; e--diesel rotational speed, rpm; f--Note: Lever position heading abbreviations are port and starboard, respectively.

in the zero position), generator field winding OVG2 (see Figure 3.24) is connected to the exciter V2 or VR armature by means of selector switch contacts 1I24 and 1I25 and field switch contacts 2PV1, 2PV2 or 2PV3, 2PV4, also connected via switch 2PV to the separate excitation winding NVO2 or NVR circuit. Thus, generator G2 field control is switched to the port GED control station. Consequently, [90] diesel generator DG2 speed control also must be switched to this same station. To do so (Figure 3.25), its electropneumatic rectifiers 1T2, 2T2 are connected by selector switch contacts 1I63-1I65 via station switches 2PP to the port main propulsion motor control stations, to which diesel generator DG2 field control also has been connected.

Constant current GEU excitation circuits. A car ferry GEU excitation circuit controlled by a constant current system also is a characteristic excitation

system with a three-winding exciter. Regulation of main propulsion motors operating in this system is more complex than are conventional systems because there is a requirement simultaneously to regulate generator and main propulsion motor excitation so that the main circuit current remains constant.

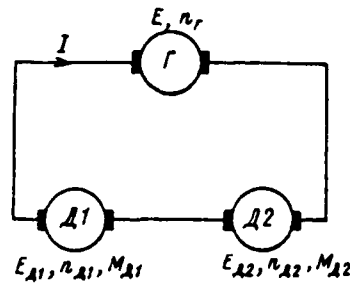


Figure 3.26. Skeleton Diagram of Generator and Main Propulsion Motor Armature Connection in a Constant Current System.

To refine what has been stated above, we will examine the circuit in Figure 3.26, in which generator G feeds two series-connected main propulsion motors D1 and D2. Given this method of connecting machinery and a conventional electric propulsion circuit, it is impossible individually to regulate the rotational speed of main propulsion motors and their individual reversal. A constant current system allows this.

We will introduce the following designations:

- $E$  -- generator emf;
- $I$  -- current in the main circuit;
- $E_{A1}, E_{A2}$  -- main propulsion motor D1 and D2 emf;
- $c, c_1, k$  -- constant values;
- $n_{A1}, n_{A2}$  -- main propulsion motor D1 and D2 rotational speed;
- $\Phi_{A1}, \Phi_{A2}$  -- main propulsion motor D1 and D2 magnetic flux;
- $M_{A1}, M_{A2}$  -- main propulsion motor D1 and D2 torque.

The following relationships hold for main propulsion motors [24]:

$$\left. \begin{aligned} E_{A1} &= cn_{A1}\Phi_{A1}; \\ E_{A2} &= cn_{A2}\Phi_{A2}; \\ M_{A1} &= c_1I\Phi_{A1}; \\ M_{A2} &= c_1I\Phi_{A2}. \end{aligned} \right\} \quad (3.3)$$

On the other hand, when the main propulsion motor runs the screw, the relationship between moment and rotational speed can be represented by expressions

$$M_{A1} = kn_{A1}^2; \quad M_{A2} = kn_{A2}^2. \quad (3.4)$$

Accepting in expressions (3.3) that  $I = \text{const}$  (regulation must occur [91] given constant voltage) and solving equations (3.3) and (3.4) jointly, one can determine that, for example, given a change in main propulsion motor D2 magnetic flux, the relationship of its emf to the magnetic flux can take the form

$$E_{A2} = c \sqrt{\frac{c_1 I}{k}} \sqrt{\Phi_{A2}} \Phi_{A2} = c \sqrt{\frac{c_1 I}{k}} \Phi_{A2}^{3/2}.$$

Having designated  $c \sqrt{\frac{c_1 I}{k}} = A$  (constant value), we get

$$E = A\Phi^{3/2}. \quad (3.5)$$

For a circuit (Figure 3.26) with an equation of emf and voltages, it will be

$$E = E_{A1} + E_{A2} + \sum IR. \quad (3.6)$$

In order that equality (3.6) remains unchanged given a change in magnetic flux,  $\Phi_{A2}$ , for instance, and consequently, also given a change in emf  $E_{A2}$ , there is a requirement to change emf  $E$  to that value at which emf  $E_{A2}$  changed, i. e., given a change in the latter to  $\Delta E_{A2}$ , we have

$$E - \Delta E_{A2} = E_{A1} + E_{A2} - \Delta E_{A2} + \sum IR.$$

In this case, current  $I$  remains unchanged, while  $E$  must be decreased to value  $\Delta E_{A2}$  through the corresponding decrease in generator magnetic flux  $\Phi$ .

In this circuit, as opposed to conventional representations, when an electric motor's magnetic flux decreases, its rotational speed does not increase. Instead, the speed drops because, given constant current  $I$  in the main circuit, based on expression (3.3) torque will decrease in proportion to the  $\Phi_{A2}$  decrease, for D2 for example, while rotational speed  $n_{A2}$  will change in proportion to  $\Phi_{A2}$ .

In the event of a  $E_{a3}$  decrease given constant  $E$ , main propulsion motor D1 may overload since, being under great voltage, it will increase rotational speed. Consequently, the resistance moment on its shaft and power delivered will increase according to the screw characteristic.

The excitation circuit of a GEU controlled by a constant current system and installed on a shuttle car ferry is depicted in Figure 3.27. The main current circuit for this electrical propulsion plant was examined in Chapter 2 (see Figure 2.17).

The ferry has two propellers and two rudders, one each at each extremity. This ferry's electrical propulsion plant consists of one 50-50 diesel generator with a 750 kW, 460 V dc generator and two 300 kW, 230 V main propulsion motors. A 110 kW, 230 V dc auxiliary generator is installed on the same shaft as the main generator.

Three-winding exciter V1 and one stand-by exciter V2 are envisaged for generator excitation. The generator field winding is connected to the exciter armatures via field switch contacts PV5-PV8. Self-excitation windings SV01 [93] and SV02 are connected to the terminals of their exciter V1 and V2 armatures. Standardizing resistors SU are cut into each winding's circuit.

Main propulsion motor field windings OVD1 and OVD2 are connected to the 220 V dc network via potentiometric regulators PUD1 and PUD2, station switches (PP9-PP24), and propulsion motor field contactor 1KVD, 2KVD contacts. Standardizing SU and additional SD resistors are connected in series to each main propulsion motor's field winding. Maximum power contactor KMM n. z. contacts are connected in parallel to resistor SD. They close and shunt resistor SD after the auxiliary generator circuit-breaker installed on the main diesel generator shaft cuts in.

Main propulsion motor fluxes are boosted, the speed of their rotation is reduced, and demand decreases in this manner.

Exciter separate excitation windings NV01 and NV02 are connected via field switch contacts PV9-PV12 and station switch contacts PP25-PP28 with two adjusting

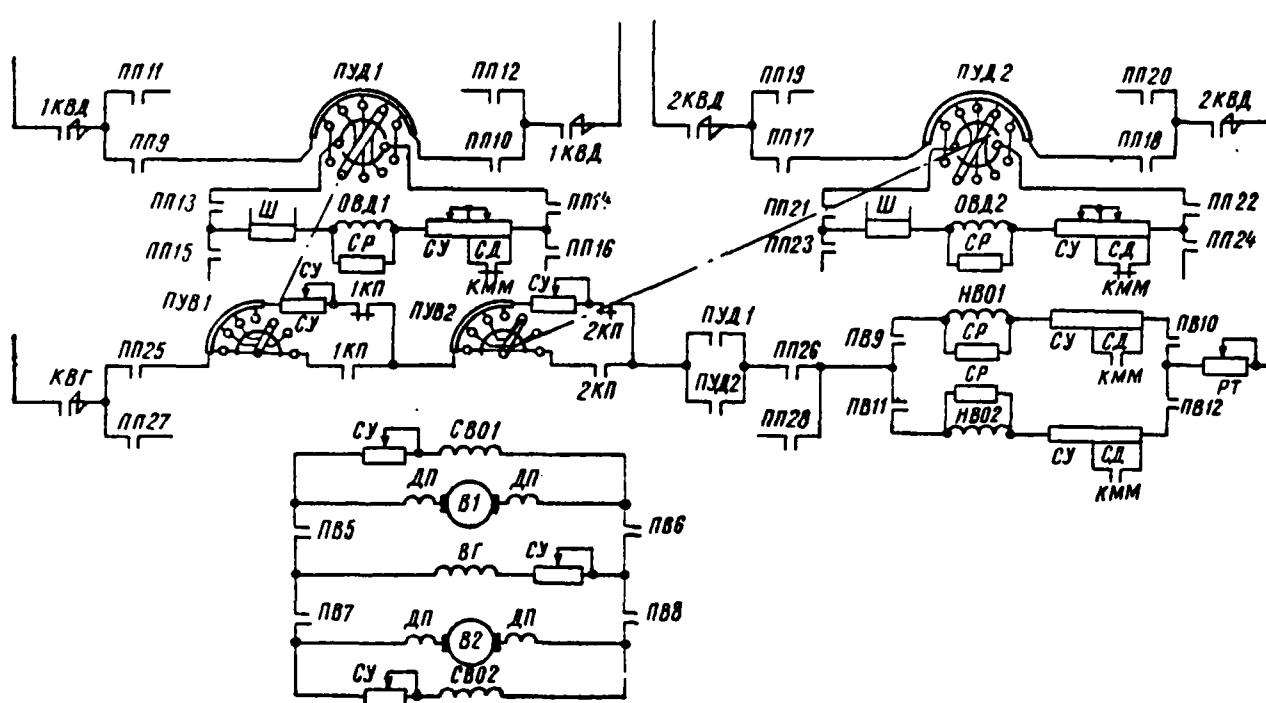


Figure 3.27. Excitation Circuit of an Electrical Propulsion Plant Operating in a Constant Current System.

resistors PUV1 and PUV2 and to the dc network by station contacts PU open in the zero position and via contactor contact KVG. Discharge resistors SR are connected in parallel with each exciter's separate field windings, while standardizing resistors SU are connected with them in series. Resistors SD are shunted by maximum power contactor contacts KMM when the auxiliary generator circuit-breaker is cut in. Contactor KMM contacts open when the auxiliary generator circuit-breaker is cut out and additional resistor SD is introduced into the field winding NV01 and NV02 circuit, which constrains generator flux, its voltage, and power delivered.

Potentiometric regulator PUD1 and adjusting resistor PUV1 are regulated by one lever simultaneously. PUD2 and PUV2 are regulated in exactly the same way. Generator and main propulsion motor excitation changes in accordance with expressions (3.3)-(3.6). Main propulsion motors are reversed by control station levers.

When control stations are in the zero position, their contacts in delay relay circuits open, which, in turn, open their contactor coil circuit n. z. contacts with a time delay. These shunt the main propulsion motor armatures, preventing these contactors from tripping when main propulsion motors are reversed. N. r. [normally open] and n. z. intermediate contactor 1KP and 2KP blocking contacts also are cut into the exciter separate excitation winding circuit. Constant current circuits similar to that shown in Figure 3.27 can be used when there are many generators and main propulsion motors.

Longitudinal field amplidynes (EMU) are used as exciters and are automated governors.

Automatic regulation of main generator and main propulsion motor exciter magnetic fluxes is envisaged in excitation circuits for GEU with two-stage EMU. This allows maintenance of a GEU electric power constancy in vessel main operating modes. GEU main circuit current and exciter voltage feedbacks are used for this purpose.

The type of static characteristics of GEU with longitudinal field EMU, given automatic regulation of main machinery field magnetic fluxes, is similar to that depicted in Figure 3.8. The GED mechanical characteristic is artificial in section AB as a result of feedback action.

We can familiarize ourselves more fully with the operation of an excitation circuit for a GEU with a two-stage longitudinal field EMU by examining, for instance, the operating principle of the GEU field circuits of "Amguema" class ships and the icebreaker "Lenin."

Ice navigation transport vessel GEU excitation circuits. An equivalent schematic diagram of one loop of the "Amguema" class vessel GEU is shown in Figure 3.28.

Master windings OZ EMUG are connected to the voltage of generator GPN via a potentiometric control station resistor. Rotation of lever PU changes the amount of voltage picked off potentiometer PU. Here, the winding OZ EMUG signal polarity is constant, while the amount changes at each PU position. The requisite amount of master n. s. OZ in the final PU position depending on GEU operating mode is set by additional resistors (not shown in Figure 3.28), connected by means of selector switches when the circuit is assembled.

The amount and polarity of the signal supplied by master winding EMUD change depending on the PU position. GED exciter polarity changes when the OZ signal polarity changes and, consequently, the direction of GED exciter flux changes. The GED reversal is accomplished in this manner.



in the OT circuit in order to improve circuit operation in transient modes. Main current bus bars are used as the primary windings of these transformers.

Voltage feedback windings OSN of exciters EMUG and EMUD improve EMU static characteristics, decreasing the magnetization curve hysteresis loop. As a result, conditions are created for more stable exciter operation. Their magnetizing [96] force is opposite generator exciter EMUG OZ n. s.

Stabilizing windings OS are connected to the diagonal of the bridge connected to EMU output voltage. Bridge arms are formed by standardizing resistors R1-R3 and stabilizing choke windings 1ST-4ST. The bridge is balanced in static modes: the stabilizing winding operates only in transient modes when bridge balance is disrupted due to appearance of an increased voltage drop in the stabilizing choke's inductance. The stabilizing winding's magnetization force either increases or weakens the OZ n. s. action, facilitating main circuit current stabilization.

Self-excitation windings SVO operate in agreement with the EMU second-stage amplifying winding. The greatest EMU gain is obtained through tuning the self-excitation circuit to the critical value. Therefore, the self-excitation circuit's resistance changes in relationship to a change in EMU load. Standardizing resistors (not shown in Figure 3.28) are used to tune the SVO circuit resistance.

Bucking winding RO EMUD is connected via a comparison potentiometer and rectifiers 2Vp and 3Vp to the difference of EMUG and GPN voltages, of tachogenerator TG and GPN, as well as directly to EMUG via rectifiers 1Vp and 4Vp. This winding's magnetization force is directed towards OZ n. s. The master winding operates when GED rotational speed exceeds the established value, when generator exciter polarity changes during a reversal, and when EMUG voltage exceeds the established level.

The GED is controlled by means of potentiometric rheostats built into the PU, with the current in the EMU exciter OZ regulated here. GED generator and armature excitation changes depending on the change of current in OZ at different control station settings.

GED excitation changes from zero to nominal from the first through ninth PU setting.

Main generator voltage changes from zero to nominal from the first through seventeenth PU setting. Generator voltage change occurs by changing diesel generator excitation and rotational speed.

Regulation of diesel generator rotational speed from 460 to 810 rpm is accomplished by electropneumatic diesel rotational speed regulation rectifiers, beginning with the ninth through seventeenth PU settings. A change in GED field current direction causes a change in propellor direction of rotation. EMU play the role of current and power regulators simultaneously.

Current feedback winding OT n. s. changes when the main circuit current changes from the assigned value. As a result, EMU excitation and generator [97] current will decrease or increase in order to bring the main circuit current back to its previous level.

Automatic regulation of GEU power constancy is accomplished by a power governor operating on the principle of maintaining constancy of main circuit current and generator voltage through regulation of GED magnetic flux. A change in main circuit current means a change in EMUG voltage, which is compared with the voltage of comparison potentiometer SPS setting.

GED speed increases when the load on the propellor decreases (transfer to the movement in open water characteristic, exposure of the propellor, and so on). Main circuit current is determined by generator voltage and GED counter emf. Consequently, main circuit current decreases when GED speed increases (given the previous magnetic flux). This will lead to a decrease in EMUG current feedback winding n. s. and, therefore, to an increase in control winding resultant magnetization force. Therefore, EMUG voltage increases. If EMUG output voltage is greater than the comparison voltage, current proportional to the difference of EMUG and comparison potentiometer setting voltages will flow through the OZ EMUD winding. As a result, EMUD voltage and GED magnetic flux decrease. In this connection, GED counter emf will decrease and main circuit current will increase to the assigned level. The current increase will lead to a slight reduction in generator EMU voltage due to intensification of current feedback winding OT action and generator voltage will be set in accordance with the new operating mode.

The new mode (given a smaller load) is characterized by greater speed, less GED magnetic flux, slightly less current in the main circuit, and increased generator voltage. Thus, joint action of generator and GED exciters provides for GED operation, given constant nominal power in the range of propellor characteristics from moored operations to movement in open water, with a slight regulation error.

Current direction in OZ EMUD changes when the PU moves from the "ahead" to the "astern" position. GED magnetic flux decreases to zero and increases in the opposite direction. The GED will rotate in the former direction, operating in the generator mode, as a result of vessel inertia. GED counter emf changes sign and acts in accordance with generator voltage. Main circuit current strives towards a radical increase. EMUG voltage decreases and GED speed is decreased due to the effect of current winding OT. This corresponds to the countercurrent flow braking mode. GED braking moment is determined by the decrease in magnetic flux and increasing current.

Winding OT reverses the magnetization of EMUG, the value of reverse voltage of which depends on the value of the main circuit current. The faster the GED counter emf drops and increases in the opposite direction, the more current [98] will flow in the main circuit and the faster the EMUG magnetization is reversed.

Generator field circuit self-induction will inhibit a rapid change in generator polarity, but the great EMUG reverse voltage will reverse the magnetization of the generator all the same. The generator changes to the motor mode and supplies kinetic energy stored in the system (after loss is deducted) to the diesel, which may cause an intolerable acceleration. There is a requirement to delay the GED counter emf change process, as well as to decrease its excitation, to constrain GEU energy recuperation.

EMUG reverse voltage is fed to regulating winding RO EMUD via rectifiers 1Vp and 4Vp for this purpose; RO n. s. arising here is opposed to OZ EMUD n. s. This leads to a decrease in resultant n. s. and, consequently, to a decrease in GED magnetic flux and counter emf. Main circuit current is constrained and GED braking occurs due to mechanical losses in it and in the diesel, as well as electrical losses in the armature circuit and the generator. GED speed gradually

drops. GED counter emf and main circuit current decrease along with it. Winding OT action decreases and EMUG changes polarity. After GED speed drops to zero, its acceleration in the opposite direction begins.

Icebreaker "Lenin" GEU excitation circuit. An equivalent schematic diagram of one loop of the icebreaker "Lenin" GEU is depicted in Figure 3.29. It contains designation of all basic power and protection regulation nodes. Powerful two-stage longitudinal field EMU analogous to the amplifiers on "Amguema" class vessels are used as main machinery exciters.

Master winding OU1 EMUG is connected to control station PU synchro SUM voltage via power limitation switch POM and rectifier 1Vp. SUM is used as a rotating transformer. Synchro output voltage changes when lever PU is moved, which leads to a change in current to OU1. The direction of OU1 EMUG n. s. action is constant and does not depend on lever PU position, the value changing only depending on the synchro turning angle. Stabilizing transformer 3ST secondary winding, whose primary winding is connected to EMUG voltage, is connected in series to the OU1 circuit to reduce the main current rate of growth in transient modes, with main current vanishing feedback also introduced by means of a magnetic amplifier.

Master winding OU1 EMUD is connected to constant voltage generator GPN voltage, has a constant magnetization force value, which changes direction with the aid of contactors KRV and KRN when the motor reverses. Stabilizing transformer 4ST secondary winding, whose primary winding is connected to EMUD voltage, is connected in series to OU1 EMUD to reduce the rate of motor magnetic flux drop.

Generator voltage increases during rapid movement of lever PU from the [99] full movement ahead to the full movement astern position after lever PU passes through zero and OU1 EMUD reversal. GED flux decreases, which can lead to an intolerable excess of main circuit current in a transient mode.

The OU4 EMUG current feedback winding is connected to the voltage drop in windings DP and KO GED. The OU4 magnetizing force is proportional to main circuit current and acts opposite to OU1 n. s., which makes it possible to obtain a main generator artificial characteristic with an electric power constraint, as well as to constrain GED mooring moment when the propellor locks.



8.5 seconds (for an average GED), delays the rise in EMUG voltage, while relay RPr contact in the magnetizing winding SU3 EMUD circuit during reversal will maintain winding SU3 open for several seconds. Therefore, GED flux during reversal mainly changes under the effect of winding OU1 EMUD.

Power limitation switch PQM has six functional positions, each limiting turbogenerator power to 10, 20, 30, 50, 70, and 100%, respectively (power limitation percentage is computed from the ratio of total power of functioning turbogenerators). Resistances limiting EMUG and generator voltage and, consequently, turbogenerator power as well, are introduced simultaneously with selection of the corresponding power in EMUG and generator master winding circuits.

### § 3.5 Excitation Circuits with Transverse Field Amplidynes

Excitation circuits with transverse field amplidynes were used widely in GEU. The special features of these field circuits will become clear from the circuits examined below.

The simplest schematic for a dc GEU using EMU as generator exciter, given a constant main propulsion motor field magnetic flux ( $\Phi_a = \text{const}$ ) is depicted in Figure 3.30.

High-speed systems and the probability of overcontrol arising as a result generates the necessity for including stabilizers in the circuit.

EMU, or generator exciter, power is selected based on the power required to excite a generator (generators), with a reserve to insure voltage boosting. Nominal EMU voltage is that exceeding generator nominal field voltage by a factor of 2-3 in order to increase the rate of generator magnetic flux growth.

Voltage from a stand-by control station is supplied to EMU master winding OZVG. This winding's magnetizing force creates the basic magnetic flux of the requisite direction. [101]

The magnetizing force of current winding OTVG is opposed to OZVG n. s. The relationship of the n. s. of these windings is such that, given a nominal

mode with nominal main circuit current  $I_{\text{ном}}$ , total EMU n. s. creates nominal magnetic flux and, correspondingly, nominal field current  $i_{\text{с.г.ном}}$  and nominal voltage  $U_{\text{г.ном}}$ . In several cases, there are no stabilizing windings.

Current winding n. s.  $F_{\text{о.т.в.г}}$  reverses EMU magnetization when main circuit current reaches the value of the mooring current. Generator voltage drops to a value equal to the voltage drop in the network and in the main propulsion motor armature, thanks to which the propulsion motor stops. The rotational speed of an idling propulsion motor, corresponding to the propeller loss mode (or of all blades at once) is limited by the generator's natural external characteristic.

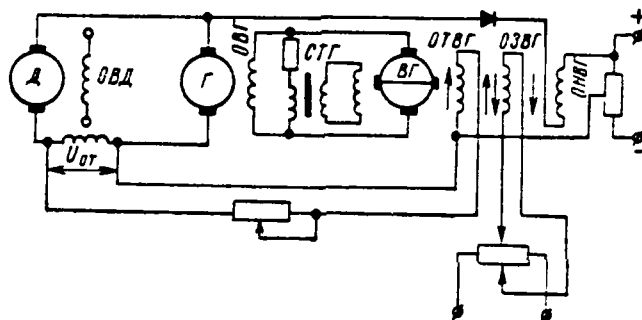


Figure 3.30. Schematic of a GEU with an EMU used as generator exciter (given that  $\Phi_{\text{д}} = \text{const}$ ).

The following must be borne in mind when constructing generator internal and external characteristics: master winding n. s.  $F_{\text{о.з.в.г}}$  (control winding n. s. must be selected beforehand) is selected with a significant reserve to provide requisite boosting and high speed. In addition, EMU must operate in the rectilinear portion of the idling characteristic, which provides more stable system operation during transient processes. In dc GEU, master and current winding n. s.,  $F_{\text{о.з.в.г}}$  and  $F_{\text{о.т.в.г}}$ , respectively, are determined by mooring current  $I_{\text{сг}}$ , which follows from Figure 3.31, in which main circuit current values lie on the Y-axis, while EMU n. s. lies in the X-axis.

Since  $F_{\text{о.з.в.г}}$  and  $F_{\text{о.т.в.г}}$  lie along one side of the Y-axis, then resultant  $F_{\text{рез.в.г}} = F_{\text{о.з.в.г}} - F_{\text{о.т.в.г}}$ .



The requirement to retain current and generator voltage constancy and, correspondingly, primary motor power constancy is met by regulating main propulsion motor magnetic flux. This is done as a function of armature circuit current and, correspondingly, as a function of the resistance moment on the screw when the circuit is used either with tight negative feedback or with the same connection, but with a cut-off.

Regulation by means of main circuit current in GEU circuits can occur either directly from a current deviation (deviation of the regulating value) or by a perturbation causing a current deviation in the armature circuit. In the former case, information sensors provide information on the regulating value [103] deviation (armature circuit current); in the latter, the systems receives information from the sensor on changes in the resistance moment on the screw and a signal proportional to the deviation of this perturbation is introduced into the regulation system. Shunts, dc transformers, and Hall sensors are used as information sensors in the former, while electromagnetic sensors, Hall sensors, and moment inductance sensors are used in the latter case.

A possible circuit with both generator and main propulsion motor regulation by means of fluxes is shown in Figure 3.33.

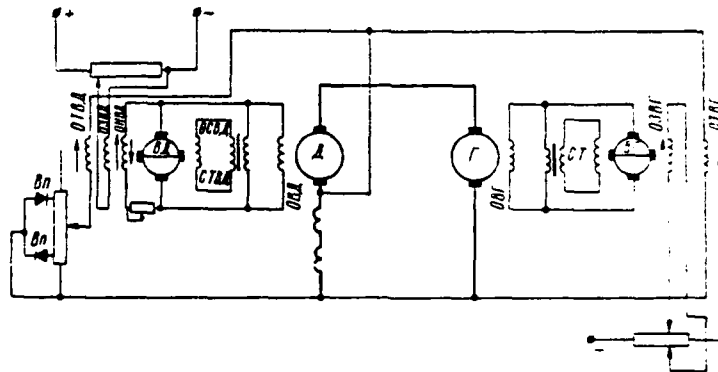


Figure 3.33. Automatic Regulation Circuit with Main Circuit Current Cut-Off.

Regulation of GED rotational speed and its reversal are accomplished by a change in generator exciter VG master winding OZVG current. GED exciter VD has four control windings: master OZVD, voltage feedback winding ONVD, current

winding OTVD connected via the current cut-off circuit, and stabilizing winding OSVD. Given currents  $0 < I < I_{\text{HOM}}$ , resultant n. s. will equal the difference in master winding OZVD and voltage winding ONVD n. s.

When  $I > I_{\text{HOM}}$ , winding OTVD goes into action and its n. s. combines with that of winding OZVD, resulting in a VD voltage and a GED flux increase. Here, current winding n. s. increases the resultant n. s. to a greater degree than voltage winding ONVD n. s. decreases it.

The circuit operates in the following way when main circuit current values exceed the nominal: given a nominal main circuit current value, generator voltage and propulsion motor flux are nominal. Armature circuit current increases and GED rotational speed decreases somewhat when the resistance moment on the screw increases. An increase in main circuit current causes an increase in GED flux, which leads to a reduction in main circuit current and GED rotational speed. [104] GED flux grows until main circuit current drops to the nominal value.

In the GEU systems we are examining, magnetic flux, which is a function of load, intensifies when the resistance moment on the screw rises. A propulsion motor's electromagnetic moment rises in proportion to the increase in magnetic flux, while rotational speed decreases accordingly. Motor counter emf remains unchanged, so main circuit current and voltage loss consequently do not change. The values of the moments, propulsion motor rotational speed, and magnetic fluxes for two modes (I and II) are determined from relationships

$$M_I n_I = M_{II} n_{II} = M_{\text{HOM}} n_{\text{HOM}} = \text{const};$$

$$n_I \Phi_I = n_{II} \Phi_{II},$$

from whence

$$\Phi_{II} = \Phi_I \frac{M_{II}}{M_I}.$$

A transverse field EMU was used as exciter in a series of "Lena" class [105] dry cargo vessels for active ice navigation and as pilot exciters in a series of "Ledokol-1" class port icebreakers.

A schematic of a single-loop GEU on "Lena" class vessels is depicted in

Figure 3.34. Propulsion motor magnetic flux is reduced simultaneously in the GEU on these vessels to increase propulsion motor efficiency when rotational speed is reduced, resulting in a decrease in field circuit losses. Main circuit current corresponding to different rotational speeds has a greater value than when propulsion motor flux is constant, resulting in main circuit current losses being diminished more slowly. A ratio with a higher efficiency at all propulsion motor rotational speeds is established between the losses in both circuits.

### § 3.6 Excitation and Control Circuits with Power Magnetic Amplifiers

Excitation circuits with magnetic amplifiers as exciters. Power magnetic amplifiers (SMU) are used as main propulsion motor and main generator pilot exciters in dc GEU field and control circuits.

SMU are not as good as semiconductor amplifiers as far as size and high speed are concerned, but have several significant advantages: they make it possible to add several unconnected control signals, are very stable and reliable, are simple to maintain, easy to adjust, have sufficient characteristic stability, resist vibrations, and are not sensitive to overloads and the effects of the environment.

The relative ease of repair of SMU used aboard ship by shipboard resources during a cruise also should be underscored. Domestic industry has assimilated manufacture of UM-3P three-phase self-saturated SMU, which meet the requirements for use directly as main propulsion motor exciters. This SUM series is intended for a standard frequency of 50 Hz, which allows them to be fed directly from the shipboard network.

Screw reversal can be accomplished in field circuits using SMU by reversing the field current either of the main propulsion motor or of the main generators.

A second method has greater advantages. The idea is that an SMU has so-called idling current, which is differentiated from zero given a non-reversing circuit. Thus, for the UM-3P, with a rise in power from 0.51 to 29.2 kVA, amplifier minimal current lies in the  $0,064/I_{\text{nom}}$  to  $0,33/I_{\text{nom}}$  range ( $I_{\text{nom}}$  — SMU nominal load current). Therefore, significant current will flow in the main circuit in the [106]

reversal variant using GED field current when the GEU circuit is ready to operate and the control station is in the zero position. This is due to the main generator bias with SMU idling current. Thus, the reversing method using main generator field current is preferable.

Generator voltage can be reversed by a reversing contact-free circuit consisting of two magnetic amplifiers. This type of circuit provides a smooth change in output current with a change in control current from  $+i_y$  to  $-i_y$ . Use of a single-contact circuit requires connection of reversing contacts to the field circuit. At the moment the control current passes through value  $i_y = 0$  and switching of reversing contacts in the field circuit, there will be a current inrush, the minimal value of which equals twice the magnetic amplifier idling current. Magnetic amplifier push-pull circuits usually are formed through differential (counter) connection of two identical magnetic amplifiers. SMU control windings are connected in anti-series here.

Field windings are connected to magnetic amplifiers using two circuits: differential circuit (Figure 3.35a) based upon subtraction of magnetizing forces. One of two field windings located on the machine's main poles is connected at the output of each single-pulse magnetic amplifier. The windings have opposed magnetic poles. The resultant n. s. will be proportional to the difference at amplifier output. Resultant n. s. equals zero when the control signal is zero. Control windings are connected in series, but in a way that an increase in current in the windings will cause an increase in load current at the output of one MU and a decrease at the other's output;

bridge circuit (Figure 3.35b), based on subtraction of currents. Two field subwindings in the circuit, rather than two ballast resistors, form the bridge, two opposed cusps of which connected to the output of one MU, while the other two are connected to the output of the other MU. The amount of resistance [107] of each ballast resistor is taken as being equal to the amount of resistance of one field subwinding since only given this equality is bridge balance possible. Identical current  $i_{\text{ном}} = 0,5(i_1 - i_2)$ , flows through both windings, directly creating the requisite field intensity.

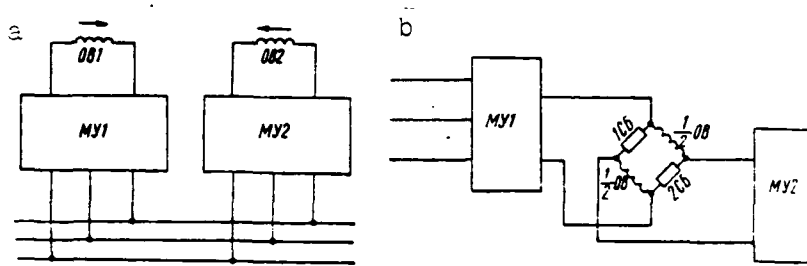


Figure 3.35. Magnetic Amplifier Push-Pull Circuits: a--Differential circuit; b--Bridge circuit.

Both circuits have approximately identical characteristics. A push-pull bridge circuit having a lesser time constant is the most applicable circuit for generator excitation systems.

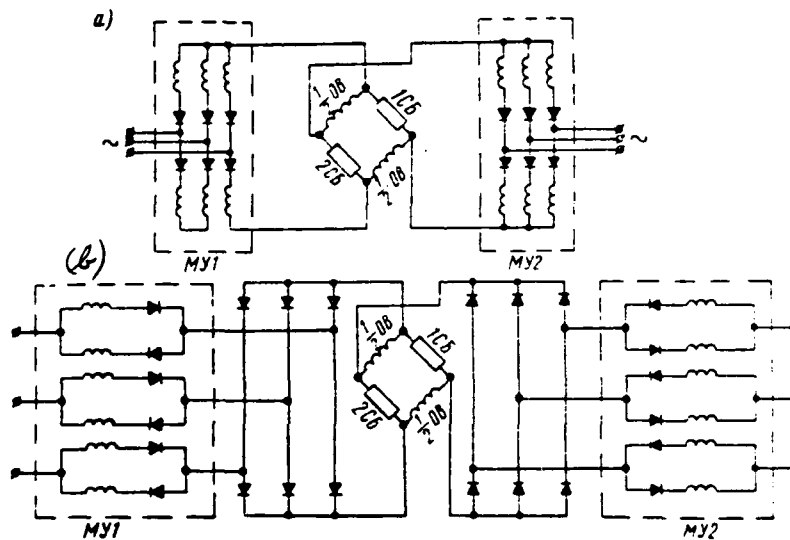


Figure 3.36. Three-Phase Reversing Circuits with Magnetic Amplifiers: a--with common load and self-saturation rectifiers; b--With an individual load rectifying bridge.

The following two six-element circuits are of interest from among the possible three-phase reversing circuits with MU control of generator magnetic flux: with common load and self-saturation rectifiers (Figure 3.36a) and with an individual load rectifying bridge (Figure 3.36b), in which operating windings and self-saturation rectifiers are connected to the feed network phases.

The advantages of the latter over the former when running a resistive-inductive load include higher current, voltage, and power gain values in static modes.

A major drawback of both circuits when main generator field windings are connected directly at a push-pull MU output is the requirement for ballast resistors, the expending power in which is approximately equal to the power the generator field windings demand.

Excitation circuits with magnetic amplifiers as pilot exciters. Magnetic [108] amplifiers are used in GEU circuits also as pilot exciters running machinery exciter field windings. In this event, power less by a factor of  $k$  than in the first case ( $k$  = exciter power gain) is consumed in the ballast resistors.

Drawbacks of circuits using MU as pilot exciters include presence in the regulation system of rotating machinery with collector devices and system speed reduction with the appearance of an additional inertial link (exciter field winding). We will examine below circuit solutions for GEU using MU as pilot exciters and excitors.

The GEU aboard the icebreakers "Leningrad" and "Moskva" are an example of such systems. A schematic of one GEU loop on the icebreaker "Moskva" is shown in Figure 3.37.

The main propulsion motor has two field windings: main OVDD and auxiliary [109] OVDD fed by additional exciter VDD. Field winding VDD is fed via a cascade of magnetic amplifiers whose input signal is main circuit current.

Additional exciter field winding OVVDD is connected to the output of main magnetic amplifier MUZ (Figure 3.38), which has intrinsic feedback and two control windings. One control winding is bias winding OSM and provides minimal load

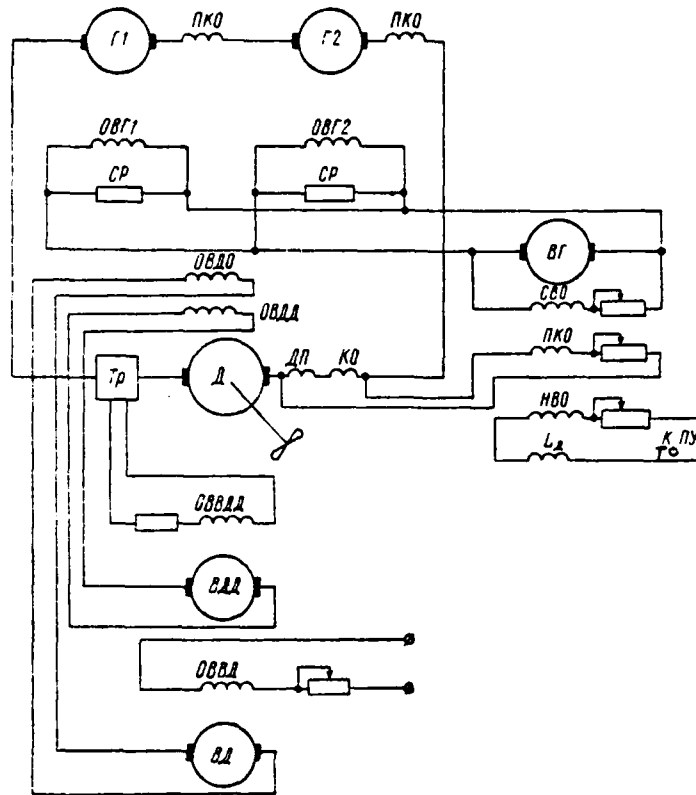


Figure 3.37. Schematic of One GEU Loop on the Icebreaker "Moskva."

current to MUZ when there is no current in the amplifier input control winding. Amplifier input winding OU is connected at the output of intermediate magnetic amplifier MU2.

Intermediate magnetic amplifier MU2 has intrinsic feedback and two control windings, one of which -- a stabilizing winding -- via a resistor and capacitance is connected to the MU3 output. It accomplishes MU3 output voltage vanishing feedback and provides dynamic stability for the automatic control system. Another amplifier MU2 control winding -- an input winding -- is connected to the difference of the standard voltage and voltage proportional to main circuit current.

The circuit operates as follows. Until the main circuit current exceeds the assigned value, the comparison system rules out the possibility of effect

on magnetic amplifiers. If the main current exceeds this value, then voltage is picked off the comparison circuit output. Intensified by the magnetic amplifiers, it is fed to the additional exciter field windings. This causes an increase in propulsion motor excitation, a decrease in its speed, an increase in torque, and a decrease in main circuit current.

The dc measuring transformer is two interleaved steel cores with windings placed on them located in a magnetic field creating main current. The transformer secondary circuit windings are connected in series and connected to ac voltage. When there is no current in the main circuit, their cores are not magnetized and winding inductive impedance is very high. In this case, very low idling current flows through the ac circuit. This current can be disregarded since this current can be made sufficiently low through corresponding selection of core material and its design.

The presence of idling current in this circuit is of no significance since elements connected to this circuit are intended for operation in proximity to points corresponding to nominal main circuit current and higher. Core magnetization increases due to an increase in main circuit current and winding inductive impedance decreases. Therefore, current in the measuring circuit rises with a rise in main circuit current.

It should be noted that a magnetic amplifier -- a regulator -- does not [111] react to main circuit current direction and the amount of current in the second loop depends only on the amount of main current. This circumstance greatly simplifies regulator design. Three protection relays and a magnetic amplifier input circuit are connected in series to the current transformer measuring circuit. The input circuit consists of transformer Tr1, rectifier Vp1, and blocking capacitor C1. Sensor rectified and filtered voltage is fed to resistor SD1.

Rectified and filtered network voltage also is fed to analogous resistor SD2. Both resistors are connected in such a way that voltage equal to the difference between standard voltage and that proportional to main circuit current is received at this circuit's output. Adjusting resistance in the standard voltage network makes it possible to establish a point of equilibrium given the requisite main circuit current value (usually nominal). The signal is fed

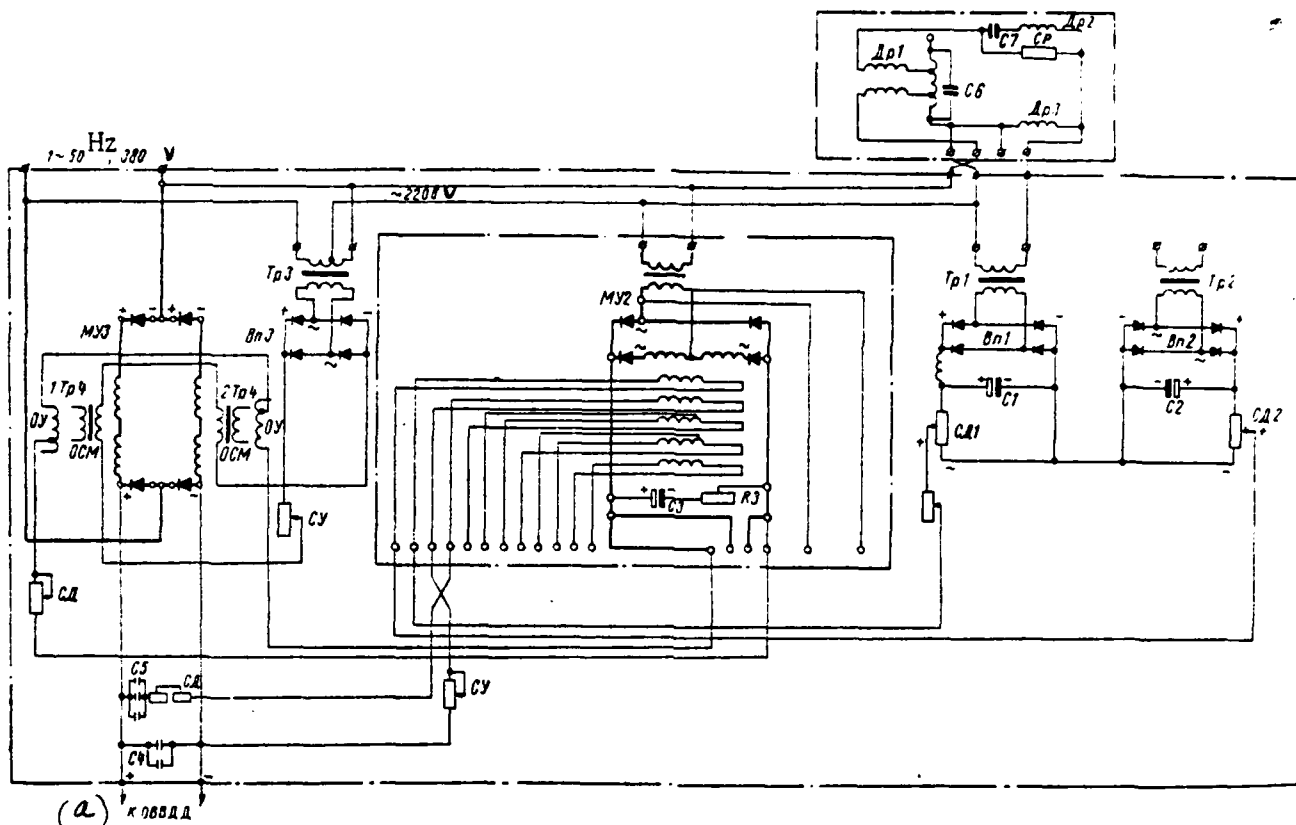


Figure 3.38. Schematic of Winding VVDD Feed. a--To OVVDD.

from the comparison circuit output to the input of the first magnetic amplifier MU2 cascade.

Positive (intrinsic) feedback, accomplished by connection of rectifiers in the ac winding, also is used to increase magnetic amplifier gain.

The signal amplified by the amplifier cascade first stage moves via filter consisting of R3C3 connected in parallel to the output and is fed to the input of the cascade's second stage. The cascade's second magnetic amplifier is built in a circuit identical to the first, the only difference being presence of bias winding OSM fed from individual transformer Tr3 with rectifier Vp3. This winding is needed to establish the operating point in the amplifier characteristic so that winding OVVDD current will equal zero given a zero signal.

Additional exciter field winding OVVD will serve as the load for the magnetic amplifier cascade's second stage. The output is shunted by rather large capacitor C4 required for rectified current pulsation smoothing.

Thus, the regulator -- the magnetic amplifier -- in an electrical propulsion plant circuit is used to boost main propulsion plant excitation given an increase in main circuit current, which will lead to a decrease in motor rotational speed and an increase in its torque. Automatic motor torque control improves propeller operating conditions when interacting with ice and insures that primary motors are protected against overloads to a known degree. The additional exciter field winding can be fed from constant voltage generator bus bars via a manually-controlled rheostat in the event the cascade of magnetic amplifiers breaks down.

A GEU automatic control circuit with a magnetic amplifier insures that a GED artificial mechanical characteristic is obtained (Figure 3.39). Power constancy is insured not only in the entire zone of screw characteristics [112] (from the moored characteristic to the movement in open water characteristic), but one considerably to the left of the moored characteristic as well.

Magnetic amplifiers used to measure main circuit current separate the high voltage circuit and the low voltage control circuit, thanks to which danger during maintenance is decreased. Here, the magnetic amplifier control current winding, electrically connected to high voltage, must be well insulated from other MU windings.

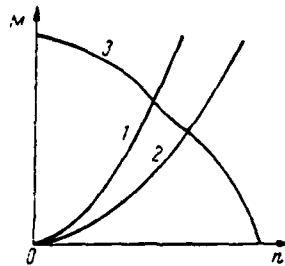


Figure 3.39. GEU Characteristics. 1--Moored characteristic; 2--Vessel movement in open water characteristic; 3--Artificial mechanical characteristic.

MU are used as main generator pilot exciters in the GEU aboard the icebreaker "Kiev." A structural diagram of an outboard GEU loop aboard "Kiev" is depicted in Figure 3.40. As opposed to the circuit on "Moskva" class icebreakers, several new elements have been introduced here to obtain dynamic characteristics providing normal GEU operation in the propellor interaction with ice mode.

As can be seen from the figure, generator field windings OVG1, OVG2 of one main current circuit are connected in parallel to the corresponding generator exciter VG.

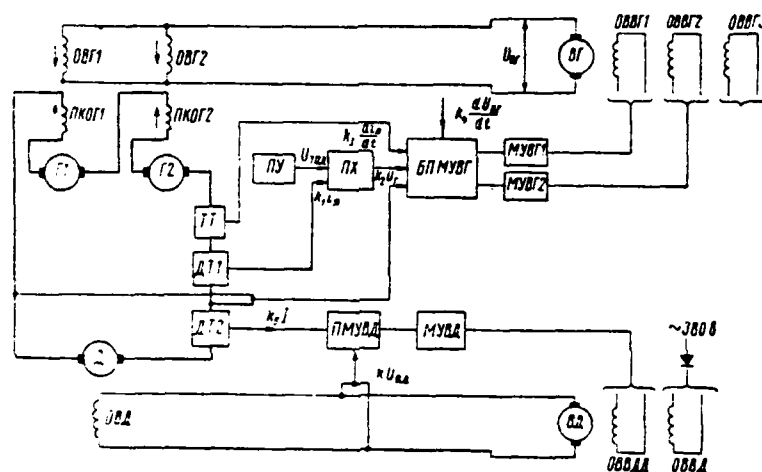


Figure 3.40. Structural Diagram of an Outboard GEU Loop on the Icebreaker "Kiev."

Generator exciter field windings OVVG1 and OVVG2 are fed by the corresponding governors with magnetic amplifiers connected by means of a push-pull circuit.

The structural diagram shows the main GEU control system connections. [113] Each field winding VG is fed by its own magnetic amplifier: OVVG1 from МУВГ1 and OVVG2 from МУВГ2. The input of these magnetic amplifiers is connected to the generator field intermediate magnetic amplifier block БПМУВГ, which adds the signals arriving from characteristics indicator PKh, from sensor TT of the derivative of current based on time  $(k_3 \frac{di_n}{dt})$ , from the main propulsion motor voltage sensor  $(k_2 U_r)$ , and signal  $k_4 \frac{dU_{n,r}}{dt}$ .

Characteristics indicator PKh adds the signals arriving from the control station ( $\dot{U}_{\text{сн}}$ ) and from current transducer DT1 in the main circuit ( $k_1 i_{\text{н}}$ ), and supplies a cumulative signal to the BPMUVG input.

Current transducer DT2 in the main circuit supplies signal  $k_5 I$  to an instrument containing main propulsion motor preliminary magnetic amplifier PMUVD. The signal is fed from the PMUVD output to the input of magnetic amplifier MUVD of main propulsion motor field current winding OVVD, which maintains virtually constant current in the main circuit when the resistance moment on the main propulsion motor shaft rises.

A third generator exciter field winding OVVG3 is included in the circuit only in the event of emergency electrical propulsion plant excitation. Emergency control serves to insure GEU operation in the event the magnetic amplifier-regulators break down. Field winding OVVG3 in this case is connected to the voltage drop at half of the propeller motor additional poles and current proportional to main circuit current flows through them. Winding OVVG3 is connected so that its magnetic flux is opposed to the magnetic fluxes of windings OVVG1 and OVVG2 and, in this case, accomplishes negative feedback through the main circuit current.

The remaining two field windings in an emergency are connected to the circuit as follows: winding OVVG1 is fed via a semiconductor full-wave rectifying bridge and contactors (for control current reversal) from a control station PU sensor and thus is the main field winding; winding OVVG3 is connected directly to exciter VG voltage and serves as a self-excitation winding.

As a result, the generator exciter operates like a three-winding electrical machinery exciter during propulsion plant emergency control.

The generator excitation system operates in the following manner during normal propulsion plant control. A control instruction in the form of master voltage  $U_{\text{сн}}$  to characteristics indicator PKh is issued with the aid of a rotating transformer from a control station PU (control stations are located in the wheel-house, top and after bridges, and maneuvering compartment).

A schematic of starboard loop control stations is presented in Figure [114] 3.41. Stations are fed from step-down transformer Tr1. One of the contactors PP1-PP4 is cut in depending on the location from which propulsion plant control occurs (from the wheelhouse, top bridge, after bridge, or maneuvering compartment).

Control stations PU1-PU4 are rotating transformers.

Voltage  $U_{3a2}$  phase and amount at rotating transformer output change depending on control station lever direction and angle of movement. This voltage is fed to characteristic indicator terminals 3, 4 (Figure 3.42), resulting in a flow of current in the transformer Tr3 winding.

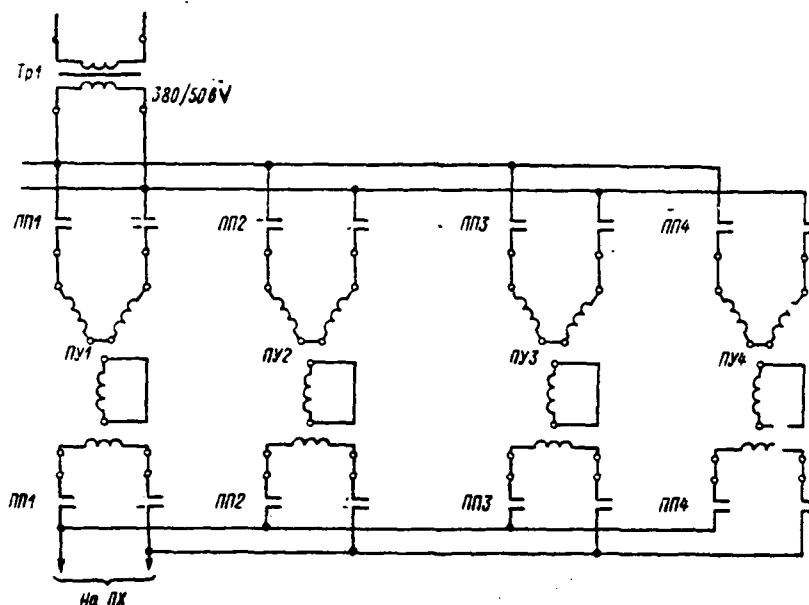


Figure 3.41. Schematic of the Starboard Loop Control Stations.

Diodes Vp5-Vp8 cut off the circuit if the rotating transformer is not set exactly in the zero position.

Reference voltage is supplied by means of transformer Tr2. As a result, a control signal, whose polarity depends on the direction of movement of the control station PU lever and whose amount depends on the amount of the rotating transformer armature turning angle, is supplied to the output of a circuit

consisting of a combination of transformers Tr2, Tr3, diodes Vp1-Vp4, and resistors R1-R4 (balancing capacitor C1 terminals).

Two control systems are envisaged for the icebreaker "Kiev" GEU: based on the principle of plant power constancy and on the principle of GED rotational speed constancy. Transfer from one system to another occurs by means of control system switch PSR, whose position in Figure 3.42 corresponds to a power con- [116] stancy system.

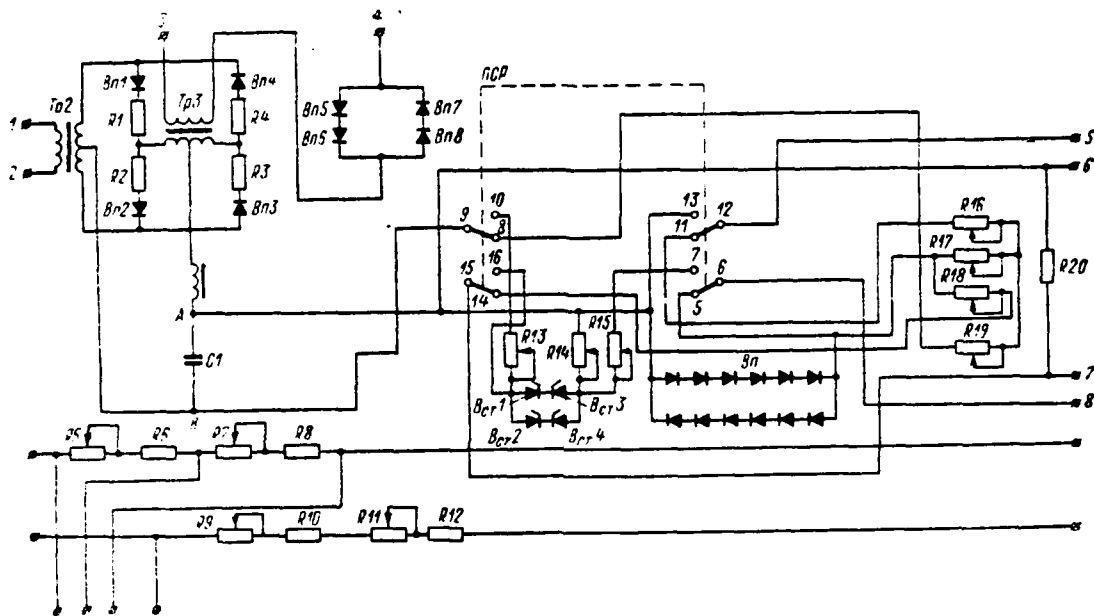


Figure 3.42. Schematic of the Characteristics Indicator.

A signal proportional to main circuit current is supplied to characteristics indicator terminals 5, 8 from the DT1 saturable reactor (see Figure 3.40). This signal's circuit is closed via resistors R16 and R17. The polarity of the voltage drop at resistor R20, stipulated by this signal, is opposite to the polarity of the control signal at capacitor C1 terminals. Thus, comparison of the control signal voltages and the voltage drop proportional to main circuit current takes place in characteristics indicator PKh given a PSR position corresponding to the power constancy system. The resultant signal is supplied to characteristics indicator output terminals 6, 7 via resistors R17-R19. Diodes Vp constrain the amount of the signal at the characteristics indicator output.

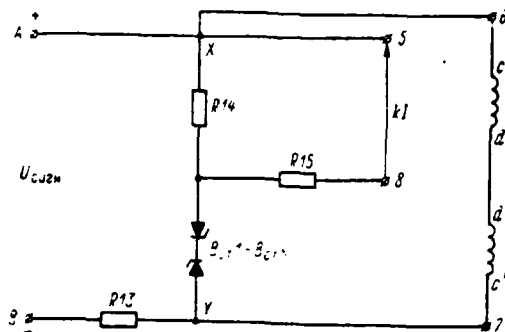


Figure 3.43. Schematic of a Control System Based on the GED Rotational Speed Constancy Principle.

Consequently, a system with negative main circuit current unity feedback with a constraint on the amount of resultant signal is used in this case.

A control system on the GED rotational speed constancy principle corresponds to the upper position of switch PSR. A schematic for this is shown separately in Figure 3.43. Control signal  $U_{cmfn}$  is supplied from the control station to capacitor C1 terminals AB (see Figure 3.42) and, via resistor R13, to control winding cd and c'd' of generator field intermediate magnetic amplifiers (PMU), which are connected in both control systems in the manner depicted in Figure 3.43 to characteristics indicator output terminals 6, 7.

Voltage proportional to the amount of main circuit current is supplied to terminals 5, 8 from the DT1 saturation choke (see Figure 3.40). Stabilizer diodes  $B_{c1}I-B_{c4}A$  (Figure 3.43) are closed and current does not flow in the circuit between points X and Y when the control station lever is turned from the zero position approximately to positions 10-15 (Figure 3.42). Therefore, even though signal kI does exist until these positions are reached, it plays no role [117] whatsoever. Voltage equal to the sum of voltage  $U_{cmfn}$  and the voltage drop at resistor R14, taking their signs into account, is applied to the terminals of stabilizer diodes  $B_{c1}I-B_{c4}A$ .

Stabilizer diode  $B_{c1}I-B_{c4}A$  voltage at the terminals will be set as equal to breakdown voltage (which corresponds to the amount of main circuit current,

equalling 3600 A) during further movement of the control station lever and stabilizer diodes  $B_{cr1}-B_{cr4}$  open, creating a circuit between points X and Y. After the stabilizer diodes open, generator exciter intermediate magnetic amplifier control windings turn out to be connected to the voltage drop at stabilizer diodes  $B_{cr1}-B_{cr4}$  and at resistor R14. This voltage remains virtually constant, in spite of a further change in control station lever position, due to a change in the voltage drop at resistor R13, since a circuit was created between points X and Y and current through resistor R13 increased as voltage  $U_{ctrl}$  changed, as well as because of a non-linear change in stabilizer diode  $B_{cr1}-B_{cr4}$  resistance. Thus, after the aforementioned stabilizer diodes arc, current in PMUVD control windings cd and c'd' (see Figure 3.40) remains virtually constant regardless of control station lever positions, to which the almost constant propulsion motor rotational speed corresponds.

The difference in the control systems (based on the power constancy and propulsion motor rotational speed constancy principles), from the circuit construction point of view, lies only in the characteristics indicator. Further explanation of the GEU excitation system applies both to control systems based on the power constancy principle, as well as to the GED rotational speed constancy principle.

Resistors R5-R12 (see Figure 3.42) located in the same block with the characteristics indicator change the value of the signal proportional to GED voltage and supplied to intermediate magnetic amplifier control windings cd and c'd' depending on the number of main generators connected to the loop.

The RC circuit consisting of a combination of capacitors and resistors R23-R27 (Figure 3.44) and also located in the same block with the characteristics indicator supplies a signal proportional to the first voltage derivative of exciter VG (see Figure 3.40) to BPMUVG (signal  $k_4 \frac{dU_{b.r}}{dt}$ ).

The signal goes from the characteristics indicator output to generator field intermediate magnetic amplifier block BPMUVG terminals. Two generator field intermediate magnetic amplifiers PMUVG (1) and PMUVG (2), the corresponding control windings of which are connected to each other in series, are included in it (see Figure 3.44). Transformer Tr4 and rectifier unit Vp9, feeding generator

exciter magnetic amplifier bias windings (final amplification stage) MUVG1 and MUVG2 (see Figure 3.40), also are included in PMUVG (1). Capacitor C2 smooths the voltage at the rectifier output.

Besides the signal from the characteristics indicator output, the following signals are supplied to the input, i. e. to the corresponding BPMUVG control windings (see Figure 3.40): 1) a signal proportional to the first main circuit current derivative ( $k_3 \frac{di_m}{dt}$ ), picked off transformer II; 2) a signal proportional to GED voltage ( $k_2 U_r$ ); 3) a signal proportional to the first generator exciter voltage derivative ( $k_1 \frac{dU_{n.r.}}{dt}$ ).

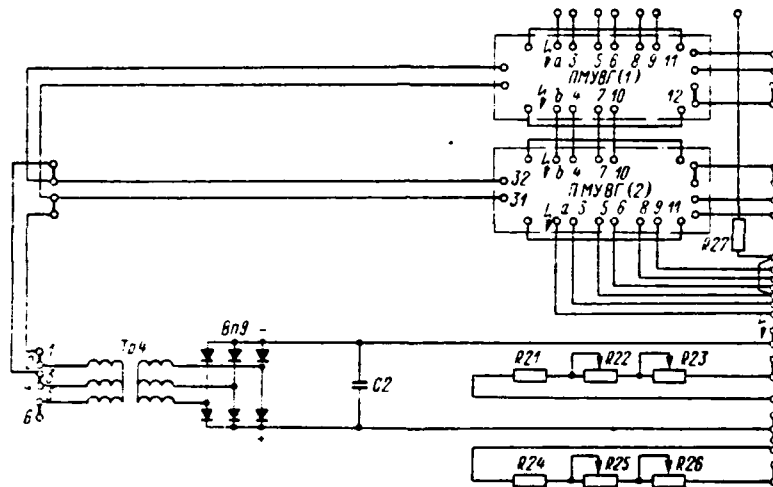


Figure 3.44. Generator Exciter Intermediate Magnetic Amplifier Block Circuit.

The magnetic amplifier PMUVG (1) circuit is presented in Figure 3.45. A signal proportional to  $U_r$  is supplied to winding ab. Winding cd is fed from the characteristics indicator output. Signal  $k_3 \frac{di_m}{dt}$  is supplied to winding e<sub>1</sub>f, and a signal proportional to the first generator exciter voltage derivative is supplied via the RC circuit (R33C3) to winding hg<sub>1</sub>.

Winding  $k_1 i_m$  is a bias winding and is fed from transformer Tr4 terminals (see Figure 3.44). One of the PMUVG is magnetized and the other, on the contrary, has its magnetization reversed, depending on the polarity of the signal at the

characteristics indicator output. Analogously, one of the magnetic amplifiers of the last stage of excitation of generator exciters MUVG1 or MUVG2 (see Figure 3.40) is magnetized, while the other has its magnetization reversed since control winding MUVG1, MUVG2 is fed from its own BPMUVG.

An MUVG circuit is depicted in Figure 3.46. The signal at the characteristics indicator output is absent when the control station lever is in the zero position and amplifiers MUVG1 and MUVG2 are magnetized identically. Therefore, identical currents flow in both generator exciter VG field windings OVVG (see Figure 3.40).

VG voltage equals zero since windings OVVG are connected in such a way that their n. s. are opposed.

Current increases in one winding OVVG when the control station lever is transposed, while that in the other drops. As a result, the polarity of the generator exciter voltage will depend on the direction to which the lever is transposed. The GED propulsion motor field winding is fed from exciter VD, which is a dc generator.

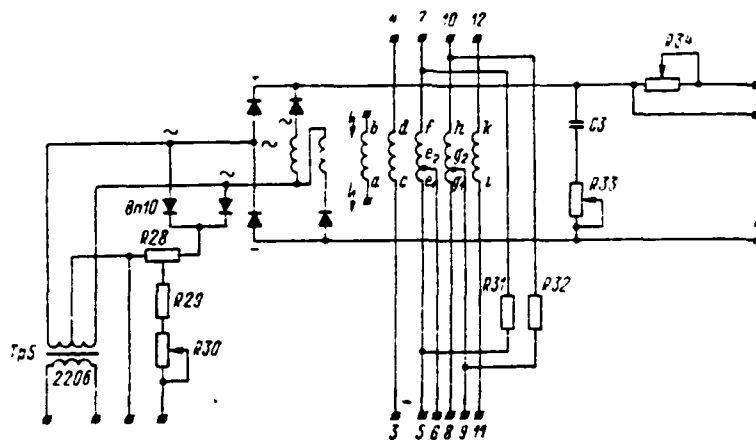


Figure 3.45. Generator Exciter Intermediate Magnetic Amplifier Circuit.

Exciter VD has main field winding OVVD, which is fed via semiconductor rectifiers assembled based on a Larionov circuit with 380 V bus bars. Therefore,

the amount of current in this winding is constant. Only slight current changes are possible in winding OVVD, stipulating mutual induction emf, given a change in current in the other winding.

Auxiliary winding OVVDD boosts propulsion motor magnetic flux. Feed to this winding is supplied from the exciter VD field control system in the magnetic amplifiers. Control is carried out in accordance with the principle of positive main circuit current unity feedback with a cut-off.

Propulsion motor magnetic flux remains constant in the icebreaker movement in open water mode, i. e., when main circuit current does not exceed the nominal value. The propulsion motor field is amplified during movement in ice modes, i. e., when the screw is operating in the ice or moored characteristic.

There is a comparison circuit in the control system. This circuit's output signal is supplied to the intermediate magnetic amplifier control winding [120] PMUVD (Figure 3.47). Final stage magnetic amplifier control winding MUVD is fed from PMUVD and feeds winding OVVDD. The magnetic amplifier MUVD circuit does not differ at all from the generator exciter field final cascade magnetic amplifier circuit depicted in Figure 3.46.

Input voltage of 380 V is transformed into 50 V by transformer Tr6 (see [122] Figure 3.47) and further is rectified by rectifier block Vp19. Capacitor C4 smooths rectifier block output voltage.

Feed is supplied from terminals 10, 12 via resistors R43-R45 to magnetic amplifier MUVD bias winding. The signal, proportional to main circuit current, is supplied from the DT2 saturation choke (see Figure 3.40) to terminals 13, 14 (Figure 3.47). This signal's polarity at the terminals of resistors R35 and R36 remains constant as a result of current passing through rectifier block Vp14-Vp17. The amount of the signal proportional to main circuit current and picked off resistors R35 and R36 is limited by stabilizer diode  $B_{cr5}$ . This signal is compared with the assigned comparison voltage picked off resistors R40 and R41, whose value is stabilized by stabilizer diode  $B_{cr6}$ .

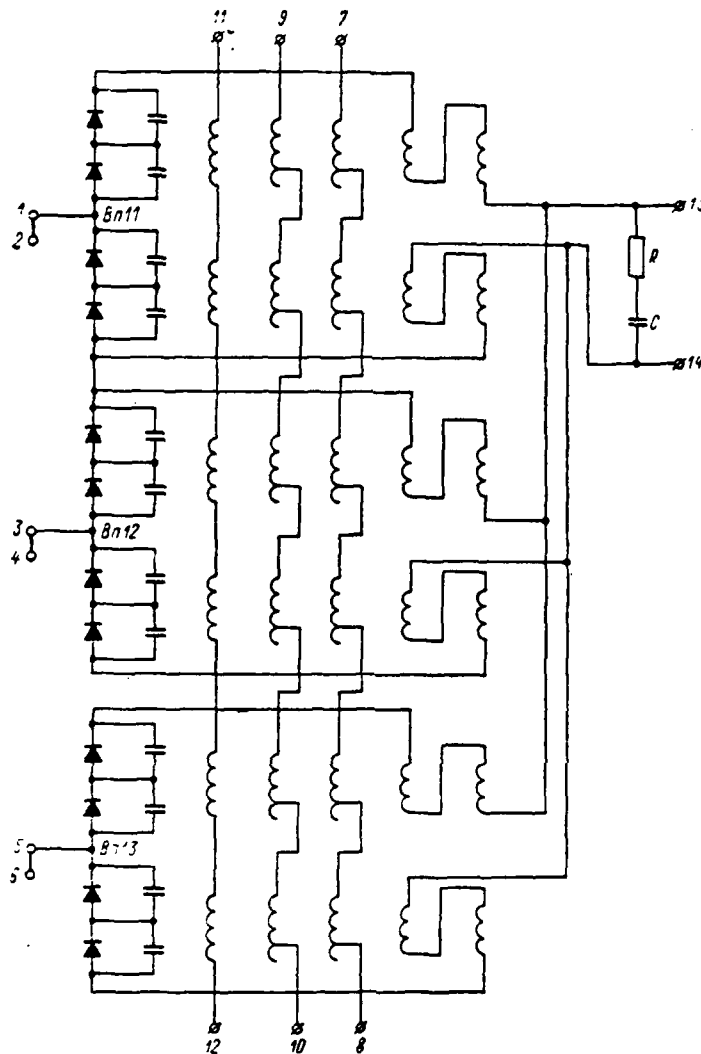


Figure 3.46. Generator Exciter Final Magnetic Amplifier (MUVG) Circuit.

Current will not flow in the PMUVD motor exciter intermediate magnetic amplifier control winding ab circuit due to the presence of diode Vp18 if the voltage picked off resistors R35 and R36 is less than the assigned voltage. Current will flow through the winding ab circuit if voltage  $U_{i_a} = k i_a$  exceeds the value of the assigned voltage, the PMUVD magnetic amplifier will magnetize, voltage at its output will increase, and the voltage at the magnetic amplifier MUVD will increase correspondingly. The latter's control winding is fed from magnetic amplifier PMUVD. As a result, propulsion motor field current will be boosted.

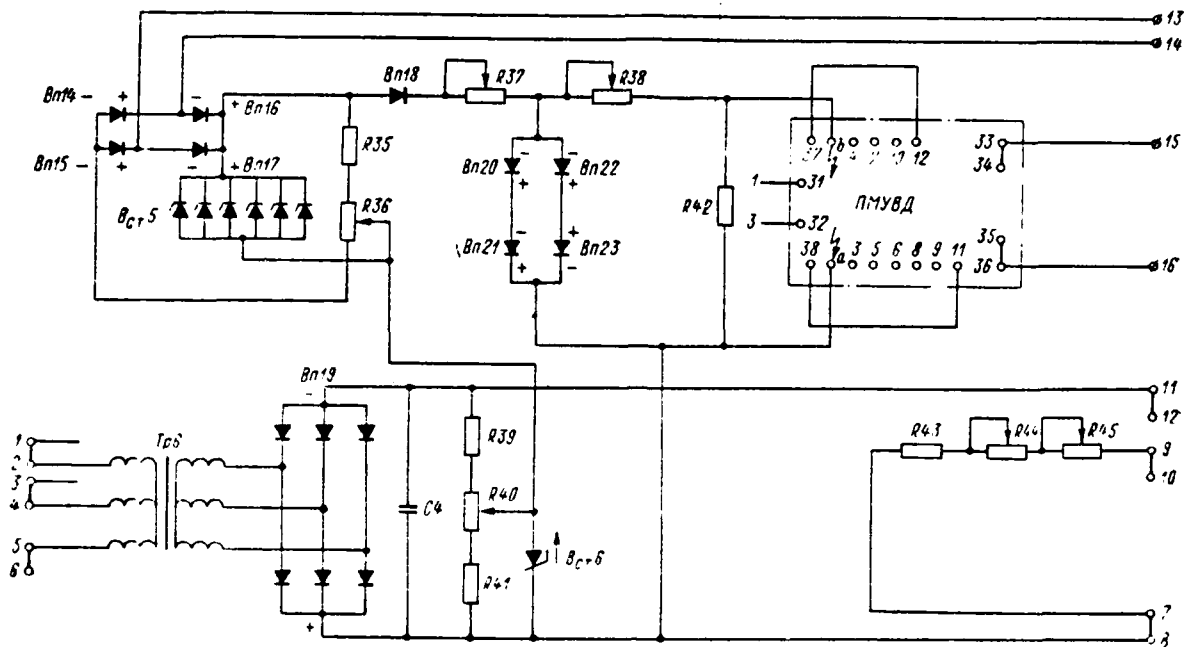


Figure 3.47. Block Diagram of a Comparison Indicator with a GED Exciter Field System with an Intermediate Magnetic Amplifier.

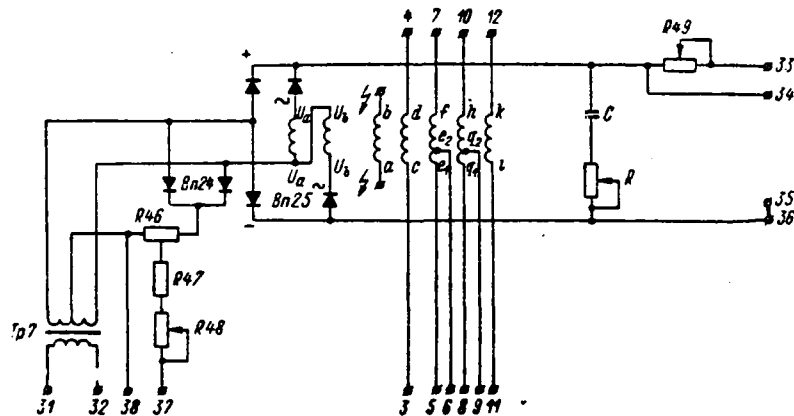


Figure 3.48. GED Exciter Intermediate Magnetic Amplifier Circuit.

The circuit for a GED exciter intermediate magnetic amplifier with a feed transformer, analogous to the circuit for a generator exciter field preliminary stage magnetic amplifier circuit, is depicted in Figure 3.48.

Figure 3.49 presents a schematic of a GEU with power magnetic amplifiers [123] used as GED exciters and as main generator pilot exciters. GED excitation occurs directly from magnetic amplifier MUZ. Contacts 1-8 are representative for control station PU in the zero position. Contacts 1-4 or 5-8, respectively, close when the PU lever is transposed to the "ahead" or "astern" position. Amplifiers MU1 and MU2 are connected to a push-pull (reversing) circuit. A balanced bridge consisting of ballast resistors 1SB and 2SB and two generator exciter field half-windings OVVG serves as their load. Generator exciter VG is a standard shipboard dc generator with individual field half-windings.

The GEU is reversed through reversal of generator excitation by changing current in control windings OU1 and OU2.

MU in this circuit are used both as main generator pilot exciters and as regulators to avoid installation of a dual MU set of great power and loss of power in ballast resistors equal to generator field power. This is an additional advantage for GEU circuits, which have several generators connected into one loop and with field windings connected in parallel. This circumstance would complicate circuit tuning taking the number of generators connected into the loop into account if one considers that MU characteristics greatly depend on load resistance. But, since identical elements of a push-pull MU will have [124] identical parameters and characteristics, changes in voltage, frequency, and environmental temperature will not disrupt MU balance and zero drift.

The steeply-dipping form of the GED mechanical characteristic is insured by the negative main circuit current close coupling acting upon the generator field.

Automatic GED field current control is insured by positive main circuit current unity feedback, which magnetizes the GED when vessel resistance to movement increases. Positive vanishing feedback acting via stabilizing transformer ST on winding OT MUZ and further on GED excitation is introduced into the GED excitation system to affect the rate of main circuit current growth and, consequently, to improve GEU dynamic characteristics.

Study of a mock-up of this circuit revealed that this circuit provides

constancy in a sufficiently broad GED shaft resistance moment range of change. Power fluctuations here do not exceed 6% of its average value.

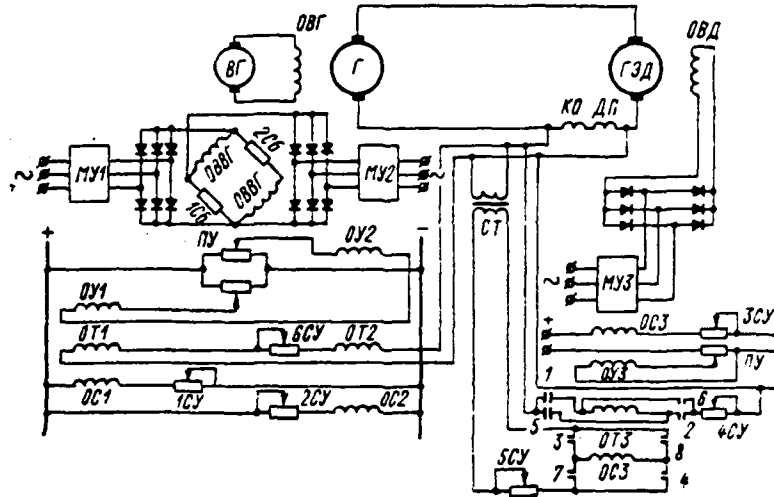


Figure 3.49 Schematic of a GEU with Power Magnetic Amplifiers in the Excitation System.

It is not rational to feed GED field windings in all operating modes only from MU since MU power here will be great. Below we examine a circuit solution for a GED excitation system in which a GED field winding is fed by total current from MU and from an ac or dc shipboard network (Figure 3.50). A field flux constant component (field flux for the movement in open water mode) is provided from the  $\sim 220$  V shipboard network, while MU1 and MU2 regulate boosting of the field flux in navigational modes with increased resistance to movement.

A dual-cascade amplifier is used here to reduce sluggishness and to [125] increase magnetic amplifier gain. Here, the time constant will equal the sum of the time constants of the first and second links of the cascade  $T_{\Sigma} = T_{MU1} + T_{MU2}$ , while gain will equal the product of the gains of both MU:

$$K_{y\Sigma} = K_{y1}K_{y2}.$$

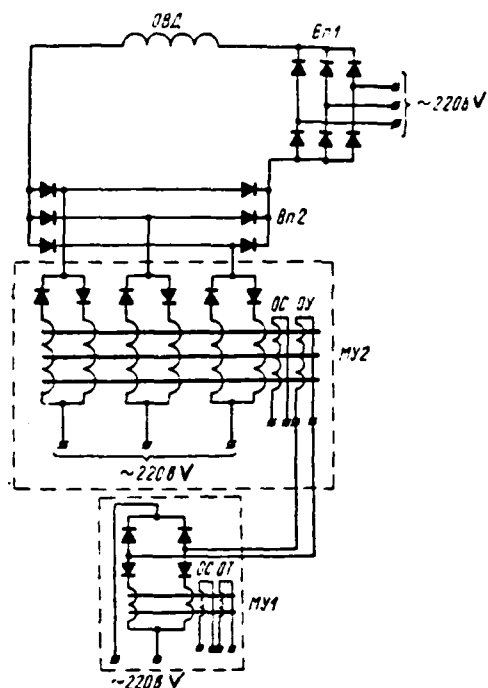


Figure 3.50. Circuit for a GEU with Power Magnetic Amplifiers in GED Excitation Systems and Feed from the Shipboard Network.

A positive main circuit current feedback winding is connected to the first cascade's magnetic amplifier.

The circuit shown in Figure 3.50 has several advantages: wide range of regulation, high gain, absence of rotating elements, and high reliability. Four feedbacks are envisaged in the circuit:

- 1) negative main circuit current unity feedback connecting main generator field MU;
- 2) positive main circuit current unity feedback regulating GED field flux during a changed in GED operating mode. Its rotational speed is reduced with an increase in propellor resistance moment, counter emf decreases, and main circuit current increases. Propulsion motor field flux  $\Phi_A$  here also will increase under the effect of positive main circuit current unity feedback.

Field flux boosting is insured in mode  $I_n > I_{n, nom}$ . Current cut-off in the feedback circuit is accomplished by a stabilizing diode. A saturation choke connected to the main current circuit is the feedback sensor.

- 3) stabilizing feedback;
- 4) GED rotational speed negative delayed feedback. A monitoring tachogenerator placed in rotation by the propellor can serve as the information source.

### § 3.7 Static Excitation Systems with Controlled Rectifiers

Control circuits with controlled rectifiers (thyristors) need not be electrically connected with anode circuits. They should be fed by individual transformers so that anode and input circuits will be electrically separated by transformers. The circuit between a controlling electrode and cathode must not be a high-resistance circuit so that anode circuit transient processes do not influence the input electrode potential via an interelectrode capacitor between the anode and the control electrode.

Control current (pulse) must have a steep leading edge due to the variation of rectifier starting characteristics in order to obtain precise blanking. The pulse method of rectifier blanking is more advisable since pulses load the rectifier and control circuit (pulse generator) little.

Pulses with a duration of about 10-50 ms are sufficient for reliable [126] blanking under an active load. Rectifier blanking under an inductive load requires longer-duration pulses due to the lower rate of current growth in the circuit. Rectifier pulse blanking requires a definite pulse current and voltage over a definite time.

Generally speaking, greater amplitude is required for shorter pulses. However, there is a minimum required pulse time. Circuit parameters must insure anode current growth to a value exceeding the minimum threshold value in the case of short control pulses, if a thyristor must change to the conducting state prior to the time the pulse ceases being active.

Experimental GEU pilot excitation system on the icebreaker "Kiev." This system was built with controlled rectifiers and was used experimentally for a short time. A block diagram of a main generator excitation system using thyristors is presented in Figure 3.51. The thyristor-based control system operates as follows. A signal from a control station, with a rotary transformer

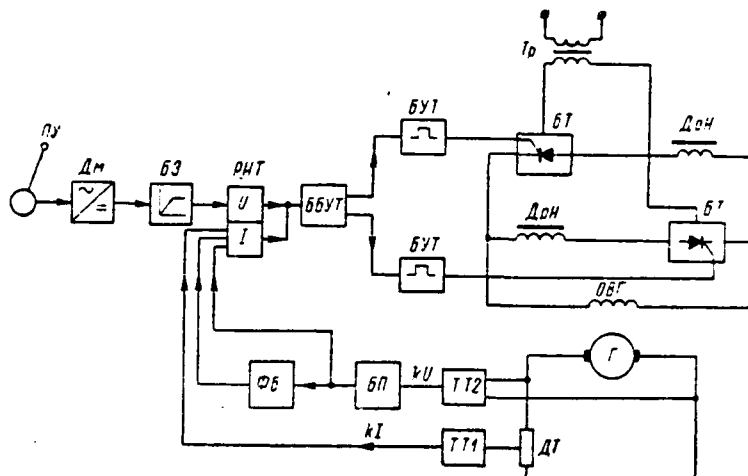


Figure 3.51. Block Diagram of a Main Generator Excitation System Consisting of Controlled Rectifiers (Thyristors).

used in this role, is supplied to demodulator Dm, whose circuit and operating principle are depicted in Figure 3.52.

A signal from the demodulator output is supplied to delay unit BZ and then on to the RNT unit, which is a GEU voltage and current regulator. GEU main circuit current is regulated in the voltage function so that power constancy is maintained, both in the normal and in intermediate modes, in a zone falling between the movement in open water characteristic and the moored characteristic. [127]

Besides the signal from the retarder output to the RNT unit, the following signals are supplied:

- a)  $kI$  -- a signal proportional to main circuit current and moving from indicator DT via dc transformer TT1;
- b) signals moving from converter unit BP and functional block FB outputs (Figure 3.51). These signals are formed as follows: main generator voltage is supplied to dc transformer TT2, where the amount of voltage is decreased and, in addition, where control circuits are decoupled galvanically from the main current circuit. Signal  $kU$  is supplied from transformer TT2 to converter unit BP, whose output signal is a function of GED voltage and the number of operating generators, as well as main diesel rotational speed.

One signal from the unit BP output is sent to block RNT, another to main circuit current block FB in a main generator voltage function and, from there, to unit RNT.

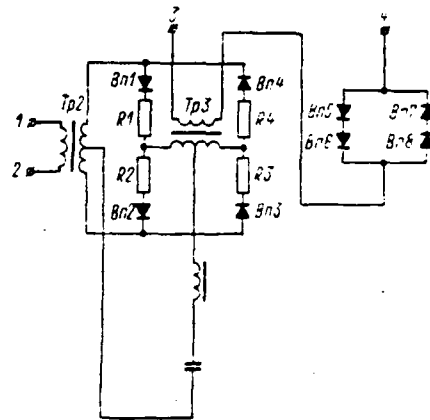


Figure 3.52. Demodulator Schematic.

The signal from the unit RNT output is supplied to the compensation (circular) current interblock unit BBUT, from whence signals are sent already to thyristor control unit BUT.

A block diagram of the propulsion motor excitation system is shown in Figure 3.53.

As can be seen from the diagram, the propulsion motor is excited directly from thyristors assembled in a Larionov circuit.

Thyristor control occurs with the aid of control unit BUT, which converts the voltage supplied to its input into the phase of the pulse at output.

The control signal at the BUT input is supplied from functional block FB, which has the following signals at its input:

- $kI$  -- a signal proportional to main circuit current;
- $U_{39Д}$  -- assigned signal;
- $U_{\text{рез}} -- residue signal supplied from the amplified voltage unit BVN, which is fed by feed transformer Tr secondary winding.$

The BVN is a rectifier unit, with a voltage at its output having a sign opposite to the sign of voltage  $U_{3a2}$ , while its amount is proportional to the thyristor transformer feed voltage.

The signs of signals  $U_{3a2}$  and  $kI$  coincide.

[128]

The input signal polarity indicated was selected so that possible feed network voltage fluctuations would not affect the nature of the thyristor control signal.

GEU pilot excitation system on the icebreaker "Murmansk." The firm Stromberg (Finland) used a pilot excitation system with controlled rectifiers (thyristors) on this icebreaker.\*

Main generator exciter field windings are fed by the shipboard network via a transformer and two thyristor bridges.

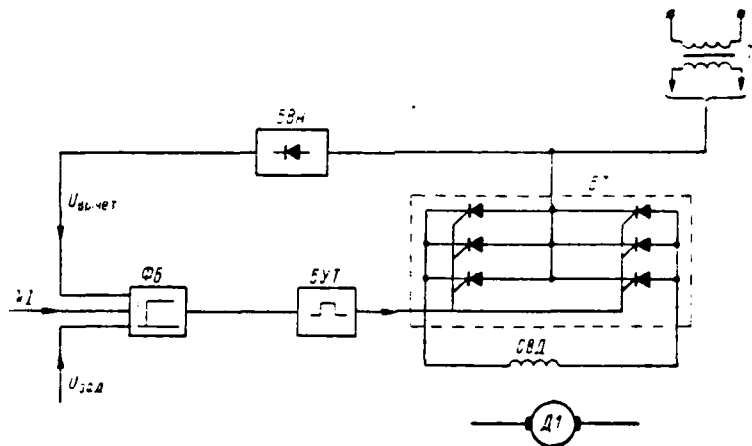


Figure 3.53. Block Diagram of a Main Propulsion Motor Excitation System Consisting of Controlled Rectifiers (Thyristors).

One of the thyristor bridges (I) operates as the icebreaker moves ahead and the other (II) during movement astern (Figure 3.54).

\*Shaft output, power distribution, and main current circuit are analogous to the GEU aboard the icebreakers "Moskva" and "Leningrad."

Main propulsion motor excitation also is accomplished based on a quadratic system, whereby the exciter has two field windings, one providing a constant field flux and the second -- a control winding -- is for amplification of the main propulsion motor magnetic flux and fed from a thyristor bridge (Figure 3.55) controlled by a field amplification regulator. In principle, generator and main propulsion motor machine exciters can be replaced by rectifier units comprising thyristor bridges, which are transistor regulators. But, a machine field unit must be envisaged here for each main current circuit in order to provide manual and emergency control.

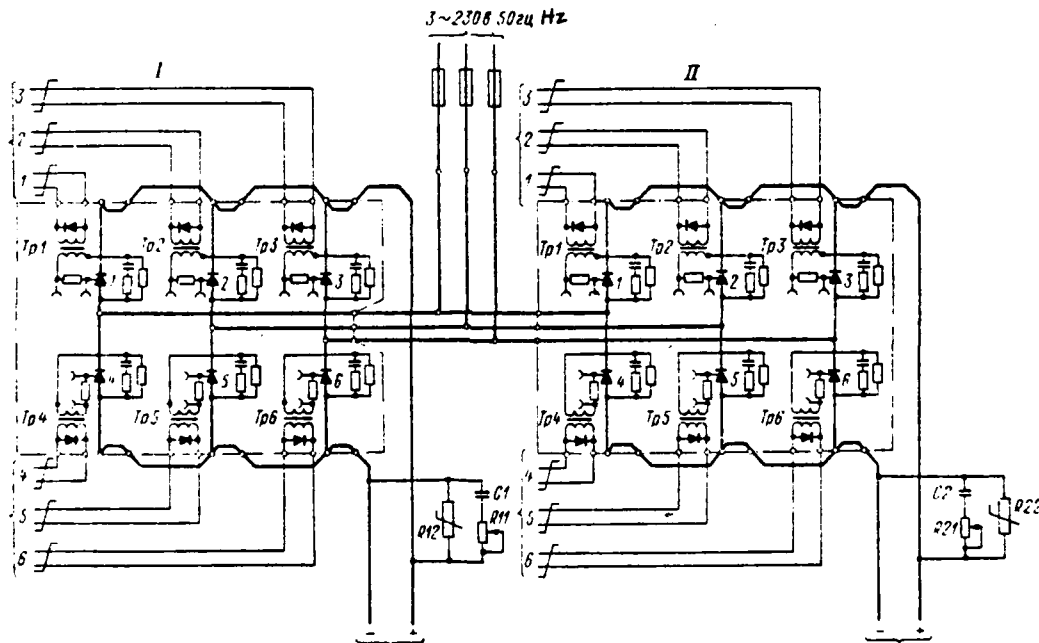


Figure 3.54. Schematic of Main Propulsion Motor Exciter Field Thyristor Bridges. 1-6--Controlled rectifiers; Tr1-Tr6--Ignition circuit feed transformers.

There is no basis upon which to recommend generator and main propulsion [130] motor excitation systems fed directly from silicon controlled rectifiers for domestic electrical propulsion plants due to lack of know-how in operating such GEU.

Use of main generator and main propulsion motor excitation systems directly

from thyristor bridges degrades commutation at the collector, which impacts particularly on machinery built with an interleaved steel stator.

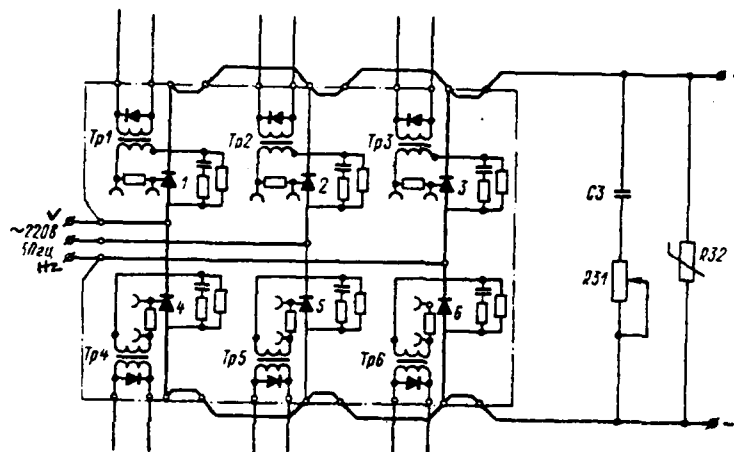


Figure 3.55. Schematic of a Bridge with Controlled Rectifiers in the Main Propulsion Motor Magnetic Field Amplification Circuit. 1-6--Controlled rectifiers; Tr1-Tr6--Rectifier ignition circuit feed transformers.

A structural diagram of the excitation for the GEU amidships loop on the icebreaker "Murmansk" is shown in Figure 3.56.

The armatures of main propulsion motor 22 are connected in series, just as are the armatures of their exciters 23. Each exciter has two field windings: one creates the main excitation field and is fed by rectifier 29, while the second is for field regulation and is fed by thyristor bridge 17.

Main propulsion motor armature current moves via dc transformer 21, which issues a signal proportional to the current, then via rectifier 25 to adding and comparison unit 27, where this signal is compared to reference voltage received from potentiometer 26. Field amplification begins after the signal received from the dc transformer exceeds the reference voltage. The combined signal is supplied to unit 28.

Unit 28 controls ignitor 16 of thyristor bridge 17, which feeds exciter second windings.

Field amplification is accomplished by two closed control loops: outer [131] and inner. The outer loop is for magnetic field regulation, while the inner is exciter armature circuit current regulation. Main propulsion motor high-speed field amplification is achieved in this manner.

The field amplification circuit is cut out for a specific time when main propulsion motors are reversed and constant voltage assigned value unit 4 changes its sign when GED direction of rotation changes. This is achieved by amplifier 2. When amplifier output voltage changes its sign, pulse circuit 1 connected beyond it transmits a disabling pulse to control unit 28.

Four generators 20 in the circuit are connected in series. Their field windings are connected in parallel and are fed by exciter 19 with two field windings. There are three control loops on the generator side: inner, middle, and outer.

The inner loop is for voltage regulation at the exciter armature terminals (exciter voltage feedback). The voltage of the exciter 19 armature is measured by constant voltage transducer 18. Transducer voltage is supplied to unit 12, which controls two ignitors 16 and two thyristor bridges 17. The thyristor bridges feed each of their own exciter field windings and the magnetizing [132] forces of these windings are opposed. Operation of the thyristor bridges and generator field polarity depend on master unit 12.

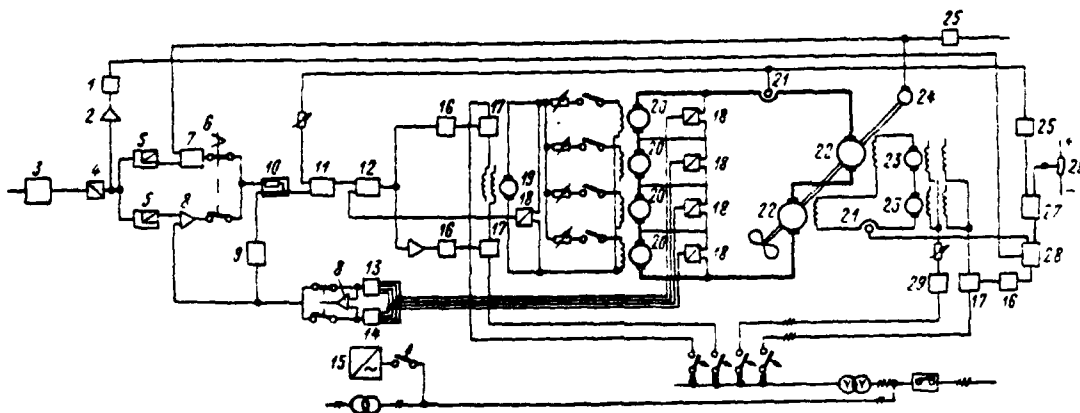


Figure 3.56. Structural Diagram of the Excitation of the Icebreaker "Murmansk" GEU Middle Loop.

The middle loop is for main generator armature current regulation (main circuit current unity feedback). The signal from the generator armature current is supplied via the same transducer, which is used for regulation of main propulsion motor field amplification. The measured armature current acts upon unit 11, which in turn provides the assigned value to inner loop device 12.

The two outer control loops are connected in parallel to regulate propulsion motor speed and main generator power, with the regulation method selected by a switch. The method of control is selected by a switch.

The propulsion motor rotational speed control loop accomplishes GED rotational speed feedback. Shaft rotational speed is measured by tachogenerator 24. Constant voltage proportional to rotational speed is fed to unit 7, which regulates rotational speed. This unit receives a signal from integrator 5 and from control device 3 and unit 4 connected to it. Unit 4 creates the assigned constant voltage value. The job of the integrator is to limit the signal change rate to a known level. Propulsion motor rotational speed and direction can be set by control device 3.

The main generator power regulation loop protects primary motors against overloads. The voltage at each main generator armature's terminals is measured by constant voltage transducer 18. The measured voltage values are supplied to the selectors of maximum 13 and minimum 14 values. Connected between selector output terminals is an amplifier, which controls the relay connected beyond the selectors so that maximum or minimum voltage at the armature terminals can pass.

This circuit's purpose is to select the voltage highest in numerical value, which is supplied to adding amplifier 8. Voltage from assigned value integrator 5 is supplied to the same amplifier. This voltage corresponds to the assigned power value, i. e., the product of the armature circuit current and one generator's voltage. However, the product within a specific range can be replaced by the sum of the aforementioned values. Then, the assigned value integrator voltage can be considered as the sum of the armature circuit current and the voltage.

On the other hand, the armature circuit current will be the adding amplifier's

output voltage if voltage with a negative sign higher in numerical value is supplied to the adding amplifier. This signal is supplied via control limiter 10 in the form of the assigned value for the armature circuit current control loop.

Consequently, power regulation occurs simultaneously with rotational speed regulation and is accomplished by setting switch 6 in the appropriate position. [133]

Armature circuit current limitation is provided by functional generator 9. Armature voltage higher in numerical value is supplied to it as assigned voltage. It supplies signals to control limiter 10 in accordance with this voltage.

Direct Current Electrical Propulsion Plant Protection,  
Indication, and Interlock Circuits

§ 4.1 GEU Protection Circuits

Abnormal modes and phenomena can arise as electrical propulsion and other electrical machinery is operated. This will lead to stoppages, breakdowns, and damage to equipment, reducing the reliability of electrical propulsion plants [GEU].

GEU protection system. Various types of protection shield electrical equipment against abnormal phenomena and modes and eliminate the possibility of their occurrence. The quality of GEU operation, reliability, and longevity depend upon correctly-designed protection.

Various emergency modes can arise in dc electrical propulsion plants. The most dangerous are short circuits in the main current circuit and locking of the propellor. Current in the main current circuit in both cases will reach an intolerably high level, which destroys generators and main propulsion motors.

Overvoltage relays connected to the main current circuit are used to protect against excessive currents. The relay breaks the contactor coil circuits in generator and main propulsion motor field circuits with its contacts when the current in the main circuit increases, the contactors cut out, and the generator and main propulsion plant circuits break.

Overvoltage relays, which can act not only to remove excitation but also on supply of signals to visual and audible warning indication circuits, /134 also are used in excitation systems with main circuit current negative feedback.

The capability to stop a main propulsion motor at current  $I_{ct} = (1.4-2.0) I_{nom}$  for a limited (usually 1-2 minutes) time is envisioned with GEU having main circuit current negative feedback. If the stoppage under current lasts longer than the time guaranteed by the electromechanical plant, machinery overheats

beyond tolerable values and can break down. Therefore, it is advisable to envisage time delay protection which cuts off or reduces generator excitation.

Main propulsion motor overloads caused by an increase in shaft resistance moment in stormy weather, when underway with a load, and so on can arise in electrical propulsion plants. A consequence of overloads will be an increase in main circuit current above the nominal level and a dangerous increase in generator and main propulsion motor overheating.

GEU protection circuits must envision an overload relay affecting a reduction in generator field current to a level at which current in the circuit does not exceed the nominal current of the machinery. Serious emergencies can occur when diesels stop suddenly. As is known from Chapter 2, most often several generators run one main propulsion motor in dc electrical propulsion plants (see Figure 2.4, for example). The generator field windings in that circuit are fed by one exciter, while the armatures in these generators are bypassed by common current.

If a primary motor stops due to breakdown, the rotational speed and emf of the generator connected to it will drop to zero, but the magnetic flux remains constant. Nominal current created by the second generator will flow in the previous direction in the armature circuit. The emergency generator in this instance transfers to the motor mode with rotation in the opposite direction and the primary motor will reverse. This reversal will cause the primary motor to break down.

Special protection in the form of a pressure relay connected to the primary motor fresh water cooling pipe is used to prevent this phenomenon. The cooling system pump is attached directly to the primary motor and the rate of its rotation is proportional to primary motor rotational speed. Pump rotational speed decreases with an increase in motor rotational speed, resulting in a pressure drop in the cooling pipe. The pressure relay trips and cuts out generator and main propulsion motor excitation.

For 40-50 years of this century, pressure relays were connected to the motor lubrication system, but this led to accidents since pressure in the

lubrication system fell slowly and the protection was unable to cut out the excitation.

A primary motor also can be protected against reversal by means of centrifugal relays or tachogenerators set on the primary motor shaft and affecting excitation cut-off. However, the design of extant centrifugal relays does not provide reliable protection.

A main propulsion motor field circuit failure (field failure) is analogous to a short circuit in the main current circuit. A field-failure relay affecting generator field cut-off is envisioned in several circuits to protect against this emergency. This type of protection is not used in modern circuits since, with three-winding exciters or amplidynes in field circuits, current feedback exists which, when the main propulsion motor field fails, will limit the current in the main circuit and, after a specific time interval, overload protection will activate. Overvoltage protection activates at high currents.

The GEU auxiliary circuit feeds generator and main propulsion motor exciter field circuits and contactor coils in their field winding circuits, as well as indication and interlock circuits.

An electrical propulsion plant stops when voltage in the auxiliary circuit disappears, since excitation is picked off generators and main propulsion motors and protection circuits open. Sudden repeat reestablishment of voltage will cause a repeat GEU start to full rotational speed. Zero protection is used to prevent such a start.

Zero protection is accomplished by a control station contact closing only in the station zero position and connected in series with the voltage relay (RN) coil. The station contact is shunted by the n. z. [normally closed] voltage relay contact.

The voltage relay coil will deenergize when voltage in the auxiliary circuit disappears, relay contacts open, and all electrical propulsion motor circuits are cut out via intermediate contactors. It is possible to connect GEU circuits after voltage is restored in the auxiliary circuit only after the control station is set in the zero position.

Generators and main propulsion motors in electrical propulsion plants with a power exceeding 1000 kW are built with forced ventilation throughout the closed and open cycle, with air cooling in the air coolers of the outboard water circulating in them. The air will overheat when the water stops circulating and the electrical machinery will heat up beyond tolerances. Protection against these malfunctions is provided by a pressure relay in the air cooler water piping network. This relay cuts out generator and main propulsion motor excitation when the pressure in the system drops and stops the electrical propulsion plant. Analogous protection also is envisaged in the bearing lubrication system for this machinery.

It is advisable to use extant circuits to familiarize ourselves with /136 protection system construction principles.

GEU protection circuits with single-winding exciters. A GEU protection system on the diesel electric ship "General Azi Aslanov," which provides protection against overloads, overvoltage protection, zero protection, and protection against primary motor reversal, is depicted in Figure 4.1.

Protection against overloads is accomplished with the aid of overload relay RP, the coil of which is connected to the voltage drop in the main propulsion motor auxiliary pole winding. The relay will trip and close its contact in the field boosting relay (RF) coil circuit when the current in the main circuit increases beyond the 1300 A to which the relay is tuned. Relay RF, tripping, will open n. r. [normally open] contact RF1 (see Figure 3.13), which shunts the resistance in the exciter field winding circuit and will close n. z. contact RF1, which shorts resistance RVb in the main propulsion motor field winding circuit (Figure 3.10). Resistor SD will be introduced into the exciter field winding circuit, causing exciter and generator voltage to decrease, main propulsion motor magnetic flux will increase due to introduction of resistance RVb, and main circuit current will decrease.

Overvoltage protection is accomplished as follows. Overvoltage relays RM1 and RM2 (Figure 4.1) trip when there is a radical change in load on the screw, which in turn causes an increase in main circuit current. Relay RM1 and RM2 coils are connected in series with diesel generator G1 and G2 armatures

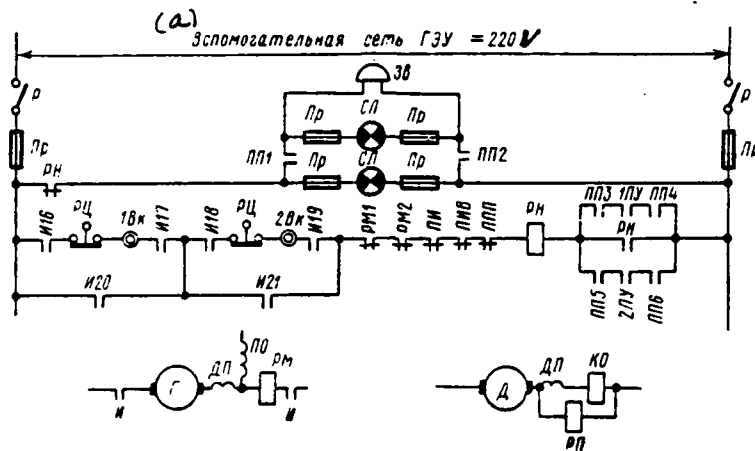


Figure 4.1. Diesel Electric Ship "General Azi Aslanov" GEU Protection Circuit. a--GEU auxiliary network=220 V.

and are set to trip at a current of 1500 A. Overvoltage relays RM1 and RM2, tripping, open their contacts in the voltage relay RN coil circuit. This relay opens its contacts in the exciter separately-excited winding potentiometric /137 regulator circuit and generator field contactor KVG coils. After the separately-excited winding loses feed, voltage at the exciter armature will drop almost to zero. In addition, the contactor KVG coil, deenergized, opens its contacts and cuts the generator field windings (see Figure 3.13) out of the exciter armature.

Zero protection and protection against a voltage decrease are accomplished by means of control stations 1PU, 2PU contacts (Figure 4.1), which close only in the zero position and are connected in parallel to the voltage relay RN open contact. If voltage in the GEU auxiliary network disappears while the electrical propulsion plant is operating (control station in the zero position), the RN coil loses feed and relay contacts in the exciter separately-excited winding and the RN coil circuits open. The RN coil circuit will open if voltage suddenly is restored, since control station 1PU, 2PU contacts are open. These contacts will close after the stations are placed in the zero position, the RN coil will obtain feed, the relay will trip, and will shunt the control station contacts with its contact. The stations can be operated again.

Centrifugal relays RTs (Figure 4.1) installed individually on each diesel

generator provide protection against primary motor reversal. Each diesel generator's protection circuits are connected in series by means of selector switch I16-I17 and I18-I19 contacts to the RN circuit, but, when a diesel generator is cut out of the overall circuit, its protection circuits are cut out of it as well.

Centrifugal relay RTs opens the RN circuit contacts when diesel generator rotational speed drops. This relay cuts out, removing excitation from the generator. Centrifugal relays are not being used now to protect against reversal since they do not provide reliable protection.

Protection in the GEU circuit for the tug "Goliath" in the main is identical to that for the diesel electric ship "General Azi Aslanov" (Figure 4.2).

Overvoltage and zero protection in this circuit are accomplished in a manner identical to that in the Figure 4.1 circuit, except that exciter field contactor KVV replaces voltage relay RN.

Protection against diesel generator reversal in this circuit is complicated by inclusion in the KVV coil circuit of oil pressure relays RDM1 and RDM2 in the lubrication systems of each diesel and of special RTs contacts connected mechanically with each diesel's shaft. Fuses protect GEU auxiliary circuits against short circuits.

Contactors KVD3, with an n. r. contact in the main propulsion motor field winding discharging resistance circuit, is an additional element introduced into this circuit. Contactor KVD3 cuts discharging resistance out during GEU operation, thus achieving a slight electric power saving, even though complicating the circuit. This contactor's blocking contact is connected to the contactor /138 KVD1 and KVD2 coil circuit, via whose contacts the main propulsion motor field circuit and GEU control circuit are fed.

If the KVD3 coil is under voltage, then its n. r. contact in the main propulsion motor field winding discharging resistance circuit opens and the KVD3 blocking contact in the KVD1 and KVD2 coil circuit closes. The latter trip, close their contacts, and supply feed to GEU control circuits and propulsion motor field windings.

Such a circuit complexity is not recommended because, if the KVD3 coil breaks or burns out, GEU operation is disrupted at a time when it could operate normally. Cutting out the discharging resistance lowers circuit reliability also because the length of the cables connecting the field winding to this resistance is increased and, consequently, the probability of a break and damage to these cables increases. Usually, discharging resistances are installed in such a way that cables connecting them to field windings are as short as possible.

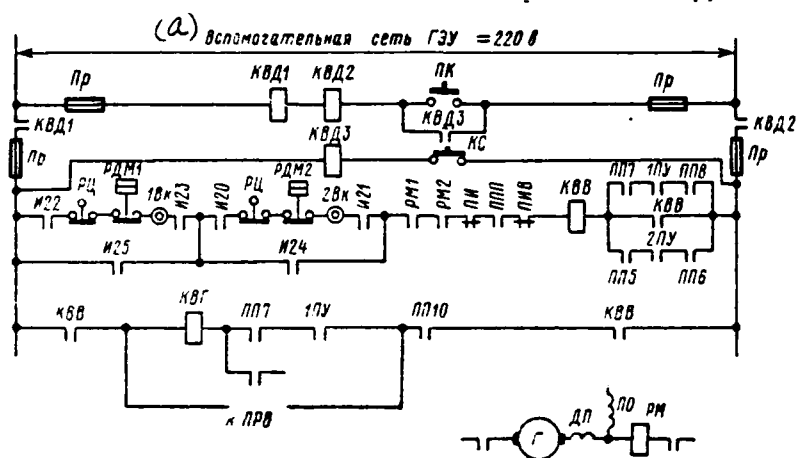


Figure 4.2. Tug "Goliasf" GEU Protection Circuit. a--GEU auxiliary network 220 V.

GEU protection circuits with three-winding exciters. A more complex protection circuit is used for the GEU aboard the ferry "Yuzhnyy" (Figure 4.3). The circuit envisions overvoltage protection affecting indication, protection against an overload, protection against primary motor reversal, zero protection, main propulsion motor field failure protection, and protection against a drop in main propulsion motor lubrication pressure.

Overvoltage protection is accomplished by a relay, the coil of which connected directly to the GEU main current circuit in series with the main propulsion motor armatures. Relay contacts are connected to a bell circuit. An indicator /139 bell rings in the engine room and pilot house if a current overload occurs.

Overload protection is provided by an excitation system with a three-winding

exciter, which, in the event of an increase in screw moment and resultant current increase in the main circuit, demagnetizes generators, in so doing reducing their voltage and main propulsion motor rotational speed in such a way that power taken from the primary motor remains almost constant.

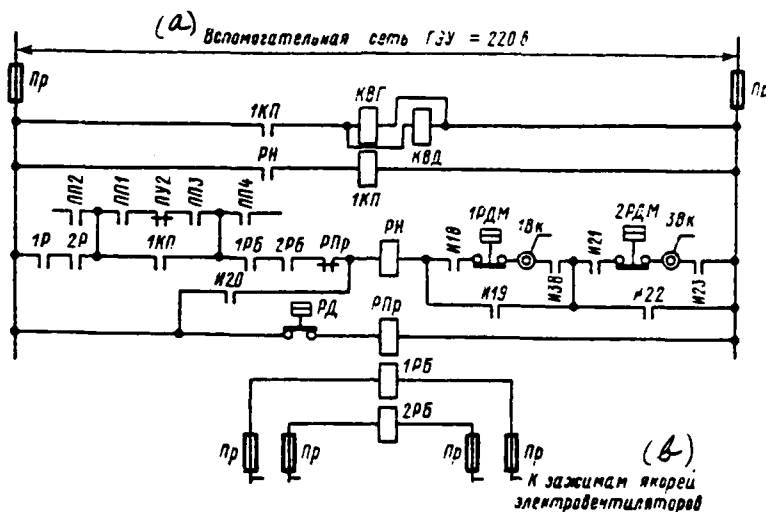


Figure 4.3. "Yuzhnyy" Class Ferry GEU Protection Circuit. a-- GEU auxiliary network 220 V; b--To electric fan armature terminals.

Protection against primary motor reversal in this circuit is accomplished by oil pressure relays 1RDM and 2RDM in each motor's system. Switches 1Vk and 2Vk, which are closed by an engineman after the diesel has been started and warmed up, are connected in series to each relay. Relays 1RDM and 2RDM break the GEU protection circuit in the event of a pressure drop in the diesel's lubrication system and cut out the entire electric propulsion circuit. This protection circuit has not proven itself and can not be recommended since oil pressure drops rather slowly and the protection is unable to trip if the diesel running at full speed stops. Thus, the motor begins to reverse. The pressure relay and diesel readiness switches are connected to the protection circuit by selector switch I18, I38 contacts (generator G1 protection) and I21, I23 contacts (generator G3 protection). Contact I19 shunts the diesel generator G1 protection circuit when it cuts out, while contact I22 does the same for the diesel generator G3 protection circuit.

Protection against a break in the main propulsion motor field is introduced into the protection circuit because the circuit envisions cutting out by means of a main propulsion motor field winding knife switch when one of the armatures breaks down. Therefore, knife switch 1R and 2R n. r. contacts are introduced /140 into the protection circuit to avoid cutting in an unexcited main propulsion motor.

Zero protection is accomplished by means of a control station PU2 contact which closes only in the zero position. When the relay RN circuit closes, it trips, closing the intermediate contactor 1KP coil circuit, the contactor trips, and the contactor KVG and KVD coil circuit closes. These contactors close the generator and main propulsion motor field windings and the contactor 1KP blocking contact shunts the zero protection PU2 contact.

Protection against main propulsion motor electric fan stoppage is provided by relays 1RB and 2RB, whose coils are connected to propulsion motor fan armature terminals. The normally closed contacts of these relays are connected to the RN circuit. When any electric fan stops, RN cuts out and removes excitation from generators and main propulsion motors.

This protection type is not used for electrical propulsion plants developed after 1953 since the circuit is complicated unnecessarily. If a main propulsion motor is operating without cooling, it begins to overheat and the appropriate indication reaches the electrical propulsion board.

The circuit envisages one other type protection -- against a pressure drop in the main propulsion motor forced lubrication system, <sup>(Fig. 4.3)</sup> When this occurs, relay RD closes its contacts in the intermediate relay RPr coil circuit, the relay trips, and closes its n. r. contact in the RN circuit.

Main propulsion motor protection elements are cut out of the circuit by a selector switch I20 contact when the diesel generators are running the shipboard network.

A maritime tug GEU protection circuit (Figure 4.4) envisions overvoltage protection, zero protection, protection against primary motor reversal, and

protection against a diesel overload and GEU power constraint during operation of auxiliary generators installed on the same diesels as are the main generators [50].

Overtoltage protection is accomplished, as in the previous circuits, by overvoltage relay RM, whose contacts break the intermediate relay IRPr circuit. The latter in turn breaks its contacts in the generator field contactor KVG and main propulsion motor field contactor KVD coil circuit. The relay IRPr contact in the KVG and KVD circuit close with a time delay to avoid false trips during transient processes -- starts and reversals, then close instantaneously.

Zero protection is accomplished by control station 1PU1-3PU1 contacts. These contacts are connected not to relay IRPr, but to the contactor KVG and KVD coil circuit and are shunted by these contactors' blocking contacts.

Protection against primary motor reversal is provided by relays IRSO and ZRSO connected to the diesel coolant water system.

Water circulation in the cooling system is provided by a pump mounted on /141 the motor. System pressure drops when diesel rotational speed decreases and a relay opens its contacts in the IRPr circuit, thus cutting the system out.

Each diesel's protection elements are connected to the circuit by selector switch contacts.

Protection against overloads is accomplished by selection of the appropriate three-winding exciter characteristics.

Auxiliary generators as well as main generators are mounted on the diesels in this circuit, as opposed to the previous ones. Therefore, the propulsion plant load is decreased in order not to overload the diesels when auxiliary generators are cut in. This is done by maximum power contactor KMM, whose coil is connected via auxiliary generator circuit breaker 1A and 2A n. z. blocking contacts. Contactor KMM, tripping when circuit breaker 1A or 2A cuts in, closes an n. z. contact, which shunts the resistance in the main propulsion motor field winding circuit, intensifying its flux, and an n. r. contact in the exciter

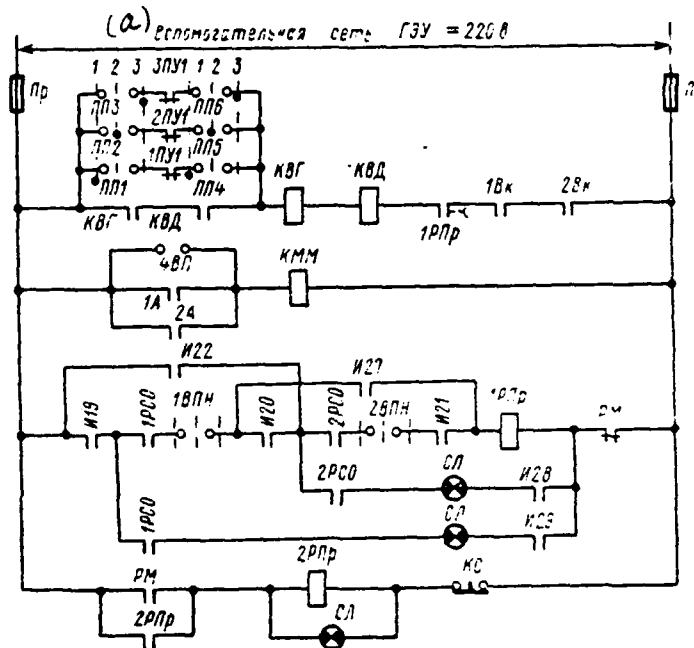


Figure 4.4. Maritime Tug GEU Protection Circuit. a--GEU auxiliary network 220 V.

separately-excited winding circuit opens, introducing additional resistance 4SD into the circuit (see Figure 3.16).

Ice navigation vessel GEU protection circuits. A "Lena" class maritime GEU protection circuit is presented in Figure 4.5 [50].

Overvoltage protection in this circuit is accomplished by overvoltage /142 relays RM1 and RM2. Relay coils are connected to shunts in each loop's main current circuit. The relay trips when main circuit current exceeds 5000 A and its contacts in exciter contactor KVV1 and KVV2 coil circuit open. These contactors in turn pick off feed from amplidyne master winding potentiometers -- generator and main propulsion motor exciters.

Contactors RMN1 and RMN2, whose coils are connected to EMU and whose contacts are connected to the contactor KVV1 and KVV2 coil circuit, trip when there is /143 an excessive increase in voltage in generator amplidyne armatures.

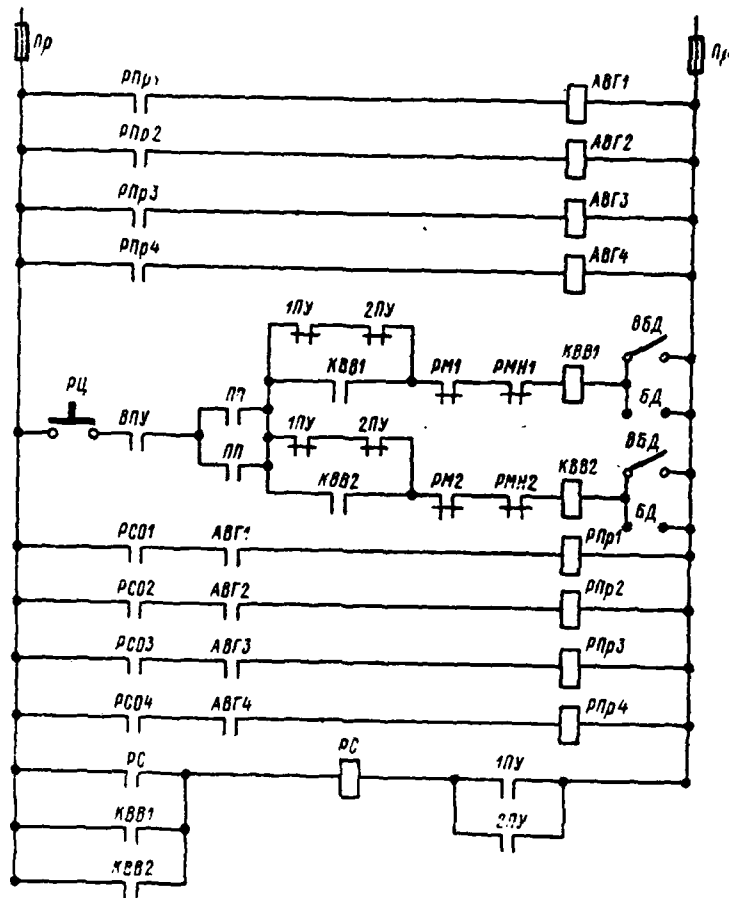


Figure 4.5. "Lena" Class Dry Cargo Ice Navigation Vessel GEU Protection Circuit.

Protection against primary motor reversals is provided by diesel rotational speed reduction relay RS01-RS04. These relays' coils are connected to the armature terminals of tachogenerators sitting on each generator's shaft. Relays RS01-RS04 open their contacts (each relay in its own intermediate relay RPr1-RPr4 coil circuit) when tachogenerator voltage drops to a value less than 50% of the nominal value. The intermediate relays in turn open the contacts in a generator field circuit breaker AVG1-AVG4 cut-off coil circuit; each cut-off coil cuts out a circuit breaker, breaking the corresponding generator's field winding circuit.

Zero protection is accomplished by control station 1PU-2PU contacts, which are closed only when the control stations are in the zero position.

Centrifugal relay RTs connected to the field contactor KVV1 and KVV2 coil circuit protects the main propulsion motor against racing. This is redundant, additional, and reserve protection provided by a main propulsion motor excitation system (by main propulsion motor EMU winding 0U). (See Figure 3.9).

A protection circuit for one loop of the GEU on an "Amguema" class active ice navigation dry cargo vessel is depicted in Figure 4.6. It differs somewhat from the previous circuit.

Overvoltage protection is provided by relays RM1 and RM2, whose coils are connected in parallel to the main propulsion motor additional pole windings and compensating winding. Relay RM1 and RM2 contacts are connected to the contactor 1KVV and 2KVV coil circuit, which connect the contacts to generator EMU control winding potentiometer circuits.

The contacts of relays RN1 and RN2 with coils connected to EMU armature terminals -- generator exciters, are connected to the same circuit. The relays cut out the 1KVV or 2KVV coil when there is an excessive increase in voltage at these terminals.

Zero protection is accomplished by control station 1PU2 and 2PU2 contacts, which are closed only in the control station zero position and are shunted by contactor 1KVV and 2KVV blocking contacts. Restoration of the GEU control circuit when voltage disappears on the constant voltage generator bus bars, from which all GEU auxiliary circuits are fed, and when it reappears is possible only after a connected control station is set in the zero position.

Diesel protection against reversal is accomplished by means of water pressure relays 7RD-8RD in the diesel cooling system.

Relays 7RD-8RD open their contacts in the intermediate relay 3RPr-4RPr circuit when the pressure in any diesel's cooling system decreases, which can occur in the event its rotational speed decreases. The corresponding relay in turn breaks the field circuit breaker 1A-4A cut-off coil circuit of the /144 corresponding diesel generator. The circuit breaker cuts the generator field winding out from the amplidyne. In addition, the circuit breaker 3A-4A blocking contact breaks the field contactor 1KVV-2KVV coil circuit.

Diesel readiness control switch 3PGD-4PGD contacts, closed by the engineman after the diesels have warmed up, also are connected in series with the 7RD-8RD contacts to the intermediate relay 3RPr-4RPr coil circuit.

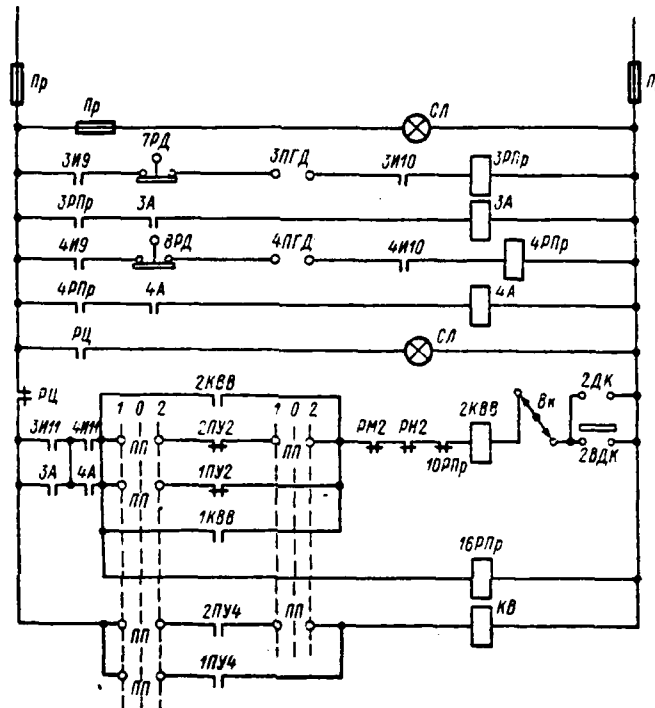


Figure 4.6. Protection Circuit for One Loop of the GEU on an "Amguema" Class Dry Cargo Ice Navigation Vessel.

GEU protection circuit for single-shaft vessels. A more complicated GEU protection circuit with four diesel generators running one main propulsion motor for the GEU on an "Aktyubinsk" class diesel electric ship is depicted in Figure 4.7. Overvoltage protection against overloads is absent from this circuit. The circuit is protected against overloads through selection of the corresponding three-winding exciter characteristics and by the appropriate construction of the field circuit, which does not, however, provide protection during short circuits.

Zero protection is accomplished by a control station 1PU1 or 2PU1 contact, which is closed only in the control station zero position. These contacts /145

are connected to the circuit via station switch PP1-PP4 contacts. Each diesel is protected against reversal by relays 1RSO-4RSO, which are tripped by a drop in cooling system pressure and protection against a pressure drop in the motor 1RD-4RD lubrication system. Each diesel's protection can be shunted by selector switch contacts.

A relay RN coil, which, deenergizing, opens its contact in the intermediate contactor KP circuit, is connected to the protection circuit. Contactor KP in turn has n. z. contact in the generator field KVG and main propulsion motor KVD contactor coil circuit. Tripping, the protection cuts generator and main propulsion motor excitation out. In addition, intermediate contactor KP has blocking contacts: normally closed in the exciter separately-excited winding circuit and normally open in the control station emergency indication circuit.

Absence of overvoltage protection in this circuit cannot be justified since even a dead-end short circuit can occur in the circuit if the differentially-compounded winding opens. Opening of the differentially-compounded winding in this circuit is possible since it is connected not in series to the main current circuit, but in parallel to the main propulsion motor additional pole winding and the compensating winding. Contact closure for the circuit shown in Figure 4.7 is presented in Table 4.1.

A protection circuit for a GEU with four diesel generators running one two-armature main propulsion motor used in the GEU on a "Mirnyy" class whaler is depicted in Figure 4.8.

Overvoltage protection also is absent in this circuit, but limitation of /146 current in the main current circuit (as in the Figure 4.3 circuit) is accomplished by the three-winding exciter.

Zero protection is provided by control station 1PU1-3PU1 contacts, which shunt field contactor KVG and KVD blocking contacts. The voltage relay RN coil is connected to the protection circuit, while the relay RN contacts are connected to the field contactor KVG and KVD circuit.

Each diesel generator is protected against reversal by means of pressure

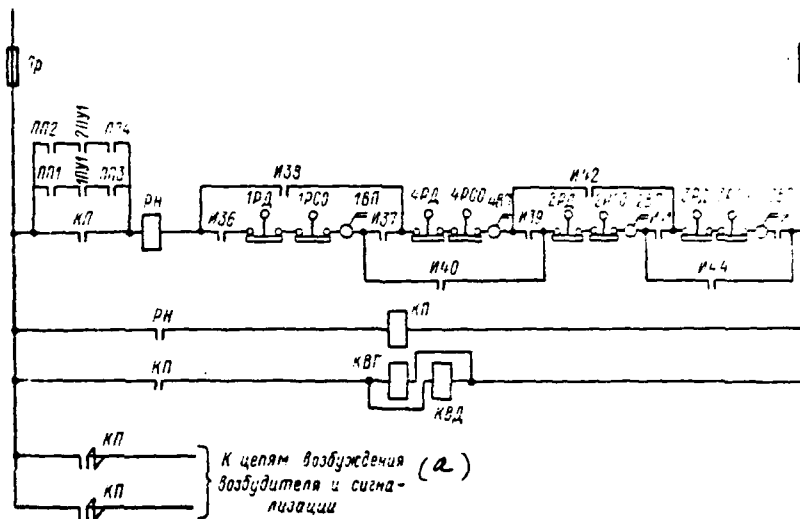


Figure 4.7. "Aktyubinsk" Class Refrigerator Ship GEU Protection Circuit. a--To exciter and indication field circuits.

relays 1RDV-4RDV in the cooling system. In addition, there are diesel readiness switches 1VPN-4VPN in each diesel generator protection circuit.

There is no need for an intermediate contactor (KP) because relay RN contacts are connected to the field contactor coil circuit. Diesel control circuits are connected to the circuit by selector switch 1I, 2I contacts in such a way that, when any diesel generator is cut out of the overall circuit, its protection circuits also are cut out. The circuit depicted in Figure 4.8 corresponds to /147 a main current circuit (Figure 2.9) with two selector switches (one for each two generators), which sharply increases the circuit's flexibility in comparison to the previous one. Selector switch contact closure is shown in Table 4.2.

GEU protection circuit operating from a constant current system. A car ferry GEU protection circuit operating from a constant current system is shown in Figure 4.9. The circuit provides overvoltage protection. The overvoltage relay coil is connected directly to the generator armature circuit, while its contact is connected to the main propulsion motor field contactor coil and intermediate contactors 1KP-2KP coil circuits. Generator and main propulsion motor field circuit feed ceases when RM trips. Current limitation protection

(a)

Положение выключателя	Режим работы (b)	(c) К схеме на рис. 3.12							(d) К схеме на рис. 4.7							
		I29	I37	I31	I42	I37	I44	I45	I47	I37	I38	I39	I40	I41	I42	I44
0																
1	G1-G4 на Дн и Дк	x	x	x	x				x	x	x					
2	G1, G3, G4 на Дн и Дк (G2 от- ключен) (2)	x			x	x			x	x						
3	G1-G3 на Дн и Дк (G4 отключен) (2)	x			x	x			x				x	x		
4	G2-G4 на Дн и Дк (G1 отк- лючен) (2)	x			x	x				x	x				x	
5	G1, G2, G4 на Дн и Дк (G3 от- ключен) (2)	x			x	x			x	x		x				
6	G1, G2 на Дн (G3 и G4 отк- лючены) (2)	x	x				x		x				x			
7	G3, G4 на Дк (G1 и G2 отк- лючены) (2)			x	x			x		x					x	

Table 4.1. Selector Switch Contact Closure. a--Selector switch [IP] position; b--Operating mode; c--For Figure 3.12 circuit; d--For Figure 4.7 circuit; e--I29-I44; 0-7: Designate generators running stern and pump motors or those that are cut out. (1) - to; (2) - cut out

is provided by a three-winding exciter, which limits the current in the main circuit to 2400 A.

Zero protection here is somewhat more complicated than in previous circuits and is accomplished by control station 1PU-2PU contacts closed in the zero position.

Delay relay 1RZm-2RZm coils are fed via these contacts. Tripping, the /148 delay relays close the 1RZm and 2RZm contacts in the 1KVD and 2KVD circuit and, in addition, contacts 1RZm and 2RZm in main propulsion motor armature shunting contactor 1KD and 2KD circuit.

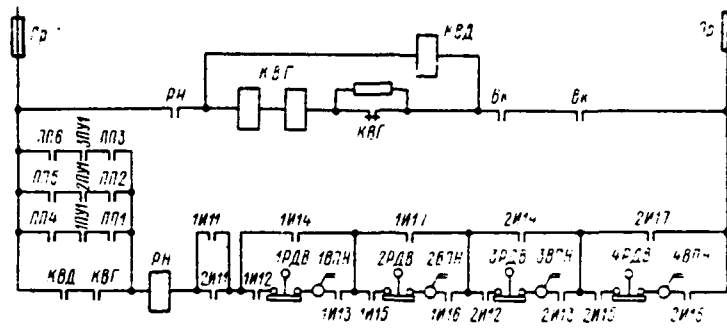


Figure 4.8. "Mirnyy" Class Whaler GEU Protection Circuit.

(a)

Поло- жение ИП	Режим работы	(c)	1И11 2И11	1И12 2И12	1И13 2И13	1И14 2И14	1И15 2И15	1И16 2И16	1И17 2И17
0									
1	Г1, Г3 на Д1, Д2		×	×	×				
2	Г1 на Д1, Д2		×	×	×				
3	Г3 на Д1, Д2								

Table 4.2. Selector Switch Contact Closure (See Figure 4.8 Circuit).  
a--Selector switch position; b--Operating mode; c--1I11-1I17 and 2I11-2I17. Designates generators running motors. (1) - to

Contactors 1KVD and 2KVD, tripping, close their contacts 1KVD and 2KVD in the main propulsion motor field winding circuit, as well as blocking contacts 1KVD and 2KVD in the intermediate contactor 1KP-2KP contact. These contactors, tripping, use their own contacts to close the contactor KVG coil circuit and, with other contacts, shunt delay relay 1RZm and 2RZm contacts in the contactor 1KVD-2KVD coil circuit. Thus, it is possible to move the control stations out of zero position after the relays and contactors trip.

1PI and 2PU contacts will open after disappearance of voltage when the control station is moved from the zero position. Relays 1RZm and 2RZm will not receive feed after repeat restoration of voltage and the circuit will not be restored. Relay 1RZm and 2RZm contacts in the contactor circuit, which shunt the main propulsion motor armatures, do not open instantaneously, but with a



GEU protection circuit for dual-shaft vessels with generator switching to both shafts. A more complex protection circuit for dual-shaft vessel GEU is one in which some of the generators can run the main propulsion motors of both shafts. A protection circuit for a similar plant is shown in Figure 4.10. The GEU's excitation circuit is examined in Chapter 3 (see Figure 3.24) and contact closure is shown in Table 4.3.

(a)

Положе- ние ШШ	Режим работы	(c)															
		1127	1128	1129	1130	1131	1132	1133	1134	1135	1136	1137	1138	1139	1140	1141	
0																	
1	Г1 и Г2 (1) на Д1	x	x	x	x												
2	Г1 на Д1, Г2 на сеть(2)	x	x			x											
3	Г1 на сеть(2) Г2 на Д1 (1)			x	x	x											
4	Г1 на сеть(2) Г2 на Д1 и Д2 (1)			x	x	x											
5	Г1 на Д1, Г2 на Д2 (1)	x	x					x	x	x	x						

Table 4.3. Selector Switch 1I and 2I Contact Closure (For the Figure 4.10 Circuit). a--Selector switch position; b--Operating mode; c--1126-1148. Designates generators running motors or the network. (1) - to; (2) - to network

The protection circuit provides overvoltage protection by means of relays RM1 and RM2, whose coils are connected in parallel to generator additional pole and compensating windings.

Relay 1RM and 2RM contacts are connected to the relay 1RN-2RN coil circuit; relay 1RN and 2RN contacts to the exciter field contactor KVV coil circuit; contactor KVV contacts to exciter separately-excited winding potentiometric regulator circuit, while the blocking contact is connected to the generator /151 field contactor KVG coil circuit. The first KVG contact is in the main propulsion motor field contactor 1KVD-2KVD coil circuit, while the second is connected



Diesel generator G2 and G4 protection circuits can be connected to the protection circuits of both main propulsion motors. For example, if G2 is running D2, then the G2 protection circuit in the D1 circuit is shunted by contact 1I31, while 1I28-1I29 are open; selector switch 2I contacts are open, with the exception of 2I34-2I36 since switch 2I must be in the zero position. The G2 protection circuit is connected to the D2 circuit by selector switch 1I32, 1I33 contacts.

The circuit (Figure 4.10) envisions protection against a pressure drop in the main propulsion motor lubrication system by means of relays 1RD-2RD, whose contacts are connected to the intermediate relay 3RPr coil circuit. The 3RPr contacts are located in the 1RN or 2RN coil circuit.

Relay 1RD or 2RD opens the contacts in the relay 3RPr coil circuit in the event of a pressure drop in the forced lubrication system, which deenergizes and breaks the 1RN or 2RN circuit. The latter removes voltage from all field circuits.

One other special feature of the circuit should be noted. When, for example, G2 is running two series-connected main propulsion motors D1 and D2, then signals from the lubrication pressure relays of both main propulsion motor are connected to the protection circuit. And, since 1I34 will open, then the circuit is closed by contact 4RPr from the D2 circuit, which in turn trips from 2RD via intermediate relay 3RPr.

Zero protection, as in all previous circuits, is accomplished by control station 1PU1 contact, which is shunted by a exciter field contactor KVV contact.

Icebreaker "Lenin" GEU protection circuit. A protection circuit for one GEU shaft on the atomic icebreaker "Lenin" is shown in Figure 4.11. The circuit envisages the following types of protection: overvoltage protection by means of relay MUZ (the relay coil is connected to the output of magnetic amplifier MUZ, relay contacts are connected to the contactor 3KZ and 4KZ coil circuit, whose contacts remove feed from all this loop's field circuits) and protection against a decrease in turbogenerator voltage by means of relays 2RST2 and 4RST2. Relays 2RST2 and 4RST2 open their contacts if turbogenerator rotational speed decreases more than 50% and cuts out all the given loop's circuits. /152



circuits since three-winding exciter current windings and amplidyne current feedback windings are connected not in series to the main current circuit, but in parallel to additional pole and compensating windings. Therefore, one cannot rule out breaks in the circuits in these windings, which lead to dead-end short circuits. Only overvoltage protection can prevent these.

Zero protection is accomplished in almost an identical manner in all of /153 circuits examined. Field contactor coils are connected to the protection circuit in some overall circuits (see Figures 4.2, 4.4-4.6, 4.9), while voltage relays acting in turn upon field contactor coils are used in others.

The recommendation should go to connecting sensitive voltage relays RN, having only one contact RN connected to the field contactor coil circuit, to the protection circuit. It is desirable to shunt of control station contacts providing overvoltage protection by means of field contactor blocking contacts, as was the case in the circuit shown in Figure 4.10. Protection with the contactors in this circuit is less reliable since the contactor coils may release their contacts during a more profound (up to 40-50%) voltage decrease, which is undesirable.

As experience showed, it is advisable to disconnect generator field windings from three-winding exciter armatures since there have been occasions of generator self-excitation when generator and main propulsion motor field circuits are cut out by auxiliary pole winding fluxes, given a collected main current circuit and rotating diesel generators, resulting in an intolerable increase in main circuit current. If generator windings are not disconnected from three-winding exciter armatures, then the latter's differentially-compounded windings counteract generator self-excitation. Thus, use of generator field contactors KVG in the circuits is not recommended since their contacts break the generator field winding circuit, disconnecting them from three-winding exciters.

Protection against primary motor reversals, accomplished in various ways, is envisioned in the circuits shown: for centrifugal relays, pressure relays in the motor lubrication system, from pressure relays in the diesel cooling system. Protection provided by a relay in the diesel cooling system has proven to be the best and therefore can be recommended.

Protection against a pressure drop in a main propulsion motor lubrication system is not present in all circuits. Malfunctions in this system can lead to serious main propulsion motor breakdowns. Therefore, one should recommend use of the aforementioned type of protection in all circuits for main propulsion motors using a forced bearing lubrication system.

One can overlook the remaining protections and, in particular, protection against main generator and main propulsion motor electric cooling fan stoppage. Malfunctions can be indicated by the indication system alone.

Automated diesel generators having automatic remote control (DAU) systems are finding more and more use in modern GEU. The requirement for protection for fresh water and oil coolant pressure decreases when a diesel generator has DAU systems since the system issues an instruction to cut out the diesel when breakdowns occur.

#### § 4.2 GEU Indication Circuits

/154

Indication types and elements in GEU systems. A light and sound indication system is used to monitor GEU electrical equipment operation to warn of impending abnormal operating modes.

Many different types of indication exist in electrical propulsion plants. We will list several:

- indication of the presence of voltage in appropriate circuits of the overall GEU circuit;
- indication of GEU operating modes;
- instruction indication -- of the requirement to carry out appropriate instructions, and response indication -- of execution of these instructions;
- warning indication -- of the imminence of abnormal modes, such as overload, overheating, and so on;
- alarm indication -- of disruption of the normal operation of individual types of GEU equipment;
- indication of the proper circuit arrangement;
- indication of correct functioning of electromagnetic interlocking;

indication of the operation of main generators and main propulsion motors, their cooling systems, bearings;

indication of the operation of diesels, of lubrication and coolant water temperature and pressure;

indication of the operation of auxiliary mechanisms, main generator and main propulsion motor electric fans, main propulsion motor and diesel oil pumps, main generator and main propulsion motor air cooler circulating coolant pumps, diesel and exciter unit air cooler circulating pumps, and so on.

Incandescent lights are the basic indication elements in electrical propulsion plant circuits.

It should be considered that indicator lights, as a rule, must be connected via their own individual fuses so that short circuits in indicator light circuits are not reflected in the operation of those circuits in the overall GEU circuitry that the indicator lights indicate.

Bells, howlers, and ratchets also are used as audible signals along with indicator lights in alarm and warning indications.

One other indicator type exists to show temperature -- heat indicators. The most widespread are the TS-100, which can provide remote temperature readings and even influence protection elements. These indication elements are used to measure main generator and main propulsion motor bearing temperatures and this machinery's coolant air temperature.

Indication usually is multistage, i. e., all required indicator types /155 are envisioned in direct proximity to the equipment whose operation is being monitored. For example, bifurcated indication elements are placed in the engine room to monitor diesel generator operation, a generalized indication of this operation is supplied to the electrical propulsion board, and so on.

We need to examine indication systems by looking at several specific examples. This will facilitate a more detailed explanation of how these systems are set up. Indication of how electrical power plant circuits are functioning is present, as a rule, in those locations where the GEU equipment is located, on the electrical propulsion board or at the central GEU control station, and in the pilot house.

Indication circuits for GEU with three-winding exciters. We will examine a "Yuzhnyy" class ferry GEU indication circuit.

Light indication at control stations was shown in Figure 3.14: light LZ (green) is on when all GEU circuits are functioning and the circuit is ready for operation; light LK (red) is on when relay RN is cut out due to protection action or when there is some other malfunction in the circuit.

The indication circuit for one GEU shaft on a "Yuzhnyy" class ferry is depicted in Figure 4.12. Indicator light LS1 shows the presence of voltage in the indication circuits: lights LS2 and LS3 are on when RP contacts are closed and indicate a pressure drop in the main propulsion plant lubrication system; light LS2 is installed on the electrical propulsion board, while LS3 is in the pilot house; lights LS4 and LS7 indicate generator G1 and G3 coolant water overheat and come on after generator G1 and G3 coolant water heat indicator 1TVG and 3TVG contacts close. Lights LS5 and LS6 come on after one of the main propulsion motor bearing oil temperature indicator 1TM-4TM contacts closes.

Indicator lights LS2-LS7 are connected in series to the RTS -- alarm indicator relay -- coil, which, when one of the signals trips, closes its own contact in the bell circuit installed in the engine room, on electrical propulsion boards, and in the pilot house, thus supplying an audible indication of a breakdown.

Resistances, which insure that alarm indicator relay RTS trips when there is any alarm signal and even when any indicator light burns out, are connected in series and in parallel with lights LS2-LS7.

Lights LS8-LS10 indicate supply of voltage to electromagnetic interlocking latches, which will be discussed below.

A diesel alarm indication circuit for the GEU aboard the ferry "Yuzhnyy" is presented in Figure 4.13. Light LS1 indicates the presence of voltage in the diesel alarm indication circuit. Lights LS2 and LS4 indicate a malfunction in the first and third diesel lubrication systems, coming on when 1TMD and 3TMD contacts close as a result of increased oil temperature in the diesel lubrication systems.

Lights LS3 and LS5 indicate a malfunction in the diesel cooling system, /156 coming on after cooling water temperature indicator 1TVD-3TVD contacts in the diesel coolant system close.

Interlock relay 1RB or 2RB trips when any of the aforementioned indications trips and closes the fire alarm GB circuit in the engine room. Indicator lights are installed on a special indication panel on the electrical propulsion board.

Padding resistor SSh, whose purpose is to insure tripping of relay RB when indicator lights burn out and tripping of the corresponding relay TMD or TVD, is connected in parallel to each indicator light.

An indication circuit showing the operation of auxiliary mechanisms and malfunctions in main GEU machinery circuits aboard "Aktyubinsk" class refrigerator ships is shown in Figure 4.14. This circuit is an improvement over those depicted in Figures 4.12 and 4.13.

Lights LS1 and LS15 indicate the presence of voltage in the indication circuits. When main propulsion motor fan electric motors start, their starter blocking contacts DV1 and DV2 close the indicator light LS2 and LS3 circuits. Electric fan starter n. r. contacts DV1 and DV2 close the red indicator light /157 LS19 circuit on the electrical propulsion board when there is an emergency disconnect of fan electric motors.

Cutting in of the main or stand-by excitation unit is indicated by white indicator light LS4 or LS5 coming on. Exciter set starter n. r. blocking contacts PVO and PVR close the red indicator light LS20 circuit when there is an emergency disconnect of the exciter sets.

White indicator lights LS6-LS9 light up on the electrical propulsion board when generator G1 and G2 electric cooling fans cut in. Indicator lights LS10-LS11 come on when main propulsion motor bearing oil pumps cut in.

Electrical machinery alarm and warning indication is accomplished by indicator lights: contacts RDM close and red indicator light LS16 on the electrical propulsion board comes on when there is a pressure drop in the main propulsion motor

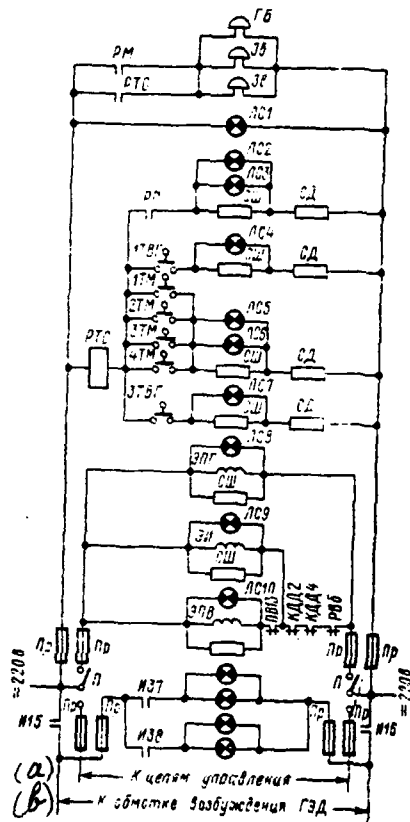


Figure 4.12. "Yuzhnyy" Class Ferry GEU Indication Circuit.  
 a--To control circuits; b--To GED field winding.

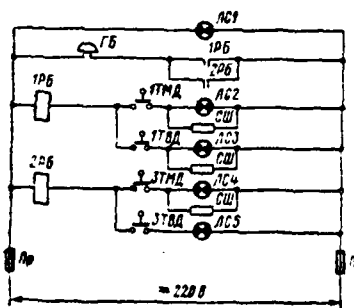


Figure 4.13. "Yuzhnyy" Class Ferry GEU Diesel Alarm Indication Circuit.

bearing lubrication system; heat indicator TVD1 or TVD2 will close its contact in the indicator light LS17 or LS18 circuit when the main propulsion motor armature cooling air temperature exceeds 60° C; heat indicator TMD1 or TMD2 will close its contact in the red indicator light LS17 or LS18 circuit on the electrical propulsion board when main propulsion motor bearings heat up above 80° C. The lights come on and indicate an abnormal situation.

Heat indicators TVG1-TVG4 are installed at the generator cooling air output, while heat indicators TMG1-TMG4, which, tripping, close the corresponding red indicator light LS21-LS24 circuit indicating a malfunction in each generator, are installed on the generator bearings.

In addition, red indicator light LS25, which comes on when the voltage relay RN coil is cut out due to any type of protection tripping, is located on this same electrical propulsion board panel.

Alarm indicator relay RTS is connected in series to each of the aforementioned lights (LS16-LS25). Relay RTS contacts close the audible indication circuit: the bell circuit in the electrical propulsion board compartment and ratchet circuit in the pilot house. An audible indication accompanies any light coming on. Audible signal cancel buttons KS1 and KS2 are connected to each audible indicator circuit so that the audible signal does not continue while the damage is being repaired. When buttons KS1 and KS2 are pushed, their lower (in the circuit) contacts close, closing the coil circuit, which will keep the button in the off position (the audible signal is cut out) until the RTS contact is opened.

Diesel indication circuit. This circuit supplying a generalized indication of a breakdown individually for each diesel is shown in Figure 4.15. Shown here is the circuit for one station installed directly by the appropriate diesel in the engine room and a circuit for a central (generalized) station for all diesels, installed in the electrical propulsion board compartment.

The indication circuit is cut in by switches VP2 (diesel individual stations) and VP1 (central station).

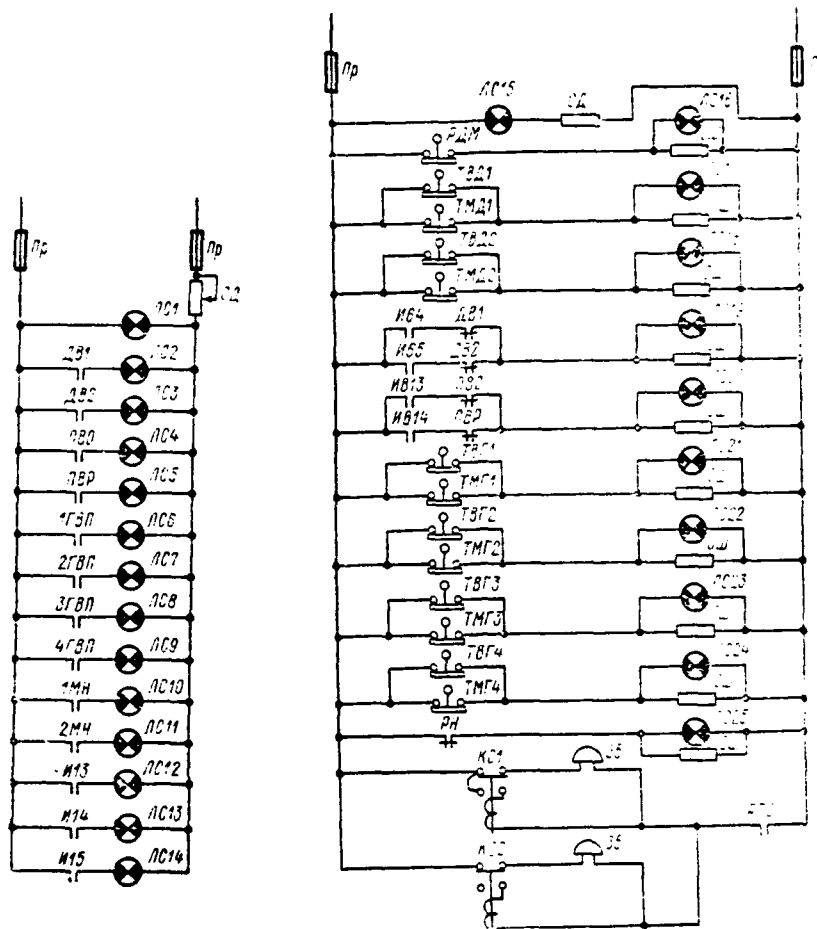


Figure 4.14. Circuit Indicating Operation of Auxiliary Mechanisms and Malfunctions in GEU Main Machinery Circuits.

Fuses in the feed circuit, switch VP2, and three relays are installed at each individual station: RTV -- cooling air temperature relay with two n. z. and one n. r. contacts, RTM -- lubrication system oil temperature relay with two n. z. and one n. r. contacts, and RDM -- lubrication system oil pressure relay with two n. r. and one n. z. contacts.

Relay RTV and RTM normally are open, relays RSDz1 and RSDz2 are deenergized, and the relay RDM contact is closed. Relay RSDz1 and RSDz2 n. r. contacts are closed (green indicator lights LSI and LS2 are on), the relay RSDz3 contact /159 is closed (green indicator light LS3 is on), and RSDz1, RSDz2, and RSDz3 second contacts in the VP2 circuit all also are open.

AD-A114 423

FOREIGN TECHNOLOGY DIV WRIGHT-PATTERSON AFB OH  
FUNDAMENTALS OF ELECTRICAL PROPULSION PLANT DESIGN. (U)  
APR 82 N A KUZNETSOV, P V KUROPATKIN  
FTD-ID(RS)T-1388-80

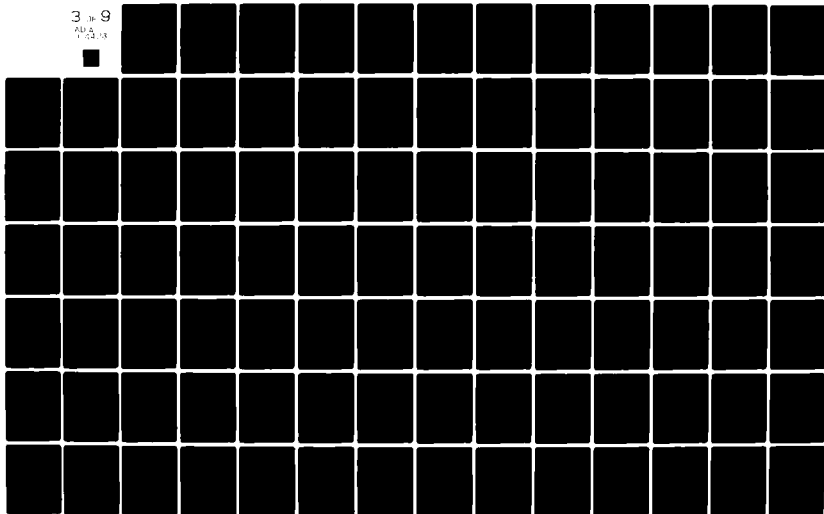
F/G 21/3

UNCLASSIFIED

NL

3 of 9

AD-A  
1703-13



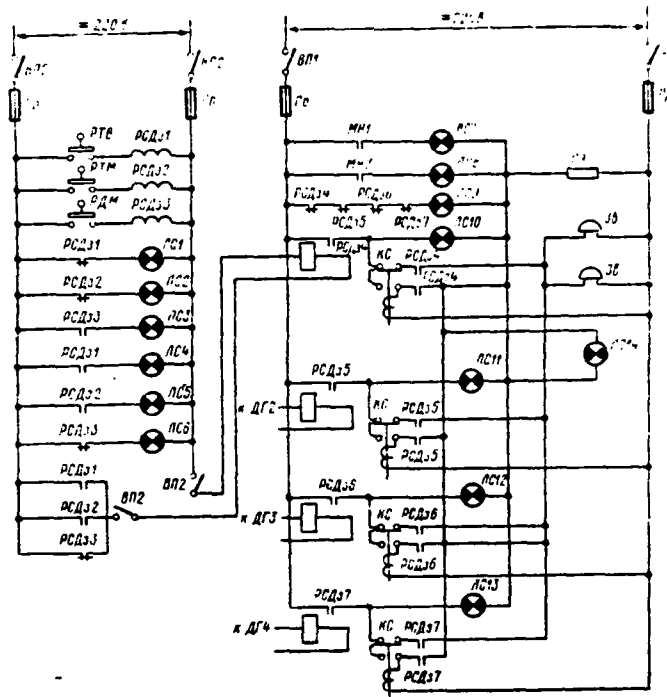


Figure 4.15. Diesel Alarm Indication Circuit.

In the event of intolerable cooling air or oil overheating or when oil pressure drops, red light LS4, LS5, or LS6 light up and one of the RSDz1, RSDz2, or RSDz3 open contacts closes and, via switch VP2, the intermediate relay RSDz4 coil on the central panel cuts in. Relay RSDz4 breaks the n. r. contact in the green indicator light LS9 circuit, the n. z. contact in the red indicator light LS10 circuit of the given diesel closes, and the RSDz4 contact in the audible signal circuit closes via button KS. Light indication is augmented by audible indications Zv in the engine room and at the electrical propulsion boards. The KS coil will keep the button in the activated state when the audible signal cancel button is pressed. Here, the audible signals circuit will be broken and they cease. Red indicator light LS14 will be cut in on the electrical propulsion board by the RSDz4 normally closed contact.

The indication circuit at the central station and from the other diesels by means of relays RSDz5, RSDz6, and RSDz7 is analogous.

As can be seen from the circuit examined, three indications are provided /160 to the individual diesel station: water temperature, oil temperature, and oil pressure, while a generalized emergency indication is supplied to the central station from the diesel, with no elaboration as to piece of equipment or reason.

This type of indication circuit presently is used for all diesels used in electrical propulsion plants.

Ice navigation vessel GEU indication circuits. This circuit on the diesel electric ship "Lena" differs somewhat from those examined above. It has the following indication types: of GEU operating mode or of the number of generators connected to the circuit, of electrical machinery overloads, of abnormal situations in the GEU, and of excessive increases in voltage and rotational speed.

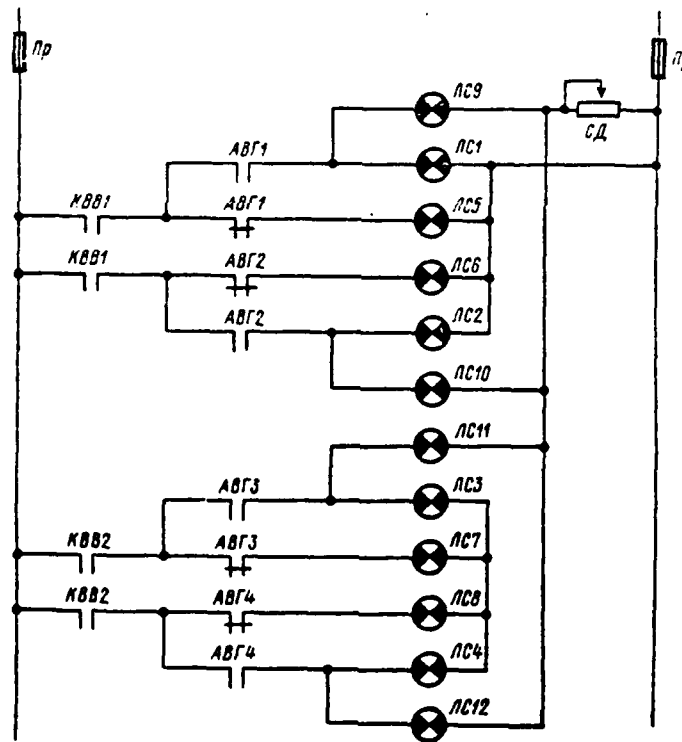


Figure 4.16. Circuit Indicating Number of Connected GEU Generators on the Diesel Electric Ship "Lena."

An indication circuit showing the number of connected generators is provided in Figure 4.16. The indication circuit is accomplished with field contactor KVV1 and KVV2 blocking contacts, field circuit breaker AVG1-AVG4 blocking contacts, and indicator lights LS1-LS12.

KVV1 and KVV2 contacts in the indication circuit close when protection /161 circuits close and coils are cut in. White indicator lights LS1-LS4 light up on the electrical propulsion board and white indicator lights LS9-LS12 come on in the pilot house after the field circuit breakers cut in. Field circuit breaker AVG1-AVG4 n. r. contacts will close when there is an emergency disconnect of any generator's field circuit breaker due to emergency reduction of diesel generator rotational speed and one red indicator light LS5, LS6, LS7, or LS8 will come on.

The indicator lights in the pilot house are connected via adjusting resistance SD, which allows the intensity of the lights to be decreased.

A GEU alarm and warning indication circuit is depicted in Figure 4.17.

Centrifugal relay RTs closes the contact in the red indicator light LS1 circuit in case of an intolerable increase in main propulsion motor rotational speed. Light LS2 comes on at the electrical propulsion board if the barring gear is not cut out (contact VPU will close). Red light LS3 comes on when the entry doors open, since contacts DK behind the electrical propulsion board will close. Indicator light LS4 or LS6 will come on if overvoltage protection RM1 or RM2 trips; current will pass simultaneously via series-connected intermediate relay RPr1-RPr3 coils. The latter close their contacts and shunt relay RM1 or RM2 contacts. The indicator lights remain on until buttons KU1, KU2 are disconnected.

Relays RN1 and RN2 will close their contacts in red indicator light LS5 and LS7 circuits installed on the electrical propulsion board in a similar manner when there is an intolerable increase in voltage at the terminals of EMU armatures -- generator exciters. And, along with this, relay RPr2-RPr4 coils connected in series with the lights shunt relay RM1 and RM2 contacts with their own RPr2-RPr4 contacts. This indication only can be removed by pushing button KU1 or KU2.

Heat indicators TVG1-TVG4 close their contacts in the indicator light LS8 circuit on the electrical propulsion board if there is an increase in generator cooling air temperature.

Increased temperature of the air cooling the main propulsion motor armatures causes heat indicator TVDV1 or TVDV2 to close and indicator light LS9 to come on; indicator light LS10 comes on if the main propulsion motor bearing temperature increases.

Delay relay RZ1 or RZ2 will trip if one of the poles in the main current circuit is grounded or leakage current to ground exceeds 5 A. The relay will close its contact in the bell circuit and an audible indication will be issued.

The audible indication will be intermittent since the relay RZ1 or RZ2 coil will open after tripping by its contacts.

GEU operating mode indication circuits. An additional type of indication /162 exists in electrical propulsion plants -- the supervisory telegraph, used to issue the GEU operating mode.

All control over the propulsion plant is exercised from the pilot house or from bridge extensions, where control stations are located, by which main /163 propulsion motor rotational speed and direction are changed.

But, it is necessary in many instances to provide "economic speed," i. e., prolonged movement at reduced speeds. It then is advantageous to decrease speed not through a change in generator excitation, but by cutting some of the generators out of the circuit or, in other words, by a change in electrical propulsion plant operating mode.

An operating mode change in extant GEU is achieved by switching selector switches on the electrical propulsion board from one mode to another; this is achieved in the engine room by starting and stopping the appropriate diesel generator units.

Instructions to change electrical propulsion plant operating modes are issued from the pilot house by so-called supervisory telegraphs.

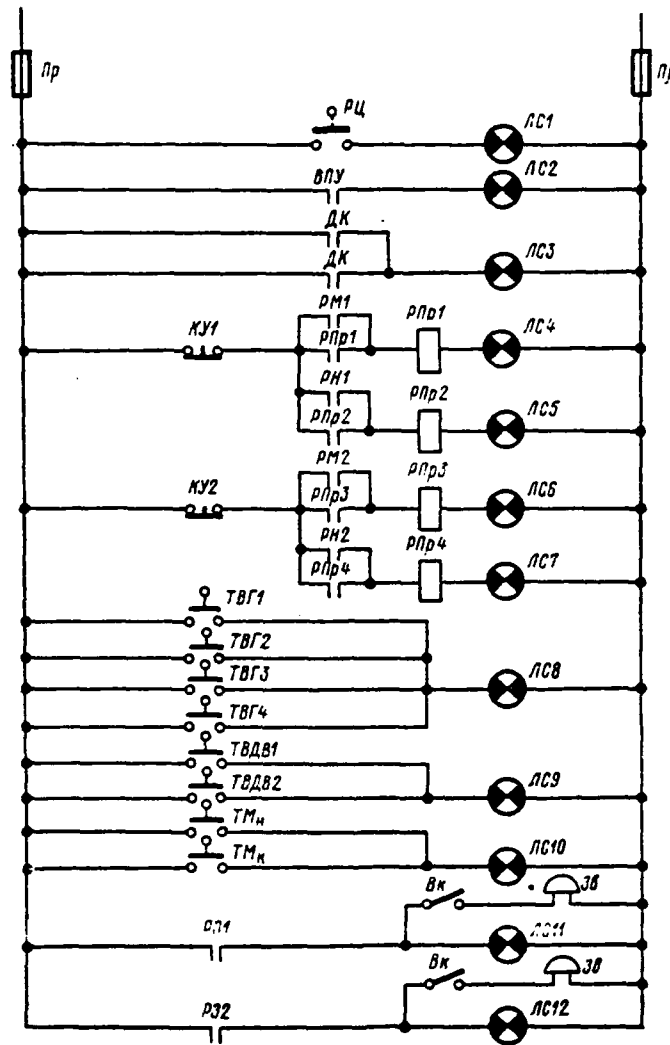


Figure 4.17. GEU Alarm and Warning Indication Circuit Aboard the Diesel Electric Ship "Lena."

The circuit for the GEU supervisory telegraph aboard a "Yuzhnyy" class ferry is shown in Figure 4.18.

An MT913 supervisory telegraph transceiver is installed in pilot house I /164 and has the following detents:

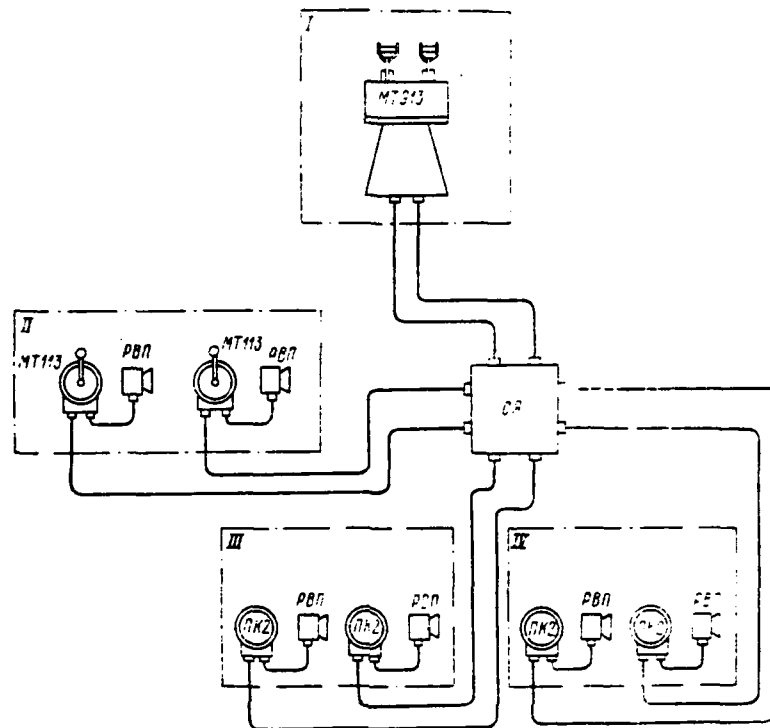


Figure 4.18. GEU Supervisory Telegraph Circuit. PK2 is the engine room telegraph receiver.

For Lever 1

DG1 and DG3 to D1

DG1 to D1, DG3 cut out

DG1 cut out, DG3 to D1

DG1 to network, DG3 cut out

DG1 cut out, DG3 to network

For Lever 2

DG2 and DG4 to D2

DG2 to D2, DG4 cut out

DG2 cut out, DG4 to D2

DG2 to network, DG4 cut out

DG2 cut out, DG4 to network

MT113 supervisory telegraph transceivers with the same detents are installed on the electrical propulsion boards II. Placement of a telegraph lever in the pilot house to a specific scale detent results in an arrow in the receiver on the electrical propulsion board being set to the same detent. An audible ratchet signal goes off automatically at both instruments.

The receiver knob must be set to the same position as the pilot house knob to shut off the audible indication. This demonstrates that the instruction was received and must be accomplished.

Recommendations on GEU indication circuit selection. Encapsulating everything said about indication circuits and generalizing the circuits examined, one can make the following recommendations.

Indications in the pilot house should be kept to a minimum and involve only signals concerning operating mode, i. e., which diesels or turbogenerators are cut in to the circuit, and a general indication of an emergency in the electrical propulsion plant circuit.

Indications at electrical propulsion boards must show which exciter sets, electric fans, and electric pumps are cut in, which selector switches are cut in to which GEU operating mode; indication of generator and main propulsion motor air overheating, of generator and main propulsion motor bearings overheating, of oil pressure in bearings or in the forced lubrication system, of protections tripping, with information on which one tripped; indication of a primary motor emergency (generalized indication).

A malfunction indication must be accompanied by an audible signal. One also should envisage cancellation of this audible indication.

Generator and main propulsion motor bearing and cooling air temperature indicators, indication of the temperature of the cooling water and oil in diesel, generator, and main propulsion motor lubrication systems, indication, with abnormal mode audible signals, of the oil pressure in the diesel lubrication system, indication of lubricant pressure in the main generator and main propulsion motor bearing forced lubrication system, and indication of the temperature, pressure, and specific resistance of the water in the electrical machinery fresh water cooling system must be envisaged in engine rooms III and IV (Figure 4.18).

#### § 4.3 GEU Interlock Circuits

Interlock types and elements in GEU circuits. Electrical propulsion plants

are complicated complexes requiring qualified care and maintenance. GEU circuits have a significant number of switches, circuit breakers, and other commutating devices, which can lead to serious emergencies and problems if not handled properly.

An electrical and mechanical interlock system is used in electrical propulsion plants to prevent improper connections and switchings.

The most important GEU circuit elements are generator selector switches, field winding switches, and station switches. Switching them under voltage can cause damage to main generators and main propulsion motors and lead to destruction of the switches themselves. Therefore, the interlock system applies primarily to this equipment.

Electromagnetic latches are used in most instances as the interlock elements. These latches restrain a special trip and, only when permitted, the electromagnet cuts in and frees the trip from its restraint.

Simplest electromagnetic interlocks. Such interlocks were shown in Figure 4.1. Contacts PP, PIV, and PPP are present in the GEU protection circuit on the diesel electric ship "General Azi Aslanov." These contacts are connected to pedals which must be pushed for switching the generator selector switch, field switch, and station switch, respectively. The trip leaves the shaped washer when the pedal is depressed, freeing the corresponding switch, and the contacts of selector switch PI, field switch PIV, or station switch PPP open at the same time. The RN coil loses feed when any of these contacts open and excitation is removed from the generators and main propulsion motor. Thus, switching will occur in the deenergized state.

In addition, generator selector switches have an electromagnetic interlock provided by electromagnetic latches that do not allow both selector switches to be set in the third and fourth positions simultaneously.

Generators G1 and G4 are connected to loading pump bus bars when the selector switches are in the third and fourth positions. Parallel operation of the generators running the loading pumps is not envisioned and is not allowed. Therefore, an electromagnetic interlock frees the shaped washer seated on the selector

switch shaft, permitting it to be set in the third and fourth positions only when the second switch is in the first, second, or fifth position, i. e., when its blocking contact in the first switch's electromagnetic latch circuit is /166 closed.

Electromagnetic interlock circuits for GEU with three-winding exciters.

The electromagnetic interlock in the GEU circuit on "Yuzhnyy" class ferries is set up somewhat differently. Figure 4.12 showed an electromagnetic latch connection circuit: EPP is a station switch, EI is a selector switch, and EPV is a field switch.

The electromagnetic latch circuit is fed when switch P is in the upper position. Feed is supplied to the main propulsion motor field windings and to exciter protection and excitation circuits when switch P is in the lower position.

Thus, removal of voltage from all field circuits precedes supply of voltage to electromagnetic latches.

Electromagnetic latch EPP, having received feed, immediately allows control station switching. A white indicator light indicates latch readiness.

Electromagnetic latch EI receives feed via field regulator RVb n. r. blocking contacts, which regulates generator voltage when it is running the shipboard network (the regulator must be always introduced), and via diesel starting contactor KDD2 and KDD4 contacts.

Starting contactors KDD1-KDD4 connect the generator armature to the starter storage battery when a generator in the role of starter turns the diesel during start-up.

The armature draws latch EI in, frees the trip, and allows the selector switch to rotate only when all the aforementioned blocking contacts are closed.

There is one more blocking contact in the field switch electromagnetic latch EPV circuit. This is PV23 -- the opposite side GEU circuit field switch

blocking contact required to prevent connection of the stand-by exciter simultaneously to the generators of both screws. If the stand-by exciter is connected to one side's circuit, then the switch PV13 contact will open and the switch itself will be connected to the opposite side's electromagnetic latch switch circuit. As is known, the stand-by exciter can be connected in place of a malfunctioning exciter from any side's GEU circuit, making the interlock with the PV13 contact necessary.

A maritime tug electromagnetic interlock circuit is depicted in Figure 4.19. The following elements in this circuit are protected by a electromagnetic interlock: knife switch R in the main current circuit by electromagnetic latch ER, station switch by electromagnetic latch EPP, selector switch by electromagnetic latch EI, and field switch by electromagnetic latch EPV. The electromagnetic latch circuit is connected by switch 1P, which, simultaneously with connection of this circuit, removes feed from generator and main propulsion motor field circuits. Having received feed, electromagnetic latches ER and EPP immediately /167 release trips and provide the opportunity for cutting out the isolator and switching the control station switch.

The field switch EPV electromagnetic latch will cut in only after the field regulator 2RVb blocking contact closes. Regulator 2RVb is for generator voltage regulation when running the shipboard network; the 2RVb contact closes when regulator 2RVb is introduced fully.

It should be noted that placement of isolator R in the GEU main current circuit increases the security of selector switch manipulation since main current contacts will not break the currents created in the residual magnetization voltage main circuit.

Electromagnetic interlock circuits for ice navigation vessels. An electromagnetic interlock circuit for one loop of the GEU aboard an "Amguema" class dry cargo ice navigation vessel is shown in Figure 4.20. Each loop's electromagnetic interlock circuit has four electromagnetic latches: 3EI for the generator G3 selector switch, 4EI for the generator G4 selector switch, 2EPV for the second loop field switch, and 2EPP for the control station switch.

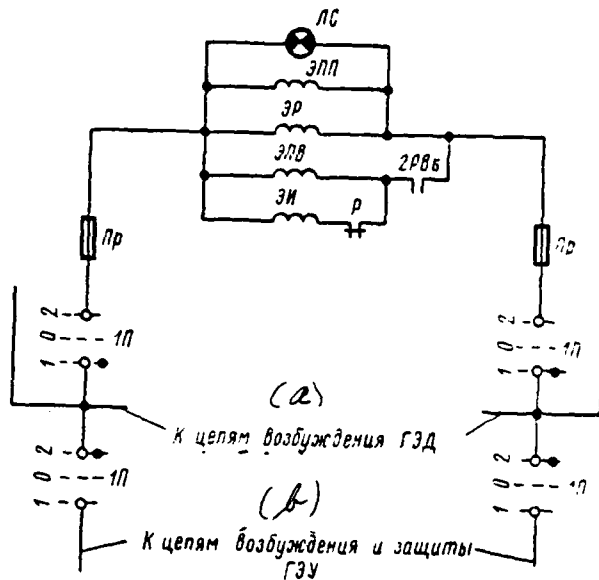


Figure 4.19. Maritime Tug Electromagnetic Interlock Circuit.  
 a--To GED field circuits; b--To GEU field and protection circuits.

Feed is supplied to the electromagnetic latch circuit from a rectifier via field switch 2V. Supplying feed to the electromagnetic latches, field /168 switch 2V with other contacts breaks the field and protection circuits. Electromagnetic latches 3EI, 4EI, and 2EPV, having received feed, release the trips from the washer grooves attached to the shafts of the corresponding switches, allowing their switching to take place.

Electromagnetic latch 2EPP receives feed via switches 1V and 2V of both loops. Thus, excitation is removed from the generators and main propulsion motor armatures of both loops.

The second loop's field switch 1V blocking contact, which prevents the possibility of connecting stand-by exciters simultaneously to both loops, is present in the 2EPV circuit.

A more complex electromagnetic interlock circuit is shown in Figure 4.21. This interlock applies to an electrical propulsion plant circuit in which two generators (one each from each pair running one main propulsion motor) can run

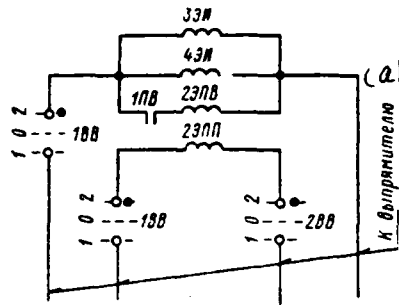


Figure 4.20. "Amguema" Class Ice Navigation Vessel GEU Electromagnetic Interlock Circuit. a--To rectifier.

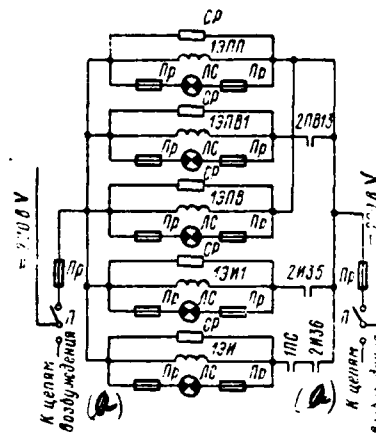


Figure 4.21. GEU Electromagnetic Interlock Circuit with Crossed Generators Running Main Propulsion Motors. a--To field circuits.

the main propulsion motors on different sides or both main propulsion motors simultaneously.

An electromagnetic interlock for the starboard main propulsion motor is shown in the figure. Feed is supplied to the electromagnetic latches via switch P, which simultaneously removes feed from generator and main propulsion motor field circuits.

There are five electromagnetic latches for each main propulsion motor's circuit. There is one electromagnetic latch 1EPP in the station switch, which allows switching to occur as soon as feed is supplied to the interlock circuits.

The field switch has two electromagnetic latches, 1EPV and 1EPV1. The former makes it possible to rotate switch 1PV to the "Main" and "Cut Off" positions as soon as feed is supplied to it; the shaped washer held by latch 1EPV1 is not allowed to rotate in the "Stand-by" position. This latch receives feed only in the event the opposite side's main propulsion motor switch is set in the "Main" and "Cut Out" positions and when its contact 2PV13 is closed. /169

Switch 1I also has two electromagnetic latches, 1EI and 1EI1, each of which

holding its own shaped washer. The switch 2I contact 2I36 is connected to electromagnetic latch circuit 1EI. This contact will close when this switch is in the 0, 1, 2, and 3 positions (i. e., when the opposite side's generators are running their own main propulsion motor).

The latch 1EI shaped washer makes it possible to rotate the selector switch, when contact 2I36 closes, only to those positions in which generators run their own main propulsion motors (i. e., 0, 1, 2, and 3). A second shaped washer held by electromagnetic latch 1EI1, which is fed via opposite side switch 2I contact 2I35, prevents rotation of the switch to positions in which one generator can run the opposite main propulsion motor. Contact 2I35 closes only in the switch 2I zero position, i. e., when all its circuits are open.

Thus, a generator can be cut in to the opposite side's main propulsion motor only when this main propulsion motor's selector switch is set in the zero position, i. e., when all of its generators are cut out.

A white signal lamp is connected through fuses in parallel to each lock; and when the lamp burns it signals that the electromagnetic lock has received power and released the detent.

Recommendations on using electromagnetic interlocks in GEU circuits. As can be seen from the interlock circuit characteristics examined, electromagnetic latches in GEU circuits are used for station switches, field switches, selector switches, and main circuit isolators.

The conclusion follows that station switches, field switches, selector switches, and main current isolators must have electromagnetic latches that permit switchings only when voltage is removed and the main circuit is deenergized. The Rules of the USSR Registry require an interlock which removes voltage from GEU circuits as it enters the electrical propulsion board.

There must be electrical as well as electromagnetic interlocks. For example, interlocks preventing connection of circuits when there is no coolant water in electrical machinery cooling systems, preventing circuit connection when diesels are not warmed up, and so on.

It should be noted in conclusion that most of the GEU circuits presented in this chapter were developed by the collective at the KhEMZ [Khar'kov Order of Lenin Electromechanical Plant] Design Bureau.

## Chapter 5

### Calculation of the Static Characteristics of Direct Current /170 Electrical Propulsion Plants

#### § 5.1 Basic Equations for GEU Statics

Basic assumptions. Proper selection of propellor electric drive parameters is of important significance during electrical propulsion plant design. Unsubstantiated parameter selection can entail increased electrical machinery dimensions, complicated electric propulsion circuits, and underutilization of primary motor power.

Optimal propellor electric drive parameters are established from the results of calculating static characteristics for all possible GEU operating modes. Those parameter values providing the fullest use of primary motor power and a normal load for electrical machinery are determined during these calculations.

Relationships  $(M, U, I) = f(n)$  in established operating modes are called an electrical propulsion plant's static characteristics.

The requirement is to compute parameters for main generators and main propulsion motors for vessels with a prolonged running mode and brief maneuvers, based on the most prolonged mode, i. e., based on the "running in open water" mode. This is applicable for the GEU aboard dry cargo vessels, refrigerator ships, floating bases, lumber ships, and tankers. The GEU aboard ferries can be added to this category, even though they do operate for a considerable time in maneuvering modes and are in the moored mode for a short time. The "running with a load" mode is most applicable for calculations for the main generators and main propulsion motors aboard tugs, which operate in this mode a majority of the time. The moored mode is used for main generators and main propulsion motor calculations for icebreakers, which operate in maneuvering and moored modes.

One needs to consider that vessel resistance to movement increases when running in stormy weather and, consequently, propellor torque increases. Therefore,

when making calculations for the "running in open water" mode, main propulsion motor moment must be increased approximately 15% and generator power 10%. This power increase can be prolonged or brief, depending on design function.

Main propulsion motor rotational speed and propellor torque with a varied number of generators operating are determined as static characteristics are calculated. /171

One should strive for fullest possible use of primary motor power, at the same time not permitting overloading of electrical machinery (main generators and main propulsion motors).

In this book, calculation of static characteristics assumes only series connection of generators. Parallel connection of generators in dc GEU circuits aboard domestic electric ships is not used because, as pointed out in Chapter 1, main generator and main propulsion motor excitation systems become complicated. This does not apply to circuits with individual loops, which we will examine below.

Initial equations for GEU circuits with separate generator excitation.  
Calculation of static characteristics for generator separate excitation circuits is based on a rotational speed equation, main propulsion motor torque equation, and screw moment of resistance equation.

The main propulsion motor rotational speed equation is:

$$n_2 = \frac{mE - I \sum R}{C_e \Phi_2}, \quad (5.1)$$

where

- m - number of series-connected generators;
- E - generator emf, W;
- I - current in the main circuit, A;
- $\sum R$  - main circuit resistance, ohms;
- $C_e$  - constant;
- $\Phi_2$  - main propulsion motor magnetic flux, Wb.

Main circuit resistance is determined from expression

$$\sum R = m(R_{a,r} + R_{b,r} + R_{k,r}) + q(R_{a,d} + R_{b,d} + R_{k,d}) + R_{no}, \quad (5.2)$$

where  $R_{a,r}$  - generator armature winding resistance, ohms;  
 $R_{b,r}$  - generator auxiliary pole winding resistance, ohms;  
 $R_{k,r}$  - generator compensating winding resistance, ohms;  
 $q$  - number of series-connected propulsion motor armatures;  
 $R_{a,d}$  - motor armature winding resistance, ohms;  
 $R_{b,d}$  - motor auxiliary pole winding resistance, ohms;  
 $R_{k,d}$  - generator compensating winding resistance, ohms;  
 $R_{cp}$  - connecting wire resistance, ohms.

If you disregard mechanical losses and losses in the main propulsion motor iron, then the shaft torque equation will take the form

$$M_d = C_m I \Phi_d, \quad (5.3)$$

where  $C_m$  - a constant in the moment equation;  
 $I$  - main circuit current, A;  
 $\Phi_d$  - main propulsion motor magnetic flux, Wb.

The screw moment of resistance equation is: /172

$$M_c = C n_d^2, \quad (5.4)$$

where  $M_c$  - screw moment of resistance, kg-m;  
 $C$  - a constant;  
 $n_d$  - main propulsion motor rotational speed, rpm.

Static characteristics are calculated in relative units. Parameter values in the nominal mode are the base units. The running in open water at top speed mode is accepted as nominal for all vessels except icebreakers and ice navigation vessels. Operation in the moored mode with full power to the screw is accepted as nominal for icebreakers and ice navigation vessels.

§ 5.2 Analytical Methods for Approximate Static Characteristic Calculations

Initial formulas for calculation of static characteristics. We will designate propellor torque, main propulsion motor rotational speed, generator emf, main circuit current, and main propulsion motor magnetic flux, respectively, in the following manner:

in the nominal mode - by  $M_{д. ном.}, n_{д. ном.}, E_{ном.}, I_{ном.},$

when running in open water  $M_{д. с.}, n_{д. с.}, E_{с.}, I_{с.}, \Phi_{д. с.},$

when operating while moored -  $M_{д. ш.}, n_{д. ш.}, E_{ш.}, I_{ш.}, \Phi_{д. ш.},$

Having accepted these designations and considering that  $M_c = M_{д.}$  in the established modes, we will rewrite equation (5.4) for the open water and moored modes

$$M_{д. с.} = C_1 n_{д. с.}^2; \quad M_{д. ш.} = C_2 n_{д. ш.}^2, \quad (5.5)$$

where  $C_1$  - is a constant in the screw torque equation when running in open water;

$C_2$  - is a constant in the screw torque equation in the moored mode.

The form of the formulas for calculation of static characteristics depends on selection of nominal mode.

Accepting the running in open water mode as nominal, with full power to the screw we have

$$M_{д. с.} = M_{д. ном.}; \quad n_{д. с.} = n_{д. ном.}$$

Having divided expression (5.5) by the equation  $M_{д. ном.} = C_1 n_{д. ном.}^2$ , we will get, in relative units,

$$M_{д. с.} = \bar{n}_{д. с.}^2 \quad \text{and} \quad \bar{M}_{д. ш.} = \frac{C_2}{C_1} \bar{n}_{д. ш.}^2. \quad (5.6)$$

Accepting the moored mode as nominal, analogous to the previous we will get /173

$$\bar{M}_{д. с.} = \frac{C_1}{C_2} \bar{n}_{д. с.}^2 \quad \text{and} \quad \bar{M}_{д. ш.} = \bar{n}_{д. ш.}^2. \quad (5.7)$$

Relative values are designated by the line above the symbol.

When primary motor full power is used both while running in open water and during moored operations, the following equality must be provided

$$\overline{M}_{x.c} \overline{n}_{x.c} = \overline{M}_{x.w} \overline{n}_{x.w} = 1. \quad (5.8)$$

Accepting  $\overline{M}_{x.c} = \overline{M}_{x.nom} = 1$ , we will get from expressions (5.6) and (5.8) main propulsion motor rotational speed in the moored mode, whereby power equality is provided:

$$\overline{n}_{x.w} = \sqrt[3]{\frac{\overline{C}_1}{\overline{C}_2}}. \quad (5.9)$$

In a general case, for any intermediate power to the screw we will have

$$\overline{n}_{x.w} = \overline{n}_{x.c} \sqrt[3]{\frac{\overline{C}_1}{\overline{C}_2}}. \quad (5.10)$$

Accepting moored operations as the nominal mode, based on an analogy with the aforementioned, from expressions (5.7) and (5.8) we get

$$\overline{n}_{x.c} = \sqrt[3]{\frac{\overline{C}_2}{\overline{C}_1}}; \quad (5.11)$$

$$\overline{n}_{x.c} = \overline{n}_{x.w} \sqrt[3]{\frac{\overline{C}_2}{\overline{C}_1}}. \quad (5.12)$$

Screw power constancy both when running in open water and during moored operations can be achieved in two ways:

- 1) by a decrease in generator emf, i. e., by a decrease in their field flux given the corresponding increase in main circuit current and constant main propulsion motor field flux;
- 2) by an increase in main propulsion motor field flux given generator constant current and emf.

In the future, for brevity the first method of power maintenance will be called "propulsion motor constant field flux" and the second "constant main circuit current." The second method mainly is used in electrical propulsion plants with automated electrical machinery. If the running in open water mode

is accepted as nominal, then propulsion motor constant field flux means that main generators and the main propulsion motor will have current overloads.

Direct current machinery usually is designed so that brief overloads are /174 permitted in order to obtain high efficiencies. Therefore, operating time in the moored mode must be coordinated with the electromechanical plant.

Motor rotational velocity decreases in proportion to the change in total generator emf, while propellor shaft power does so in proportion to the cube of the rotational speed when some of the generators are cut out of the circuit. Consequently, main propulsion motor field flux must be decreased by cutting resistance in to the field winding in order to increase generator load.

A similar picture unfolds for a change in generator rotational speed as well.

The amount of resistance is selected in such a way that main circuit current and generator emf remain constant.

Considering that generator emf will change proportionally with a change in their rotational speed and accepting the running in open water mode as nominal, it is possible in accordance with equation (5.1) to write the following expression for nominal rotational speed:

$$n_{d, \text{НОМ}} = \frac{mE_{\text{НОМ}} - I_{\text{НОМ}} \sum R}{C_e \Phi_{d, \text{НОМ}}} \quad (5.13)$$

When  $k$  generators are cut out and their rotational speed is decreased to  $n$  rpm, we will have the following for the running in open water mode

$$n_{d, c} = \frac{(m-k) E_{\text{НОМ}} \frac{n}{n_{\text{НОМ}}} - I_{\text{НОМ}} \sum R_k}{C_e \Phi_{d, c}} \quad (5.14)$$

where  $n_{\text{НОМ}}$  — is nominal generator rotational speed, rpm;

$\sum R_k$  — main circuit resistance during operation of  $m - k$  generators, ohms:

$$\sum R_k = (m-k) (R_{a, r} + R_{b, r} + R_{c, r}) + q (R_{a, d} + R_{b, d} + R_{c, d}) + R_{np};$$

$\Phi_{d, c}$  — propulsion motor field flux when running in open water.

Having divided equation (5.14) into (5.13), we get the equation for main propulsion motor rotational speed in relative units:

$$\bar{n}_{\text{д.с}} = \frac{(m-k)\bar{n} - \sum \bar{R}_k}{(m - \sum \bar{R}) \Phi_{\text{д.с}}}, \quad (5.15)$$

where  $\bar{n} = \frac{n}{n_{\text{НОМ}}}$  is the relative generator rotational speed;

$\sum \bar{R} = \frac{\sum R}{R_{\text{НОМ}}}$  — is the relative main circuit resistance when m generators are running;

$R_{\text{НОМ}} = \frac{E_{\text{НОМ}}}{I_{\text{НОМ}}}$  — is hypothetical nominal resistance;

$\sum \bar{R}_k = \frac{\sum R_k}{R_{\text{НОМ}}}$  — is relative main circuit resistance when m -- k generators are running.

In accordance with equation (5.3), main propulsion motor moment in relative units in the case being examined will take the form

$$\bar{M}_{\text{д.с}} = I_c \bar{\Phi}_{\text{д.с}}. \quad (5.16)$$

It is necessary that  $I_c = I_{\text{НОМ}} = 1$ , to insure full primary motor loading. Then considering equation (5.16), we get

$$\bar{M}_{\text{д.с}} = \bar{\Phi}_{\text{д.с}} = \bar{n}_{\text{д.с}}^2. \quad (5.17)$$

Substituting value  $\bar{\Phi}_{\text{д.с}}$  from equation (5.17) in equation (5.15) and solving it for  $\bar{n}_{\text{д.с}}$ , we get

$$\bar{n}_{\text{д.с}} = \sqrt[3]{\frac{(m-k)\bar{n} - \sum R_k}{m - \sum R}}. \quad (5.18)$$

Assuming in equation (5.18) k equals zero and replacing  $\sum \bar{R}_k$  for  $\sum R$  in the numerator, we get the equation for main propulsion motor rotational speed given a decrease in rotational speed of m operating generators to n and constant current in the main circuit.

Assuming in equation (5.18)  $n$  equals one, we get the equation for main propulsion motor rotational speed given  $m - k$  operating generators and constant current in the main circuit.

Substituting value  $n_{x.c}$  from equation (5.18) in equation (5.10), we get the expression for main propulsion motor rotational speed in the moored mode:

$$\bar{n}_{x.w} = \bar{n}_{x.c} \sqrt[3]{\frac{C_1}{C_2}} = \sqrt[3]{\frac{(m-k)\bar{n} - \sum R_k}{m - \sum \bar{R}} \cdot \frac{C_1}{C_2}} \quad (5.19)$$

If power constancy when running in open water and in moored operations is maintained given main propulsion motor constant magnetic flux equalling  $\Phi_{z.ном}$ , then main propulsion motor rotational speed will be determined from expression

$$n_{x.w} = \frac{mE_w - I_w \sum R}{C_1 \Phi_{z.ном}} \quad (5.20)$$

Having divided equation (5.20) into equation (5.13) and having made the transformations, we get the following, in relative units

$$\bar{n}_{x.w} = \frac{m\bar{E}_w - \bar{I}_w \sum \bar{R}}{m - \sum \bar{R}}, \quad (5.21)$$

where

$$\bar{E}_w = \frac{E_w}{E_{ном}}; \quad \bar{I}_w \sum \bar{R} = \frac{I_w}{I_{ном}} \cdot \frac{\sum R}{R_{ном}}$$

Solving equation (5.21) for  $\bar{E}_w$ , we get an expression for determination of generator emf in the moored mode and given main propulsion motor constant magnetic flux: /176

$$\bar{E}_w = \frac{\bar{n}_{x.w} (m - \sum \bar{R}) - \bar{I}_w \sum \bar{R}}{m}, \quad (5.22)$$

where:  $\bar{n}_{x.w}$  is determined from equation (5.9) and  $\bar{I}_w$  given main propulsion motor constant flux from equation (5.6) and equality  $\bar{M}_{x.w} = \bar{I}_w$ , i. e.,

$$\bar{I}_w = \bar{M}_{x.w} = \frac{C_2}{C_1} \bar{n}_{x.w}^2 \quad (5.23)$$

Thus, it is possible to calculate the parameters of all propulsion plant operating modes using equations (5.6), (5.9), (5.10), (5.16)-(5.19), (5.22), and (5.23), i. e., given the different number of generators, envisaged by the circuit, running one main propulsion motor. Results of the calculations will be consolidated into a table.

If one accepts the moored mode as nominal, then we will have main propulsion motor rotational speed equations analogous to the previous one:

a) in the moored mode when  $m - k$  generators are operating and the relative speed of their rotation equals  $n$ ,

$$\bar{n}_{r, w} = \sqrt[3]{\frac{(m-k)\bar{n} - \sum \bar{R}_k}{m - \sum \bar{R}}}; \quad (5.24)$$

b) in the running in open water mode given  $m - k$  generators running and the relative speed of their rotation equals  $n$ ,

$$\bar{n}_{z, c} = \sqrt[3]{\frac{(m-k)\bar{n} - \sum \bar{R}_k}{m - \sum \bar{R}} \cdot \frac{C_2}{C_1}}. \quad (5.25)$$

Initial formulas for calculation of a GEU with automated electrical machinery and with regulation of GED electromagnetic flux. The equations presented above also are applicable for calculation of the static characteristics of electrical propulsion plants with automated electrical machinery and with regulation of main propulsion motor magnetic flux, but they require refinements and additions.

Refinements for these formulas are stipulated by the fact that main propulsion motor magnetic flux is boosted in circuits with automated electrical machinery to decrease main circuit current when the screw is operating in the moored modes. Main propulsion motor flux in these plants is regulated by so-called shut-off circuits. This signifies that as long as the current in the main circuit is less than nominal, no magnetic flux regulation occurs. The circuit begins to act as soon as the main circuit current exceeds its nominal value.

Creation of a main propulsion motor magnetic flux control system which would maintain precise constant current in the main circuit is possible, but /177 it is enormous. Therefore, the systems mentioned are built in such a way that main circuit current is increased somewhat in the moored mode compared to the

running in open water mode. Usually, the increase in current cannot exceed 10% (i. e.,  $1.1 I_{\text{НОМ}}$ ), which is not dangerous for electrical machinery since it is built to withstand a 10% overload for 2 hours. No primary motor overloads will occur since main generator voltage must be decreased in proportion to the current increase. Consequently, power must remain constant.

The amount of main propulsion motor magnetic flux which provides an increase in main circuit current to  $1.1 I_{\text{НОМ}}$  when the screw transfers from the "running in open water" characteristic to the "moored operations" characteristic can be determined from expression (5.3).

Having accepted the running in open water mode as nominal, given main propulsion motor constant flux we get

$$M_{\lambda, w} = C_M I_w \Phi_{\lambda, c} \quad (5.26)$$

In order to decrease current  $I_w$  to  $1.1 I_c$ , one must increase main propulsion motor magnetic flux to  $\bar{\Phi}_{\lambda, w}$ , i. e.,

$$M_{\lambda, w} = C_M 1.1 I_c \Phi_{\lambda, w} \quad (5.27)$$

Equating the right-hand portions of equations (5.26) and (5.27), we get  $I_w \Phi_{\lambda, c} = 1.1 I_c \Phi_{\lambda, w}$ . Solving this expression for  $\Phi_{\lambda, w}$  and converting it into relative units, we get

$$\bar{\Phi}_{\lambda, w} = 0.91 \frac{I_w}{I_c} \bar{\Phi}_{\lambda, c} \quad (5.28)$$

Values  $I_w$  and  $I_c$  were determined given main propulsion motor constant magnetic flux. Therefore, they can be replaced by values  $M_{\lambda, w}$  and  $M_{\lambda, c}$ . Then

$$\bar{\Phi}_{\lambda, w} = 0.91 \frac{M_{\lambda, w}}{M_{\lambda, c}} \bar{\Phi}_{\lambda, c} = 0.91 \bar{M}_{\lambda, w} \bar{\Phi}_{\lambda, c} \quad (5.29)$$

Substituting  $\bar{n}_{\lambda, w}$  from equation (5.9) in equation (5.8), we get

$$\bar{M}_{\lambda, w} = \sqrt[3]{\frac{C_2}{C_1}} \quad (5.30)$$

Substituting  $M_{x.w}$  from equation (5.30) in (5.29), finally we will have

$$\bar{\Phi}_{x.w} = 0,91 \sqrt[3]{\frac{C_2}{C_1}} \bar{\Phi}_{x.c}. \quad (5.31)$$

Based on expression (5.15) and considering expression (5.31), we can write the following equation for rotational speed in the moored mode, given regulation of main propulsion motor magnetic flux,  $m - k$  generators operating, and generator rotational speed  $\bar{n}$  rpm: /178

$$\bar{n}_{x.w} = \frac{0,91 (m - k) \bar{n} - 1,1 \sum \bar{R}_k}{0,91 (m - \sum \bar{R}) \sqrt[3]{\frac{C_2}{C_1}}},$$

or

$$\bar{n}_{x.w} = \frac{(m - k) \bar{n} - 1,21 \sum \bar{R}_k}{m - \sum \bar{R}} \sqrt[3]{\frac{C_1}{C_2}}, \quad (5.32)$$

where coefficient 0.91 in the first member of the right side's numerator considers the decrease in generator emf to  $0,91 E_{nom}$  to avoid overloading the primary motor when the main circuit current increases to  $1,1 I_{nom}$ .

Main propulsion motor field currents from its magnetization curve are determined for values  $M_{x.w}$ ,  $\bar{n}_{x.w}$ ,  $\bar{\Phi}_{x.w}$  found from expressions (5.30)-(5.32). Analytical determination of field currents is impossible due to the nonlinear relationship between main propulsion motor magnetic flux and field current. The control system is computed based on the main propulsion motor field currents obtained.

Field currents and the amounts of standardizing and additional resistances are determined taking into account the computed values of the basic parameters compiled into a table by modes. We have two different GEU modes  $I$ ,  $E_r$ ,  $\Phi_r$ ,  $\Phi_x$ ,  $n_x$ ,  $M_x$  from the table of basic parameters computed from the aforementioned equations. Knowing these values, it is possible to calculate all GEU circuit resistances and remaining parameters.

#### Calculation of additional and standardizing resistances in GEU field circuits.

A GEU schematic is presented in Figure 5.1. Calculation of circuit resistances should begin with the main propulsion motor field winding circuit. It is advisable

when calculating main propulsion motor circuits to select field winding resistance in such a way that nominal field current will be provided at a voltage comprising 0.6-0.8 of the feed source voltage for the possibility for boosting the excitation. Excess voltage must be suppressed in standardizing resistance SU.

Knowing main propulsion motor magnetic flux  $\Phi_1$ , one will find main propulsion motor field current from the magnetization curve or from the idling characteristic (Figure 5.2). For example, emf  $E_1$  corresponds to field current  $i_1$ ,  $E_{НОМ}$  corresponds to  $i_{НОМ}$ . Voltage in the main propulsion motor field winding is  $U_{в.д} = i_{в.д} r_{в.д}$  (Figure 5.1). Discharging resistance SR, whose value  $r_{п.д}$  is accepted usually as equal to  $r_{п.д} = (6-10) r_{в.д}$ , is connected in parallel to the field winding. Taking discharging resistance into consideration, current in the main propulsion motor field circuit will equal

$$i_2 = \frac{U_{в.д}(r_{в.д} + r_{п.д})}{r_{в.д} r_{п.д}}$$

Standardizing SU and additional SD resistances are connected in series /179 with the main propulsion motor field winding.

The amount of standardizing resistance intended, as pointed out above, for suppression of an excess of voltage in the field winding and to set the requisite field current value, is taken as equal to

$$r_{с.д} = (0,2 - 0,3) \frac{U_{в.д} r_{п.д}}{r_{в.д} + r_{п.д}}$$

The value of the additional resistance intended to weaken main propulsion motor magnetic flux in several modes is taken as equal to

$$r_{д.д} = 0,6 \frac{r_{в.д} r_{п.д}}{r_{в.д} + r_{п.д}}$$

with the capability for fine adjustment, which makes it possible to change field current 60%.

Calculation of generator field circuits will occur in an identical way. Requisite field current  $i_f$  will be found from the idling characteristic for

emf  $E_g$  (Figure 5.2) and voltage in the generator field winding  $U_{g,r} = i_r r_f$ .  
 Current in the generator field circuit considering discharging resistance equals

$$i_r = \frac{U_{g,r} (r_f + r_{p,r})}{r_f r_{p,r}}$$

where  $r_f$  is generator field winding resistance.

Additional resistances, as a rule, are not connected to generator field /180 windings. The values of the standardizing resistances in generator field winding circuits are calculated from expression

$$r_{y,r} = 0,3 \frac{r_f r_{p,r}}{r_f + r_{p,r}}$$

Two generator field windings are connected to the field armature in the circuit (Figure 5.1). Therefore, current in the exciter armature circuit will be  $i_{a,r} = 2i_r$ .

Exciter electromotive force will be determined from the expression

$$E_B = 2i_r' (r_{a,a} + r_{a,b} + r_{np}) + i_r' \frac{r_f r_{p,r}}{r_f + r_{p,r}} + i_r' r_{y,r}$$

where  $r_{a,a}$  is exciter armature winding resistance;  $r_{a,b}$  is exciter auxiliary pole winding resistance;  $r_{np}$  is connecting wire resistance;  $r_{y,r}$  standardizing resistance portion introduced in the generator field winding.

The recommendation is to take exciter electromotive force as equalling 1.5-2.0 of the voltage in the generator field winding for the capability of adjusting characteristics as the circuit is tuned.\*

### § 5.3 Graphic-Analytical Method of Calculating Static Characteristics of GEU with Three-Winding Exciters

Initial data for a graphic-analytical construction. As was mentioned above,

---

\*The exciter voltage reserve for icebreaker GEU is increased to a value larger by a factor of 3-5.

GEU with three-winding exciters having three field windings found wide use in domestic practice in 1949-1950. They are separate excitation, self-excitation, and differentially-compounded windings.

Calculation of the static characteristics of GEU main generators with three-winding exciters is impractical using the methods enumerated in § 5.2 due to the non-linearity of the relationships of electromotive forces, magnetic fluxes, and generator and exciter field currents.

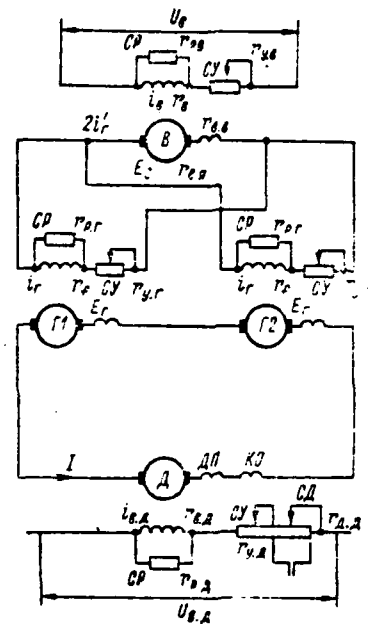


Figure 5.1. GEU Schematic.

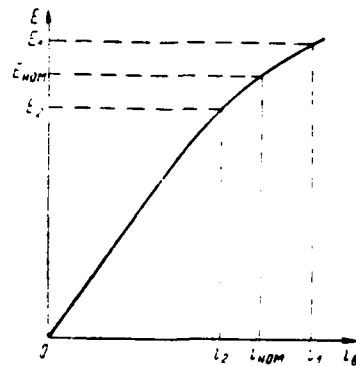


Figure 5.2. DC Machine Idling Characteristic.

emf  $E_g$  (Figure 5.2) and voltage in the generator field winding  $U_{g.f} = i_f r_f$ .  
 Current in the generator field circuit considering discharging resistance equals

$$i'_f = \frac{U_{g.f} (r_f + r_{p.f})}{r_f r_{p.f}}$$

where  $r_f$  is generator field winding resistance.

Additional resistances, as a rule, are not connected to generator field windings. The values of the standardizing resistances in generator field winding circuits are calculated from expression

$$r_{y.f} = 0,3 \frac{r_f r_{p.f}}{r_f + r_{p.f}}$$

Two generator field windings are connected to the field armature in the circuit (Figure 5.1). Therefore, current in the exciter armature circuit will be  $i_{a.e} = 2i'_f$ .

Exciter electromotive force will be determined from the expression

$$E_b = 2i'_f (r_{a.a} + r_{a.p} + r_{np}) + i'_f \frac{r_f r_{p.f}}{r_f + r_{p.f}} + i'_f r_{y.f}$$

where  $r_{a.a}$  is exciter armature winding resistance;  $r_{a.p}$  is exciter auxiliary pole winding resistance;  $r_{np}$  is connecting wire resistance;  $r_{y.f}$  - standardizing resistance portion introduced in the generator field winding.

The recommendation is to take exciter electromotive force as equalling 1.5-2.0 of the voltage in the generator field winding for the capability of adjusting characteristics as the circuit is tuned.\*

### § 5.3 Graphic-Analytical Method of Calculating Static Characteristics of GEU with Three-Winding Exciters

Initial data for a graphic-analytical construction. As was mentioned above,

---

\*The exciter voltage reserve for icebreaker GEU is increased to a value larger by a factor of 3-5.

The graphic-analytic method can be used to calculate the static characteristics of GEU with three-winding exciters. It is necessary to have the relationships  $M_x = f(n_x)$  of the screw when running in open water and during moored operations and the screw nominal moment of resistance and rotational speed  $M_{x, \text{nom}}, n_{x, \text{nom}}$ , corresponding to full propellor shaft power.

On propeller curves  $M_x = f(n_x)$  we plot a curve equal to power  $M_x n_x = \text{const.}/181$  from which we determine propellor torque and rotational speed in the moored mode  $M_{x, \text{w}}, n_{x, \text{w}}$ .

The following must be determined for each operating mode: generator emf  $E$ , main circuit current  $I$ , generator field current  $i_f$ , and exciter emf  $E_e$ .

Main propulsion motor characteristic  $M_x = f(n_x)$  when generators are excited from a three-winding exciter must be calculated in such a way as to provide propellor shaft power constancy from the running in open water to the moored operation mode.

One should have 10-15% less current in the main circuit than the nominal rated current for nominal generator voltage for the running in open water mode to avoid large electrical machinery current overloads in the moored mode.\*

In accordance with what has been stated, we have:

a) for the running in open water mode

$$M_{x, c}, n_{x, c}, E_c = E_{\text{nom}}, I_c \approx 0,85 I_{\text{nom}},$$

where  $I_{\text{nom}}$  is main propulsion motor current from data supplied by the electro-mechanical plant;

b) for the moored mode

$$M_{x, w}, n_{x, w}, E_w = E \frac{I_{\text{nom}}}{I_w}, I_w = I_{\text{nom}} \frac{M_{x, w}}{M_{x, c}}.$$

The corresponding field currents  $i$  for the running in open water and moored

---

\*If the purpose for which the system is designed does not call for prolonged operation in the moored mode, it is permissible to accept  $I_{\text{nom}} = I_c$ . Operating time in the moored mode in this case is coordinated with the electromechanical plant.

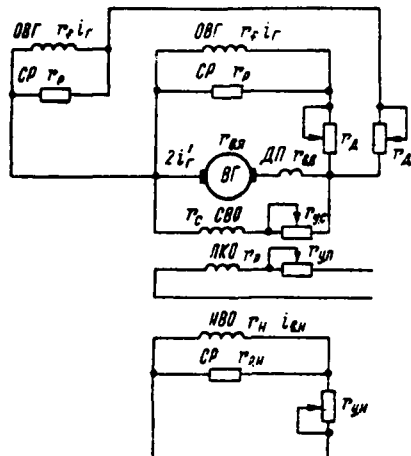


Figure 5.3. Main Generator Field Winding Connection Circuit.

modes are determined in accordance with accepted generator emf values  $E_c$  and  $E_w$  based on the idling characteristic.

It should be kept in mind that direct determination of generator field currents from the idling characteristic is permissible only for compensated machinery. Electromechanical plants must supply curves  $U = f(i_f)$  where  $I = \text{const}$  for values  $I = 0,5 I_{\text{НОМ}}$ ;  $I = I_{\text{НОМ}}$ ;  $I = 1,25 I_{\text{НОМ}}$  to do calculations for uncompensated generators.

One must consider discharging and additional resistances connected in series and in parallel to field windings (Figure 5.3) when determining exciter emf.

Given  $m$  generators, exciter armature circuit total resistance comprises /182

$$r = r_{\text{в.к}} + r_{\text{н.к}} + r_{\text{оп}} + \frac{r_{\text{а}}}{m} + \frac{r_f r_p}{m(r_f - r_p)}, \quad (5.33)$$

where  $r_{\text{оп}}$  is connecting wire resistance.

Current in the generator and discharging resistance field winding circuit equals

$$i_r' = i_r \left( \frac{r_l + r_p}{r_p} \right). \quad (5.34)$$

Exciter electromotive force will be determined from equation

$$E_s = m i_r r \left( \frac{r_l + r_p}{r_p} \right). \quad (5.35)$$

If the electromechanical plant does not supply the data, the following values can be accepted for the discharging and additional resistances:

$$r_p = (6-10) r_f; \quad r_{200n} = 0,1 r_f.$$

A graphic-analytical construction of generator external characteristics.

We will construct exciter idling characteristic  $E_s = f(F)$  —, the relationship of exciter n. s. to field n. s. (curve 1 in Figure 5.4), to determine three-winding exciter winding n. s. We plot one generator's field current  $i_{f_1}$  along the X-axis of this curve along with exciter n. s. in an undefined scale. We will construct the relationship of generator field current to exciter emf  $i_r' = f(E_s)$ , curve 2, and the main generator idling characteristic  $E = f(i_r)$ , curve 3, on these same coordinate axes from equation (5.35).

We drop perpendiculars  $aa_2$  and  $bb_2$  on the X-axis from points  $a_2$  and  $b_2$  in the generator idling characteristic, which correspond to the emf when running in open water and during moored operations. Segments  $Oa$  and  $Ob$  will equal generator field currents  $i_{fc}$  and  $i_{fm}$ , respectively.

We get the corresponding exciter emf  $E_{s.c}$  and  $E_{s.m}$  (segments  $aa_1$  and  $bb_1$ ) at points  $a_1$  and  $b_1$  where lines  $aa_2$  and  $bb_2$  intersect lines  $OA$ .

We run straight line  $cc_2$  parallel to the X-axis through point  $a_1$ . Segment  $cc_1$  equals exciter total n. s. when running in open water at full speed:

$$cc_1 = F_n + F_{cB} - F_n. \quad (5.36)$$

Knowing the number of differentially-compounded winding turns  $w_n$  and main

circuit current  $I_c$  when running in open water, it is possible to determine the n. s. created by the differentially-compounded winding:

a) when the differentially-compounded winding is connected directly to the main current circuit

$$F_n = \omega_n I_c; \quad (5.37)$$

b) when the differentially-compounded winding is connected in parallel to the main propulsion motor compensating winding and auxiliary pole winding. /183 In this case, we do the calculation in the following manner.

We find the voltage drop in main propulsion motor windings:

$$\Delta U_{n. k. a} = I_c (R_{n. a} - R_{k. a}). \quad (5.38)$$

We determine the current in the differentially-compounded winding considering the voltage drop in connecting wires, which we accept as equalling 1 V:

$$i_n = \frac{\Delta U_{n. k. a} - 1}{r_a + r_n} = \frac{I_c (R_{n. a} - R_{k. a})}{r_a + r_n}. \quad (5.39)$$

where  $r_a$  is the standardizing resistance in the differentially-compounded /184 winding intended for n. s. adjustment;  $r_n$  is differentially-compounded winding resistance.

Differentially-compounded winding n. s. then will equal

$$F_n = \omega_n i_n. \quad (5.40)$$

We plot segment  $c_1 c_2$  equal to  $F_n$  on an extension of straight line  $cc_1$  to the right of point  $c_1$ . Thus, segment  $cc_2$  will equal the sum of the separate winding and self-excitation winding n. s.

Running through point  $b_1$ , segment  $dd_2$ , a portion of which equals the sum of exciter n. s. in the moored mode, and having plotted from point  $d_1$  to the right segment  $d_1 d_2$ , equal to differentially-compounded winding n. s. in the moored mode, we get segment  $dd_2$  equal to the sum of the separate n. s. and self-excitation n. s.

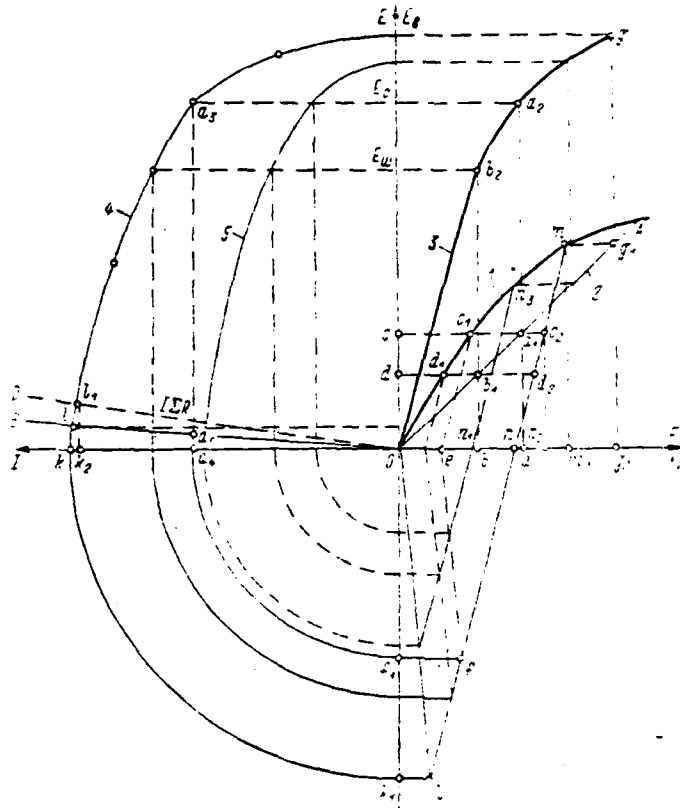


Figure 5.4. Graphic Calculation of a Generator's External Characteristic. 1--Exciter idling characteristic  $E_b = f(I_f)$ ; 2--Relationship of generator field current to exciter emf  $i_f = f(E_b)$ ; 3--Idling characteristic  $E = f(I_f)$ ; 4--Generator external characteristic  $E = f(I)$ ; 5--Generator external characteristic given decreased current in the exciter separate excitation winding.

Having joined points  $c_2d_2$  of the straight line and having continued it to the intersection with the exciter idling characteristic and the X-axis, we get line  $mn$ , providing the sum of separate excitation and self-excitation winding n. s. Having dropped perpendicular  $mm_1$  to the X-axis from point  $m$ , we get segment  $Om_1$  equal to the sum of separate excitation winding  $On$  n. s. and self-excitation winding  $nm_1$  n. s., with an open differentially-compounded winding.

Segment  $Og_2$  equals the field current, while segment  $gg_2$  equals the emf of the main generator when the differentially-compounded winding circuit is broken.

Segments of straight lines parallel to the X-axis included between the exciter idling characteristic and line mn equal the differentially-compounded winding n. s. and, on a certain scale, the main circuit current. Thus, segment  $c_1c_2$  on a certain scale equals current  $I_c$ , segment  $d_1d_2$  equals current  $I_w$ , and segment On equals main propulsion motor moored current.

Running straight lines parallel to the X-axis and measuring the length of the segments included between the exciter idling characteristic and line mn, we get the value of the currents in the main circuit. Dropping perpendiculars from the points of intersection of these segments from straight line OA to the X-axis and continuing them to the intersection with the generator idling characteristic, we get the corresponding generator emf.

Relationship  $E = f(I)$ , curve 4, will be constructed from the resultant data.

The voltage drop in the main circuit  $I\sum R$ , represented by line QB (Figure 5.4), is calculated from the ordinates of this relationship.

The ordinates of line OB decrease by a factor of m, i. e., they will equal  $\frac{I\sum R}{m}$ , given m series-connected generators.

Relationship  $E = f(I)$  of a generator can be constructed graphically.

We plot current I on an arbitrary scale to the left of point O (Figure 5.4). We draw a circle from point O with radius Ok, corresponding to main propulsion motor moored current, to the intersection with the Y-axis (point  $k_1$ ). We run line  $k_1h$  from point  $k_1$  parallel to the X-axis to the intersection with the continuation of line mn. We connect point h of the intersection of these lines to point O. All preliminary constructions are concluded with this action.

We accomplish further construction in the following way. We draw segment  $c_1c_2$ . We draw line  $c_1e$  from point  $c_1$  parallel to line mn; line ef is drawn from point e parallel to line Oh. From point f we drop a perpendicular to the Y-axis; we draw a circle with radius  $Of_1$  from point O to the intersection with

the X-axis at point  $a_4$ . Segment  $Oa_4$  corresponds in the accepted scale to current in the main circuit. We draw line  $aa_2$  perpendicular to the X-axis via point  $a_1$  where segment  $c_1c_2$  intersects line  $OA$ ; segment  $aa_2$  will equal generator emf.

Drawing line  $a_3a_4$  parallel to the Y-axis and line  $a_2a_3$  parallel to the X-axis, we get desired point  $a_3$  of relationship  $E = f(I)$  at the point where they intersect.

We construct the main propulsion motor's mechanical characteristic from the resultant relationship.

We determine main circuit current and propulsion motor emf from the generator relationship  $E = f(I)$  for arbitrary points. For example, for point  $a_3$ , segment  $Oa_4 = I$ , segment  $a_3a_5 = E_a$ , and segment  $a_4a_5 = \frac{I \sum R}{m}$ , where  $\sum R$  is the main current circuit resistance.

#### Graphic-analytical construction of generator external characteristic.

Having main propulsion motor plant nominal data, it is possible to determine nominal torque

$$M_{\text{НОМ}} = \frac{P_{\text{д.НОМ}} \cdot 975}{n_{\text{д.НОМ}}}, \quad (5.41)$$

where  $P_{\text{д.НОМ}}$  is main propulsion motor nominal power based on plant data;  $n_{\text{д.НОМ}}$  is nominal rotational speed based on plant data.

Nominal torque in the GEU nominal operating mode is determined from expression  $M_{\text{д.НОМ}} = M'_{\text{НОМ}}$ .

In addition, from equation (5.3) we find

$$M_{\text{д}} = C_M / \Phi_{\text{д.НОМ}}, \quad (5.42)$$

from whence nominal torque in the GEU nominal operating mode

$$M_{\text{д.НОМ}} = C_M / \Phi_{\text{д.НОМ}}'. \quad (5.43)$$

Having divided expression (5.42) into (5.43) and solving for M, we get

$$M_d = M_{d, \text{НОМ}} \frac{I}{I_{\text{НОМ}}}. \quad (5.44)$$

Knowing propulsion motor nominal moment and current, it is possible to determine from expression (5.44) main propulsion motor torque for any current value taken based upon the generator's external characteristic.

Main propulsion motor rotational speed: /186

$$n_d = \frac{E_d}{C_e \Phi_d}, \quad (5.45)$$

where  $E_d$  is main propulsion motor emf.

Nominal main propulsion motor rotational speed:

$$n_{d, \text{НОМ}} = \frac{E_{d, \text{НОМ}}}{C_e \Phi_d}. \quad (5.46)$$

Main propulsion motor nominal electromotive force can be determined from the expression

$$E_{d, \text{НОМ}} = U_{\text{НОМ}} - I_{\text{НОМ}} (R_{\text{я. д}} + R_{\text{н. д}} + R_{\text{к. д}}), \quad (5.47)$$

where  $U_{\text{НОМ}}$  is main propulsion motor nominal voltage based on plant data.

Having divided expression (5.45) into (5.46) and multiplying both parts by  $n_{\text{НОМ}}$ , we get

$$n_d = n_{d, \text{НОМ}} \frac{E_d}{E_{d, \text{НОМ}}}. \quad (5.48)$$

From expression (5.48) it is possible to calculate main propulsion motor rotational speed for different values  $E_d$  taken from relationship  $E = f(I)$ .

Determining for several points of the generator's external characteristic values  $E_d$  and  $I$ , as well as  $M_d$  and  $n_d$  of the main propulsion motor corresponding to them, we construct main propulsion motor relationship  $M_d = f(n_d)$  (Figure 5.5).

The proportionality between the flux and shaft power remains constant  $M \propto I$  when  $m - k$  generators are running and main propulsion motor magnetic flux is constant. Main propulsion motor electromotive force equals:

when  $m$  generators are running

$$E_a = mE - I \sum R; \quad (5.49)$$

when  $m - k$  generators are running

$$E'_a = (m - k)E - I \sum R_k. \quad (5.50)$$

Disregarding the change in main circuit resistance when  $m - k$  generators are running, i. e., having assumed  $R = R_k$ , and subtracting equation (5.50) from equation (5.49), we get

$$\Delta E_a = E_a - E'_a = mE - I \sum R - (m - k)E - I \sum R = kE \quad (5.51)$$

or  $E'_a = E_a - kE.$

Main propulsion motor rotational speed when  $m - k$  generators are running

$$n'_a = n_a \frac{E'_a}{E_a}. \quad (5.52)$$

Here, the abscissas of the  $M_a = f(n_a)$  curve (Figure 5.5) must be changed based on equation (5.52) for the identical shaft powers. The new curve (2) /188 is depicted in Figure 5.6. The value of the main propulsion motor moored current when  $m - k$  generators are running must be refined. The voltage drop in the main circuit  $I \sum R$  in this case will be distributed not to  $m$ , but to  $m - k$  generators. Consequently, the ordinates of straight line OB in Figure 5.4 must be increased in the ratio  $m/(m - k)$ . In Figure 5.4, straight line OD will be drawn with ordinates greater by a factor of  $m/(m - k)$  than the ordinates of straight line OB. Perpendicular  $l_1 k_1$  is dropped from point  $l_1$  of the intersection of straight line OD with generator relationship  $E = f(I)$  to the X-axis. Segment  $Ok_2$  provides the value of the moored current when  $m - k$  generators are running.

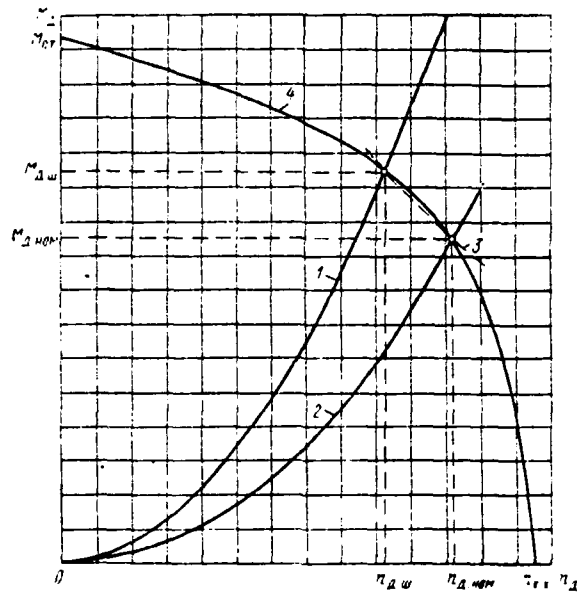


Figure 5.5. Construction of a Main Propulsion Motor's Mechanical Characteristic. 1--Screw characteristic during moored operations; 2--Screw characteristic when running in open water; 3--Relationship  $M_x n_x$  when all diesels are running the main propulsion motor; 4--Main propulsion motor mechanical characteristic  $M_x = f(n_x)$ .

Relationship  $M_x = f(n_x)$  obtained from Figure 5.6 when  $m - k$  generators are running does not provide a full primary motor load.

Main propulsion motor rotational speed must be increased by weakening magnetic flux in order to increase the primary motor load.

Construction of characteristic  $M_x = f(n_x)$ , which provides a full primary motor load, involves drawing horizontal straight line AE to the intersection with curve 2 at point B and with the Y-axis at point E in Figure 5.6 from point A, the intersection of the curve construction from the equation  $M_x n_x \frac{m-k}{m}$ , with the curve of screw torque when running in open water.

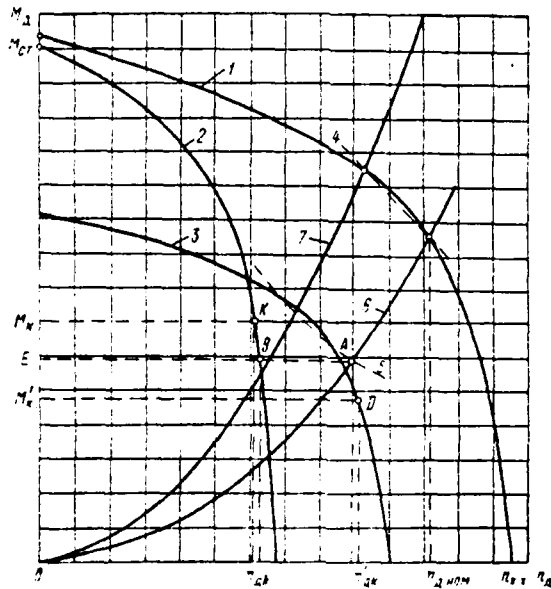


Figure 5.6. Graphic Construction of Main Propulsion Motor Mechanical Characteristics With a Varying Number of Generators Running. 1--Main propulsion motor mechanical characteristic when all diesel generators are running; 2--Main propulsion motor mechanical characteristic when half the generators are running and magnetic flux is constant; 3--Main propulsion motor mechanical characteristic when half the generators are running and flux is weakened; 4--Curve  $M_1 n_1 = \text{const}$  when all diesel generators are running; 5--Curve  $M_1 n_1 \frac{n_1}{n_2} = \text{const}$  when half the diesel generators are running; 6--Screw characteristic when running in open water; 7--Screw characteristic during moored operations.

Main propulsion motor magnetic flux  $\Phi_1'$  at which normal machinery load is provided must equal

$$\Phi_1' = \Phi_1 \frac{BE}{AE} \quad (5.53)$$

Curve 2 points are recalculated using equation (5.53) for the new flux value.

For arbitrary point K in curve 2, we find rotational speed  $n_{2K}$  and  $M_K$  moment, while we determine their corresponding values given flux  $\Phi_1$  from ratios

$$n'_{2K} = n_{2K} \frac{\Phi_1}{\Phi_1'} = n_{2K} \frac{AE}{BE}; \quad M'_K = M_{2K} \frac{\Phi_1}{\Phi_1'} = M_K \frac{BE}{AE}. \quad (5.54)$$

We construct point D of new relationship  $M_2 = f(n_2)$  from coordinates  $n'_{2K}$  and  $M'_K$ . Performing similar recalculations for several points, we construct curve 3 (Figure 5.6).

Precise determination of GED torque. All constructions of mechanical characteristic  $M_2 = f(n_2)$  presented above were accomplished with the assumption that main propulsion motor effective shaft power equals the electromagnetic moment, with losses in the iron and main propulsion motor mechanical losses not considered.

In this event, when the electromechanical plant furnishes the curves for the losses in the iron and mechanical losses, it is possible to do precise calculations of moment. This is done as follows: values I and E are written for /189 several points based on generator relationship  $E = f(I)$  (see Figure 5.4). Demand is determined:

$$P_{\text{торп}} = [mE - I(R_{a,r} + R_{b,r} - R_{k,r}) - R_{np}I] I \cdot 10^{-3} \text{ kW}. \quad (5.55)$$

Main propulsion motor emf is determined:

$$E_1 = mE - I \sum R \text{ V}. \quad (5.56)$$

Main propulsion motor rotational speed is calculated from expression (5.48).

All types of losses in the main propulsion motor are determined:

a) losses in copper

$$P_{\text{Cu}} = I^2 (R_{a,2} + R_{b,2} - R_{k,2}) \cdot 10^{-3} \text{ kW}. \quad (5.57)$$

b) losses in the commutator

$$P_{\text{кн}} = I \Delta V \cdot 10^{-3} \text{ kW}. \quad (5.58)$$

where  $\Delta V$  for carbon brushes equals 2 V and is 0.6 V for copper-carbon brushes;

c) additional losses:

for compensated machinery  $P_{206} = 0,005 P_{\text{НОМ}}$  ;

for uncompensated machinery  $P_{206} = 0,01 P_{\text{НОТР}}$  ;

d) losses in the iron and mechanical losses were taken from curves provided by the electromechanical plant for different field currents and different main propulsion motor rotational speed.

The sum of losses in the main propulsion motor:

$$\sum P = P_{\text{Сш}} + P_{\text{к.л}} - P_{206} + P_{\text{Fe-мех.}} \quad (5.59)$$

Full main propulsion motor shaft power:

$$P_A = P_{\text{НОТР}} - \sum P. \quad (5.60)$$

Main propulsion motor torque:

$$M_A = \frac{975 P_A}{n_A}. \quad (5.61)$$

When a main propulsion motor has  $q$  armatures, expressions (5.48) and (5.49) must be divided by  $q$  and expression (5.55) multiplied by  $q$ .

Basic electrical propulsion plant parameters:  $M_A$ ,  $n_A$ ,  $\Phi_A$ ,  $E_r$ ,  $I$ ,  $\Phi$  are determined from the aforementioned graphic-analytical constructions for each mode and compiled in Table 5.1.

One must calculate resistances in field circuits to obtain these parameters.

Calculation of resistances in pilot excitation circuits. If calculation of resistances in generator and main propulsion motor field circuits is done as described in § 5.2, then calculation of resistances in pilot excitation circuits has a certain specificity. Having determined exciter emf  $E_e$  from expression (5.35), total exciter n. s. is determined from the idling characteristic:  
 $F = F_H - F_c - F_{\pi}.$

Режим работы	Примерная схема главной цепи	Режим хода судна	Гребной электродвигатель					Дизель-генератор						
			Момент на валу, кг·м	Скорость вращения, об/мин	Мощность, кВт	Поток возбуждения, %	К. п. д., %	Напряжение, в	Ток, а	Мощность, кВт	Поток возбуждения, %	К. п. д., %	Мощность на валу, л. с.	
1		Свободная вода (n)	(f)	(g)	(h)	(i)	(j)	(k)	(l)	(m)				
		Швартовый (o)												
2		Свободная вода (n)												
		Швартовый (o)												
3		Свободная вода (n)												
		Швартовый (o)												

Table 5.1. Results From Calculation of GEU Static Characteristics. a--Operating mode; b--Approximate main circuit circuitry; c--Vessel running mode; d--Main propulsion motor; e--Diesel generator; f--Shaft power, kg-m; g--Rotational speed, rpm; h--Power kW; i--Field flux, %; j--Efficiency, %; k--Voltage, V; l--Current, A; m--Diesel shaft power, hp; n--Open water; o--Moored.

Separate excitation winding n. s.  $F_n$  -- segment On, self-excitation winding n. s.  $F_c$  -- segment nn<sub>2</sub>, and differentially-compounded winding n. s.  $F_n$  -- segment c<sub>1</sub>c<sub>2</sub> are determined for the nominal mode from curve 1 and line mn (see Figure 5.4). Currents in exciter three-winding field windings will be found from known n. s.:

$$i_{в.н} = F_n/\omega_n; \quad i_{в.с} = F_c/\omega_c; \quad i_{н.н} = F_n/\omega_n.$$

Figure 5.3 depicts the circuit for three-winding exciter windings.

Given a known field current in separate excitation winding  $i_{b.n}$ , standardizing resistance in this winding  $r_{y.n}$  can be determined from expression

$$r_{y.n} = \frac{U_{p.n}}{i_{b.n}(r_n - r_{p.n})} - \frac{r_n r_{p.n}}{r_n - r_{p.n}} \quad (5.62)$$

Standardizing resistance in a differentially-compounded winding is determined from expression

$$r_{y.n} = \frac{\Delta U_{b.k.d} - 1 - i_{b.n} r_n}{i_{b.n}}, \quad (5.63)$$

where  $\Delta U_{b.k.d}$  is the voltage drop in main propulsion motor auxiliary pole windings and compensating winding, while the digit 1 considers the voltage drop in the /191 connecting wires.

Standardizing resistance in self-excitation windings is determined from expression

$$r_{y.c} = \frac{E_n - i_r'(r_{n.n} - r_{n.c})}{i_{b.c}} - r_c \quad (5.64)$$

Mechanical characteristics of intermediate mode GED. Generator and main propulsion motor parameters for intermediate control station positions are determined graphically from Figure 5.4, in which line  $n_1 n_3$  is drawn parallel to line  $mn$ . Segment  $n_1 n$  corresponds to decreased exciter separate excitation winding n. s., so

$$\frac{F_n'}{F_n} = \frac{O n_1}{O n}$$

The construction is done in Figure 5.4. As a result of this construction, we get the generator external characteristic (curve 5). The main propulsion motor mechanical characteristic given decreased separately-excited winding n. s. is constructed in a manner analogous to that described above.

Special features of a construction of the static characteristics of GEU with three-winding exciters. In those instances when GEU are called upon to operate for a prolonged period in the moored mode, current exceeding the nominal flows in main current circuits, causing excessive overheating of main generator and main propulsion motor windings and their premature destruction.

As pointed out above, current in the main current circuit in circuitry with main generator three-winding exciters is proportional to main propulsion motor shaft power, i. e.,

$$I_{\text{ш}} = I_{\text{н}} \frac{M_{\text{д. ш}}}{M_{\text{д. н}}}$$

In accordance with the aforementioned expressions, when main propulsion motor field flux is constant, the current in the main circuit in the moored operation mode equals

$$I_{\text{ш}} = I_{\text{ном}} \frac{M_{\text{д. ш}}}{M_{\text{д. ном}}}$$

A three-winding exciter, all three field windings of which cut in concordantly, can be used for main propulsion motor excitation to reduce current in the main circuit in the moored mode.

The compounded winding of a main propulsion motor three-winding exciter is cut in via a magnetic amplifier to the voltage drop in the auxiliary pole and compensating windings. The magnetic amplifier is tuned so that current will not flow via the compound winding when the amount of current in the main /192 propulsion motor armature circuit is less than  $I_{\text{ном}}$  and corresponds to the running in open water mode. Current amplifying the main propulsion motor field will flow via the compounded winding when the current in the main circuit exceeds  $I_{\text{ном}}$ . Direction of the current in a three-winding exciter's compounded winding does not change when current direction in the main circuit changes. Consequently, the compounded winding examined above will also amplify the flux of its field when current in the main circuit increases after reversal of the main propulsion motor (with a change in generator polarity).

The magnetizing forces of main propulsion motor three-winding exciter field windings can be calculated graphically using the following method.

Main propulsion motor idling characteristic  $E_{\text{д}} = f(i_{\text{д}})$ , given  $n = n_{\text{с}}$ , where  $n_{\text{с}}$  is main propulsion motor rotational speed when running in open water (curve 1), is constructed on the right side in Figure 5.7. The main propulsion motor

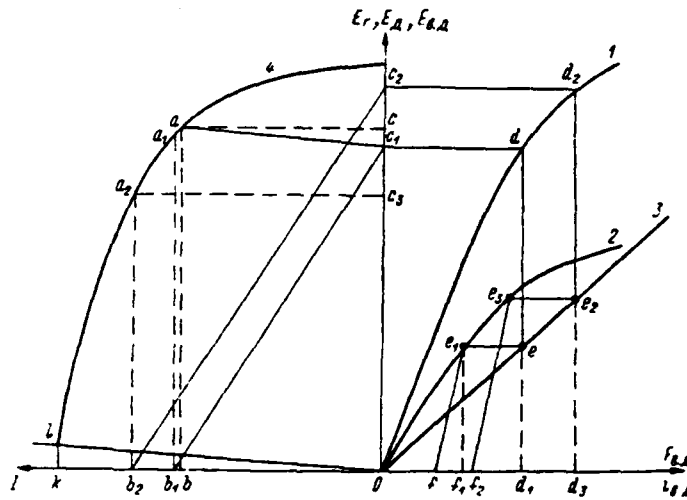


Figure 5.7. Graphic Determination of a Main Propulsion Motor Exciter Compounded Winding Magnetization Force.

exciter idling characteristic (curve 2) and the relationship of main propulsion motor field current to exciter emf  $i_{a, a} = f(E_{a, a})$  (straight line 3) will be constructed in the same quadrant.

Construction of relationship  $i_{a, a} = f(E_{a, a})$  is analogous to construction of this relationship for generators from expressions (5.34) and (5.35) with formulation in them of the parameters of the main propulsion motor field circuit. To the left of the Y-axis we will construct curve 4 -- the relationship of generator emf to main circuit current  $E_r = f(I)$ , calculated using the graphic method explained above (see Figure 5.4). Further constructions are made as follows: line 01 corresponding to the voltage drop in the main circuit is drawn in the /193 accepted scale; segment 0b equal in the accepted scale to main circuit current  $I_c$  when running in open water is plotted from point 0; segment  $Ob_1$  equal to  $1.1I_c$  and segment  $Ob_2$  equal to main circuit current  $I_w$  during moored operations and main propulsion motor constant field flux are plotted. Lines ab,  $a_1b_1$ , and  $a_2b_2$  are drawn from points b,  $b_1$ , and  $b_2$  parallel to the Y-axis to the intersection with relationship  $F_r = f(I)$ . These segments will correspond to generator emf given a vessel running in open water, current  $1.1I_c$ , and moored operation and main propulsion motor constant field flux.

Line  $ac_1$ , parallel to line 01 and determining voltage drop in the main

circuit, is drawn from point a. Segment  $Oc_1$  equals emf  $E_x$  given that the vessel is running in open water. A line is drawn from point  $c_1$  parallel to the X-axis to the intersection with the main propulsion motor idling characteristic at point d. Perpendicular  $dd_1$  is dropped to the X-axis from point d. Segment  $Od_1$  equals main propulsion motor field current for a vessel running in open water.

Line  $ee_1$  is drawn parallel to the X-axis to the intersection with the exciter idling characteristic (curve 2) from point e of line  $dd_1$  intersection with line 3. Perpendicular  $e_1f_1$  is dropped to the X-axis from point  $e_1$ . Segment  $Of_1$  equals the sum of the magnetizing forces of exciter separate excitation and self-excitation windings required to create main propulsion motor emf  $E_x$ . We usually use  $F_n = 65 \div 70\% F$ , and  $F_{cs} = 35 \div 30\% F$  where  $F = F_n + F_{cs}$ , to find winding n. s.

As noted above, the increase in current in the moored mode can be assumed to be up to  $1,1 I_{НОМ}$ . Considering this, to the left of point O we plot to the X-axis segment  $Ob_1$  equal in the accepted scale to  $1,1 I_{НОМ}$ . In order that current in the moored mode not exceed  $1,1 I_{НОМ}$ , it is necessary to increase main propulsion motor field flux in the ratio

$$\Phi_x = \Phi_{x, НОМ} \frac{Ob_2}{Ob_1},$$

where segment  $Ob_2$  equals the current in the main circuit in the moored mode given main propulsion motor constant flux. This flux increase must be accomplished through compounded winding n. s.

Compounded winding n. s. are determined graphically: in Figure 5.7 we will draw line  $b_1c_1$  connecting point  $b_1$  corresponding to current  $1,1 I_{НОМ}$  in the main current circuit and point  $c_1$  corresponding to main propulsion motor emf for a vessel running in open water. Line  $b_2c_2$  is drawn parallel to line  $b_1c_1$ . Line  $c_2d_2$  will be drawn via point  $c_2$  of line  $b_2c_2$  intersection with the Y-axis to the intersection at point  $d_2$  with the main propulsion motor idling characteristic. Line  $d_2e_2$  will be drawn perpendicular to the X-axis via point  $d_2$  to the intersection at point  $e_2$  with straight line 3. Line  $e_2e_3$  will be drawn

via point  $e_2$  parallel to the X-axis to the intersection with the main propulsion motor exciter idling characteristic (curve 2). Line  $e_3f_2$  is drawn via point  $e_3$  parallel to line  $e_1f$ . Resultant segment  $ff_2$  will equal to compounded winding n. s.  $F_k$  necessary to create flux  $\Phi_a$ , which provides a reduction in main circuit current to value  $1,1/I_{\text{НОМ}}$ .

Current in the compounded winding is determined from known compounded winding n. s. from expression

$$i_k = \frac{F_k}{w_k}.$$

#### § 5.4 Graphic-Analytical Method of Calculation of the Static Characteristics of Automated GEU

Initial assumptions. This paragraph is devoted to calculation of the static characteristics of automated dc GEU, whose field circuits envisage a change in main machinery field magnetic fluxes.

The method of calculation is set up so that solution of the problem will be applicable for GEU systems with three-winding exciters and with amplidyne (it is assumed that the control and excitation circuit circuitry is analogous, i. e., they have an equal number of exciter field circuits with an identical type of action).

We will examine the foundation of the method relative to construction of generator and GED characteristics.

##### Graphic-analytical construction of the generator external characteristic.

The analytical expression for calculation of a generator's external characteristic taking its exciter with several windings into consideration can be obtained from the following expressions:

1) exciter n. s. equation

$$a_n \Phi_n = F_n + F_{c_n} - F_n - F_{p_n} = 2w_n i_n + 2w_{c_n} - 2w_n i_n - 2w_{a_n} i_{n,r} \quad (5.65)$$

where  $a_n$  is the proportionality factor between exciter n. s. and magnetic flux;  $\Phi_n$  is exciter magnetic flux;  $w_n$  is the number of field separate master winding

turns per pole;  $\omega_{cs}$  is the number of voltage feedback (self-excitation) winding turns per pole;  $\omega_n$  number of current feedback winding (differentially-compounded winding) turns per pole;  $i_n = \delta I_a$  current in the current winding (determined by the number of parallel branches given direct connection to the main current PKO winding, while when the current winding is fed from a shunt in the main circuit,  $i_n$  is determined by voltage  $\Delta U_{un}$ ; in the former  $\delta = 2a_n$ , while in the latter  $\delta = \frac{r_{un}}{R_n}$ ;  $F_{p,n}$  is armature reaction n. s. equalling  $I_a \omega_a'$ ;  $I_a$  is main circuit armature current;  $\omega_a'$  is the equivalent number of armature turns creating the reaction;  $i$  is the current in the winding circuits; /195

2) exciter emf equation

$$E_s = C_e n_s K_s \Phi_s = \varphi_s \Phi_s, \quad (5.66)$$

where  $E_s$  is exciter emf;  $C_e$  is a design factor;  $n_s$  is exciter rotational speed;  $K_s$  is a proportionality factor (for EMU);  $\varphi_s = C_e n_s K_s$  is a proportionality factor between emf and magnetic flux;

3) main generator n. s. equation

$$a_r \Phi_r = F_{s,r} = 2\omega_{s,r} i_{s,r} - 2\omega_{ar}' I_a, \quad (5.67)$$

where  $a_r$  is a proportionality factor between n. s. and magnetic flux;  $\Phi_r$  is main generator field magnetic flux;  $\omega_{s,r}$  is the number of generator field winding turns per pole;  $i_{s,r}$  is the generator field current;  $\omega_{ar}'$  is the equivalent number of armature turns creating the reaction;

4) main generator emf equation

$$E_r = C_{er} n_r \Phi_r = \varphi_r \Phi_r, \quad (5.68)$$

where  $E_r$  is main generator emf;  $C_{er}$  is a design factor;  $n_r$  is generator rotational speed;  $\varphi_r = C_{er} n_r$  a proportionality factor between emf and magnetic flux.

Having determined from equation (5.65) value  $\Phi_s$  and having substituted it in equation (5.66), we get

$$E_s = \frac{2\omega_n \varphi_s}{a_s} i_s + \frac{2\omega_{cs} \varphi_s}{a_s} i_{cs} - \frac{2\omega_n \varphi_s}{a_s} \delta I_a - \frac{2\omega_a' \varphi_s}{a_s} i_{s,r}$$

or, instead of currents, having substituted their values, we get

$$U_o + i_{a,r} R_{aa} = E_o = \frac{2\omega_a \Phi_B}{a_b R_n} U_a + \frac{2\omega_{cs} \Phi_n}{a_b R_{cs}} U_o - \frac{2\omega_n \Phi_B}{a_b R_n} R_n \delta I_a - \frac{2\omega_a' \Phi_B}{a_b R_{b,r}}$$

where  $R_n$  is separate master winding resistance;  $U_a$  is voltage supplied from a control station to master control winding;  $R_{cs} = R_{cs} + R_{aa} + r_i$  is the voltage winding circuit impedance;  $R_n$  is current winding resistance.

If designations are introduced:

$$K_{cs} = \frac{2\omega_{cs} \Phi_n}{a_b R_{cs}} \quad \text{voltage gain from the voltage feedback winding;}$$

$$K_{k,b} = \frac{2\omega_a' \Phi_B}{a_b R_{b,r}} \quad \text{voltage gain from the armature reaction;}$$

$$K_n = \frac{2\omega_n \Phi_B}{a_b R_n} \quad \text{voltage gain from the master winding;} \quad /196$$

$$K_n = \frac{2\omega_n \Phi_B}{a_b R_n} \quad \text{voltage gain from current feedback winding,}$$

then

$$U_o = \frac{K_n U_a - K_n R_n \delta I_a - i_{a,r} R_{aa}}{1 - K_{cs} + K_{k,b}} \quad (5.69)$$

Analogously, determining value  $\Phi_r$  from equation (5.67) and substituting it in equation (5.68), we get

$$E_r = K_r U_o - K_{k,r} I_a, \quad (5.70)$$

where  $K_r = \frac{2\omega_{a,r} \Phi_r}{a_r R_{b,r}}$  is generator voltage gain;  $K_{k,r} = \frac{2\omega_{ar} \Phi_r}{a_r}$  is a factor considering the presence of an armature reaction.

Substituting equation (5.69) in equation (5.70), we get the analytical expression of the equation for the generator external characteristic when the field winding is fed by an exciter with voltage and main circuit current feedbacks:

$$E_r = \frac{K_r}{1 - K_{cs} K_{k,b}} (K_n U_a - K_n R_n \delta I_a - i_{a,r} R_{aa}) - K_{k,r} I_a. \quad (5.71)$$

However, calculation of a generator's external characteristic using equation

(5.71) is relatively complicated, since, given the non-linearity of generator and exciter characteristics, input factors  $K_{c,r}, K_u, K_{k,b}, K_n, K_{k,r}$  will be variables. Therefore, these characteristics should be subdivided into several linear sections for the purpose of simplifying the calculations.

The following graphical method of calculating a generator's external characteristic based on the relationships between the values established by equations (5.69)-(5.71) is proposed.

Construction  $E_r = f(I_a)$  is shown in a coordinate system in Figure 5.8.

A generator's idling characteristic ( $U_s$  is accepted for a generator warm field winding), curve 1, taking the presence of residual magnetization into account, has been constructed in the first quadrant. Exciter magnetization characteristic  $U_s = f(F)$  when operating load  $R_n = R_{s,r}$ , curve 2\*, has been constructed in the fourth quadrant.

It should be noted that characteristic  $U_s = f(F)$  must be accepted for the given specific tuning of the voltage feedback winding circuit. Acceptance of this very characteristic simplifies the construction later on because it would be necessary to draw the volt-ampere characteristic of the voltage feedback winding circuit and continually take it into consideration during construction if the voltage feedback winding and master winding action is separated. /197  
Characteristic  $U_s = f(F_n)$  also is constructed taking the presence of residual magnetization into consideration.

Plotted in the third quadrant on the X-axis is point  $O_1$ , the origin of the generator armature current reading. Moreover, it is selected in such a way that the point corresponding to assigned main propulsion motor moored current with motor braked will coincide with point 0.

Then, the nominal points of all values a, b, c, d, and e are plotted on the coordinate axes. Angle  $\alpha$  characterizing the action of current feedback

---

\*This characteristic must be constructed as a function of control winding n. s. when an EMU is used as generator exciter.

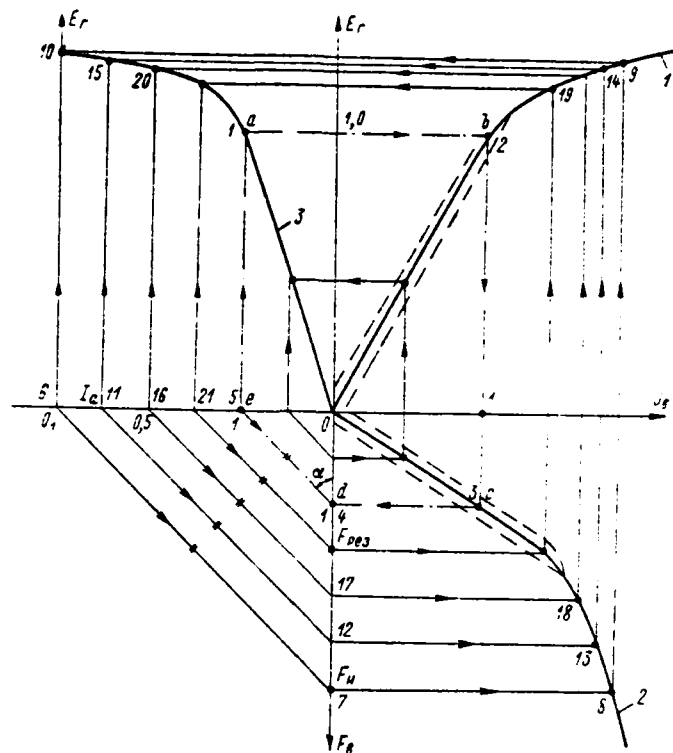


Figure 5.8. Graphic Construction of a Generator's External Characteristic.

is determined by drawing path *de*. If path *6-7* is drawn from point *O* parallel to path *de*, then segment *O-7* determines exciter field master winding *n. s. F<sub>H</sub>*. Knowing the number of this winding's turns per pole  $\omega_n$ , current  $i_n = \frac{F_H}{2\omega_n}$  is computed and, further, given known shipboard network voltage  $U = U_0$ , one finds resistance

$$R_n = \frac{U_0}{i_n}.$$

When the propellor jams and current in the generator armature circuit is  $I_a = I_{cr}$ ,  $F_H = F_{n,cr}$  can be accepted as approximate. Then, based on known values  $F_{n,cr}$  and  $I_{cr}$ , the required number of current winding turns per pole is determined:

$$\omega_n = \frac{F_{n,cr}}{2 I_{cr}}.$$

The sequence of generator external characteristic  $E_r = f(I_a)$  construction, curve 3, is indicated by arrows and designated by numbers. The construction has been drawn only from the average branches of generator and exciter characteristics for the purposes of clarity.

Graphic-analytical construction of a GED mechanical characteristic. This characteristic is determined from the following analytical relationships:

$$M_A = C_{m.a} I_a \Phi_a \kappa \Gamma M; \quad (5.72)$$

$$n_A = \frac{E_r - I_a R_a'}{C_{e.a} \Phi_a} \text{ об/мин}, \quad (5.73)$$

where  $M_A$  is GED shaft power;  $n_A$  is GED rotational speed;  $C_{e.a}$  and  $C_{m.a}$  are GED design factors;  $R_a'$  is main circuit impedance.

Corresponding values  $E_r$  and  $I_a$  from curve 3 (Figure 5.8) are substituted in equations (5.72) and (5.73) and  $M_A = f(n_A)$  is determined for assigned values  $\Phi_a$ . Different characteristics  $E_r = f(I_a)$ , and, consequently, different characteristics  $M_A = f(n_A)$ , as well, correspond to the different control station lever positions. In addition, the form of mechanical characteristic  $M_A = f(n_A)$  is determined by the value of GED field magnetic flux. When there is staged control of  $\Phi_a$  characteristics  $M_A = f(n_A)$  should be calculated with this factor considered.

However, graphic construction also can be proposed for determination of the GED mechanical characteristic. Two GED quadrants are envisioned for this: current and rotational speed (Figure 5.9).

Characteristic  $E_r = f(I_a)$  - curve 1, is constructed in the current quadrant and path  $I_a$  is determined based on known impedance in main machinery armature circuit.

Propellor characteristics 3 and 4 for the running in open water and moored modes are constructed in the rotational speed quadrant.

After these characteristics are constructed and scales selected, points a, b, c, ..., n, corresponding to GEU nominal operating mode, are plotted. Here, segment  $ab = O_1c$  equals main propulsion motor counter emf given nominal

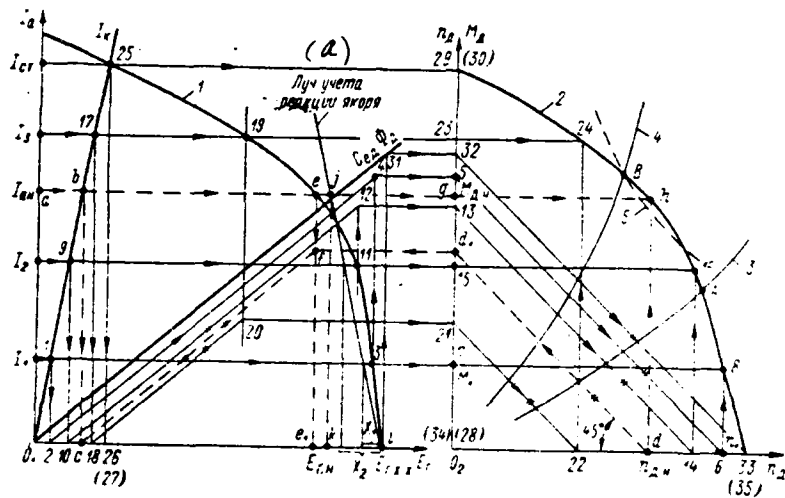


Figure 5.9. Graphic formulation of mechanical GED characteristic at  $\Phi_a = \text{const}$  and  $\Phi_f = \text{var.}$   
 (a) Path of armature reaction

magnetic flux and nominal rotational speed. Path  $cd$  determines the slope of path  $C_{e2}\Phi_2$ , which establishes the relationship of counter emf for  $\Phi_2 = \text{const}$  and GED rotational speed. Since  $\Phi_2 = \text{const}$ , in this case, then  $M_2 = I_{a2}$ . /199  
 Therefore, points  $a$  and  $g$  lie on the same horizontal. Another path  $C_{e2}\Phi_2$  slope will correspond to another GED field magnetic flux (given staged control). Although current  $I_{a2}$  and moment  $M_2$  points will remain on the same horizontal, given another  $\Phi_2$ , value  $M_2$  will differ, which is determined by equation (5.72).

The sequence of plotting GEU nominal operating mode points in Figure 5.9 follows the Latin alphabet.

A main propulsion motor's mechanical characteristic (curve 2) is constructed in the following manner. Having selected random main circuit current value  $I_1$ , we determine  $\Delta U_{a1}$  -- segment  $0_1 2$ . We find the emf value corresponding to current  $I_1$ , point 3, based on characteristic  $E_r = f(I_a)$ . The intersection of the verticals passing through point 3 and of the sloping path passing through point 2 parallel to path  $C_{e2}\Phi_2$ , determines the position of point 4. Horizontally drawing path 4-5 and further on path 5-6 parallel to path  $dd_1$  (path  $dd_1$  slope is selected randomly), we find rotational speed value  $n_1$ . Point 7 along the current  $I_1$  horizontal determines GED electromagnetic moment value  $M_1$ . Intersection of the horizontal passing through point 7 and the verticals passing through point 6 determines point 8 of the GED mechanical characteristic. Further, having selected another current value  $I_2$ , an analogous construction is made, resulting in determination of point 16, and so forth. The construction sequence is indicated by arrows and designated by numbers.

Equations (5.72) and (5.73) confirm the correctness of the proposed graphic construction of the GED mechanical characteristic.

The points of intersection of screw characteristics with the GED mechanical characteristic (points A and B) determine GEU operating indicators for the corresponding vessel operating modes. /200

Since GEU main machinery usually is compensated, there is no need to consider armature reaction when constructing characteristics  $E_r = f(I_a)$  and  $M_2 = f(n_2)$ . If any piece of machinery lacks a compensating winding, then construction should

be accomplished taking armature reaction into account. Otherwise, the resultant curve  $M_2 = f(n_2)$  will differ somewhat from the actual curve.

If, for example, the main generator lacks a compensating winding, it will be necessary, prior to drawing the verticals through points 3, 11, 19, and so on, to plot to the left segments  $x_1, x_2$ , and so forth, which take into account a decrease in generator emf due to the decrease in resultant field magnetic flux  $\Phi_r$  from the demagnetizing action of the armature reaction. A path which considers armature reaction will be introduced in the graph for this purpose. This path is drawn through point i, which corresponds to idling emf, and point j, which is determined by nominal current and by armature reaction triangle data; segment ik equals the decrease in generator emf due to armature reaction at nominal current load.

Consideration of armature reaction. The reaction of a GED armature also can be considered in the corresponding manner. One can see from Figure 5.9 that the GED mechanical characteristic in section AB of curve 2 differs from the hyperbole (curve 5). Consequently, GEU power in this circuit does not remain constant. If one also considers electrical machinery hysteresis, then the GEU power fluctuation in section AB can reach 15-20%.

Graphic-analytical calculation of a GED mechanical characteristic given simultaneous control of generator and GED field fluxes. Simultaneous regulation of the field magnetic fluxes of both a generator and a GED is used in some GEU to avoid a significant overload in armature current of the main electrical machinery. In this case, it is possible to provide GEU electric power constancy and, in so doing, to increase the economy of plant operation.

Main propulsion motor characteristic  $\Phi_1 = f(I_a)$  is determined in general by the following relationships (if the GED exciter control regulating winding is fed by resistance  $r_w$  in the main circuit):

1) exciter n. s. equation

$$a_{w, \Delta} \Phi_{\Delta} = \pm F_{ch} + F_{p, o} + F_H - F_{p, \Delta} = \pm 2\omega_{ch} i_{ch} + 2\omega_{p, o} i_{p, \Delta} + 2\omega_H i_H - 2\omega_{\Delta} i_{\Delta} \quad (5.74)$$

2) exciter emf equation

$$E_{a, d} = C_p n_{b, d} \Phi_{b, d} = \Phi_{b, d} \Phi_{d, d}; \quad (5.75)$$

3) main propulsion motor emf equation

$$a_d \Phi_{d, d} = F_{b, d} = 2\omega_{b, d} i_{b, d} - \omega_{a, d} I_a. \quad (5.76)$$

From equations (5.74)-(5.76) we get

/201

$$\Phi_{d, d} = \frac{K_d}{1 - K_{cb} - K_{k, d}} (K_{11} U_c + K_p \sigma \omega I_a - i_{b, d} R_{ab, d} - K_{p, d} I_a), \quad (5.77)$$

where  $K_1 = \frac{2\omega_{b, d}}{a_d R_{b, d}}$  - is GED gain;  $K_{k, d} = \frac{2\omega_{ab, d} i_{b, d}}{u_{b, d} R_{b, d}}$ ;  $K_{p, d} = \frac{2\omega_{a, d}}{a_d}$ ;  $K_{p, o} = \frac{2\omega_{p, d} i_{b, d}}{u_{b, d} R_{p, d}}$ .

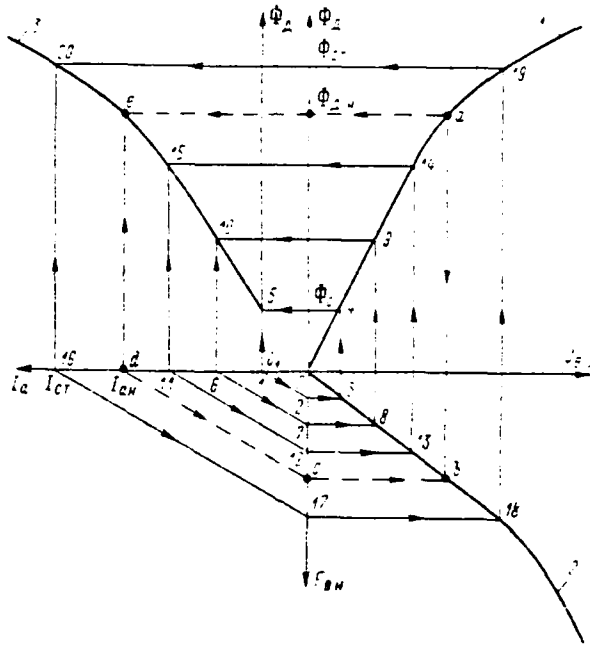


Figure 5.10. Graphic Construction of Characteristic  $\Phi_d = f(I_a)$ .

All value designations in the above equations are the same as those used above for a generator.

Equation (5.77) makes it possible analytically to calculate characteristic  $\Phi_d = f(I_a)$ , and, using this same characteristic, knowing nominal GED data, it

is possible to determine the ratio of exciter winding parameters which provide the assigned range of magnetic flux change when main circuit current changes from  $I_{a \text{ nom}}$  to  $I_{cr}$ .

However, analytical solution of a similar problem presents well-known difficulties. Therefore, graphic construction  $\Phi_x = f(I_a)$  is proposed below. The selection of GED exciter winding parameters is based on results of this construction.

The GED magnetization characteristic (curve 1) is plotted in the first quadrant in Figure 5.10. The motor exciter load characteristic when running /202 a constant resistance of load  $R_{n,r} = R_{a,x} = \text{const}$  (curve 2) has been constructed in the fourth quadrant. This characteristic is the relationship of exciter voltage  $U_{a,x}$  to field separate winding n. s. when the voltage feedback winding is cut in. Characteristics 1 and 2 are depicted without consideration for the presence of residual magnetization in order to simplify the figure. We select random point  $O_1$  on the X-axis running to the left and plot the armature current scale. Next, we plot the points corresponding to GED nominal operating mode (points a, b, c, d, and e). Connecting points c and d, we get a path determining the proportionality between armature current and current winding n. s. The sequence of plotting the nominal mode points is designated by arrows. Next, given various armature current values from zero to  $\beta$ , we accomplish the graphical construction of curve 3, characteristic  $\Phi_a = f(I_a)$ . The construction sequence is designated by numbers and indicated by arrows.

After the construction, one should indicate the separate winding and control winding n. s. on the n. s. axis  $F_{b,n}$  for determination of the requisite bucking [starting] winding (RO) parameters. Segment Oc determines resultant exciter field n. s. taking the presence of voltage feedback into account. Segment O—2 determines assigned value  $F_{b,n}$ . Therefore, we get

$$i_u = \frac{F_{b,n}}{2W_n} = \frac{U_n}{R_n + r},$$

where one of the values must be given. If value  $U_n$  is known and the selected number of separate winding turns per pole is  $w_n$ , then it is simple to determine  $R_n + r$ . This winding's wire section must correspond to current  $i_u$ .

Winding RO parameters are determined by the magnetizing force from segment s-2:

$$i_{p.o} = \frac{F_{p.o}}{2W_{p.o}} = \frac{r_{w}I_a}{R_{p.o}}$$

If as a result of the construction of characteristic  $\Phi_a = f(I_a)$  it is established that, at current  $I_{cr}$ , moment  $M_{cr}$  differs from the assigned value, then value  $\Phi_{cr}$  should be changed, making a corresponding change in winding RO action necessary.

It should be noted that, at current  $I_a = 0$ , motor field magnetic flux is determined only by the action of the separate winding n. s. Therefore, value  $\Phi_a$  can be significantly less than  $\Phi_{a.n}$ . However, this is quite acceptable since the GED when started initially operates in the idling mode.

Figure 5.11 presents the graphic construction of the mechanical characteristic of a GED for a GEU circuit with controlled main machinery fluxes. Here, path  $I_{kr}$ , generator external characteristic (curve 1), and screw characteristics (curves 3 and 4) are constructed and the points of the GEU nominal mode plotted in a manner analogous to those shown in Figure 5.9. Because the circuit envisions a change of  $\Phi_a$  in the main current function, the path of the proportionality  $M_{cr} / I_a$  between GED torque and depiction of current and magnetic flux (path  $C_{m.a} I_a \Phi_a$ ) has been constructed in the current quadrant. Point g, corresponding to the amount of nominal value  $M_{a.n}$  is determined for the selected GED moment scale. Next, point h is determined from known value  $I_{ah}$  and path  $C_{e2} \Phi_a$

Intersection of the vertical passing through point h and the horizontal passing through point g will provide point j. Path  $C_{m.a} I_a \Phi_a$  will pass through center  $O_1$  and point j. This path will have a constant slope and is the link between armature current and GED torque. Since GED magnetic flux changes in current function  $I_a$ , then the slope of path  $C_{e2} \Phi_a$  will change. There is a third quadrant with center  $O_3$  for determination of the slope of path  $C_{e2} \Phi_a$ , corresponding to the different values of magnetic flux  $\Phi_a$ . Armature current is plotted in this quadrant along the Y-axis and magnetic flux  $\Phi_a$  along the X-axis. Any current scale can be selected, while the scale of magnetic flux  $\Phi_a$  lies in strict dependence on the slope of path  $C_{e2} \Phi_a$ . Point i obtained as a result of the intersection

of path  $C_{eA}\Phi_A$  with the horizontal  $fd_1$  on the X-axis in the quadrant with center  $O_3$  corresponds to point  $k$  of nominal value  $\Phi_{A, \text{HOM}}$ . The scale for  $\Phi_A$  on the X-axis also is determined by this. If now value  $\Phi_1$  corresponding to point  $I_1$  is to be determined from characteristic  $\Phi_A = f(I_a)$ , then the intersection of the vertical passing through the point corresponding to this value  $\Phi_1$ , with horizontal  $fd_1$ , will determine the point through which path  $C_{eA}\Phi_A$  from center  $O_1$  will pass. Horizontal  $fd_1$  is common for determination of path  $C_{eA}\Phi_A$  slope at different values of  $\Phi_A$ .

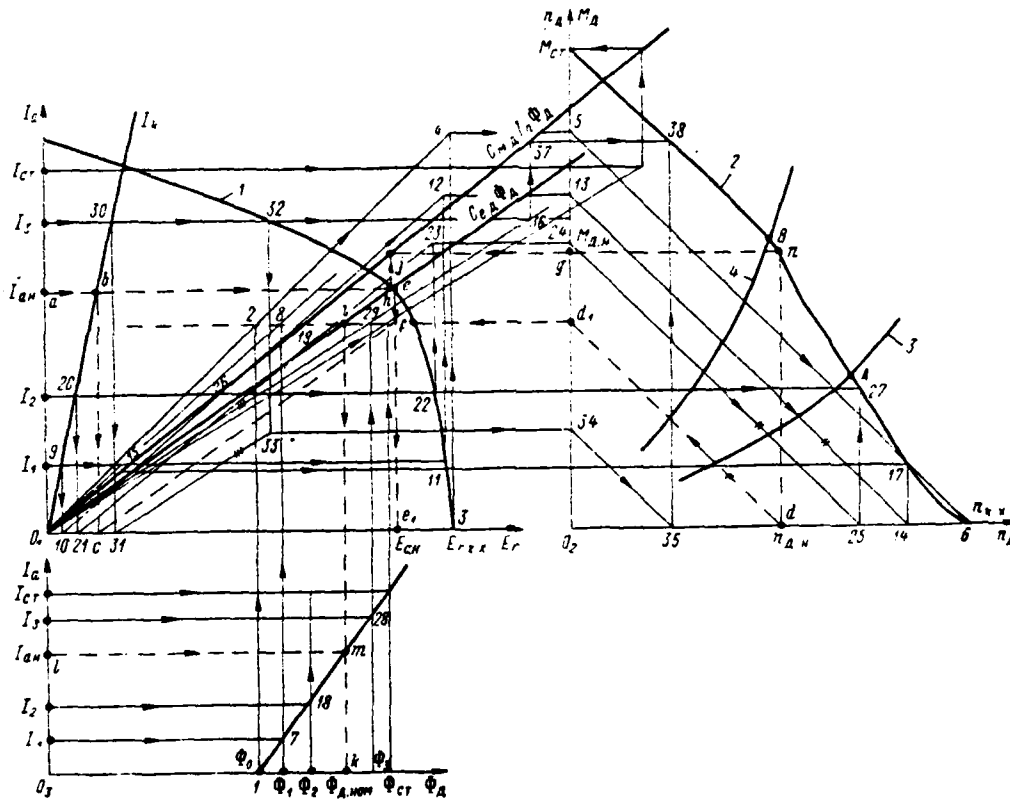


Figure 5.11. Graphic Construction of the GED Mechanical Characteristic Where  $\Phi_A = \text{var}$  and  $\Phi_r = \text{var}$ .

Graphical determination of value  $n_A$  from selected value  $I_a$  is made analogously to the method shown in Figure 5.9, only the change in path  $C_{eA}\Phi_A$  slope is considered.

Graphic determination of value  $M_2$  based on selected value  $I_a$  occurs in the following manner (Figure 5.11). After determination of the path  $C_{e2}\Phi_2$  position, a horizontal is drawn from the Y-axis using selected current value  $I_a$  to path  $C_{e2}\Phi_2$ . Next, a vertical is drawn through this resulting point to path  $C_{m2}/I_a\Phi_2$ . The point obtained on path  $C_{m2}/I_a\Phi_2$  will be plotted along the horizontal to the axis of the moments in the quadrant with center  $O_2$  and the intersection of this horizontal with the vertical for the rotational speed value obtained in this manner will determine the point of the GED mechanical characteristic. The construction sequence in Figure 5.11 is designated by numbers and indicated by arrows.

The entire construction corresponds to the physical essence of electrical propulsion plant operation. The GED mechanical characteristic in section AB has a concave form and, given the corresponding selection of exciter winding parameters and generator and GED magnetization characteristics, can coincide with the hyperbole of GEU power constancy.

One must consider the action of current coupling when constructing a generator's external characteristic and characteristic  $\Phi_x = f(I_a)$ , given the presence of shut-offs for the purposes of current feedbacks. Construction of the GED mechanical characteristic from resultant  $E_r = f(I_a)$  and  $f(I_a)$  /205 remains identical to that depicted in Figure 5.11.

Analytical relationships for elements of GEU with two-stage longitudinal field EMU. If multistage amplidynes (any type) are used as exciters, then their magnetization characteristics when operating on a load need to be plotted in exciter quadrants. The calculation principle is retained. The nature of the action of feedbacks and their number are determined during graphical construction from the corresponding paths in exciter quadrants.

The analytical relationships of all nodes are examined below using the automated GEU with a two-stage longitudinal field EMU aboard the atomic icebreaker "Lenin" (see Figure 3.29), which are used for graphical calculation of this GEU's static characteristics, as our example.

We will compile statics equations for all GEU elements on the icebreaker "Lenin" (analogously for "Amguema" class vessels).

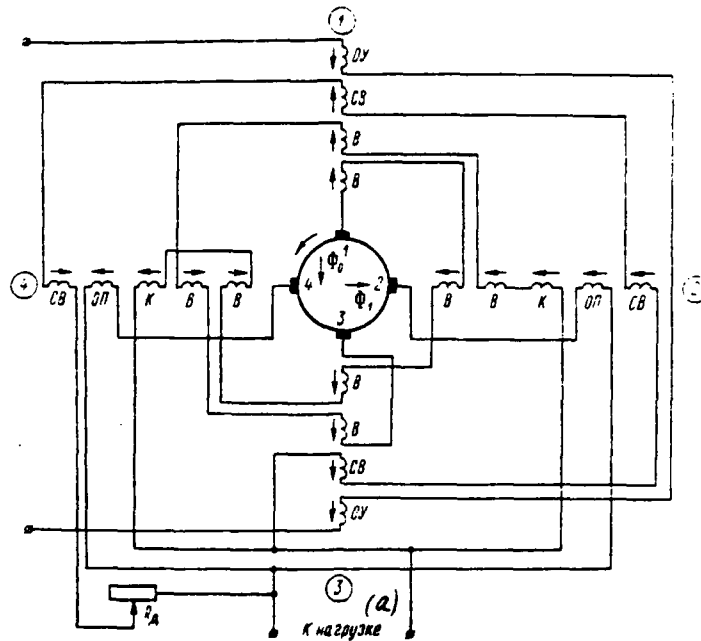


Figure 5.12. Schematic of a Two-Stage Longitudinal Field EMU.  
a--To load.

Two-stage longitudinal field EMU (rototrol amplifier). The basic equations for each EMU stage are compiled and specific relationships used in analytical calculation of GEU static characteristics are established in accordance with the schematic (Figure 5.12). The operating principle of this EMU and its /206 characteristics are examined in [27].

EMU first stage. Exciter magnetic flux along the axis of poles 1-3 is created as a result of the action of control winding OU magnetizing force and of the magnetizing force of the armature reaction from circulating current  $I_{24}$ :

$$a_s \Phi_0 = 2\omega_y i_y - \omega_a i_{24}, \quad (5.78)$$

where  $\omega_y$  and  $i_y$  are the number of turns per pole and control winding current;  $\omega_a$  is the number of armature turns creating the reaction from current  $I_{24}$ .

Armature rotation in magnetic flux creates emf equalling  $\Phi_0$

$$U_{13} = C_p n_s \Phi_0 = \varphi_s \Phi_0, \quad (5.79)$$

where  $\varphi_s = \frac{PN}{a^30} n_s$  is the proportionality factor between emf and magnetic flux.

If the circuit of brushes 1-3 from the EMU circuit is closed (Figure 5.12), circulating current  $I_{13}$  arises, which creates the magnetizing force of the field four-pole output system

$$i_{13} = \frac{U_{13}}{R_{13}} = \frac{K_y U_y - K_1 U_{24}}{R_{13}}, \quad (5.80)$$

where  $R_{13}$  is circuit 1-3 impedance.

As circulating current  $I_{13}$  flows, armature reaction magnetizing force appears along the axis of poles 2-4, creating flux  $\Phi_1$ :

$$a_s \Phi_1 = i_{13} (\omega_a - 2\omega_k) - i_{24} \omega_{on}, \quad (5.81)$$

where  $\omega_k$  and  $\omega_{on}$  are the number of compensating and opposed winding turns.

When an armature turns in flux  $\Phi_1$  emf arises

$$U_{24} = \varphi_s \Phi_1. \quad (5.82)$$

Substituting equation (5.81) in equation (5.82), we get

$$U_{24} = \frac{K_k U_{13}}{1 - K_{on}}. \quad (5.83)$$

Substituting equation (5.83) into the equation for  $U_{13}$  from (5.80), taking certain conversions into account we get

$$U_{13} = \frac{K_y (1 + K_{on})}{(1 + K_{on} + K_1 K_k)} U_y. \quad (5.84)$$

Current in the brushes 1-3 circuit is determined now from equation

$$i_{13} = \frac{K_y (1 + K_{on})}{(1 + K_{on} + K_1 K_k) R_{13}} U_y. \quad (5.85)$$

EMU second stage. Second-stage EMU field magnetizing force is created

as a result of the presence of circulating current  $I_{13}$ . This magnetizing force determines magnetic flux, taking the presence of self-excitation winding SV into account: /207

$$a_b \Phi_b = 2\omega_n i_{13} + 2\omega_{cb} i_{cb}. \quad (5.86)$$

When an armature rotates in magnetic flux  $\Phi_b$  emf arises

$$U_b = \varphi_b \Phi_b. \quad (5.87)$$

Substituting equation (5.86) into equation (5.87), we get

$$U_b = \frac{K_b}{1 - K_{cb}} U_{13}. \quad (5.88)$$

If equation (5.84) is substituted in equation (5.88), then we get the equation for calculation of the static characteristics of a two-stage EMU with a longitudinal field:

$$U_b = \frac{K_y K_b (1 + K_{on})}{(1 - K_{cb})(1 - K_{on} - K_1 K_k)} U_y = K_y K_{\Sigma M S} U_a. \quad (5.89)$$

The following designations were used in the above equations:

$$K_y = \frac{2\omega_y \varphi_n}{a_b R_y}; \quad K_k = \frac{(\omega_a - 2\omega_k) \varphi_n}{a_n R_{13}};$$

$$K_1 = \frac{\omega_a \varphi_n}{a_n R_{24}}; \quad K_{o.n} = \frac{2\omega_{on} \varphi_n}{a_n R_{24}}.$$

Equation (5.89) shows that the presence of a self-exciting winding makes it possible to increase the value of factor  $K_{\Sigma M S}$ , while undercompensation of armature reactions from current  $i_{13}$  and  $i_{24}$  will lead to a considerable decrease in this factor. Therefore, there is a requirement to tune EMU compensation carefully when the EMU is installed.

Presence of different feedbacks is characteristic of the electrical propulsion plant circuit aboard the atomic icebreaker "Lenin." Therefore, one must introduce appropriate additions into equation (5.89) due to the presence of main circuit armature negative current feedback and EMU negative voltage feedback:

$$U_{n,r} = K_{\Sigma M S} \Gamma [K_{o,y1} U_{n,y} - K_{o,y4} (R_{2,n} + R_{k,o}) I_a - K_{o,y3} U_{n,r}] \quad (5.90)$$

A main propulsion motor EMU exciter requires introduction into equation (5.89) of additions stipulated by the presence of EMU negative voltage feedback (control winding  $OU_1$ ) and EMU negative voltage feedback of a generator with a shut-off:

$$U_{b.1} = K_{ЭМВД} [K_{o.y1} U_{o.y2} U_{b.1} - (U_{b.r} - U_{срвн}) K_{o.y3}] \quad (5.91)$$

Current is absent from control winding OZ when  $U_{b.r} < U_{срвн}$  due to the presence of a semiconductor rectifier.

Main generator. Main propulsion motor armature feed from two dual-armature generators is envisioned in the GEU circuit aboard the atomic icebreaker "Lenin."

The magnetizing force equation (without considering armature reaction) /208 has the form

$$a_r \Phi_r = 2\omega_{b.r} i_{b.r} \quad (5.92)$$

When an armature rotates in magnetic flux  $\Phi_r$ , emf arises

$$E_r = \varphi_r \Phi_r \quad (5.93)$$

Substituting equation (5.92) in equation (5.93), we get

$$E_r = \frac{2\omega_{b.r} \varphi_r}{a_r} i_{b.r} \quad (5.94)$$

On the basis of the GEU generator main current circuit and field winding circuits, equation (5.94) can take the form

$$E_{r.2} = 2K_r U_{b.r} \quad (5.95)$$

where

$$k_r = \frac{2\omega_{b.r} \varphi_r}{a_r R_{b.r}}; \quad \varphi_r = C_{er} n_r; \quad R_{b.r} = R_{b.n} + R_{a.}$$

As a result of the substitution of equation (5.90) in (5.95), we get the equation of the main (equivalent) generator taking the two-stage EMU with a longitudinal field (with EMU main circuit current and voltage feedbacks) into consideration:

$$E_{r.2} = K_{ЭМВД} 2K_r [K_{o.y1} U_{n.y} - K_{o.y4} (R_{b.n} + R_{k.o}) I_a - K_{o.y3} U_{b.r}] \quad (5.96)$$

It is possible to determine generator external characteristic  $E_{r.2} = f(I_a)$  from equation (5.96).

Main propulsion motor. Since main propulsion motor field magnetic flux changes due to the decrease in icebreaker resistance to movement from the moored to the running in open water mode, this should be taken into account when calculating the mechanical characteristic.

The magnetizing force equation (without considering armature reaction) has the form

$$a_d \Phi_d = 2w_{b,d} i_{b,d}. \quad (5.97)$$

Equation (5.97) can be reduced to the form

$$\Phi_d = \frac{2w_{b,d}}{a_d R_{b,d}} U_{b,d} = K_d U_{b,d}. \quad (5.98)$$

where

$$K_d = \frac{2w_{b,d}}{a_d R_{b,d}}; \quad R_{b,d} = R_{b,d} + R_a.$$

Substituting equation (5.91) in equation (5.98), we get

$$\begin{aligned} \Phi_d = K_{\text{ЭМУД}} K_d [K'_{o,y1} U'_{n,y} - K'_{o,y2} U_{b,d} - \\ - (U_{b,\Gamma} - U_{\text{срвв}}) K_{o,y3}]. \end{aligned} \quad (5.99)$$

The characteristic of the change in main propulsion motor field magnetic /209 flux  $\Phi_d = f(I_d)$  is determined from equation (5.99).

Calculation of the GED mechanical characteristic. It is possible analytically to calculate the GED armature mechanical characteristic from the equations of the generator mechanical characteristic and motor magnetic flux equation (5.99):

$$M_d = C_{m,d} I_d \Phi_d; \quad (5.100)$$

$$n_d = \frac{E_{r,d} - I_d R_d}{C_{e,d} \Phi_d}. \quad (5.101)$$

It should be noted that generator external characteristic  $E_{r,d} = f(I_d)$  and GED characteristic  $\Phi_d = f(I_d)$  need to be calculated with consideration taken of the hysteresis of all electrical machinery and the non-linearity of their magnetization characteristics. This denotes that equations (5.96) and (5.99) have variable factors.

Solution of a similar problem, i. e., determination of the GEU mechanical

characteristic by means of an analytical calculation from equations with variable coefficients, is complex and labor intensive.

Graphic construction of the mechanical characteristic of a GED with two-stage longitudinal field EMU. It is possible to use a graphic method based upon the machinery statics equations obtained above for calculation of the EMU mechanical characteristic.

The principle of graphic construction of the GED mechanical characteristic for the icebreaker "Lenin" GEU (see Figure 3.29) is depicted in Figure 5.13. Construction occurs in nine quadrants.

The characteristics of the first stage of two-stage longitudinal field EMU showing the relationship of amplifying winding n. s. to control winding n. s.  $F_s = f(F_v)$  taking negative voltage feedback into account are plotted in the first and sixth quadrants. Characteristics  $F_a = f(F_v)$  must be obtained experimentally since the actual degree of armature reaction compensation against circulating currents will be considered here.

The load characteristics of two-stage longitudinal field EMU when operating a constant load resistance (generator field winding and GED field winding) are plotted in the second and seventh quadrants. These characteristics show the relationship of second-stage output voltage to amplifying winding n. s. (or to self-excitation winding n. s. given independent feed)  $U_s = f(F_a)$ .

The main generator magnetization characteristic (x.x.x) is depicted in the third quadrant.

The paths of short circuit  $I_{sc}$ , counter emf, and GED electromagnetic moment are plotted in the fourth quadrant. Total generator emf  $E_r$  is laid along the X-axis of this quadrant. Path  $I_a$  determines the relationship of the voltage drop in the GEU main circuit to the amount of current and will be constructed in a manner analogous to that indicated in the preceding paragraph. Since GED field magnetic flux changes when the main circuit current is less than the /211 nominal, two auxiliary paths are drawn in the GED current quadrant. One of

these, moment path  $C_{m,1} I_d \Phi_A$  remains constant during the constructions, while the other, a path determining GED counter emf, has a varied slope given different  $\Phi_A$ .

Screw characteristics are constructed in the fifth quadrant: 1 -- for the moored mode, and 2 -- for the running in open water mode. The GED mechanical characteristic will be constructed in this quadrant.

The GED magnetization characteristic is constructed in the eighth quadrant.

The ninth quadrant is the auxiliary for consideration of the change in the slope of the counter emf path  $C_{c,2} \Phi_A$  depending upon the amount of GED field magnetic flux.

Negative main circuit current feedback path  $S_1$  is constructed in the first quadrant. This path is drawn via point a corresponding to nominal n. s. of the EMU control master winding -- generator exciter -- and a point on the Y-axis of the first quadrant corresponding to to point  $I_{cr}$  (see the horizontal from point  $I_{cr}$  in the fourth quadrant to the Y-axis of the first quadrant). The presence of EMU negative voltage feedback is taken into account by characteristic  $F_s = f(F_y)$ .

Self-excitation winding path  $S_2$ , whose slope depends on the amount of resistance in this circuit, is drawn in the second quadrant. Path  $O_2 P_2$  establishes the relationship between magnetizing forces  $F_m$  of the first and second quadrants. Path  $O_2 P_2$  will run at a  $45^\circ$  angle if the scale along axis  $F_m$  in the first and second quadrants is identical.

Path  $O_3 P_3$  of the proportionality between exciter voltage and generator field current is drawn in the third quadrant. This path will be drawn through the origin of coordinate  $O_3$  and point i, which is determined by the intersection of a vertical from point j corresponding to the field current flowing in the generator field winding at exciter voltage  $U_{e.r.m.}$ .

Path mn in the fifth quadrant is for translation of a point from one axis to another for the purpose of subsequent determination of GED counter emf. The amount of path mn slope can be selected arbitrarily.

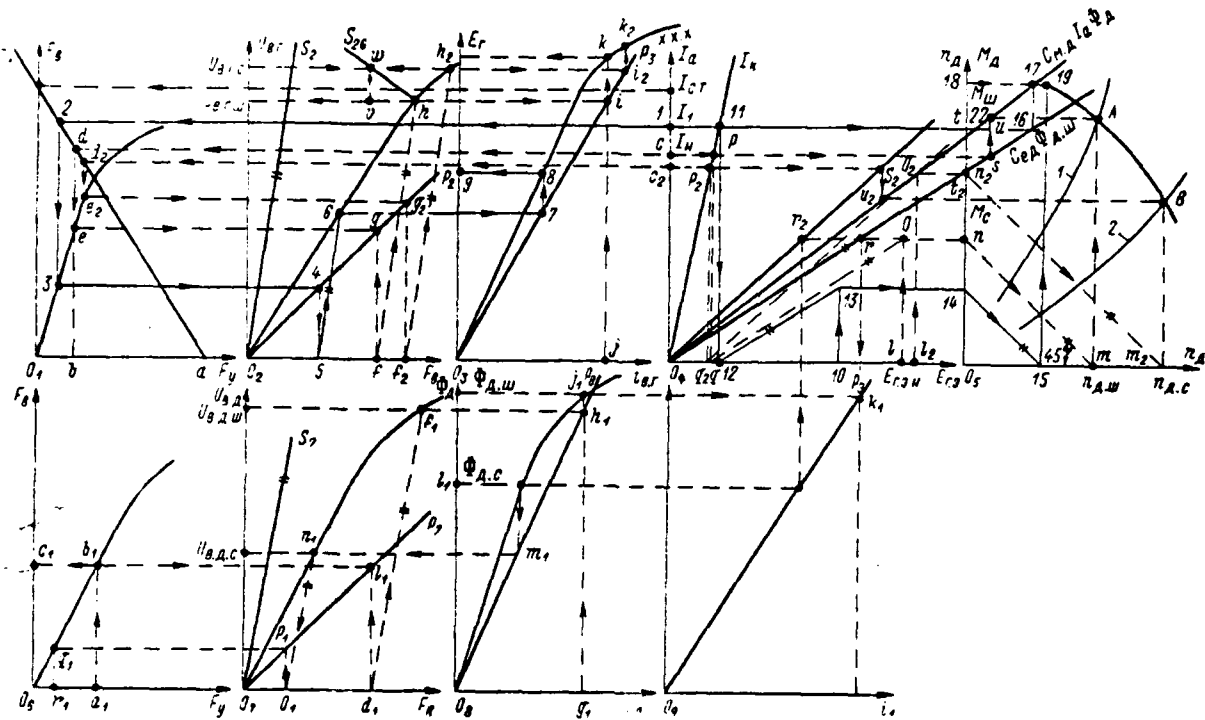


Figure 5.13. Principle of Graphic Construction of the Mechanical Characteristic of an Automated GEU GED.

Self-excitation winding path  $S_7$  is drawn in the seventh quadrant, while path  $Q_7P_7$  establishes the relationship between  $n, s$   $F_n$  of the sixth and seventh quadrants (analogous to path  $O_2P_2$ ).

Path  $O_8P_8$  in the eighth quadrant determines the proportionality between exciter voltage and current in the GED field winding circuit (analogous to path  $O_3P_3$ ).

Path  $O_9P_9$  in the ninth quadrant determines the proportionality between the amount of GED field magnetic flux and the slope of path  $C_{e2}D_A$  in the fourth quadrant.

Path  $S_{26}$  in the second quadrant considers the presence of generator exciter negative voltage feedback acting upon the GED exciter.

Points a, b, ..., w, u,  $a_1, b_1, \dots, k_1$  correspond to GEU nominal operating mode (in this case, this is the moored mode of operation). Points  $l_1, m_1, \dots, r_1$  and points  $c_2, d_2, \dots, u_2$  are plotted based on known value for main circuit current for a vessel running in open water and based on the amount of GED field magnetic flux for this mode. The sequence of plotting the points follows the letters of the Latin alphabet and is indicated by arrows in the figure.

Interconnection among quadrants is determined by the corresponding GEU machinery equations. Segment  $r_1 a_1$  on the X-axis of the sixth quadrant equals the n. s. created by the feedback winding from the generator exciter EMU output in the vessel running in open water mode. These provide automatic reduction of GED field flux to value  $\Phi_{x.c.}$ .

Path  $S_{26}$ , determining the proportionality between generator EMU voltage growth and motor EMU feedback winding n. s. regulating GED field magnetic flux, for simplicity of calculations is drawn in the second quadrant. Path  $S_{26}$  is determined by voltage  $U_{n.r.c.}$  and by segment  $h v = r_1 a_1$  (from the sixth quadrant) and passes through points h and w.

Construction of the GED mechanical characteristic point begins with acceptance of arbitrary main circuit armature current value  $I_1$  (point 1). Next, considering negative feedback  $S_1$  and other negative feedbacks, emf of the equivalent generator is determined (point 9). Points 1 and 9 determine one of the points of the generator's external characteristic.

If a point corresponding to the selected current value is located below point  $I_n$  (point  $c_2$ ), the subsequent construction occurs considering the fifth, sixth, seventh, eighth, and ninth quadrants in a manner analogous to the procedure for plotting points  $l_1, m_1, \dots, r_1$  (only in reverse order) after determination of the corresponding segment based on path  $S_{26}$  for the resultant value of generator exciter voltage. If the point corresponding to the selected current value is located above point  $I_n$ , then subsequent construction (after point 12) occurs without consideration of lower quadrants and without a change in the slope of path  $C_{r.A} \Phi_A$  (based on path  $C_{r.A} \Phi_{x.w}$ ).

One construction cycle for a selected value of current  $I_1$  is shown in Figure 5.13. These constructions result in one of the points of the GED mechanical characteristic (point 19). Further construction of the points of the GED mechanical characteristic occurs in a manner analogous to the aforementioned taking the interconnection between the quadrants and path  $S_{26}$  into account.

Thus, accepting different values for main circuit current from zero to  $I_{cr}$ , the mechanical characteristic of an automated GEU GED is constructed. Non-linearity of the magnetization characteristics of GEU electrical machinery and its hysteresis are taken into account here. Machinery characteristics in Figure 5.13 are plotted without considering hysteresis to simplify the construction and impart clarity to the graph. Construction should be reduced to the appropriate branches of the magnetization characteristics for determination of a GED mechanical characteristic taking hysteresis into consideration.

The mechanical characteristic of the GEU aboard the icebreaker "Lenin," /213 obtained from the aforementioned graphic construction, is depicted in Figure 5.14. The calculation was made from design data prior to final adjustment of the GEU without considering GED protection circuits.

As can be seen from the figure, the GEU must have a node for protection against an excessive increase in GED rotational speed when propellor shaft power is reduced (loss of a screw or its exposure). Curves depicted in this figure in intervals of a load less than the load while running in open water are theoretical. The discontinuity of the characteristic for  $n_2$  with a translation through infinity is depicted theoretically as well in the assumption that a GED can have unlimited rotational speed.

A reduction in load current, as is known, occurs as an icebreaker transitions from the moored mode to the running in open water mode. Further reduction in main circuit current during the calculation was accepted in the assumption that it occurs either when the screw is exposed or one of its blades breaks off. It follows from the calculation that, in this case, given an EMU -- GED exciter load current of 5,500 A, voltage will drop to zero. Therefore, the GED will be without excitation given somewhat increased generator voltage (due to weakened current winding action with reduced main circuit current). It is known that /214

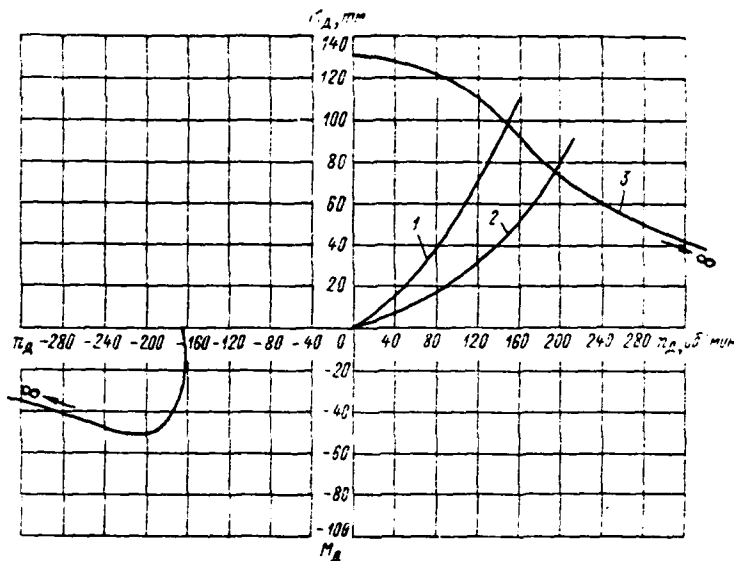


Figure 5.14. Mechanical Characteristics of a GED and Amidships Screw of the Atomic Icebreaker "Lenin." 1--Screw characteristic during moored operations; 2--Screw characteristic when running in open water; 3--Mechanical characteristic.

a motor with excitation removed when idling in the event voltage in the armature circuit is nominal will "run away."

Graphic construction of the GEU static characteristics of "Lena" and "Anguema" class vessels is analogous to that shown in Figure 5.13, while their static characteristics are similar to those of the icebreaker "Lenin" GEU.

Preparatory calculations and constructions. Methodology for calculation of the static characteristics of GEU with magnetic amplifiers is very similar to that for calculation of GEU with amplidynes examined in §5.4. However, there are differences, as can be seen from the example depicted in Figure 5.15.

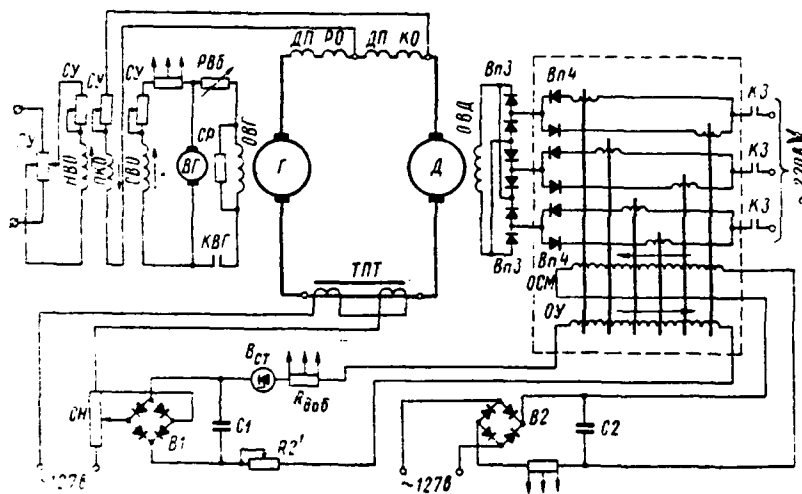


Figure 5.15. Schematic of a Port Icebreaker GEU (Variant with MU as GED Exciter).

Graphic construction is shown in Figure 5.16.

The characteristic of the equivalent generator's idling is constructed in the first static characteristics quadrant at coordinates  $U_{r,0}$ ,  $U_{b,r}$ , where  $U_{r,0}$  - is the equivalent generator's voltage equalling  $m_r U_r$  ( $m_r$  - is the number of series-connected generator armatures in the loop examined);  $U_{b,r}$  - is generator field voltage.

If characteristic  $E_r = f(i_{b,r})$  is given, then along the X-axis in this quadrant we plot  $U_{b,r} = i_{b,r} r_{b,r}$ , where  $r_{b,r}$  - is generator field winding equivalent resistance, with  $r_{b,r} = \frac{r_{b,r}}{m_r}$  of one generator

We plot the equivalent generator  $E_{r,3}$  equal to  $E_{r,3} = m_r E_r$  along the Y-axis.

Given a series of main current values and using the reactive triangle of the equivalent generator (we consider PKO action in the reactive triangle), we construct a series of equivalent generator load characteristics corresponding to the selected current values.

Based on data from the selected generator type, we establish the demagnetizing of the armature reaction in the nominal mode corrected to field current  $i_{pa}$  and PKO demagnetizing action in the nominal mode, corrected to field current:

$$i_n = \frac{I_{nom} \omega_n i_r}{2p \omega_{b,r} i_r}$$

where  $I_{nom}$  - is main generator nominal current;  $\omega_n$  - number of PKO turns;  $i_r$  generator field current;  $2p$  - number of poles;  $\omega_{b,r}$  number of main generator field winding turns.

The joint demagnetizing action of the armature reaction and of the differentially-compounded winding in the nominal mode is expressed by the sum  $i_{pa3M} = i_{pa} + i_n$ .

The voltage drop in the equivalent generator circuit comprises  $\Delta U_{r,3} = I_{nom} \sum R$ , where  $\sum R$  is armature circuit resistance in the hot state equalling  $\sum R = 1,2 (R_n + R_{b,n} + R_{pa3M})$ .

We determine the sides of the reactive triangle in the nominal mode:

$$\Delta U_{b,r} = m_r i_{pa3M} r_r; \Delta U_{r,3} = I_{nom} \sum R.$$

We assume that characteristic triangle abc constructed for the nominal mode is proportional to load current.

In the second quadrant we construct characteristic 4 of the voltage drop in the propulsion motor circuit  $\Delta U_2 = f(I)$ . Here,  $\Delta U_2 = I (R_{n,2} + R_{b,2} + R_{a,2})$ .

We construct generator exciter idling characteristic 7 in the fourth quadrant.

We construct main generator exciter load characteristic 6 from the reactive triangle.

Here, we compute the voltage drop in the exciter circuit from data for machinery selected from series  $\Delta U = 0.275 \frac{U_{B.r.}}{R_{B.r.}}$  for nominal exciter voltage.

Magnetizing forces of the armature reaction demagnetizing action corrected for exciter field n. s. are determined from formula

$$F_{p.n} = 2.89 \frac{U_{B.r.}}{R_{B.r.}}$$

We determine the position of volt-ampere characteristic 5 of current feedback in the main circuit in the third quadrant from points corresponding to moored mode current  $I_w$ , anchorage current  $I_{cr}$ , resultant anchorage n. s.  $F_{cr}$ , and resultant moored mode n. s.  $F_w$ .

Given several load current values, we construct the equivalent generator external characteristic in the second quadrant (curve 3) using the methods enumerated above. The construction sequence is indicated by arrows in the first through fourth quadrants and designated by the digits 1-5.

Subtracting the voltage drop in the propulsion motor armature circuit from the ordinates of the generator external characteristic, we get characteristic  $E_A = \bar{i}(I)$ , curve 2.

We construct propulsion motor screw characteristics 11 and 12 for the given mode in the tenth quadrant.

We construct propulsion motor magnetization curve 9 from plant-supplied data in the fifth quadrant.

We determine the required amount of main propulsion motor field flux for the moored mode:

$$\Phi_{A.w} = \frac{E_{A.w}}{C_e n_{A.w}}$$

where  $C_e = \frac{p \cdot N}{60 \pi}$  - is the machine's design constant; value  $E_{A.w}$  is determined

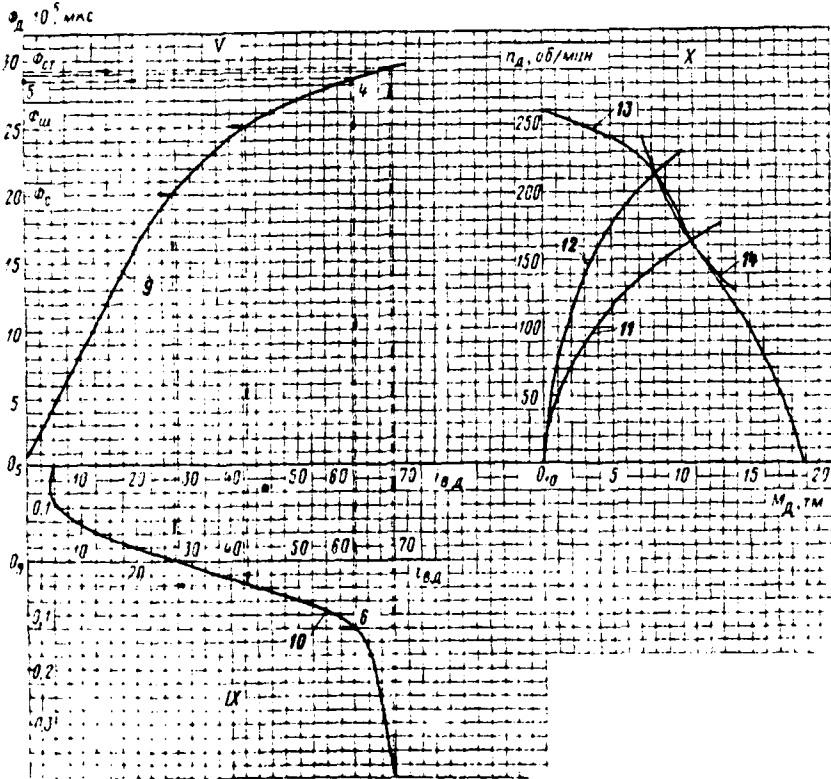
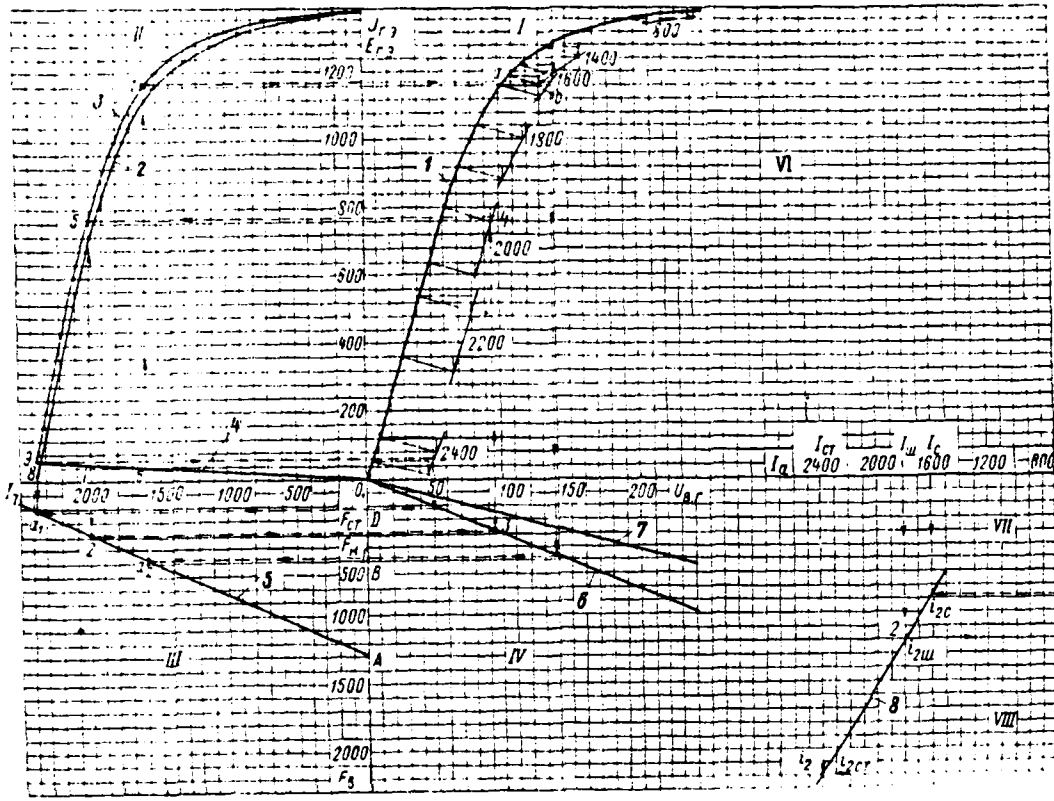


Figure 5.16.  
Graphic Construction  
of Static Charac-  
teristics.

based on  $I_w$  from characteristic  $E_A = f(I)$ , constructed in the second quadrant (curve 2).

We assume that current in open water equals  $I_c = I_w - \Delta I$ , where  $I_w$  - is current in the moored mode; value  $\Delta I$  is assumed in accordance with the selected scale.

We determine the required amount of main propulsion motor field flux for the open water mode:

$$\Phi_{A.c} = \frac{E_{A.c}}{C_{pA.c}},$$

where value  $E_{A.c}$  is determined from the trace in the second quadrant.

In the fifth quadrant, we determine the amount of propulsion motor field current for the moored mode and when a vessel is running in open water based on the values found and on the main propulsion motor magnetization curve.

The appropriate magnetic amplifier is selected based on the amount of field current (based on power) for the moored mode considering brief boosting of magnetic flux when the GED stops (on the order of  $1.5\Phi_{A.w}$ ).

We construct the magnetic amplifier load characteristic using the methodology presented in [55].

We calculate the magnetic amplifier bias winding circuit, which provides at the MU output load current equal to main propulsion motor field current for the vessel running in open water mode, with the control winding signal absent.

We find the value of bias current  $i_{cm}$  from the MU load characteristic /219 for the basic mode (when all generators are running the main propulsion motor). The bias winding is connected via a rectifier. Its total resistance equals

$$\sum R_{cm} = \frac{UK}{i_{cm}},$$

where K is MU gain.

Knowing MU bias winding resistance, we determine additional resistance in the bias winding circuit from relationship  $R_{2, \text{bias}} = \sum R_{\text{cm}} - R_{\text{cm}}$ .

The resultant magnetic amplifier characteristic is constructed in the ninth quadrant.

The value of the main circuit current is plotted in the seventh quadrant along the X-axis on a scale convenient for construction.

The value of the amount of current in the magnetic amplifier control winding is determined from value  $\Phi_{\text{a.w}}$ . The construction sequence for this determination is shown in the figure.

The position of the positive current feedback volt-ampere characteristic 8 is determined in the eighth quadrant from points corresponding to

$$I_{\text{a.w}}, I_{\text{ct}}, I_{\text{ct}}$$

Construction of a GED mechanical characteristic. Having completed the preparatory calculations and constructions described above, we convert to construction in the tenth quadrant of the main propulsion motor mechanical characteristic (curve 13).

We are given the actual value of the load current and we determine the electromotive force of the motor from characteristic 2  $E_{\text{a}} = \bar{f}(I)$  in the second quadrant.

We plot the actual current value in the seventh quadrant from positive current feedback volt-ampere characteristic 8 and magnetic amplifier load characteristic 6. We determine propulsion motor field current and then, using the magnetization curve 9, the field flux. Construction progress is depicted in the drawing by arrows and is designated by digits 1-5. If the values of the armature circuit current are less than the current when the vessel is running in open water, then motor magnetic flux will be constant and equal to the flux in the vessel running in open water mode since a silicon stabilitron accomplishes current cut-off in the magnetic amplifier control winding circuit.

From the values found for  $E_A$  and  $\Phi_A$ , we determine motor moment  $M_A$  and its rotational speed  $n_A$ :

$$M_A = C_{m, A} I_{A1} \Phi_{A1}; \quad n_{A1} = \frac{E_{A1}}{C_{eA} \Phi_{A1}}$$

where  $C_{m, A} = \frac{P \cdot \lambda}{6,81 \cdot \pi \cdot 2a}$  and  $C_{eA}$  are design constants.

We construct propulsion motor mechanical characteristic 13 from the resultant points.

Data from calculation of the main propulsion motor mechanical characteristic are compiled in tabular form (Table 5.2).

$I_{A1}, a$	$\Phi_{A1} \cdot 10^6, \frac{US}{MKS}$	$E_{A1}, V$	$M_{A1}, m.M$	$n_{A1}, \frac{rpm}{0,2 \cdot MIN}$

Table 5.2. Data for Construction of the GED Mechanical Characteristic.

Static characteristics for all other GEU operating modes are calculated /220 in an analogous manner.

Calculation of the main propulsion motor positive current feedback node.  
Regulation of the main propulsion motor field flux as a function of main circuit current is shown in the Figure 5.15 diagram.

We will calculate the current node.

We determine (approximately) the main propulsion motor field winding time constant, using known formula

$$T_s = \sqrt[3]{\frac{1000 P_{A, NOM}}{n_{A, NOM} (2p)^2}} \text{ сек.}$$

where  $P_{A, NOM}$  is rated power;  $n_{A, NOM}$  is rated rotational speed;  $2p$  is the number of poles.

We select the method of connecting the magnetic amplifier control winding to obtain a signal proportional to main circuit current.

First variant. We connect the magnetic amplifier control winding to the voltage drop at the propulsion motor commutating poles and compensating winding. Here, the total voltage drop at the commutating poles and compensating winding equals  $\sum R_{\alpha, \beta, \gamma, \delta} = R_{\beta, \alpha} + R_{\delta, \gamma}$ .

The voltage drop at anchorage current  $I_{cr}$  comprises  $\Delta U_{cr} = I_{cr} \sum R_{\alpha, \beta, \gamma, \delta}$ .

The voltage drop with the vessel running in open water mode current  $I_c$  equals  $\Delta U_c$ .

A silicon stabilitron with parameters  $U_c = 18$  V,  $I_c = 700$  mA can be used in the vessel running in open water mode for cut-off of main circuit current in the magnetic amplifier control winding circuit.

Correlation of the amounts of voltage drop in propulsion motor compensating winding and commutating poles at different operating modes with the voltage drop in the stabilitron may indicate that this method is unacceptable due to the limited capability to tune the current cut-off.

Second variant. We will use bus bar instrument transformers as a dc transformer to obtain a signal proportional to the current in the propulsion motor circuit.

We construct characteristic  $i_2 = f(I_a)$  from the core material magnetization characteristic. Using a known methodology for calculation of magnetic /221 amplifiers proposed by M. A. Rozenblat, for the purposes of simplification we draw an approximation of it with a segment of straight line 8.

Calculation process. 1. Current in the transformer's secondary winding from characteristic  $i_2 = f(I_a)$  will be  $i_{2c}$  when main circuit current in the vessel running in open water mode is  $I_c$ .

Stabilitron rectified voltage can be assumed to equal  $U_{cr} = 18$  V. Then,

for a full-wave single-phase circuit, the voltage drop in tuned resistance will equal  $\Delta U'_{R_2} = \frac{U_{ct6}}{K}$ , where  $K = 0.9$ .

The voltage drop in the entire resistance  $R_2$  will comprise  $\Delta U_{R_2} = i_2 R_2$ .

We determine the value of tuned resistance  $R_2'$ :

$$R_2' = \frac{R_2 \Delta U'_{R_2}}{\Delta U_{R_2}}$$

2. Current in the transformer's secondary circuit from characteristic  $i_2 = f(I_a)$  will be  $i_{2w}$  for the moored mode when main circuit current is  $I_w$ .

We determine voltage drop  $\Delta U'_{R_2}$  in the tuned resistance:  $R_2 = i_{2w} R_2'$ .

Rectified voltage equals  $U_R = K \Delta U'_{R_2}$ .

Then the voltage drop in the magnetic amplifier control winding and additional resistance will equal  $\Delta U_v = \Delta U'_{R_2} - U_{ct6}$ , where  $U_{ct6}$  is voltage drop in the stabilatron.

Total control winding resistance and additional resistance:

$$\sum R_{v+206} = \frac{\Delta U}{i_{y.w}}$$

where  $i_{y.w}$  is the current in the control winding in the moored mode, whose value is taken from the drawing.

The value of the additional resistance in the control winding circuit comprises  $R_{206} = \sum R_{v+206} - R_y$ , where  $R_y$  is control winding resistance.

3. For the anchorage under current mode where main circuit current is  $I_{ct}$ , current in the transformer's secondary winding  $i_2$  is determined from characteristic  $i_2 = f(I_a)$ .

Voltage drop  $\Delta U_{R_2}$  in tuned resistance  $R_2'$ :  $U_{R_2'} = i_{2ct} R_2'^2$ .

Rectified voltage  $U_R = U'_{R_3} \cdot K$  .

The voltage drop in the control winding and in the additional resistance:

$$\Delta U_{y+\text{доб}} = U'_R = -U_{\text{cr}}$$

Control winding circuit current in the anchorage under current mode: /222

$$i_{y, \text{cr}} = \frac{\Delta U}{\sum R_{y+\text{доб}}}$$

We determine control winding circuit equivalent resistance:

$$R_3 = \frac{U'_R}{i_{y, \text{cr}}}$$

We find the magnetic amplifier time constant:

$$T_{y,3} = \frac{T_y R_y}{R_3}; T_{y,3} \ll T_y$$

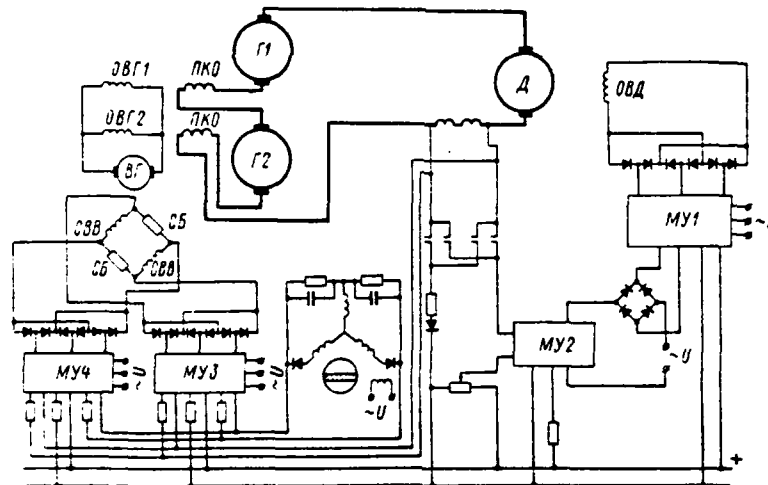


Figure 5.17. Schematic of a GEU with MU as Generator and GED Pilot Exciters.

Special features of calculating the static characteristics of GEU with magnetic amplifiers as GED exciters and main generator pilot exciters. We will examine certain special features of calculating the static characteristics of GEU circuits in which power magnetic amplifiers are used as GED exciters and

main generator pilot exciters. These special features appear mainly in calculations of negative and positive feedbacks.

We will present the calculation methodology relative to the schematic (Figure 5.17) for the basic mode.

Construction of characteristic  $E_a = f(I)$ . . Graphic-analytical construction occurs in four quadrants (Figure 5.18).

We construct the load characteristic of a push-pull generator field MU in the first quadrant and the characteristic of generator exciter VG idling /223 in the second quadrant. We construct the path linking values  $I_{b.r}$  in the first and second quadrants.

We construct the equivalent generator idling characteristic  $m_r E_r = f(I_{b.r})$  in the third quadrant. We draw the connecting path, found from the equation for the voltage equilibrium for the field circuit in the established mode  $E_{b.r} - m_r I_{b.r} R_{b.r} = I_{b.r} R_{b.r}$ .

We assume during this construction that the circuit operates in the rectilinear portion of the characteristics both of magnetic amplifier VG and the generator exciter.

We construct relationship  $E_a = f(I_a)$  in the fourth quadrant. We accomplish the construction in the following sequence:

1. We determine the voltage drop in the main circuit for  $I_a = I_{cr}$  (usually it is assumed that  $I_{cr} = 1.5 I_{nom}$ ). We construct path 1-2 (Figure 5.18) from point  $I_a = I_{cr}$  to point  $E_a = I_{cr} \sum R$  in the same quadrant.

We determine the amount of current in the push-pull MU master winding. The sequence of  $i_{y,cr}$  location is indicated by digits 1-8 and by arrows (Figure 5.18).

2. From point 9, corresponding to  $I_a = I_w$ , we plot the amount of motor magnetic flux in the moored mode from ratio

$$\Phi_{a.w} = \frac{M_{a.w}}{m_r C_w I_w}$$

and GED emf in the moored mode

$$E_{\lambda, \omega} = \frac{C_{\lambda} n_{\lambda} \Phi_{\lambda, \omega}}{\sigma}$$

From point 11, corresponding to values  $I_{\omega}$  and  $E_{\lambda, \omega}$ , we construct a path parallel to path 1—2 of the voltage drop in the main circuit and we find generator emf  $E_{r, \omega} = E_{\lambda, \omega} - \Delta U$  and its corresponding exciter current  $i_{\lambda, r, \omega}$ , as well as exciter emf  $E_{\lambda, r}$ . From value  $E_{\lambda, r}$ , we determine  $i_{\lambda, r}$  and MU control current  $i_{y, \omega}$  corresponding to it. The sequence of determination of  $I_{y, \omega}$  is denoted by the digits 9—17 and by arrows.

Following determination of MU — main generator pilot exciter control current (the total amount of current of the two control windings, master and current), one can determine the current in the master winding corresponding to the nominal mode. Here, the following ratios are used: current winding voltage  $U_{o, \tau} = I (R_{o, \lambda} + R_{o, \omega})$  (for cases where the current winding is connected to the total voltage drop in additional poles and in the compensating winding) and current winding circuit total resistance

$$R_{o, \tau} = \frac{R_{\lambda, \kappa, \lambda} (I_{ct} - I_{\omega})}{i_{y, \omega} - i_{y, ct}}$$

The amount of current in the feedback winding, given anchorage current, equals

$$i_{o, c, ct} = \frac{R_{\lambda, \kappa, \lambda} I_{ct}}{R_{o, \tau}}$$

Current in the master winding must be greater than  $i_{o, c, ct}$  by value  $i_{y, ct}$  /226 since only in this case will anchorage current  $I_{ct}$  equal  $K I_{nom}$ , where K is a factor, usually  $K = 1.5$ . Thus,  $i_{\lambda, o} = i_{o, c, ct} + i_{y, ct}$ .

We plot master winding current in the first quadrant along axis  $i_{\lambda}$ . We draw the current feedback path at angle  $\alpha = 45^\circ$  from point  $i_{\lambda, o}$  since we assume the equality of scales  $i_y$  in the first and fourth quadrants. From point  $i_{y, ct}$  we construct a straight line perpendicular to axis  $i_y$  to the intersection with the current feedback path at point C. We plot the value of this segment in the fourth quadrant on the perpendicular from point  $I_{ct}$ . We draw a straight line from the origin of coordinate  $O_4$  through the end of the segment, which also will be current feedback characteristic  $I_{o, c, \tau} = f(I_{\lambda})$ .

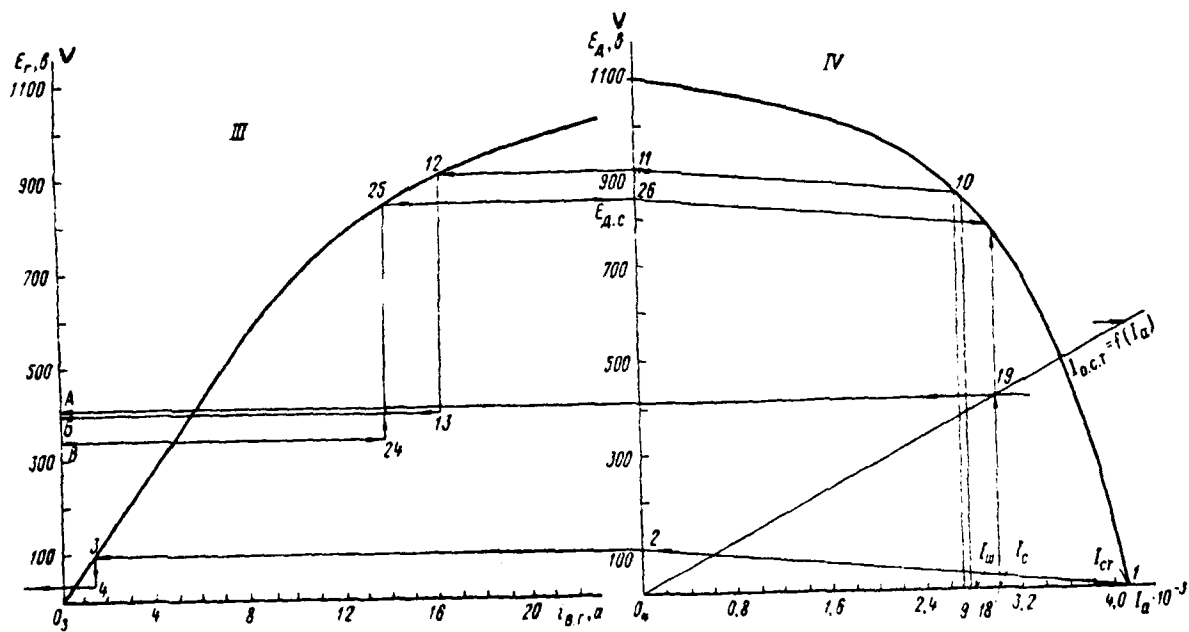
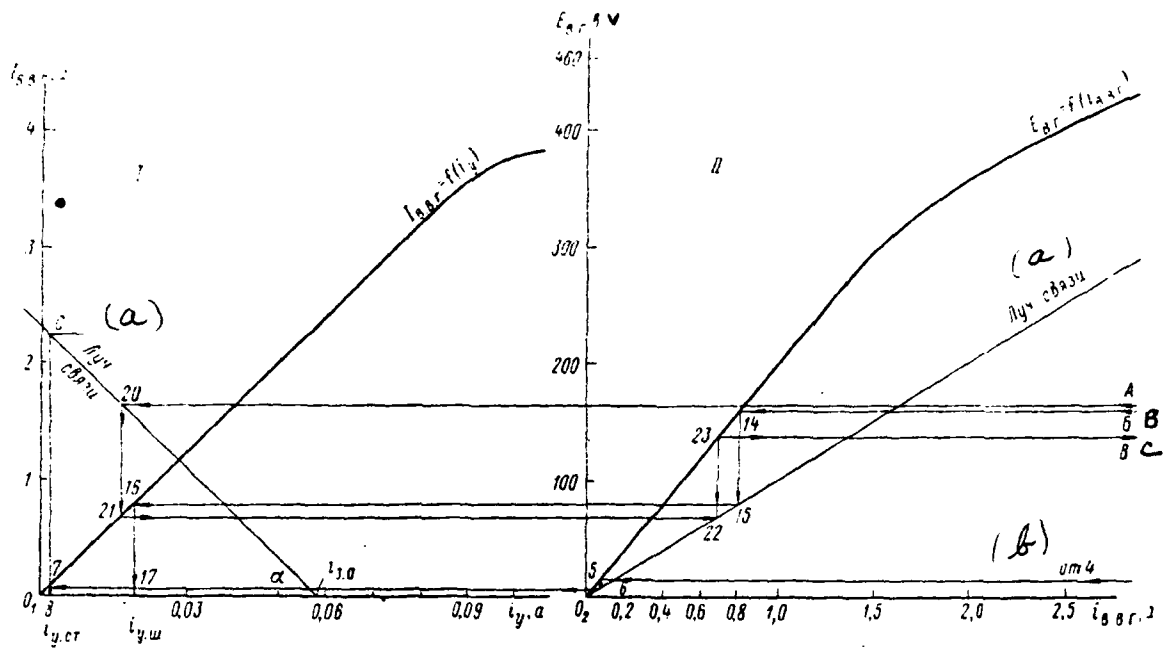


Figure 5.18. Graphic Construction of Characteristic  $I_a = f(I)$ .  
 a—Connecting path; b—From 4.

Since regulation occurs as a function of current, then we use  $\Delta I_a$  to designate the difference between armature circuit current values in the moored mode and in the vessel running in open water mode:  $\Delta I_a = I_w - I_c$ ; here,

$$\Delta i_y = i_{o.c.w} - i_{o.c.c} = \frac{R_{b.z+k.z}(I_w - I_c)}{R_{o.r}},$$

i. e.,

$$i_{y.c} = i_{y.w} + \Delta i_y, \text{ a } \Phi_{d.c} = \frac{M_{d.c}\sigma}{m_r C_M/c} \text{ и } E_{d.c} = \frac{C_e R_{d.c} \Phi_{d.c}}{\sigma}.$$

From the characteristics, we determine the magnitudes of the values in each quadrant, sequentially drawing a path from the point corresponding to magnitudes  $I_c$  and  $E_{d.c}$  (points 18—26).

Construction of characteristic  $\Phi_d = f(I)$ . For the assumed GED field circuit (Figure 5.17) and for subsequent calculation simplification, first we construct the characteristic coupling the "input" and "output" of a GED exciter dual-cascade MU:  $U_{b.a} = f(i_{y1})$ , where  $i_{y1}$  is the current in the control winding of the MU first cascade. For a vessel running in open water  $U_{b.a} = U_{b.a.c}$ . This is provided by the corresponding values of the currents in the bias windings of both cascades.

$\Phi_{d.c}$  corresponds to value  $U_{b.a.c}$ .

We accomplish the construction in three quadrants: relationship  $U_{b.a} = f(i_{y1})$ ;

in the first; magnetization characteristic  $\Phi_d = f(i_{b.a})$  and connecting path  $U_{b.a} = K_{b.a} i_{b.a}$ ; in the second; characteristic  $\Phi_d = f(I_d)$  must be constructed in the third quadrant. The construction is accomplished in the following sequence:

1. We plot a segment equal to  $\Phi_{d.w}$ , i. e., a positive feedback signal to the output of the first MU must have a value given a current change from  $I_c$  to  $I_w$ , so that  $\Phi_d$  will increase from value  $\Phi_{d.c}$  to  $\Phi_{d.w}$ , in the third quadrant from a point corresponding to value  $I_w$ .

Sequentially drawing the path from the third quadrant to the first, we determine value  $i_{y1}$ . The construction sequence is shown by arrows and designated by digits 5—13.

2. The amount of current winding circuit resistance is determined by /228 the expression

$$R_{o.r} = \frac{R_{b.z+k.z} \Delta i_y}{i_{y.r}}$$

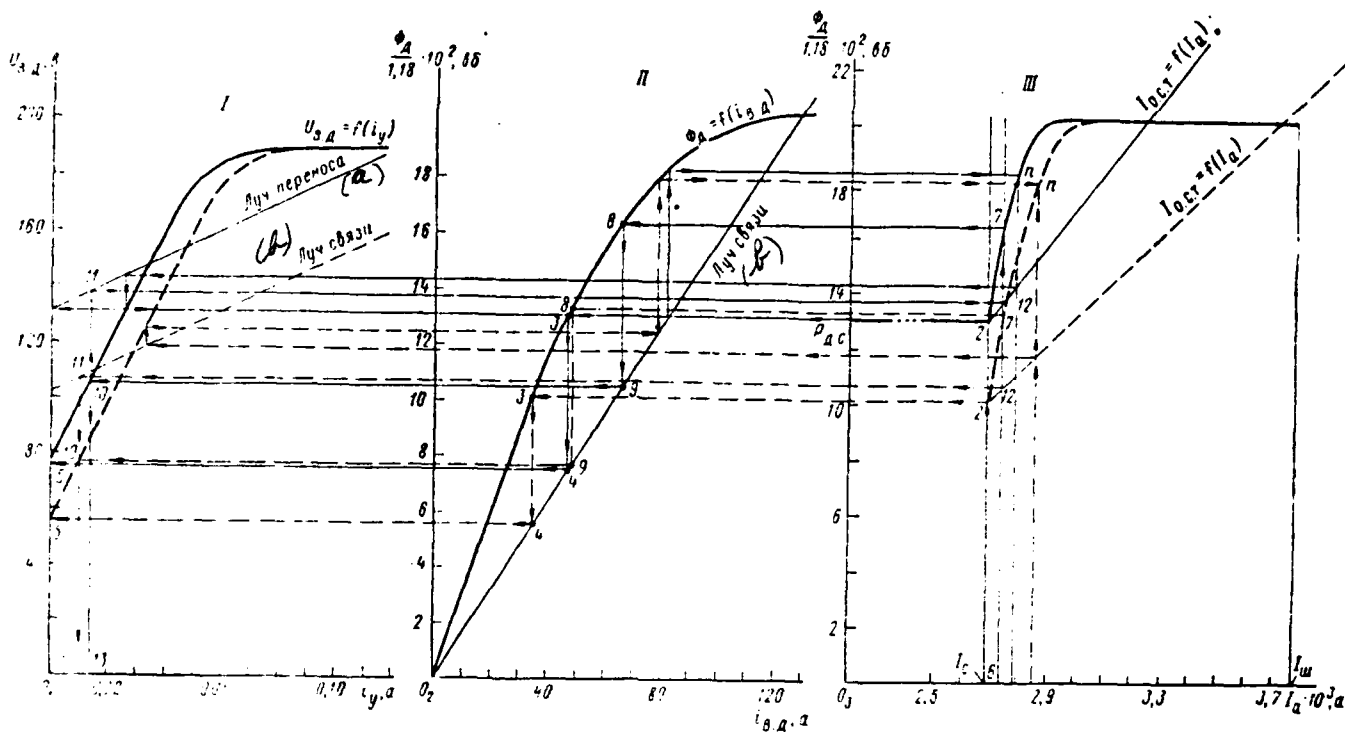


Figure 5.19. Graphic Construction of Characteristic  $\Phi_A = f(I_A)$ .  
 a—Translation path; b—Connecting path.

3. We construct the current feedback characteristic in the third quadrant. We plot the amount of feedback current along the vertical. We construct the characteristic from points  $I_c$  and  $\Phi_{A.c.}$ .

4. We construct a translation path, which originates from a point lying on the axis  $U_{A.d}$  and on one horizontal from the origin of characteristic  $I_{0.c.r.} = f(I_A)$ , in the first quadrant.

The construction sequence for one point  $n$  of characteristic  $\Phi_A = f(I_A)$  is shown by arrows.

Construction of characteristic  $M_A = f(n_A)$ . The GED mechanical characteristic is calculated using characteristics  $E_A = f(I_A)$  and  $\Phi_A = f(I_A)$ , previously constructed. This is the calculation sequence:

1. A series of main circuit current values  $I_{Ai}$  is given.
2. The corresponding values  $I_{Ai}$  of values  $E_{Ai}$  and  $\Phi_{Ai}$  are determined.
3. GED electromagnetic moment values for selected values  $I_{Ai}$  and  $\Phi_{Ai}$  are determined from expression  $M_{Ai} = m_w C_w I_{Ai} \Phi_{Ai}$ .

4. GED rotational speed for the corresponding values  $E_{Ai} = f(\Phi_{Ai})$  are determined from expression

$$n_{Ai} = \frac{E_{Ai}}{C_e \Phi_{Ai}}$$

Static characteristics for all GEU operating modes are determined from an analogous methodology.

#### § 5.6 Static Characteristics of GEU With Controlled Rectifiers (Thyristors)

Special features of the excitation system. The following special features of an excitation system must be considered when calculating the static characteristics of GEU with silicon controlled rectifiers (thyristors):

1. Rectified voltage  $U_d$  depending upon rectifier control angle  $\alpha$  has a character similar to that of the external characteristic of an exciter with constant negative current feedback, i. e., it has a convex curve. In this connection, full use of generator power at nominal amounts of main circuit current and voltage is possible either in the moored mode or in the vessel running in open water mode. If one assumes that the vessel running in the open water mode is the basic GEU operating mode, then use of full plant power during the /229 transition to the moored mode is possible only given a slight increase in main circuit current and a corresponding reduction in voltage. The excitation system, considering combined regulation of generator and main propulsion motor field fluxes, makes it possible to achieve current and voltage fluctuations from nominal values within a range of several percent.

2. Considering that generators used in GEU as a rule are equipped with compensating windings, we disregard the influence of an armature transverse reaction when performing the calculation.

3. Given generator characteristic  $E_r = f_1(i_r)$  and main propulsion motor characteristic  $\Phi_{s_2} = f_2(F_2)$  must be reconstructed into characteristics  $E_r = f_3(U_{s,r})$  and  $\Phi_{s_2} = f_4(U_{s,r})$ , where  $U_{s,r}$  is the voltage at the generator exciter thyristor output;  $U_{s,r}$  is the voltage at the main propulsion motor exciter thyristor output.

4. The main propulsion motor mechanical characteristic is constructed from data on the volt-ampere characteristics of negative and positive feedbacks.

Initial data for construction of static characteristics. Some of the information that must be available prior to beginning the construction are:

- a) for main generators and main propulsion motors: main current circuitry and basic modes, machinery nominal data, winding data, idling characteristics;
- b) for thyristors: type, nominal current (average rectified), switching voltage at 120° C and amplitude reverse test voltage of at least 1,200 V, nominal

operating voltage (amplitude);

c) for uncontrolled rectifiers (silicon diodes): type, maximum permissible operating voltage amplitude, nominal value of the average rectified voltage, as well as type of capacitors and resistors, maximum permissible forward voltage for group G, ultimate voltage, typical voltage, forward leakage current; typical current equalling 1 mA, reverse leakage current;

d) for the magnetic amplifier selected as saturation choke: type, nominal alternating voltage in volts, nominal frequency, prolonged permissible load current;

e) for propellers: characteristics for vessel running in open water  $M_{a.c} = f(n_a)$  and for moored operations  $M_{a.w} = f(n_a)$ .

Preparatory calculations and constructions for GEU main operating modes (reversing in the GED field circuit). The calculation of static characteristics is done relative to the circuit shown in Figure 3.57.

Generator armature winding circuit total resistance comprises

$$R_{\Sigma r} = m_r (R_{a.r} + R_{a.n} + R_{k.o} + R_{n.k.o}),$$

where  $m_r$  is the number of series-connected generators in the loop;

$R_{a.r}, R_{a.n}, R_{k.o}, R_{n.k.o}$  is the resistance of the armature, additional poles, /230 compensating winding, and differentially-compounded winding, respectively.

Given generator idling characteristic  $E_r = f(i_r)$  is reconstructed in coordinates  $E_r = f(U_{a.r})$ , where  $U_{a.r} = i_r R_{a.r}$ , while

$$R'_{a.r} = \frac{R_{a.r} - R_{c.p}}{m_r},$$

where  $R'_{a.r}$  is generator field winding equivalent resistance;  $R_{c.p}$  is adjusting resistance in the generator field circuit.

The equivalent generator's idling characteristic is constructed in the first quadrant (Figure 5.20).

In the fourth quadrant, we construct the exciter load characteristic, the characteristic of a three-phase thyristor rectifier operating an active-inductive load obtained from relationship  $\frac{E_{da}}{E_{do}} = f(\alpha^c) \quad i_y = f(\alpha^c)$ ,

where  $E_{d\alpha}$  is the average amount of rectified voltage given different control angles;  $E_{d0}$  is the maximum amount of rectified voltage;  $i_y$  is saturation choke control current.

Here, the X-axis is common for the equivalent generator's idling characteristic  $E_r = f(U_{s,r})$  and exciter load characteristic  $U_{s,r} = f(i_y)$ .

The main propulsion motor magnetization characteristic  $\Phi_a = f(i_{s,a})$  is reconstructed in coordinates  $\Phi_a = f(U_{s,a})$ . The GED idling characteristic is the initial information here.

Conversion occurs based on formulas

$$E_a = C_e n_a \Phi_a \quad \text{and} \quad U_{s,a} = i_{s,a} R'_{s,a}$$

where  $C_e$  is the proportionality factor between GED emf, field flux, and rotational speed equalling

$$C_e = -\frac{pn \cdot 10^{-8}}{60a}; \quad R'_{s,a} = R_{s,a} + R_{s,a} \cdot \alpha \cos^2$$

The calculation is accomplished in the form of Table 5.3.

$U_{s,a}, V$	$i_{s,a}, a$	$\Phi_a, 10^6, \text{Wb}$	$U_{s,a}, V$

Table 5.3. Data for Construction of the GED Magnetization Characteristic.

The GED magnetization characteristic is constructed in the seventh quadrant.

In the eighth quadrant, we construct the GED exciter load characteristic /232 obtained in a manner analogous to the generator exciter load characteristic.

The X-axis is common for the characteristics in the seventh and eighth quadrants.

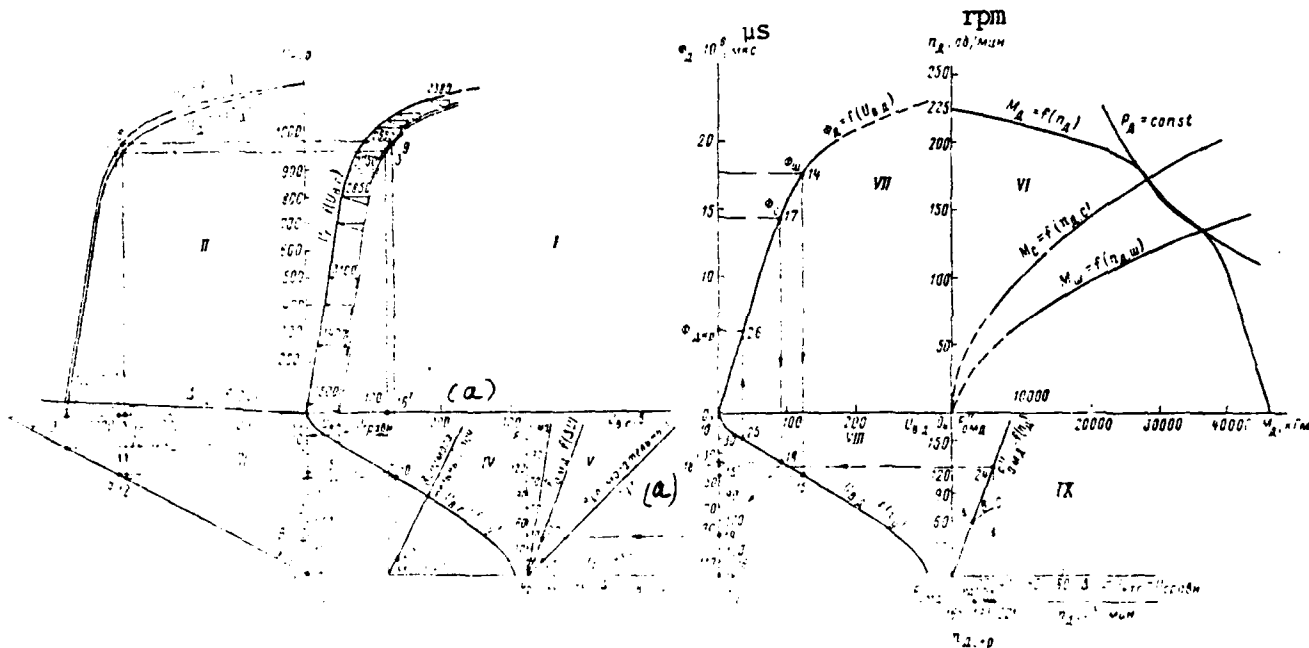


Figure 5.20. Graphic Construction of Static Characteristics.  
a - auxiliary path

We construct the characteristic of the propeller in the moored mode  $M_w = f(n_{A,w})$  and in the open water mode  $M_c = f(n_{A,c})$  in the sixth quadrant.

The next stage of the calculation is construction of the generator external characteristic  $U_r = f(I)$ . We start from the requirement for full generator power use in both the moored and running in open water modes. We assume that the current will change to value  $\Delta I$  during the transition from the moored to the vessel running in open water mode. Then, given that power constancy is retained, current while the vessel is running in open water will equal  $I_c = I_w - \Delta I$ , while voltage is

$$U_c = \frac{I_w U_w}{I_w - \Delta I}$$

We construct points 2 and 8 in the second quadrant from current values  $I_a = I_w$ . Generator external characteristic  $U_r = f(I_a)$  must pass through these points.

Next, we construct a series of equivalent generator load characteristics

for different armature current values  $I_a$ . Construction of load characteristics occurs with the aid of a triangle, whose vertical leg corresponds to the voltage drop in the generator armature circuit  $\Delta U_r = I \sum R_r + \Delta U_m$  (for the purposes of simplification, the drop in the brushes of each generator  $U_m$  is assumed to equal 2 V and is independent of the amount of load current), while the horizontal leg is a certain equivalent voltage increment, to which the voltage at the exciter output must be increased in order to compensate for the demagnetizing action of negative main circuit current feedback.

The magnitude of the voltage increment for an equivalent generator is calculated from formula

$$\Delta U_s = \frac{2I\omega_n R_{s,r}}{B\omega_n r},$$

where B is the number of PKO parallel branches.

We construct the equivalent generator's load characteristics  $U_r = f(I_a)$  taking into account triangle parameters in the first quadrant computed for various values  $I_a$ .

We determine the requisite amount of exciter voltage and requisite resultant control n. s.  $F_y$  for conditions  $I_a = I_{\text{НОМ}} = I_w$ ,  $U_r = U_w$ ,  $I_a = I_c$ ,  $U_r = U_c$  from the load characteristics which correspond to them. Following this, we draw lines through points 5 and 11 to their intersection in the third quadrant with the corresponding verticals passing through points 1 and 7 ( $I_{\text{НОМ}}$  and  $I_c$ ).

We draw a straight line through resultant points 6 and 12 to its intersection with the Y-axis at point 13. This point determines the full n. s. of the generator exciter master winding (OZG) taking into consideration the demagnetizing action of the current winding (OTG).

Straight line 6—12 is the volt-ampere characteristic of the current winding (OTG) feedback circuit, while  $\text{tg}$  of the slope  $\beta$  of this straight line to the Y-axis is proportional to the winding OTG resistance.

Segments  $O_1-5$  and  $O_1-11$  on the Y-axis of the fourth quadrant in the control

n. s. scale is the required n. s. at the control unit input:

for the moored mode

$$F_{o.r.r} = F_{o.s.r} - F_{p.w.}$$

for the running in open water mode

$$F_{o.r.r} = F_{o.s.r} - F_{p.w.}$$

Given that the feed for the electrical propulsion plant control and indication circuits occurs in each loop via an isolation transformer with use of a one-phase rectifier bridge, feed voltage is determined from formula  $U_{\text{rect}} = U_{\text{rep}} K \sigma$ , where  $K = 0.9$  for a one-phase rectifier.

Calculation of generator control winding circuit parameters. From construction  $i_y$  (points 0—13) we have

$$i_y = \frac{F_{o.s.r}}{w_{o.s.r}} \alpha; \quad \sum R = \frac{U}{i_y} \text{ ohms}; \quad R_x = \sum R - R_{o.s.r} \quad \text{ohms}$$

OTG n. s. in the moored mode  $F_{o.r.w.}$  is determined from the construction.

We use a device comprising a dc transformer (TPT) and voltage divider to obtain a signal proportional to the main circuit current.

The TPT comprises two bus bar instrument transformers, whose secondary windings are connected in series in accordance with the circuit shown.

It follows from the TPT characteristic that the TPT is saturated at values  $I_2$ , equalling  $I_2$  and above.

We determine  $R_2 = U/I_2$  at value  $I_2 = 6$  A.

We calculate the OTG parameters for the mooring mode.

From the TPT characteristic where  $I_m = I_2$ , we find the voltage drop at  $R_2$  from the expression  $U_2 = \bar{R}_2 I_2$ .

We assume that  $R_x = \bar{R}_{o.r.r}$  ohms.

We find value  $i_{y.m}$  in milliamperes, then  $U_m = i_y (R_{o.r.r} + R_x)$  V.

We determine the value of the voltage drop at resistance  $R_2$ , from which the rectifier bridge must be fed:  $R_2 = U_{nep}/I_2$ , where  $U_{nep} = U_w/K$ .

We determine OTG current when the current bump in the main loop is /234  
 $I_{maxc} = 1,8I_{nom}$ ;  $U_{nep} = R_2 I_2$ ;  $U_1 = U_{nep} K$ . Then,  $I_2 = U_1/R_2$ , which corresponds to nominal OTG current and, consequently, to nominal n. s. Thus, given double and triple shock currents, due to TPT saturation OTG winding n. s. loads will not exceed OZG winding n. s. loads, which eliminates the need for an upper current shut-off (initially, the proposal was to connect stabilitrons in parallel to OTG).

After determination of the position of the current winding OTG volt-ampere characteristic, given a series of load current values, we construct the generator's entire external characteristic. This characteristic passes through points 2 and 8, which correspond to full use of plant power in the moored mode and in the vessel running in open water mode with the assigned accuracy in maintaining main circuit current constancy.

Construction of the power constancy hyperbole. To determine anchorage current, in the second quadrant we construct the main propulsion motor armature circuit voltage drop characteristic:  $\Delta U_a = f(I_a)$  or  $\Delta U_a = I_a R_a$ .

We draw a straight line through the origin of the coordinates and the resultant point.

The magnitude of the anchorage current value  $I_{cr}$  is determined from the point of intersection of this characteristic with the generator external characteristic  $U_r = f(I_a)$ . Subtracting the GED armature circuit voltage drop characteristic from the generator external characteristic, we construct the motor electromotive force characteristic  $U_x = f(I_{a,x})$ .

From the resultant data, we find motor emf values for operation in open water  $E_{a,c}$  and in the moored mode  $E_{a,w}$  (we disregard losses in the iron and additional losses):

$$P_A = E_{a,c} I_c = E_{a,w} I_w = \text{const.}$$

We construct the hyperbole of constant power  $P_A = \text{const.}$  in the sixth quadrant, where screw characteristics already are constructed. We use this formula to do so

$$M_A = \frac{q \cdot 975 \cdot P_A}{n_A},$$

where  $q$  is the number of main propulsion motor armatures.

Calculation of GED magnetic flux. Having constructed the constant power hyperbole, we determine the value of screw rotational speed for operation in open water  $n_{c.u}$  and in the moored mode  $n_w$ , which the main propulsion motor must develop given that full power is used.

Having obtained values  $E_c, n_c$  and  $E_w, n_w$  from the formula for emf, we calculate the values of main propulsion motor field flux, which automatically must be provided by the control system when plant operating conditions change: for the vessel running in open water mode

$$\Phi_A = \frac{E_c}{C_e n_{A.c}};$$

for the moored mode

/235

$$\Phi_{A.w} = \frac{E_w}{C_e n_{A.w}}.$$

We determine the resulting exciter control n. s. from the main propulsion motor magnetization curve and motor exciter load characteristic:  $F_{\text{pes.c}}$  for the vessel running in open water mode and  $F_{\text{pes.w}}$  for the moored mode.

The static exciters assumed in the circuit essentially are inertia-free and the duration of the transient process will be determined by the motor exciter winding's own time constant. Therefore, it suffices to assume that the motor exciter control winding boosting factor falls within the limits of 2—3. We assume  $k_\Phi = 2.6$ .

We determine motor master control winding (OZD) nominal n. s. from the selected boosting factor and plot it in scale on the Y-axis in the eighth quadrant:

$$F_{\text{OZD}} = k_\Phi F_{\text{pes.nom}}, \text{ where } F_{\text{pes.nom}} \text{ is nominal n. s. when } \Phi_{\text{A.OZD}} = \Phi_{\text{A.nom}}.$$

We connect resultant point 16 to point 15 in the exciter load characteristic, which corresponds to

$$\Phi_{a.w} = \Phi_{a.ном.}$$

Straight line 15—16 is the volt-ampere characteristic of the voltage unity feedback circuit (OND), the origin of which translates from point  $O_3$  to point 16. We determine the OND magnetization characteristic given  $\Phi_{a.c} = \Phi_{a.w}$  from construction  $F_{o.n.2} = O_3 - 16 - O_2 - 15$ .

Calculation of GED exciter control winding circuit parameters. Control master winding (OZD). From the construction we find value  $i_y$ , then

$$\sum R = \frac{U}{i_y},$$

where  $\sum R$  is the resistance of the entire OZD winding circuit;  $U$  is feed voltage,  $V$ . Consequently,  $R_1 = \sum R - R_{o.z.d.}$ .

Motor exciter voltage feedback winding (OND). From the construction we find  $i_{y.pez}$ , then  $i_{o.n.2} = i_{o.z.d.} - i_{y.pez}$ .

In accordance with the construction, exciter voltage in the moored mode will be  $U_{a.w.}$ , then total OND winding circuit resistance equals

$$\sum R = \frac{U_{a.w.}}{i_{y.uz}}$$

and consequently,  $\sum R - R_{o.n.2}$ .

OND winding n. s. are determined, when the voltage differs from  $U_{a.w.}$ ; from the construction of straight lines parallel to straight line 15—16 through the points of the motor exciter load characteristic corresponding to voltage value data. Thus, for example,  $F_{o.n.2.c}$  for the running in open water mode is determined in the appropriate scale from segment 19—18.

Since in the static mode for a vessel running in open water resultant /236 motor exciter control n. s. is determined by the interaction of three control windings: OZD, OND, and OMD (motor power control winding), then, using the

OND and OZD n. s. values for this mode obtained during the calculation, we will find values  $F_{o.m.a.c.}$ , which the OMD winding must create when operating in the vessel running in open water mode (points 16—19).

It is assumed in the calculation that, in the moored mode,  $U_g = U_{\text{срвнн}}$ , OMD winding current equals zero, and  $\Phi_w = \Phi_{\text{ном}}$ .

We plot comparison voltage equal to generator exciter voltage in the moored mode (segment  $O_1-16$ ). We construct the axes of the fifth quadrant in such a way that the X-axis coincides with point 16 at the Y-axis ( $F_y$ ) of the eighth quadrant.

We determine the generator field voltage excess in relationship to comparison voltage. The resultant increase  $\Delta U = U_{b,r} - U_{\text{срвнн}}$  in the vessel running in open water mode is translated from the fourth quadrant to the fifth with the aid of auxiliary paths, whose slopes to the X-axis equal  $\alpha_1 = 64^\circ$ ,  $\alpha_2 = 45^\circ$ . This makes it possible to coordinate varied voltage scales  $U_{b,r}$  and  $\Delta U$ .

The construction process in Figure 5.20 is designated by the digits 10—20—22—19.

We draw broken line 19—22—21—20 through point 19 to its intersection with the vertical passing through point 20, which determines the voltage increment in the running in open water mode  $\Delta U_{\text{срвнн}}$ . The voltage increment in the moored mode  $\Delta U_w = 0$  is from a condition assumed during the calculation.

Through points  $O_2$  and 22 we draw a straight line, which determines the position of the resultant volt-ampere characteristic of the OMD winding's first circuit  $F_{o.m.a.} = f(\Delta U)$  - of the OMD winding connected to the difference in voltages  $U_{b,r}$  and  $U_{\text{срвнн}}$ .

Due to the insignificant resistance of the silicon diodes used as shut-off rectifiers in the OMD winding circuit, we do not consider their characteristics during the construction.

The desired volt-ampere characteristic must pass through the origin of

AD-A114 423

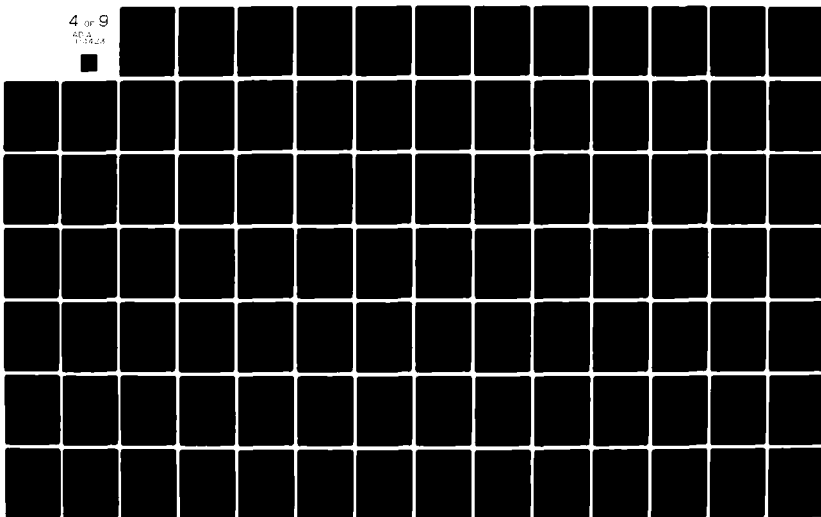
FOREIGN TECHNOLOGY DIV WRIGHT-PATTERSON AFB OH  
FUNDAMENTALS OF ELECTRICAL PROPULSION PLANT DESIGN, (U)  
APR 82 N A KUZNETSOV, P V KUROPATKIN  
FTD-ID(RS)T-1388-80

F/G 21/3

UNCLASSIFIED

NL

4 of 9  
AD-A  
75824



the coordinates. Otherwise, the assigned accuracy in main circuit current control will not be provided.

Calculation of the first circuit of the OMD power control winding. From the construction, OMD current in the vessel running in open water mode will be determined as equalling  $i_y$  and  $\Delta U = U_{в.г} - U_{срвнн}$ .

OMD winding circuit impedance equals

$$\sum R = \frac{\Delta U}{i_{y.c}}$$

Following accomplishment of constructions determining the position of the characteristics of all basic circuit elements, it is possible to calculate the main propulsion motor's entire mechanical characteristic (in a range of current changes from zero to the anchorage current value) without considering the action of the OMD winding's second circuit connected to the voltage differences of /237 the monitoring tachogenerator KTG and  $U_{срвнн}$ . The calculation sequence is as follows:

1. We are given a series of values for the load current in the main circuit from  $I = I_w$  and greater to  $I_{с.г}$ . We calculate the section of the characteristic from  $n_w$  to  $n_{с.г} = 0$ . Motor field flux in this case equals  $\Phi_x = \Phi_{x.w}$  (from the condition that  $U_{в.г.w} = U_{срвнн}$ ).

2. We determine propulsion motor emf from the given values of current  $I_a$  from the construction based on characteristic  $E_x = f(I_a)$ .

3. We determine main propulsion motor rotational speed and the amount of torque, where  $K = 2$  — the number of loops, from the values found for  $\Phi_{x1}$ ,  $E_{x1}$ , and  $I_{a1}$ . The calculation is compiled in Table 5.4.

$I_a, a$	$E_x, v$	$n_x, \frac{rpm}{об/мин}$	$M_x, \frac{kGm}{R/L}$

Table 5.4. Data for Construction of the GED Mechanical Characteristic.

4. We are given a series of current values in the interval  $I_w > I_a > I_{с.г}$ . For example,  $I_a = 2700 a$ . From the construction in the second quadrant, we determine that  $E_x = 947 v$ . Since generator field voltage in this case is greater

than comparison voltage  $U_{b,r} > U_{\text{ср.ср.}}$ , then, with the aid of additional paths, we translate the voltage difference  $\Delta U$  to the fifth quadrant and, based on the magnitude of the resultant increment, we determine OMD winding n. s.

5. Next, we translate resultant n. s. value  $F_{o.m.a}$  to the ordinate of the eighth quadrant and draw a straight line (19—18) through the resultant point parallel to the OMD winding volt-ampere characteristic to its intersection with the motor exciter field load characteristic  $U_{b,a} = f(i_y)$ . We determine the amount of motor field flux  $\Psi_a$  from the construction.

Construction of the GED mechanical characteristic. We determine GED rotational speed  $n_a$  and torque  $M_a$  in a manner analogous to that above. Here, the curve of the mechanical characteristic runs somewhat above the constant power hyperbole.

The influence of the KTG — OMD winding circuit node on the main propulsion motor mechanical characteristic can be considered as follows: we construct the OMD winding circuit volt-ampere characteristic in the ninth quadrant at coordinates  $F_{o.m.a}$  and  $\Delta U = U_{k.r.r} - U_{\text{ср.ср.}}$ . We obtain the magnitude of the OMD winding circuit resistance value  $R_{o.m.a} + R_{\text{доп}}$  analogously to the previous calculation. We construct the OMD characteristic exactly as was done in the fifth quadrant.

It is possible conditionally to divide the GED mechanical characteristic  $M_a = f(n_a)$  in a range of load change from zero to the vessel running in open water mode into two sections.

Both OMD winding circuits influence the amount of motor field flux in /238 the first section to the critical current  $I_{xp}$  value, when  $U_b > U_{\text{ср.ср.}}$ . In the second section, when  $U_b < U_{\text{ср.ср.}}$ , OMD winding current is stipulated only by the KTG voltage excess above the comparison voltage.

We select a series of main circuit load current  $I_a$  values in the  $I_r - I_{\text{до}}$  range for calculation of the first section of the characteristic. Then we determine values  $E_a$ ,  $U_{b,a}$  and  $F_{o.m.a}$  created by the first OMD winding circuit based upon this current.

Next, we are given a series of GED rotation values in the  $n_a > n_{a.c}$ .

range and, for each of these values  $n_{\Delta i}$  from previously-found value  $E_{\Delta i}$ , we determine the amount of GED field flux from the formula

$$\Phi_{\Delta i} = \frac{E_{\Delta i}}{C_e n_{\Delta i}}.$$

We determine those amounts of resultant n. s. which the OMD winding must create from the construction in the seventh and eighth quadrants based on the motor magnetization curve  $\Phi_{\Delta} = f(U_{\Delta})$  and from load characteristic  $U_{\Delta} = f(i_{\Delta})$ . Subtracting the first circuit's n. s. from the total OMD, we get n. s. which must be provided by the OMD winding second circuit:  $F_{o.m.\Delta} = \sum F_{o.m.\Delta} - \Delta F'_{o.m.\Delta}$ .

It is necessary for the construction to determine the rotational speed scale in the quadrant. We assume that  $n_{\Delta} = 165$  rpm.

We are given in the ninth quadrant  $\Delta U = 20$  V; then

$$\Delta n_{\Delta} = \frac{n_{\Delta} \Delta U}{U_{\text{ср.вн}}}.$$

From this we determine the rotational speed scale in the ninth quadrant.

We find the critical current value for determination of  $n_{\Delta}$  in a section where OMD acts only from the KTG. In the calculation of the OMD first circuit, it was assumed that  $I_{kp} = I_{\text{ср.вн}}$ , where  $U_{\text{ср.вн}} = U_{\Delta}$ . We are given several rotational speed values where  $I_{kp}$ , for example,  $n_{\Delta} = 179, 193,$  and  $207$  rpm. In order to determine  $n_{\Delta, kp}$  from the construction, we find motor field flux  $\Phi_{\Delta}$ , where  $I_{kp}$  and  $U_{\Delta}$  for these rotational speeds; then

$$\Phi_{\Delta} = \frac{E_{\Delta}}{C_e n_{\Delta}}.$$

Flux, in accordance with the selected rotational speed values, equals, for example:  $\Phi_{\Delta} = 13.4 \times 10^6, 12.4 \times 10^6,$  and  $11.6 \times 10^6$  mcs.

Having plotted in the ninth quadrant three points corresponding to the three GED rotational speed values, we determine  $n_{\Delta, kp}$  from the construction, using the GED magnetization curve and the motor exciter load characteristic. This will be at the point where the OMD volt-ampere characteristic and curve ABC intersect.

From the construction, we find that:  $n_{д.кР} = 187 \text{ rpm}$ ,  $\Phi_{д.кР} = 12.7 \times 10^6$  mcs, and  $U_{д.кР} = 963 \text{ V}$ .

We subtract the torque where  $n_{д.кР}$  equal to  $M_{д.кР} = KC_M I_{д.кР} \Phi_{д.кР}$ . /239

Having determined  $M_{д.кР}$  and  $n_{д.кР}$ , we plot the point of the screw mechanical characteristic in the sixth quadrant. We are given rotational speed values exceeding  $n_{д.кР}$  and, for them, we find the moment via emf and GED field flux. These parameters are determined from the construction. Figure 5.20 shows the calculation process for  $n_{д.кР} = 207 \text{ rpm}$ . Construction sequence is depicted by arrows and designated by digits 23 — 26.

We determine motor emf from the given value and from that found from the construction for  $\Phi_{д}$ . We determine motor current from the emf value and screw torque from expression  $M_{д} = KC_M I \Phi_{д}$ .

We compile the calculation in Table 5.5.

$I_{д}, \text{ a}$	$n_{д}, \text{ rpm}$ $\text{об/мин}$	$\Phi_{д}, \mu\text{S}$ $10^6, \text{ мкс}$	$V$ $E_{д}, \text{ в}$	$\text{kGm}$ $M_{д}, \text{ кгм}$

Table 5.5. Data for Construction of GED Electromagnetic Torque.

Calculation of a variant of the GEU circuit for the main mode concludes with construction of this section of the characteristic.

The static characteristics of all GEU operating modes are calculated in an analogous manner.

#### § 5.7 Methodology for Calculation of Icebreaker GEU Static Characteristics

Propellor interaction with ice mode. Study of this mode is linked to correct selection of propellers and shafts, as well as of electrical plant elements, which provide economic and accident-free operation of vessels navigating in ice.

A screw often is called upon to operate in an interaction with ice mode as a vessel navigates through ice. Under these conditions, the screw moment of resistance to movement increases sharply, which is accompanied by rapid changes in the speed of its rotation and its complete stop, i. e., jamming, in spite of the presence of significant propulsion motor torque. Propellor blade strikes against ice and screw jamming are the most difficult propulsion plant operating modes and are accompanied by frequent damage to propellers and shafts, which puts the vessel out of action.

A large amount of experimental and other materials characterizing propulsion plant operation during various types of propellor -- ice interaction has been /240 generalized at the present time. Analysis of test materials and observation of icebreaker and ice navigation vessel operations make it possible to express the following thoughts about types of propellor -- ice interaction.

Operation in sludge (small ice rafts). Such navigational conditions, as a rule, are encountered in ports and river estuaries. An additional moment of resistance to movement arises on screw blades when a screw operates in small ice rafts. This gradually decreases propulsion motor rotational speed to a value depending apparently on the propulsion motor's ability to change torque when the rotational speed changes (i. e., on the type of motor static characteristic and the entire system's dynamic properties). In this event, the screw seems to be operating in a more dense medium.

Operation in smooth ice fields. Moving in an ice field, an icebreaker punches out chunks of ice floes with its bow. These chunks, following the ship's lines, will end up in a vertical position. Here, some of the ice floes, initially compressed between the ice field and the icebreaker, come in contact with the propellor blades as they surface near the stern. Also, ice floes sunk by the icebreaker's bow and moving through the area along the bottom where the screws are housed come in contact with the propellor blades.

The screw -- ice interaction process as icebreakers operate in smooth ice fields demonstrates that quite regular periodic changes in screw angular rotational speed occur with radical increases and decreases, alternating essentially exactly four times per screw rotation (if it is a four-bladed screw). Thus, each screw

blade in a specific position comes in contact with the ice, breaks it, and, having turned here to a particular angle, ceases contact with the ice, continuing to rotate in open water. The moment of resistance in accordance with this also changes, considerably increasing as the blade breaks the ice and decreasing as it rotates in open water.

It is evident that, if the force required to break the ice with a blade is greater than the force required to throw aside an ice floe with a blade with a given angular rotational speed, then the ice floe, without breaking, will be thrown aside or submerged as it is turned by the propellor blade. If the amount of moment of resistance exceeds the nominal value, then the plant will not be able for a prolonged period to surmount such an ice load and, after a certain period has passed, will become jammed, i. e., the propellor will be jammed by the ice floes ending up under its blades. It is quite apparent that jamming time and turning angle for this period will depend on such factors as the propulsion motor static characteristic, the system's dynamic properties, the kinetic energy reserve of the rotating masses, the amount of additional moment of resistance and duration of its action, and so on.

If two blades rather than one are in contact with the ice floe at the /241 same time, then there is a decrease in propellor angular rotational speed without significant oscillations. One can see in oscillograms less radical and, over a prolonged period of time, continual decreases in angular rotational speed.

Operation in small packed floes. Fields of small ice floes, as a rule, include frozen hummocked ice floes, "inflows," and perennial packed ice floes. The operation of icebreaker and ice navigation vessel GEU in such ice is similar to operation in smooth ice fields. However, the periodicity of propellor — ice interaction is disrupted radically here.

Observation of propulsion plant operation as icebreakers navigate in smooth and in small packed ice fields demonstrated that propellor blades slice and shape ice floes hitting them.

The depth a propellor blade cuts into ice depends on many random factors that are difficult to take into account. However, as numerous observations

have shown, the maximum observed depth stern propellers cut as they slice into ice does not exceed 500 — 800 mm. These data are confirmed by results of dock inspections of propellers, where it was observed that the tips of the blades had been ground down to a glitter by the ice to approximately 1/4 — 1/3 of the propeller's radius from the periphery.

Stoppage of the propeller while the vessel is moving is the most dangerous phenomenon that can lead to propeller or shaft damage since, in this instance, the blades "tow" encountered ice without breaking or throwing it aside.

In cases where a large ice floe resting against an ice field encounters a blade, forces received by the blade can turn out to be so great that they will damage the propeller or shaft. This confirms the importance of predetermining, through calculations, the magnitude of ice loads acting upon propeller blades. Knowing the ice loads, it is possible correctly to calculate the propeller complex (propeller — shaft) and provide that main propulsion motor torque which eliminates stoppage (jamming) of the propeller.

Correct calculation of GEU static characteristics to a considerable degree increases the reliability of icebreaker and ice navigation vessel operations.

As pointed out above, stoppage of the propeller (jamming) while a vessel is moving can lead to propeller or shaft breakdown.

Data determining the link between propeller moments of resistance and its rotational speed are the initial sources of information for calculation of static characteristics. Initial data for icebreakers and ice navigation vessels are the characteristics of propeller moment of resistance to rotation in open water  $M_R = f(n_R)$  and the characteristics of the moment of resistance stipulated by /242 propeller — ice interaction,  $M_{i1} = f(n_R)$ :

$$M_{con} = M_R + M_{i1} = f(n_R).$$

The propulsion plant mechanical characteristic  $M_a = f(n_a)$ , selected from characteristic  $M_{con} = f(n_a)$  must satisfy all possible plant operating modes. Therefore, selection of characteristic  $M_a = f(n_a)$  must occur based on the total moment of resistance characteristic.

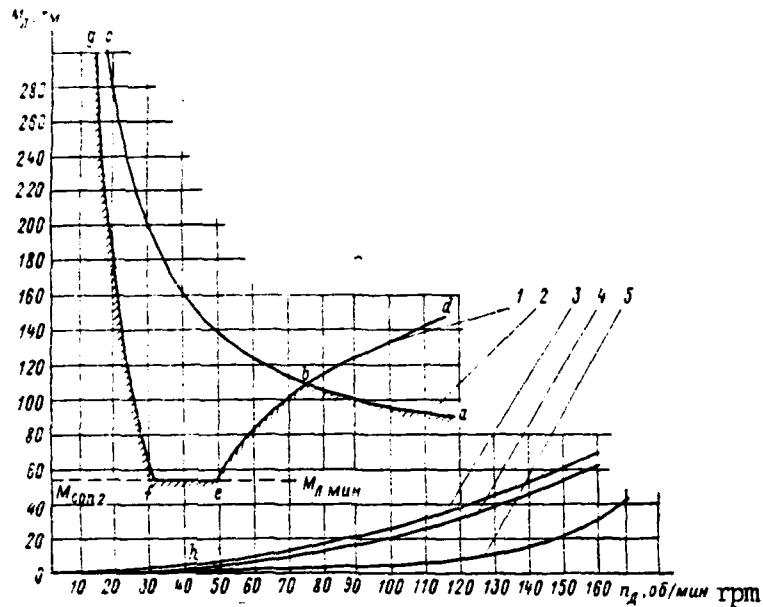


Figure 5.21. Curves of Relationships  $M_n = f(n_n)$  and  $M_b = f(n_n)$ .

1—Characteristic gfc of the relationship of total propeller power to its rotational speed; 2—Characteristic cba of the relationship of shaft power while breaking ice on propeller rotational speed; 3—Moored characteristic; 4—Characteristic as icebreaker is underway at 4.5 knots; 5—Characteristic of vessel running in open water.

Selection of optimal form of a GED mechanical characteristic. The ultimate value of main propulsion motor rotational speed (for example, in the event of propeller loss) must correspond to the requirements of the USSR Registry (or of other qualified societies establishing norms for GEU construction) and technical conditions for main propulsion motor construction.

The mechanical characteristic must coincide with the power constancy hyperbole in the range of propeller characteristics (Figure 5.21) from running in open water (curve 5) to moored (curve 3).

In a propeller rotational speed range from  $n_{n1}$ , which corresponds to the moored mode (curve 3), to  $n_{n2}$ , which corresponds to the zero stop (point h), the mechanical characteristic must pass as close as possible to the power constancy hyperbole, intersecting characteristic  $M_{con} = M_b + M_n$  (curve 1) at the point in which  $M_{con1} \approx M_{con2}$ , where  $M_{con2}$  corresponds to the torque for propeller /243 rotational speed at the zero stop. Here, main propulsion motor motive moment equalling  $M_{con2}$  is maximum.

Selection of parameters and calculation of main propulsion motor, generator, and excitation system characteristics must consider the aforementioned icebreaker GEU static characteristic special features.

The minimal value of ice moment in Figure 5.21 corresponds to the force for cutting an ice floe with a propellor blade only with a rib. This phenomenon is observed when propellor rotational speed approximates speed at the zero stop.

Further reduction in propellor rotational speed causes an increase in braking torque and the propellor can be damaged due to its stopping.

Proper GEU design entails obtaining that amount of GED electromagnetic moment at which motor rotational speed in propellor — ice interaction modes does not drop below the speed corresponding to the zero stop.

The following recommendations on calculation of static characteristics can be made on the basis of experiments and full-scale tests run on icebreakers and vessels operating in ice:

1. An almost regular periodic process of propulsion motor angular rotational speed change, with radical increases and decreases alternating for each rotation of the propellor in accordance with the number of blades, is observed as propellor blades interact with a large individual ice floe. It is quite apparent that, in this event, both the jamming time and the propellor turning angle during the "jamming" will depend on the motor static characteristic, propulsion plant dynamic properties, kinetic energy reserve, and so forth.
2. Operation of a propellor in small ice rafts (sludge) is similar to propellor operation in a more dense medium. Here, propellor moment of resistance to rotation changes in proportion to the square of the change in its angular velocity.
3. Removal of propulsion motor torque during the propellor blade interaction process as the vessel moves can lead to propellor or shaft breakdown.
4. Propulsion plant operating reliability and efficiency as the propellor interacts with ice should be looked upon as one basic criterion during selection of plant control system equipment and calculation of dynamic characteristics.
5. It is possible to use characteristic  $M_n = f(n_n)$  in selection of the parameters of a GEU with that mechanical characteristic that would make it possible

to eliminate propellor jamming. This, in turn, to a significant degree will decrease the number of propellor breakdowns and thereby increase icebreaker and ice navigation vessel overall reliability.

The complete methodology for calculation of icebreaker GEU static characteristics is presented in [77, 78].

## Electrical Propulsion Plant Stability and Control Quality

§ 6.1 Special Features of Analysis of the Stability  
of Automated GEU

The following problems are examined when doing engineering calculations for electrical propulsion plant automated control systems, just as when doing calculations for other automated control systems: system stability, nature of the transient process, deviation of controlled values from the assigned values, duration of the control process, effect of individual parameters on the quality of the control process as a whole, and, finally, study of the influence of transient processes in all of the electric ship's interconnected loops.

Basic parameters to be calculated when studying dc GEU are main propulsion motor rotational speed and the amounts of torque developed by main propulsion motors during the control process.

Calculation of the control system involves compilation of differential or integro-differential equations describing the functional changes of variable values in an electrical propulsion plant during the control process.

Frequency methods and mathematical modeling are used most widely for analysis of the stability and quality of propellor electric drive automated systems. Known idealization of equations describing control processes is permitted during analytical study of these systems. It is natural, of course, that a precise account of all phenomena and their mathematical description so complicate the analytical expressions of the process that it is extremely difficult to use the results of a mathematical description for specific analysis. Therefore, in the future, only extant factors characterizing the conduct of the electrical propulsion plant in dynamic modes are considered.

One principle special feature of these plants is that they are an autonomous power system comprising primary motors, generators, main propulsion motors, and other aggregates, all elements of which automatically controlled in their interaction.

A primary motor and a generator in electrical propulsion plants, as a rule, are equal in power and a change in generator load is accompanied by a change /245 in primary motor rotational speed. Coming into play here is a system for automatic control of primary motor rotational speed constancy.

A change in primary motor rotational speed in turn leads to a change in generator voltage and, consequently, to a change in main propulsion motor load current and torque. Therefore, one must consider a change in primary motor rotational speed when studying electrical propulsion plant control processes in the primary motor — generator — main propulsion motor — propellor complex. This circumstance leads to a requirement for simultaneous examination of electromagnetic and electromechanical processes of propellor automated electric drive jointly with the mechanical processes of thermal engines and their systems of automatic rotational speed control. This study is complicated, as a rule, by the presence of several generators and main propulsion motors connected in series or in parallel running the propellor. Mathematical description of the general nature of the system's motion is complicated also by the fact that many relationships are expressed in nonlinear functions.

Known methods of stability analysis are used for the more characteristic standard GEU circuitry, including a standard circuit with two individual loops (when two or more series-connected generators run the armature of a paired main propulsion motor).

Analysis of plant operation in dynamic modes, analysis of the stability of the entire system in particular, must be accomplished by joint examination of electromagnetic and electromechanical processes in the electric transmission, the mechanical processes of the primary motor and its governor, as well as of the hydrodynamic processes of the propellor in interaction with the hull of the vessel. And, for icebreaker GEU, it also is necessary to consider the processes arising during interaction of the propellor with the ice coming in contact with its blades.

Established modes for joint operation of the primary motor, generator, main propulsion motor, and propellor are determined by the position of the points of intersection of the curves of the hydrodynamic characteristics of the propellor

and the characteristics of the generator and main propulsion motor automatic control systems. Here, GEU automatic control systems, especially for the plants on icebreakers, ice navigation vessels, harbor tugs, and so on, are required to provide full use of primary motor power as the propellor operates in the full range of characteristics corresponding to changing navigational conditions.

Hydromechanical characteristics of the propellor for icebreakers and ice navigation vessels can, as is known, change in the interval between the characteristic corresponding to zero speed of vessel movement (moored characteristic) /246 and the ice navigation characteristic calculated in such a way that the propulsion plant develops full power as the vessel moves at slow speed in ice. But, when the vessel operates in open water, the propulsion plant must also develop full power for a prolonged period. These two circumstances also determine the requirement for automatic maintenance of ice navigation vessel propulsion plant power constancy in a very broad interval of propellor characteristics.

Icebreaker and ice navigation vessels also have increased requirements relative to transient modes for high maneuverability and the capability for rapid alteration of the direction of motion.

GEU operating modes as the vessel reverses can correspond to any point of the area limited by propellor and propellor drive characteristics. Main propulsion motors and generators allow significant current and torque overloads; primary motors used in electrical propulsion plants have stricter overload limitations. Since propellor operating modes are brief during vessel reversing, the electrical propulsion plant automatic control system must provide full use of primary motor power during permissible generator and main propulsion motor current and torque overloads for the purpose of obtaining the greatest effect during vessel reversing.

As already noted, a propellor often is called upon to operate in direct interaction with ice as a vessel navigates through ice. A radical increase here in moment of resistance is accompanied by a radical change in propellor rotational speed. The GEU automatic control system must provide efficiency in surmounting possible propellor jammings by ice when full primary motor power is used and during a permissible generator and main propulsion motor overload.

The task of studying processes occurring in an automated propellor electric drive involves establishing the nature of the change of regulated values over time (in our case, current, power, main propulsion motor torque, and its rotational speed) given the assigned nature of input value change. The combination of all equations of the elements and their links comprising the propellor electric drive system and reflecting the nature of the course of the process bears the name electrical propulsion plant control process equations. Since the processes occurring in an automated propellor electric drive, generally speaking, are described by nonlinear equations with nonlinear coefficients, then the law of change of controlled values over time cannot be represented in general form analytically.

One often turns to study of a linear problem when nonlinear equations /247 are approximated by linear or piecewise functions, i. e., are linearized. Linearization of a problem and disregard for certain factors may lead to a known deviation of obtained results from the real nature of the course of a process, but there are simpler ways to study the control system and to solve several complex problems relating to control.

It should be noted that there are modes in an automated electric drive in which deviations of the regulated values from assigned values turn out to be significant. A separate chapter will be devoted to examination of these modes.

Obtaining true results involves mainly correct description of the physical processes occurring in a system and subject to examination, and depend on correct mathematical representation of all electromagnetic, electromechanical, thermal, and hydrodynamic processes occurring in the propellor electric drive.

Solving jointly the system of equations for individual links of an automated propellor electric drive and eliminating intermediate variables, we get the electrical propulsion plant control equation. Selection of generalized coordinates, i. e., selection of those variables independent of one another which are required and sufficient for full description of those values, whose significance fully determine the state of the system at any moment in time and also determine the number of degrees of freedom of the given system, precedes investigation of the control system.

Having noted the generalized coordinates, there should be a further stipulation on the origin and direction of reading generalized coordinate increments. Since equations are compiled in increments, the equilibrium state of the control system must be assumed to be the origin of the account. It is possible to determine the value of a deviation either from the initial state of equilibrium or from a new state of equilibrium which the system reaches upon conclusion of the control process.

When studying a control system and beginning from the initial state of equilibrium, mathematical processing will result in an inhomogeneous differential equation, whose solution also determines the amount of regulated value in the new state. This approach is of interest for static control systems for which non-reduction of the regulated value to the nominal is characteristic. If a new equilibrium state of the system is assumed, then there is a homogeneous equation to solve.

Thus, the methodology of compilation of equations of a system's transient process in deviations includes:

- determination of the relationship between generalized coordinates for the system's state of equilibrium (statics equation);
- compilation of the transient mode equation (dynamics equation), /248 considering the equilibrium state to be disrupted;
- obtaining the expression characterizing the transient mode in increments, i. e., subtracting statics equations from dynamics equations;
- linearization of nonlinear characteristics, if when compiling the transient process equation elements are encountered whose transient processes are described as nonlinear equations (nonlinear function characterizing conduct of a link in a transient process. For this purpose, the increments should be expanded in terms of degrees of increment and, discarding members on an order above the first, obtaining an approximate link equation; partial derivatives in the resultant expansion, given minor coordinate deviations, can be considered constant factors; thus, the result may be a linear differential equation);
- study of the conduct of the control system in the entire operating range, for which the latter is divided into several small intervals, within which are partial derivatives are assumed to be constant.

This methodology for compilation of the control equation and its study are explained below using examples of standard automated electrical propulsion plants.

## § 6.2 Equations of Standard Automated GEU Links

Equation of motion of the "primary motor" link. Thermal engines, diesels in particular, are used, as a rule, as primary motors in ac and dc electric ships. The equation of motion for this type of primary motor is presented below. The term motor equation will be used for the equation of the change of a regulated parameter during transient processes. In the example shown, the motor shaft angular rotational speed is the controlled parameter.

The established (static) motor operating mode is characterized by the constancy of the crankshaft rotational speed at a given load. Maintenance of this mode is possible only given equality of torque  $M_{дз}$ , developed by the motor and moment of resistance  $M_{соп. ном}$ , transmitted to the motor shaft. Thus, there is equality

$$M_{дз. ном} = M_{соп. ном} \quad (6.1)$$

We assume

$$M_{соп. ном} = M_{г. ном} + M_{г. н. ном} + M_{т. дг. ном} \quad (6.1a)$$

where  $M_{г. ном}$  is established (nominal for a given mode) braking torque developed by the main generator;  $M_{г. н. ном}$  is the established (nominal for the given mode) braking (for the motor) torque developed by the installed generator;  $M_{т. дг. ном}$  is the established (for the given mode) transmission line friction torque: primary motor — generator.

Disruption of the established motor operating mode can occur due to a change in the torque it develops or a change in the braking torque developed by the main and attached generators. A change in torque developed by a primary motor in electrical propulsion plants, as well in shipboard power plants overall, is caused by changes in the water resistance to vessel movement (in established modes).

If you designate the moment of inertia of the motor and aggregates linked with it (armatures of the main generator and attached generator) transferred to the shaft as  $J_{\Delta 23}$ , then the equation of the dynamic equilibrium of the moments compiled in accordance with the d'Alembert principle will take the form

$$J_{\Delta 23} \frac{d\omega_{\Delta 23}}{dt} = \frac{GD_{\Delta 23}^2}{375} \frac{dn_r}{dt} = m_{\Delta 23} - m_r - m_{r, H} - m_{r, \Delta r}, \quad (6.2)$$

where  $GD_{\Delta 23}^2$  is the moment of gyration of the rotating parts of the diesel motor and generators transmitted to the motor shaft;  $n_r = n_{\Delta 23}$  is generator rotational speed which, given the absence of a reduction-gear transmission between them, equals motor-diesel rotational speed;  $m_{\Delta 23}$ ,  $m_r$ ,  $m_{r, H}$ ,  $m_{r, \Delta r}$  are instantaneous values of the corresponding moments.

Having substituted instead of instantaneous values of variable amounts their expressions in increments and having subtracted termwise the static mode equation, we get the moment equilibrium equation of the primary motor -- generator system expressed in increments:

$$J_{\Delta 23} \frac{d \Delta \omega_{\Delta 23}}{dt} = \frac{GD_{\Delta 23}^2}{375} \frac{d \Delta n_r}{dt} = \Delta m_{\Delta 23} - \Delta m_r - \Delta m_{r, H} - \Delta m_{r, \Delta r}. \quad (6.3)$$

Motor torque  $m_{\Delta 23}$  depends on the speed and load modes of its operation. The speed operating mode is characterized by motor crankshaft angular rotational speed ( $\omega_{\Delta 23}$  or  $n_r$ ), while the load mode is characterized by the torque developed by the motor which, in turn, depends on the amount of fuel  $\Delta q$ , supplied per cycle to the motor and on motor effective efficiency in the given mode. The supply of fuel is determined by position  $h$  of the fuel pump actuator and, consequently, by position  $\xi$  of the governor clutch for direct control or position  $\phi$  of the servomotor piston for indirect control. Consequently, motor torque is a function of angular velocity  $\omega_{\Delta 23}$  and position  $\xi$  of the clutch or  $\phi$  of the servomotor piston, i. e.,

$$m_{\Delta 23} = f(\omega_{\Delta 23}; \xi)$$

or

/250

$$m_{\Delta 23} = f_1(\omega_{\Delta 23}; \phi). \quad (6.4)$$

It is possible to obtain the motor torque increment by expansion of function  $m_{23}$  into a Maclaurin series. In this event, expansion of the first of the presented functions has the form

$$m_{23} = M_{23, \text{НОМ}} + \Delta m_{23} = M_{23, \text{НОМ}} + \left( \frac{\partial m_{23}}{\partial \omega_{23}} \right) \Delta \omega_{23} + \dots + \left( \frac{\partial^n m_{23}}{\partial \omega_{23}^n} \right) \frac{\Delta^n \omega_{23}}{n!} + \left( \frac{\partial m_{23}}{\partial \xi} \right) \Delta \xi + \dots + \left( \frac{\partial^n m_{23}}{\partial \xi^n} \right) \frac{\Delta^n \xi}{n!}. \quad (6.5)$$

Derivatives of function  $m_{23} = f(\omega_{23}; \xi_{\text{НОМ}})$ , included in the resultant series must be determined in a position of an equilibrium (established) motor and governor operating mode  $(\omega_{23, \text{НОМ}}; \xi_{\text{НОМ}})$ , in which condition  $M_{23, \text{НОМ}} = M_{\text{соп. НОМ}}$  is accomplished.

Presented in Figure 6.1 is a graph in which motor characteristics (curves 1—4) are combined with moment of resistance characteristics (curves I—IV). The points of intersection of these curves A, B, C, D, and so on characterize established modes since they satisfy statics condition (6.1).

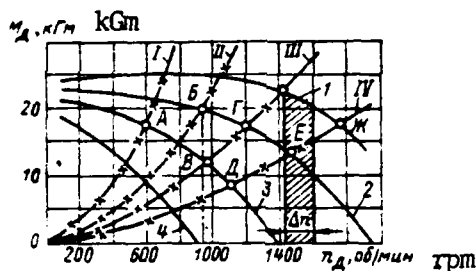


Figure 6.1. Combined Graph of Motor Characteristics and Propeller Resistance.

The resultant expansion into terms, given a sufficient number of expansion members, makes it possible to obtain with considerable accuracy the relationship of torque in any selected range of increments  $\Delta \omega_{23}$  and  $\Delta \xi$ . However, consideration of all expansion members will lead to expression (6.3) in nonlinear form. Disregarding in (6.5) members of the highest order of infinitesimals, one can write

$$m_{23} = M_{23, \text{НОМ}} + \Delta m_{23} = M_{23, \text{НОМ}} + \left( \frac{\partial m_{23}}{\partial \omega_{23}} \right) \Delta \omega_{23} + \left( \frac{\partial m_{23}}{\partial \xi} \right) \Delta \xi$$

or

$$\Delta m_{23} = \left( \frac{\partial m_{23}}{\partial \omega_{23}} \right) \Delta \omega_{23} + \left( \frac{\partial m_{23}}{\partial \xi} \right) \Delta \xi. \quad (6.6)$$

In the event of non-direct control, expression (6.6) has the form

$$\Delta m_{23} = \frac{\partial m_{23}}{\partial \omega_{23}} \Delta \omega_{23} + \frac{\partial m_{23}}{\partial \varphi} \Delta \varphi. \quad (6.7)$$

Essentially, this denotes that the real motor characteristic AB in section  $\Delta \omega_{23}$  (Figure 6.1) is replaced by the segment applicable to it. It is clear from Figure 6.1 that the error from such a replacement will be smaller, the smaller the amount of deviation. The corrected replacement when the real curve is replaced by the one relating to it at the operating mode point is one linearization /251 method widely used in dynamics.

Examining the circuit given absence of attached generators and disregarding friction torque  $m_{r, dr}$ , one can write

$$m_{con} = m_r = C_{m, r} \Phi_r i_n = f(\Phi_r, i_n), \quad (6.8)$$

where  $C_{m, r} = \frac{P_r N}{2\pi a_r}$ , if torque is expressed in electrical values.

Substituting the amount of moment of resistance from expression (6.8) in initial equation (6.1), we get the equation for torque dynamic equilibrium

$$J_{A3} \frac{d\omega_{23}}{dt} = \frac{GD_{A3}^2}{375} \frac{dn_r}{dt} = m_{A3} - m_{con} = m_{A3} - C_{m, r} \Phi_r i_n. \quad (6.9)$$

The static mode equation will have the form

$$M_{23, nom} = C_{m, r} \Phi_{r, nom} I_{r, nom}. \quad (6.9a)$$

The generator torque increment can be obtained by expansion of function (6.8) into a Maclaurin series and by disregarding members of the highest orders of infinitesimals. We will examine two approaches to linearization, which in essence involve the identical mathematical method, for a case of generator torque increment. Expanding (6.8) into a Maclaurin series, we get

$$m_r = M_{r, nom} + \Delta m_r = M_{r, nom} + \frac{\partial m_r}{\partial \Phi_r} \Delta \Phi_r + \frac{\partial m_r}{\partial i_n} \Delta i_n \quad (6.10)$$

or

$$\Delta m_r = \frac{\partial m_r}{\partial \Phi_r} \Delta \Phi_r + \frac{\partial m_r}{\partial i_n} \Delta i_n. \quad (6.11)$$

Having expressed all variables through an increment, i. e.

$$\left. \begin{aligned} m_r &= M_{r, \text{НОМ}} + \Delta m_r; \\ \Phi_r &= \Phi_{r, \text{НОМ}} + \Delta \Phi_r; \\ i_a &= I_{a, \text{НОМ}} + \Delta i_a. \end{aligned} \right\} \quad (6.12)$$

and having substituted them in (6.8), we will subtract termwise the statics equation (6.9a). Thus, we will get the moments equation expressed in increments:

$$\Delta m_r = C_{m, r} \Phi_{r, \text{НОМ}} \Delta i_a + C_{m, r} I_{a, \text{НОМ}} \Delta \Phi_r. \quad (6.13)$$

Determining partial derivatives  $\frac{\partial m_r}{\partial \Phi_r}$  and  $\frac{\partial m_r}{\partial i_a}$  for a nominal mode we will find

$$\frac{\partial m_r}{\partial \Phi_r} = C_{m, r} I_{a, \text{НОМ}} \quad \text{и} \quad \frac{\partial m_r}{\partial i_a} = C_{m, r} \Phi_{r, \text{НОМ}}. \quad (6.14)$$

Consequently, expressions (6.13) and (6.11) are identical. In the future, we will use the second method to obtain equations in increments.

Substitution of (6.6) or (6.7) in (6.13) will lead to equality

$$\begin{aligned} \frac{\partial m_{дз}}{\partial \xi_{дз}} \Delta \xi_{дз} + \frac{\partial m_{дз}}{\partial n_r} \Delta n_r &\approx C_{m, r} \Phi_{r, \text{НОМ}} \Delta i_a + \\ &+ C_{m, r} I_{a, \text{НОМ}} \Delta \Phi_r + \frac{GD_{a, r}^2}{375 dt} \Delta n_r. \end{aligned} \quad (6.15)$$

We will represent variable values from expression (6.15) in relative units, having selected their nominal values as the base values. Then

$$\begin{aligned} \frac{\partial m_{дз}}{\partial \xi_{дз}} \xi_{дз, \text{НОМ}} \frac{\Delta \xi_{дз}}{\xi_{дз, \text{НОМ}}} + \frac{\partial m_{дз}}{\partial n_r} n_{r, \text{НОМ}} \frac{\Delta n_r}{n_{r, \text{НОМ}}} &= \\ = \frac{C_{m, r} \Phi_{r, \text{НОМ}} \Delta i_a}{I_{a, \text{НОМ}}} I_{a, \text{НОМ}} + C_{m, r} I_{a, \text{НОМ}} \frac{\Delta \Phi_r}{\Phi_{r, \text{НОМ}}} \Phi_{r, \text{НОМ}} + \\ + \frac{GD_{a, r}^2}{375} n_{r, \text{НОМ}} \frac{d \frac{\Delta n_r}{n_{r, \text{НОМ}}}}{dt}. \end{aligned} \quad (6.16)$$

We introduce the following designations:

$$\frac{\Delta \xi_{дз}}{\xi_{дз, \text{НОМ}}} = \Delta \bar{\xi}_{дз} \quad - \text{relative displacement of the actuator controlling the fuel supply;}$$

$$\frac{\Delta n_r}{n_{r, \text{НОМ}}} = \Delta \bar{n}_r \quad - \text{relative change in primary motor rotational speed;}$$

$$\frac{\Delta i_a}{I_{a, \text{НОМ}}} = \Delta \bar{i}_a \quad - \text{relative change in main circuit current;}$$

$$\frac{\Delta \Phi_r}{\Phi_{r, \text{НОМ}}} = \Delta \bar{\Phi}_r \quad - \text{relative change in generator field flux;}$$

$\frac{\frac{\partial m_{23}}{\partial \xi_{23}} \xi_{23, \text{ном}}}{C_{\text{м.г}} \Phi_{\text{г.ном}} / \text{я.ном}} = \bar{m}_{\xi_{23}}$  - relative torque stipulated by displacement of the actuator controlling the fuel supply (transfer factor of the primary motor during displacement of this actuator);

$\frac{\frac{\partial m_{23}}{\partial n_r} n_{\text{г.ном}}}{C_{\text{м.г}} \Phi_{\text{г.ном}} / \text{я.ном}} = \bar{m}_{n_r}$  - relative torque stipulated by the change in generator rotational speed (transfer factor of the primary motor - generator link rotational speed);

$T_{\text{м.г}}$  - electromechanical time constant of the primary motor - generator link. /253

Taking previously used and newly introduced designations into account, equation (6.16) is written in the following way:

$$\bar{m}_{\xi_{23}} \Delta \bar{\xi}_{23} - \bar{m}_{n_r} \Delta \bar{n}_r = \Delta \bar{i}_a + \Delta \bar{\Phi}_r + T_{\text{м.г}} \frac{d \Delta \bar{n}_r}{dt} \quad (6.17)$$

or in operator form given zero initial conditions:

$$\Delta \bar{n}_r(\rho)(T_{\text{м.г}}\rho + \bar{m}_{n_r}) = -\Delta \bar{i}_a(\rho) - \Delta \bar{\Phi}_r(\rho) - \bar{m}_{\xi_{23}} \Delta \bar{\xi}_{23} \quad (6.18)$$

or

$$\bar{m}_{n_r} \Delta \bar{n}_r(\rho)(T_{\text{м.г}}\rho + 1) = -\Delta \bar{i}_a(\rho) - \Delta \bar{\Phi}_r(\rho) + \bar{m}_{\xi_{23}} \Delta \bar{\xi}_{23}(\rho), \quad (6.18a)$$

where

$$T_{\text{м.г}}' = \frac{T_{\text{м.г}}}{\bar{m}_{n_r}}. \quad (6.18b)$$

Given constant generator field flux, expressions (6.18) and (6.18a), respectively, will take the form

$$\Delta \bar{n}_r(\rho)(T_{\text{м.г}}\rho + \bar{m}_{n_r}) = -\Delta \bar{i}_a(\rho) + \bar{m}_{\xi_{23}} \Delta \bar{\xi}_{23}; \quad (6.19)$$

$$\bar{m}_{n_r} \Delta \bar{n}_r(\rho)(T_{\text{м.г}}\rho + 1) = -\Delta \bar{i}_a(\rho) + \bar{m}_{\xi_{23}} \Delta \bar{\xi}_{23}(\rho). \quad (6.20)$$

If one examines control processes given constant primary motor rotational speed and given constant flux, then equations (6.18) and (6.20), respectively, take the form

$$\Delta \bar{i}_a(\rho) + \Delta \bar{\Phi}_r(\rho) = \bar{m}_{\xi_{23}} \Delta \bar{\xi}_{23}(\rho); \quad (6.21)$$

$$\Delta \bar{i}_n(\rho) = \bar{m}_{\text{ca}}, \Delta \bar{\xi}_{\text{ca}}(\rho). \quad (6.22)$$

Equation of motion of primary motor velocity regulator. In the most general form, this equation in operator form is written this way:

$$P(\rho) \Delta \bar{\xi}_{\text{ca}}(\rho) = K_p \Delta \bar{n}_r(\rho), \quad (6.23)$$

where  $P(\rho)$  and  $K_p$  are polynomials of  $P$ .

If one keeps in mind the "Woodward" plus-integral [PI] element direct action hydraulic speed governor system with a unilateral servomotor widely used on electric ships, then the differential equation of motion and time constants for this type of governor are determined in the following way. A change in diesel rotational speed is accomplished by acting upon the governor spring. The speed governor equation is deduced next taking into account the degree of residual irregularity  $\delta_p$ , obtained given the presence of a unity feedback lever. The governor equation in simplified form is obtained from the following expressions:

1) sensing element equation of motion, which, without considering the mass of the cargo and friction, will take the form

$$\Delta \bar{x} = K_p \Delta \bar{n}_r - K_{o.c.} \bar{\xi}_{\text{ca}} - K_y \Delta \bar{h}, \quad (6.24)$$

where  $\Delta \bar{x} = \frac{\Delta x}{\Delta H}$  is the relative value of an increment of governor clutch shift;

$\Delta \bar{h} = \frac{\Delta h}{\Delta H}$  is the relative value of an increment of vertical displacement of dead center and of connection of the lever to unity feedback;  $K_p$ ;  $K_{o.c.}$ ;  $K_y$  are transfer factors for  $\Delta \bar{n}_r$ ,  $\Delta \bar{m}$ ,  $\Delta \bar{h}$ ; respectively;

2) servomotor equation of motion

$$T_s \frac{d \Delta \bar{\xi}_{\text{ca}}}{dt} = \Delta \bar{\eta} K_y, \quad (6.25)$$

where  $T_s$  is a servomotor time constant, sec;  $\Delta \bar{\eta}$  - is relative opening of the slide-valve port;

3) equation of motion of a slide-valve with PI-element

$$K_y \Delta \bar{\eta} = \Delta \bar{x} - \Delta \bar{I}_\sigma, \quad (6.26)$$

where  $\Delta \bar{I}_\sigma$  is relative displacement of the slide-valve journal box;

4) elastic feedback (PI-element) equation, which, without considering the movable parts (slide-valve journal boxes and compensating piston), can be written as follows:

$$T_i \frac{d \Delta \bar{I}_\sigma}{dt} + \Delta \bar{I}_\sigma = T_i \frac{d \Delta \bar{\xi}_{\text{ca}}}{dt}, \quad (6.27)$$

where  $T_i$  is the PI-element time constant, sec.



Equation of regulation of a primary motor with speed regulator [governor].

The equation of regulation of a diesel generator with speed governor is obtained by joint solution of equations (6.33) and (6.18a):

$$[T_S T_i \rho^2 + (T_S + T_i + \delta_p T_i) \rho + \delta_p] \Delta \bar{\xi}(\rho) = (T_i \rho + 1) [\Delta \bar{n}_r(\rho) - L_s]; \quad (6.34)$$

$$\begin{aligned} \bar{m}_{n_r} \Delta \bar{n}_r(\rho) (T_{m_r} \rho + 1) &= \\ &= \bar{m}_{\xi_{33}} \Delta \bar{\xi}_{33}(\rho) - \Delta \bar{i}_n(\rho) - \Delta \bar{\Phi}_r(\rho). \end{aligned}$$

For a closed control system, we change the sign of  $\Delta \bar{\xi}(\rho)$  in the lower equation (6.34) to the opposite and, substituting  $\Delta \bar{\xi}(\rho)$  from the first in the second equation, we get

$$\bar{m}_{n_r} \Delta \bar{n}_r(\rho) (T_{m_r} \rho + 1) = - \frac{(T_i \rho + 1) [\Delta \bar{n}_r(\rho) - L_s]}{[T_S T_i \rho^2 + (T_S + T_i + T_i \delta_p) \rho + \delta_p] - \Delta \bar{i}_n(\rho) - \Delta \bar{\Phi}_r(\rho)} \quad (6.35)$$

and

$$\begin{aligned} \bar{m}_{n_r} \Delta \bar{n}_r(\rho) (T_{m_r} \rho + 1) [T_S T_i \rho^2 + (T_S + T_i + T_i \delta_p) \rho + \delta_p + \\ + (T_i \rho + 1) [\Delta \bar{n}_r(\rho) - L_s]] = - [\Delta \bar{i}_n(\rho) + \Delta \bar{\Phi}_r(\rho)] \times \\ \times [T_S \rho^2 T_i + (T_S T_i + T_i \delta_p) \rho + \delta_p]. \end{aligned} \quad (6.36)$$

We will designate

$$\begin{aligned} R(\rho) &= [T_S T_i \rho^2 + (T_S + T_i + T_i \delta_p) \rho + \delta_p]; \\ \bar{\Phi}(\rho) &= \bar{m}_{n_r} (1 + T_{m_r} \rho) R(\rho) - (T_i \rho + 1); \end{aligned} \quad (6.37)$$

then the equation of motion of a diesel generator with speed governor will be written in this way:

$$\bar{\Phi}(\rho) \Delta \bar{n}_r(\rho) = -R(\rho) [\Delta \bar{i}_n(\rho) + \Delta \bar{\Phi}_r(\rho) - (T_i \rho + 1) L_s]. \quad (6.38)$$

In particular cases, the equation has the form:

given constant generator field flux

$$\bar{\Phi}(\rho) \Delta \bar{n}_r(\rho) = -R(\rho) [\Delta \bar{i}_n(\rho) + (T_i \rho + 1) L_s]; \quad (6.39)$$

given constant generator rotational speed

$$R(\rho) \Delta \bar{i}_n(\rho) = L_s (T_i \rho + 1). \quad (6.40)$$

The values of time constants  $T_i$  and  $T_S$  depend on governor tuning and, therefore, can change over a broad range. Linearization of the speed governor

equation will lead to averaging of values  $T_i$  and  $T_s$ , which change along with transfer of the rod from a position corresponding to a decrease (closing) of the fuel supply to a position corresponding to an increase (opening) of the fuel supply. Therefore, values  $T_i$  and  $T_s$  in the corrected equation should be looked upon as averaged obtained as a result of linearization of the servomotor and PI-element equations.

Equation of motion of the "main propulsion motor" link. The propellor shaft line torque equation has the form

$$m_d = \frac{GD_d^2}{375} \cdot \frac{dn_d}{dt} + m_b + m_r, \quad (6.41)$$

where main propulsion motor torque is a nonlinear function of armature circuit current  $i_a$  and of magnetic flux  $\Phi_d$ :

$$m_d = C_{m,d} i_a \Phi_{b,d} = f(i_a; \Phi_{b,d}); \quad (6.42)$$

propellor moment of resistance is in general a nonlinear function of the speed of its rotation and vessel speed:

$$m_b = f(n_d; V). \quad (6.43)$$

For the performance characteristic, it can be considered approximately constant, considering vessel speed,

$$m_b = kn_d^2. \quad (6.44)$$

When there is a change in the propellor hydrodynamic characteristic under the influence of external conditions, for example in the case of an increase in water resistance to vessel movement, one should consider a change in the value both of factor  $k$  as well as of rotational speed  $n_d$ . Meanwhile,  $m_r$  (friction torque in the shaft line) is accepted as constant equal to a certain share of nominal torque  $(0.5-1)\% M_{d, \text{nom}}$ . Therefore, it is possible not to consider this component in dynamic modes, limiting oneself to a decrease in torque  $m_d$  0.5-1%.

Having jointly solved (6.41) and (6.42) and having replaced variable values with their expressions in increments, we get

$$C_{m,d} (i_{a, \text{nom}} + \Delta i_a) (\Phi_{b,d, \text{nom}} + \Delta \Phi_{b,d}) = \frac{GD_d^2}{375} \frac{d(n_{d, \text{nom}} + \Delta n_d)}{dt} + (k_{\text{nom}} + \Delta k) (n_{d, \text{nom}} + \Delta n_d)^2 \quad (6.45)$$

or

$$\begin{aligned}
 & C_{m, \Delta} I_{я, \text{НОМ}} \Phi_{в. \Delta, \text{НОМ}} - C_{m, \Delta} I_{я, \text{НОМ}} \Delta \Phi_{в. \Delta} + C_{m, \Delta} \Phi_{в. \Delta, \text{НОМ}} \Delta i_{я} + \\
 & + C_{m, \Delta} \Delta \Phi_{в. \Delta} \Delta i_{я} = \frac{GD_{\Delta}^2}{375} \frac{d \Delta n_{\Delta}}{dt} + k_{\text{НОМ}} n_{\Delta, \text{НОМ}}^2 - \\
 & - 2k_{\text{НОМ}} n_{\Delta, \text{НОМ}} \Delta n_{\Delta} + k_{\text{НОМ}} \Delta n_{\Delta}^2 + n_{\Delta, \text{НОМ}}^2 \Delta k + 2n_{\Delta, \text{НОМ}} k_{\text{НОМ}} \Delta n_{\Delta} - \\
 & + \Delta k (\Delta n_{\Delta})^2.
 \end{aligned} \tag{6.46}$$

Disregarding members  $\Delta k (\Delta n_{\Delta})^2$ ;  $2n_{\Delta} \Delta k \Delta n_{\Delta}$ ;  $C_{m, \Delta} \Delta \Phi_{в. \Delta} \Delta i_{я}$  and  $k_{\text{НОМ}} (\Delta n_{\Delta})^2$ , as values of the second order of infinitesimals, we get the propellor shaft torque equilibrium equation (the "main propulsion motor — propellor shaft — propellor" link).

$$\begin{aligned}
 & C_{m, \Delta} I_{я, \text{НОМ}} \Phi_{в. \Delta, \text{НОМ}} + C_{m, \Delta} I_{я, \text{НОМ}} \Delta \Phi_{в. \Delta} + C_{m, \Delta} \Delta i_{я} \Phi_{в. \Delta, \text{НОМ}} = \\
 & = \frac{GD_{\Delta}^2}{375} \frac{d \Delta n_{\Delta}}{dt} + k_{\text{НОМ}} n_{\Delta, \text{НОМ}}^2 - 2k_{\text{НОМ}} n_{\Delta, \text{НОМ}} \Delta n_{\Delta} + n_{\Delta, \text{НОМ}}^2 \Delta k
 \end{aligned} \tag{6.47}$$

or expressed in increments

$$\begin{aligned}
 & C_{m, \Delta} I_{я, \text{НОМ}} \Delta \Phi_{в. \Delta} - C_{m, \Delta} \Delta i_{я} \Phi_{в. \Delta, \text{НОМ}} = \frac{GD_{\Delta}^2}{375} \frac{d \Delta n_{\Delta}}{dt} - \\
 & - \Delta k n_{\Delta, \text{НОМ}}^2 - 2k_{\text{НОМ}} n_{\Delta, \text{НОМ}} \Delta n_{\Delta}.
 \end{aligned} \tag{6.48}$$

Expression (6.48) can be written also in the following way, taking constant parameters into account:

$$k_1 \Delta i_{я}(\rho) + k_2 \Delta \Phi_{в. \Delta}(\rho) = (T'_{м \Delta \rho} + 1) \Delta n_{\Delta}(\rho) - k_3 \Delta k(\rho), \tag{6.49}$$

where

$$\begin{aligned}
 k_1 &= \frac{C_{m, \Delta} \Phi_{в. \Delta, \text{НОМ}}}{2k_{\text{НОМ}} n_{\Delta, \text{НОМ}}}; & k_2 &= \frac{C_{m, \Delta} I_{я, \text{НОМ}}}{2k_{\text{НОМ}} n_{\Delta, \text{НОМ}}}; \\
 k_3 &= \frac{n_{\Delta, \text{НОМ}}^2}{2k_{\text{НОМ}}}.
 \end{aligned}$$

Converting in expression (6.48) to relative units and taking as base values the nominal values of variables, and, considering that

$C_{m, \Delta} I_{я, \text{НОМ}} \Phi_{в. \Delta, \text{НОМ}} = k_{\text{НОМ}} n_{\Delta, \text{НОМ}}^2$ , we get

$$\begin{aligned}
 \frac{\Delta \Phi_{в. \Delta}}{\Phi_{в. \Delta, \text{НОМ}}} + \frac{\Delta i_{я}}{I_{я, \text{НОМ}}} &= \frac{GD_{\Delta}^2}{375} \frac{n_{\Delta, \text{НОМ}}}{M_{\Delta, \text{НОМ}}} \frac{d \left( \frac{\Delta n_{\Delta}}{n_{\Delta, \text{НОМ}}} \right)}{dt} + \\
 &+ \frac{\Delta k}{k_{\text{НОМ}}} + 2 \frac{\Delta n_{\Delta}}{n_{\Delta, \text{НОМ}}}.
 \end{aligned} \tag{6.50}$$

We introduce designations:

$$\begin{aligned}
 \frac{\Delta \Phi_{в. \Delta}}{\Phi_{в. \Delta, \text{НОМ}}} &= \Delta \bar{\Phi}_{в. \Delta} \text{ - relative increment of electric motor flux;} \\
 \frac{\Delta i_{я}}{I_{я, \text{НОМ}}} &= \Delta \bar{i}_{я} \text{ - relative increment of main circuit current;}
 \end{aligned}$$

/258

$\frac{GD_1^2}{375} \cdot \frac{n_{\Sigma \text{ ном}}}{M_{\Sigma \text{ ном}}} = T_{\Sigma, \Sigma}$  - electromechanical time constant of the "main propulsion motor — propellor shaft line — propellor and water entrapped by the propellor" link;

$\frac{\Delta k}{k_{\text{ном}}} = \Delta \bar{k}$  - relative change in the coefficient of the propellor hydrodynamic characteristic;

$2 \frac{\Delta n_{\Sigma}}{n_{\Sigma \text{ ном}}} = 2\Delta \bar{n}_{\Sigma}$  - relative increment of main propulsion motor rotational speed.

Taking previously used and newly introduced designations into account, equation (6.50) is brought to the form

$$\Delta \bar{\Phi}_{\Sigma, \Sigma} + \Delta \bar{i}_{\Sigma} = T_{\Sigma, \Sigma} \frac{d \Delta \bar{n}_{\Sigma}}{dt} + \Delta \bar{k} + 2\Delta \bar{n}_{\Sigma}. \quad (6.51)$$

We will write this expression in operator form:

given non-zero initial conditions

$$\Delta \bar{\Phi}_{\Sigma, \Sigma}(\rho) + \Delta \bar{i}_{\Sigma}(\rho) = T_{\Sigma, \Sigma} \rho \Delta \bar{n}_{\Sigma}(\rho) - T_{\Sigma, \Sigma} \Delta \bar{n}_{\Sigma}(0) + \Delta \bar{k}(\rho) + 2\Delta \bar{n}_{\Sigma}(\rho)$$

or

$$\Delta \bar{\Phi}_{\Sigma, \Sigma}(\rho) + \Delta \bar{i}_{\Sigma}(\rho) = \Delta \bar{n}_{\Sigma}(\rho) (2 + T_{\Sigma, \Sigma} \rho) + \Delta \bar{k}(\rho) - T_{\Sigma, \Sigma} \Delta \bar{n}_{\Sigma}(0), \quad (6.52)$$

taking zero initial conditions into account

$$(6.53)$$

where  $\Delta \bar{\Phi}_{\Sigma, \Sigma}(\rho) + \Delta \bar{i}_{\Sigma}(\rho) = 2\Delta \bar{n}_{\Sigma}(\rho) (1 + \rho T'_{\Sigma, \Sigma}) + \Delta \bar{k}(\rho)$ ,

$$T'_{\Sigma, \Sigma} = \frac{T_{\Sigma, \Sigma}}{2}.$$

Given constant main propulsion motor field flux, the propellor shaft line torque equilibrium equation can be obtained from equation (6.53) if one adds to it  $\Delta \Phi_{\Sigma, \Sigma}(\rho) = 0$ . Taking earlier used designations into account, the torque equilibrium equation can be written in operator form:

$$\Delta \bar{i}_{\Sigma}(\rho) = \Delta \bar{n}_{\Sigma}(\rho) 2(1 + \rho T'_{\Sigma, \Sigma}) + \Delta \bar{k}(\rho) - T_{\Sigma, \Sigma} \Delta \bar{n}_{\Sigma}(0) \quad (6.54)$$

and, given zero initial conditions,

$$\Delta \bar{i}_{\Sigma}(\rho) = \Delta \bar{n}_{\Sigma}(\rho) 2(1 + \rho T'_{\Sigma, \Sigma}) + \Delta \bar{k}(\rho). \quad (6.55)$$

It is possible to obtain the torque equation for a two-loop circuit with one paired main propulsion motor if you take into account that  $m_x = m_{x1} + m_{x2} / 259$  and  $i_x = i_{x1} - i_{x2}$ . Meanwhile, given constant motor field flux  $m_{x1} = C_{eD} i_{x1}$ ;  $m_{x2} = C_{eD} \Delta i_{x2}$  or in increments

$$\begin{cases} \Delta m_{x1} = C_{eD} \Delta i_{x1}; \\ \Delta m_{x2} = C_{eD} \Delta i_{x2}. \end{cases} \quad (6.56)$$

and it is possible to assume for the established mode

$$I_{1 \text{ NOM}} = I_{2 \text{ NOM}} = I_{\text{NOM}}; \quad (6.57)$$

then

$$\frac{1}{2} (\Delta \bar{i}_{x1} + \Delta \bar{i}_{x2}) = T_{m.x} \frac{d \Delta \bar{n}_x}{dt} + 2 \Delta \bar{n}_x + \Delta \bar{k}, \quad (6.58)$$

where

$$C_{eD} I_{x1 \text{ NOM}} = C_{eD} I_{x2 \text{ NOM}} = \frac{1}{2} M_{D \text{ NOM}} = \frac{1}{2} n_{D \text{ NOM}}^2 k_{\text{NOM}} \quad (6.59)$$

A more complete expression for the propellor shaft equilibrium equation can be obtained stemming from the following relationship:

$$m_s = f(n_x; V). \quad (6.60)$$

Expanding this function into a Maclaurin series and disregarding members of the highest order of infinitesimals, we get

$$\Delta m_s = \frac{\partial m_s}{\partial n_x} \Delta n_x + \frac{\partial m_s}{\partial V} \Delta V. \quad (6.61)$$

Then, disregarding propellor shaft line friction torque  $m_f$ , we will write the equilibrium equation in this form:

$$\begin{aligned} C_{m.D} I_{x \text{ NOM}} \Delta \Phi_D + C_{m.D} \Phi_{D \text{ NOM}} \Delta i_x &= \frac{GD_D}{375} \frac{d \Delta n_x}{dt} + \\ &+ \frac{\partial m_s}{\partial n_x} \Delta n_x + \frac{\partial m_s}{\partial V} \Delta V. \end{aligned} \quad (6.62)$$

We will present equation (6.62) in relative units:

$$\begin{aligned} C_{m.D} I_{x \text{ NOM}} \Phi_{D \text{ NOM}} \frac{\Delta \Phi_D}{\Phi_{D \text{ NOM}}} + C_{m.D} I_{x \text{ NOM}} \Phi_{D \text{ NOM}} \frac{\Delta i_x}{I_{x \text{ NOM}}} &= \\ = \frac{GD_D^2}{375} n_{D \text{ NOM}} \frac{d \Delta \bar{n}_x}{dt} + \frac{\partial m_s}{\partial n_x} \frac{\Delta n_x}{n_{D \text{ NOM}}} n_{D \text{ NOM}} + \frac{\partial m_s}{\partial V} \frac{\Delta V}{V_{\text{NOM}}} V_{\text{NOM}}. \end{aligned} \quad (6.63)$$

We introduce designations:

$$\frac{\frac{\partial m_s}{\partial n_x} n_{D \text{ NOM}}}{M_{D \text{ NOM}}} = \gamma_{2n} \quad \text{- transfer factor of the system for propellor rotational speed;}$$

$$\frac{\frac{\partial m_s}{\partial V} V_{\text{NOM}}}{M_{D \text{ NOM}}} = \gamma_{2V} \quad \text{- transfer factor of the system for vessel speed.}$$

Taking these and earlier accepted designations into account, we will /260  
write the propellor shaft line torque equilibrium equation expressed in relative  
units and in increments:

$$\Delta\bar{\Phi}_{v, \lambda} + \Delta\bar{i}_n = T_{m, \lambda} \frac{d\Delta n_{\lambda}}{dt} + \gamma_{2n} \Delta\bar{n}_{\lambda} + \gamma_{2V} \Delta\bar{V}. \quad (6.64)$$

The equation looks like this in operator form

$$T_{m, \lambda} p \Delta\bar{n}_{\lambda}(p) + \gamma_{2n} \Delta\bar{n}_{\lambda}(p) = \Delta\bar{\Phi}_{v, \lambda}(p) + \Delta\bar{i}_n(p) - \gamma_{2V} \Delta\bar{V}(p) + T_{m, \lambda} \Delta\bar{n}_{\lambda}(0), \quad (6.65)$$

and, given zero initial conditions, using designation  $T_{m, \lambda} = \frac{T_{m, \lambda}}{\gamma_{2n}}$ , it is possible to write

$$\gamma_{2n} \Delta n_{\lambda}(p) (T_{m, \lambda} p + 1) = \Delta\bar{\Phi}_{v, \lambda}(p) + \Delta\bar{i}_n(p) - \gamma_{2V} \Delta\bar{V}(p). \quad (6.66)$$

The torque equilibrium equation will have this form, given constant main propulsion motor field flux:

given variable vessel speed 
$$\Delta\bar{i}_n(p) = \gamma_{2n} \Delta\bar{n}_{\lambda}(p) (T_{m, \lambda} p + 1) + \gamma_{2V} \Delta\bar{V}(p); \quad (6.67)$$

given constant vessel speed during the period electrical propulsion plant transient processes occur

$$\Delta\bar{i}_n(p) = \gamma_{2n} \Delta\bar{n}_{\lambda}(p) (T_{m, \lambda} p + 1). \quad (6.68)$$

The G—D system armature circuit: 
$$e_r = r_n i_n + L_n \frac{di_n}{dt} + e_x, \quad (6.69)$$

where  $e_r$  is generator emf;  $r_n = r_{n,r} + r_{n,x}$  is armature circuit resistance;

$L_n = L_{n,r} + L_{n,x}$  is armature circuit inductivity  $e_x = C_{e\lambda} \Phi_{v, \lambda} n_{\lambda}$  is main propulsion motor counter emf;  $C_{e\lambda}$  is motor machinery constant.

Converting to increments in the operator form of recording and considering that

we get 
$$\Delta e_x(p) = C_{e\lambda} \Phi_{v, \lambda, \text{ном}} \Delta n_{\lambda}(p) + C_{e\lambda} n_{\lambda, \text{ном}} \Delta \Phi_{\lambda}(p),$$

$$\Delta e_r(p) = r_n \Delta i_n(p) + L_n p \Delta i_n(p) + C_{e\lambda} \Phi_{\lambda, \text{ном}} \Delta n_{\lambda}(p) + C_{e\lambda} n_{\lambda, \text{ном}} \Delta \Phi_{v, \lambda}(p) \quad (6.69a)$$

or

$$\Delta i_n(p) (T_n p + 1) = \frac{1}{r_n} \Delta e_r(p) - k_4 \Delta n_{\lambda}(p) - k_5 \Delta \Phi_{v, \lambda}(p), \quad (6.70)$$

where  $T_n = \frac{L_n}{r_n}$  is an armature circuit time constant;  $k_4 = \frac{C_{e\lambda} \Phi_{\lambda, \text{ном}}}{r_n}$ , and

$k_5 = \frac{C_{e\lambda} n_{\lambda, \text{ном}}}{r_n}$  are factors.

The GED motor field winding voltage equilibrium equation has the form

$$U_{b, \lambda} = i_{b, \lambda} r_{b, \lambda} + 2p_{b, \lambda} \sigma_{b, \lambda} \dot{\omega}_{b, \lambda} \frac{d\Phi_{b, \lambda}}{dt}, \quad (6.71)$$

where  $U_{b, \lambda}$  — is field winding voltage;  $i_{b, \lambda}$  — is field winding current;  $r_{b, \lambda}$  — is field winding resistance;  $p_{b, \lambda}$  — is the number of motor pole pairs;  $\sigma_{b, \lambda}$  — is a motor field winding equilibrium factor;  $\dot{\omega}_{b, \lambda}$  is the number of field winding turns per pole.

Motor field flux equals  $\Phi_{b, \lambda} = C_{\lambda} i_{b, \lambda} \dot{\omega}_{b, \lambda}$ , where  $C_{\lambda} = \frac{\partial f(\sum F_{b, \lambda})}{\partial (\sum F_{b, \lambda})}$ ;  $\sum F_{b, \lambda}$  is the proportionality factor determined from the motor magnetization curve at the operating point.

Converting to recording in increments and in operator form having considered that  $\Delta\Phi_{b, \lambda}(\rho) = C_{\lambda} \dot{\omega}_{b, \lambda} \Delta i_{b, \lambda}(\rho)$ , we get  $\Delta U_{b, \lambda}(\rho)$

$$= r_{b, \lambda} \Delta i_{b, \lambda}(\rho) + 2p_{b, \lambda} \sigma_{b, \lambda} \dot{\omega}_{b, \lambda} \rho \Delta\Phi_{b, \lambda}(\rho) \quad \text{or} \\ (T_{b, \lambda} \rho + 1) \Delta\Phi_{b, \lambda}(\rho) = k_{\lambda} \Delta U_{b, \lambda}(\rho), \quad (6.72)$$

where  $T_{b, \lambda} = \frac{2p_{b, \lambda} \sigma_{b, \lambda} \dot{\omega}_{b, \lambda} C_{\lambda}}{r_{b, \lambda}}$  is a field winding time constant;  $k_{\lambda} = \frac{C_{\lambda} \dot{\omega}_{b, \lambda}}{r_{b, \lambda}}$  — is a factor.

We obtain the general propulsion motor equation, having jointly solved equations (6.49), (6.70), and (6.72) relative to increments of armature current  $\Delta i_n(\rho)$  and rotational speed  $\Delta n_n(\rho)$ .

From (6.49) we have

$$\Delta n_n(\rho) = \frac{k_1 \Delta i_n(\rho) + k_2 \Delta\Phi_{b, \lambda}(\rho) - k_3 \Delta k(\rho)}{T_{m, \lambda} \rho + 1}$$

and substituting in (6.70)

$$(T_{n, \lambda} \rho + 1) \Delta i_n(\rho) = k_7 \Delta e_r(\rho) - \frac{k_1 k_4 \Delta i_n(\rho) + k_2 k_4 \Delta\Phi_{b, \lambda}(\rho) - k_3 k_4 \Delta k(\rho)}{T_{m, \lambda} \rho + 1} - \\ - k_5 \Delta\Phi_{b, \lambda}(\rho);$$

from which

$$\Delta\Phi_{b, \lambda}(\rho) = \frac{k_7 (T_{m, \lambda} \rho + 1) \Delta e_r(\rho) - [(T_{n, \lambda} \rho + 1)(T_{m, \lambda} \rho + 1) k_1 k_4] \Delta i_n(\rho) - k_3 k_4 \Delta k(\rho)}{k_2 k_4 - k_5 (T_{m, \lambda} \rho + 1)}$$

we substitute in (6.72)

$$k_{\lambda} (T_{m, \lambda} \rho + 1) (T_{b, \lambda} \rho + 1) \Delta e_r(\rho) - (T_{b, \lambda} \rho + 1) [(T_{n, \lambda} \rho + 1)(T_{m, \lambda} \rho + 1) + k_1 k_4] \Delta i_n(\rho) + (T_{b, \lambda} \rho + 1) k_3 k_4 \Delta k(\rho) = \\ = [k_{\lambda} k_4 k_5 + k_3 k_5 (T_{m, \lambda} \rho + 1)] \Delta U_{b, \lambda}(\rho).$$

Finally

/262

$$\begin{aligned} & (T_{m, \mu p} + 1) [(T_{n p} + 1)(T_{m, \mu p} + 1) + k_1 k_6] \Delta i_m(\rho) = \\ & = k_7 (T_{m, \mu p} + 1)(T_{n p} + 1) \Delta e_r(\rho) - [k_1 k_4 k_6 + k_6 k_6 (T_{m, \mu p} + \\ & + 1)] \Delta U_{m, \mu}(\rho) + k_3 k_4 (T_{m, \mu p} + 1) \Delta k(\rho); \end{aligned} \quad (6.73)$$

relative to rotational speed  $n_n$  we have from (6.69)

$$\Delta i_m = \frac{(T_{m, \mu p} + 1) \Delta n_n(\rho) - k_2 \Delta \Phi_{m, \mu}(\rho) + k_3 \Delta k(\rho)}{k_1}$$

and we substitute in (6.70)

$$\begin{aligned} & (T_{n p} + 1)(T_{m, \mu p} + 1) \Delta n_n(\rho) - k_2 (T_{n p} + 1) \Delta \Phi_{m, \mu}(\rho) + \\ & + k_3 (T_{n p} + 1) \Delta k(\rho) = k_1 k_7 \Delta e_r(\rho) - k_1 k_4 \Delta n_n(\rho) - \\ & - k_2 k_3 \Delta \Phi_{m, \mu}(\rho); \end{aligned} \quad (6.74)$$

from whence

$$\begin{aligned} & \Delta \Phi_{m, \mu}(\rho) = \\ & = \frac{(T_{n p} + 1)(T_{m, \mu p} + 1) \Delta n_n(\rho) + k_3 (T_{n p} + 1) \Delta k(\rho) - k_1 k_7 \Delta e_r(\rho) + k_1 k_4 \Delta n_n(\rho)}{k_2 (T_{n p} + 1) - k_1 k_6} \end{aligned}$$

we substitute in (6.72), then

$$\begin{aligned} & (T_{m, \mu p} + 1) [(T_{n p} + 1)(T_{m, \mu p} + 1) + k_1 k_6] \Delta n_n(\rho) = \\ & = k_1 k_7 (T_{m, \mu p} + 1) \Delta e_r(\rho) + [k_1 k_6 (T_{n p} + 1) - \\ & - k_1 k_3 k_6] \Delta U_{m, \mu}(\rho) - k_3 (T_{m, \mu p} + 1)(T_{n p} + 1) \Delta k(\rho). \end{aligned} \quad (6.75)$$

Equation of motion of the "main generator" link. Generator field magnetic flux is a function of generator field mmf [magnetomotive force] and the equation written in increments and in operator form has the form

$$\Delta \Phi_r(\rho) = C_r' w_{m, r} \Delta i_{m, r}(\rho), \quad (6.76)$$

where  $C_r' = \frac{df(\sum F_{m, r})}{d(\sum F_{m, r})} \sum F_{m, r, 0}$  is a factor determined from characteristic

$\Phi_r = f(F_{m, r})$  in the operating point.

The field circuit emf equation: 
$$U_{m, r} = r_{m, r} i_{m, r} + 2p_r \sigma_r w_{m, r} \frac{d\Phi_r}{dt}. \quad (6.77)$$

Written in increments and in operator form, it has the form

$$\Delta U_{m, r}(\rho) = r_{m, r} \Delta i_{m, r}(\rho) + 2p_r \sigma_r w_{m, r} \rho \Delta \Phi_r(\rho), \quad (6.78)$$

where  $U_{m, r}$  is generator field circuit voltage;  $r_{m, r}$  field circuit resistance;  $i_{m, r}$  is generator field current;  $p_r$  is the number of pole pairs;  $w_{m, r}$  is the number of field winding turns per pole;  $\Phi_r$  is field winding flux.

The relationship among rotational speed, magnetic flux, and generator in increments is determined by expression

$$\Delta e_r(\rho) = C'_{n,r} [\Delta n_r(\rho) + \Delta \Phi_r(\rho)] \quad (6.79)$$

and, given constant generator rotational speed, by the expression

$$\Delta e_r(\rho) = C_r \Delta \Phi_r(\rho), \quad (6.80)$$

where  $C_r = \frac{P_r N_a a n_r}{60 a}$ ;  $N_a$  - are the number of armature active conductors;  $a$  is the number of armature winding parallel branch pairs;  $n_r$  - armature rotational speed, rpm.

We solve equations (6.76)–(6.80) jointly. From (6.76) we have

$$\Delta i_{n,r}(\rho) = \frac{\Delta \Phi_r(\rho)}{C_r w_{n,r}}$$

and we substitute it in (6.78):

$$\Delta U_{n,r}(\rho) = \frac{r_{n,r}}{C_r w_{n,r}} \Delta \Phi_r(\rho) + 2\rho_r \sigma_r w_{n,r} \rho \Delta \Phi_r(\rho);$$

then

$$\Delta \Phi_r(\rho) = \frac{\Delta U_{n,r}(\rho)}{\left( \frac{r_{n,r}}{C_r w_{n,r}} + 2\rho_r \sigma_r w_{n,r} \rho \right)}$$

we will substitute in (6.79), then

$$\left( \frac{r_{n,r}}{C_r w_{n,r}} + 2\rho_r \sigma_r w_{n,r} \rho \right) \Delta e_r(\rho) = C_r \Delta U_{n,r}(\rho).$$

Finally

$$(T_r \rho + 1) \Delta e_r(\rho) = k_r \Delta U_{n,r}(\rho), \quad (6.81)$$

where  $T_r = \frac{2\rho_r C_r \sigma_r w_{n,r}^2}{r_{n,r}}$  is a generator time constant;  $k_r = \frac{w_{n,r} C_r C_r'}{r_{n,r}}$  is a generator transmission factor.

Equation of motion of the "generator exciter" link(Figure 6.3). The master winding (NVO) equation is:

$$U_{n\Delta} = i_{n\Delta} (r_{n.o,r} + r_{c,y}) + 2\rho_{n,r} \sigma_{n.o,r} \frac{d\Phi_{n.o,r}}{dt},$$

where  $U_{n\Delta}$  is the voltage in the generator field master winding;  $i_{n\Delta}$  is master winding current;  $r_{n.o,r}$  is master winding dc resistance;  $r_{c,y}$  is standardizing resistance;  $\rho_{n,r}$  is the number of pole pairs;  $\sigma_{n.o,r}$  is a winding dispersal factor;  $\Phi_{n.o,r}$  is exciter field flux.

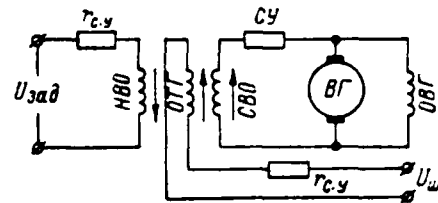


Fig. 6.3. Link of system for automatic control of "generator exciter"

Converting to increments and to the operator form of recording (in /264 form, when  $U_{\text{зад}} = \text{var}$ ), we get

$$\begin{aligned} \Delta U_{\text{зад}}(p) - (r_{\text{н.о.г}} + r_{\text{с.г}}) \Delta i_{\text{зад}}(p) - \\ - 2p_{\text{п.г}} \sigma_{\text{н.о.г}} \omega_{\text{н.о.г}} p \Delta \Phi_{\text{п.г.г}}(p) = 0. \end{aligned} \quad (6.82)$$

The current feedback winding (OTG) equation is:

$$U_{\text{ш}} = i_{\text{о.т.г}}(r_{\text{о.т.г}} + r_{\text{с.г}}) - 2p_{\text{п.г}} \sigma_{\text{о.т.г}} \omega_{\text{о.т.г}} \frac{d\Phi_{\text{п.г.г}}}{dt},$$

where  $U_{\text{ш}}$  is voltage picked off main propulsion motor additional poles and the compensating winding proportional to main circuit current (if one disregards the inductivity of the additional poles and compensating winding):  $i_{\text{о.т.г}}$  is winding current,  $r_{\text{о.т.г}}$  is winding resistance;  $r_{\text{с.г}}$  is standardizing resistance;  $p_{\text{п.г}}$  is the number of pole pairs;  $\sigma_{\text{о.т.г}}$  is the dispersal factor;  $\omega_{\text{о.т.г}}$  is the number of OTG winding turns per pole. Converting to increments and in the operator form of recording, we get

$$\Delta U_{\text{ш}}(p) - (r_{\text{о.т.г}} + r_{\text{с.г}}) \Delta i_{\text{о.т.г}}(p) + 2p_{\text{п.г}} \sigma_{\text{о.т.г}} \omega_{\text{о.т.г}} p \Delta \Phi_{\text{п.г.г}}(p) = 0. \quad (6.83)$$

The self-excitation winding (SVO) equation is:

$$U_{\text{св}} = U_{\text{п.г}} = i_{\text{св}}(r_{\text{св}} + r_{\text{с.г}}) + 2p_{\text{п.г}} \sigma_{\text{св}} \omega_{\text{св}} \frac{d\Phi_{\text{п.г.г}}}{dt},$$

where  $U_{\text{св}}$  is voltage in the winding equal to  $U_{\text{п.г}}$ ;  $i_{\text{св}}$  is self-excitation winding current;  $r_{\text{св}}$  is winding resistance;  $r_{\text{с.г}}$  is standardizing resistance.

Converting to increments and to the operator form of recording, we get

$$\Delta U_{\text{п.г}}(p) - (r_{\text{св}} + r_{\text{с.г}}) \Delta i_{\text{св}}(p) - 2p_{\text{п.г}} \omega_{\text{св}} \sigma_{\text{св}} p \Delta \Phi_{\text{п.г.г}}(p) = 0. \quad (6.84)$$

The field flux equation in increments and in the operator form is:

$$\begin{aligned} \Delta \Phi_{\text{п.г.г}}(p) = C_{\text{п.г}} \left[ \omega_{\text{н.о.г}} \Delta i_{\text{зад}}(p) + \omega_{\text{св}} \Delta i_{\text{св}}(p) - \right. \\ \left. - \omega_{\text{о.т.г}} \Delta i_{\text{о.т.г}}(p) \right], \end{aligned} \quad (6.85)$$

where  $C_{\text{п.г}}$  is a factor determined from characteristic  $\Phi_{\text{п.г.г}} = f(\sum F_{\text{п.г.г}})$  in the operating point.

The constraint equation between emf and flux in increments and in the operator form (where  $n_{\text{п.г}} = \text{const}$ ):

$$\Delta e_{\text{п.г.г}}(p) = C_{\text{п.г.г}} \Delta \Phi_{\text{п.г.г}}(p), \quad (6.86)$$

where  $C_{\text{п.г.г}} = \frac{p_{\text{п.г}} N n_{\text{п.г}}}{60a}$ ,  $N$  are the number of armature active conductors;  $a$  is the number of armature parallel branch pairs;  $n_{\text{п.г}}$  is armature rotational speed, rpm.

Constraint equation of emf and voltage. In this case it is possible /265 for simplicity to disregard current flowing through the self-excitation winding since  $i_{b.r} = i_{cb}$ , as well as inductivity of the generator exciter armature, since  $L_{n.b.r} = L_{b.r}$ . Then the constraint between emf and generator field voltage in increments and in operator form will be expressed in the following way:

$$\Delta U'_{b.r}(\rho) = \Delta e_{b.r}(\rho) - r_{n.b.r} \Delta i_{b.r}(\rho),$$

here, from (6.78) and (6.81) we have

$$\Delta i_{b.r}(\rho) = \frac{\Delta U_{b.r}(\rho)}{r_{b.r}(T_{b.r}\rho + 1)}.$$

Then

$$\Delta e_{b.r}(\rho) = \Delta U'_{b.r}(\rho) + \frac{r_{n.b.r} \Delta U_{b.r}(\rho)}{r_{b.r}(T_{b.r}\rho + 1)}$$

or

$$r_{b.r}(T_{b.r}\rho + 1) \Delta e_{b.r}(\rho) = (r_{b.r} - r_{n.b.r} + r_{b.r} T_{b.r} \rho) \Delta U_{b.r}(\rho);$$

finally

$$(T_{b.r}\rho + 1) \Delta U_{b.r}(\rho) = \alpha_1 (T_{b.r}\rho + 1) \Delta e_{b.r}(\rho);$$

$$T_{b.r} = \frac{r_{b.r}}{r_{b.r} - r_{n.b.r}} T_{b.r} = \alpha_1 T_{b.r}; \quad (6.87)$$

$$\alpha_1 = \frac{r_{b.r}}{r_{b.r} - r_{n.b.r}}.$$

Solving equations (6.82) — (6.87) jointly, we will find:

$$\text{from (6.82)} \quad \Delta i_{3a2}(\rho) = \frac{\Delta U_{3a2}(\rho) - 2\rho r_{n.o.r} \omega_{n.o.r} \rho \Delta \Phi_{b.r}(\rho)}{r_{n.o.r} - r_{c.y}}$$

and when

$$\Delta U_{3a2}(\rho) = 0$$

$$\Delta i_{3a2}(\rho) = - \frac{2\rho r_{n.o.r} \omega_{n.o.r} \rho \Delta \Phi_{b.r}(\rho)}{r_{n.o.r} - r_{c.y}};$$

from (6.83)

$$\Delta i_{o.t.r}(\rho) = \frac{\Delta U_{\omega}(\rho) - 2\rho r_{o.t.r} \omega_{o.t.r} \rho \Delta \Phi_{b.r}(\rho)}{r_{o.t.r} - r_{c.y}};$$

from (6.84)

$$\Delta i_{cb}(\rho) = \frac{\Delta U_{b.r}(\rho) - 2\rho r_{cb} \omega_{cb} \rho \Delta \Phi_{b.r}(\rho)}{r_{cb} - r_{c.y}}$$

we will substitute in equation (6.85) and we get

$$[(T_{n.o.r} + T_{cb} + T_{o.t.r})\rho + 1] \Delta \Phi_{b.r}(\rho) = k_{n.o.r} \Delta U_{3a2}(\rho) - k_{cb} \Delta U_{b.r}(\rho) - k_{o.t.r} \Delta U_{\omega}(\rho)$$

and when

$$\Delta U_{3a2}(\rho) = 0$$

$$[(T_{n.o.r} + T_{cb} + T_{o.t.r})\rho + 1] \Delta \Phi_{b.r}(\rho) = k_{cb} \Delta U_{b.r}(\rho) - k_{o.t.r} \Delta U_{\omega}(\rho).$$

From equation (6.86)

$$\Delta \Phi_{b.r}(\rho) = \frac{\Delta e_{b.r}(\rho)}{C_{b.r}},$$

/266

then

$$(T_{\rho} + 1) \Delta e_{b.r}(\rho) = k_{n.o.r} \Delta U_{3a2}(\rho) + k_{cb} \Delta U_{b.r}(\rho) - k_{o.t.r} \Delta U_{\omega}(\rho)$$

(6.88)

and when  $\Delta U_{322}(\rho) = 0$   
 where  $(T_{\Sigma}\rho + 1)\Delta e_{n,r}(\rho) = k_{cb}\Delta U_{n,r}(\rho) - k_{o,t,r}\Delta U_w(\rho)$ , (6.89)

$T_{\Sigma} = T_{n,o,r} + T_{cb} + T_{o,t,r}$ ;  $T_{n,o,r} = \frac{2\rho_{n,r}\sigma_{n,o,r}C'_{n,r}w_{n,o,r}^2}{r_{n,o,r} + r_{c,y}}$  is a master winding time constant;  
 $T_{cb} = \frac{2\rho_{n,r}\sigma_{cb}C'_{n,r}w_{cb}^2}{r_{cb} + r_{c,y}}$  is a self-excitation winding time constant;  
 $T_{o,t,r} = \frac{2\rho_{n,r}\sigma_{o,t,r}C'_{o,t,r}w_{o,t,r}^2}{r_{o,t,r} + r_{c,y}}$  is a current feedback winding (OTG) time constant;

$$\left. \begin{aligned} k_{n,o,r} &= \frac{C'_{n,r}w_{n,o,r}C_{n,r}}{r_{n,o,r} + r_{c,y}} \\ k_{cb} &= \frac{C'_{n,r}w_{cb}C_{n,r}}{r_{cb} + r_{c,y}} \\ k_{o,t,r} &= \frac{k_w C'_{o,t,r}w_{o,t,r}C_{n,r}}{r_{o,t,r} + r_{c,y}} \end{aligned} \right\} \text{are winding gain.}$$

From equation (6.87)

$$\Delta e_{n,r}(\rho) = \frac{(T'_{n,r}\rho + 1)\Delta U_{n,r}(\rho)}{\alpha_1(T_{n,r}\rho + 1)}$$

we substitute in (6.88)

$$(T_{\Sigma}\rho + 1)(T'_{n,r}\rho + 1)\Delta U_{n,r}(\rho) = \alpha_1(T_{n,r}\rho + 1) \times [k_{n,o,r}\Delta U_{322}(\rho) + k_{cb}\Delta U_{n,r}(\rho) - k_{o,t,r}\Delta U_w(\rho)]$$
 (6.90)

and when  $\Delta U_{322}(\rho) = 0$

$$[(T_{\Sigma}\rho + 1)(T'_{n,r}\rho + 1) - k_{cb}(T_{n,r}\rho + 1)]\Delta U_{n,r}(\rho) = -(T_{n,r}\rho + 1)k_{o,t,r}\Delta U_w(\rho)$$
 (6.91)

here, we consider that  $\Delta U_{n,r}(\rho) = \Delta U_{n,c}(\rho)$ , and, since  $r_{n,r} \gg r_{cb}$ , then  $\alpha_1 = 1$ .

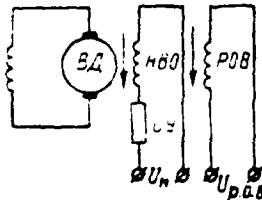


Figure 6.4. Automated Control System "Main Propulsion Motor" Link.

Equations of motion of the "main propulsion motor" link (Figure 6.4).

The independent winding (NVO) equation is:

$$U_n = i_n(r_n + r_{c,y}) + 2\rho_{n,r}\sigma_n w_n \frac{d\Phi_{n,r}}{dt}$$

where  $U_H$  is winding voltage;  $i_H$  is winding current;  $r_H$  is winding resistance;  $r_{c.y}$  is additional winding resistance;  $p_{b.d}$  is number of exciter pole pairs;  $\sigma_H$  is a dispersal factor;  $\Phi_{b.p.d}$  is flux of one pole. /267

Converting to increments and an operational notation, we have

$$\Delta U_H(p) - (r_H + r_{c.y}) \Delta i_H(p) - 2p_{b.d} \sigma_H \omega_H p \Delta \Phi_{b.p.d}(p) = 0. \quad (6.92)$$

When  $\Delta U_H(p) = 0$  (having assumed  $U_H = \text{const}$ )

$$0 = (r_H + r_{c.y}) \Delta i_H(p) + 2p_{b.d} \sigma_H \omega_H p \Delta \Phi_{b.p.d}(p). \quad (6.93)$$

The current feedback winding (OTD) equation is:

$$U_{o.t.d} = i_{o.t.d} r_{o.t.d} - 2p_{b.d} \sigma_{o.t.d} \omega_{o.t.d} p \frac{d\Phi_{b.p.d}}{dt}$$

where  $U_{o.t.d}$  is winding voltage (we assume accordingly that voltage at the armature terminals  $U_{o.t.d} \approx e_{o.t.d}$ );  $i_{o.t.d}$  winding current;  $r_{o.t.d}$  winding resistance;  $p_{b.d}$  is the number of pole pairs;  $\sigma_{o.t.d}$  is winding dispersal factor.

Converting to increments and to an operational notation, we have

$$\Delta U_{o.t.d}(p) - r_{o.t.d} \Delta i_{o.t.d}(p) + 2p_{b.d} \sigma_{o.t.d} \omega_{o.t.d} p \Delta \Phi_{b.p.d}(p) = 0. \quad (6.94)$$

The magnetic flux equation in increments and in an operational notation, is:

$$\Delta \Phi_{b.p.d}(p) = C'_{b.d} [\omega_H \Delta i_H(p) - \omega_{o.t.d} \Delta i_{o.t.d}(p)]. \quad (6.95)$$

where  $C'_{b.d}$  is a factor from characteristic  $\Phi_{b.d} = f(\sum F_{b.d})$  in an operating point.

The constraint equation between emf and magnetic flux in increments and in an operational notation (with  $n_{b.d} = \text{const}$ ) is:

$$\Delta e_{b.d}(p) = C_{b.d} \Delta \Phi_{b.p.d}(p), \quad (6.96)$$

where  $C_{b.d} = \frac{p_{b.d} N_a \sigma_{b.d}}{60a}$ ;  $p_{b.d}$  is the number of pole pairs;  $N_a$  is the number of exciter armature conductors;  $n_{b.d}$  is exciter rotational speed, rpm;  $a$  is the number of parallel branch pairs.

We obtain the constraint equation between emf and voltage in the following way. We disregard  $L_{a.b.d}$ , since  $L_{a.b.d} \ll L_{b.p.d}$ . Then we can write in increments and in an operational notation  $\Delta U_{b.d}(p) = \Delta e_{b.d}(p) - r_{a.b.d} \Delta i_{b.d}(p)$ .

Solving jointly with (6.72), we will find

$$r_{b.d} (T_{b.d} p + 1) \Delta e_{b.d}(p) = (r_{b.d} + r_{a.b.d} - r_{b.d} T_{b.d} p) \Delta U_{b.d}(p)$$

and, finally

$$(T'_{b.z} p + 1) \Delta U_{b.z}(p) = \alpha_1 (T_{b.z} p + 1) \Delta e_{b.z}(p), \quad (6.97)$$

where, taking (6.72) into account

$$\alpha_1 = \frac{r_{b.z}}{r_{b.z} + r_{a.b.z}}; \quad T'_{b.z} = \alpha_1 T_{b.z}.$$

Solving equations (6.92) and (6.93) — (6.97) jointly, we have: /268  
from (6.92)

$$\Delta i_H(p) = \frac{\Delta U_H(p) - 2p_{b.z} \sigma_H \omega_H p \Delta \Phi_{b.v.z}(p)}{r_H - r_{c.y}};$$

from (6.93) 
$$\Delta i_H(p) = - \frac{2p_{b.z} \sigma_H \omega_H p \Delta \Phi_{b.v.z}(p)}{r_H - r_{c.y}};$$

from (6.94) 
$$\Delta i_{o.t.z}(p) = \frac{\Delta U_{o.t.z}(p) - 2p_{b.z} \sigma_{o.t.z} \omega_{o.t.z} p \Delta \Phi_{b.v.z}(p)}{r_{o.t.z}}. \quad (6.98)$$

Having substituted (6.98) in (6.97), we get

$$[(T_H - T_{o.t.z}) p + 1] \Delta \Phi_{b.v.z}(p) = k_H \Delta U_H(p) - k_{o.t.z} \Delta U_{o.t.z}(p).$$

From (6.96) we have

$$\Delta \Phi_{b.v.z}(p) = \frac{\Delta e_{b.z}(p)}{C_{b.z}}$$

and, having substituted this equality in the previous expression, we get

$$(T'_{z.p} + 1) \Delta e_{b.z}(p) = k_H \Delta U_H(p) - k_{o.t.z} \Delta U_{o.t.z}(p) \quad (6.99)$$

and when  $\Delta U_H(p) = 0$

$$(T'_{z.p} - 1) \Delta e_{b.z}(p) = -k_{o.t.z} \Delta U_{o.t.z}(p),$$

where  $T'_{z.p} = T_H - T_{o.t.z}$  is an exciter field circuit time constant;

$T_H = \frac{2p_{b.z} C_{b.z} \sigma_H \omega_H^2}{r_H - r_{c.y}}$  is winding NVO time constant;  $T_{o.t.z} = \frac{2p_{b.z} C_{b.z} \sigma_{o.t.z} \omega_{o.t.z}^2}{r_{o.t.z}}$  is winding ROV time constant;  $k_H = \frac{C_{b.z} C_{b.z} \sigma_H \omega_H^2}{r_H - r_{c.y}}$  is winding NVO gain;  $k_{o.t.z} = \frac{C_{b.z} C_{b.z} \sigma_{o.t.z} \omega_{o.t.z}^2}{r_{o.t.z}}$  is winding ROV gain.

From equation (6.97) we have

$$\Delta e_{b.z}(p) = \frac{(T'_{b.z} p - 1) \Delta U_{b.z}(p)}{\alpha_1 (T_{b.z} p - 1)}$$

and, having substituted in (6.99), we get

$$(T'_{z.p} - 1) (T'_{b.z} p + 1) \Delta U_{b.z}(p) = \alpha_1 (T_{b.z} p + 1) [k_H \Delta U_H(p) - k_{o.t.z} \Delta U_{o.t.z}(p)]$$

or

$$(T'_{z.p} + 1) (T'_{b.z} p + 1) \Delta U_{b.z}(p) = \alpha_1 k_{o.t.z} (T_{b.z} p + 1) \cdot \left[ \frac{k_H}{k_{o.t.z}} \Delta U_H(p) - \Delta U_{o.t.z}(p) \right] \quad (6.100)$$

and, when  $\Delta U_n(p) = 0$

/269

$$(T_{\Sigma p} + 1)(T_{\Sigma p} - 1)\Delta U_{\Sigma p}(p) = -\alpha_1 (T_{\Sigma p} + 1)k_{0. \tau. \Sigma} \Delta U_{0. \tau. \Sigma}(p). \quad (6.101)$$

Equation of motion of the "transverse field amplidyne" link (Figure 6.5).

The equation for the resulting magnetic flux along longitudinal axis  $\Phi_1$  in increments and in an operational notation is:

$$\Delta \Phi_1(p) = C_1 [\omega_{0. \Sigma} \Delta i_{0. \Sigma}(p) + \omega_{0. c. \Sigma} \Delta i_{0. c. \Sigma}(p) - \omega_{0. \tau} \Delta i_{0. \tau}(p) - \omega_{0. c} \Delta i_{0. c}(p)], \quad (6.102)$$

where  $\omega_{0. \tau} \Delta i_{0. \tau}(p)$ ,  $\omega_{0. c} \Delta i_{0. c}(p)$ ,  $\omega_{0. \Sigma} \Delta i_{0. \Sigma}(p)$ ,  $\omega_{0. c. \Sigma} \Delta i_{0. c. \Sigma}(p)$  are EMU control winding mmf;  $C_1 = \frac{\partial \Phi_1}{\partial \sum F_1} \sum F_{10}$  is a proportionality factor between magnetic flux and mmf along the longitudinal axis of amplifier F.

The equation of the resultant magnetic flux along the longitudinal axis in increments and in an operational notation is

$$\Delta \Phi_2(p) = C_2 \omega_{\Sigma} \Delta i_{\Sigma}(p), \quad (6.103)$$

where  $\omega_{\Sigma} \Delta i_{\Sigma}$  is armature mmf along the transverse axis due to a current increment;

$C_2 = \frac{\partial \Phi_2}{\partial \sum F_2} \sum F_{20}$  is a proportionality factor between magnetic flux  $F_2$  and mmf along the transverse axis.

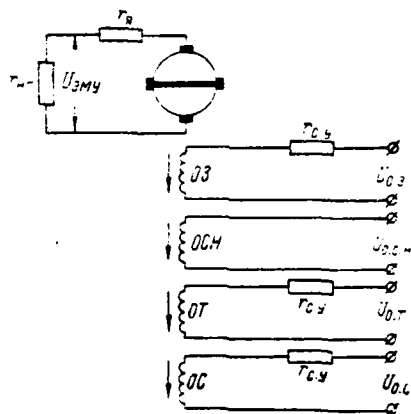


Figure 6.5. Automatic Control System "Amplidyne" Link.

The equations of control winding emf in increments and in an operational notation are:

$$\Delta U_{0. \Sigma}(p) - (r_{0. \Sigma} + r_{c. \Sigma}) \Delta i_{0. \Sigma}(p) - 2p_{\Sigma} \sigma_{0. \Sigma} \omega_{0. \Sigma} \Delta \Phi_1(p) = 0 \quad (6.104)$$

and, when  $U_{0.3} = \text{const}$

$$0 = (r_{0.3} + r_{c.y}) \Delta i_{0.3}(\rho) + 2\rho_{\text{ЭМУ}} \sigma_{0.3} \omega_{0.3} \rho \Delta \Phi_1(\rho); \quad (6.105)$$

$$\Delta U_{0.c.H}(\rho) - r_{0.c.H} \Delta i_{0.c.H}(\rho) - 2\rho_{\text{ЭМУ}} \sigma_{0.c.H} \omega_{0.c.H} \rho \Delta \Phi_1(\rho) = 0; \quad (6.106)$$

$$\Delta U_{0.T}(\rho) - (r_{0.T} + r_{c.y}) \Delta i_{0.T}(\rho) + 2\rho_{\text{ЭМУ}} \sigma_{0.T} \omega_{0.T} \rho \Delta \Phi_1(\rho) = 0; \quad (6.107)$$

$$\Delta U_{0.c}(\rho) - (r_{0.c} + r_{c.y}) \Delta i_{0.c}(\rho) + 2\rho_{\text{ЭМУ}} \sigma_{0.c} \omega_{0.c} \rho \Delta \Phi_1(\rho) = 0. \quad (6.108)$$

The equation for shorted circuit emf in increments and in an operational notation is:

$$C_{\text{ЭМУ}} \Delta \Phi_1(\rho) - r_{к3} \Delta i_{к3}(\rho) - 2\rho_{\text{ЭМУ}} \sigma_{к3} \omega_{к3} \rho \Delta \Phi_2(\rho) = 0, \quad (6.109)$$

where  $C_{\text{ЭМУ}} = \frac{P_{\text{ЭМУ}} N_n}{60\alpha}$  is a proportionality factor between emf and magnetic flux. /270

From equations (6.102)–(6.109), we get the following current values:

from (6.104)

$$\Delta i_{0.3}(\rho) = \frac{\Delta U_{0.3}(\rho) - 2\rho_{\text{ЭМУ}} \sigma_{0.3} \omega_{0.3} \rho \Delta \Phi_1(\rho)}{r_{0.3} + r_{c.y}}$$

and

$$\Delta i_{0.3}(\rho) = - \frac{2\rho_{\text{ЭМУ}} \sigma_{0.3} \omega_{0.3} \rho \Delta \Phi_1(\rho)}{r_{0.3} + r_{c.y}};$$

from (6.106)

$$\Delta i_{0.T}(\rho) = \frac{\Delta U_{0.T}(\rho) - 2\rho_{\text{ЭМУ}} \sigma_{0.T} \omega_{0.T} \rho \Delta \Phi_1(\rho)}{r_{0.c.H}}$$

from (6.107)

$$\Delta i_{0.T}(\rho) = \frac{\Delta U_{0.T}(\rho) + 2\rho_{\text{ЭМУ}} \sigma_{0.T} \omega_{0.T} \rho \Delta \Phi_1(\rho)}{r_{0.T} + r_{c.y}};$$

from (6.108)

$$\Delta i_{0.c}(\rho) = \frac{\Delta U_{\text{ЭМУ}}(\rho) + 2\rho_{\text{ЭМУ}} \sigma_{0.c} \omega_{0.c} \rho \Delta \Phi_1(\rho)}{r_{0.c} + r_{c.y}}$$

We will substitute the resultant equations in (6.102) and, after conversions, we will find

$$[(T_{0.3} + T_{0.c.H} - T_{0.T} + T_{0.c}) \rho + 1] \Delta \Phi_1(\rho) = k_{0.3} \Delta U_{0.3}(\rho) + k_{0.c.H} \Delta U_{0.c.H}(\rho) - k_{0.T} \Delta U_{0.T}(\rho) - k_{0.c} \Delta U_{0.c}(\rho), \quad (6.110)$$

where

$$T_{0.3} = \frac{2\rho_{\text{ЭМУ}} \sigma_{0.3} \omega_{0.3}^2 C_1'}{r_{0.3} + r_{c.y}} - \text{voltage master winding time constant};$$

$$T_{0.c.H} = \frac{2\rho_{\text{ЭМУ}} \sigma_{0.c.H} \omega_{0.c.H}^2 C_1'}{r_{0.c.H}} - \text{control winding time constant};$$

$$T_{0.T} = \frac{2\rho_{\text{ЭМУ}} \sigma_{0.T} \omega_{0.T}^2 C_1'}{r_{0.T} + r_{c.y}} - \text{EMU current winding time constant};$$

$$\begin{aligned}
 T_{o.c} &= \frac{2p_{\Sigma} \omega_{o.c} \omega_{o.c}^2 C_1}{r_{o.c} + r_{c.y}} && \text{- stabilizing winding time constant} \\
 k_{o.s} &= \frac{\omega_{o.s} C_1}{r_{o.s} + r_{c.y}} \\
 k_{o.c.H} &= \frac{\omega_{o.c.H} C_1}{r_{o.c.H}} \\
 k_{o.T} &= \frac{\omega_{o.T} C_1}{r_{o.T} + r_{c.y}} \\
 k_{o.c} &= \frac{\omega_{o.c} C_1}{r_{o.c} + r_{c.y}}
 \end{aligned}$$

- amplifier first-stage voltage gain from the corresponding control windings;

$T_{\Sigma \Sigma \Sigma} = T_{o.s} + T_{o.c.H} + T_{o.T} + T_{o.c}$  - amplifier field circuit overall time constant,

then

$$(T_{\Sigma \Sigma \Sigma} p + 1) \Delta \Phi_1(p) = k_{o.s} \Delta U_{o.s}(p) + k_{o.c.H} \Delta U_{o.c.H}(p) - k_{o.T} \Delta U_{o.T}(p) - k_{o.c} \Delta U_{o.c}(p) \quad (6.111)$$

and, when  $\Delta U_{o.s}(p) = 0$

$$(T_{\Sigma \Sigma \Sigma} p + 1) \Delta \Phi_1(p) = k_{o.c.H} \Delta U_{o.c.H}(p) - k_{o.T} \Delta U_{o.T}(p) - k_{o.c} \Delta U_{o.c}(p). \quad (6.112)$$

From (6.109) we have

$$\Delta i_{k3}(p) = \frac{C_{\Sigma \Sigma \Sigma} \Delta \Phi_1(p) - 2p_{\Sigma} \sigma_H \omega_H^2 \Delta \Phi_2(p)}{r_{k3}}$$

and, having substituted in (6.103), we will find

$$\Delta \Phi_2(p) = \frac{C_2 C_{\Sigma \Sigma \Sigma} \omega_H \Delta \Phi_1(p)}{r_{k3}} - \frac{2p_{\Sigma} C_2 \sigma_H \omega_H^2 p \Delta \Phi_1(p)}{r_{k3}}$$

or

$$(T_{k3} p + 1) \Delta \Phi_2(p) = k_2 \Delta \Phi_1(p) \quad (6.113)$$

and

$$\Delta U_{\Sigma \Sigma \Sigma}(p) = k_3 \Delta \Phi_2(p), \quad (6.114)$$

where  $T_{k3} = \frac{2p_{\Sigma} C_2 \sigma_H \omega_H^2}{r_{k3}} = \frac{L_{k3}}{r_{k3}}$  is amplifier shorted circuit time constant;

$k_2 = \frac{C_2 C_{\Sigma \Sigma \Sigma} \omega_H}{r_{k3}}$  is amplifier second-stage voltage gain.

In this case, for simplicity in compilation of the amplifier equation, we are not considering armature reaction along the transverse axis caused by load current, assuming full compensation of armature reaction along the amplifier's longitudinal axis:

$$r_{o.T} \gg r_k; r_H \gg r_H + r_{d.H} + \frac{r_k r_{o.T}}{r_k + r_{o.T}}$$

Solving (6.111)–(6.114) jointly, we will find for  $\Delta U_{\Sigma \Sigma \Sigma}(p)$

$$\Delta U_{\Sigma \Sigma \Sigma}(p) = \frac{k_{o.c.H} \Delta U_{o.c.H}(p) - k_{o.T} \Delta U_{o.T}(p) - k_{o.c} \Delta U_{o.c}(p)}{(T_{k3} p + 1)(T_{\Sigma \Sigma \Sigma} p + 1)} \quad (6.115)$$

where

$$k_{o.c.H} = k_{o.c.H} k_2; k_{o.T} = k_{o.T} k_2; k_{o.c} = k_{o.c} k_2$$

Next, we assume that a change in the control circuit occurs only in amplifier control current winding OT. Then, the equation's final form will be

$$\Delta U_{\Sigma \text{ЭМВ}}(\rho) = \frac{-k_{\text{о.т}} \Delta U_{\text{о.т}}(\rho)}{(T_{\text{ЭМВ}} \rho + 1)(T_{\Sigma \text{ЭМВ}} \rho + 1)}. \quad (6.116)$$

Equation of motion of the "amplidyne stabilizing winding bridge circuit" link (Figure 6.6). The bridge equilibrium condition is /272

$$\frac{R_1}{R_1 + R_4} = \frac{R_2}{R_2 + R_3}.$$

We obtain an inference of this link's equation

$$\begin{aligned} U_{\text{ЭМВ}} &= U_1 - U_2 = \frac{R_3}{R_2 + R_3} U_{\text{BX}} - \frac{R_4 - L\rho}{R_1 + R_4 + L\rho} U_{\text{BX}} = \\ &= \left( \frac{R_3}{R_2 + R_3} - \frac{R_4}{R_4 + R_1} \cdot \frac{1 - T'\rho}{1 - T\rho} \right) U_{\text{BX}}, \end{aligned}$$

where  $T' = \frac{L}{R_4}$  is a winding RO time constant;  $T = \frac{L}{R_1 + R_4}$  is a winding RO circuit time constant.

Next

$$U_{\text{ЭМВ}} = \frac{R_3}{R_2 + R_3} \left[ \frac{1 - T\rho - \frac{R_2 + R_3}{R_1 + R_4} \frac{R_4}{R_3} (1 - T'\rho)}{T\rho + 1} \right] U_{\text{BX}}$$

or

$$\begin{aligned} U_{\text{ЭМВ}} &= \frac{R_3}{R_2 + R_3} \left[ 1 - \frac{R_2 + R_3}{R_1 + R_4} \frac{R_4}{R_3} + \left( T - \frac{R_2 + R_3}{R_2} T \right) \rho \right] U_{\text{BX}} = \\ &= \frac{R_3}{R_2 + R_3} \left[ \frac{1 - \frac{R_2 + R_3}{R_1 + R_4} \frac{R_4}{R_3} - \frac{R_2}{R_3} T\rho}{T\rho + 1} \right] U_{\text{BX}}, \end{aligned}$$

if  $\frac{R_3}{R_2 + R_3} = \frac{R_4}{R_1 + R_4}$ , then, finally

$$\Delta U_{\text{ЭМВ}}(\rho) = -\frac{\alpha_{\text{o.c.}} T_{\text{o.c.}} \rho}{1 + T_{\text{o.c.}} \rho} \Delta U_{\text{BX}}(\rho) \quad (6.117)$$

where  $\alpha_{\text{o.c.}} = \frac{\bar{R}_2}{R_2 + R_3}$ ;  $T_{\text{o.c.}} = T$ .

Equations of motion of the "three-stage longitudinal field amplidyne" link.

A schematic of a circuit for a GEU with an amplifier with main circuit current and diesel rotational speed feedbacks is shown in Figure 6.7. The following assumptions are made in the calculation: the amplifier is compensated fully; dispersal fluxes changed with the same sign as do effective fluxes; there is no residual magnetization; commutation along all cascades is rectilinear; comparison source voltage fluctuations and eddy fluxes are not considered; amplifier rotational speed is a constant.

The equation for mmf along the control axis in the first stage of amplification has the form

$$\alpha \Delta\Phi_1 = 2\omega_{0,y} \Delta i_{0,y} - 2\omega_{0,r} \Delta i_{0,r} - 2\omega_{0,c,c} \Delta i_{0,c,c} - 2\omega_{0,c} \Delta i_{0,c}, \quad (6.118)$$

where  $\alpha$  is a proportionality factor between mmf and magnetic flux;  $\Delta\Phi_1$  is /273 the increments of magnetic flux along the control axis (along the axis of poles 1-3);  $\omega_{0,y}$  is the number of control winding turns per pole;  $\Delta i_{0,y}$  increments of current in the OU.

The emf equation for the winding OU circuit (first loop):

$$\Delta i_{0,y} r_{0,y} - 2p' \sigma \omega_{0,y} \frac{d \Delta\Phi_1}{dt} = 0,$$

from which

$$-\Delta i_{0,y} = \frac{2p' \sigma \omega_{0,y}}{r_{0,y}} p \Delta\Phi_1. \quad (6.119)$$

The transformer primary winding emf equation for the second loop's winding OS circuit is:

$$C_1 \Delta\Phi_3 - \Delta i_{r1} r_{r1} - \sigma_r \omega_{r1} \frac{d \Delta\Phi_r}{dt} = 0, \quad (6.120)$$

where  $C_1$  is a proportionality factor between emf and amplifier flux for load characteristic ( $C' = C_r n$ );  $\Delta\Phi_3$  is an increment of amplifier field basic flux;  $\Delta i_{r1}$  is an increment of current in the transformer primary winding;  $r_{r1}$  is the transformer primary winding circuit resistance;  $\omega_{r1}$  is the number of transformer primary winding turns;  $\sigma_r$  is a transformer magnetic flux dispersal factor;  $\Delta\Phi_r$  is the increment of transformer total flux.

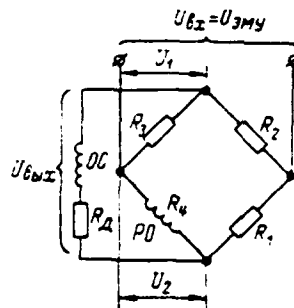


Figure 6.6. "EMU Stabilizing Winding Bridge Circuit" Link.

The emf equation for the transformer's secondary winding is:

$$\sigma_r \omega_{r2} \frac{d \Delta\Phi_r}{dt} - \Delta i_{0,c,c} r_{0,c,c} + \sigma 2p' \omega_{0,c} \frac{d \Delta\Phi_1}{dt} = 0, \quad (6.121)$$

where  $\omega_{r2}$  is the number of transformer secondary winding turns;  $2p'$  is the /274 number of amplifier first cascade input poles.



The fourth loop's winding OSS circuit emf equation is:

$$\Delta U_{\tau\tau} - \Delta i_{o.c.c} r_{o.c.c} + \sigma 2p' \omega_{o.c.c} \frac{d \Delta \Phi_1}{dt} = 0,$$

from which

$$\Delta i_{o.c.c} = \frac{\Delta U_{\tau\tau}}{r_{o.c.c}} + \frac{\sigma 2p' \omega_{o.c.c}}{r_{o.c.c}} \rho \Delta \Phi_1, \quad (6.126)$$

where  $\Delta U_{\tau\tau} = C_{e\tau\tau} \Phi_{\tau\tau} \Delta n_{\tau\tau}$  is an increment of tachogenerator voltage;  $C_{e\tau\tau}$  is a tachogenerator design factor;  $\Delta n_{\tau\tau}$  is an increment of tachogenerator rotational speed;  $\Phi_{\tau\tau}$  tachogenerator field flux.

Substituting the magnitude of the current increments in the windings /275 obtained from equations (6.119), (6.124), (6.125), and (6.126) in (6.118), we will find

$$\begin{aligned} \Delta \Phi_1 = & - \frac{2\sigma 2p' \omega_{o.y}^2}{a r_{o.y}} \rho \Delta \Phi_1 - \frac{2\omega_{o.c} k_{\tau}}{a r_{o.c}} \cdot \frac{T_{\tau\tau} \rho}{1 - T_{\tau\tau} \rho} C' \Delta \Phi_3 - \\ & - \frac{2\omega_{o.c} \alpha}{a 2\omega_{o.c}} \cdot \frac{T_{o.c} (1 - T_{\tau\tau} \rho)}{1 - T_{\tau\tau} \rho} \rho \Delta \Phi_1 - \frac{2\omega_{o.\tau} \Delta U_{\text{III}}}{a r_{o.\tau}} - \\ & - \frac{2\sigma 2p' \omega_{o.\tau}^2}{a r_{o.\tau}} \rho \Delta \Phi_1 - \frac{2\omega_{o.c.c} \Delta U_{\tau\tau}}{a r_{o.c.c}} - \frac{2\sigma 2p' \omega_{o.c.c}^2}{a r_{o.c.c}} \rho \Delta \Phi_1. \end{aligned}$$

As a result of conversions and introduction of designations, we get the equation for the first stage of EMU amplification

$$\begin{aligned} \Delta \Phi_1 \left[ 1 + T_s \rho + \frac{T_{o.c} (1 - T_{\tau\tau} \rho)}{(1 - T_{\tau\tau} \rho)} \rho \right] = & - \frac{k_{o.\tau} \Delta U_{\text{III}}}{C} - \\ & + \frac{k_{o.c.c} \Delta U_{\tau\tau}}{C} - \frac{k_{o.c} C_1 k_{\tau}}{C} \frac{T_{\tau\tau} \rho}{(1 - T_{\tau\tau} \rho)} \Delta \Phi_3, \end{aligned} \quad (6.127)$$

where  $T_s = T_{o.y} + T_{o.\tau} + T_{o.c.c}$  is control winding overall time constant;

$k_{o.c} = \frac{2\omega_{o.c} C}{a r_{o.c}}$  is winding OS voltage gain;  $k_{o.\tau} = \frac{2\omega_{o.\tau} C}{a r_{o.\tau}}$  winding OT voltage gain;  
 $k_{o.c.c} = \frac{2\omega_{o.c.c} C}{a r_{o.c.c}}$  is winding OSS voltage gain;  $C = C_e n 10^{-8} = \frac{P}{a} \frac{1}{60} n$  is a proportionality factor between emf and amplifier flux ( $C \approx C'$ ).

The equation for the second stage of EMU amplification has the form

$$\Delta \Phi_2 (1 + T_1 \rho) = k_1 \Delta \Phi_1, \quad (6.128)$$

where  $k_1 = \frac{2\omega_a C}{a r_{1-3}}$  is second stage direction gain;  $\omega_a$  is the number of armature winding turns per pole;  $r_{1-3}$  is EMU brush 1-3 circuit impedance;

$T_1 = \frac{2 \cdot 2p' \omega_a^2}{a r_{1-3}}$  is a brush 1-3 circuit time constant;  $\Delta \Phi_2$  is the increment of magnetic flux along the axis of poles 2-4.

The self-excitation winding circuit emf equation is:

$$C \Delta \Phi_2 - 2p' \sigma \omega_{en} \frac{d \Delta \Phi_2}{dt} - \Delta i_{e3} (r_{13} + r_a) - \Delta i_{e4} r_a = 0. \quad (6.129)$$

where  $2p'$  is the number of third-stage amplification poles;  $\omega_{cb}$  is the number of self-excitation winding turns per pole;  $r_{cb}$  is self-excitation winding circuit resistance;  $r'_a$  is amplifier armature circuit impedance to load current;  $\Delta i_{cb}$  is the increment of current in the winding SVO circuit;  $\Delta i_{b,r}$  is the increment of current in the generator field winding circuit.

The amplifier load circuit (generator field winding circuit) emf equation is:

$$C \Delta \Phi_3 - (r'_a - r_{o.b.r}) \Delta i_{b,r} - \Delta i_{cb} r'_a - L_{o.b.r} \frac{d \Delta i_{b,r}}{dt} = 0, \quad (6.130)$$

where  $r_{o.b.r}$  is generator field winding resistance;  $L_{o.b.r}$  is generator field winding inductivity (we disregard amplifier armature winding inductivity).

The amplifier field basic system (output cascade) emf equation is:

$$\alpha \Delta \Phi_3 = 2\omega_{cb} \Delta i_{cb} + 2\omega_B \Delta i_{2-4}, \quad (6.131)$$

where  $\omega_B$  is the number of amplifying winding V (not shown in the figure) turns per pole;  $\Delta i_{2-4}$  is the increment of current in the brush 2—4 circuit:

The brush 2—4 circuit emf equation is:

$$C \Delta \Phi_2 - \Delta i_{2-4} r_{2-4} - \sigma 2p' \omega_B \frac{d \Delta \Phi_2}{dt} = 0,$$

from which

$$\Delta i_{2-4} = \frac{C \Delta \Phi_2}{r_{2-4}} - \frac{\sigma 2p' \omega_B}{r_{2-4}} \rho \Delta \Phi_3. \quad (6.132)$$

We substitute the magnitude of flux increment  $\Delta \Phi_1$  from (6.127) in (6.128) and solve for  $\Delta \Phi_2$ :

$$\begin{aligned} \Delta \Phi_2 = & \frac{k_1}{(1 - T_7 \rho)} \left[ \frac{-k_{o,\tau}(1 - T_7 \rho)}{C[(1 - T_7 \rho) - T_3 \rho(1 - T_7 \rho) + T_{o,c\rho}(1 - T_{11} \rho)]} \Delta U_{\tau} + \right. \\ & \left. + \frac{k_{o,c,c}(1 - T_7 \rho)}{C[(1 - T_7 \rho) + T_3 \rho(1 - T_7 \rho) - T_{o,c\rho}(1 - T_{11} \rho)]} \Delta U_{\pi} - \right. \\ & \left. - \frac{k_{o,c} k_{\tau} T_{11} \rho}{[(1 - T_7 \rho) - T_3 \rho(1 - T_7 \rho) + T_{o,c\rho}(1 - T_{11} \rho)]} \Delta \Phi_3 \right]. \quad (6.133) \end{aligned}$$

From (6.129) we determine  $\Delta i_{cb}$ :

$$\Delta i_{cb} = \frac{C \Delta \Phi_3}{r_{cb} - r'_a} - \frac{\sigma 2p' \omega_{cb}}{r_{cb} - r'_a} \rho \Delta \Phi_3 - \frac{r'_a}{r_{cb} - r'_a} \Delta i_{b,r}. \quad (6.134)$$

Solving equations (6.130)—(6.134) jointly for  $\Delta i_{b,r}$ , we get

$$\begin{aligned} \Delta i_{b,r} = & \frac{k_{o,\tau} k_1 k_B (1 - T_7 \rho) (1 - T'_{cb} \rho)}{(r'_a - r_{o.b.r}) N(\rho) [(1 - T_{o,b,r} \rho) (1 - k_{cb} - T_3 \rho) - k'_{cb} (1 - T'_{cb} \rho)] + (r'_a - r_{o.b.r}) (1 + T_{o,b,r} \rho) k_3 T_{11} \rho} \Delta U_{\omega} - \\ & + \frac{k_{o,c} k_1 k_B (1 - T_7 \rho) (1 - T'_{cb} \rho) \Delta U_{\pi}}{(r'_a - r_{o.b.r}) N(\rho) [(1 + T_{o,b,r} \rho) (1 - k_{cb} - T_3 \rho) - k'_{cb} (1 - T'_{cb} \rho)] + (r'_a - r_{o.b,r} \rho) (1 + T_{o,b,r} \rho) k_3 T_{11} \rho} \quad (6.135) \end{aligned}$$

where  $k_B = \frac{2\omega_B C}{\alpha r_{2-4}}$  is amplifier winding V voltage gain:

$$k_{CB} = k_{CB} \frac{r_a'}{r_a' - r_{o.B.R.}};$$

$k_{CB} = \frac{2\omega_{CB} C}{\alpha (r_{CB} - r_a')}$  is amplifier self-excitation winding voltage gain;

$$T_{CB} = T_{CB} \frac{r_a'}{(r_{CB} - r_a') k_{CB}};$$

$T_{CB} = \frac{2\sigma 2p \omega_{CB}^2}{\alpha (r_a' - r_{CB})}$  is a self-excitation winding circuit time constant;  $T_B = \frac{2\sigma 2p \omega_B^2}{\alpha r_{2-4}}$  is an amplifier amplifying winding V time constant;  $T_3 = T_B - T_{CB}$  is the

overall time constant;  $k_3 = \frac{k_o \cdot k_r \cdot k_1 \cdot k_B C'}{C}$  is equivalent voltage gain;  $T_{o.B.R.} = \frac{L}{r_a' - r_{o.B.R.}}$  is a generator field winding time constant;

$$N(p) = [(1 - T_3 p)(1 - T_2 p) - T_{o.B.R.} p (1 - T_1 p)] (1 - T_1 p) \quad (6.136)$$

This approximation  $\frac{r_{CB}}{r_{CB} - r_a'} \approx 1$  was assumed when solving equations

(6.130)–(6.134) since  $r_{CB} \approx r_a'$ ;  $\frac{(r_a')^2}{(r_{CB} - r_a')(r_{o.B.R.} - r_a')} \approx 0$  since  $(r_a')^2 \ll r_{CB} \cdot r_{o.B.R.}$ .

Equation of motion of the "generator--three-stage longitudinal field amplidyne field winding" link. The generator field system mmf equation is:

$$a_r \Delta \Phi_r = 2\omega_{o.B.R.} \Delta i_{gr}, \quad (6.137)$$

where  $a_r$  is a proportionality factor between mmf and generator flux;  $\omega_{o.B.R.}$  is the number of generator field winding turns per pole;  $\Delta \Phi_r$  is the increment of generator field flux.

Substituting (6.135) in (6.137) and solving for  $\Delta \Phi_r$ , we get the equation of motion of the "generator field winding -- three-stage longitudinal field EMU with main circuit current, diesel rotational speed, and vanishing constraint feedbacks with amplifier output to the control winding" link

$$\Delta \Phi_r = Q(p) \Delta i_a + R(p) \Delta U_{gr} \quad (6.138)$$

where

$$Q(p) = \frac{k_3 r_{gr}}{C_{gr}} \cdot \frac{(1 - T_{CB} p)(1 - T_2 p)}{N_1(p)}; \quad (6.139)$$

/278

$$R(p) = \frac{k_4}{C_{gr}} \frac{(1 + T_{CB} p)(1 + T_2 p)}{N_1(p)}; \quad (6.140)$$

$$\left. \begin{aligned} k_3 &= k_{o.r} k_1 k_B k_r; \\ k_4 &= k_{o.c.c} k_1 k_B k_r; \end{aligned} \right\} \quad (6.141)$$

$$C_{gr} = C_{gr} n_r = \frac{p}{\alpha} \frac{N}{60} n_r; \quad (6.142)$$

$k_r = \frac{2\omega_{o. s. r} C_{er}}{\alpha_r (r'_a - r_{o. s. r})}$  is generator voltage gain;

$$N_1(p) = N(p) [(1 + T_{o. s. r} p)(1 - k_{cs} + T_3 p) + k_{cs} (1 + T'_{cs} p)] + k_3 T_{r1} p (1 + T_{o. s. r} p). \quad (6.143)$$

Equation of motion of the "magnetic amplifier" link. The fundamentals of the layout and operating principles of magnetic amplifiers, and well as the special features of different circuits, were examine in detail in [55] and other works.

We will examine relationships characterizing a magnetic amplifier (MU) as a link in an automated control system.

Mathematical description of transient processes in MU encounters particular difficulties due to the presence of direct and alternating currents coupled inductively with iron. Therefore, one resorts to a series of assumptions and simplifications. So, in particular, if one disregards the phenomena of hysteresis and eddy currents, as well as the sluggishness of ac circuits, this one should consider that MU sluggishness is determined by processes in the control winding.

The following differential equation is justified for a control circuit:

$$U_y = i_y r_y + L_{y. p} \frac{di_y}{dt} + w_y \frac{d\Phi_0}{dt}, \quad (6.144)$$

where  $L_{y. p}$  is control winding inductivity caused by dispersal currents;  $r_y, w_y$  is resistance and the number of control winding turns;  $\Phi_0$  is the average magnitude of the magnetic flux in the core.

Using the formula for an ideal magnetic amplifier [55]

$$I_{\infty cp} w_{\infty cp} = i_y w_y \quad (6.145)$$

and, having replaced  $i_y$  in (6.144) with new variable  $I_{\infty cp}$ , we get

$$U_y = \frac{w_{\infty cp} r_y}{w_y} I_{\infty cp} + \frac{w_{\infty cp} L_{y. p}}{w_y} \frac{dI_{\infty cp}}{dt} + w_y \frac{d\Phi_0}{dt} \frac{dI_{\infty cp}}{dt}. \quad (6.146)$$

Having in mind that  $U_{\infty} = I_{\infty r_n} - e_s$  and  $U_{\infty}$  of the network does not depend on  $I_{\infty}$ , we get

$$r_n = \frac{de_s}{dI_{\infty}}$$

Converting to average values, we have

$$\begin{aligned} r_{11} &= \frac{dE_{\infty \text{ cp}}}{dl_{\infty \text{ cp}}}; & /279 \\ E_{\infty \text{ cp}} &= 4f\omega_{\infty}\Phi_0; \\ \frac{d\Phi_0}{dl_{\infty \text{ cp}}} &= \frac{r_{11}}{4f\omega_{\infty}}. \end{aligned} \quad (6.147)$$

Having solved (6.146) and (6.148) jointly, we will find

$$U_y = \frac{\omega_{\infty} r_y}{\omega_y} I_{\infty \text{ cp}} + \left( \frac{\omega_{\infty} L_{y.p}}{\omega_y} + \frac{\omega_y r_{11}}{4f\omega_{\infty}} \right) \frac{dl_{\infty \text{ cp}}}{dt}.$$

In operational form and in increments, the equation will take the form

$$\Delta U_y(\rho) = \left[ \frac{\omega_{\infty} r_y}{\omega_y} + \left( \frac{\omega_{\infty} L_{y.p}}{\omega_y} + \frac{\omega_y r_{11}}{4f\omega_{\infty}} \right) \rho \right] \Delta I_{\infty \text{ cp}}(\rho), \quad (6.148)$$

from which

$$\Delta I_{\infty \text{ cp}}(\rho) = \frac{\Delta U_y(\rho) \omega_y}{r_y \omega_{\infty}} \frac{1}{1 + \rho T_{MY}} = \frac{\Delta I_{\infty \text{ ycr}}(\rho)}{1 + \rho T_{MY}}, \quad (6.149)$$

where  $T_{MY} = \frac{L_{y.p}}{r_y} + \frac{r_{11} \omega_y^2}{4f r_y \omega_{\infty}^2}$  is an amplifier time constant;  $I_{\infty \text{ ycr}} = \frac{U_y}{r_y} \frac{\omega_y}{\omega_{\infty}}$  is established load current.

Disregarding the first term in the expression for the time constant and in view of its minor magnitude (due to the insignificant amount of dispersal flux) compared to the second, we get

$$T_{MY} = \frac{r_{11} \omega_y^2}{4f r_y \omega_{\infty}^2}. \quad (6.150)$$

It is apparent from the last expression that time constant  $T_{MY}$  is inversely proportional to the ac frequency  $f$ . In this connection, magnetic circuits in slightly-sluggish MU usually are fed by alternating current of a higher frequency ( $f = 500 \text{ Hz}$ ).

Thus, MU in dynamic processes given known assumptions are looked upon as a delayed-action link of the first order. MU sluggishness is determined mainly by the time lag for a current change in the control winding from a voltage change supplied to the amplifier input.

Magnetic amplifier schematics are depicted in Figure 6.8: without feedback and with external and intrinsic feedbacks.

Examining MU without feedback (Figure 6.8a) with a resistive (and, in many cases, a resistive-inductive) load and series-connected ac windings  $w_n$ , it is easy to establish that load current  $i_{nr}$  lags in time behind control current  $i_y$ , since relationship  $i_n w_n = w_y i_y$  is justified for an unsaturated core at any moment in time.

Examining MU with  $n$  control windings and assuming that amplifier idling voltage equals zero or looking upon  $U_{nr}$  as an increment of voltage in a load, the transient process equation for the linear portion of an MU characteristic can be written in the form

$$U_{nr}(1 + pT_{MV}) = \sum_{i=1}^n k_{U_i} U_{y_i}, \quad (6.151)$$

and, in increments and in operational form

$$\Delta U_{nr}(p)(1 + pT_{MV}) = \sum_{i=1}^n k_{U_i} \Delta U_{y_i}(p), \quad (6.152)$$

where  $T_{MV} = \sum_{i=1}^n T_i$  is an MU time constant;  $T_i$  is a time constant of the  $j$ -th control winding or of a winding coupled with it inductively;  $k_{U_i}$ ,  $U_{y_i}$  are the voltage gain and the signal voltage of the  $j$ -th control winding;  $U_{nr}$  is the load voltage.

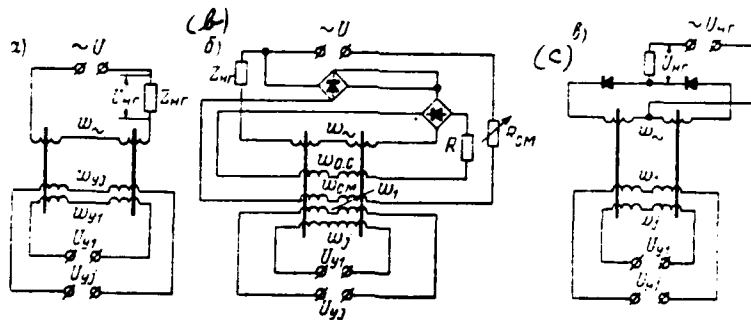


Figure 6.8. Magnetic Amplifier Circuits: a—Without feedback; b—With external feedback; c—With intrinsic feedback.

Expression (6.150) is used to make an approximate determination of the time constant of the  $j$ -th winding of an MU with external feedback (Figure 6.8b).

For amplifiers with intrinsic feedback (Figure 6.8c)  $T_i = \frac{kL_1 \omega y_1}{2\eta f \omega}$ ,

where  $\eta = \frac{R_L}{R}$  load circuit efficiency;  $R_{nr}$  is load resistance;  $R$  is the entire circuit's resistance;  $f$  is the ac frequency of the operating winding;  $w$  is the number of operating winding turns.

Equations of motion of the "synchros and synchro resolver" link. Alternating current induction electrical machinery is referred to as synchros. Synchros are used as measurement elements in automatic control systems. In design, /281 they are categorized as contact and non-contact. In turn, contact synchros are subdivided into homogeneous (or single-phase) and differential (or three-phase) depending on the nature of the windings located on the stator and rotor. For the former here, one of the windings is primary and is single-phase (located either on the stator or on the rotor). Another winding (secondary) is three-phase. In the latter type of synchro, both windings, stator and rotor, are three-phase.

Single-phase synchros are the most common. They are used for remote transmission of the turning angle (display mode), as well as for measurement of error angles (transformer mode). Non-contact synchros, which have a single-phase (primary) winding and a three-phase (secondary) winding on the stator and a rotor built in the form of a specially-designed cylindrical magnetic circuit, have an identical purpose in automatic control systems and in servos.

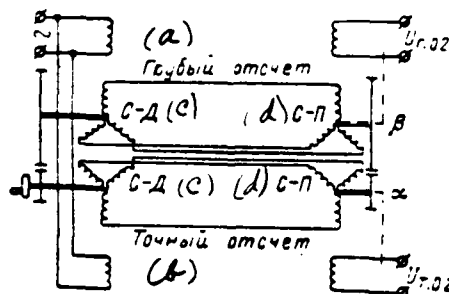


Figure 6.9. Schematic of a Two-axis Error Angle Measurement Circuit: master  $\alpha$  and slave  $\beta$ . a—Coarse; b—Fine.

The principle for use of two synchros to measure the error angle of two axes is explained by the following circuit (Figure 6.9).

If rotors S--D [synchro-transmitter] and S--P [synchro-receiver] are mismatched, then voltage proportional to the error angle will be induced in the S--P homogeneous winding. This is called the transformer mode. We introduce the following assumptions for inference of the static relationship between  $U_2$  and the error angle of axis  $\theta_1 = (\alpha - \beta)$ :

rotor and stator windings are separate and distribution of induction in the gap between machinery bears a sinusoidal character;

we disregard losses in rotor and stator steel, as well as saturation of the magnetic system;

we disregard rotor S--D magnetic flux;

we disregard rotor rotation emf.

The last assumption is justified when rotor S--D rotational speeds are low.

The S--D field winding magnetic flux induces in its rotor's phase windings emf, which can be written:

$$\left. \begin{aligned} E_1 &= E_{\text{max}} \cos \alpha; \\ E_2 &= E_{\text{max}} \cos(\alpha + 120^\circ); \\ E_3 &= E_{\text{max}} \cos(\alpha - 120^\circ). \end{aligned} \right\} \quad (6.153)$$

The following ratios are justified for phase currents:

$$I_1 = \frac{E_1}{2Z}; \quad I_2 = \frac{E_2}{2Z}; \quad I_3 = \frac{E_3}{2Z},$$

where  $Z$  is rotor S--D and S--P (each in isolation) winding phase resistance. These currents create variable magnetic fluxes which, in a synchro-receiver single-phase stator winding, will induce emf equalling

$$\left. \begin{aligned} E'_1 &= AI_1 \cos \beta; \\ E'_2 &= AI_2 \cos(\beta + 120^\circ); \\ E'_3 &= AI_3 \cos(\beta - 120^\circ), \end{aligned} \right\} \quad (6.154)$$

where  $A$  is a proportionality factor.

Total emf in a stator S--P single-phase winding is determined by equation

$$\begin{aligned} U_2 &= E'_1 + E'_2 + E'_3 = A [I_1 \cos \beta + I_2 \cos(\beta + 120^\circ) + \\ &+ I_3 \cos(\beta - 120^\circ)] = \frac{E_{\text{max}}}{2Z} A [\cos \alpha \cos \beta + \cos(\alpha + 120^\circ) \times \\ &\times \cos(\beta + 120^\circ) + \cos(\alpha - 120^\circ) \cos(\beta - 120^\circ)] = \frac{3}{4} \frac{AE_{\text{max}}}{Z} \times \end{aligned} \quad (6.155).$$

$$(\cos \alpha \cos \beta + \sin \alpha \sin \beta) = \frac{3}{4} \frac{AE_{\text{max}}}{Z} \cos(\alpha - \beta) = U_{\text{max}} \cos(\alpha - \beta).$$

Consequently, the voltage at the terminals of a synchro-receiver single-phase winding depends on rotor error angle. If rotor S—P is braked, then it is possible to judge the error angle from the amount of voltage. Here,  $U_2$  will be maximum when  $\alpha - \beta = 0$ . For  $\alpha - \beta = 0$  and  $U_2$  to equal zero, they create an initial  $90^\circ$  shift between rotor axes and an error angle of  $\theta = 90 + \alpha - \beta$ . In this case,

$$U_2 = U_{\text{max}} \cos(\theta - 90) = U_{\text{max}} \sin \theta. \quad (6.156)$$

This relationship within the boundaries of small angles  $\theta$  (up to  $15^\circ$  with an accuracy of up to 1%) is linear. Thus, this formula is justified for small angles

$$U_2 = k\theta. \quad (6.157)$$

Synchros in the transformer mode essentially are inertia free, i. e., relationship (6.157) is justified in transient processes. The principle of operation of the synchro pair in the transformer mode when non-contact synchros are used does not differ from that examined above. However, in this case, the rotor turn does not change the mutual position of the rotor and stator windings, changing only the direction of the field magnetic flux relative to the three- /283 phase winding due to the change in the direction of the axis of the greatest permeance.

When synchros are used for remote transmission of an angle (display mode), the electrical schematic for their connection has the formed depicted in Figure 6.10. The synchro-transmitter is coupled with master axis a, while the synchro-receiver is coupled to slave b. The field windings of both synchros are connected to the ac network. Single-phase alternating current feeding the field winding creates a pulsating magnetic flux in each synchro's magnetic system. Electromotive forces are induced in the three-phase windings due to the influence of this flux.

The magnitude of these emf in each phase depends on the position of the phase in space. If synchro rotors are matched, then identical emf are induced in the analogous phase windings. Since these emf are opposed, there will be no currents in the three-phase windings. If the synchro-transmitter and synchro-receiver rotors are mismatched, then currents which, interacting with

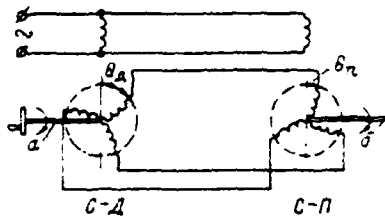


Fig. 6.10. Electrical schematic of connections when synchros are used for remote angle transmission (display mode)

the field winding magnetic fluxes, create torque, will flow in the three-phase windings. The latter strive to place the rotors in a matched position. Since the synchro-transmitter rotor is in a fixed position, then under the influence of electromagnetic moment, which is referred to as synchronizing, the synchro-receiver rotor will turn. Synchronizing torque for synchros essentially is proportional to the sine of the error angle:

$$m_{cx} = M_{\max} \sin \theta, \quad (6.158)$$

where  $m_{cx}$  is synchronizing torque;  $M_{\max}$  is maximum synchronizing torque;  $\theta = \theta_{c-d} - \theta_{c-p}$  is the error angle;  $\theta_{c-d}$  is synchro-transmitter rotor turning angle;  $\theta_{c-p}$  is synchro-receiver rotor turning angle.

Where  $\theta = 0$  and  $\theta = 180^\circ$   $m_{cx} = 0$ . However, when  $\theta = 0$ , deflection  $-\Delta\theta$  corresponds to positive synchronizing torque, while  $-\Delta\theta$  corresponds to negative synchronizing torque. In both cases, under the influence of these torques a deflected rotor strives to return to the starting (initial) position.

When  $\theta = 180^\circ$ , negative synchronizing torques correspond to deflection  $-\Delta\theta$ , while positive synchronizing torques correspond to deflection  $-\Delta\theta$ , i. e., deflections in both cases increase under the influence of these torques.

Synchro resolvers (VT) are single-phase induction machines similar in design to synchros. The rotor and stator are cylindrical and distributed single-phase windings are dropped in the slots. The total number of windings can reach four (two each on the rotor and stator). VT are used for measurement of angular deflections, angular errors, as well as sine-cosine mechanisms. A two-winding VT (Figure 6.11) provides a sinusoidal relationship between secondary winding emf and rotor turning angle  $E_2 = E_{2 \max}$  where  $Z_{\text{HT}} = \infty$ . When a load is present, this relationship is distorted considerably mainly due to the transverse component of the rotor flux. Distortions are decreased in three-winding sine-cosine synchro resolver (SKVT), a schematic for the connection of which is shown in Figure 6.12. Where  $Z_a = Z_b = \infty$

$$E_a = E_{a \max} \cos \alpha; \quad E_b = E_{b \max} \sin \alpha.$$

Connection of a load in this circuit as well introduces a distortion into the aforementioned relationship, but it is less than in a two-winding VT.

One circuit for a four-winding linear VT, which can provide a static relationship between input and output values close to linear (within boundaries up to 60-70%), is shown in Figure 6.13.

As can be seen from the circuit, the stator and rotor each have two single-phase windings. One stator winding  $w_1$  is a field winding and is connected to /285 the ac network. The other  $w_k$  is connected in series with load  $Z_{nr}$  and with the operating winding of rotor  $w_1$ .

Winding  $w_2$  is for compensation of the rotor's transverse field and closes at ballast resistance  $Z_6$ .

In this circuit, the voltage at load will change depending on rotor turning angle in accordance with the following law:

$$U_2 = \frac{K_1 \sin \alpha}{1 - K_2 \cos \alpha}, \quad (6.159)$$

where  $\alpha$  is rotor turning angle;  $K_1$  and  $K_2$  are factors depending on the VT parameter.

Relationship (6.159) is much closer to being linear than sinusoidal. So, when  $K_2 = 0.5$  with an accuracy of up to 1%, the relationship is linear within boundaries up to 60° of the rotor turn.

Equations of motion of the "two-phase induction motor" link. Two-phase induction motors are used in automatic control systems as slaves and in electromechanical compensators as elements. Two-phase induction motors with a squirrel-cage rotor in the form of a hollow thin-walled cylinder have found especially wide use. The motor's stator has two windings dropped in such a way that their magnetic axes for a two-pole machine are mutually perpendicular. Figure 6.14 presents a diagram of a two-phase induction motor. Motor field winding  $w_1$  is connected to a fixed voltage ac feed source. Control winding  $w_2$  usually is fed by voltage of the same frequency as that of the field voltage, but via control amplifier UU. Creation of a rotating magnetic field requires that both voltages shift in phase relative to each other about 90°. The shift is accomplished either in control amplifier UU or by connection to the capacitor

field winding circuit. Control signal  $U_y$  serves as the induction motor input value, while motor shaft turning angle  $\theta_2$  is the output value.

A system of equations describing the physical processes in a two-phase induction motor is nonlinear. However, considering the slight influence of rotor rotation emf on the amount of current in the field winding, especially in the area of operating rotational speed differing greatly from a synchronous motor, as well as the fact that the rotor circuit time constant is much less than the stator time constant, i. e.,  $T_{\text{rot}} \ll T_{\text{cr}}$ , this system can approximate a linear system of differential equations with variable factors. Given these simplifications, the constraint between input and output values is determined fully by the synchronous motor transfer function [10]:

$$W(p) = \frac{\theta_2(p)}{U_y(p)} = K \frac{a_1 p^2 - a_2 p + a_3}{[T_{a.s} p - 1] \left[ \left( p + \frac{1}{T_{\text{cr}}} \right)^2 + \omega^2 \right] p}, \quad (6.160)$$

where

$$K = \frac{1}{R} \frac{I_1 K_p T_p \omega \mu}{2\rho (1 - \omega^2 T_{\text{cr}}^2) + I_1^2 K_{\text{por}} T_{\text{por}} \mu};$$

$$a_1 = \cos \varphi + \frac{1}{\omega T_{\text{cr}}} \sin \varphi;$$

$$a_2 = \frac{2}{T_{\text{cr}}} \cos \varphi + \sin \varphi \left( \frac{1}{\omega T_{\text{cr}}} - \omega \right);$$

$$a_3 = 2\omega^2 \cos \varphi \left( 1 + \frac{1}{\omega^2 T_{\text{cr}}^2} \right);$$

$T_{a.s}$  is a motor electrical time constant;

$$T_{a.s} = \frac{2J(1 + \omega^2 T_{\text{cr}}^2)}{2\rho (1 - \omega^2 T_{\text{cr}}^2) + I_1^2 K_{\text{por}} \mu};$$

$\varphi$  is the phase shift among control field voltages;  $\omega$  is field angular rotational speed;  $T_{\text{cr}}$  is a stator winding electrical time constant;  $T_{\text{por}}$  is a rotor electrical time constant;  $R$  is control winding resistance;  $\rho$  is a viscous friction factor;  $\mu$  is an interinduction factor between stator and rotor circuits;  $K_{\text{por}} = \mu / Z_{\text{res}}$ ;

$Z_{\text{res}}$  is resultant rotor inductivity;  $I_1$  is field winding current.

Expression (6.160) considers both the electromechanical time constant and transient electrical processes in motor windings, the occurrence rate which is stipulated by the magnitude of time constant  $T_{\text{cr}}$ . It has been established through calculations and experiments that, when  $\varphi = 90^\circ$  and the frequency of rounding

control signal  $\omega \leq 300$  rads per second, the influence of  $T_{cr}$  can be disregarded. Then, it is possible for practical calculations to use the transfer function of a two-phase synchronous motor in the form

$$W_{a,x}(p) = \frac{\theta_x(p)}{U_y(p)} = \frac{K_R}{p(1 + T_{a,x}p)}, \quad (6.161)$$

where  $K_R$  is motor gain.

When a two-phase induction motor is used as a compensator in devices where motor sluggishness can be disregarded, a two-phase induction motor can be looked upon as an integrating link with a transfer function:

$$W_{a,x}(p) = \frac{K_R}{p}.$$

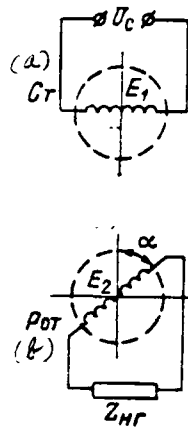


Figure 6.11. Two-Phase Synchro Resolver Diagrams. a—Stator; b—Rotor.

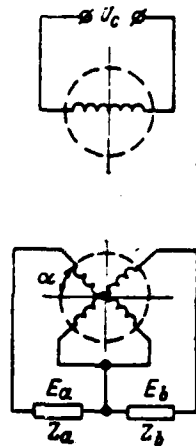


Figure 6.12 Schematic for Connection of Three-Winding Sine-Cosine Synchro Resolvers.

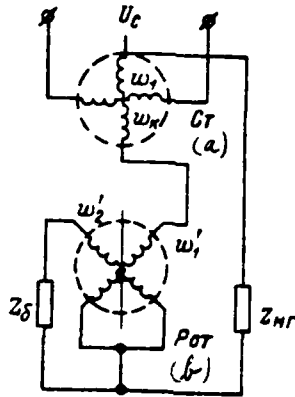


Figure 6.13. Four-Winding Linear Synchro Resolver Circuit.  
a—Stator; b—Rotor

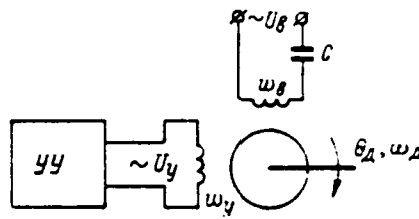


Figure 6.14. Two-Phase Induction Motor Circuit.

### § 6.3 Equations of Motion and Transfer Functions of Standard Direct Current GEU Systems

The methodology of using the standard link equations obtained in § 6.2 for analysis of the stability and evaluation of the quality of automated propellor electric drive is illustrated through examination of standard circuits.

GEU with longitudinal field amplidyne. The GEU circuit shown in Figure 6.15 does not have main propulsion motor rotational speed feedbacks and is closed based on main circuit current and power regulation. Main propulsion motor EMU and generator exciter master winding voltages for a given mode are considered constant and their increments equal zero.

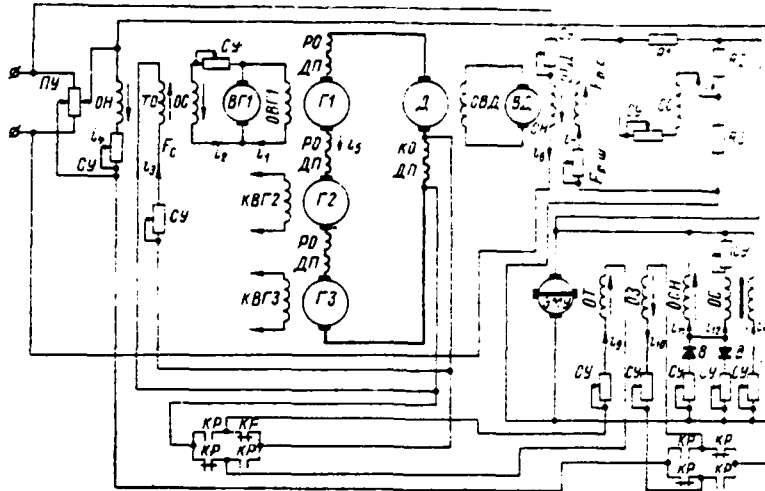


Figure 6.15. Schematic of a GEU with Electrical Machinery Automation.

GED rotational speed changes caused by a change in propellor moment of resistance automatically change motor electromagnetic torque, as well as GED current and magnetic flux.

Initial system of equations. Below we present the initial system of equations for basic GEU links (Figure 6.15) considering constant magnitudes of exciter VG1 master winding, EMU pilot exciter, and exciter VD field independent winding voltages:

equation of motion of the "generator exciter" link /288

$$(T_{\Sigma p} + 1)(T_{b.r.p} + 1)\Delta\bar{U}_{b.r.}(p) = (T_{b.r.p} + 1)[k_{c.b}\Delta\bar{U}_{b.r.}(p) - k_{o.t.r}\Delta\bar{i}_n(p)]; \quad (I)$$

equation of motion of the "main generator" link

$$(T_r p + 1)\Delta\bar{e}_r(p) = k_r\Delta\bar{U}_{b.r.}(p); \quad (II)$$

equation of motion of the "main propulsion motor" link, solved for  $\Delta\bar{i}_n$ , expressed in increments and in operational form is:

$$(T_{b.z.p} + 1)[(T_{\Sigma p} + 1)(T_{m.z.p} + 1) + k_1 k_4]\Delta\bar{i}_n(p) = k_r(T_{m.z.p} + 1) \times \\ \times (T_{b.z.p} + 1)\Delta\bar{e}_r(p) - [k_2 k_4 k_6 + k_3 k_6(T_{m.z.p} + 1)]\Delta\bar{U}_{b.z.}(p) + \\ + k_3 k_6(T_{b.z.p} + 1)\Delta\bar{k}(p); \quad (III)$$

equation of motion of the "main propulsion motor" link, solved for  $\Delta n_2$  is:

$$\begin{aligned} (T_{B.2}p + 1)(T_{A.2}p + 1)(T_{M.2}p + 1) + k_1k_4] \Delta \bar{n}_2(p) = k_1k_2(T_{B.2}p + 1) \times \\ \Delta \bar{e}_r(p) + [k_2k_3(T_{A.2}p + 1) - k_1k_3k_6] \Delta \bar{U}_{B.A}(p) - k_3 \times \\ \times (T_{B.2}p + 1)(T_{A.2}p + 1) \Delta \bar{k}(p); \end{aligned} \quad (IV)$$

equation of motion of the main propulsion motor exciter (two-winding which has the main winding connected to voltage  $U_{ном} = \text{const}$ , resulting in the second winding only participating in the control) is described from (6.100), but considering  $U_{ном} = \text{const}$  is:

$$(T_{\Sigma}p + 1)(T_{B.2}p + 1) \Delta U_{B.A}(p) = -\alpha_1 k_{o.r.a} (T_{B.B.2}p + 1) \Delta U_{o.r.a}(p); \quad (V)$$

transverse field amplidyne equation in accordance with (6.115), but considering the connection circuit (Figure 6.15), i. e., given

$$\Delta U_{o.c.n}(p) = \Delta U_{\Sigma M \Sigma}(p), \quad \Delta U_{o.r}(p) = k_{\omega 1} \Delta i_a(p),$$

where

$$k_{o.r} = k_{o.r} k_{\omega 1}; \quad \Delta U_{o.c}(p) = \Delta U_{\Sigma M \Sigma}(p) \text{ и } \Delta U_{o.s}(p) = 0;$$

and, finally

$$\begin{aligned} (T_{\Sigma M \Sigma}p + 1)(T_{A.2}p + 1) \Delta U_{\Sigma M \Sigma}(p) = k_{o.c.n} \Delta U_{\Sigma M \Sigma}(p) - \\ - k_{o.r} \Delta i_a(p) - k_{o.c} \Delta U_{\Sigma M \Sigma}(p) \end{aligned} \quad (VI)$$

bridge circuit equation in accordance with (6.117), considering conditions  $\Delta U_{B.A}(p) = \Delta U_{\Sigma M \Sigma}(p)$  and  $\Delta U_{B.M \Sigma}(p) = \Delta U_{o.r.a}(p)$ :

$$(T_{o.c1}p + 1) \Delta U_{o.r.a}(p) = \alpha_{o.c1} T_{o.c1} p \Delta U_{\Sigma M \Sigma}(p). \quad (VII)$$

The system of link equations will be reduced to one equation of motion /289 by eliminating intermediate variables. Then, the resultant equation is solved for the controlled parameter, i. e., the expression reflecting the relationship of the controlled parameter to disturbances for a closed and an open system will be found. Presented below are expressions for armature circuit current and main propulsion motor rotational speed:

$$\begin{aligned} \Delta \bar{i}_a(p) = \frac{k_{11} k_{o.3} p B(p) \Gamma(p) (T_r p + 1) \Delta U_{o.3}(p) - k_3 k_4 (T_r p + 1) A(p) B(p) \Delta k(p)}{A(p) B(p) B(p) \Delta(p) (T_r p + 1) - k_1 k_{o.r} (T_{o.r} p + 1) (T_{\omega} p + 1) A(p) \Delta(p) - k_{11} k_{o.r} p (T_r p + 1) \Gamma(p) B(p)}; \\ \Delta \bar{n}_2(p) = \frac{k_{o.3} \Phi(p) [k_{o.r} H(p) \Gamma(p) - k_{o.r} X(p) \Gamma(p) - H(p) R(p) \Delta U_{o.3}(p) - T(p) [k_{o.r} \Phi(p) H(p) k_4 - k_{o.r} X(p) k_4 - (T_{A.2} p + 1) R(p) \Delta k(p)]}{A(p) B(p) B(p) \Delta(p) R(p) (T_r p + 1)} \end{aligned}$$

where the corresponding designations are:

$$\begin{aligned}
 A(p) &= [(T_{\Sigma \text{ЭМВ}} p + 1)(T_{\text{к3}} p + 1) - (k_{o.c.m} - k_{o.c})]; \\
 Б(p) &= [(T_{\Sigma} p + 1)(T_{\text{в.т}} p + 1) - k_{cB}(T_{\text{в.т}} p + 1)]; \\
 B(p) &= [(T_{\text{я}} p + 1)(T_{\text{м}} p + 1) - k_1 k_4]; \\
 \Gamma(p) &= [k_2 k_4 k_6 + k_5 k_6 (T_{\text{м}} p + 1)]; \\
 Д(p) &= [(T_{\Sigma} p + 1)(T_{\text{в.з}} p + 1)(T_{o.c1} p + 1)]; \\
 И(p) &= [k_2 k_6 (T_{\text{я}} p + 1) - k_1 k_5 k_6]; \\
 \Phi(p) &= k_{11} (T_{\text{т}} p + 1) p Б(p); \\
 X(p) &= k_1 (T_{\text{в.т}} p + 1) A(p) Д(p); \\
 R(p) &= [A(p) Б(p) B(p) Д(p) (T_{\text{т}} p + 1) + k_1 k_{o.t.r} (T_{\text{в.т}} p + 1) \times \\
 &\quad \times (T_{\text{м}} p + 1) A(p) Д(p) + k_{11} k_{o.t} (T_{\text{т}} p + 1) \Gamma(p) Б(p)]; \\
 k_1 &= k_1 \alpha_1 k_r k_i; \quad k_{11} = \alpha_1 \alpha_{o.c} T_{o.c} k_{o.t.r}(p).
 \end{aligned}$$

Structural diagram and transfer functions. Structural diagrams are compiled on the basis of the schematic for each operating mode. A structural diagram for a mode corresponding to three generators running the main propulsion motor is presented in Figure 6.16.

Link transfer functions corresponding to the Figure 6.16 diagram for a mode where one generator armature runs the main propulsion motor have the form

$$W_{21}(\rho) = \frac{k_1 k_7}{(T_{2\rho} - 1)(T_{2\rho} - 1) + k_1 k_4} = \frac{\Delta n_2(\rho)}{\Delta e_r(\rho)};$$

$$W_{22}(\rho) = \frac{k_2 k_6 (T_{2\rho} - 1) - k_1 k_3 k_6}{(T_{2\rho} - 1)[(T_{2\rho} - 1)(T_{2\rho} + 1) - k_1 k_4]} = \frac{\Delta n_2(\rho)}{\Delta U_{2,2}(\rho)};$$

$$W_{23}(\rho) = -\frac{k_9 (T_{2\rho} + 1)}{(T_{2\rho} - 1)(T_{2\rho} + 1) + k_1 k_4} = \frac{\Delta n_2(\rho)}{\Delta k(\rho)};$$

$$W_{24}(\rho) = \frac{(T_{2\rho} - 1) k_4}{k_1 k_4 - (T_{2\rho} - 1)(T_{2\rho} + 1)} = \frac{\Delta i_n(\rho)}{\Delta e_r(\rho)};$$

$$W_{25}(\rho) = -\frac{k_2 k_4 k_6 - k_3 k_6 (T_{2\rho} - 1)}{(T_{2\rho} + 1)[(T_{2\rho} - 1)(T_{2\rho} + 1) + k_1 k_4]} = \frac{\Delta i_n(\rho)}{\Delta U_{2,2}(\rho)};$$

$$W_{26}(\rho) = \frac{k_2 k_6}{(T_{2\rho} + 1)(T_{2\rho} + 1) + k_1 k_4} = \frac{\Delta i_n(\rho)}{\Delta k(\rho)};$$

$$W_r(\rho) = \frac{k_r}{T_{2,r\rho} + 1} = \frac{\Delta e_r(\rho)}{\Delta U_{2,r}(\rho)};$$

$$W_{2,r}(\rho) = \frac{k_{0,r,r}}{(1 - k_{cB}) \left( \frac{T_e}{1 - k_{cB}} \rho + 1 \right)} = \frac{\Delta U_{2,r}(\rho)}{\Delta U_{2,r}(\rho)};$$

$$W_{2,\Delta}(\rho) = \frac{a_1 k_{0,r,\Delta} (T_{2,\Delta\rho} - 1)}{(T_{2,\Delta\rho} - 1)(T_{2,\Delta\rho} - 1)} = \frac{\Delta U_{2,\Delta}(\rho)}{\Delta U_{0,r,\Delta}(\rho)};$$

$$W_{\Sigma M \nu}(\rho) = \frac{k_{0,r}}{(T_{\Sigma,3\rho} - 1)(T_{\Sigma \Sigma M \nu \rho} + 1)} = \frac{\Delta U_{\Sigma M \nu}(\rho)}{\Delta U_{0,r}(\rho)};$$

$$W_{0,c1}(\rho) = -\frac{a_{0,c1} T_{0,c1} \rho}{T_{0,c1} \rho - 1} = \frac{\Delta U_{0,c1}(\rho)}{\Delta U_{0,c1}(\rho)};$$

$$W_{0,c2}(\rho) = \frac{a_{r,c} T_{r,c} \rho}{T_{r,c} \rho - 1}; \quad W_w(\rho) = r_w.$$

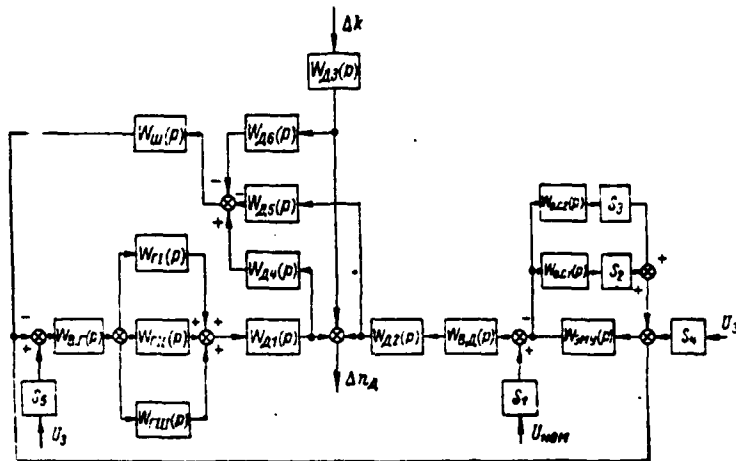


Figure 6.16. Structural Diagram of Three Generators Running the GED.

Besides transfer functions, the structural diagram will contain the /291 following multiplier constants:

$$S_1 = \frac{k_H}{k_{o.t.d}}; \quad S_2 = \frac{k_{o.c}}{k_{o.t.d}};$$

$$S_3 = \frac{k_{o.c.u}}{k_{o.t.d}}; \quad S_4 = \frac{k_{o.z}}{k_{o.t.d}}; \quad S_5 = \frac{k_{H.o.c}}{k_{o.t.f}}$$

GEU with longitudinal field amplidyne. Link operational equations. These equations are written relative to the GEU schematic (Figure 6.17) considering the equations obtained in § 6.2.

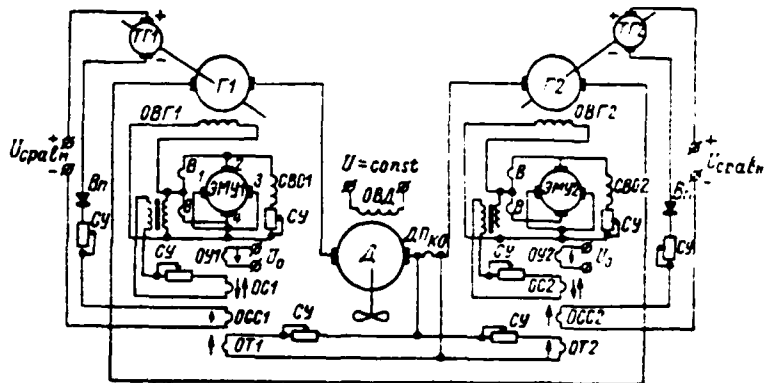


Figure 6.17. Schematic of an Automated Propellor Electric Drive with Longitudinal Field EMU.

We will compile the main generator equation in accordance with expression (6.81).

We will write the equation for the first stage of EMU amplification using (6.127), without considering the effect of the stabilizing winding and having noted that  $\Delta U_0(p) = 0$ :

$$\Delta e_{\text{ЭМВ}1}(p)(T_{\text{ЭМВ}}p + 1) = -k_{o,r} \Delta U_{\text{ш}}(p) + k_{o,c,c} |\Delta U_{r,r}(p) - \Delta U_{\text{срвн}}(p)|,$$

where  $T_{\text{ЭМВ}} = T_{o,y} + T_{o,r} + T_{o,c,c}$  - is control winding circuit total time constant.

The equation for the second stage of amplification of a longitudinal field EMU in accordance with (6.128) is:

$$\Delta \Phi_2 (T_1 p + 1) = k_1 \Delta \Phi_1$$

or

$$(T_1 p + 1) \Delta e_{\text{ЭМВ}2}(p) = k_2 \Delta e_{\text{ЭМВ}1}(p).$$

We will find the equation for the third stage of EMU amplification, using (6.14):

$$(T_{\text{ЭМВ}}p + 1)(T_1 p + 1)T_2 p \Delta e_{\text{ЭМВ}}(p) = -k_{o,r} \Delta U_{\text{ш}}(p) + k_{o,c,c} |\Delta U_{r,r}(p) - \Delta U_{\text{срвн}}(p)|,$$

where  $T_2 = T_{\text{св}} + T_{\text{в}}$  - is the total time constant.

The main propulsion motor equation is compiled in the following way. /292 Based on the Figure 6.17 diagram where  $\Phi_{\text{в,д}} = \text{const}$  and correspondingly  $\Delta \Phi_{\text{в,д}}(p) = 0$ , then, using (6.75), we get expressions:

for a propulsion motor rotational speed increment

$$\Delta n_{\text{д}}(p) [(T_{\text{д}} p + 1)(T_{\text{м}} p + a) + 1] = k_{\text{д}} \Delta e_r(p) - k_{\text{д}}' \Delta k(p) (1 + p T_{\text{д}}),$$

where

$$a = \frac{2n_{\text{д, ном}} k_{\text{ном}}}{C_{\text{д}} C_{\text{м}}}; \quad k_{\text{д}} = \frac{1}{C_{\text{д}}}; \quad \text{и } k_{\text{д}}' = \frac{n_{\text{д, ном}}^2}{C_{\text{д}} C_{\text{м}}};$$

for an armature circuit current increment, converting (6.73),

$$\begin{aligned} \Delta i_{\text{д}}(p) [(T_{\text{д}} p + 1)(T_{\text{м}} p + a) + 1] = \\ = \frac{1}{r_{\text{д}}} (T_{\text{м}} p + a) \Delta e_r(p) + k_{\text{д}}' C_{\text{д}} \Delta k(p). \end{aligned}$$

The primary motor (diesel) equation is:

$$(T_{\text{д}} p + 1) \Delta n_{\text{д}}(p) = -a_1' \Delta e_r(p) - a_2' \Delta i_{\text{д}}(p).$$

The equation system when two generators (GI and GII) run one motor D.

The main propulsion motor rotational speed change equation is:

$$\begin{aligned} [(T_{\text{np}} p + 1)(T_{\text{wp}} + a) + 1] \Delta n_{\text{r}}(p) &= k_{\text{r}} \times \\ &\times [\Delta e_{\text{rI}}(p) + \Delta e_{\text{rII}}(p)] - (T_{\text{np}} + 1) \Delta k(p) k_{\text{r}}. \end{aligned}$$

The equation for a current change in the propulsion motor armature circuit is:

$$\begin{aligned} \Delta i_{\text{r}}(p) &= \frac{T_{\text{wp}} + a}{(T_{\text{np}} + 1)(T_{\text{wp}} + a) + 1} \cdot \frac{\Delta e_{\text{rI}}(p) + \Delta e_{\text{rII}}(p)}{r_{\text{r}}} - \\ &- \frac{k_{\text{r}}' C_{\text{e}}}{[(T_{\text{np}} + 1)(T_{\text{wp}} + a) + 1]} \Delta k(p). \end{aligned} \quad (6.162)$$

The diesel rotational speed change equation is:

(6.163)

$$\begin{aligned} (T_{\text{zsl}} p + 1) \Delta n_{\text{zsl}}(p) &= -a_{11}' \Delta e_{\text{rI}}(p) - a_{21}' \Delta i_{\text{r}}(p); \\ (T_{\text{zslI}} p + 1) \Delta n_{\text{zslI}}(p) &= -a_{11} \Delta e_{\text{rII}}(p) - a_{21} \Delta i_{\text{r}}(p). \end{aligned} \quad (6.164)$$

The generator and exciter equations are:

$$\begin{aligned} \Delta i_{\text{I}}(p) \Delta e_{\text{rI}}(p) &= k_{11} \left[ \frac{k_{21}}{k_{11}} \Delta U - \frac{k_{21}}{k_{11}} \right] \times \\ &\times \Delta U_{\text{wI}}(p) - \Delta U_{\text{cpoBII}}(p) \Delta U_{\text{rI}}(p); \end{aligned} \quad (6.165)$$

$$\begin{aligned} \Delta i_{\text{II}}(p) \Delta e_{\text{rII}}(p) &= k_{11} \left[ \frac{k_{21}}{k_{11}} \Delta U_{\text{oII}}(p) - \right. \\ &\left. - \frac{k_{21}}{k_{11}} \right] \Delta U_{\text{wII}}(p) - \Delta U_{\text{cpoBII}}(p) + \Delta U_{\text{rII}}(p). \end{aligned} \quad (6.166)$$

The generator and exciter equation considering motor current feedback.

When inferring this equation, one should consider it advisable for simplification of the control system structural diagram to replace propulsion motor current /293 feedback with generator equivalent voltage feedback. Accomplishment of this replacement requires elimination of the following voltages in equations (6.165) and (6.166):

$$\begin{aligned} \Delta U_{\text{wI}}(p) &= r_{\text{wI}} \Delta i_{\text{r}}(p); \\ \Delta U_{\text{wII}}(p) &= r_{\text{wII}} \Delta i_{\text{r}}(p), \end{aligned}$$

having expressed propulsion motor current value  $\Delta i_{\text{r}}(p)$  via voltages to generators GI and GII.

Having solved (6.162) and (6.165) jointly, we get

$$\begin{aligned} \Delta_i(p) \Delta e_{r1}(p) &= k_{11} \left\{ \frac{k_{31}}{k_{11}} \Delta U_{01}(p) - \right. \\ &- \frac{(T_{mp} + ar_n)}{(T_{\Sigma n} p + 1)(T_{mp} + ar_n) + 1} \cdot \frac{r_{w1} k_{21}}{r_{\Sigma n} k_{11}} \times \\ &\times [\Delta e_{r1}(p) + \Delta e_{r11}(p)] - \frac{1}{(T_{\Sigma n} p + 1)(T_{mp} + a) + 1} \times \\ &\left. \times \frac{r_{w1} k_{21}}{r_{\Sigma n} k_{11}} C_{c.a} \Delta n_c(p) + \Delta U_{tr1}(p) - \Delta U_{cрaвн.1}(p) \right\}. \end{aligned} \quad (6.167)$$

As can be seen from equation (6.167), propulsion motor current feedback can be represented in the form of GI and GII voltage feedback. If you introduce designations:

$$W_{11}(p) = \frac{k_{11}}{\Delta_i(p)} -$$

- transfer function from control winding OUI

$$k_{o.c1} W_{22}(p) = \frac{r_{w1} k_{21}}{r_{\Sigma n} k_{11}} \cdot \frac{T_{mp} - a}{(T_{\Sigma n} p + 1)(T_{mp} + ar_n) + 1} -$$

- voltage feedback equivalent transfer function transferred to control winding OUI;

$$k_{o.c1} = \frac{r_{w1} k_{21}}{r_{\Sigma n} k_{11}} -$$

- feedback factor,

then the equation can be written in the form

$$\begin{aligned} [1 + W_{11}(p) k_{o.c1} W_{22}(p)] \Delta e_r(p) &= W_{11}(p) k_{o.c1} W_{22}(p) \times \\ &\times \left[ \frac{\frac{k_{31}}{k_{11}} \Delta U_{01}(p) - \Delta U_{cрaвн.1}(p) - \Delta U_{tr1}(p)}{k_{o.c1} W_{22}(p)} - \right. \\ &\left. - \Delta e_{r11}(p) - \frac{C_{c.a}}{T_{mp} + a} \Delta n_n(p) \right]. \end{aligned} \quad (6.168)$$

If you introduce designations:

/294

$$\Delta U'_{01}(p) = \frac{k_{31}}{k_{11}} \Delta U_{01}(p) - \text{master voltage transferred to control winding OUI;}$$

- equivalent voltage change caused by a change

$$\Delta U_{m.c}(p) = \frac{C_{c.a}}{T_{mp} + a} \Delta n_n(p) \quad \text{in moment of resistance;}$$

$$W_{22}(p) = \frac{C_{c.a}}{T_{mp} + a} - \text{equivalent link transfer function;}$$

$$\Delta U_{\Sigma 1}(p) = \frac{1}{k_{o.c1} W_{22}(p)} [\Delta U'_{01}(p) - \text{equivalent voltage change,}$$

-  $\Delta U_{cрaвн.1}(p) - \Delta U_{tr1}(p)]$  -  
then, on the basis of equation (6.168), one can represent the structural diagram of the control system's inner loop as shown in Figure 6.18a. If you use

$$W_i(p) = \frac{W_{11}(p) k_{o.c1} W_{22}(p)}{1 + W_{11}(p) k_{o.c1} W_{22}(p)}$$

to designate the converted inner loop's transfer function, then you can express the generator and exciter structural diagram, considering propulsion motor current feedback, as shown in Figure 6.18b, and you can write the equation in the form

$$\Delta e_{r1}(p) = \frac{\Delta W_1(p)}{k_{o.c11} W_{\Delta 2}(p)} [\Delta U_{01}(p) + \Delta U_{\tau r 1}(p) - \Delta U_{c p a m 1}(p)] - \Delta W_1(p) \times \\ \times \Delta e_{r11}(p) - \Delta W_1(p) W_{\Delta 2}(p) \Delta n_2(p). \quad (6.169)$$

Having solved equations (6.166) and (6.169) jointly analogously to the manner shown above, we get the generator GII and exciter equation considering current feedback in the form

$$\Delta e_{r11}(p) = \frac{\Delta W_{11}(p)}{k_{o.c11} W_{\Delta 2}(p)} [\Delta U_{011}(p) + \Delta U_{\tau r 11}(p) - \Delta U_{c p a m 1}(p)] - \\ - \Delta W_{11}(p) \Delta e_{r1}(p) - \Delta W_{11}(p) W_{\Delta 2}(p) \Delta n_2(p), \quad (6.170)$$

where

$$\Delta W_{11} = \frac{W_{11}(p) k_{o.c11} W_{\Delta 2}(p)}{1 - W_{11}(p) k_{o.c11} W_{\Delta 2}(p)};$$

$$W_{11} = \frac{k_1}{A_{11}(p)}; \quad k_{o.c11} = \frac{r_{m11} k_{211}}{r_{\Sigma n} k_{111}};$$

$$k_{o.c11} W_{\Delta 2}(p) = \frac{r_{m11} k_{211}}{r_{\Sigma n} k_{111}} \cdot \frac{(T_{\Sigma n} p - a r_n)}{(T_{\Sigma n} p + 1)(T_{M} p + a) + 1}.$$

Obtained below is the equation coupling the diesel rotational speed /295 change with the voltage change in generators GI and GII and with the change in moment of resistance  $\Delta m_s$  to the propulsion motor shaft.

In order to obtain the equation coupling the diesel rotational speed change with the voltage change in generators GI and GII and with the change in moment of resistance to the propulsion motor shaft, it is necessary in equations (6.163) and (6.164) to express the change in propulsion motor current via the corresponding generator GI and GII voltage changes and the change in moment of resistance to the propulsion motor shaft, using equation (6.162) for this.

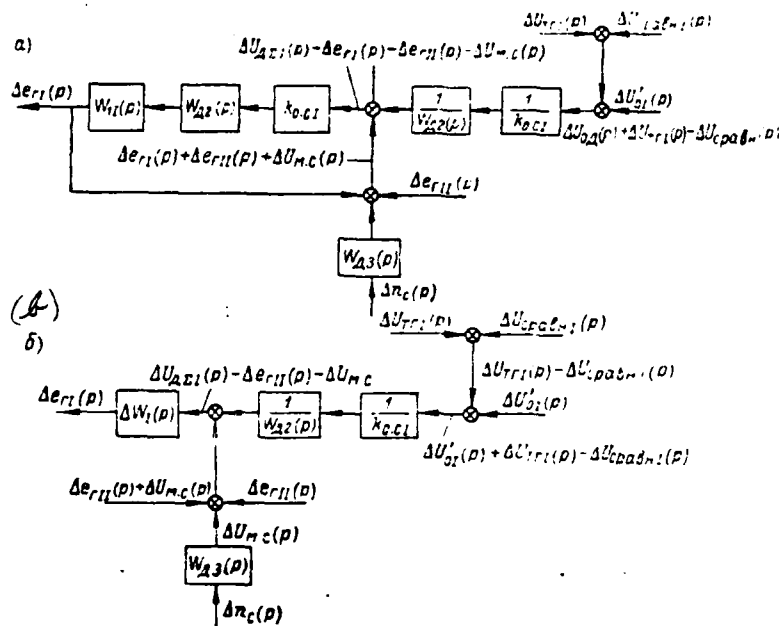


Figure 6.18. Control System Structural Diagram: a—Internal loop; b—Considering main circuit current feedback.

Having solved equations (6.163) and (6.164) jointly, for the diesel we get the equation

$$\begin{aligned}
 (T_{\Sigma 31} p + 1) \Delta n_{\Sigma 31}(p) &= -a_{11} \Delta e_{r1}(p) \frac{T_{\Sigma 31} p - a}{(T_{\Sigma 31} p - 1)(T_{\Sigma 31} p - a) - 1} \cdot \frac{a_{11}}{r_{\Sigma 31}} \\
 &\times \left[ \Delta e_{r1}(p) + \Delta e_{r11}(p) - \frac{T_{\Sigma 31} p - a}{(T_{\Sigma 31} p - 1)(T_{\Sigma 31} p - a) - 1} \right. \\
 &\left. \times \frac{a_{211}}{r_{\Sigma 31}} \cdot \frac{C'_{eD}}{T_{\Sigma 31} p - a} \right] \Delta n_c(p).
 \end{aligned} \tag{6.171}$$

If you introduce designations:  $W_{\Sigma 31}(p) = \frac{T_{\Sigma 31} p + a}{(T_{\Sigma 31} p - 1)(T_{\Sigma 31} p - a) - 1}$ ;  $k_1 = \frac{a_{211}}{a_{11} r_{\Sigma 31}}$ ;

$$W_{\Sigma 32} = \frac{C'_{eD}}{T_{\Sigma 31} p - a}; \quad W_{\Sigma 33}(p) = \frac{a_{11}}{T_{\Sigma 31} p - a},$$

then we get an equation in the form

$$\begin{aligned}
 -\Delta n_{\Sigma 31}(p) &= W_{\Sigma 31}(p) [1 + k_1 W_{\Sigma 32}(p)] \Delta e_{r1}(p) + \\
 &+ W_{\Sigma 31}(p) k_1 W_{\Sigma 32}(p) [\Delta e_{r11}(p) + W_{\Sigma 33}(p) \Delta n_c(p)].
 \end{aligned} \tag{6.172}$$

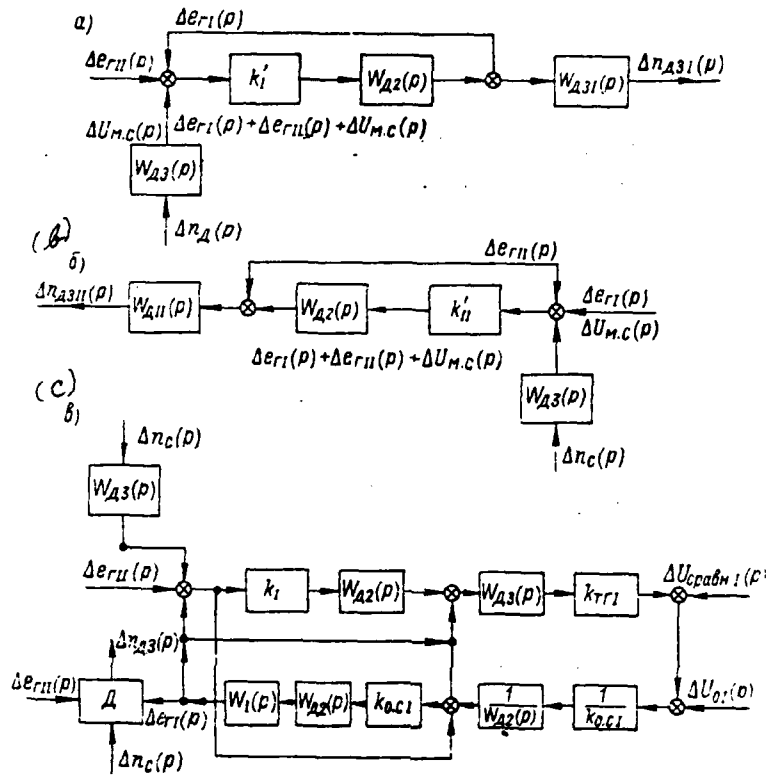


Figure 6.19. Diesel Generator Structural Diagram. a—Diesel structural diagram considering the generator effect; b—Diesel DzII structural diagram; c—Diesel and generator automatic control structural diagram.

The structural diagram of a diesel considering the effect of generator emf and moment of resistance can be represented as shown in Figure 6.19a.

Having solved equations (6.162) and (6.164) jointly analogously to the /297 manner shown above, we get the equation for diesel DzII in the form

$$\begin{aligned}
 -\Delta n_{d311}(p) &= W_{d311}(p) [1 + k'_{11} W_{d2}(p)] \Delta e_{r11}(p) - \\
 &+ W_{d311}(p) k'_{11} W_{d2}(p) [\Delta e_{r1}(p) - W_{d3}(p) \Delta n_2(p)],
 \end{aligned}
 \tag{6.173}$$

where

$$W_{a311}(\rho) = \frac{a_{11}}{T_{a311}\rho - a};$$

$$k_{11} = \frac{a_{21}}{r_{\Sigma} a_{11}};$$

$$W_{a2}(\rho) = \frac{T_{m\rho} - a}{(T_{\Sigma a}\rho + 1)(T_{m\rho} - a) - 1};$$

$$W_{a3}(\rho) = \frac{C_{12}}{T_{m\rho} + a}.$$

Figure 6.19b shows the DzII structural diagram.

The equation for generator GI and GII emf change. It is possible to obtain the equation for generator GI emf change if you solve equations (6.169) and (6.172) jointly and consider that the voltage in tachogenerator TGI equals

$$\Delta U_{TGI}(\rho) = k_{TGI} \Delta n_{a3}(\rho).$$

As a result, we get

$$\left[ 1 + \Delta W_1(\rho) k_{TGI} W_{a31}(\rho) \frac{1 - k_1 W_{a2}(\rho)}{k_{o.c1} W_{a2}(\rho)} \right] \Delta e_{r1}(\rho) = \frac{\Delta W_1(\rho)}{k_{o.c1} W_{a2}(\rho)}$$

$$\times [\Delta U_{01}(\rho) - \Delta U_{срaвн1}(\rho)] - \Delta W_1(\rho) \left[ 1 + \frac{k_{TGI} k_1}{k_{o.c11}} W_{a31}(\rho) \right]$$

$$\times \Delta e_{r1}(\rho) - \Delta W_1(\rho) W_{a3}(\rho) \left[ 1 + \frac{k_{TGI} k_1}{k_{o.c1}} W_{a31}(\rho) \right] \Delta n_{a3}(\rho). \quad (6.174)$$

It is possible to compile the structural diagram of the diesel DzI and generator GI automatic control system, as shown in Figure 6.19c, based on equation (6.174) and the structural diagrams presented in Figures 6.19a and 6.19b.

If you introduce designations:

$$W_{c1}(\rho) = \frac{1 - \frac{k_{o.c1}}{k_{TGI} k_1 W_{a31}(\rho)}}{1 + \frac{k_1 W_{a2}(\rho)}{k_{o.c11}}};$$

$$W_{a1}(\rho) = \frac{1}{[1 + k_1 W_{a2}(\rho)] W_{a21}(\rho) k_{TGI}};$$

$$W_1(\rho) = \Delta W_1(\rho) k_{TGI} W_{a31}(\rho) \frac{1 - k_1 W_{a2}(\rho)}{k_{o.c1} W_{a2}(\rho)},$$

then equation (6.174) can be written in the form

/298

$$[1 + W_1(\rho)] \Delta e_{r1}(\rho) = W_1(\rho) W_{a1}(\rho) [\Delta U_{01}(\rho) - \Delta U_{срaвн1}(\rho)] -$$

$$- W_1(\rho) W_{c1}(\rho) \Delta e_{r11}(\rho) - W_1(\rho) W_{c1}(\rho) W_{a3}(\rho) \Delta n_{a3}(\rho). \quad (6.175)$$

Based on equation (6.175), the diesel DzI and generator GI control system structural diagram can be reduced to the form shown in Figure 6.20.

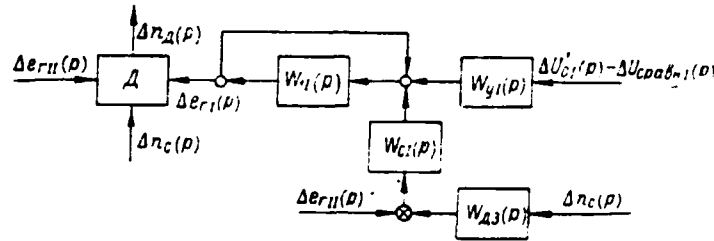


Figure 6.20. Converted Diesel and Generator Control Structural Diagram.

Having solved equations (6.170) and (6.173) jointly analogously to the manner shown above, we get the equation for generator GII emf change in the form

$$\begin{aligned}
 [1 + W_{II}(p)] \Delta e_{rII}(p) = & W_{yII}(p) W_{II}(p) \times \\
 & \times [\Delta U'_{0II}(p) - \Delta U_{cpa3II}(p)] - W_{II}(p) \times \\
 & \times W_{cII}(p) \Delta e_{rI}(p) - W_{II}(p) W_{cII}(p) W_{A3}(p) \Delta n_c(p),
 \end{aligned}
 \tag{6.176}$$

where

$$\begin{aligned}
 W_{II}(p) = & \Delta W_{II}(p) k_{\tau II} W_{A3II}(p) \frac{1 + k_{II} W_{A2}(p)}{k_{o.cII} W_{A3}(p)}; \\
 W_{yII}(p) = & \frac{1}{[1 + k_{II} W_{A2}(p)] W_{A3II}(p) k_{\tau II}}; \\
 W_{cII}(p) = & \frac{1 + \frac{k_{o.cII}}{k_{\tau II} k_{II} W_{A3II}(p)}}{1 + \frac{1}{k_{II} W_{A2}(p)}}.
 \end{aligned}$$

Control system equation when two generators GI and GII run one motor D.

Having solved equations (6.175) and (6.176) jointly, it is possible to get the emf change formula:

for generator GI

$$\begin{aligned}
 \left[ 1 - \frac{W_I(p)}{1 + W_I(p)} W_{cI}(p) \frac{W_{II}(p) W_{cII}(p)}{1 + W_{II}(p)} \right] \Delta e_{rI}(p) = \\
 = \frac{W_I(p)}{1 + W_I(p)} W_{yI}(p) [\Delta U'_{0I}(p) - \Delta U_{cpa3I}(p)] -
 \end{aligned}$$

$$\begin{aligned}
& - \frac{W_1(p)}{1+W_1(p)} W_{c1}(p) \frac{W_{11}(p)}{1+W_{11}(p)} W_{y11}(p) \times \\
& \times [\Delta U'_{011}(p) - \Delta U_{\text{сравн}11}(p)] - \frac{W_1(p)}{1+W_1(p)} \times \\
& \times W_{c1}(p) W_{\text{зп}}(p) \left[ 1 + \frac{W_{11}(p)}{1+W_{11}(p)} W_{c1}(p) \right] \Delta n_x(p);
\end{aligned} \tag{6.177}$$

for generator GII

/299

$$\begin{aligned}
& \left[ 1 - \frac{W_1(p)}{1+W_1(p)} W_{c1}(p) \frac{W_{11}(p)}{1+W_{11}(p)} W_{c11}(p) \right] \Delta e_{r11}(p) \\
& = \frac{W_{11}(p)}{1+W_{11}(p)} W_{y11} [\Delta U'_{011}(p) - \Delta U_{\text{сравн}11}(p)] - \\
& - \frac{W_{11}(p)}{1+W_{11}(p)} W_{c11}(p) \frac{W_1(p)}{1+W_1(p)} W_{y1}(p) \times \\
& \times [\Delta U'_{01}(p) - \Delta U_{\text{сравн}1}(p)] - \frac{W_{11}(p)}{1+W_{11}(p)} \times \\
& \times W_{c11}(p) W_{\text{зп}}(p) \left[ 1 + \frac{W_1(p)}{1+W_1(p)} W_{c1}(p) \right] \Delta n_x(p).
\end{aligned} \tag{6.178}$$

Based on equations (6.177) and (6.178) and the structural diagrams presented in Figures 6.19 and 6.20, it is possible to represent the full structural diagram as shown in Figure 6.21. A converted control system structural diagram compiled from the Figure 6.20 and 6.21 diagrams is presented in Figure 6.22.

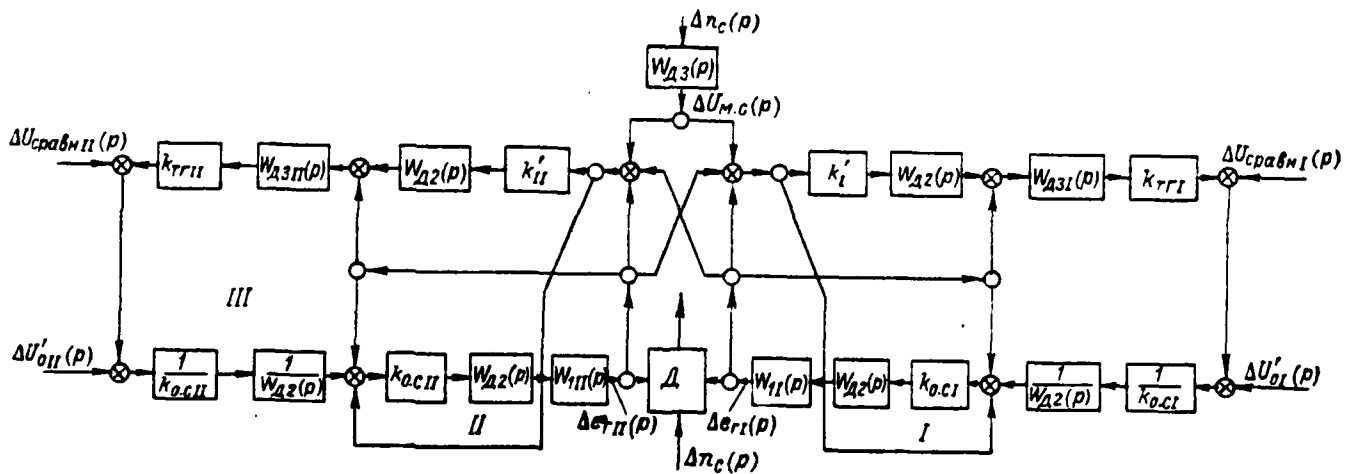


Figure 6.21. Complete Control Structural Diagram. I—III are internal control loops.

GEU with MU in a field and control system. Initial system of operational equations. This system is described relative to GEU whose schematic is shown in Figure 6.23.

The main propulsion motor equation considering two field windings will be obtained from the following general equations:

$$(6.179)$$

$$(T_M p + 1) \Delta n_d(p) = k_1' \Delta i_n(p) + k_2' \Delta \Phi_d(p) - k_3' \Delta k(p),$$

where

$$T_M' = T_M \frac{C_e C_m}{2k_{\text{л.д. ном}} r_a}; \quad k_1' = C_m I_{\text{н. ном}}; \quad k_2' = C_m \Phi_{\text{д. ном}};$$

$$\text{и } k_3' = n_{\text{д. ном}}^2;$$

$$(T_{\text{в.д}} p + 1) \Delta i_n(p) = k_4' \Delta e_r(p) - k_5' \Delta n_d(p) - k_6' \Delta \Phi_d(p), \quad (6.180)$$

where  $k_4' = 1/r_n$ ;  $k_5' = C_e \Phi_{\text{д. ном}} / r_n$ ;  $k_6' = \frac{C_e n_{\text{д. ном}}}{r_n}$ ,

and, for the field circuit

/301

$$(T_{\text{в.д}} p + 1) \Delta \Phi_d(p) = k_7' \Delta U_{\text{в.д. доп}}(p), \quad (6.181)$$

where  $T_{\text{в.д}} = T_{\text{осн}} + T_{\text{доп}}$  - GED excitation overall time constant.

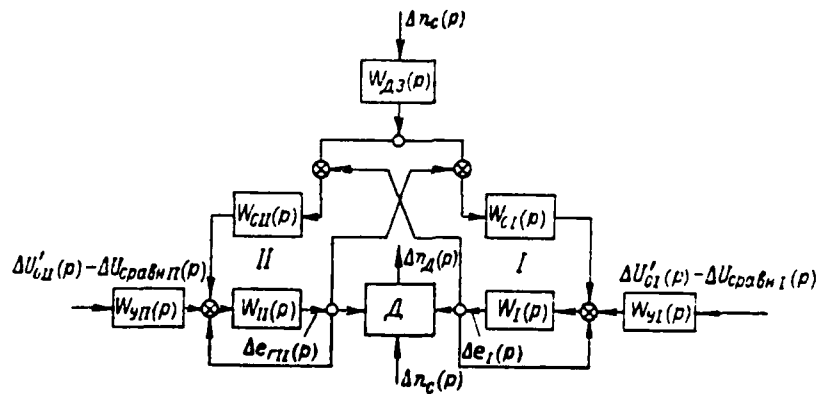


Figure 6.22. Converted Complete Control Structural Diagram.

The GED basic winding time constant is:

$$T_{\text{осн}} = \frac{2p_2 \sigma_2 \cdot \text{осн} \omega_{\text{в.д. осн}}^2 C_2}{r_{\text{в.д. осн}}}$$

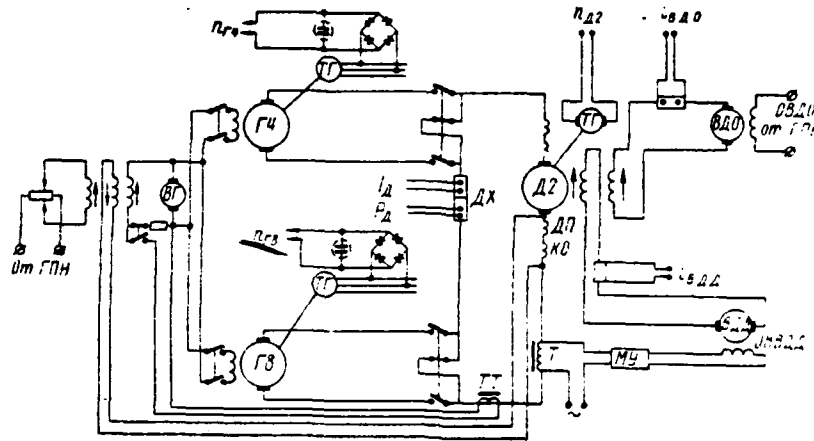


Figure 6.23. Schematic for a GEU with Magnetic Amplifiers in GED Field Circuits.

The GED additional winding time constant is:

/302

$$T_{\text{доп}} = \frac{2\rho_{\text{д. доп}} \omega_{\text{в. д. доп}}^2 C_{\text{д}}}{r_{\text{в. д. доп}}}$$

$$k_{7\text{доп}} = \frac{C_{\text{д}} \omega_{\text{в. д. доп}}}{r_{\text{в. д. доп}} T_{\text{в. д. доп}}}$$

Having solved the system for armature circuit current in accordance with (6.73), we get

$$\begin{aligned} & (T_{\text{в. дп}} p + 1) [k_5 k_1 + (T_{\text{мп}} p + 1) (T_{\text{рп}} p + 1)] \Delta i_{\text{а}}(p) = \\ & = k_4 (T_{\text{мп}} p + 1) (T_{\text{в. дп}} p + 1) \Delta e_{\text{r}}(p) + k_5 k_5 (T_{\text{в. дп}} p + 1) \Delta k(p) \cdot \\ & - [k_{7\text{доп}} k_2 k_5 + k_{7\text{доп}} k_6 (T_{\text{мп}} p + 1)] \Delta U_{\text{в. д. доп}}(p). \end{aligned} \quad (6.182)$$

Having solved the system for rotational speed in accordance with (6.75), we get

$$\begin{aligned} & (T_{\text{в. дп}} p + 1) [k_5 k_5 + (T_{\text{рп}} p + 1) (T_{\text{мп}} p + 1)] \Delta n_{\text{а}}(p) = \\ & = - (T_{\text{в. дп}} p + 1) k_3 \Delta k(p) + k_1 k_4 (T_{\text{в. дп}} p + 1) \Delta e_{\text{r}}(p) + \\ & + [k_{7\text{доп}} k_2 (T_{\text{рп}} p + 1) - k_1 k_6 k_{7\text{доп}}] \Delta U_{\text{в. д. доп}}(p). \end{aligned} \quad (6.183)$$

The equation for a three-winding exciter considering that  $\Delta U_{\text{в. д. доп}}(p) = 0$

in accordance with (6.91), but without considering speed feedback of the main circuit current change, has the form

$$\begin{aligned} (T_2 p + 1) (T_{s.r} p + 1) \Delta U_{s.r}(p) = \\ = (T_{s.r} p + 1) [k_{c.s} \Delta U_{s.r}(p) - k_{o.s.r} \Delta i_s(p)]. \end{aligned}$$

The equation for the equivalent main generator in accordance with (6.81) is:

$$(T_r p + 1) \Delta e_r(p) = k_r \Delta U_{s.r}(p).$$

The equation for the GED field additional winding pilot excitation is:

$$(T_{n.d} p + 1) \Delta e_{n.d}(p) = k'_n \Delta U_n(p),$$

where

$$\begin{aligned} k'_n &= k_n T_{n.d}; \\ k_n &= \frac{C_{s.v.d}}{2\rho_{s.v.d} \sigma_{n.d} W_{s.v.d}}; \\ T_{n.d} &= \frac{2\rho_{s.v.d} \sigma_{n.d} W_{s.v.d}^2 C'_{s.v.d}}{r_n}. \end{aligned}$$

The equation for the magnetic amplifier circuit in first approximation /303 has the form

$$(T_{M.V} p + 1) \Delta U_{M.V}(p) = k'_{12} \Delta i_n(p),$$

where  $U_{M.V}$  is MU output voltage magnitude;  $k'_{12} = k_{12} T_{M.V}$ ,  $T_{M.V}$  is a link time constant.

The equation system's transfer functions are:

$$\begin{aligned}
 W_{a1}(\rho) &= \frac{k_1 k_4}{k_5 k_1 + (T_M \rho + 1)(T_N \rho + 1)} = \frac{\Delta i_n(\rho)}{\Delta e_r(\rho)}; \\
 W_{a2}(\rho) &= \frac{k_{720n} k_2 (T_N \rho + 1) - k_{720n} k_6 k_1}{(T_{B.A} \rho + 1) [k_5 k_1 + (T_M \rho + 1)(T_N \rho + 1)]} \\
 &= \frac{\Delta i_n(\rho)}{\Delta U_{B.A}(\rho)}; \\
 W_{a3}(\rho) &= \frac{-k_3 (T_N \rho + 1)}{k_5 k_1 + (T_M \rho + 1)(T_N \rho + 1)} = \frac{\Delta i_n(\rho)}{\Delta k(\rho)}; \\
 W_{a4}(\rho) &= \frac{k_4 (T_M \rho + 1)}{k_5 k_1 + (T_M \rho + 1)(T_N \rho + 1)} = \frac{\Delta i_n(\rho)}{\Delta e_r(\rho)}; \\
 W_{a5}(\rho) &= \frac{-k_{720n} k_5 k_2 - k_{720n} k_6 (T_M \rho + 1)}{(T_{B.A} \rho + 1) [k_5 k_1 + (T_M \rho + 1)(T_N \rho + 1)]} \\
 &= \frac{\Delta i_n(\rho)}{\Delta U_{B.A}(\rho)}; \\
 W_{a6}(\rho) &= \frac{k_3 k_5}{k_5 k_1 + (T_M \rho + 1)(T_N \rho + 1)} = \frac{\Delta i_n(\rho)}{\Delta k(\rho)}; \\
 W_{r1}(\rho) &= \frac{k_8}{T_{B.r}(\rho) + 1} = \frac{\Delta e_r(\rho)}{\Delta i_n(\rho)}; \\
 W_{r2}(\rho) &= -\frac{C_r C_r w_{o.r.r}}{T_{B.r}(\rho) + 1} = \frac{\Delta e_r(\rho)}{\Delta U_{B.r}(\rho)}; \\
 W_{B.r}(\rho) &= -\frac{k_9}{T_{\Sigma} \rho + 1} = \frac{\Delta U_{B.r}(\rho)}{\Delta U_r(\rho)}; \\
 W_{B.A.A}(\rho) &= \frac{k_{11}}{T_{H.A} \rho + 1} = \frac{\Delta e_{B.A}(\rho)}{\Delta U_H(\rho)} \\
 &= \frac{\Delta e_{B.A}(\rho)}{\Delta U_{MY}(\rho)}; \\
 W_{K.o}(\rho) &= k_{13} = \frac{1}{2} \rho_{K.o} = \frac{\Delta U_T(\rho)}{\Delta i_n(\rho)}; \\
 W_{MY}(\rho) &= \frac{k_{12}}{T_{MY} \rho + 1} = \frac{\Delta U_{MY}(\rho)}{\Delta i_n(\rho)}.
 \end{aligned}
 \tag{6.184}$$

§ 6.4 Analysis of the Stability of Standard GEU Systems /304

GEU with transverse field amplidyne. Calculation of stability (relative to the equations of motion obtained in § 6.3) is accomplished for all basic operating modes. The methodology presented is for a mode in which one diesel generator runs the aft main propulsion motor (the sequence of the calculation for all other operating modes is analogous).

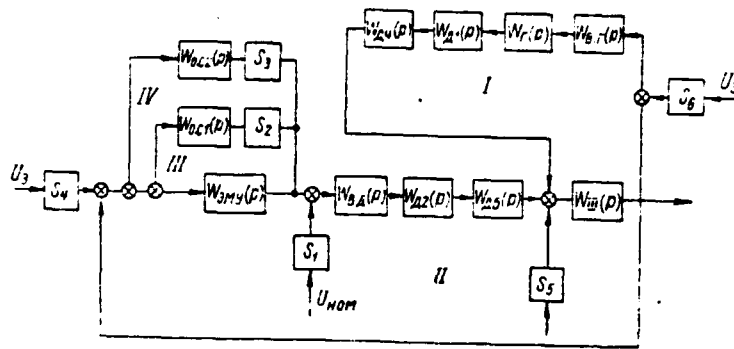


Figure 6.24. Converted Structural Diagram.

Stability analysis is done in the following sequence:

1. We compile a structural diagram on the basis of the main current circuit and field circuit, as well as the link equations (transfer functions).
2. Having converted the structural diagram for simplified characteristics calculation, we get the diagram shown in Figure 6.24, which sets forth four closed loops (I—IV).
3. Using the appropriate link equations and their transfer functions, we compile equivalent loop transfer functions:

loop I transfer function

where

$$W_{\text{кв. I}}(p) = W_{\text{III}}(p) W_{24}(p) W_{21}(p) W_{1r}(p) W_{16}(p),$$

then

$$W_{\text{кв. I}}(p) = W_{\text{III}}(p) W_{\text{o.c.}}(p), \text{ а } W_{\text{o.c.}}(p) = W_{24}(p) W_{21}(p) W_{1r}(p) W_{16}(p).$$

$$W_{\text{кв. I}}(p) = \frac{r_{\text{ш}}(T_{\text{мD}} + 1) k_1 k_7 k_r k_{\text{o. r. r}}}{k_1 [(T_{\text{нD}} + 1)(T_{\text{мD}} + 1) k_1 k_4] (T_{\text{в. rD}} + 1) (1 - k_{\text{св}}) \left( \frac{T_{\Sigma}}{1 - k_{\text{св}}} p + 1 \right)}; \quad (6.185)$$

loop II transfer function  $W_{\text{II}}(p) = W_{9A}(p) W_{22}(p) W_{25}(p)$  /305

we multiply with feedback transfer function  $W_{\text{o.c.}}(p)$ , as a result of which we get

$$\begin{aligned} W_{\text{кв. II}} &= \frac{W_{\text{II}}(p)}{W_{\text{o.c.}}(p)} = \frac{W_{9A}(p) W_{22}(p) W_{25}(p)}{W_{24}(p) W_{21}(p) W_{1r}(p) W_{16}(p)} = \\ &= \frac{\alpha_1 k_{\text{p.o.}} (T_{\text{в. нD}} - 1) [k_2 k_5 (T_{\text{нD}} - 1) - k_1 k_4 k_6] [k_2 k_4 k_8 - k_1 k_8 (T_{\text{мD}} - 1)]}{(T_{\Sigma} - 1) (T_{\text{в. нD}} - 1) (T_{\text{в. нD}} - 1) [(T_{\text{нD}} - 1) (T_{\text{мD}} - 1) - k_1 k_4]} \\ &\times \frac{k_1 (T_{\text{нD}} + 1) (T_{\text{мD}} - 1) + k_1 k_4 (T_{\text{мD}} + 1) (1 - k_{\text{св}}) \left( \frac{T_{\Sigma}}{1 - k_{\text{св}}} p + 1 \right)}{[k_2 k_5 (T_{\text{нD}} + 1) - k_1 k_4 k_6] (T_{\text{мD}} - 1) k_1 k_7 k_r k_{\text{o. r. r}}} \end{aligned} \quad (6.186)$$

Analogously, we determine the following equivalent functions for the loops without considering the stabilizing transformer loop (see loop IV in Figure 6.24):

$$W_{\text{кв III}}(p) = W_{\Sigma \text{МВ}}(p) W_{\text{о.сI}}(p) S_2 = \frac{k_{\text{о.т}} a_{\text{о.сI}} T_{\text{о.сI}} p k_{\text{о.с}}}{(T_{\text{к.з}} p - 1)(T_{\Sigma \text{МВ}} p - 1)(T_{\text{о.с}} p - 1) k_{\text{р.о}}}; \quad (6.187)$$

$$W_{\text{кв IV}}(p) = \frac{1}{W_{\text{о.сI}}(p) S_2} = \frac{a_{\text{о.сI}} T_{\text{о.сI}} k_{\text{о.с}} p}{(T_{\text{о.с}} p - 1) k_{\text{р.о}}}. \quad (6.188)$$

4. We construct amplitude and phase responses for all equivalent transfer functions.

5. Using a Nichols chart for an open system's responses with loop I transfer function  $W_{\text{кв I}}(p)$  and loop II transfer function  $W_{\text{кв II}}(p)$ , we construct amplitude  $L$  and phase  $\varphi$  responses for the closed system's corresponding loops.

6. Having added  $L_{\text{о.сI}}$  to  $L_{\text{о.сI}}(L_{\text{кв I}})$  and  $\varphi_{\text{о.сI}}$  to  $\varphi_{\text{о.сI}}(\varphi_{\text{кв I}})$ , we get the amplitude ratio and phase responses of the corresponding loops with unitary feedback. We get  $L_{\text{кI}}$ ,  $L_{\text{кII}}$  and  $\varphi_{\text{кI}}$ ,  $\varphi_{\text{кII}}$  (Figures 6.25 and 6.26) for the first and second loops,  $L_{\text{кв II}}$  and  $\varphi_{\text{кв II}}$  (Figure 6.27), the logarithmic amplitude and phase characteristics, respectively, for the second loop.

7. Having added the responses of both loops  $L_{\text{кI}}$  and  $L_{\text{кII}}$ ,  $\varphi_{\text{кI}}$  and  $\varphi_{\text{кII}}$ , we determine system stability without a stabilizing transformer as one diesel generator is run (responses  $L'$  and  $\varphi'$  in Figure 6.27). Response  $\varphi'$  intersects line  $-180^\circ$  (point c) at a frequency at which the amplitude response has a positive value (a—b), i. e., in this case, the system is unstable; the unstable state of the system in the mode examined is explained by the fact that the generator exciter is operating in the unsaturated portion of its characteristic. A variant with a stabilizing transformer, whose Bode diagrams are shown in Figure 6.28, can be used to stabilize the system.

8. Having added amplitude responses  $L_{\text{кII}}$  and  $L_{\text{с.т}}$  and using a Nichols /308 chart, we determine the closed system's responses. Having added them to the stabilizing transformer's back characteristics, we get new loop III responses (Figure 6.29). Having added  $L_{\text{кII}}$  and  $\varphi_{\text{кII}}$  to  $L_{\text{кI}}$  and  $\varphi_{\text{кI}}$ , we get resultant responses  $L$  and  $\varphi$  (see Figure 6.27).

It is evident from the chart that phase response  $\varphi$  does not intersect

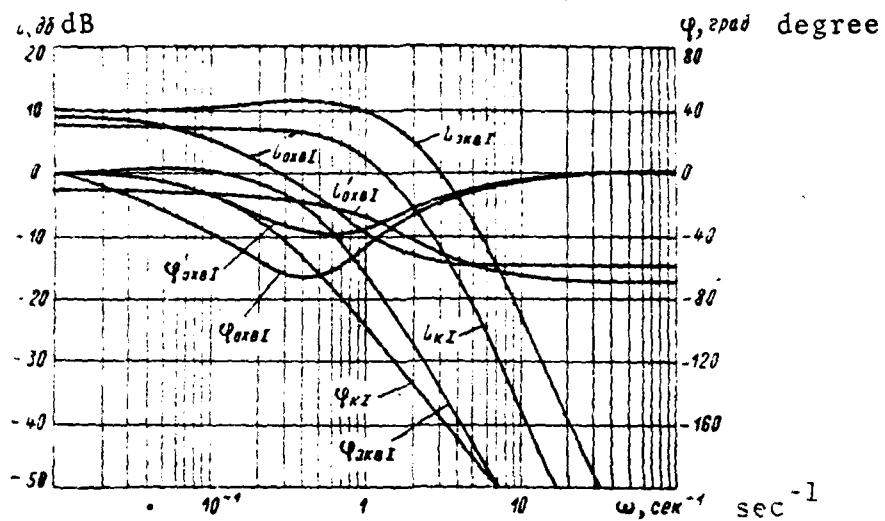


Figure 6.25. Loop I Closed System Log-Magnitude and Phase-Angle Plots.

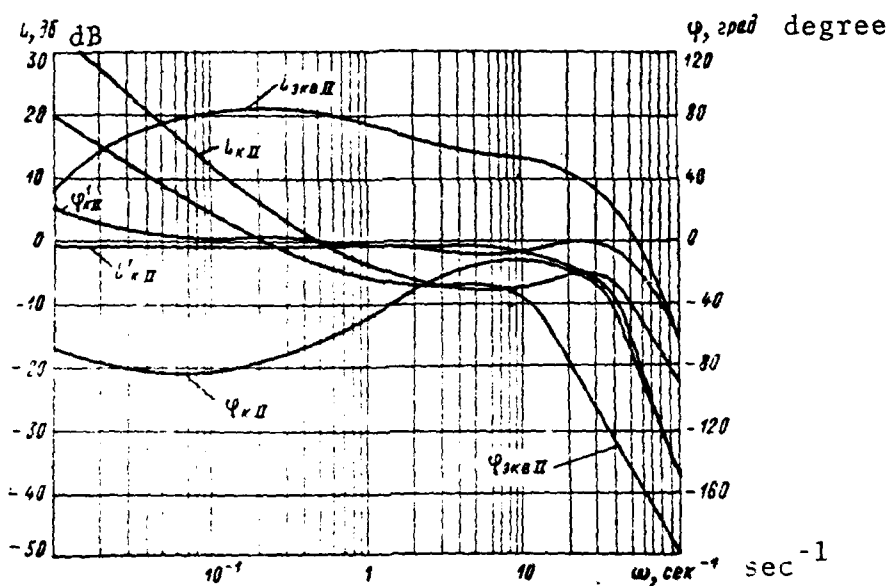


Figure 6.26. Loop II Closed System Log-Magnitude and Phase-Angle Plots.

line —<sup>π</sup> at a frequency at which the amplitude response is positive, i. e., the system became stable after introduction of a stabilizing transformer.

GEU with longitudinal field amplidynes. The methodology used is applicable to the equations of motion obtained in § 6.3, with the use of frequency responses.

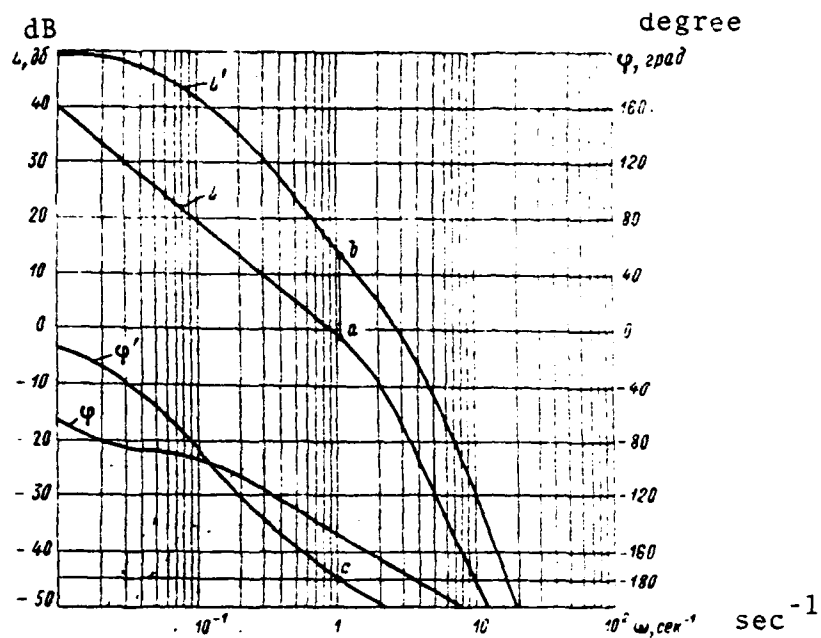


Figure 6.27. Log-Magnitude and Phase-Angle Plots of a Control System Without a Stabilizing Transformer and When One Diesel Generator is Running.

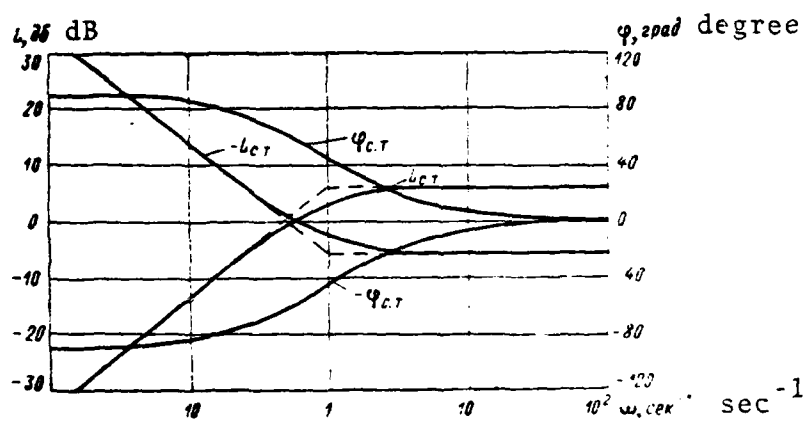


Figure 6.28. Stabilizing Transformer Bode Diagram.

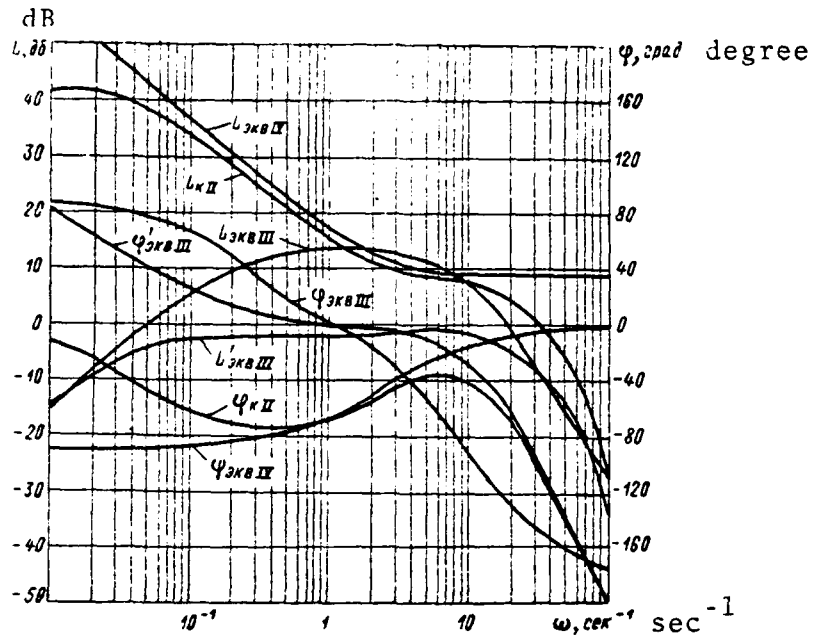


Figure 6.29. Closed System Bode Diagram.

It is known that the curvature of a significant number of responses decreases when they are constructed on a logarithmic scale. This can be used for an approximation of amplitude and phase responses constructed on a logarithmic scale by using broken lines compiled from rectilinear segments. Computational work is decreased greatly by so doing.

One must study the stability of a system's individual loops in order to judge the stability of the entire system's operation. Each loop (I—III) consists of series-connected links (see Figure 6.21). We construct amplitude responses based on conjugating frequencies for each link, then, based on these /309 responses, we construct the open loop's amplitude response. Finally, we construct the loop's frequency response based on its amplitude response, using a logarithmic grid.

Using a nomogram for determination of the closed system's log-magnitude and phase-angle plots based on the open loop's transfer locus, next we construct the closed loop's amplitude and phase response. We judge the loop's stability and stability reserve from the resultant responses.

Investigation of loop I stability. 1. The transfer function for this loop (see Figure 6.21 and 6.22) can be written as follows:

$$W_1(p) = W_r(p) + W'_{\text{ЭМВ}}(p).$$

The amplitude response of this loop is constructed in Figure 6.30 from conjugate frequencies computed for the specific system.

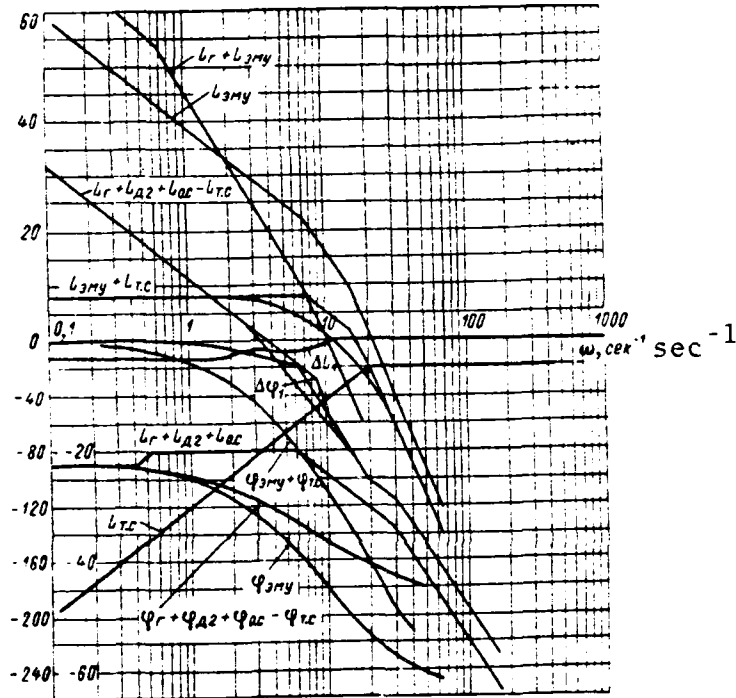


Figure 6.30. Loop I Log-Magnitude Plots.

Since the loop's amplitude-ratio response intersects the X-axis at a  $\omega = 310$  large angle, the loop is unstable, just as is the entire system. Compensation must be introduced to make this inner loop stable (see Figure 6.22). The amplidyne is "enclosed" by vanishing feedback for this purpose. The compensator characteristic is selected so that loop stability will be insured. A stabilizing transformer can be selected as compensator in this case.

A loop comprising  $W'_{\text{ЭМВ}}$  and  $W_{r,r}$ , is stable. Its phase stability reserve is about  $40^\circ$ .

Investigation of loop II stability (see Figure 6.21). We determine the

conjugate frequencies and bring the transfer function to the form

$$W_{22}(p) = \frac{T_M p + a}{(T_{\Sigma} p + 1)(T_M p + a) + 1} = \frac{T_M p + 1}{1 + \frac{T_M}{a} p + 1} \cdot \frac{a}{1 + a}.$$

We construct the general logarithmic amplitude response of the entire open loop (Figure 6.30) and we determine its phase response.

Using a Nichols chart, we find the closed loop's amplitude and phase response (Figure 6.30).

It is evident from the figure that the phase stability reserve is about 60°.

Investigation of loop III stability (Figure 6.21). After determination of conjugate frequencies, we bring the transfer function to that form in which time constants and frequencies have the form

$$\begin{aligned} T_1' &= \frac{T_M T_{\Sigma}}{1 + (1 + k_1) a}; \\ T_2' &= \frac{a T_{\Sigma} + T_M + k_1 T_M}{1 + a(1 + k_1)}; \\ \beta &= \frac{1 + a(1 + k_1)}{1 + a}; \\ T_1'' &= \frac{T_M T_{\Sigma}}{1 + a}; \\ T_2'' &= \frac{T_{\Sigma} - T_M}{1 + a}; \\ \omega_2'' &= \frac{1}{T_2''}; \quad \omega_1'' = \frac{1}{T_2''}; \\ \omega_1' &= \frac{1}{T_1'}; \quad \omega_1 = \frac{1}{T_1'}. \end{aligned}$$

The amplitude responses of the loop's links and  $L_{21}$ , the amplitude-ratio response of the entire open loop are constructed in Figure 6.31. Using a logarithmic grid, we find the open loop's phase response. /311

We use a Nichols chart to find the closed loop's amplitude and phase responses  $L_{22}$  and  $\varphi_{22}$ . It is apparent from their mutual location that the system has a large (about 40°) phase stability reserve.

Investigation of the stability of system operation as two generators jointly



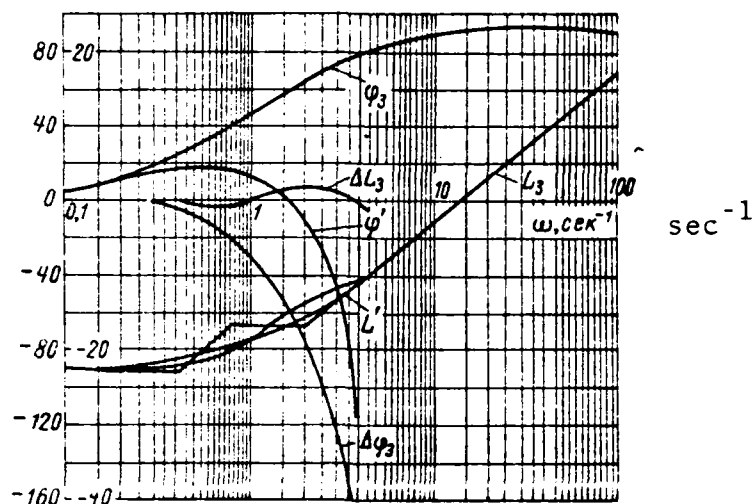


Figure 6.32. Open Control System Log-Magnitude and Phase-Angle Plots.

It is apparent from Figure 6.32 that phase response  $\varphi_3$  in the area where  $L_3 > 0$  does not intersect the straight line parallel to the frequency axis and separated from it by value  $-\pi$ . Consequently, the loop is stable in the closed state. The stability of this loop can be checked based on both the amplitude and phase responses of the closed system. To do so, using a Nichols chart, we construct  $L'$  and  $\varphi'$ , log-magnitude and phase-angle plots. It is evident from their common position that the system is stable. If we construct the closed loop's transfer locus, then it will have a spiral form (since the module also increases due to the increase in angle). It follows from the Mikhaylov criterion for an open system that the system is stable. Since all loops individually /313 are stable, the overall system also is stable.

GEU with magnetic amplifiers. The analysis was done relative to the equations of motion obtained in § 6.3 with the use of log-magnitude and phase-angle plots.

Using Bode diagrams, we construct the characteristics of the system's individual links. Adding log-magnitude and phase-angle plots of the individual links, we get the automatic control system's Bode diagrams. Comparing the open control system's log-magnitude and phase-angle plots, one can judge the stability of the closed control system.

A structural diagram is presented in Figure 6.33a and its conversion is depicted in Figure 6.33b.

Loop I Bode diagrams (Figure 6.33b). The transfer function:

$$W_{\text{SAR I}}(p) = \frac{W_{\text{A4}}(p) 4W_{\text{r2}}(p)}{1 + W_{\text{A4}}(p) 4W_{\text{r2}}(p)} \cdot \frac{1}{4W_{\text{r2}}(p)}$$

The transfer locus is:

$$W_{\text{SAR I}}(j\omega) = \frac{W_{\text{A4}}(j\omega) 4W_{\text{r2}}(j\omega)}{1 + W_{\text{A4}}(j\omega) 4W_{\text{r2}}(j\omega)} \cdot \frac{1}{4W_{\text{r2}}(j\omega)} = \frac{W'(j\omega)}{1 + W'(j\omega)}$$

We construct the Bode diagrams of the links of an open SAR [automatic control system] with transfer function  $W'(p) = W_{\text{A4}}(p) 4W_{\text{r2}}(p)$ .

The multiplier's Bode diagrams are:

$$4W_{\text{r2}}(j\omega) = \frac{4C_r C_r' \omega_{o.r.r.}}{T_{n.r} j\omega - 1}$$

Taking the logarithm of the latter, we get

$$20 \lg 4W_{\text{r2}}(j\omega) = 20 \lg 4C_r C_r' \omega_{o.r.r.} - 20 \lg |1 + j\omega T_{n.r}|$$

The log-magnitude plot [LACHKh] is determined by the absolute magnitude of the right side of the equation:

$$L_1 = 20 \lg 4C_r C_r' \omega_{o.r.r.} - 20 \lg |1 + j\omega T_{n.r}|$$

Investigating the second term

$$20 \lg |1 + j\omega T_{n.r}|$$

having determined the point of intersection of LACHKh asymptotes and its slope, we construct the LACHKh multiplier  $\frac{1}{T_{n.r} j\omega - 1}$  and, "raising" it to the magnitude of gain  $k = 20 \lg 4C_r C_r' \omega_{o.r.r.}$ , we get LACHKh multiplier

$$\frac{4C_r C_r' \omega_{o.r.r.}}{T_{n.r} j\omega - 1}$$

The phase-angle plot (LFChKh) is determined from Table 6.1 data.

/315

In future, we will use the above table for construction of logarithmic phase-angle plots. For determination of  $\omega$ , at which given angle  $\varphi$  has significance, we will divide value  $U$  into the corresponding time constant. Meanwhile, for a  $\frac{1}{j\omega T - 1}$  type multiplier phase has a negative sign, while it has a positive sign for a  $j\omega T - 1$  type multiplier.

Due to the minor magnitudes of correction  $\delta$  to LACHKh, we will disregard it in future.

$(a)$ При $U = T_n \cdot r \omega$									
$U$	0,07	0,1	0,2	0,4	0,6	0,8	1	2	3
$\varphi_1(\omega)$	-4	-5,7	-11,3	-21,8	-31	-38,7	-45	-63,4	-71,5
$U$	4	6	8	10	20	40	60	100	
$\varphi_1(\omega)$	-76	-80,5	-82,9	-84,3	-87,1	-88,5	-89	-89,4	
$(a)$ При $\xi = 0,565$									
$U$	0,06	0,1	0,2	0,4	0,5	0,7	0,9	1	1,25
$\varphi_2(\omega)$	-3,8	-6,4	-13	-28	-36,5	-57	-79,5	-90	-112,5
$U$	2	3	5	8	10	20	30	50	100
$\varphi_2(\omega)$	-144	-158	-167,5	-171,9	-173,5	-176,9	-177,9	-178,8	-179,3

Table 6.1. Data for Construction of Phase Responses. a—When.

The transfer function is:

$$W_{\text{дд}}(p) = \frac{k_4 (T_n p - 1)}{k_5 k_1 + (T_n p - 1)(T_m p - 1)}$$

The multiplier's Bode diagram is

$$W_{\text{дд}}(p) = \frac{k_4}{k_5 k_1 + (T_n p - 1)(T_m p - 1)}$$

We convert this expression's denominator:

/316

$$\begin{aligned} k_5 k_1 + (T_n p - 1)(T_m p - 1) &= k_5 k_1 + T_n T_m p^2 + T_n p + T_m p + 1 = \\ &= [T_n T_m p^2 + (T_n + T_m) p + 1 + k_5 k_1] (1 + k_5 k_1) = \\ &= \left[ \frac{T_n T_m}{1 + k_5 k_1} p^2 + \frac{T_n + T_m}{1 + k_5 k_1} p + 1 \right] (1 + k_5 k_1) = \\ &= \left[ \frac{(1 - k_5 k_1) T_n T_m}{(1 + k_5 k_1)^2} p^2 + \frac{T_n + T_m}{1 + k_5 k_1} p + 1 \right] (1 + k_5 k_1). \end{aligned}$$

We will designate

$$1 + k_5 k_1 = a; T_{z, n} = \frac{T_n}{a}; T_{z, m} = \frac{T_m}{a},$$

then, the denominator will take the form

$$(a T_{z, n} T_{z, m} p^2 + T_{z, n} p + T_{z, m} p + 1) a.$$

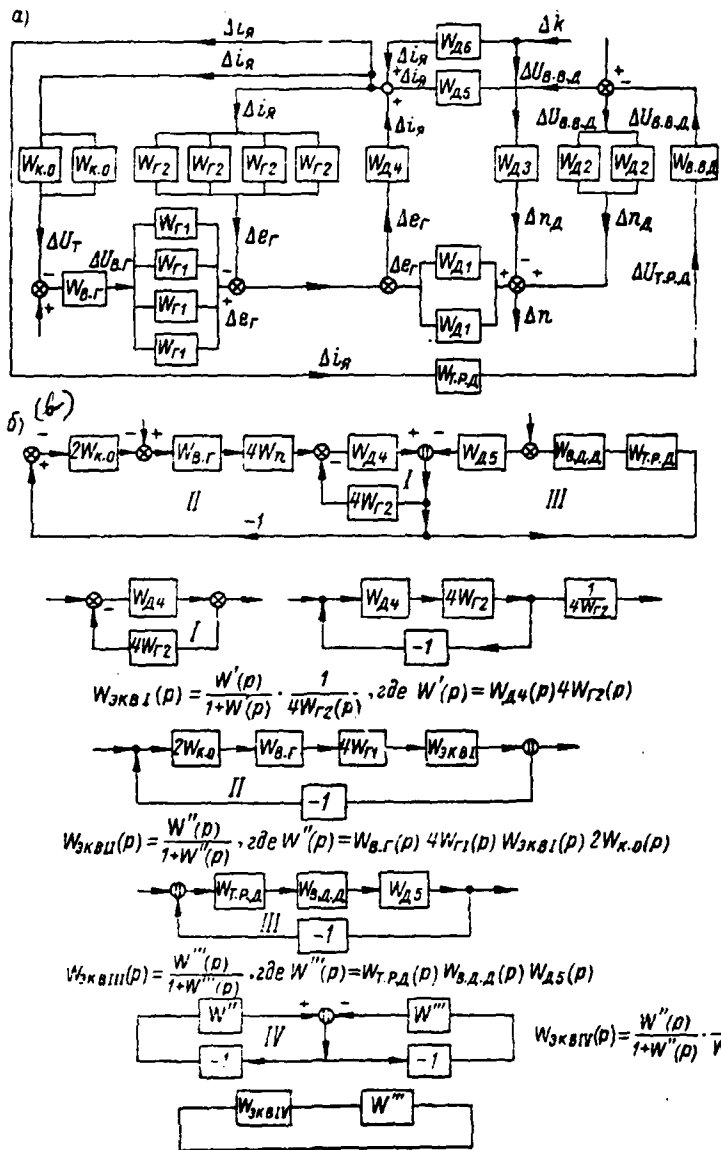


Figure 6.33. Structural Control Systems: a—Structural diagram of the entire system; b—Structural diagrams of the conversion.

We designate

$$aT_{n.3}T_{u.3} = c^2; \quad c = \sqrt{aT_{n.3}T_{u.3}};$$

$$T_{n.3} + T_{u.3} = c_3\xi,$$

where

$$\frac{T_{n.3} + T_{u.3}}{2c} = \xi; \quad k_4 = \frac{k_4}{a}.$$

Following the accepted designations

$$aT_{n.3}T_{u.3}p^2 + (T_{n.3} + T_{u.3})p + 1 = c^2p^2 + c_3\xi p + 1.$$

Now we get an expression convenient for construction of Bode diagrams:

$$W_{24}(p) = \frac{k_4^*}{aT_{\pi,3}T_{\mu,3}p^2 + (T_{\pi,3} + T_{\mu,3})p + 1} = \frac{k_4^*}{c^2p^2 + c_2^*p + 1}$$

The transfer locus is:

$$W_{24}(j\omega) = \frac{k_4^*}{aT_{\pi,3}T_{\mu,3}(j\omega)^2 + (T_{\pi,3} + T_{\mu,3})j\omega + 1} = \frac{k_4^*}{c^2(j\omega)^2 + c_2^*j\omega + 1}$$

The amplitude-ratio response is:

$$L_2 = 20 \lg k_4^* - 20 \lg |aT_{\pi,3}T_{\mu,3}(j\omega)^2 + (T_{\pi,3} + T_{\mu,3})j\omega + 1|$$

When  $\omega \ll 1$ , we have

$$20 \lg |aT_{\pi,3}T_{\mu,3}(j\omega)^2 + (T_{\pi,3} + T_{\mu,3})j\omega + 1| \approx 20 \lg 1 = 0,$$

but, when  $\omega \gg 1$ , disregarding the unit, we get

$$20 \lg |aT_{\pi,3}T_{\mu,3}\omega^2 + (T_{\pi,3} + T_{\mu,3})j\omega|$$

Disregarding value  $T_{\pi,3}$  as compared to  $c T_{\mu,3}$ , we get

$$20 \lg |T_{\mu,3}\omega^2 + a^2T_{\pi,3}^2T_{\mu,3}\omega^4| = 20 \lg |T_{\mu,3}\omega^2(1 + a^2T_{\pi,3}^2\omega^2)|$$

Again disregarding the unit, we have

/317

and, when  $\omega = \frac{1}{T_{\mu,3}T_{\pi,3}a^2}$ , we get  $20 \lg 1 = 0$  (i. e., we get the point of intersection of LACHKh asymptotes).

Phase-angle plot  $\varphi_2$  will be constructed from data present in Table 6.1 (given calculated value  $\xi = 0,565$ ). Since  $U = c\omega$ , we will get values  $\omega$ , with division  $U/c$ , for which values  $\varphi$  for type multipliers have a negative sign, while those of this type  $c^2(j\omega)^2 + c_2^*j\omega + 1$  have a positive sign.

The Bode diagram of multiplier  $T_{\mu}p - 1$   $L_3 = 20 \lg |T_{\mu}\omega^2 - 1|$  has a point of intersection with the X-axis  $\omega = \frac{1}{T_{\mu}}$ . Response  $\varphi_3$  will be constructed from tabular data [10, 72].

Adding the LACHKh and LFChKh of multipliers  $L_1, L_2, L_3$  and  $\varphi_1, \varphi_2, \varphi_3$ , we get resultant open system LACHKh  $L'$  and LFChKh  $\varphi'$  (Figure 6.34), from the compilation of which it follows that the open system is stable and, consequently, so is the closed system.

The latter occurs because, given a crossover frequency, the phase shift is  $154^\circ$ . Consequently, this system's locus does not encompass the critical point with coordinates  $(-1; j0)$ .

Using a nomogram for determination of a closed system's amplitude-ratio

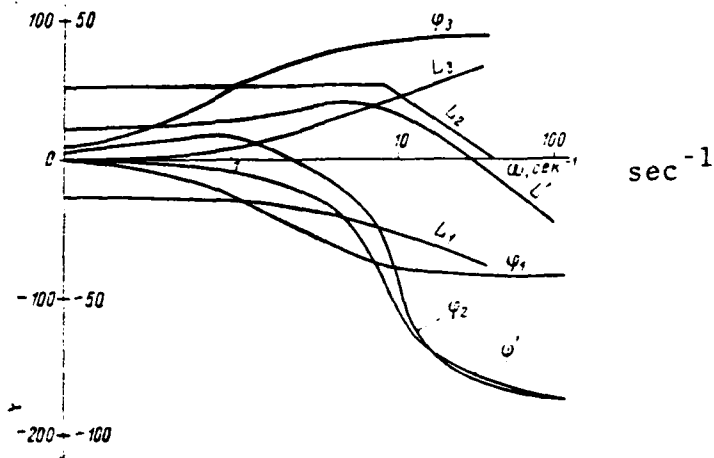


Figure 6.34. Control System Link (Loop I) Bode Diagrams.

$\omega, \text{сек}^{-1}$ (a)	0.1	0.3	0.4	0.6	0.1	1	2	3	4.6	6
$L'(\omega), \text{дБ}$ (b)	11	11.5	12	12.6	13	14	16.5	18.5	20	19.6
$\varphi'(\omega), \text{град}$ (c)	6	12	13.8	16	16	14	3	-9	-24	-38
$B_1(\omega), \text{дБ}$ (b)	-2.15	-2	-1.62	-1.8	-1.75	-1.6	-1.2	-0.95	-0.76	-0.72
$\psi_1(\omega), \text{град}$ (c)	1.2	2.6	2.5	3.2	3	2.3	0	0	-2.1	-3.5
$\omega, \text{сек}^{-1}$ (a)	8	10	12	14	16	20	24	30	50	80
$L'(\omega), \text{дБ}$ (b)	18	16	12.5	10	7.5	3.8	0	-4	-12.5	-21.3
$\varphi'(\omega), \text{град}$ (c)	-62	-30	-123	-132	-140	-149	-155	-161	-169	-174
$B_1(\omega), \text{дБ}$ (b)	-0.55	-0.12	1.07	1.65	2.7	5.1	7.82	2.75	-10.5	-20.5
$\psi_1(\omega), \text{град}$ (c)	-6	-9	-12.5	-17	-22	-37	-78	-132	-165	-174

Table 6.2. a—sec<sup>-1</sup>; b—дБ; c—град

and phase responses, based on the open system's transfer locus we will /319  
 construct the closed system's LChKh  $B_1$  and LFChKh  $\psi_1$  (Figure 6.35a), whose  
 transfer locus equals

$$\frac{W_{d0}(j\omega) 4W_{r2}(j\omega)}{1 + W_{d0}(j\omega) 4W_{r2}(j\omega)} \cdot \frac{1}{4W_{r2}(j\omega)}$$

Next, composing them from the LChKh ( $L_4$ ) and LFChKh ( $\varphi_4$ ) of the multiplier  $\frac{1}{4W_{r2}(j\omega)}$ , we get LChKh  $A_1$  and LFChKh  $\varphi_1$  of the SAR loop I (Figure 6.35a).

Bode diagrams  $L_4$  and  $\varphi_4$  of multiplier  $\frac{1}{4W_{r2}(j\omega)}$ , are constructed as a mirror image of diagrams  $L_1$  and  $\varphi_1$  of multiplier  $4W_{r2}(j\omega)$ .

Loop II Bode diagrams. The transfer function is:

$$W_{\text{кв II}}(\rho) = \frac{W_{\text{н.г}}(\rho) 4W_{r1}(\rho) W_{\text{кв I}}(\rho) 2W_{\text{к.о}}(\rho)}{1 + W_{\text{н.г}}(\rho) 4W_{r1}(\rho) W_{\text{кв I}}(\rho) 2W_{\text{к.о}}(\rho)} = \frac{W''(\rho)}{1 + W''(\rho)}$$

The transfer locus is:

$$W_{\text{кв II}}(j\omega) = \frac{W''(j\omega)}{1 + W''(j\omega)} = \frac{W_{\text{н.г}}(j\omega) 4W_{r1}(j\omega) W_{\text{кв I}}(j\omega) 2W_{\text{к.о}}(j\omega)}{1 + W_{\text{н.г}}(j\omega) 4W_{r1}(j\omega) W_{\text{кв I}}(j\omega) 2W_{\text{к.о}}(j\omega)}$$

The Bode diagram of multiplier  $W_{\text{н.г}}(j\omega) = \frac{k_x}{T_x j\omega + 1}$  has the form

$$L_5 = 20 \lg k_x - 20 \lg |T_x j\omega + 1|$$

For  $\omega \ll 1$

$$20 \lg |T_x j\omega + 1| \approx 20 \lg 1 = 0.$$

For  $\omega \gg 1$

$$20 \lg |T_x j\omega + 1| = 20 \lg T_x \omega.$$

The point of intersection of LChKh asymptotes for  $\omega \ll 1$  and  $\omega \gg 1$  occurs when  $\omega = 1/T_x$ .

The phase-angle plot will be constructed from tabular data (Table 6.3). Here,  $\varphi_5$  is determined for given value  $T_x$ .

The Bode diagram of multiplier

$$4W_{r1}(j\omega) = \frac{4k_3}{T_{\text{н.г}} j\omega + 1}$$

has the form

$$L_6 = 20 \lg 4k_3 - 20 \lg |T_{\text{н.г}} j\omega + 1|$$

For  $\omega \ll 1$ , we have

$$20 \lg |T_{\text{н.г}} j\omega + 1| = 20 \lg 1 = 0,$$

and for  $\omega \gg 1$

$$20 \lg |T_{\text{н.г}} j\omega + 1| \approx 20 \lg T_{\text{н.г}} \omega.$$

/321

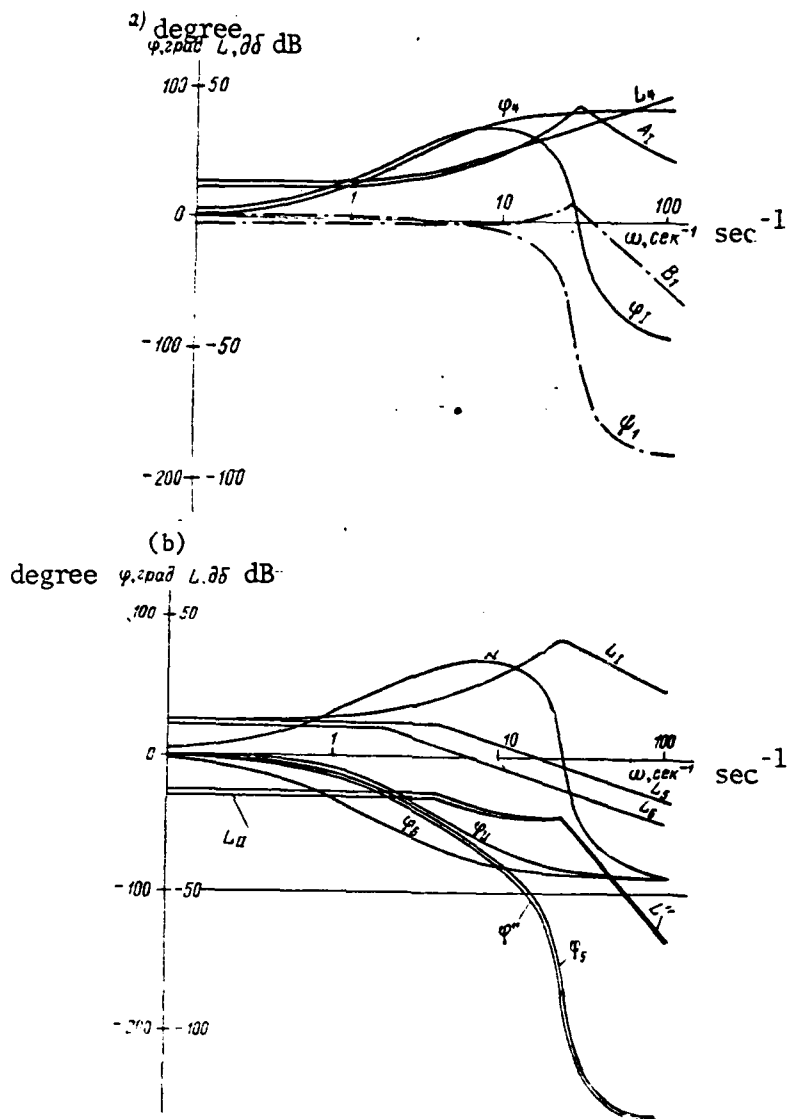


Figure 6.35. Bode Diagrams: a—Closed control system (loop I) resultant LChKh; b—Loop II Bode diagrams.

The LACHKh point of change is

$$\omega = \frac{1}{T_{\text{в.р.}}}$$

The phase-angle plot will be constructed in accordance with tabular data (Table 6.3). Meanwhile,  $\varphi_0$  is determined for given value  $T_{\text{в.р.}}$ . The Bode diagram of multiplier

$$2W_{\text{к.о}}(j\omega) = 2k_{13}$$

has the form

$$L_7 = 20 \lg 2k_{13}$$

The phase response is

$$\varphi_7 = 0,$$

since this link's transfer locus is only gain, while the magnitude of the gain does not affect phase shift.

$\omega, \text{сек}^{-1}$ (a)	0,5	1	1,6	2	2,5	3	4	5
$L''(\omega), \text{дБ}$ (b)	-13	-13	-13	-13	-13	-13	-13,5	-15
$\varphi''(\omega), \text{град}$ (c)	-4	-10	-20	-25	-32	-38	-47	-54
$L_{11}(\omega), \text{дБ}$ (b)	-14,8	-14,8	-14,8	-14,8	-14,7	-14,6	-14,8	-16
$\varphi_{11}(\omega), \text{град}$ (c)	-3	-8	-16	-20	-26	-31	-39	-48
$\omega, \text{сек}^{-1}$ (a)	7	9	12	16	20	25	30	50
$L''(\omega), \text{дБ}$ (b)	-18	-19	-20,5	-21,5	-22	-22	-30	-45
$\varphi''(\omega), \text{град}$ (c)	-66	-74	-86	-101	-118	-154	-220	-250
$L_{11}(\omega), \text{дБ}$ (b)	-19	-19,2	-20,5	-21,5	-22	-22	-30	-45
$\varphi_{11}(\omega), \text{град}$ (c)	-59	-67	-80	-96	-114	-152	-220	-250

Table 6.3. Data for Construction of Closed Loop Responses. a-- $\text{sec}^{-1}$ ; b--дБ; c--deg.

Adding the Bode diagrams of all links comprising the second loop, we get resultant Bode diagrams  $L''$  and  $\varphi''$  (Figure 6.35b). Analyzing them, we come to the conclusion that the closed loop is stable since the open loop has a large stability reserve. However, this loop's gain is very small, resulting in this turning out not to be a good quality of the control system.

The closed loop's responses  $L_{11}$  and  $\varphi_{11}$  (Table 6.3 and Figure 6.35b) will be constructed from extant open loop responses.

Loop III Bode diagrams. The transfer function is:

$$W_{\text{зкв III}}(p) = \frac{W^*(p)}{1 + W^*(p)} = \frac{W_{\text{в.з.д}}(p) W_{\text{т.д}}(p) W_{\text{дз}}(p)}{1 + W_{\text{в.з.д}}(p) W_{\text{т.д}}(p) W_{\text{дз}}(p)}$$

The transfer locus is:

$$W_{\text{зкв III}}(j\omega) = \frac{W^*(j\omega)}{1 + W^*(j\omega)} = \frac{W_{\text{в.з.д}}(j\omega) W_{\text{т.д}}(j\omega) W_{\text{дз}}(j\omega)}{1 + W_{\text{в.з.д}}(j\omega) W_{\text{т.д}}(j\omega) W_{\text{дз}}(j\omega)}$$

Determination of the multipliers' Bode diagrams and construction of LACHh

and LFChKh for loop III are analogous to that described above for loops I and II.

Construction of Bode diagrams from transfer function  $W_{\text{зкв IV}}(p)$ :

$$W_{\text{зкв IV}}(p) = \frac{W^*(p)}{1 + W^*(p)} \cdot \frac{1}{W^*(p)}$$

These closed system responses are designated  $B_4$  and  $\psi_4$  in Figure 6.36a. Adding them to the responses of multipliers  $\frac{1}{W^*(p)}$ ,  $-\psi^*$  and  $\frac{1}{L^*}$ , we will construct responses  $L_{IV}$  and  $\varphi_{IV}$ . It follows from the construction that  $L_{IV} = 0$  and  $\varphi_{IV} = 0$ , i. e., the stability of the GEU middle loop's SAR is determined only by loop III.

Loop II, stable in and of itself, does not influence the stability of the entire SAR.

Next, breaking the loops with transfer functions  $W_{\text{зкв IV}}(p)$  and  $W^*(p)$ , we will construct the Bode diagrams of the entire open SAR:  $L^*$  and  $\Phi^*$  (Figure 6.36b). Here,  $W^*(j\omega)$  — is the transfer locus of the open system

$$W^*(p) = W_{\text{в.д.д}}(j\omega) W_{\text{т.р.д}}(j\omega) W_{\text{дб}}(j\omega) W_{\text{д.к}}(j\omega)$$

and, correspondingly,  $\Phi^*$  is the open system's phase response.

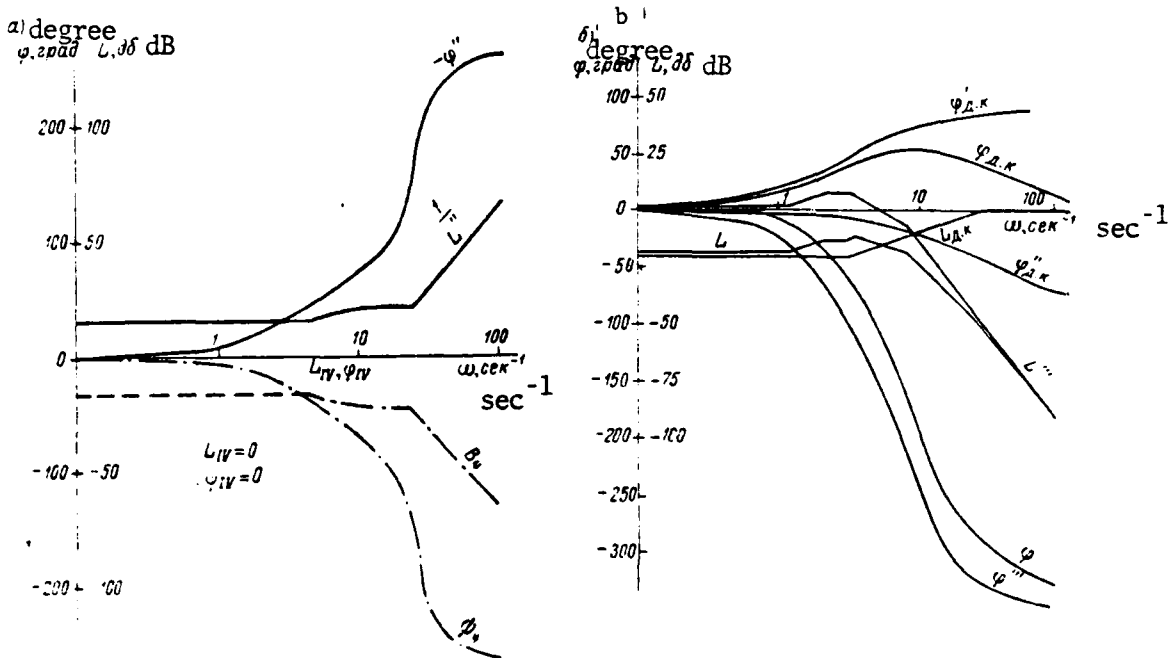


Figure 6.36. Bode Diagrams: a—Closed control system; b—Considering the stabilizing loop.

The designations in Figure 6.36b are:  $L_{\text{д.к}}$  and  $\varphi_{\text{д.к}}$  the stabilizing loop's frequency response. Here, response  $\varphi_{\text{д.к}}$  is constructed for values  $T = T_{\text{д.к}}$  и  $\varphi'$  and  $\varphi''$  for values  $T = \frac{\alpha}{T_{\text{д.к}}}$ , where  $\alpha = \frac{R_1 + R_2}{R_2}$ ;  $R_1$  and  $R_2$  are differentiating loop resistances ( $R_2$  is determined by the amount of magnetic amplifier control master winding resistance).

Thus, an icebreaker's automatic control system satisfies the stability condition since the phase shift comprises in our example  $160^\circ$  and the locus of this system does not enclose the critical point with coordinates  $(-1, j0)$ . However, as a result of a small stability reserve, the requirement to add a stabilizer is evident.

Transient Processes in Direct Current Electrical Propulsion Plants  
(Theory, Analytical, and Graphic-Analytical Calculation Methods)

§ 7.1 Purpose of the Calculations and Special Features  
of Transient Processes

Determination of transient processes in GEU and their significance for insuring the maneuvering qualities of electric ships. The operation of any, including propulsion, plant or electric drive system is characterized by its conduct in established and transient modes. Transition from one established operating mode or equilibrium state to another is accompanied by specific phenomena occurring in mechanical, electrical, and hydrodynamic elements of the plant (system). These phenomena arising as a result of a change in external effects on the system, as well as the changes within it, are called transient processes.

During the course of transient processes, the operation of specific GEU elements is characterized by extraordinarily large, and in some cases excessive, indicators. Introduction of automatic control elements into a propulsion plant system manifests itself clearly in the nature of the transient processes: on the one hand, it makes it possible to avoid the appearance of intolerable modes. On the other hand, it may lead to appearance of some undesirable phenomena.

Thus, transient processes occurring in automated electric propulsion /325 plants are complex and require comprehensive study and the ability to predetermine them by means of calculations. A special section of propeller electric drive theory, electric propulsion plant dynamics, will be devoted to study of the objective laws to which transient processes in different electrical propulsion plant systems are subordinate and methods of acting upon them.

All ships with propeller electric drives can be subdivided into the following groups depending on the role the transient processes play in insuring the appropriate maneuvering qualities:

1. Ships operated on prolonged voyages with fixed machinery operating modes. Time these ships spend in moored operations is insignificant compared



with total ship operating time. It is presumed that such ships do make frequent port calls and the time they navigate in narrows, canals, and the like is minimal. This category includes large ocean-going dry cargo ships, large-displacement tankers, passenger liners, and so on.

2. Ships which spend significant amounts of time in moored and other maneuvering operations, i. e., ships with radically changing machinery operating conditions. This category includes tugs, ferries, floating cranes, ships intended for mixed ocean and river navigation, dredges, floating docks, trawlers, seiners, and so on.

3. Ships whose normal activities call for maneuvering modes. Their machinery operates in transient modes for extended periods of time. This category includes icebreakers and active ice navigation vessels, harbor and special tugs, and so on.

There are instances when ships in the first two categories have such high demands for safe navigation placed on their maneuvering characteristics that they should be relegated to the third category.

Origin and nature of the course of transient processes. The course and duration of a transient process are determined both by the nature and the special features of the electrical propulsion plant system, in particular by the number and magnitudes of lags the system possesses. Machinery and system time-lag properties are rated by a so-called time constant, the magnitude of which, measured in seconds, depends on the basic indicators of propeller electric drive machinery, shafting line, propeller, and water entrapped by the screw. The following time constants exist: electromechanical, electromagnetic, and thermal, designations corresponding to the types of inertias involved.

The onset of transient processes in an electrical propulsion plant is caused, on the one hand, by a change of electromagnetic energy in its electrical /326 circuits and, on the other, by a change in the kinetic energy of the gyrating masses of the main propulsion motor, shafting line, propeller, and the water entrapped by the screw during the time of transition from one established mode to another. Here, either accumulation or expenditure of accumulated energy occurs in the system, with the duration of the transient process over time depending on the ratios of system parameters.

In a main propulsion motor transient process condition, changes in its rotational speed, accelerations, current, voltages, and other indicators occur simultaneously. It is very important for a GEU transient process to flow stably, i. e., that an electric propellor drive come to a new state of equilibrium or stable state following a period of disturbance. This will take place if the controlled magnitude during the transient process changes, for example, following an exponential curve, approximating the established value or when the controlled parameter changes, achieving aperiodic damped oscillations. A controlled magnitude during an unstable transient process increases without constraint over time, either increasing in accordance with an aperiodic law or achieving oscillations with increasing amplitude. A transient process also can occur in the form of undamped oscillations. Such a process is the boundary between a stable and unstable process and is unacceptable for GEU systems.

Actually, transient processes in an electrical propulsion plant take a more complex form due to the complex combination of electromagnetic, electro-mechanical, and hydrodynamic characteristics of electric propellor drive system elements.

Besides transient process duration, velocity and acceleration oscillations causing the onset of mechanical stresses in the electric propellor drive, current bumps, losses of energy, and associated generator and main propulsion motor heating also occur here. The magnitude of parameter overshoot relative to tolerable values is significant.

Requirements levied on the nature of transient processes when designing GEU. During early development of electrical propulsion plants, the main indicator for main propulsion motor power selection was power determined from static characteristics, i. e., from the prolonged load mode. Today, things are different. Selection of main propulsion motor power and the form of its mechanical characteristic to a significant degree are determined by the system's conduct during transient processes due to the great complexity of propellor electric drive control circuits and introduction of automated elements, especially for icebreakers, active ice navigation vessels, and tugs. The problems to be solved here include not only the link between plant transient processes and electric ship maneuvering properties, but also the problem of system stability, the /327 quality of the transient process course, and selection of correctional methods.

Specific requirements are levied relative to maximum permissible currents, accelerations, rotational speeds, torque overload capability, and so on when designing a main propulsion motor and shafting line, just as for the transient processes occurring in an electric propellor drive.

Individual operations in modern electric propulsion plants and the transient processes occurring in them must be carried out, where possible, in short time intervals with constrained overload norms for electrical machinery, primary motors, and the system as a whole. Achievement of the minimum time for propellor racing, reversing, and braking is linked on the one hand with an increase in accelerations. On the other hand, it is tied in with the special hydraulic features of shipboard propulsion equipment. However, reliability considerations and safe plant operation dictate definitive constraints relative to tolerable mechanical and electrical loads and overloads.

Besides this, the problem of obtaining optimal accelerations can not be solved rationally without consideration of plant primary motor characteristics.

In several instances, requirements levied on electrical propulsion plants involve not only high speed, i. e., main propulsion motor acceleration and reversing time and the number of reversals per hour, but also relative to fulfillment of special conditions such as operating conditions based on the law of power constancy or torque when navigating in ice or in open water, during movement with and without cargo, during navigation of vessels with different drafts, and so on.

Electrical propulsion plant design and proper operation most completely satisfying very diverse and sometimes even contradictory requirements are impossible without the knowledge and ability, through calculations, to predetermine all phenomena occurring during the transient processes.

Investigation of transient processes provides the capability, with the requisite completeness, to reveal the conduct of generators, main propulsion motors, and primary motors, to achieve their optimum use, and to establish the necessity for introduction of changes for the purpose of improving main generator, main propulsion motor, and excitation system characteristics.

Study of electric propellor drive transient processes for the purpose of determining starting, braking, and reversal duration, duration of the transition from one state to another, as well as to obtain data required for construction of so-called load diagrams, i. e., when establishing the relationships of torque, power, current, and main propulsion motor rotational speed to time:  $\bar{m}_x = f_1(t)$ ;  $\bar{p}_x = f_2(t)$ ;  $\bar{i}_x = f_3(t)$ ;  $\bar{n}_x = f_4(t)$ , is of great significance.

Figures 7.1 and 7.2 show the curves of the transient processes of the /328 dry cargo vessel "Dneproges" GEU during a reversal in open water. The hatched areas correspond to the overload energy of generator G2 (Figure 7.1) and generator G3 (Figure 7.2), as well as to the recuperation energy. Curves  $i_n = f(t)$  make it possible to discover the conduct of protected equipment during overcurrents, machinery commutation, voltage drop, and so forth. From curves  $\bar{m}_x = f(t)$  and  $\bar{i}_n = f(t)$  one can judge generator and main propulsion motor heating. Curve  $\bar{n}_x = f(t)$  can be used to determine acceleration and mechanical stresses in individual plant elements, and, finally, use of these characteristics permits solution of the problem of determining the maneuvering characteristics of the vessel itself, considering the dynamic characteristics of the electric propellor drive.

Transient process load diagrams reveal both instantaneous electric propellor drive overloads and the circumstances of its heating.

Study of the transient processes in automated electric propellor drive circuits being used more and more widely in contemporary electric ships is of exceptionally important significance.

Purpose of the calculations and mathematical description of the transient processes in GEU. Complete analysis of transient processes provides the capability:

- to select, for a propellor drive, the optimal combination of main propulsion motor mechanical (operating and maneuvering) characteristics and propellor hydrodynamic characteristics;
- to find the most improved principles of automatic electric propulsion plant control from the point of view of primary motor, generator, and main propulsion motor utilization;
- to establish specific requirements for control equipment, primary motor governors, and other links in the automated electric propellor drive system.

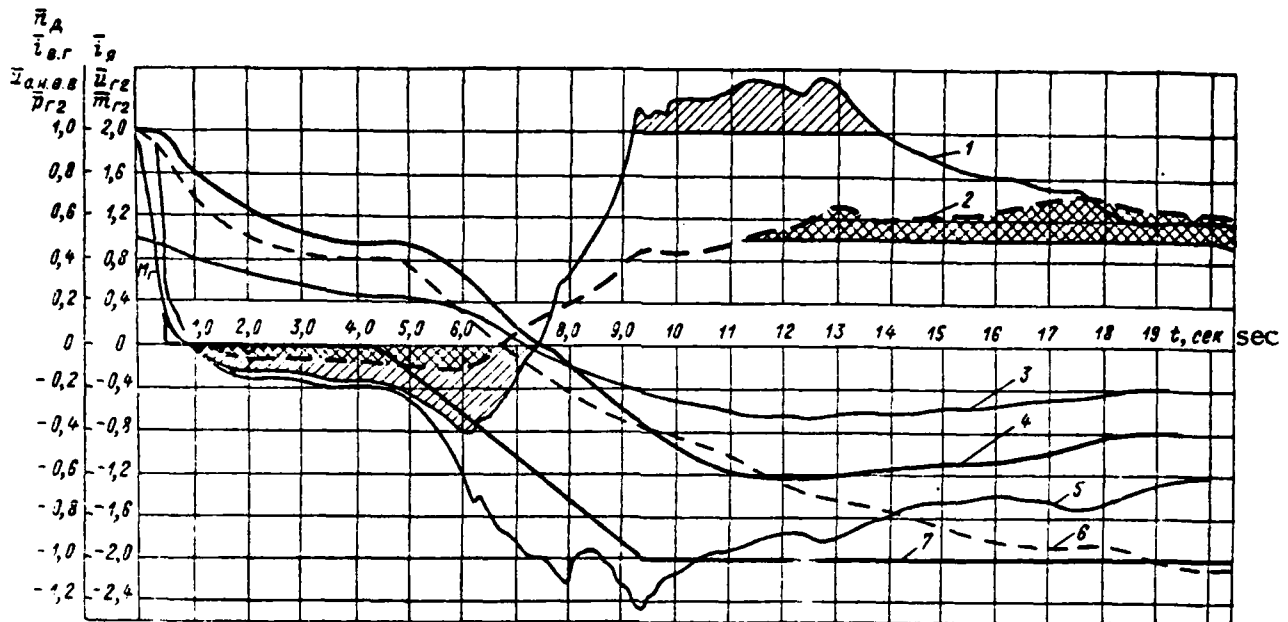


Figure 7.1. Dry Cargo Ship "Dneproges" GEU Transient Processes During Reverse. 1—Generator power change curve  $\bar{p}_{r2}$  ; 2—Generator torque change curve  $\bar{m}_{r2}$  ; 3—GED rotational speed change curve  $\bar{n}_1$  ; 4—Generator voltage change curve  $\bar{u}_{r2}$  ; 5—Main circuit current change curve  $\bar{i}_a$  ; 6—Generator excitation change curve  $\bar{u}_{e1}$  ; 7—Exciter independent field winding voltage change curve  $\bar{u}_{e1}$  .

Theoretical examination of the transient processes of modern electric propellor drives considering all factors impacting on them in many cases is exceptionally difficult.

In the most general form, transient processes can be described mathematically by a system of nonhomogeneous nonlinear differential equations with variables. This equation system can be reduced to one differential equation, the order of which turning out to be rather high. In addition, analytical solution of such an equation is complicated by the presence of a considerable number of significant nonlinearities. In several instances, solution even turns out to be impossible.

It is possible to bring the system of differential equations to a linear

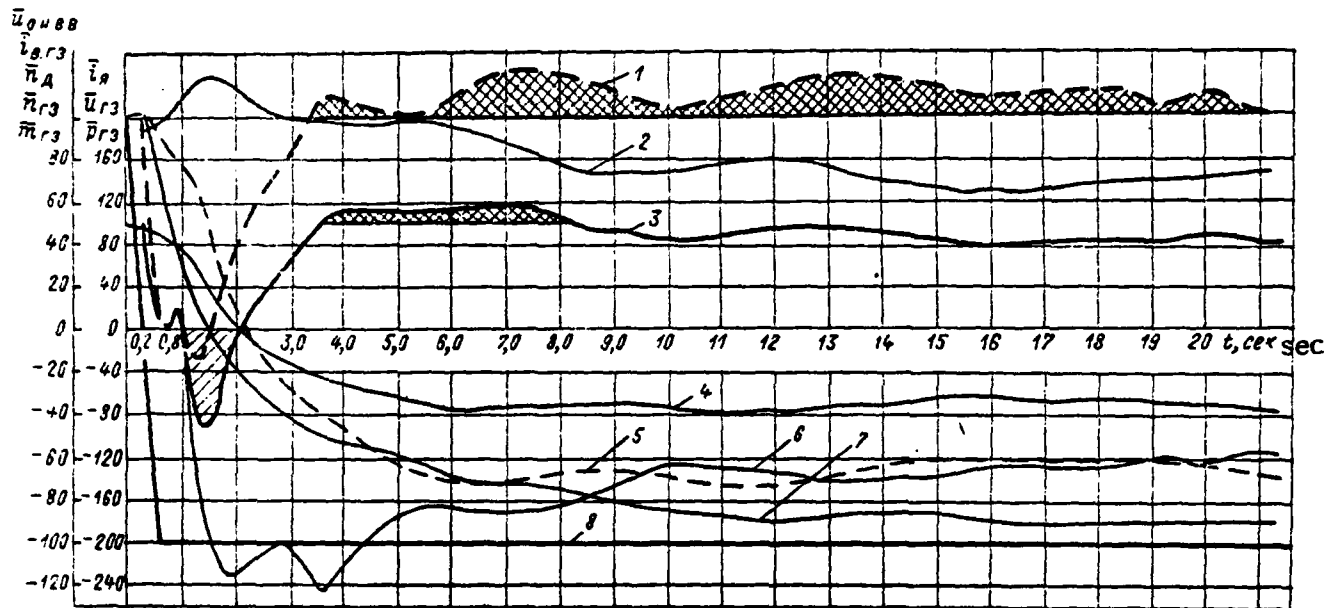


Figure 7.2. Dry Cargo Ship "Dneproges" GEU Transient Processes During Reverse and Rapid Transposition of a Control Station Lever. 1—Generator torque curve  $\bar{m}_{r3}$  ; 2—Generator rotational speed change curve  $\bar{n}_{r3}$  ; 3—Generator power change curve  $\bar{p}_{r3}$  ; 4—Generator voltage curve  $\bar{u}_{r3}$  ; 5—GED rotational speed curve  $\bar{n}_2$  ; 6—Armature circuit current change curve  $\bar{i}_{a,r3}$  ; 7—Generator field current change curve  $\bar{i}_n$  ; 8—Generator exciter field independent winding voltage change curve  $\bar{u}_{o.n.p.}$  .

form at the stage of preliminary calculations for certain electrical propulsion plant circuits. Physically, this signifies that, in a qualitative sense, the nature of the processes occurring in a system will not depend here on their intensity.

Calculation of the transient processes requires a knowledge of the /331 hydrodynamic characteristics of the propellor and the vessel's hull and the electric propellor drive's electromechanical characteristics.

The parameters of an electric propellor drive, which consists of primary motors, generators, main propulsion motors, and exciters, are provided with sufficient accuracy: at the first stage by calculation data and at the second

stage by plant bench test data. Propellor properties are expressed by a family of hydrodynamic characteristics representing the relationship of propellor moment of resistance and thrust to the velocity of its rotation at different vessel translational speeds. The degree of reliability of these characteristics is not always high since it is impossible to consider all factors influencing them.

During design of electrical propulsion plants, especially in its first stage, as well as during their operation, it is permissible to solve complex problems involving calculation of transient processes considering only the basic factors influencing their character, disregarding factors of secondary significance. One can find an engineering method of solving assigned problems only under these conditions. In particular, for example, we will be able to consider the degree of nonuniformity of primary motor governors only in certain cases.

All variables except time will be expressed in relative values, with either nominal values or values of variables during a short circuit assumed as the base values.

Calculated predetermination of transient processes in dc electric propulsion plants is accomplished by analytical and graphical methods developed relative to GEU and by a method of mathematical and combined modelling.

The most promising of the analytical methods are an approximate calculation based on frequency responses and an engineering method based on a body of mathematics using approximation by iteration widely-used for circuits, the transient processes in which describable by nonlinear differential equations not exceeding the fifth order.

The foundations of the theory of transient processes in dc GEU and their engineering calculation based on the aforementioned two analytical methods and a graphic-analytical method are presented below relative to such systems. The most general and undoubtedly most promising is a method based on use of analog computers and combined modelling. These methods are presented separately in Chapter 8 and illustrated by examples of calculation of complex GEU circuits.

Combined modelling is the term used to describe a method based on use of physical modelling of main circuit circuitry and mathematical modelling of GED control and load systems.

§ 7.2 The Process of Starting and Reversing  
a Direct Current Electric Drive

/332

Starting the main propulsion motor. After the GEU circuit has been set up, the main propulsion motor is started by rearrangement of the control post lever from the zero position to any position corresponding to a main propulsion motor specific rotational speed or to a specific power (the control station layout into positions can be accomplished based on one of the aforementioned principles). Since main propulsion motor acceleration occurs during a time incommensurably less than the time of vessel acceleration, it then is possible approximately to consider that propellor racing occurs on a non-moving ship, i. e., it occurs based on the moored characteristic. Therefore, the control station lever should not immediately be set to the position corresponding to full speed since, in the moored characteristic, torque considerably exceeding the nominal corresponds to propellor full rotational speed (nominal). Overload of the main propulsion motor, generator, and primary motor is unavoidable in this starting method.

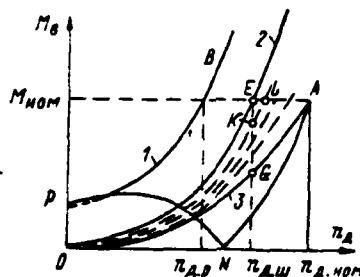


Figure 7.3. Propellor Static Characteristics. 1—Reverse (curve BPNA); 2—Moored; 3—Basic.

The velocity to which a main propulsion motor can be accelerated for a stationary vessel is determined by value  $n_{н.н}$  corresponding to nominal torque in the moored characteristic (Figure 7.3).

Propellor moment of resistance decreases as the vessel accelerates under the effect of main propulsion motor torque. Decrease in propellor moment of resistance during the transition to an intermediate characteristic to point K is accompanied by a corresponding decrease in main circuit current. The capability then arises for a further increase in the rotational speed of control station lever rearrangement to a new position until main circuit current reaches the nominal value. This new mode corresponds to point L. Consequently, gradually increasing propulsion motor rotational speed, it is possible to accomplish the start at the nominal current value. Here, the propellor will operate sequentially at points E, L, ..., A, i. e. will transition from one characteristic to another along straight line ELA.

Starting also can be accomplished given presence of powerful and rapid /333 enough main circuit current feedback and given rapid transposition of the control station lever from the zero position to "full ahead."

The propellor line (main propulsion motor, propellor shaft, screw, and water entrapped by the screw) mechanical time constant is incommensurable with the exciter field circuit and generator electromagnetic time constant. Therefore, a simultaneous increase in generator emf and main propulsion motor rotational speed occurs.

Starting occurs with considerable overcontrol in GEU with automated electrical machinery in field systems thanks to very high speed and gain. And, in spite of the presence of main circuit current feedbacks, considerable primary motor overloads can occur during starting.

Reversing the main propulsion motor. Reversal of the main propulsion motors in dc electrical propulsion plants is accomplished by turning the control station lever from the "ahead" to the "astern" position. Here, just as during starting, one should not bring propulsion motor rotational speed in the opposite direction to the nominal value since torque exceeding the nominal by several factors corresponds in the reversing characteristic to negative nominal rotational speed. Therefore, rotational speed in the opposite direction is constrained by value  $n_{d.p}$ , which corresponds to nominal torque in the screw's reversing characteristic. The consideration is that screw reversal for a stationary vessel occurs based on the moored characteristic.

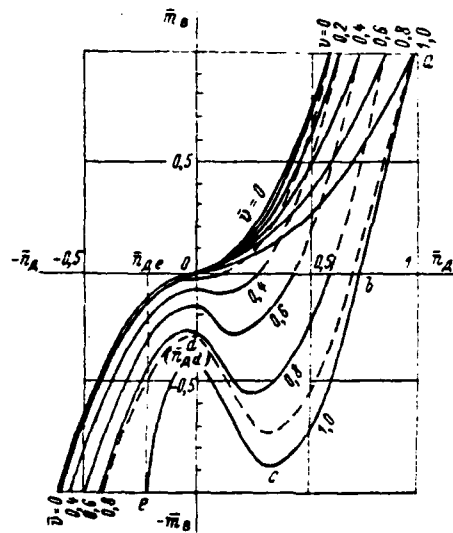


Figure 7.4. Relationship of Water Moment of Resistance to Ship Movement to Propellor Rotational Speed During Reversal.

We will describe the nature of the process during a reversal. The screw moment of resistance and velocity of its rotation will change in accordance with section *ab* (Figure 7.4) of the example reversal characteristic during the decrease to zero of the torque applied to the main propulsion motor of a vessel underway ahead at nominal speed. The propellor begins to develop negative moment of resistance (i. e. propelling torque) when rotational speed decreases further. In this mode, the screw operates on the water turbine principle in section /334 *bcd*. It is assumed here that vessel speed remains constant and equals  $\bar{v} = 1$  (in relative units). When screw rotational speed equals zero, its torque is expressed by section *od*. The screw will develop reverse-direction speed in section *de* given fixed forward speed equalling  $\bar{v} = 1$ . In actuality, vessel speed during main propulsion motor reversal will drop and the operation of the screw will occur with a gradual transition from curve  $\bar{v} = 1$  to curves  $\bar{v}_1 = 0.99$ ;  $\bar{v}_2 = 0.98$ , and so forth.

Most effective braking requires that the screw pass through section *abcd* as rapidly as possible (i. e., it will reach  $\bar{n}_x = 0$  developing with a certain negative speed  $\bar{n}_{xe}$  nominal braking torque and the corresponding braking thrust (here, the main propulsion motor will operate with nominal current and a certain speed  $\bar{n}_{xe} < \bar{n}_{x, nom}$ ). Screw operation will be characterized by a gradual transition

to operation based on reversal characteristics at vessel speeds of  $\bar{v} = 0,91$ ;  $\bar{v} = 0,9$  and so forth as the vessel's forward speed decreases, with gradually increasing propellor rotational speed. The limit will be the operating mode based on the moored characteristic ( $\bar{v} = 0$ ), since the vessel here is expending its kinetic energy of translational motion forward. It should be kept in mind that it is advisable to develop nominal braking torque at speed  $n_{2r}$  of the screw reversal curve, since:

— it is inadvisable to brake a vessel when the screw is operating in the reversal curve in the lower right quadrant since the braking thrust in this area is less than nominal and drops with a decrease in vessel speed;

— in the lower right quadrant, a screw operating like a water turbine imparts the corresponding torque to the main propulsion motor. The motor, losing torque, transitions to the generator mode, imparting its kinetic energy obtained from the screw to the generator. The generator, transitioning to the motor mode, imparts its energy to the primary motor (diesel). The latter, due to its irreversibility, begins to increase rotational speed, which given known circumstances, may reach an intolerable magnitude.

The term reversal time of a main propulsion motor should be understood to mean the time occurring from the moment of transposition of the control station lever (given the absence of timing dashpots) from ahead to the moment when the main propulsion motor will develop constant (nominal) braking torque for a certain established screw reverse rotational speed.

It should be borne in mind when establishing reversal time that a very rapid reverse can initiate transient process  $\bar{i}(t)$  with intolerable main machinery overloads. Extraordinary prolongation of the transient process has a deleterious effect on the vessel's maneuvering qualities and can elicit an intolerable /335 increase in generator and primary motor rotational speed.

The example physical picture of the electrical propulsion plant reversal process presented and main propulsion motor—screw interaction during reversal lacks numerical analysis. Therefore, the numerical value of the influence of the screw's reversal characteristic on GEU transient processes is a mandatory element of calculation methodology.

§ 7.3 Methodology for Calculation of Transient Processes  
Based on Frequency Characteristics

Formulas linking transient process characteristics with frequency responses.

A frequency method developed by Soviet scientist V. V. Solodovnikov [61] relative to investigation and calculation of a broad circle of automatic control problems, investigation of control system qualities in particular, forms the foundation of the development of the frequency method of transient processes in electric propeller drive. The method makes it possible in an uncomplicated way to provide an approximate evaluation of a transient process during starting and reversal of a main propulsion motor and to determine all qualitative indicators characterizing the system. The transient process evaluation is based on use of the real frequency response of a closed system's transfer locus  $\Phi(j\omega)$  completely determining all the system's dynamic properties during the harmonic external action on the part of the load or on the part of the driving element.

We will establish the link between the transient process' curve and the closed system's frequency response, given step action.

The control process is determined by a Laplace reverse transform:

$$Z_n(t) = \frac{1}{2\pi j} \int_{-\infty}^{+\infty} \Phi(p) \frac{F}{p} e^{pt} dp.$$

If we relate function  $Z_n(t)$  to the value of a unitary function at input  $F$ , we get the expression for the transfer function

$$\varphi(t) = \frac{Z_n(t)}{F} = \frac{1}{2\pi j} \int_{-\infty}^{+\infty} \Phi(p) \frac{e^{pt}}{p} dp. \quad (7.1)$$

The transient process caused by the unitary function, which lies in the harmonic series, will correspond to expression (7.1) if we replace  $p$  with  $j\omega$  the expression  $j\omega$ :

$$\varphi(t) = \frac{1}{2\pi j} \int_{-\infty}^{+\infty} \Phi(j\omega) \frac{e^{j\omega t}}{\omega} d\omega, \quad (7.1a)$$

where  $\Phi(j\omega) = P(\omega) - jQ(\omega)$  is a function assuming complex values.

Functions  $P(\omega)$  and  $jQ(\omega)$  are called, respectively, real and imaginary frequency responses. Introducing the concept of the value of the complex function given zero frequency  $\Phi(0)$ , we can write

$$\varphi(t) = \frac{\Phi(0)}{2\pi j} \int_{-\infty}^{+\infty} \frac{e^{j\omega t}}{\omega} d\omega + \frac{1}{2\pi j} \int_{-\infty}^{+\infty} \frac{\Phi(j\omega) - \Phi(0)}{\omega} e^{j\omega t} d\omega.$$

Since expansion of the unitary function into a continuous spectrum of harmonics is expressed by the equality

$$\frac{1}{2\pi j} \int_{-\infty}^{+\infty} \frac{e^{j\omega t}}{\omega} d\omega = 1(t),$$

then we get

$$\varphi(t) = \Phi(0) \cdot 1(t) + \frac{1}{2\pi j} \int_{-\infty}^{+\infty} \frac{\Phi(j\omega) - \Phi(0)}{\omega} e^{j\omega t} d\omega.$$

Replacing

$$e^{j\omega t} = \cos \omega t + j \sin \omega t; \quad \Phi(j\omega) = P(\omega) + jQ(\omega),$$

we get

$$\varphi(t) = \Phi(0) \cdot 1(t) + \frac{1}{2\pi j} \int_{-\infty}^{+\infty} \frac{P(\omega) + jQ(\omega) - \Phi(0)}{\omega} (\cos \omega t + j \sin \omega t) d\omega.$$

Having opened the parentheses and keeping in mind that, since the left portion of the equality is a real value, the imaginary components of the right side must equal zero, we will find

$$\begin{aligned} \varphi(t) &= \Phi(0) \cdot 1(t) + \frac{1}{2\pi} \int_{-\infty}^{+\infty} \frac{P(\omega)}{\omega} \sin \omega t d\omega + \\ &+ \frac{1}{2\pi} \int_{-\infty}^{+\infty} \frac{Q(\omega)}{\omega} \cos \omega t d\omega - \frac{1}{2\pi} \int_{-\infty}^{+\infty} \frac{\Phi(0)}{\omega} \sin \omega t d\omega. \end{aligned}$$

Considering that all integrands are even, that  $\Phi(0) = P(0)$ , and that /337 when  $t < 0$  value  $1(t) = 0$ , we get

$$\begin{aligned} \varphi(t) &= P(0) \cdot 1(t) + \frac{1}{\pi} \int_0^{\infty} \frac{P(\omega)}{\omega} \sin \omega t d\omega + \\ &+ \frac{1}{\pi} \int_0^{\infty} \frac{Q(\omega)}{\omega} \cos \omega t d\omega - \frac{1}{\pi} \int_0^{\infty} \frac{P(0)}{\omega} \sin \omega t d\omega. \end{aligned} \quad (7.2)$$

Since the disturbance was equal to zero at moment  $t = 0$ , then, consequently,

prior to this the system was at rest, i. e.,  $(t) = 0$  when  $t < 0$ . Therefore, having replaced  $t$  in (7.2) by  $-t$ , we get

$$0 = -\frac{1}{\pi} \int_0^{\infty} \frac{P(\omega)}{\omega} \sin \omega t d\omega + \frac{1}{\pi} \int_0^{\infty} \frac{Q(\omega)}{\omega} \cos \omega t d\omega + \frac{1}{\pi} \int_0^{\infty} \frac{P(0)}{\omega} \sin \omega t d\omega. \quad (7.3)$$

Subtracting equality (7.3) termwise from (7.2), we get

$$\varphi(t) = P(0) + \frac{2}{\pi} \int_0^{\infty} \frac{P(\omega)}{\omega} \sin \omega t d\omega - \frac{2}{\pi} \int_0^{\infty} \frac{P(0)}{\omega} \sin \omega t d\omega, \quad (7.4)$$

but

$$\int_0^{\infty} \frac{\sin \omega t}{\omega} d\omega = \frac{\pi}{2},$$

consequently,

$$\varphi(t) = \frac{2}{\pi} \int_0^{\infty} \frac{P(\omega)}{\omega} \sin \omega t d\omega. \quad (7.5)$$

Adding equalities (7.2) and (7.3), we get

$$\varphi(t) = P(0) + \frac{2}{\pi} \int_0^{\infty} \frac{Q(\omega)}{\omega} \cos \omega t d\omega. \quad (7.6)$$

Formulas (7.5) and (7.6) are linked by an identical relationship to the function of unitary transient process  $\varphi(t)$  with the real  $P(\omega)$  and imaginary  $Q(\omega)$  parts of the closed system's transfer locus  $\Phi(j\omega)$ , given a unitary step disturbance. The frequency method of investigating GEU transient processes being examined is based upon use of formula (7.5).

Use of expression (7.5) requires the expansion of real response  $P(\omega)$ . /338 The response can be obtained from the closed system's transfer locus  $\Phi(j\omega)$  expression.

The real frequency response also can be represented as the algebraic sum of the trapezoidal frequency responses.

Since the frequency method is applicable to linear differential equation systems, in future we will use the procedure for linear approximation of individual nonlinear functions. Obtaining frequency responses for the linear sections, we will construct the transient process by section with subsequent "fitting" of results obtained.

Frequency method of calculating transient processes of GEU with a three-winding generator exciter. We will examine the methodology for investigation of transfer loci for calculation of transient processes of GEU with a three-winding generator exciter.

Dividing propellor hydrodynamic characteristic  $m_n = f(n_n)$  into linear sections of the type  $m_n = -m_{n0} + k_r n_n$  and assuming applied voltage to exciter field independent winding  $u_{nx}$  (GEU system input) and moments of resistance on the propellor  $m_0$  with unitary functions in the event of instantaneous transposition of the control station lever, we get Laplace transform differential equations for a GEU system with a three-winding exciter in relative units, given non-zero initial conditions approximately describing the transient process:

for output value  $\bar{n}_n(t)$

$$\begin{aligned} (T_4 p^4 + T_3 p^3 + T_2 p^2 + T_1 p + k) \bar{n}_n(p) &= k_{n_n} u_{nx} \frac{1}{p} + \\ &+ k_{n_0} m_0 \frac{1}{p} + \bar{n}_n(0) (T_4 p^3 + T_3 p^2 + T_2 p + T_1) + \\ &+ \bar{n}_n'(0) (T_4 p^2 + T_3 p + T_2) + \bar{n}_n''(0) (T_4 p + T_3) + \bar{n}_n'''(0) T_4 \end{aligned} \quad (7.7)$$

for output value  $\bar{i}_n(t)$

$$\begin{aligned} (T_4 p^4 + T_3 p^3 + T_2 p^2 + T_1 p + k) \bar{i}_n(p) &= k_i u_{nx} \frac{1}{p} + k_i T_4 \bar{u}_{nx}(p) - \\ &- k_i T_4 u_{nx}(0) + k_i m_0 \frac{1}{p} + \bar{i}_n(0) (T_4 p^3 + T_3 p^2 + T_2 p + T_1) + \\ &+ \bar{i}_n'(0) (T_4 p^2 + T_3 p + T_2) + \bar{i}_n''(0) (T_4 p + T_3) + \bar{i}_n'''(0) T_4 \end{aligned} \quad (7.8)$$

where  $T_4, T_3, T_2, T_1, T_n$  are system link time constants;  
 $k, k_{n_n}, k_{n_0}, k_i, k_{i_0}, m_0$  dimensionless constant factors;  
 $\bar{n}_n(0); \bar{i}_n(0), u_{nx}(0)$  initial relative function values;  
 $\bar{n}_n'(0), \bar{n}_n''(0), \bar{n}_n'''(0), \bar{i}_n'(0), \bar{i}_n''(0), \bar{i}_n'''(0)$  are initial values of  
 derivative functions  $\bar{n}_n(t)$  and  $\bar{i}_n(t)$ .

From expressions (7.7) and (7.8), we get GEU system generalized transfer functions:

/339

$$\frac{n_n(p)}{F_p} = \bar{n}_{n0}(p) = \frac{k_n u_{nx} + k_{n0} m_0 + p A_0(p)}{k W(p)}; \quad (7.9)$$

$$\frac{i_n(p)}{F(p)} = \bar{i}_{n0}(p) = \frac{k_i u_{nx} - k_{i0} m_0 + p k_i T_{nx} u_{nx} + p B_0(p) - p C_0(p)}{k W(p)}, \quad (7.10)$$

where

$$\begin{aligned} A_0(p) &= \bar{n}_n(0) (T_4 p^3 + T_3 p^2 + T_2 p + T_1) + \\ &+ \bar{n}'_n(0) (T_4 p^2 + T_3 p + T_2) + \bar{n}''_n(0) (T_4 p + T_3) + \bar{n}'''_n(0) T_4; \\ k W(p) &= T_4 p^4 + T_3 p^3 + T_2 p^2 + T_1 p + k; \\ B_0(p) &= i(0) (T_4 p^3 + T_3 p^2 + T_2 p + T_1) + \\ &+ \bar{i}'(0) (T_4 p^2 + T_3 p + T_2) + \bar{i}''(0) (T_4 p + T_3) + \bar{i}'''(0) T_4; \\ C_0(p) &= k_i T_{nx} u_{nx}(0); \quad F(p) = \frac{1}{p}. \end{aligned}$$

Substituting  $j\omega$  instead of  $p$  in expressions (7.9) and (7.10), we will get generalized real frequency response  $\bar{n}_{n0}(j\omega)$  or  $\bar{i}_{n0}(j\omega)$ .

Extracting the real portions from  $\bar{n}_{n0}(j\omega)$  or  $\bar{i}_{n0}(j\omega)$ , we get generalized real frequency response  $P_{n_x}(\omega)$  or  $P_{i_n}(\omega)$ , the values from which we use to construct the transient process for a given linear section  $\{\bar{n}_n(t)$  or  $i_n(t)\}$ .

The initial conditions for each section are determined as the finite values of desired functions  $\bar{n}_n(t)$  or  $i_n(t)$  of the previous section.

It is simplest of all to determine initial values of the derivatives included in expressions  $A_0(p)$  and  $B_0(p)$  through graphic differentiation of the end of the transient process of the previous section: here, it is sufficient for calculation simplification to consider only the first derivative, disregarding the highest ones since consideration of the highest derivatives essentially has a minor effect on calculation results.

In accordance with the methodology suggested in [71] and assuming that the station lever is transposed at a constant speed, the GEU system input function  $u_{nx}(t)$  can be represented analytically in the form of the sum

$$u_{nx}(t) = u_{nx1}(t) + u_{nx2}(t),$$

where, for the starting mode

$$u_{bx1}(t) = \begin{cases} u_{bx} \frac{t}{\tau}; & t < \tau \\ 0 & t > \tau \end{cases}; \quad (7.11)$$

$$u_{bx2}(t) = \begin{cases} 0 & t < \tau \\ u_{bx0} & t > \tau \end{cases}; \quad (7.12)$$

for the reversal mode

/340

$$u_{bx1}(t) = \begin{cases} u_{bx0} - 2u_{bx0} \frac{t}{\tau} & t < \tau \\ 0 & t > \tau \end{cases}; \quad (7.13)$$

$$u_{bx2}(t) = \begin{cases} 0 & t < \tau \\ -u_{bx0} & t > \tau \end{cases}. \quad (7.14)$$

The following designations were used in expressions (7.11)--(7.14):

- $u_{bx0}$  — constant value equalling the nominal relative value of the input voltage;
- $\tau$  — control station lever transposition time;
- $t$  — current time value.

The following will be the Laplace transform of  $u_{bx1}(t) = u_{bx0} \frac{t}{\tau}$  type action:

$$L\{u_{bx1}(t)\} = \frac{u_{bx0}}{\tau} \cdot \frac{1}{p^2}. \quad (7.15)$$

The Laplace transform of the input (desired) function of the GEU system considering a  $u_{bx1}(t)$  action can be written

$$X(p) = \frac{X_0(p)}{p^2}, \quad (7.16)$$

where  $X(p)$  is the Laplace transform of the output (desired) function of the system;  $X_0(\bar{p})$  is the Laplace transform of function  $[\bar{n}_x(p)$  and  $\bar{i}_x(p)]$  reflecting the dynamic properties of the system considering action  $u_{bx1}(t)$  and not having special features in the entire right half-plane and on the imaginary axis, including coordinates of the origin.

As follows from expression (7.16), function  $X(p)$  has a pole of the second

order where  $p = 0$ . Therefore, formula (7.1a) is inapplicable for calculation of transient processes since, in this case

$$\lim_{t \rightarrow \infty} Z(t) = \lim_{p \rightarrow 0} pX(p) = \lim_{p \rightarrow 0} \frac{X_0(p)}{p} = \infty, \quad (7.17)$$

i. e., function  $Z(t)$  when  $t \rightarrow \infty$  strives towards  $\infty$ . In view of the presence of a pole of the second order when  $p = 0$ , function  $X(p)$  has an irregular part

$$X_n(p) = \frac{X_0(0)}{p^2}. \quad (7.18)$$

We will represent function  $X(p)$  in the form of two terms

$$X(p) = X_r(p) - X_n(p), \quad (7.19)$$

where  $X_r(p)$  is a regular part, i. e., a function comprising all poles of  $X(p)$  located in the left half-plane (the roots of the denominator of  $X(p)$  having negative real parts);  $X_n(p)$  is an irregular part, i. e. a function comprising all poles of  $X(p)$ , located in the right half-plane and on the imaginary axis, /341 including the origin of the coordinates (the roots of the denominator of  $X(p)$ ) having positive real parts or parts equalling zero.

Evidently, in our case  $\lim_{t \rightarrow \infty} Z_n(t)$  is a diverging function;

$\lim X_r(t) = 0$  is a transient function of  $t$ .

Substituting (7.18) in (7.19) considering (7.16) for the regular part of  $X_r(p)$ , we will have

$$X_r(p) = X(p) - X_n(p) = \frac{X_0(p)}{p^2} - \frac{X_0(0)}{p^2}. \quad (7.20)$$

Assuming here that  $p = j\omega$  and considering that  $X_0(0) = P_0(0)$  since  $P_0(0) = 0$ , we will get

$$P_r(\omega) + jP_r(\omega) = \frac{P_0(\omega) + jP_0(\omega) - P_0(0)}{-\omega^2} = \frac{P_0(0) - P_0(\omega)}{\omega^2} - j \frac{P_0(\omega)}{\omega^2}$$

from which

$$P_r(\omega) = \frac{P_0(0) - P_0(\omega)}{\omega^2}; \quad (7.21)$$

$$P_r(\omega) = \frac{-P_0(\omega)}{\omega^2}. \quad (7.22)$$

Since

$$X_r(t) = -\frac{2}{\pi} \int_0^{\infty} P_r(\omega) \sin \omega t \, d\omega \quad (7.23)$$

when  $t > 0$ , then, substituting (7.22) in (7.23), we will get

$$X_r(t) = \frac{2}{\pi} \int_0^{\infty} \frac{P_0(\omega)}{\omega} \cdot \frac{\sin \omega t}{\omega} \, d\omega. \quad (7.24)$$

Since  $X_n(t) = P_0(0)$ , then, when  $t > 0$ , the transient process formula has the form

$$X(t) = X_n(t) + X_r(t) = P_0(0) + \frac{2}{\pi} \int_0^{\infty} \frac{P_0(\omega)}{\omega} \cdot \frac{\sin \omega t}{\omega} \, d\omega. \quad (7.25)$$

We will designate  $\frac{P_0(\omega)}{\omega} = P(\omega)$ , in (7.25), then the final formula for the desired functions's transient process, given the action of input function of the  $u_{0x1}(t) = u_{0x0} \frac{t}{\tau}$  type is:

$$X(t) = P_0(0) + \frac{2}{\pi} \int_0^{\infty} P(\omega) \frac{\sin \omega t}{\omega} \, d\omega. \quad (7.26)$$

Expanding the system's frequency response considering action of the  $u_{0x1}$  type and using the trapezoidal frequency response method, we will construct the transient process in the interval  $t = 0 - \tau$ .

We have  $u_{0x}(t) = u_{0x0} l(t)$  when  $t > \tau$ . /342

The transient process is calculated given unitary action considering initial conditions.

It also is possible to represent function  $u_{bx}(t)$  comprising two functions:  
 $u_{bx}(t) = u_{bx1}(t) + u_{bx2}(t)$ , where  $u_{bx1}(t)$  is the initial part of an exponent whose  
time constant equals transposition time  $\tau$ ; ; and  $u_{bx2}(t)$ , a time constant equalling  
 $u_{bx0}$  .

Here, for starting we will have

$$u_{bx1}(t) = \begin{cases} 1,6u_{bx0}(1 - e^{-t/\tau}) & \text{with } t < \tau; \\ 0 & \text{with } t > \tau; \end{cases} \quad (7.27)$$

$$u_{bx2}(t) = \begin{cases} 0 & \text{with } t < \tau; \\ u_{bx0} & \text{with } t > \tau. \end{cases} \quad (7.28)$$

Factor 1.6 when  $u_{bx0}$  in function  $u_{bx1}(t)$  stems from a property of the exponent  
in which an exponential function is achieved in the time equal to a time constant  
of a value comprising 0.632 of amplitude value  $u_{bx0}$  .

In our case,  $u_{bx0} = 0,632u'_{bx0}$  or  $u'_{bx0} = 1,6u_{bx0}$  . For reverse

$$u_{bx}(t) = \begin{cases} -2,2u_{bx0} + 3,2u_{bx0}e^{-t/\tau} & \text{при } t < \tau; \\ 0 & \text{with } t > \tau; \end{cases} \quad (7.29)$$

$$u_{bx2}(t) = \begin{cases} 0 & \text{with } t < \tau; \\ -u_{bx0} & \text{with } t > \tau. \end{cases} \quad (7.30)$$

In fact

$$u_{bx1}(t) = -(u'_{bx0} - u_{bx0}) + u_{bx0}e^{-t/\tau}.$$

Since

$$2u_{bx0}(t) = 0,63u'_{bx0}$$

and

$$u'_{bx0} = \frac{2}{0,63}u_{bx0} = 3,2u_{bx0},$$

then

$$u_{bx1}(t) = -2,2u_{bx0} + 3,2u_{bx0}e^{-t/\tau}.$$

This will be the Laplace transform of function  $u_{bx1}(t)$  :

$$L[u_{bx1}(t)] = 1,6u_{bx0} \frac{1}{p} - 1,6u_{bx0} \frac{1}{p - \alpha}; \quad (7.31)$$

during a reverse

$$L\{u_{bx1}(t)\} = -2,2u_{bx0} \frac{1}{p} + 3,2u_{bx0} \frac{1}{p + \alpha}, \quad (7.32)$$

where  $\alpha = 1/\tau$ .

The Laplace transform of the GEU system's output (desired) function considering action  $u_{bx1}(t)$  in our case will have a simple pole of the first order at the origin of coordinates.

#### § 7.4 Analytical Method of Calculating the Transient Processes /343 of Automated GEU Nonlinear Systems

Several theoretical assumptions. Methods of analyzing transient processes in dc electrical propulsion plants examined earlier are based on solution of linear differential equations with constant factors. However, equations reflecting actual electric propellor drive operating conditions will contain variable factors of the differential equations. Therefore, analysis built on the assumption of the constancy of these factors can, in some instances, provide a noticeable error compared to processes taking place in reality in GEU during transient modes. Use of an approximate method is recommended, however, only in the early stage of plant design or in cases that require obtaining reference data.

Among the variable factors is one dependent upon the amount of magnetic flux  $\Phi$  which, in a linear system of differential equations, is assumed to be proportional to field current  $i_f$ . In actuality, as already pointed out above, the saturation of the magnetic current greatly influences the amount of dc machinery magnetic flux. Therefore, relationship  $\Phi = f(i_f)$  cannot be expressed in the form of a linear relationship.

Also falling in the category of variable factors are losses to eddy currents, additional losses in teeth and windings, armature reaction, and so on, which under certain conditions also can influence the factors of differential equations.

Professor V. I. Kas'yanov [19, 20] developed an engineering method of calculating the electromechanical transient processes of starting, braking,



We will accept as the first approximation

$$y_1 = y_0(t) + L \int_0^t k(t-\tau) p_m[y_0(t)] d\tau = y_0(t) + z_1(t);$$

$$y_2 = y_0(t) + L \int_0^t k(t-\tau) p_m[y_1(t)] d\tau = y_0(t) + z_2(t).$$

Since sequential approximations will diverge because the distance between two sequential approximations will strive towards zero, then, if the subtracted error does not exceed the tolerable, one can stop at that approximation.

Calculation of transient processes of GEU systems given direct introduction of the main current circuit into the pilot excitation system. Direct current electrical propulsion plant systems with main circuit current unity feedback (see § 3.3) have been used widely both in domestic and foreign practice.

The transient processes of electric propellor drive starting and reversing can be described by the following initial system of differential equations.

We obtained the diesel generator torque equation, disregarding forces of /345 inertia in the diesel control system and considering that the supply of fuel without delay changes proportionally to generator electromagnetic moment. Then the torque equation in accordance with (6.2) can be written in this form:

$$m_{дг} = M_{дг. ном} = m_{г. дг} + m_{г} + m_{дг. дмн}.$$

The propellor line torque equation has the form (6.41).

The equilibrium equation of voltages in the main current circuit based on (6.69) will be written

$$me_r = qe_d + \sum r_n i_n + L \frac{di_n}{dt} + \sum \Delta u_{n. \omega} + r_{д. п+к. о} i_n - \\ - 2p_n \omega_r \sigma_n \frac{d\phi_n}{dt} + (r_{\alpha. \tau} + r_{\alpha. \tau. ном}) i_n + L_{д. п+к. о} \frac{di_n}{dt}.$$

Accordingly, the equilibrium equation of voltages in the generator field circuit in accordance with (6.78) has the form

$$e_{g,r} = m \left( r_{g,r} i_{g,r} + L_{g,r} \frac{di_{g,r}}{dt} + (r_{g,r} + r_{g,r, \text{доб}}) i_{g,r} + 2p_g \omega_{g,r} \sigma_r \frac{d\phi_r}{dt} + \Delta u_{g,r, \text{ш}} \right).$$

The equilibrium equation of exciter self-excitation winding voltages in accordance with (6.84) will be

$$e_{g,r} = r_{g,r} i_{g,r} + L_{g,r} \frac{di_{g,r}}{dt} + (r_{g,r} + r_{g,r, \text{доб}}) i_{g,r} + r_{g,r} i_{g,r} m + 2p_g \omega_{g,r} \sigma_g \frac{d\phi_g}{dt} + \Delta u_{g,r, \text{ш}}.$$

The equilibrium equation of independent field (master) winding voltages from expression (6.82) has the form

$$u_{h,g} = (r_{h,g, \text{доб}} + r_{h,g}) i_{h,g} + 2p_h \omega_{h,g} \sigma \frac{d\phi_h}{dt}.$$

Exciter field flux is determined by the equality

$$\phi_g = 2a_g (\omega_{h,g} i_{h,g} + \omega_{g,r} i_{g,r} - \omega_{o,r} i_{o,r}).$$

Significant generator braking moments, and sometimes torques, arise during transient processes, especially when a main propulsion motor is reversed. These cause a change in primary motor rotational speed. The degree of change of this speed depends on the form of the drive motor characteristic and the magnitude of the diesel generator gyrating mass' moment of gyration.

The same designations as were used in the corresponding expressions in /346 Chapter 6 are used in this system. Therefore, we list below only the additional designations:

- l — control rack motion;
- $m_{g,r}$  — diesel generator friction loss torque;

$m_r$  — generator braking torque equalling

$$m_r = \frac{N_r p_g}{2\pi a} \phi_r i_g = C_m \phi_r i_g;$$

$m_{дг. дмн}$  — diesel generator dynamic torque equalling

$$m_{дг. дмн} = \frac{GD_{дг}^2}{375} \cdot \frac{dn_r}{dt};$$

$GD_{дг}^2$  — diesel generator moment of gyration;

$m_d$  — main propulsion motor electromagnetic moment equalling

$$m_d = C_m \phi_d i_d;$$

$m_{в.т}$  — shafting line friction torque;

$m_b$  — propellor hydrodynamic moment (characteristic), a complex function of vessel speed and screw rotational speed

$$m_b(v, n_d).$$

Note: Keeping in mind that the transient processes in propellor electric drive occur during almost constant vessel speed, in future the propellor hydrodynamic characteristic everywhere is considered only as a function of the speed of its rotation  $m_b = f(n_d)$  (as was the case previously);

$m$  — number of series-connected generators;

$q$  — number of series-connected main propulsion motor armatures;

$e_r$  — generator electromotive force equalling

$$e_r = \frac{N_r p_r}{60 a_r} n_r \phi_r = C_{er} n_r \phi_r;$$

$e_d$  — main propulsion motor electromotive force equalling

$$e_d = \frac{N_d p_d}{60 a_d} n_d \phi_d = C_{ed} n_d \phi_d;$$

$e_{в.т}$  — generator exciter electromotive force equalling

$$e_{в.т} = \frac{P_{в.т} n_{в.т}}{60 a_{в.т}} n_{в.т} \phi_{в.т} = C_{ev} n_{в.т} \phi_{в.т}.$$

We will designate the sum of the voltage drops in the resistance of the G—D [generator—diesel] armature circuit by

$$r_n i_n + r_{д. п+к. дг} i_n + (r_{о.т} + r_{о.т. дмн}) i_n = \sum R i_n.$$

Using the aforementioned designations, we will compile the following initial

system of equations describing transient processes relative to the circuit depicted in Figure 3.14:

$$\begin{aligned}
 m_{\Delta \Sigma} \dot{n} &= m_{r, \tau} + m_{\tau} + \frac{GD_{\Delta r}^2}{325} \cdot \frac{dn_r}{dt}; \\
 m_{\Delta} &= C_{\Phi \Delta} i_{\Delta} = \frac{GD_{\Delta}^2}{375} \cdot \frac{dn_{\Delta}}{dt} + m_{\Sigma}(n_{\Delta}); \\
 e_r &= e_{\Delta} + \sum R i_{\Delta} + L_{\Delta} \frac{di_{\Delta}}{dt} + \sum \Delta u_{\text{ш}} - 2\rho_{\Sigma} \omega_{o, \tau} \sigma_{\Sigma} \frac{d\phi_{\Sigma}}{dt}; \\
 e_{\Sigma, r} &= r_{\Sigma, \Sigma} i_{\Sigma, r} + L_{\Sigma, \Sigma} \frac{di_{\Sigma, r}}{dt} + (r_{\Sigma, r} + \\
 &+ r_{\Sigma, r, \text{доб}}) i_{\Sigma, r} + 2\rho_{\Sigma} \omega_{\Sigma, r} \sigma_{\Sigma} \frac{d\phi_{\Sigma}}{dt} + \Delta u_{\Sigma, \Sigma}; \\
 e_{\Sigma, r} &= r_{\Sigma, \Sigma} i_{\Sigma, \Sigma} + L_{\Sigma, \Sigma} \frac{di_{\Sigma, \Sigma}}{dt} + (r_{\Sigma, \Sigma} + \\
 &+ r_{\Sigma, \Sigma, \text{доб}}) i_{\Sigma, \Sigma} + 2\rho_{\Sigma} \omega_{\Sigma, \Sigma} \sigma_{\Sigma} \frac{d\phi_{\Sigma}}{dt} + \Delta u_{\Sigma, \Sigma}; \\
 u_{\Sigma, \Sigma, r} &= (r_{\Sigma, \Sigma} + r_{\Sigma, \Sigma, \text{доб}}) i_{\Sigma, \Sigma} + 2\rho_{\Sigma} \omega_{\Sigma, \Sigma} \sigma_{\Sigma} \frac{d\phi_{\Sigma}}{dt}.
 \end{aligned} \tag{7.36}$$

We will write the reduced system of equations in relative units, having accepted as base values the nominal values of the torques and the nominal value of the exciter independent field winding voltage.

The initial system of equations given motor field constant flux

$$\begin{aligned}
 \text{a) } \bar{M}_{\Delta \Sigma, \text{ном}} \dot{n} &= \bar{m}_{\Delta r, \tau} + \bar{m}_{\tau} + T_{\Sigma, r} \frac{d\bar{n}_r}{dt}; \\
 \text{(б) } \bar{i}_{\Delta} &= T_{\Sigma, \Delta} \frac{d\bar{n}_{\Delta}}{dt} + \bar{m}_{\Sigma}(\bar{n}_{\Delta}); \\
 \text{(в) } \bar{E}_{r, \text{ном}} \bar{\phi}_r \bar{n}_r &= \bar{E}_{\Delta, \text{ном}} \bar{n}_{\Delta} + \bar{e}_{r, \tau} I_{\Delta, \text{ном}} + T_{\Delta r} \frac{d\bar{i}_{\Delta}}{dt} + \\
 &+ T_{o, \tau} \frac{d\bar{\phi}_{\Sigma}}{dt} + \sum \Delta u_{\text{ш}}; \\
 \text{(г) } \bar{E}_{\Sigma, \text{ном}} \bar{\phi}_{\Sigma} &= \bar{E}_{\Sigma, r, \text{ном}} \bar{i}_{\Sigma, r} + (\bar{e}_{\Sigma, \Sigma} \bar{e}_{\Sigma, r}) \bar{\phi}_{\Sigma} + \\
 &+ T_{\Delta \Sigma} \frac{d\bar{i}_{\Delta}}{dt} + T_{\Sigma, r} \frac{d\bar{\phi}_r}{dt} + \Delta u_{\text{ш}}; \\
 \text{(д) } \bar{E}_{\Sigma, \text{ном}} \bar{\phi}_{\Sigma} &= \bar{i}_{\Sigma, \Sigma} (\bar{e}_{\Sigma, \Sigma} + \bar{e}_{\Delta r}) + T_{\Delta \Sigma} \frac{d\bar{i}_{\Delta}}{dt} + \\
 &+ \bar{e}_{\Sigma, r, \text{ном}} \bar{\phi}_{\Sigma} + T_{\Sigma, \Sigma} \frac{d\bar{\phi}_{\Sigma}}{dt}; \\
 \text{(е) } \bar{u}_{\Sigma, \Sigma} &= \bar{E}_{\Sigma, \text{ном}} \bar{i}_{\Sigma, \Sigma} + T_{\Sigma, \Sigma} \frac{d\bar{\phi}_{\Sigma}}{dt}; \\
 \text{(ж) } \bar{\phi}_{\Sigma} &= a(\omega_{\Sigma, \Sigma} \bar{i}_{\Sigma, \Sigma} + \omega_{\Sigma, \Sigma} \bar{i}_{\Sigma, \Sigma} - \omega_{o, \tau} \bar{i}_{\Delta}),
 \end{aligned} \tag{7.37}$$

- where
- $\bar{M}_{ДЗ.НОМ} = \frac{\bar{M}_{ДЗ.НОМ}}{M_{Г.НОМ}}$  — diesel torque nominal value;
  - $\bar{m}_{ДГ.Г} = \frac{m_{ДГ.Г}}{M_{Д.НОМ}}$  — time of diesel generator idling loss;
  - $\bar{m}_Г = \frac{m_Г}{M_{Г.НОМ}}$  — generator torque ( $\bar{m}_Г = \bar{\varphi}_Г \bar{i}_Г$ ) ;
  - $\frac{GD_{ДГ.НОМ}^2 n_{Г.НОМ}}{375 M_{Д.НОМ}} = T_{М.Г}$  — diesel generator electromechanical time constant, sec;
  - $\bar{n}_Г$  — generator rotational speed;
  - $\frac{i_Г}{I_{Г.НОМ}} = \bar{i}_Г$  — main circuit current;
  - $\frac{GD_{Д.НОМ}^2 n_{Д.НОМ}}{375 M_{Д.НОМ}} = T_{М.Д}$  — propellor shafting electromechanical time constant, sec;
  - $\frac{m_в(n_Д)}{M_{в.НОМ}(n_Д)} = \bar{m}_в(\bar{n}_Д)$  — screw moment of resistance and function from the speed of its rotation;
  - $\frac{E_{Г.НОМ}}{U_{в.в.НОМ}} = \bar{E}_Г$  — main generator emf nominal value;
  - $\frac{\Phi_в + \Phi_Г}{\Phi_{Г.НОМ}} = \bar{\phi}_Г$  — main generator magnetic flux;
  - $\frac{\Phi_{в.в} - \Phi_в}{\Phi_{в.НОМ}} = \bar{\phi}_в$  — generator exciter magnetic flux;
  - $\frac{E_{Д.НОМ}}{U_{в.в.НОМ}} = \bar{E}_Д$  — main propulsion motor armature emf nominal value;
  - $\frac{\sum R I_{Г.НОМ}}{U_{в.в.НОМ}} = \bar{e}_{Г.Г}$  — overall active drop of main circuit voltage given nominal current;
  - $\frac{L_a I_{Г.НОМ}}{U_{в.в.НОМ}} = \frac{L_a}{r_a} \frac{I_{Г.НОМ} r_a}{U_{в.в.НОМ}} = T'_a$  — armature circuit electromagnetic time constant, sec;
  - $L_a$  — main circuit overall inductivity, H;
  - $r_a$  — main circuit overall impedance;
  - $\frac{\sum \Delta u_{цл}}{U_{в.в.НОМ}} = \Delta \bar{u}_{цл.Г}$  — voltage drop in main generator two-way make-before-break contacts;
  - $\frac{2p_в \omega_в \gamma \sigma_в \Phi_{в.НОМ}}{U_{в.в.НОМ}} = T_{\sigma.Г}$  — current (differentially-compounded) winding electromagnetic time constant, sec;
  - $\frac{E_{в.НОМ}}{U_{в.в.НОМ}} = \bar{E}_в$  — generator field emf nominal value;
  - $\frac{r_{Г.в} I_{в.Г.НОМ}}{U_{в.в.НОМ}} = \bar{e}_{Г.в}$  — voltage drop in exciter armature given nominal generator field current  $I_{в.Г.НОМ}$ , relative units;
  - $\frac{(r_{в.Г} - r_{в.Г.ДОБ}) I_{в.Г.НОМ}}{U_{в.в.НОМ}}$  — voltage drop in the generator field winding circuit given nominal field current  $I_{в.Г.НОМ}$ , relative units;

$$\frac{\Delta u_{\text{ш. в.}}}{U_{\text{в. в. ном}}} = \bar{\Delta u}_{\text{ш. в.}} \quad \text{— voltage drop in generator exciter two-way make-before-break contacts;}$$

$$\frac{2\rho_{\text{г}}\omega_{\text{в. г.}}\sigma_{\text{г}}\Phi_{\text{г. ном}}}{U_{\text{в. в. ном}}} = T_{\text{в. г.}} \quad \text{— field winding circuit electromagnetic time constant, sec;}$$

$$\frac{r_{\text{я. в.}} I_{\text{св. ном}}}{U_{\text{в. в. ном}}} = \bar{e}_{\text{св}} \quad \text{— voltage drop in the exciter armature given self-excitation winding nominal current;}$$

$$\frac{L_{\text{я. в.}} I_{\text{св. ном}}}{U_{\text{в. в. ном}}} = \frac{L_{\text{я. в.}}}{r_{\text{ав}}} \frac{I_{\text{св. ном}} r_{\text{ав}}}{U_{\text{в. в. ном}}} = T'_{\text{ав. св.}} \quad \text{— exciter armature circuit electromagnetic time constant given self-excitation winding nominal current;}$$

$$\frac{L_{\text{я. в.}} I_{\text{св. ном}}}{U_{\text{в. в. ном}}} = \frac{L_{\text{я. в.}}}{r_{\text{ав}}} \frac{I_{\text{св. ном}} r_{\text{ав}}}{U_{\text{в. в. ном}}} = T_{\text{ав. г.}} \quad \text{— exciter armature circuit electromagnetic time constant given nominal current in the generator field winding, sec;}$$

$$\frac{(r_{\text{св.}} + r_{\text{св. доб}}) I_{\text{св. ном}}}{U_{\text{в. в. ном}}} = \bar{e}_{\text{св}} \quad \text{— voltage drop in the self-excitation winding given nominal current of this winding } I_{\text{св. ном}} ;$$

$$\frac{2\rho_{\text{э}}\omega_{\text{св}}\sigma_{\text{св}}\Phi_{\text{св. ном}}}{U_{\text{в. в. ном}}} = T_{\text{св}} \quad \text{— self-excitation winding electromagnetic time constant, sec;}$$

$$\frac{(r_{\text{н. в.}} + r_{\text{н. в. доб}}) I_{\text{н. в. ном}}}{U_{\text{в. в. ном}}} = \bar{e}_{\text{н. в.}} \quad \text{— voltage drop in the field independent winding given nominal current of this winding } I_{\text{н. в. ном}} ;$$

$$\frac{2\rho_{\text{в. в.}}\omega_{\text{н. в.}}\sigma_{\text{н. в.}}\Phi_{\text{н. в. ном}}}{U_{\text{в. в. ном}}} = T_{\text{н. в.}} \quad \text{— exciter independent field winding electromagnetic time constant, sec;}$$

$$\left. \begin{aligned} F_{\text{н. в.}} &= \frac{2\omega_{\text{н. в.}} I_{\text{н. в. ном}}}{F_{\text{ном}}} \\ F_{\text{св.}} &= \frac{2\omega_{\text{св.}} I_{\text{св. ном}}}{F_{\text{ном}}} \\ F_{\text{о. г.}} &= \frac{2\omega_{\text{о. г.}} I_{\text{я. ном}}}{F_{\text{ном}}} \end{aligned} \right\} \quad \text{— mmf nominal value for the field independent winding, self-excitation winding, and current winding.}$$

For the rectified portion of the generator magnetization curve we have

$$\phi_{\text{г}} = a_{\text{г}} 2\omega_{\text{в. г.}} i_{\text{в. г.}}$$

or (in relative units)

$$\bar{\phi}_{\text{г}} = \bar{i}_{\text{в. г.}}$$

on the other hand

$$\phi_{\text{в. г.}} = a'_{\text{г}} 2\omega_{\text{св.}} i_{\text{св.}}$$

or (in relative units)

$$\bar{\phi}_{\text{в.г}} = \bar{i}_{\text{св}}$$

Solving equations a, b, c, and d from system (7.37) for the derivatives and disregarding the inductive drop in exciter armature winding voltage, we will get

$$\left. \begin{aligned} \frac{d\bar{n}_r}{dt} &= \frac{\bar{M}_{\text{дв.ном}} - \bar{m}_{\text{дг.г}} - \bar{q}_r \bar{i}_a}{T_{\text{м.г}}}, & \frac{d\bar{n}_d}{dt} &= \frac{\bar{i}_a - \bar{m}_a(\bar{n}_d)}{T_{\text{м.д}}}, \\ \frac{d\bar{i}_a}{dt} &= \frac{\bar{E}_{\text{г.ном}} \bar{\phi}_r \bar{n}_r - \bar{E}_{\text{д.ном}} \bar{n}_d \bar{n}_{\text{ом}} - \bar{e}_r \bar{i}_a \bar{n}_{\text{ом}} - T_{\text{о.г}} \frac{d\bar{\phi}_a}{dt} \sum \Delta \bar{u}_{\text{ш}}}{T_{\text{аг}}}, \\ \frac{d\bar{\phi}_r}{dt} &= \frac{\bar{E}_{\text{в.ном}} \bar{\phi}_a - (\bar{e}_{\text{н.в}} + \bar{e}_{\text{в.г}}) \bar{\phi}_r - \Delta \bar{u}_{\text{ш}}}{T_{\text{вг}} + T_{\text{ав}}}. \end{aligned} \right\} \quad (7.38)$$

From expressions e and f of system (7.37), we will find

/350

$$\bar{i}_{\text{св}} = \frac{\bar{E}_{\text{в.ном}} \bar{\phi}_a \bar{n}_r - \bar{e}_{\text{а.в.г}} \bar{i}_a \bar{n}_{\text{ом}} T_{\text{св}} \frac{d\bar{\phi}_a}{dt}}{\bar{e}_{\text{а.св}} + \bar{e}_{\text{св}}};$$

$$\bar{i}_{\text{н.в}} = \frac{\bar{u}_{\text{н.в}} - T_{\text{н.в}} \frac{d\bar{\phi}_a}{dt}}{\bar{e}_{\text{н.в}}}.$$

Having substituted the values found for generator exciter field currents in expression g of system (7.37) and having solved it for the magnetic flux derivative  $\frac{d\bar{\phi}_a}{dt}$ , we will get

$$\frac{d\bar{\phi}_a}{dt} = \frac{(\bar{e}_{\text{а.св}} + \bar{e}_{\text{св}}) F_{\text{н.в}} \bar{u}_{\text{н.в}} + (\bar{e}_{\text{н.в}} F_{\text{св}} \bar{e}_{\text{а.св}} - \bar{e}_{\text{св}}) \times \bar{e}_{\text{н.в}} \bar{\phi}_a \bar{n}_r - \bar{e}_{\text{а.в.г}} \bar{e}_{\text{н.в}} F_{\text{св}} \bar{\phi}_r - (\bar{e}_{\text{а.св}} + \bar{e}_{\text{св}}) \bar{e}_{\text{н.в}} F_{\text{о.г}} \bar{i}_a}{\bar{e}_{\text{н.в}} F_{\text{св}} T_{\text{св}} + (\bar{e}_{\text{а.св}} + \bar{e}_{\text{св}}) F_{\text{н.в}} T_{\text{н.в}}}. \quad (7.39)$$

Equations (7.38) and (7.39) obtained can be solved using the approximation by iteration method. Beforehand, we will introduce these designations for convenience in writing the equations:

- $m \bar{E}_{\text{г.ном}} = \bar{E}_{\Sigma \text{г.ном}}$  — overall nominal value of series-connected generator emf;
- $q \bar{E}_{\text{д.ном}} = \bar{E}_{\Sigma \text{д.ном}}$  — overall nominal value of main propulsion motor series-connected armature emf;
- $\bar{e}_{\text{н.в}} + \bar{e}_{\text{в.г}} = \bar{e}_{\Sigma \text{в.г}}$  — overall value of the voltage drop (given nominal generator field current voltage) in the generator field winding and in the exciter armature from generator field winding circuit current;

- $\bar{e}_{a_{cb}} + \bar{e}_{cb} = \bar{e}_{\Sigma_{cb}}$  — overall value of the voltage drop (given nominal self-excitation winding current) in the exciter self-excitation winding and in the exciter armature winding from the self-excitation winding circuit current;
- $T_{\Sigma_{cb}} = T_{a_{cb}} + T_{\Sigma_{cb}}$  — overall generator field winding and exciter armature circuit time constant.

If one also accepts the voltage drop in the brush contact as a constant magnitude which can be considered when calculating generator and exciter emf, then, finally, the system of equations describing dc GEU transient processes, given main current unity feedback and direct input of the main current circuit to the generator exciter, solved relative to the increments of the variables, will take the form

/351

$$\Delta \bar{\phi}_{v.g} = \frac{\bar{e}_{\Sigma_{cb}} F_{н.в} \bar{u}_{н.в.ср} + (\bar{e}_{н.в} F_{cb} - \bar{e}_{\Sigma_{cb}}) \times \bar{e}_{н.в} \bar{\phi}_{в.ср} - \bar{e}_{a_{cb}} \bar{e}_{н.в} F_{cb} \bar{\phi}_{г.ср} - \bar{e}_{\Sigma_{cb}} \bar{e}_{н.в} F_{о.т} \bar{i}_{я.ср}}{\bar{e}_{н.в} F_{cb} T_{cb} + \bar{e}_{\Sigma_{cb}} F_{н.в} T_{н.в}} \Delta t;$$

$$\Delta \bar{\phi}_{г} = \frac{\bar{e}_{н.в} \bar{\phi}_{в.ср} - \bar{e}_{\Sigma_{cb}} \bar{e}_{н.в} \bar{\phi}_{г.ср}}{T_{\Sigma_{cb.g}}} \Delta t;$$

$$\Delta \bar{i}_{я} = \frac{\bar{E}_{г.ном} \bar{\phi}_{г.ср} \bar{n}_{г.ср} - \bar{E}_{д.ном} \bar{n}_{д.ном.ср} - \bar{e}_{г} \bar{i}_{я.ном.ср} - T_{о.т} \frac{d\bar{\phi}_{в}}{dt}}{T_{а.г}} \Delta t;$$

$$\Delta \bar{n}_{д} = \frac{\bar{i}_{я.ср} - \bar{m}_{в} (\bar{n}_{д.ср})}{T_{м.д.}} \Delta t;$$

$$\Delta \bar{n}_{г} = \frac{\bar{M}_{дв.ном} \bar{i}_{ср} - \bar{m}_{дв} T_{ср} - \bar{\Psi}_{г.ср} \bar{i}_{я.ср}}{T_{м.г}} \Delta t.$$

The instantaneous values of the variables of the magnitudes in time interval  $\Delta t$  are assumed to be their average values.

Voltage in the generator exciter independent winding during starting is assumed to be increasing automatically (based on the exponent).

Calculation of a reversal was accomplished considering that the increase in voltage in the generator exciter field independent winding occurs in 1 second (the control station lever is transposed from one extreme position of "full ahead" to another extreme position "full astern" in 2 seconds).

(a)	(a)											
$\Delta t, \text{сек}$	$t, \text{сек}$	$u_{\text{в.п}}$	$\Delta \bar{\phi}_{\text{в.п}}$	$\bar{\phi}_{\text{в.п}}$	$\Delta \bar{\phi}_{\text{г.п}}$	$\bar{\phi}_{\text{г.п}}$	$\Delta \bar{I}_{\text{в.п}}$	$\bar{I}_{\text{в.п}}$	$\bar{m}_{\text{в.п}}$	$\frac{\partial \bar{m}_{\text{в.п}}}{\partial n_{\text{г.п}}}$	$\Delta \bar{n}_{\text{г.п}}$	$n_{\text{г.п}}$
0,1	0,1								0	0	0	0
0,1	0,2											
0,1	0,3											
—	—	1,0	—	—	—	—	—	—	—	—	—	—
—	—	1,0	—	—	—	—	—	—	—	—	—	—

Table 7.1. Tabular Form for Construction of a Transient Process as a Main Propulsion Motor is Started (In Relative Units). a—Seconds.

(a)	(a)											
$\Delta t, \text{сек}$	$t, \text{сек}$	$u_{\text{в.п}}$	$\Delta \bar{\phi}_{\text{в.п}}$	$\bar{\phi}_{\text{в.п}}$	$\Delta \bar{\phi}_{\text{г.п}}$	$\bar{\phi}_{\text{г.п}}$	$\Delta \bar{I}_{\text{в.п}}$	$\bar{I}_{\text{в.п}}$	$\bar{m}_{\text{в.п}}$	$\frac{\partial \bar{m}_{\text{в.п}}}{\partial n_{\text{г.п}}}$	$\Delta \bar{n}_{\text{г.п}}$	$n_{\text{г.п}}$
0,1	0,0	1,0	0,0	1,0	0,0	1,0	0,0	1,0	1,0		0,0	1,0
0,1	0,1											
—	—	—	—	—	—	—	—	—	—	—	—	—
—	—	—	—	—	—	—	—	—	—	—	—	—
0,1	—	-1,0										
0,1		-1,0										

Table 7.2. Tabular Form for Construction of a Transient Process as a Main Propulsion Motor is Reversed (In Relative Units). a—Seconds.

Calculations will be made in tabular form. Tables 7.1 and 7.2 are filled in as follows:

1) for reverse, the initial values of all variables are entered on the first line. If reverse is accomplished at vessel full speed ahead, then the nominal values (in relative units, this will be ones) will be the initial conditions; increments of the variables here equal zero;

2) the values of time variables are entered in the first column of Tables 7.1 and 7.2. The smaller the time interval  $\Delta t$  selected, the more precise the calculation;

3) the sum of the  $\Delta t$  increments from the previous line and this line is entered in the second column;

4) the values of the voltages in the exciter field independent winding are entered in the third column. A change in this voltage can be assumed to be either linear with regular intervals and with general reverse time  $\bar{U}_{b.p.}$  equal to the time of control station level transposition or in accordance with any preassigned law;

5) next, the table is filled in as follows, using line two as our example: from the design formula for  $\Delta\bar{\phi}_{b.p.}$  we find its value when  $\Delta t = 0.1$  second. Meanwhile, values  $\bar{\phi}_{b.p.}$  and  $\bar{i}_{n.p.}$  for determination of  $\Delta\bar{\phi}_{b.p.}$  will be taken from /353 the previous line, i. e., line one. Value  $\bar{\phi}_b$  for the second line will be found from the sum of  $\bar{\phi}_b$  from the previous line (in this case, the first line) and  $\Delta\bar{\phi}_b$  obtained for the second line. From the design formula for  $\Delta\bar{\phi}_{r.p.}$  we calculate its value for line two. Values  $\bar{\phi}_{b.p.}$ ,  $\Delta\bar{\phi}_{b.p.}$ , and  $\bar{\phi}_{r.p.}$  will be taken from the previous line (in this case, from line one). Value  $\bar{\phi}_{r.p.}$  of the second line comprises the sum of  $\bar{\phi}_{r.p.}$  of the previous line (line one in this instance) and the value found for  $\Delta\bar{\phi}_{r.p.}$ . Analogously, using the design formula for  $\Delta\bar{i}_{n.p.}$ , we will find its value, having substituted  $\bar{\phi}_{r.p.}$ ,  $\Delta\bar{\phi}_{r.p.}$ ,  $\bar{n}_{x.p.}$  and  $\bar{i}_{n.p.}$  their values from the previous line. Accordingly, value  $\bar{i}_{n.p.}$  for the second line will equal the sum of  $\bar{i}_{n.p.}$  from the previous line and obtained value  $\Delta\bar{i}_{n.p.}$ . Values  $\Delta\bar{n}_{x.p.}$  and  $\bar{n}_{x.p.}$  are determined in the same way. Meanwhile, value  $\bar{m}_{b.p.}$  will be taken each time from characteristic  $\bar{m}_{b.p.} = f(\bar{n}_{x.p.})$  in accordance with value  $\bar{n}_{x.p.}$  of the previous line. A more accurate result will be obtained if one begins with average values, namely:

$$\left. \begin{aligned} \bar{\phi}_{b.p. (i)} &= \bar{\phi}_{b.p. (i-1)} + \frac{\Delta\bar{\phi}_{b.p. (i)}}{2}; \\ \bar{\phi}_{r.p. (i)} &= \bar{\phi}_{r.p. (i-1)} + \frac{\Delta\bar{\phi}_{r.p. (i)}}{2}; \\ \bar{i}_{n.p. (i)} &= \bar{i}_{n.p. (i-1)} + \frac{\Delta\bar{i}_{n.p. (i)}}{2}; \\ \bar{n}_{x.p. (i)} &= \bar{n}_{x.p. (i-1)} + \frac{\Delta\bar{n}_{x.p. (i)}}{2}, \end{aligned} \right\} (7.40)$$

where  $i$  is the number of lines in the calculation table.

Calculation of GEU transient processes given differentially-connected main circuit current unity feedback. A schematic of such a plant is presented in Figure 3.4. In such systems, a current field winding fulfilling the function of main circuit current unity feedback is connected to the overall voltage drop in the compensating winding and main propulsion motor additional pole winding.

The initial system of equations using our assumed designations in relative units can be written if one assumes the nominal values of the variables as the basic magnitudes, while for the magnetizing force [n. s.] of individual field windings we assume a nominal value of overall mmf  $F_{\text{НОМ}}$ , then

$$\bar{m}_{23} = \bar{m}_{r, 23} + \bar{m}_r + T_{\text{н. r}} \frac{d\bar{n}_r}{dt}. \quad (7.41)$$

Given main propulsion motor field constant magnetic flux, the main propulsion motor--screw line torque equation will take the form

$$\bar{i}_n = \bar{m}_{r, n} + \bar{m}_n (\bar{n}_n) + T_{\text{н. n}} \frac{d\bar{n}_n}{dt}. \quad (7.42)$$

For the main current circuit

$$E_{r, \text{НОМ}} \bar{e}_r = \bar{e}_n E_{n, \text{НОМ}} + \Delta \bar{u}_{\text{н. ш}} + \bar{i}_n I_{\text{н. НОМ}} r_n + L_n I_{\text{н. НОМ}} \frac{d\bar{i}_n}{dt}$$

or

$$\bar{e}_r = \bar{e}_n \bar{e}_n + \Delta \bar{u}_{\text{н. ш}} + \bar{i}_n \bar{e}_{\text{н. r2}} + T_n \frac{d\bar{i}_n}{dt} \bar{e}_{\text{н. r2}}. \quad (7.43)$$

$\bar{e}_r = \bar{\phi}_r$  and  $\bar{e}_n = \bar{n}_n$ , will be for conditions of primary motor constant rotational speed (in relative units), then the last equation will be written

$$\bar{\phi}_r = \bar{n}_n \bar{e}_n + \Delta \bar{u}_{\text{н. ш}} + \bar{i}_n \bar{e}_{\text{н. r2}} + T_n \frac{d\bar{i}_n}{dt} \bar{e}_{\text{н. r2}}. \quad (7.44)$$

If one assumes that field equipment rotational speed is constant and keeps in mind that  $\bar{\phi}_r = \bar{i}_{\text{н. r}}$  is for the unsaturated portion of the idling characteristic in relative units, then the equilibrium equation for generator field circuit emf will have the form

$$\begin{aligned} \bar{\phi}_s = & \bar{\phi}_r \bar{e}_{s, r} + \Delta \bar{u}_{\text{ш. в}} + \bar{i}_{cs} \bar{e}_{s, cs} + \bar{e}'_{s, s1} T_{s, s1} \frac{d\bar{\phi}_r}{dt} + \\ & + T_{s, s2} \bar{e}_{s, s2} \frac{d\bar{i}_{cs}}{dt} + T_{s, r} \frac{d\bar{\phi}_r}{dt}. \end{aligned} \quad (7.45)$$

The equilibrium equation of self-excitation winding circuit emf will take on an analogous form

$$\begin{aligned} \bar{\phi}_s = & \bar{i}_{cs} \bar{e}_{s, cs} + \bar{\phi}_r \bar{e}_{s, r} + T_{s, s1} \bar{e}_{s, s1} \frac{d\bar{\phi}_r}{dt} + \\ & + T_{s, s2} \bar{e}_{s, s2} \frac{d\bar{i}_{cs}}{dt} + T_{cs} \frac{d\bar{\phi}_s}{dt} + \Delta \bar{u}_{\text{ш. в}}. \end{aligned} \quad (7.46)$$

For the independent field winding circuit

$$\bar{u}_{s, s} = \bar{e}_{s, s} \bar{i}_{o, s, s} + T_{o, s, s} \frac{d\bar{\phi}_s}{dt}. \quad (7.46a)$$

For the current unity feedback circuit

$$\begin{aligned} \frac{i_n}{I_{n, \text{НОМ}}} I_{n, \text{НОМ}} r_{\text{д. п+к. о}} + L_{\text{д. п+к. о}} I_{n, \text{НОМ}} \frac{di_n}{dt} = k_{o, \tau} \frac{i_n}{I_{n, \text{НОМ}}} \times \\ \times I_{n, \text{НОМ}} (r_{\text{д. п-к. о}} + r_{o, \tau}) - 2\rho_s \omega_{o, \tau} \sigma_s \bar{\Phi}_{s, \text{НОМ}} \frac{d\bar{\phi}_s}{dt} \end{aligned}$$

or

$$\begin{aligned} \bar{i}_n + T_{\text{д. п+к. о}} \frac{d\bar{i}_n}{dt} = - \frac{2\rho_s \omega_{o, \tau} \sigma_s \bar{\Phi}_{s, \text{НОМ}}}{I_{n, \text{НОМ}} (r_{\text{д. п+к. о}} - k_{o, \tau} (r_{\text{д. п+к. о}} + r_{o, \tau}))} \frac{d\bar{\phi}_s}{dt} = \\ = - T_{o, \tau} \frac{d\bar{\phi}_s}{dt}. \end{aligned} \quad (7.46b)$$

The initial equation for exciter field flux in relative units may be written /355

$$\bar{\phi}_s = \bar{F}_{s, s} \bar{i}_{n, s} + \bar{F}_{cs} \bar{i}_{cs} - \bar{F}_{o, \tau} \bar{i}_{o, \tau}, \quad (7.46c)$$

where

$$\begin{aligned} \bar{F}_{s, s} = \frac{\omega_{s, s} I_{n, s, \text{НОМ}}}{F_{\text{НОМ}}}, \quad \bar{F}_{cs} = \frac{\omega_{cs} I_{cs, \text{НОМ}}}{F_{\text{НОМ}}}, \quad \bar{F}_{o, \tau} = \frac{\omega_{o, \tau} I_{o, \tau, \text{НОМ}}}{F_{\text{НОМ}}}, \\ \bar{e}_d = \frac{E_{d, \text{НОМ}}}{E_{r, \text{НОМ}}} \quad - \text{proportionality factor between propulsion motor} \\ \text{counter emf and generator emf;} \end{aligned}$$

- $$\bar{\Delta U}_{\text{ш}} = \frac{\Delta U_{\text{ш}}}{E_{\text{г. ном}}}$$
 — relative voltage drop in generator brush two-way make-before-break contacts expressed in fractions of  $E_{\text{г. ном}}$  ;
- $$\bar{\epsilon}_{\text{я. г1}} = \frac{I_{\text{я. ном}} r_{\text{я}}}{E_{\text{г. ном}}}$$
 — relative voltage drop in the armature circuit caused by the flow of nominal current;
- $$T_{\text{я. г1}} \bar{\epsilon}_{\text{я. г1}} = \frac{L_{\text{я}}}{r_{\text{я}}} \cdot \frac{I_{\text{я. ном}} r_{\text{я}}}{r_{\text{я}} I_{\text{я. кз}}} = \frac{L_{\text{я}}}{r_{\text{я}}} \cdot \frac{I_{\text{я. ном}}}{I_{\text{я. кз}}}$$
 — derivative of factor  $\bar{\epsilon}_{\text{я. г1}}$  to armature circuit time constant;
- $$\bar{\epsilon}_{\text{я. г2}} = \frac{I_{\text{я. ном}}}{I_{\text{я. кз}}}$$
 — proportionality factor between main circuit current nominal value and this current's value during a short circuit;
- $$\bar{\epsilon}_{\text{в. в. г}} = \frac{(r_{\text{в. г}} + r_{\text{я. в}}) I_{\text{в. г. ном}}}{E_{\text{в. ном}}}$$
 — relative voltage drop in the generator field winding circuit caused by the flow of field nominal current;
- $$\bar{\Delta U}_{\text{ш. в}} = \frac{\Delta U_{\text{ш. в}}}{E_{\text{в. ном}}}$$
 — relative voltage drop in exciter brush two-way make-before-break contacts;
- $$\bar{\epsilon}_{\text{я. св}} = \frac{r_{\text{я. в}} I_{\text{св. ном}}}{E_{\text{в. ном}}}$$
 — relative voltage drop in the armature circuit from the flow of nominal self-excitation circuit current value;
- $$\bar{\epsilon}_{\text{я. в1}} = \frac{I_{\text{в. г. ном}}}{I_{\text{в. г. кз}}}$$
 — proportionality factor between generator field current value and this parameter during a short circuit;
- $$T_{\text{я. в1}} \bar{\epsilon}_{\text{я. в1}} = \frac{L_{\text{я. в1}}}{r_{\text{я. в1}}} \cdot \frac{I_{\text{я. в1 ном}} r_{\text{я. в1}}}{r_{\text{я. в1}} I_{\text{я. в1 кз}}} = \frac{L_{\text{я. в1}}}{r_{\text{я. в1}}} \cdot \frac{I_{\text{я. в1 ном}}}{I_{\text{я. в1 кз}}}$$
 — derivative of factor  $\bar{\epsilon}_{\text{я. в1}}$  to exciter armature /356 circuit time constant;
- $$\bar{\epsilon}_{\text{в. св1}} = \frac{(r_{\text{я. в}} - r_{\text{св}}) I_{\text{св. ном}}}{E_{\text{в. ном}}}$$
 — relative voltage drop in the self-excitation circuit;
- $$\bar{\epsilon}_{\text{я. в. г}} = \frac{r_{\text{я. в}} I_{\text{в. г. ном}}}{E_{\text{в. ном}}}$$
 — relative voltage drop in the armature circuit from the flow of nominal generator field current;
- $$\bar{\epsilon}_{\text{я. в2}} = \frac{I_{\text{св. ном}}}{I_{\text{св. кз}}}$$
 — proportionality factor between nominal self-excitation winding circuit current value and this parameter during a short circuit;
- $$T_{\text{я. в2}} \bar{\epsilon}_{\text{я. в2}} = \frac{L_{\text{я. в}}}{r_{\text{я. в}}} \cdot \frac{I_{\text{св. ном}}}{I_{\text{св. кз}}} = \frac{L_{\text{я. в}}}{r_{\text{я. в}}} \cdot \frac{I_{\text{св. ном}}}{I_{\text{св. кз}}}$$
 — derivative of factor  $\bar{\epsilon}_{\text{я. в2}}$  to self-excitation winding circuit time constant.

The magnitude of the time constant in additional poles and compensating winding is determined from expression

$$T_{д. п+к. о} = \frac{L_{д. п+к. о}}{[r_{д. п+к. о} - k_{о. т} (r_{д. п+к. о} + r_{о. т})]}$$

The expression for exciter field nominal n. s. has the form

$$F_{ном} = a (\omega_{о. н. в} I_{о. н. в. ном} + \omega_{о. св} I_{о. св. ном} - \omega_{о. т} I_{о. т. ном}).$$

Transient processes in electrical propulsion plants occur during a slight change in primary motor rotational speed. Here, the action of the speed governor can be calculated in the following manner.

A speed governor engages when the primary motor achieves rotational speed corresponding to the established mode, striving to keep primary motor rotational speed constant. Given a known assumption, one can accept the fact that diesel effective horsepower changes in jumps during rotational speed transpositions. Then the magnitude of primary motor (diesel) excess torque can be determined as a value proportional to the difference between power  $N_e$  corresponding to the set rotational speed value and shaft power at a given moment in time: /357

$$\begin{aligned} M_{дз. ном} - m_{дз} &= 60.75 \frac{N_{дз. ном} - N_{дз. н. в. ном}}{m_{дз} 2\pi n_{г. ном}} = \\ &= 60.75 \frac{N_e}{2\pi n_{г. ном} M_{дз. ном} n_{г. ном}} - \frac{60.75 N_{ном}}{2\pi n_{г. ном} M_{дз. ном}} \end{aligned}$$

from which

$$\bar{m}_{дз} = \frac{60.75 N_e}{2\pi n_{г. ном} M_{дз. ном} n_{г. ном}} = \frac{\bar{N}_e}{n_{г. ном}}$$

where  $\bar{N}_e$  is the relative magnitude of internal combustion engine power in fractions of conditional power corresponding to generator nominal electromagnetic moment and primary motor nominal rotational speed:

$$\bar{N}_e = 60.75 \frac{N_e}{2\pi n_{г. ном} M_{дз. ном}}$$

Value  $\bar{N}_e$  changes in accordance with the diesel operating mode. Introducing into the system of equations corresponding relationships, having solved them for finite increments of exciter and generator flux, diesel generator and main propulsion motor rotational speed, as well as armature circuit current, we will get the design system of equations:

$$\Delta \bar{n}_r = \frac{\bar{m}_{дз.ср} - \bar{m}_{т.дз.ср} - \bar{m}_{г.ср}}{T_{м.г}} \Delta t; \quad (7.47)$$

$$\Delta \bar{n}_д = \frac{\bar{i}_{я.ср} - \bar{m}_{т.д.ср} - \bar{m}_{в.ср}(\bar{n}_д)}{T_{м.д}} \Delta t; \quad (7.48)$$

$$\Delta \bar{i}_я = \frac{\bar{\phi}_r.ср - \bar{e}_{д.ном}\bar{n}_д.ср - \bar{i}_{я.ср}\bar{e}_{я.гд} - \Delta \bar{u}_{ш.ш}}{T_{я}\bar{e}_{я.гд}} \Delta t; \quad (7.49)$$

$$\Delta \bar{\phi}_r = \frac{\bar{\phi}_{в.ср} - \bar{\phi}_r.ср\bar{e}_{в.г} - \bar{i}_{св.ср}\bar{e}_{я.св} - \Delta \bar{u}_{ш.в}}{T_{в.г} + \bar{e}_{я.в1}T_{я.в1}} \Delta t. \quad (7.50)$$

Equation (7.48) is obtained given the condition that one disregards the inductive voltage drop in the exciter armature.

We get the equation for the exciter field flux change rate through joint solution of (7.46), (7.46a), and (7.46b) after disregarding the inductive voltage drop in the exciter armature:

$$\begin{aligned} \phi_a = & \frac{\bar{E}_{н.в}\bar{\phi}_a\bar{F}_{св} - \bar{\phi}_r\bar{e}_{н.в}\bar{r}\bar{F}_{св} - T_{сн}\bar{F}_{св}}{\bar{e}_{н.св}} \frac{d\bar{\phi}_a}{dt} - \\ & - \frac{\Delta \bar{u}_{ш.в}\bar{F}_{св}}{\bar{e}_{н.св}} + \frac{\bar{u}_{н.в}\bar{F}_{н.в} - T_{н.в}\bar{F}_{н.в}}{\bar{e}_{н.в}} \frac{d\bar{\phi}_a}{dt} - \frac{\bar{i}_{я}\bar{e}_{ш}\bar{F}_{о.т} - T_{о.т}\bar{F}_{о.т}}{\bar{e}_{о.т}} \frac{d\bar{F}_a}{dt}. \end{aligned}$$

Solving the expression obtained jointly with (7.46c), we will find /358

$$\begin{aligned} \bar{\phi}_a = & \frac{\bar{E}_{н.в}\bar{\phi}_a\bar{F}_{св} - \bar{\phi}_r\bar{e}_{н.в}\bar{r}\bar{F}_{св} - T_{сн}\bar{F}_{св}}{\bar{e}_{н.св}} \frac{d\bar{\phi}_a}{dt} - \frac{\Delta \bar{u}_{ш.в}\bar{F}_{св}}{\bar{e}_{н.св}} + \\ & + \frac{\bar{u}_{н.в}\bar{F}_{н.в} - T_{н.в}\bar{F}_{н.в}}{\bar{e}_{н.в}} \frac{d\bar{\phi}_a}{dt} - \frac{\bar{i}_{я}\bar{e}_{ш}\bar{F}_{о.т} - T_{о.т}\bar{F}_{о.т}}{\bar{e}_{о.т}} \frac{d\bar{\phi}_a}{dt} \end{aligned}$$

or, having solved the equation for  $\frac{d\bar{\phi}_a}{dt}$ , we get

$$\begin{aligned} \frac{d\bar{\phi}_a}{dt} (T_{сн}\bar{e}_{н.в}\bar{e}_{о.т}\bar{F}_{св} + T_{н.в}\bar{e}_{н.св}\bar{e}_{о.т}\bar{F}_{н.в} - T_{о.т}\bar{e}_{н.св}\bar{e}_{н.в}\bar{F}_{о.т}) = \\ = \bar{\phi}_a (\bar{E}_{н.в}\bar{e}_{н.в}\bar{e}_{о.т}\bar{F}_{св} - \bar{e}_{н.св}\bar{e}_{о.т}\bar{e}_{н.в}) - \bar{\phi}_r\bar{e}_{н.в}\bar{r}\bar{e}_{н.в}\bar{e}_{о.т}\bar{F}_{св} - \\ - \Delta \bar{u}_{ш.в}\bar{e}_{н.в}\bar{e}_{о.т}\bar{F}_{св} + \bar{u}_{н.в}\bar{e}_{н.св}\bar{e}_{о.т}\bar{F}_{н.в} - \bar{e}_{ш}\bar{i}_{я}\bar{e}_{н.св}\bar{e}_{н.в}\bar{F}_{о.т}. \end{aligned}$$

The latter design expression in finite increments will have the form

$$\Delta \bar{\phi}_a = \frac{\bar{u}_{н.в}\bar{e}_{н.св}\bar{e}_{о.т}\bar{F}_{н.в} + \bar{\phi}_a.ср (\bar{E}_{н.в}\bar{e}_{н.в}\bar{e}_{о.т}\bar{F}_{св} - \bar{e}_{н.св}\bar{e}_{о.т}\bar{e}_{н.в}) - \bar{\phi}_r.ср\bar{e}_{н.в}\bar{r}\bar{e}_{н.в}\bar{e}_{о.т}\bar{F}_{св} - \Delta \bar{u}_{ш.в}\bar{e}_{н.в}\bar{e}_{о.т}\bar{F}_{св} - \bar{i}_{я.ср}\bar{e}_{ш}\bar{e}_{н.св}\bar{e}_{н.в}\bar{F}_{о.т}}{T_{сн}\bar{e}_{н.в}\bar{e}_{о.т}\bar{F}_{св} + T_{н.в}\bar{e}_{н.св}\bar{e}_{о.т}\bar{F}_{н.в} - T_{о.т}\bar{e}_{н.св}\bar{e}_{н.в}\bar{F}_{о.т}} \Delta t. \quad (7.51)$$

The average values of the variables in design equations (7.47)--(7.50) are determined from expressions (7.40a).

### § 7.5 Graphic-Analytical Method of Transient Process Calculation

Assumptions. We will examine construction of the transient processes of individual links prior to examining construction of the transient process of the GEU as a whole. Here, the following assumptions are made: leakage and main fluxes change with an identical sign; electrical machinery resistances are constant during construction of transient processes.

All static characteristics of system links and their parameters, as well as nominal data, are assumed as given.

Calculation of the emf increase in a single-winding exciter (of a conventional dc generator). Conventional dc machinery with independent excitation is used in several systems as main machinery exciters. Such systems are the simplest /359 since they do not have any feedbacks. The GEU aboard the tanker "General Azi Aslanov" is an example.

Let all exciter (generator) parameters be known:  $n_r$  is rotational speed, rpm;  $C_e$  is a design factor;  $N$  is the number of armature active conductors;  $w_p$  is the number field winding turns per pole;  $2p$  is the number of poles;  $2a$  is the number of armature winding parallel branches;  $R_f$  is field winding resistance, ohms;  $u_e$  is exciter voltage, V;  $u_0$  is voltage applied to the field winding via potentiometer PU, V.

Voltage  $u_0$  will be applied to NVO during an instantaneous transposition of the control station lever. The increase in magnetic flux here will be determined in the following way.

The equilibrium equation for the winding NVO circuit emf in a transient mode has the form

$$u_0 = i_f R_f + 2p w_p \sigma \frac{d\phi_f}{dt}. \quad (7.52)$$

We will multiply both parts of equation (7.52) by  $2w_s$  :

$$2w_s u_0 = 2w_s i_s R_s + 2 \cdot 2p w_s^2 \sigma \frac{d\phi_s}{dt}. \quad (7.53)$$

We will transpose the first member of the right side of the equation to the left side and we will divide all members of equation (7.53) by  $R_s$  :

$$\frac{u_0}{R_s} 2w_s - 2w_s i_s = \frac{2 \cdot 2p w_s^2 \sigma}{R_s} \cdot \frac{d\phi_s}{dt}. \quad (7.54)$$

At the same time, it is known that  $u_s = C_s n \phi_s$  .

After substitution of  $du_s = \Delta u_s$  and  $dt = \Delta t$  and several transformations from (7.54), we will get

$$\frac{u_0}{R_s} 2w_s - 2w_s i_s = k_s \frac{\Delta u_s}{\Delta t}, \quad (7.55)$$

where  $k_s = \frac{2 \cdot 2p w_s^2 \sigma}{R_s \varphi_s}$ ;  $\varphi_s = C_s n$  .

From equation (7.55) we will compile the proportion

$$\frac{\Delta u_s}{\left( \frac{u_0}{R_s} \cdot 2w_s - i_s 2w_s \right)} = \frac{\Delta t}{k_s}. \quad (7.56)$$

Since  $k_s = \text{const}$ , then, given selected fixed interval  $\Delta t = \text{const}$ , it is possible to designate

$$\frac{\Delta m_{em}}{k_s m_U} = \text{tg } \alpha_s. \quad (7.57)$$

The numerator of the left side of equation (7.56) determines the increase (increment) of exciter voltage for assumed time interval  $\Delta t$ . The denominator of the left side of this equation determines the difference between established exciter field n. s. and the current exciter field n. s. value.

Thus, the ratio of the exciter voltage increment to the difference in /360 n. s. values  $F_{s, \text{ver}} - F_{s, \text{рекум}}$  equals the tangent of angle  $\alpha_s$  . Since the difference in n. s.  $F_{s, \text{ver}} - F_{s, \text{рекум}}$  is determined by the nature of the current increase in exciter winding NVO, which is determined by the parameters of this winding's

circuit, then angle  $\alpha_b$  determines the proportionality of increase  $\Delta u_b$  for given time interval  $\Delta t$  (Figure 7.5).

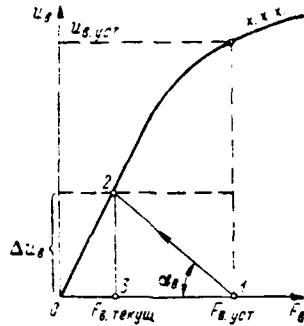


Figure 7.5. Explanation of the Principle of Transient Process Construction.

It is evident from the figure that

$$\frac{\Delta u_b}{F_{b, \text{уст}} - F_{b, \text{текущ}}} = \text{tg } \alpha_b.$$

Consequently, given known magnetization characteristic (x.x.x.), the transient process of increase  $u_b$  is determined "step-by-step" through construction by iteration, beginning with point 1 (Figure 7.5) on the n. s. axis corresponding to value  $u_{01}$  supplied from the PU to the intersection with x.x.x. (point 2). Segment 03 on the corresponding scale then will be  $F_{b, \text{текущ}}$ .

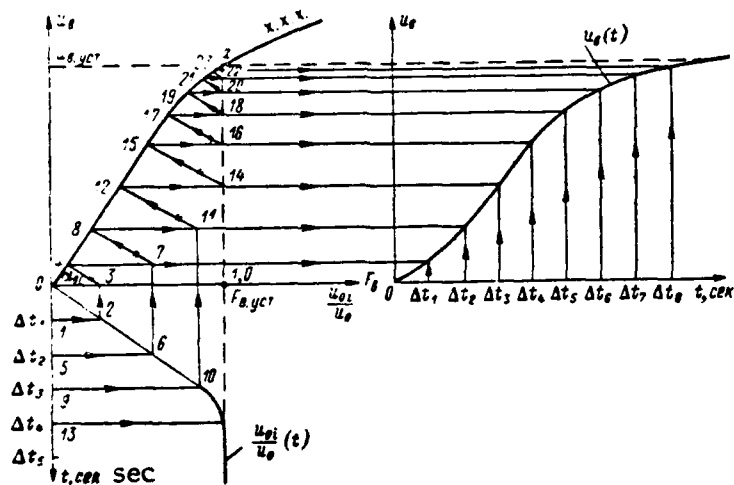


Figure 7.6. Process Construction Considering Master Voltage Increase Time.

If voltage  $u_0$  increases in the time function as the control station lever is transposed, then the construction should be done considering curve  $u_0(t)$ , which must be known. Construction  $u_s(t)$  considering  $u_0(t)$  is shown in Figure 7.6, where curve  $u_{0i}/u_0$  is presented in relative units in the time function for convenience in construction.

Value  $u_{0i}/u_0$  is plotted along the X-axis, while time in seconds is plotted below along the Y-axis. The time axis is divided into interval  $\Delta t$ . Curve  $u_s(t)$ , obtained from a calculation, is plotted on the right in Figure 7.6. A slow increase in emf caused by the corresponding increase in  $u_0$  as the control station lever is transposed occurs in the initial portion of curve  $u_s(t)$ .

The presence of voltage increase factor  $u_0$  over time influences the transient process and, during calculations, this circumstance should be considered. It is necessary when making oscillograms of transient processes during experiments to record value  $u_0(t)$  on the oscillogram simultaneously with recording remaining curves.

Consideration of the presence of feedbacks occurs by means of the corresponding change in the slope of the construction path, as well as by introduction of feedback paths.

It is possible when determining the value of factor  $k_s$  (7.55) to use the approximation method to consider the influence of eddy current on the transient process. If you introduce the equivalent loop with time constant  $T_f$ , which considers the delay in exciter field magnetic flux increase due to damping caused by the presence of the magnetic flux of eddy currents, then the value of factor  $k_s$  input to (7.57) will equal

$$k_s = \frac{a_s}{\varphi_s} (T_s + T_f), \quad (7.58)$$

where

$$T_f = \frac{4l_j a^2 b^2}{\pi \rho 2\delta_s (a^2 + b^2)} \text{сек};$$

$l_j$  is the length of the path of magnetic flux in a poured frame for a pair of poles;  $a$ ,  $b$  are the sides of a frame section equidimensional rectangle;  $\rho$  is frame material specific resistance;  $\delta_s$  is the equivalent air gap.

Calculation of the reversal of exciter (generator) emf. The calculation begins with the point of the established mode (point a in Figure 7.7) and plotting of the vertical of the given n. s. during a reversal (a vertical passing through point a at distance  $F_{n, \text{вст}}$ ) determined by the given field voltage  $u_0$ . Presented in Figure 7.7 is an instantaneous change in field voltage to the same value, but with opposite polarity. A graphic construction path at angle  $\alpha_s$ , determined from formula (7.57), is drawn from point 1 determined by the intersection of the horizontal of the initial value of exciter voltage and the vertical of the given n. s. As a result of the constructions, the curve was obtained for emf reversal depicted on the right in Figure 7.7.

It is possible during the transient process constructions presented above to consider the presence of time during which change  $u_0$  occurs [6].

Calculation of the transient processes of an exciter with voltage feedback (with a self-excitation winding). A shunt winding can be both magnetizing as well as demagnetizing. We will examine a case in which a self-excitation winding (SVO) is connected and matched with an exciter independent winding (NVO). In this case, the transient process construction is complicated somewhat in /362 comparison with the previous instance. The construction path slope is determined by the following equations:

independent winding emf equation

$$u_0 = i_s R_s + 2p w_s \sigma \frac{d\phi_s}{dt}; \quad (7.59)$$

shunt winding emf equation

$$u_s = i_m R_m + 2p w_m \sigma \frac{d\phi_s}{dt}, \quad (7.60)$$

where  $i_m$ ,  $R_m$ ,  $w_m$  is shunt winding current, resistance, and number of turns per pole.

Multiplying the first equation by  $2w_s$  and dividing by  $R_s$ , and the second correspondingly by  $2w_m$  and  $R_m$ , we get

$$\frac{u_0}{R_s} 2w_s - 2w_s i_s = \frac{2 \cdot 2p w_s^2 \sigma}{R_s} \cdot \frac{d\phi_s}{dt}; \quad (7.61)$$

$$\frac{u_s}{R_m} 2w_m - 2w_m i_m = \frac{2 \cdot 2p w_m^2 \sigma}{R_m} \cdot \frac{d\phi_s}{dt}. \quad (7.62)$$

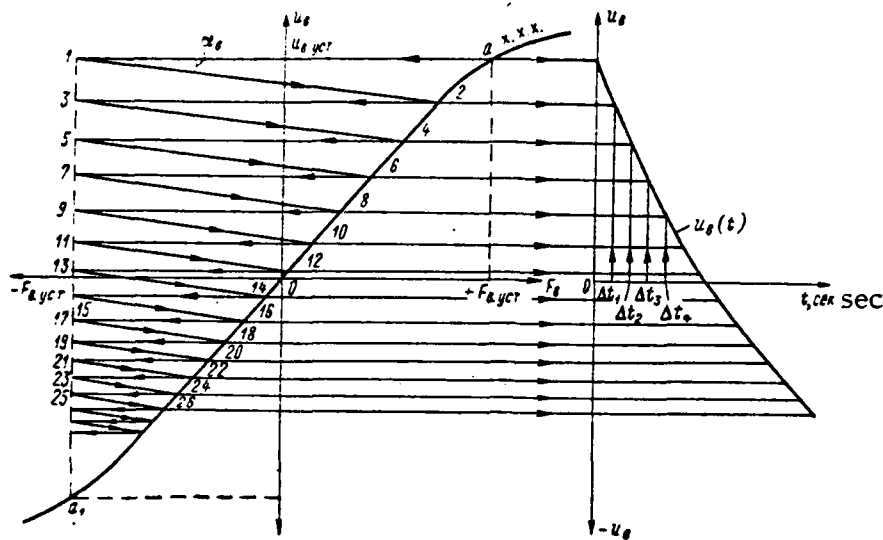


Figure 7.7. EMF Reversal Curve Construction.

Substituting  $\phi_n = \frac{u_n}{\Phi_n}$  in (7.61) and (7.62), transforming to finite increments  $\Delta$ , and adding, we will get

$$\begin{aligned} \left( \frac{u_n}{R_n} \cdot 2w_n + \frac{u_n}{R_{in}} 2w_{in} \right) - (2w_n i_n + 2w_{in} i_{in}) = \\ = \left( \frac{2 \cdot 2p w_n^2 \sigma}{\Phi_n R_n} + \frac{2 \cdot 2p w_{in}^2 \sigma}{\Phi_n R_{in}} \right) \frac{\Delta u_n}{\Delta t} \end{aligned}$$

We will introduce designation

/363

$$k_n = \frac{2 \cdot 2p \sigma}{\Phi_n} \left( \frac{w_n^2}{R_n} + \frac{w_{in}^2}{R_{in}} \right); \quad (7.63)$$

then, analogous to what was done above, we will get

$$\frac{\Delta u_n}{\left( \frac{u_n}{R_n} 2w_n + \frac{u_n}{R_{in}} 2w_{in} \right) - (2w_n i_n + 2w_{in} i_{in})} = \frac{\Delta t}{k_n} = \text{tg } \alpha_n'. \quad (7.64)$$

Thus, the increase in exciter voltage with a shunt winding is determined by the tangent of the path slope. The first term of the denominator on the left side of (7.64) determines the established magnitude of the overall exciter field n. s. value, while the second determines the actual value of exciter field n. s.

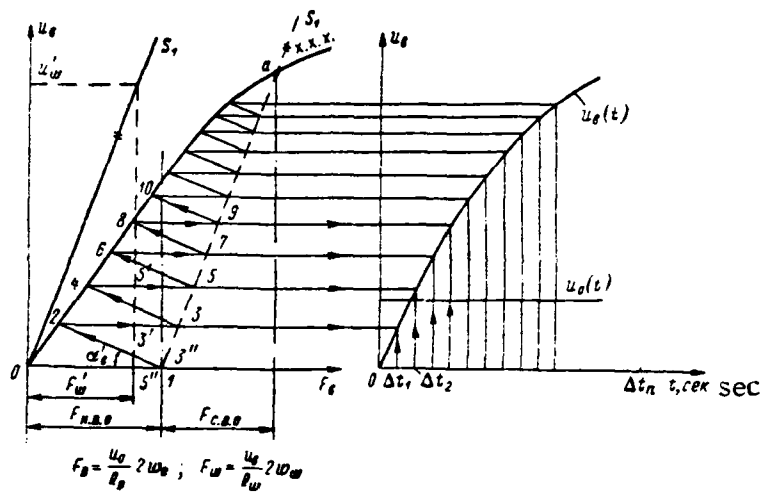


Fig. 7.8. Construction of transition process of two field winding

A construction of the increase in exciter voltage with two field windings (NVO and SVO) is depicted in Figure 7.8. The idling characteristic is plotted on the Y-axis as a function of field n. s. to a pair of poles. Next, path OS<sub>1</sub>, determined by a certain value of voltage  $u_w$  and by the emf corresponding to it, is plotted.

It should be considered that, given the presence of additional resistance in the shunt winding circuit, it should be added with the resistance of the SVO coils themselves since the slope of path OS<sub>1</sub> will depend upon this. The presence of shunt winding SVO itself leads to the fact that  $k_n > k_s$  and, consequently,  $\alpha_s < \alpha_n$ . Essentially, this signifies that the exciter time constant when positive voltage feedback is cut in increased to the magnitude of the time constant of this winding. Actually:

$$k_s = \frac{2 \cdot 2 p w_s^2 \sigma a_s}{\Phi_s R_s a_s} = \frac{a_s}{\Phi_s} T_s.$$

In Figure 7.8, segment 3'—3 determines the actual value of shunt winding /364 n. s. at the end of first time interval  $\Delta t$ . Characteristic  $u_s(t)$ , obtained as a result of a graphical calculation, is constructed on the right in Figure 7.8. Path 2—3 is drawn to the vertical passing through point 1 in the absence of feedback.

When voltage increase time  $u_0$  is present, the construction is done in a manner analogous to that in Figure 7.6.

Calculation of the voltage reversal of an exciter with positive voltage feedback. Calculation of the reversal considering the presence of increase time  $u_0(t)$  for an exciter with positive voltage feedback is depicted in Figure 7.9 [5, 6].

Point 1 and then point 2 in curve  $u_0(t)$  are determined in accordance with interval  $\Delta t_1$ . We will get initial point 4 for construction of the emf drop from the new independent winding n. s. value (point 3) obtained, retaining the shunt winding n. s. value at the first moment. Path 4—5 is drawn from point 4 at angle  $\alpha'_s$ . The construction will be drawn to the descending branch of the magnetization characteristic to consider the presence of hysteresis.

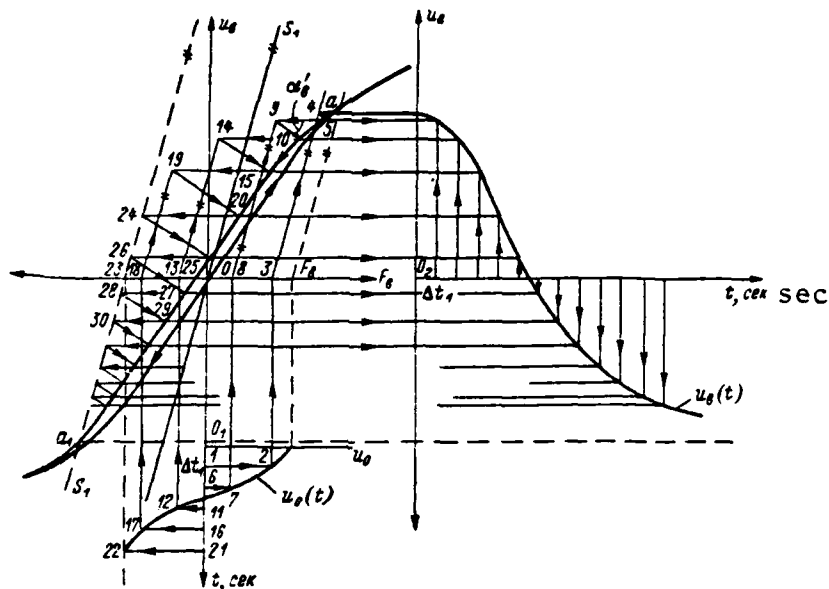


Figure 7.9. Construction of the Two-Winding Exciter Reversal Process.

Consideration of the influence of residual magnetization on the transient process using the aforementioned method during a graphic construction is very simple, while, at the same time, this greatly complicates solution of the problem during calculations using analytical methods.

The values of the exciter field independent winding  $n. s.$  are determined /365 on the X-axis in accordance with the actual value of time  $t_1$  from curve  $u_0(t)$ . Paths parallel to  $OS_1$  to the previous states (values) of exciter output voltage are drawn from the points obtained on the X-axis. The construction sequence is designated by numbers and indicated by arrows. After establishment of value  $u_0$ , the construction becomes analogous to construction of the emf increase in Figure 7.9 (after point 25).

Curve  $u_e(t)$  obtained as a result of the constructions is depicted on the right in Figure 7.9.

If the voltage feedback is negative, then feedback path  $OS_1$  must be drawn on the left of the Y-axis.

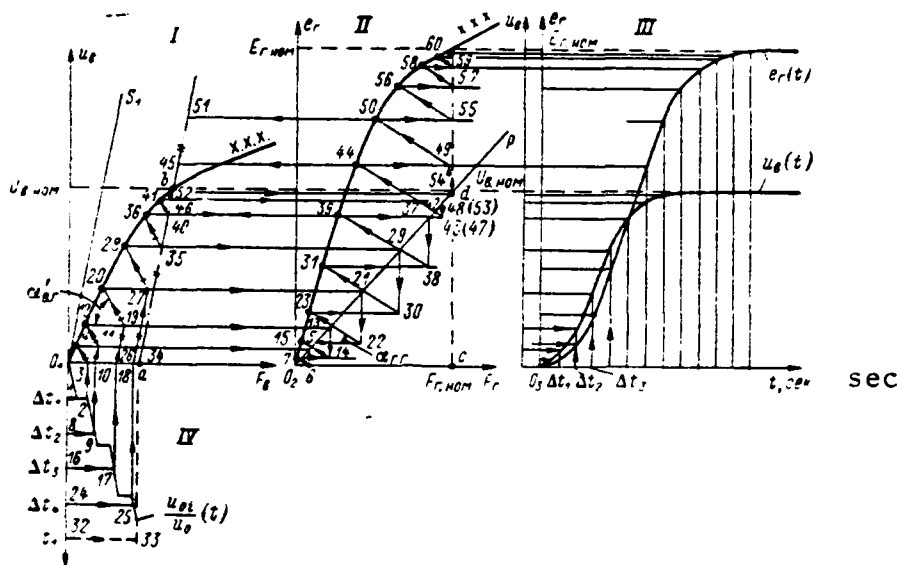


Figure 7.10. Construction of the Generator EMF Increase Given Excitation from a Two-Winding Exciter.

Calculation of the generator emf increase with an exciter with a shunt winding. The generator transient process is determined for this circuit by increase time  $u_g(t)$  and a current increase in winding OVG. Given the assigned nature of increase  $u_0(t)$ , the transient process for the exciter output at the assigned time interval is determined analogously to that shown above [5, 6].

Construction of the transient process of generator and exciter voltage given the assigned random nature of voltage increase  $u_0(t)$  is depicted in Figure 7.10. The exciter idling characteristic and path  $O_1S_1$  of the exciter shunt winding circuit volt-ampere characteristic are constructed in quadrant I. Point a on the X-axis corresponds in the established mode to nominal exciter independent winding NVO n. s. given specific value  $u_0$ . Characteristic  $\frac{u_{g1}}{u_0} = f(t)$  is constructed in quadrant IV of the same coordinate system with center  $O_1$ . We divide axis  $O_1t$  into parts corresponding to selected time interval  $\Delta t$ .

The exciter quadrant and the generator quadrant are linked via path  $O_2P$  (quadrant II) determined in the corresponding way. A path is drawn from point

a parallel to path  $O_1S_1$ . Point b in the exciter characteristic determines nominal voltage  $U_{B.HOM}$ . The specific magnitude of generator field winding n. s. corresponds to this voltage:

$$F_{r.HOM} = \frac{U_{B.HOM}}{R_{O.B.r}} 2u_{O.B.r}$$

where  $U_{B.HOM}$  corresponds to the voltage value given an exciter load.

Intersection of the horizontals passing through point b and verticals through point c provides point d. Path  $O_2P$ , passing through point d, determines the proportionality between exciter voltage and established generator field n. s.

The construction begins from point 1 corresponding to first time interval  $\Delta t_1$  on the Y-axis in the fourth quadrant of the first system of coordinates. Point 2 in curve  $\frac{u_{of}}{u_0}(t)$  corresponds to interval  $\Delta t_1$ . Next, point 3 of the value of exciter field independent winding established n. s. is determined. Path 3—4 is drawn from point 3 at angle  $\alpha'_{B.r}$  to the exciter idling characteristic. A horizontal is drawn from point 4 to path  $O_2P$ , followed by the drawing of vertical 5—6 determining the generator field winding n. s. value. Path 6—7 is drawn from point 6 at angle  $\alpha_{r,r}$  to the generator x.x.x. Points 4 and 7 determine exciter and generator voltage values corresponding to first time interval  $\Delta t_1$ . The first cycle of the constructions concludes when point 7 is obtained.

Next, the second cycle of constructions is accomplished for  $\Delta t_2$  in an analogous manner. The difference between this and the first cycle is addition of a consideration for an increase in overall exciter field n. s. due to presence of a shunt winding by drawing path 10—11 to the horizontal of the previous exciter output voltage state, i. e., to path 4—5. Path 13—14 is drawn in the same generator's quadrant to the previous state of generator output emf, i. e., to the horizontal passing through point 7. Next, the rest of the construction is analogous to the second cycle. Construction sequence in Figure 7.10 is designated by numbers and indicated by arrows.

Curves  $u_b(t)$  and  $e_r(t)$  obtained from graphical constructions are shown in quadrant III of Figure 7.10. The lag of curve  $u_b(t)$  is determined by the nature of increase  $u_0(t)$ , while that for curve  $e_r(t)$  is determined by the nature of increase  $u_b(t)$  considering the presence of  $u_0(t)$ .

There is nothing special about the construction of the generator reversal for the given circuit, but the reversal was examined above individually for each link in the system (exciter and generator), while the tie-in among quadrants via path  $O_2P$  is depicted clearly in the example just presented. /367

Graphic construction of the transient processes of a GEU with a three-winding exciter. Using the principle of graphic construction demonstrated above for all GEU links, it is possible to construct the entire system's transient processes. The principle of transient process construction as a GED is started is shown in Figure 7.11. Each GEU link is represented by its corresponding quadrant.

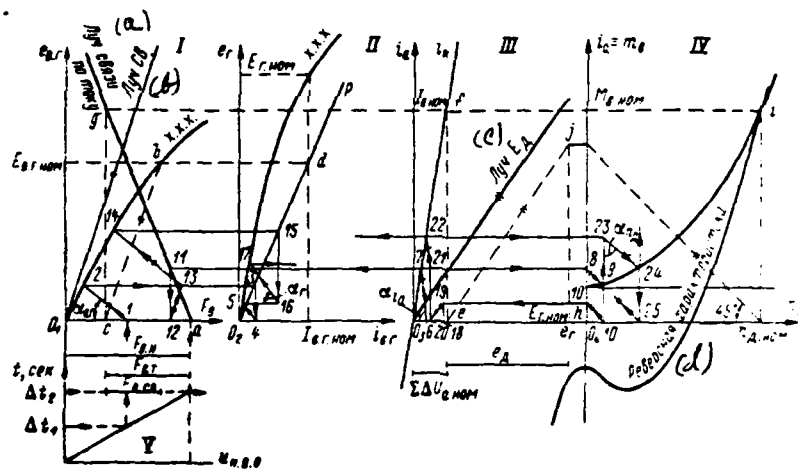


Figure 7.11. Principle of Graphic Construction of GEU Transient Processes During Starting of a GED with a Generator Three-Winding Exciter. a—Current coupling path; b—Path CB; c—Path  $E_d$ ; d—Reversing characteristic.

The slope of the path of transient process constructions for a generator three-winding exciter is determined considering the presence of winding SVO and negative generator armature current feedback.

Using the transforms shown above for the three-winding exciter winding circuit equations, we will get [6, 28]

$$\frac{\Delta e_{b,r}}{\left(\frac{u_{b,0,b}}{R_b} 2\omega_H + \frac{e_{b,r}}{R_{cb}} 2\omega_{cb} - \frac{\Delta u_{cb}}{R_n} 2\omega_n\right) - (i_H 2\omega_H + i_{cb} 2\omega_{cb} - i_n 2\omega_n)} = \frac{\Delta m_{ab}}{k_b m_b} = \operatorname{tg} \alpha_b,$$

where

$$k_b = \frac{2 \cdot 2p\sigma}{\psi_b} \left( \frac{\omega_H^2}{R_b} + \frac{\omega_{cb}^2}{R_{cb}} + \frac{\omega_n^2}{R_n} \right);$$

$m_{ab}$ ,  $m_b$  are the exciter characteristic graph scales;  $R_b$ ,  $R_{cb}$ ,  $R_n$  are impedances of windings NVO, SVO, and PKO.

The three-winding exciter feedback paths and characteristic x.x.x. are plotted in the first quadrant in Figure 7.11.

The slope of the construction path in the second quadrant (for the main /368 generator) is determined from the field winding circuit equation.

Following determinate transforms of this equation for the main generator OVG circuit, we will get

$$\frac{\Delta e_r}{\frac{e_{b,r}}{R_{o,b,r}} - R_{ab} - i_{b,r}} = \frac{\Delta m_i}{k_r m_E} = \operatorname{tg} \alpha_r,$$

where

$$k_r = \frac{2p\sigma\omega_{o,b,r}}{R_{o,b,r} - R_{ab}};$$

$m_i$  and  $m_E$  are generator characteristic graph scales.

Exciter and generator quadrants are coupled by path  $O_2P$ . This path is drawn through point d determining nominal generator field current given a nominal exciter emf value.

Two quadrants, current (third) and propellor (fourth), are used for determination of armature circuit current and GED rotational speed.

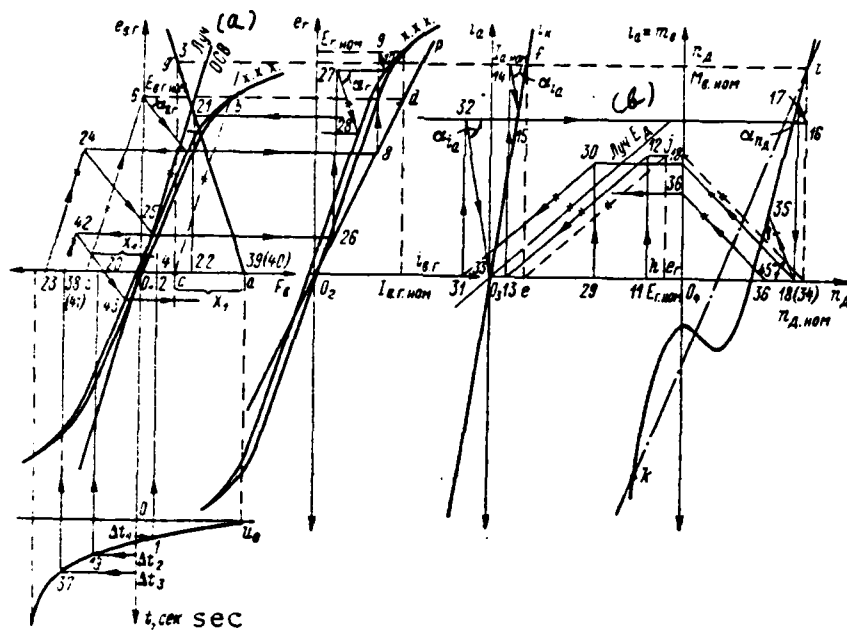


Figure 7.12. Principle of Graphic Construction of GEU Transient Processes During Reversal of a GED with a Generator Three-Winding Exciter. a—Path OSV; b—Path  $E_d$ .

For the current quadrant, using emf control of the main machinery armature after certain transforms we will get the expression determining the graphic construction of transient processes:

$$\frac{\Delta i_a}{e_r - i_a R_a' - e_a} = \frac{\Delta m_E}{L_a m_I} = \operatorname{tg} \alpha_{i_a}, \quad (7.65)$$

where  $m_I$  and  $m_E$  are the third quadrant's current and emf scales;  $R_a'$  and  $L_a'$  /369 are main machinery armature circuit resistance and inductivity.

The left portion of equation (7.65) will contain values that vary: generator emf  $e_r$  changes in the time function and, for each time interval  $\Delta t$  is determined by the construction in the first and second quadrants; the current in the generator armature circuit is determined by the magnitude of generator emf and main propulsion motor counter emf at the given moment, while the increment of current will depend on the increment of generator emf  $e_r$  for time interval  $\Delta t$  and armature circuit inductivity  $L_a'$ ; main propulsion motor counter emf  $e_a = C_{e2} \phi_a n_a$  when  $\phi_a = \text{const}$

will depend only on GED rotational speed. Thus, path  $i_k$  determining the voltage drop in the armature circuit and the path of the proportionality between  $e_a$  and  $n_a$  should be plotted in the propulsion motor's current quadrant. The slopes of these paths can be determined either through the tangents and scales or by another, simpler, method.

The voltage drop in the armatures  $\Delta U_{a \text{ HOM}} = I_{a \text{ HOM}} R_a$  is determined from known values of nominal current in the armature circuit and armature circuit impedance. Segment  $O_3e$  equalling  $\Delta U_{a \text{ HOM}}$  is plotted along the X-axis from point  $O_3$ . We get point  $f$  by drawing a vertical through point  $e$  and a horizontal through the point on the Y-axis corresponding to nominal current. The path passing through point  $f$  is path  $i_k$ . It is possible from the known value of generator emf (point  $h$ ) and established GED rotational speeds to determine point  $j$  by drawing a vertical through point  $h$  and a horizontal through point  $n_{a \text{ HOM}}$ . Segment  $eh$  on the voltage scale equals GED counter emf. Connecting points  $j$  and  $e$ , we get the slope of path  $e_a$ . Thus, paths  $i_k$  and  $e_a$  will be constructed simply and with a reflection of the physical essence. Generator emf ( $O_3h$ ) equals the sum of the voltage drop in the main circuit ( $O_3e$ ) and motor counter emf ( $eh$ ).

The propellor characteristic for one vessel operating mode (moored, for example) is constructed in the quadrant with center  $O_4$ . Since vessel inertia is considerably greater than GED inertia, the starting calculation should be done based on the moored propellor characteristic, which must be given.

One can assume  $m_a = i_a$  when  $\phi_a = \text{const}$ , therefore  $i_a \equiv n_a^2$ .

The angle of proportionality of the propulsion motor rotational speed increase during an increase in current (analogously as during reversal) is determined from the torque equation

$$m_a - m_b = \frac{\sum GD_a^2}{375} \cdot \frac{dn_a}{dt}, \quad (7.66)$$

where  $m_a$  is propulsion motor propelling torque without considering loss torque;  $m_b$  is propellor moment of resistance.

One should double the propelling torque in equation (7.66) if the main propulsion motor is of two-armature construction.

From equation (7.66) we will get

/370

$$\frac{\Delta n_n}{C_{m. \Delta} \phi_a i_a - k n_n^2} = \frac{\Delta t}{\frac{\sum GD_n^2}{375}} = \operatorname{tg} \alpha_{n_n}.$$

The tangent of the slope of the path of rotational speed increase constructions in the diagram is determined taking scales into consideration:

$$\operatorname{tg} \alpha_{n_n} = \frac{\Delta C_{m. \Delta} \phi_a}{\frac{\sum GD_n^2}{375}} \cdot \frac{m i_a}{m n_n} \beta,$$

where  $\beta$  is a factor considering the number of GED armatures.

The presence of negative current feedback (PKO) stipulates introduction of a link between the first and third quadrants via path ag (current coupling path) [6]. Current coupling path construction is based on data from calculation of static characteristics, from which the ratio of exciter field independent (NVO), shunt (SVO), and differentially-compounded (PKO) winding n. s. is known. In Figure 7.11, segment  $O_1 a$  corresponds to independent winding n. s., segment ac to differentially-compounded winding n. s. given nominal main circuit current. Intersection of the horizontals drawn through point f (quadrant III) on the axis of the currents corresponding to the nominal value and verticals drawn through point c determine the direction and slope of the current coupling path passing through points a and g. Actually, when  $I_a = 0$ , PKO n. s. equals zero and, given  $I_{a \text{ nom}}$ , PKO n. s. equals the nominal. Thus, the current coupling path establishes a directly-proportional relationship between generator armature current and PKO n. s. The slope of path CB is determined by the magnitude of this winding's circuit resistance.

The points of the nominal (established) GEU operating mode, for which the calculation of transient processes will be made, will be plotted after construction of the characteristics and drawing of the corresponding paths in the quadrants. These points are designated by letters of the Latin alphabet.

The fifth quadrant, in which construction of GEU transient processes begins, is available for consideration of the time of PU lever transposition.

The magnitude of winding NVO n. s. (point 1) is determined from selected

time interval  $\Delta t$ . This is followed by graphic construction sequentially in all quadrants.

Construction sequence is designated by numbers and indicated by arrows.

The operation to determine the magnitude of PKO n. s. given the corresponding values of main circuit current is added to the second cycle of constructions. For the amount of current corresponding to point 7 in the third quadrant, we will plot on the current coupling path point 11, which was projected to the X-axis. We get the amount of PKO n. s. ← segment a—12. From point 12 we will draw path 12—13, which considers the presence of winding SV0. Next, the entire construction is carried out analogously to the previous, taking into account the previous magnitudes of the values in all quadrants. Construction sequence is indicated by arrows and designated by numbers.

The principle for construction of the GED reversal transient process /372 for a GEU circuit with a three-winding exciter is shown in Figure 7.12. In this case, the presence of the NVO is considered by subtraction of PKO n. s. from the NVO n. s. value, which corresponds to given time interval  $\Delta t$ . For instance, for  $\Delta t_1$ , NVO n. s. decreased as a result of PU lever transposition to value  $O_2-2$ , while PKO n. s. still equals the nominal (segment a—c =  $x_1$ ). Having placed segment  $x_1$  on the left of point 2 and drawing path 5—6 parallel to the self-excitation winding (OSV) path, we determine initial point 6 for construction of the exciter emf dip.

Next, the construction is analogous to that shown for GED starting. The course of the constructions is shown by arrows and designated by numbers. Figure 7.12 shows that, in the field and generator quadrants, construction occurs based on the magnetization curves considering hysteresis loops, while in the propellor quadrant -- considering the nonlinearity of the propellor reversal characteristic. And, there is no need to approximate the last path,  $i_k$  for instance, because is not simplified in so doing.

The corresponding construction path slopes in the quadrants of all links were determined from the parameters of all GEU machinery aboard the tug "Atlant" for example purposes. The transient process curves presented in Figure 7.13

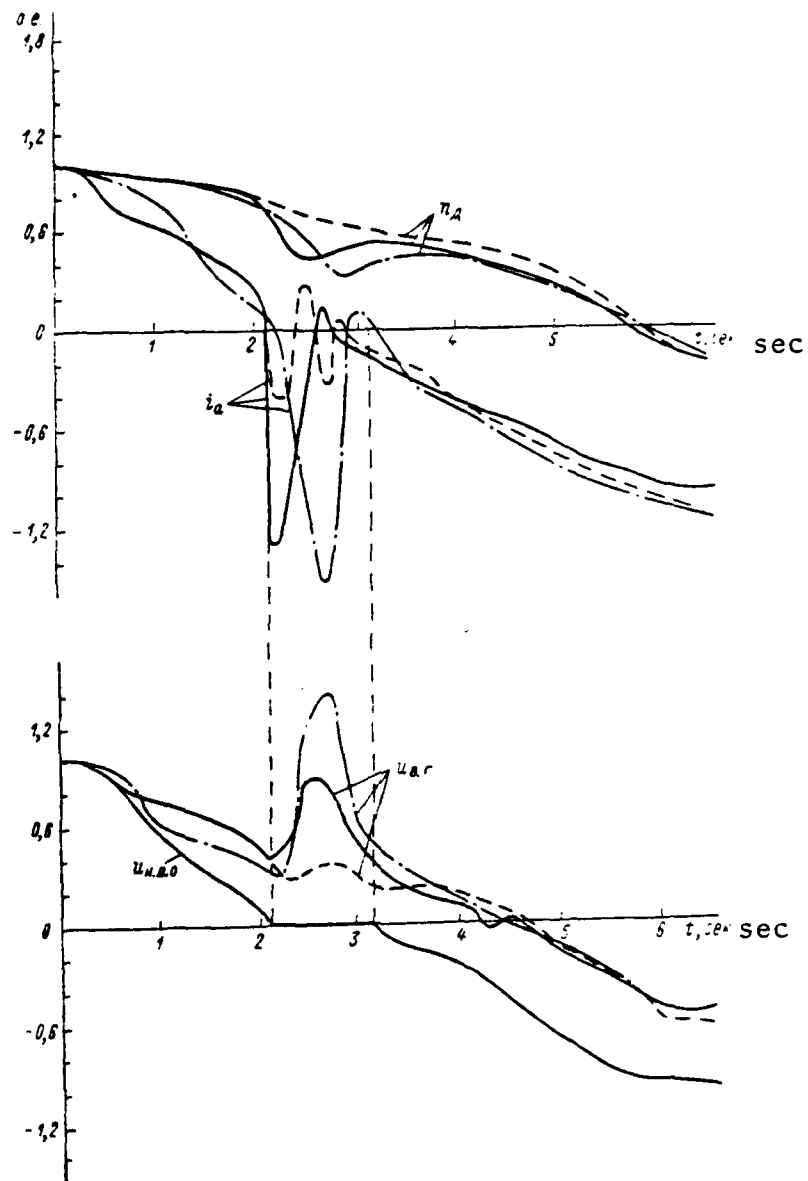


Figure 7.13. Curves of the GED Reversal Transient Process. Solid lines are design curves for a circuit with KVG disconnected; dashed lines are design curves for a circuit without the KVG disconnected; dot-dash lines are test curves with KVG disconnected.

were obtained from calculation of GED reversal for various variants of the winding OVG connection circuit.

## § 7.6 Reversal Time Calculation Using the Loss Evaluation Method

Characteristics of GEU diesel primary motors. We will examine the requirements levied on the primary motors of electrical propulsion plant diesels stemming from the conditions of their reversal.

Diesel motor plants use dc and three-phase ac. Most plants operate on dc. An ac power plant is used only on several ships in the transportation fleet.

Diesel operation in GEU circuits, especially dc circuits, is very complicated and special requirements are levied on them. Satisfaction of these requirements is mandatory for them to operate normally. Diesels, rotating generators, must have:

- 1) an all-mode speed governor making it possible to maintain any speed ranging from nominal to minimal;
- 2) a limiting governor, which cuts off the supply of fuel when rotational speed exceeds the nominal.

Floating control characteristics (4—6) are depicted in Figure 7.14. Diesel power in the control characteristic is changed by a speed governor depending on shaft output by changing the fuel supply. Power  $N$  is changed from /373 minimum to maximum, corresponding to the external characteristic (1—3).

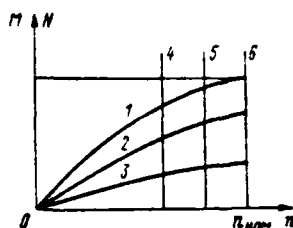


Figure 7.14. Diesel External (1—3) and Control (4—6) Characteristics.

A limiting governor must cut off the fuel supply at increased rotational speed caused by a transformation of a generator into a motor and a motor into a generator when the G—D system stops or it is reversed.

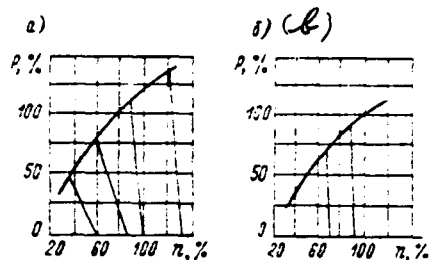


Figure 7.15. Diesel Motor Power Characteristics: a—Control and external given all-mode control, static; b—Same, floating.

Static (a) and floating (b) control characteristics essentially occurring and causing a decrease in rotational speed during an increase in load on the motor from maximum to zero are depicted in Figure 7.15. The constant-error response at nominal speed usually does not exceed 5-8%. The constant-error response value must be in the 7% range in accordance with Register Rules.

Diesel acceleration during reversals can reach a considerable magnitude. Therefore, one must know rotational speed thresholds when the G—D systems stops or when it is operating in the reverse mode so that rotational speed does not drop into the critical speed zone.

Special attention should be paid to diesel operating modes during propellor starts, braking, and reversals and to creating additional technical requirements placed on them, taking the special features of diesel operation into account.

These requirements, mainly in the area of separating the critical speed zone from operating zones, can follow these trends:

- a change  $GD^2$  in the gyrating masses of the generator flywheel and armature connected to the diesel;
- a change in operating rotational speed with proportional decrease in power given constant torque;
- a change in the diameter of the generator shaft or location of its armature's gyrating masses ( $GD^2$ );
- a change in one of two generator bearing structures connected to the diesel.

The most essential problem concerning generator diesel operation is determination of the operating speed zone of its rotation.

Maximum and critical diesel rotational speeds. When a propulsion motor /374 stops, its operation in the generator mode occurs both when its rotational speed is brought to zero and when it is in the reversal mode. A phenomenon of this type is observed in all dc plants operating in the G—D system.

It is possible to use a motion equation to determine generator diesel threshold runaway rotational speed.

The generator aggregate's acceleration operation stipulated by the energy output from the stopped propulsion motor equals

$$A = \frac{J_r \omega^2}{2} \text{ J}$$

where  $J_r$  is the dynamic torque of the inertia equalling  $\frac{GD_r^2}{4}$ , kgf/m<sup>2</sup>;  
 $\omega = \frac{\pi n}{30}$  rad/s.

From there, the energy accumulated in the main propulsion motor will be determined by expression

$$A_s = \frac{GD_A^2 n_{A, \text{nom}}^2}{730 \cdot 9,81} \text{ J} \quad (7.67)$$

If there were no losses, then the equilibrium equation would look like this:

$$(GD_r^2 + GD_{A^2}) (n_{np}^2 - n_{r, \text{nom}}^2) = GD_A^2 n_{A, \text{nom}}^2,$$

where  $n_{np}$  is diesel threshold rotational speed.

Thus, the energy accumulated in the main propulsion motor when it is stopped from nominal speed  $n_{A, \text{nom}}$  to zero would cause the generator diesel to accelerate from nominal  $n_{r, \text{nom}}$  to threshold speed  $n_{r, np}$ . Consequently,

$$n_{r, np} = \sqrt{n_{r, \text{nom}}^2 + \frac{GD_{A^2}}{GD_r^2 + GD_{A^2}} n_{A, \text{nom}}^2} \quad (7.68)$$

This expression determines the maximum possible theoretical value of the aggregate's runaway speed. However, this actually only would occur when there are no losses in the G—D circuit.

We only will consider the main machinery in the first approximation of efficiency. We will introduce their values into expression (7.68) and will consider that  $\eta_A \eta_r \eta_{AB}$  is the efficiency of the propulsion motor, generator, and mechanical -- of the diesel ( $\eta_{AB} \approx 0,85$ ); then, considering that diesel generator kinetic energy given an increment of its speed must equal the loss of stopped propulsion motor's kinetic energy, as well as considering losses in the system, we can write

$$\frac{(n_{r, np}^2 - n_{r, nom}^2)}{2} (GD_r^2 + GD_{AB}^2) = \frac{n_{A, nom}^2}{2} (GD_A^2) \eta_A \eta_r \eta_{AB}, \quad (7.69)$$

where  $n_{r, np}$  is diesel generator threshold rotational speed: /375

$$n_{r, np} = \sqrt{n_{r, nom}^2 + \frac{GD_A^2}{(GD_r^2 + GD_{AB}^2)} n_{A, nom}^2 \eta_A \eta_r \eta_{AB}}. \quad (7.70)$$

This expression is used to determine diesel generator (DG) possible threshold rotational speed.

It should be noted when explaining GEU reversing conditions that DG runaway rotational speed will not correspond always to the electrical propulsion plant's nominal operating mode.

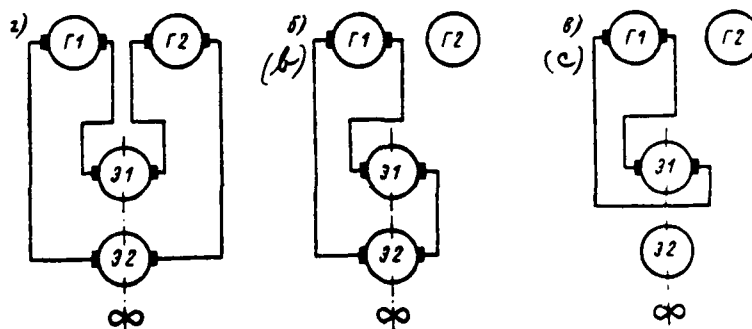


Figure 7.16. Direct Current GEU Operating Mode Circuits: a—Basic mode; b—Economic speed mode; c—Emergency mode.

We will examine a case in which a dc GEU is operating in a circuit depicted in Figure 7.16. We assume:

for the basic mode (Figure 7.16a)

$$GD_A^2 = 1; \quad GD_r^2 + GD_{As}^2 = 1 + 1 = 2; \quad \bar{n}_A = 1;$$

$$k_1 = \frac{GD_A^2}{GD_r^2 + GD_{As}^2} n_A^2 = \frac{1}{2} \cdot 1 = 0,5;$$

for the economic speed mode (Figure 7.16b)

$$GD_A^2 = 1; \quad GD_r^2 + GD_{As}^2 = 1; \quad \bar{n}_A \approx 0,8;$$

$$k_2 = \frac{GD_A^2}{GD_r^2 + GD_{As}^2} n_A^2 \approx \frac{1}{1} \cdot 0,8^2 = 0,64;$$

for the emergency mode (Figure 7.16c)

$$GD_A^2 = 1; \quad GD_r^2 + GD_{As}^2 = 1; \quad \bar{n}_A \approx 0,7; \quad k_3 = 0,49.$$

Thus, the circuit depicted in Figure 7.16b is the most complicated one and should be our reference point during calculations.

The phenomenon of generator diesel acceleration occurs during stops and /376 reversals. Diesel acceleration can reach great magnitudes. Therefore, there is a requirement to know the value of threshold rotational speed so that this speed does not drop into the range of critical speeds.

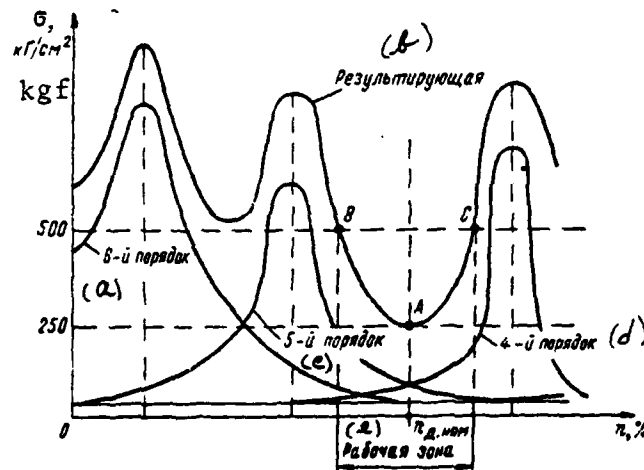


Figure 7.17. Relationship of Mechanical Stresses in Diesel Shaft Material to the Order of the Torsional Vibrations. a—Sixth order; b—Resultant; c—Fifth order; d—Fourth order; e—Operating zone.

If the rotational speed calculated from expression (7.70) turns out to be higher than that determined from point C, then it is necessary to take measures to restrict the reversal time by introducing a device which automatically slows the reversal process, either by increasing the time of control station lever transposition acting upon generator excitation or the exciter, or by other means.

Calculation of reversal time using the loss evaluation method for a G—D system. The infinite increment method examined above is sufficiently labor intensive and requires considerable time to carry out. Here, one should consider that, in some cases, it is necessary to find several runaway speeds for calculation of a tolerable reversal time in order to have the capability to find and construct the curve of the relationship of the infinite speed value to reversal time.

As already pointed out above, the kinetic energy accumulated in a propulsion motor armature must be expended on covering diesel generator runaway energy and to cover losses in the system. Extending the reversal process time, it is possible in so doing to increase losses in the system and, correspondingly /377 to decrease the kinetic energy increment in the aggregate.

To avoid primary motor runaway, the power transmitted to it from the screw must not exceed the power of all the losses which can take place in a system during the reversal period.

We will examine the influence of losses in a G—D system and the relationship of the operation of these losses to assumed reversal time values.

1. During a reversal in the plugging mode, the energy of the screw will be expended partially on heating the generator--main propulsion motor circuit. The resistance of this circuit is low. Therefore, the expended power of the losses in the copper (machinery armatures, network, and differentially-compounded winding) will comprise

$$P_{\text{пот. u}} = I^2 \sum R \quad J \quad (7.71)$$

The tolerable current value equals  $2I_{s, \text{nom}}$ . If you consider that a change in current will occur mainly in accordance with a linear law, then its root-mean-square value equals  $\frac{2}{3} I_{s, \text{nom}}$ .

The voltage drop in the armature circuit and network equals 5-7% of generator voltage  $U_{\text{НОМ}}$ . Therefore,

$$P_{\text{ПОТ. Ц}} \approx \frac{2}{3} I_{\text{а. НОМ}} 0,07 U_{\text{НОМ}} \approx 0,1 I_{\text{а. НОМ}} U_{\text{НОМ}} J$$

comprising 10% of the generator power.

2. Losses in machinery iron will occur due presence of propulsion motor field constant flux  $\phi_a$ . One can consider losses in iron as proportional to rotational speed. Considering this, one can assume that

$$P_{\text{ж}} = 0,5 P_{\text{ж. НОМ}}, \quad (7.72)$$

i. e., that losses in the propulsion motor iron equal one-half of nominal iron losses.

3. Mechanical losses in a main propulsion motor change proportionally to rotational speed. Consequently,

$$P_{\text{д. мех}} \approx 0,5 P_{\text{д. мех. НОМ}} \quad (7.73)$$

4. Iron losses in a generator given almost constant rotational speed will change proportionally to  $\phi_r^2$ . Since generator field flux will drop sharply, one can disregard the influence of iron losses.

5. Mechanical losses in a generator can be taken as equal to the nominal since generator rotational speed changes in relatively small ranges, i. e.,

$$P_{\text{г. мех}} = P_{\text{г. мех. НОМ}} \quad (7.74)$$

6. Mechanical losses  $P_{\text{дл. тр}}$  should be taken into account for a diesel. Power losses to friction in a diesel generator are approximately constant. Therefore, they are determined by the diesel's mechanical efficiency.

Losses to friction in a diesel will equal /378

$$P_{\text{дл. тр}} \approx 0,15 P_{\text{НОМ}} \quad (7.75)$$

The overall loss value is determined by expression

$$\sum \rho_{\text{пот}} = \rho_{\text{пот. и}} + \rho_{\text{ж}} + \rho_{\text{д. мех}} + \rho_{\text{г. мех}} + \rho_{\text{дз. тр.}} \quad (7.76)$$

The reversal should be carried out not instantaneously, but gradually over a certain period of time, if there is a requirement to decrease the diesel generator runaway speed. Then the main propulsion motor energy and the mass of the screw and water attracted by it will be expended not only on diesel generator runaway, but also on additional losses in the system.

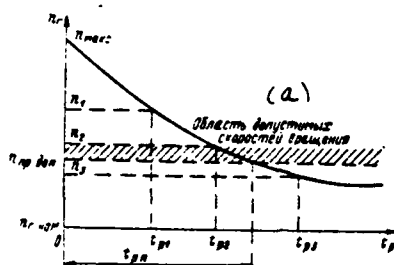


Figure 7.18. Curve  $n_r = f(t_p)$  of Runaway Rotational Speed and Threshold Speed Values. a—Area of tolerable rotational speeds.

The work of the losses must be covered by a reserve of propulsion motor kinetic energy. Then, we can write

$$\frac{(GD_r^2 + GD_{дз}^2)(n_{r.ном}^2 - n_{r.ном}^2)}{730 \cdot 9.81} + \sum \rho_{\text{пот}} t_p = \frac{GD_A^2 n_A^2}{730 \cdot 9.81} \quad (7.77)$$

Solving expression (7.77) for runaway rotational speed  $n_{r.ном}$ , we will get

$$n_{r.ном} = \sqrt{n_{r.ном}^2 + \frac{GD_A^2}{GD_r^2 + GD_{дз}^2} n_A^2 - \frac{9.81 \cdot 730 \sum \rho_{\text{пот}} t_p}{GD_r^2 + GD_{дз}^2}} \quad (7.78)$$

The curve of the relationship of diesel generator threshold runaway speed (Figure 7.18) to assumed reversal time  $n_r = f(t_p)$  can be constructed as a result of the calculation. Plotted on this curve are the values of the constrained speeds permitted based on the torsional vibrations taken from the curve presented

in Figure 7.17. The assumed reversal time value  $t_{p.n}$  will make it possible to determine the time of control station lever transposition given based on the circuit. The calculation is done in tabular form (Tables 7.3 and 7.4).

$\Delta t$ , сек (a)	$t$ , сек (a)	$m_d$ , кгм (b)	$m_p$ , кгм (b)	$m_{dyn}$ , кгм (b)	$\Delta n_d$ , об/мин (c)	$n_d$ , об/мин (c)	$P_d$ , квт (d)
----------------------------	------------------	-----------------------	-----------------------	---------------------------	---------------------------------	--------------------------	-----------------------

Table 7.3. Calculation of a Direct Current Electrical Propulsion Plant Reversal. a—sec; b—kg-m; c—rpm; d—kW.

$\Delta t$ , сек (a)	$t$ , сек (b)	$P_d$ , квт (d)	$m_r$ , кгм (c)	$m_p$ , кгм (c)	$m_{dyn}$ , кгм (c)	$\Delta n_r$ , об/мин (d)	$n_r$ , об/мин (d)
----------------------------	------------------	-----------------------	-----------------------	-----------------------	---------------------------	---------------------------------	--------------------------

Table 7.4. Calculation of Diesel Generator Runaway Speed. a—sec; b—kW; c—kg-m; d—rpm.

Transient process curves from given time intervals  $\Delta t$  will be constructed based on the above tables.

Mathematical Modelling for Analysis and Synthesis of  
Electrical Propulsion Plant Transient Processes

§ 8.1 General Assumptions

Special features of GEU transient processes and their calculation using modelling methods. Development of automatic control systems and their wide use in electrical propulsion plants require solution of several problems linked with rational selection of the structures of the electrical propulsion plant circuits themselves and of the characteristics of individual elements, stability calculations considering the influence of variable external navigational conditions, and evaluation of the influence of individual parameters on the course of propulsion plant transient processes and electric ship maneuvering characteristics.

Investigation of dynamic modes presents great difficulties and requires expenditure of a great deal of time even for the simplest GEU systems, transient processes in which with known assumptions described by linear differential equations. These difficulties grow immeasurably for the very complex modern automated propulsion plants, similar for example to the atomic icebreaker "Lenin," ice navigation electric cargo ships, a series of port icebreakers, and several other vessels, if one keeps in mind the presence in these plants of elements with nonlinear characteristics and variable parameters. This also means consideration of the complex form of the hydrodynamic characteristic of the propeller, as well as the continually and radically changing vessel external navigating conditions (variable external disturbances).

Use of modelling methods and equipment makes it possible at a definite stage of analytical investigation of GEU dynamic processes with significantly less time and equipment expenditures to solve the majority of problems involving analysis and synthesis of the dynamics of automated electrical propulsion plants.

Physical, mathematical, and combined modelling are being used at the present time [11, 12, 22, 29].

Physical modelling is founded on the principle of the study of phenomena in models having an identical physical nature as does the prototype. For instance, during design of propellers and rudders based on wind-tunnel test materials, during the study and calculation of the resistance of water to vessel movement using models tested in tanks, and when replacing modelled powerful generators /380 with low-power generators, in all such instances, the model must have parameters whose values change based on the laws of physical modelling. Since here the physical nature of the process does not change, the model recreates the entire complex of phenomena accompanying and characterizing the investigated process.

A similar investigation also might include those aspects of phenomena, the control process in particular, which do not lend themselves to mathematical description and cannot be considered when compiling a system of differential equations describing the transient processes occurring. This can apply in particular to electrical propulsion plants and to consideration of the phenomenon of the separation of the stream of water on the propeller blades during reverse. Therefore, when studying a complex of phenomena, physical modelling makes it possible to intensify the comprehension of these phenomena and refine the mathematical description of individual processes. Physical modelling methods are used widely for solution of problems concerning study of powerful electrical systems and large electrical machinery, in aero- and hydrodynamics, and in construction technology [24].

This method has the following advantages: here, the properties of the control system are reproduced more fully than when mathematical modelling is used since the latter is based to a known degree on idealized description of the dynamics of the control process; the control apparatus can be connected to the investigated model without using convertors, which can introduce additional errors and distortions.

However, the significant shortcomings of the physical modelling method should be noted: each investigated process requires creation of a special model; a change in a parameter of the modelled object elicits the requirement for labor-intensive reworking of the model and even its complete replacement; models of complicated objects (main propulsion motors, primary motors) are very expensive.

In this connection, during investigation of electrical propulsion plant transient processes, physical modelling methods have not found wide use both due to their high cost and lack of standardization, as well as the complexity of manufacturing their hydrodynamic complex mainly.

The physical modelling method is less widespread than the mathematical modelling method but, all the same, use of this method turns out to be very effective in many instances. Investigations by Academician M. P. Kostenko [24] and Professor V. I. Venikov [11] into physical modelling of control processes, as well as of various non-stationary modes in power systems are well known in our country.

Special features in using the mathematical modelling method. The mathematical modelling method has been used very widely in recent years in the study of the dynamics of electrical propulsion plant systems. This method is based upon the identity of differential equations describing phenomena occurring in a /381 model and in a prototype. The method provides the opportunity to use standard devices making it possible to solve an entire class of problems, provides speed and ease in transition from solution of one problem to that of another, and makes it possible to introduce variable parameters into different initial conditions. Its use eliminates the influence of the model equipment's own parameters on the accuracy of problem solution, simplicity in introduction of varied disturbances is achieved, and the possibility of studying dynamic processes link-by-link is provided [22, 29].

The mathematical modelling method also is convenient because there is an opportunity to use any time scale, i. e., the solution can be achieved in an artificial time scale. In addition, it is possible to consider changes in the parameters of individual elements in the investigated system and reveal the influence of these changes on the nature of transient process flow.

It sometimes turns out to be advisable to combine systems which serve mathematical and physical modelling in order to obtain a single modelling system making it possible to combine the advantages of both methods.

The original approach in the mathematical modelling method is mathematical

description of the process, while the mathematical models themselves can be looked upon as devices realizing the given mathematical ratios, i. e., like computers.

Use of mathematical computers pursues in this case the goal of speeding up the calculations of electrical propulsion plant dynamics, easing experimental investigation and tuning of the plant circuitry, and revealing the influence of individual elements and advisability of their use. In all the aforementioned instances, standard electronic models are used as the mathematical model of an electrical propulsion plant as a whole or of its individual elements.

Development of mathematical modelling methods led to the appearance of both digital and analog standard computers. An electronic computer is referred to as analog (electronic model) if the mathematical operations in the computer occur in continually-changing magnitudes. A computer is referred to as digital (electronic digital computer) if the mathematical operations in the computer occur in discretely-changing magnitudes.

Appearance of these computers not only made it possible to solve mathematical problems describing transient processes in dc and ac electrical propulsion plants previously insoluble due to the enormous volume of computations, but also led to a fundamental change in views on the advisability of carrying out such calculations and on the field of use of mathematical methods of calculation, which made it possible to look upon computers as a mechanism of mental labor.

Obtaining a solution for any type of equation with the aid of units /382 means connecting them into a closed system, the processes in which described by a given equation (by a given system of equations). This type of operation is called an equation set in a computer. Prior to forming a set, it is necessary ahead of time to determine:

- how many and which units are needed for solution of a given equation;
- how should the units be connected;
- which parameters must all units used for the solution have.

Depiction of a schematic of a set of equations for analog computers (AVM).  
For convenience, first the circuit is depicted on paper. After analysis and

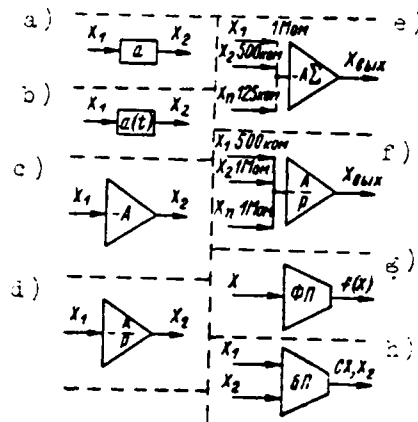


Figure 8.1. Unit Conditional Designations.

correction, the equations are input in the machine in accordance with the selected circuit. This circuit is called the set flow chart. Each computer unit in the circuit is depicted by specific conditional designations: unit interconnection is shown by means of lines with arrows. Since all input and output units have one common ground, the circuit is depicted as single wire (Figure 8.1). The circuit includes:

- a) a multiplier by a constant factor of the potentiometer type:  $x_1$  is input value;  $x_2$  is output value;  $a$  is the value of the factor established for the unit (always positive and less than one);
- b) multiplier by a variable factor:  $a(t)$  is the law of factor change set in the unit;
- c) multiplier by a constant factor with an electronic amplifier:  $A$  is a factor set in the unit (it has a negative sign);
- d) integrator:  $-\frac{A}{P}$  - integration factor (always with a "minus" sign);
- e) adder:  $-A \sum$  - factor considering the action of negative feedback ("minus" sign) and the magnitude of the resistance in the feedback circuit  $R_1 = 1 \text{ M}\Omega$  corresponds to  $A = 1$ . This then means that  $R_0 = 0.1 \text{ M}\Omega$  corresponds to  $A = 0.1$ , and so forth; the magnitudes of input resistances  $R_i$  ( $i = 1, 2, \dots, n$ ) are designated at each input; the factor by which input value  $x_1$  is multiplied is determined by the formula

$$a_i = \frac{A}{R_i},$$

where  $R_i$  is the amount of input resistance,  $M\Omega$ ;

f) parameters of the adding integrator, just as in the adder, are /383 determined by feedback circuit parameters, while the magnitudes of the input resistances are designated at each input; usually it is assumed that when  $C = 1.0 \mu F$ ,  $A = 1$ . Then, accordingly, when  $C = 0.1 \mu F$ ,  $A = 10$  and so on. The factor by which input magnitude  $x_1$  is multiplied, as in the adder, equals

$$\beta_i = \frac{A}{R_i},$$

where  $R_i$  is expressed in megohms;

g) function generator: at the unit output there must be specification of the factor with which the assigned function in the unit was set;

h) product unit.

## § 8.2 Mathematical Modelling of the Dynamic Characteristics of Icebreaker GEU with Magnetic Amplifiers in the Pilot Excitation System in the Propellor-Ice Interaction Mode

Initial data. A methodology is presented for analysis and selection of optimum characteristics for an icebreaker electrical propulsion plant with magnetic amplifiers in the main generator and main propulsion motor pilot excitation system. A schematic of the plant is shown in Figure 8.2.

Assumed designations and initial data are:

$$E_{г. ном}, E_{д. ном}, U_{г. ном}, n_{г. ном}, n_{д. ном}, I_{г. ном}, P_{г. ном}, P_{д. ном}, \Phi_{г. ном}, \Phi_{д. ном}, \omega_{г. ном}, \omega_{д. ном}, M_{г. ном}, M_{д. ном}$$

are nominal values of the following main circuit parameters in the movement in open water mode: main generator and main propulsion motor emf, generator voltage, main generator and main propulsion motor rotational speeds, main circuit current, generator and main propulsion motor powers, main generator and main propulsion motor field fluxes, main generator and main propulsion motor angular rotational speeds, and main generator and GED electromagnetic moments.

$$GD_A^2, J_A, L_{г. л}, L_{д. л}, R_{г. л}, R_{д. л}, \omega_{о. г. л}, \omega_{о. д. л}, \omega_{о. в. д}, R_{о. в. г}, R_{о. в. д}, L_{в. г}, L_{в. д}, \Phi_{в. г. ном}, \Phi_{в. д. ном}, E_{в. г. ном}, U_{в. г. ном}, E_{в. д. ном}, U_{в. д. ном}$$

are shafting line moment of gyration, shafting line moment of /384

inertia, generator armature (including PKO windings) ohmic resistances, number of generator armature turns and of generator and GED field winding turns (per pole), generator and GED field winding ohmic resistances, generator and GED field circuit inductivities, generator and GED exciter field flux nominal values, emf nominal values, and generator and GED exciter voltages.

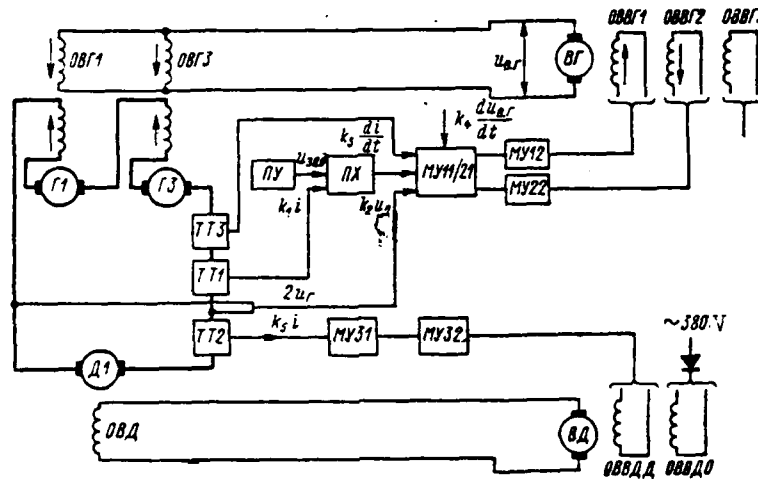


Figure 8.2. Schematic of a GEU with Magnetic Amplifiers as Pilot Exciters and Governors.

$I_{в.г.ном}, I_{в.д.ном}, I_{в.в.г.ном}, I_{в.в.д.о}, I_{в.в.д.д}$  are the nominal values of generator and main propulsion motor field circuit currents and GED exciter field and main generator exciter fields (GED exciter field main and additional windings);

$$L_{я.в.г}, L_{я.в.д}, R_{я.в.г}, R_{я.в.д}, L_{в.в.г}, L_{в.в.д}, R_{в.в.г}, R_{в.в.д}, \omega_{о.в.в.г}, \omega_{о.в.в.д}, U_{в.в.г.н}, U_{в.в.д.о}, U_{в.в.д.д}, F_{в.в.г}, F_{в.в.д}, F_{в.г}$$

$F_{МУ11}$  are generator and GED field armature inductivities and ohmic resistances, generator and GED exciter field inductivities and ohmic resistances, number of generator exciter field winding, main winding, and GED additional exciter turns, generator and main propulsion motor exciter field, main, and additional winding voltages, generator and GED exciter field magnetizing force, generator and МУ11 field magnetizing force;

$U_{с.г}, U_{в.в.д.о}, U_{в.в.д.д}, I_{г.н}, I_{г.д}, I_{МУ11}$  are voltages: standard in the МУ31 circuit, of GED exciter field main winding feed source, master from the magnetic field /385

switch, and values of OUG1, OUG2, and MU11 winding currents;

$L_{3\Delta\Delta}, L_{\tau. y. r}, L_{y. r1}, L_{y. r2}, R_{3\Delta\Delta}, R_{\tau. y. r}, \bar{R}_{y. r1}, \bar{R}_{y. r2}, R_{y. r. \Delta}, R_{\tau. r. r}$   
 are transformer magnetic field and secondary winding switch inductivities, winding UG1 and UG2 circuit overall inductivity, transformer magnetic field and secondary winding circuit resistances, winding UG1, UG2, UGD2 winding circuit overall resistance, and winding OUG1 (MU11) and transformer series-connected resistance;

$\omega_{\tau p}, \omega_{\tau. y. r}, \omega_{y. r1}$  - are the number of transformer primary winding, secondary winding, and OUG1 (MU21) control winding turns.

Designations indexed «CB» correspond to the icebreaker open water operating mode, those indexed «ШВ» - to the moored operating mode, and «Л» to the operating in ice mode. Generator and GED field flux factors are determined from expressions

$$\lambda = \frac{\omega_{o. r. \Delta}}{\omega_{o. \Delta. r}}; \quad (8.1)$$

$$\phi_r = \frac{u_r}{n_r} \frac{30}{\pi} \text{ V}\cdot\text{sec} \quad (8.2)$$

$$\phi_{\Delta} = \frac{u_{\Delta}}{n_{\Delta}} \frac{30}{\pi} \text{ V}\cdot\text{sec} \quad (8.3)$$

Corresponding parameter designations bearing a line across the top indicate their values in relative units, if their nominal values in the moored mode were assumed as the base values. For example:

$$\bar{\phi}_r = \frac{\phi_r}{\Phi_{r. \text{ном. ШВ}}};$$

$$\bar{u}_r = \frac{u_r}{U_{r. \text{ном. ШВ}}};$$

$$\bar{n}_{\Delta} = \frac{n_{\Delta}}{n_{\Delta. \text{ном. ШВ}}};$$

$$\bar{\omega}_{\Delta} = \frac{\omega_{\Delta}}{\omega_{\Delta. \text{ном. ШВ}}}.$$

Calculation of dynamic characteristics requires that one have available, along with the numerical values of all aforementioned parameters, main generator, GED, exciter, and pilot exciter (MU) magnetization (or idling) characteristics, which can be provided in the following tabular form:

$i_{\text{в.д.}} \text{ a}$	$\frac{u_{\text{д}}}{n_{\text{д}}} \cdot \text{V} \cdot \text{rpm}$	$\phi_{\text{д}} = \frac{u_{\text{д}}}{n_{\text{д}}} \cdot \frac{30}{\pi} \cdot \text{V} \cdot \text{sec}$

GED Magnetizing Characteristic.

$i_{\text{в.г}} - \lambda i_{\text{в.д.}} \text{ a}$	$\frac{u_{\text{г}}}{n_{\text{г}}} \cdot \text{V} \cdot \text{rpm}$	$\phi_{\text{г}} = \frac{u_{\text{г}}}{n_{\text{г}}} \cdot \frac{30}{\pi} \cdot \text{V} \cdot \text{sec}$

Main Generator Magnetization Characteristic.

$F_{\text{в.}} \text{ aW}$	$u_{\text{в.}} \text{ V}$

Exciter Idling Characteristic.

$i_{\text{г.}} \text{ mA}$	$E_{\text{МУ}} \text{ V}$

MU Magnetization Characteristic.

Calculation of the GEU static mode. Main propulsion motor excitation.

In the navigation in open water mode, when only one (the main) exciter field winding is operating at field current  $I_{\text{в.д.}} \text{ a}$ , A, the magnetic flux will be  $\Phi_{\text{в.д.}}$ . Then the electromagnetic moment in the air space at armature circuit current  $I_{\text{в.д.}}$  will be determined by expression

$$M_{\text{в.д.}} = \Phi_{\text{в.д.}} I_{\text{в.д.}} \quad \text{kW} \times \text{sec.} \quad (8.4)$$

Here, angular velocity equals

$$\omega_{\lambda, \text{cs}} = \frac{d\Phi_{\lambda, \text{cs}}}{dt} = \frac{m_r U_r - R_{\lambda, \text{cs}} I_{\lambda, \text{cs}}}{\Phi_{\lambda, \text{cs}}} \quad \text{sec}^{-1} \quad (8.5)$$

and

$$n_{\lambda, \text{cs}} = \omega_{\lambda, \text{cs}} \frac{30}{\pi} \quad \text{rpm.} \quad (8.6)$$

Voltage of series-connected generators will be:

$$\Phi_{\lambda, \text{cs}} \frac{d\Phi_{\lambda, \text{cs}}}{dt} = m_r U_r - R_{\lambda, \text{cs}} I_{\lambda, \text{cs}}. \quad (8.7)$$

Considering idling losses and friction losses, as well as having assumed  $\eta_{\lambda} = 0,975$ , we will find the mechanical power transmitted by the main propulsion motor to the propeller:

$$\eta_{\lambda} P_{\lambda, \text{cs}} = \eta_{\lambda} M_{\lambda, \text{cs}} \omega_{\lambda, \text{cs}} \quad \text{kW} \quad (8.8)$$

Then, the power of generators G1 and G2 must equal

/387

$$P_{r, \text{cs}} = P_{r1} + P_{r2} = P_{\lambda, \text{cs}} + I_{\lambda, \text{cs}}^2 R_{\lambda, \text{cs}}. \quad (8.9)$$

In the navigating in ice mode, the motor must develop in the nominal mode at equal generator power rotational speeds  $n_{\lambda, \text{cs}}$  and  $\frac{d\Phi_{\lambda, \text{cs}}}{dt} = \omega_{\lambda, \text{cs}} \text{ sec}^{-1}$ , nominal electromagnetic torque

$$M_{\lambda, \text{cs}} = \Phi_{\lambda, \text{cs}} I_{\lambda, \text{cs}} \quad \text{kW} \times \text{sec}, \quad (8.10)$$

meanwhile

$$\Phi_{\lambda, \text{cs}} = \frac{m_r U_r - R_{\lambda, \text{cs}} I_{\lambda, \text{cs}}}{\omega_{\lambda, \text{cs}}}. \quad (8.11)$$

Field current  $I_{\lambda, \text{cs}}$  is required to create flux  $\Phi_{\lambda, \text{cs}}$  in accordance with the magnetization characteristic.

Exciter VD in the navigation in open water mode must develop emf equalling

$$E_{\text{в.д.св}} = I_{\text{в.д.св}}(R_{\text{в.д}} + R_{\text{в.д.н}}) \quad \text{V}$$

which corresponds, in accordance with the exciter characteristic, to magnetizing force  $F_{\text{в.д.св}}$ . Here, the number of turns based on the main winding must comprise  $\omega_{\text{в.д.св}} n \eta$  at  $I_{\text{в.д.св}}$  A.

In the navigation in ice mode at current value  $I_{\text{в.д.л}}$ , exciter VD must develop emf equalling  $E_{\text{в.д.л}}^{\text{в}}$  V, which, in accordance with the exciter characteristic, requires an n. s. of  $F_{\text{в.д.л}}$  or field current

$$I_{\text{в.д.л.о}} + I_{\text{в.д.л.л}} = \frac{F_{\text{в.д.л.л}} + F_{\text{в.д.л.о}}}{\omega_{\text{в.д.л.о}} + \omega_{\text{в.д.л.л}}} \quad \text{A}$$

i. e., when navigating in ice, winding 0VVD with resistance  $R_{\text{в.д.л.л}}$  must receive from MU32 voltage

$$U_{\text{в.д.л.л}} = R_{\text{в.д.л.л}}(I_{\text{в.д.л.о}} + I_{\text{в.д.л.л}}) \quad \text{V.}$$

Main generator excitation. The following voltages are brought to control circuit A1 of series-connected MU11 and MU21 (Figure 8.3): from the magnetic field reversing switch voltage  $u_{\text{мр}}$  and opposite to it voltage from the transformer secondary winding equalling  $u_{\text{т}}$  and proportional voltage of the main circuit current change rate, and, from dc transformer T1 (see Figure 8.2), voltage  $u_{\text{т.т1}}$  proportional to main circuit current  $u_{\text{т.т1}} = \epsilon i_{\text{т}}$ .

The voltage from T1 equals

$$u_{\text{т.т1}} = \frac{R_{\text{т.т.т}}}{1+r} i_{\text{т.т1}} + \frac{\epsilon i_{\text{т}}}{1+r}, \quad (8.12)$$

where

$$r = \frac{R_{\text{т.т.т}}}{R_{\text{т.т.т}}}$$

Transformer T1 primary circuit current induces in the secondary winding /388

voltage

$$u_{T.y.r} = R_{T.y.r} i_{y.r} + L_{T.y.r} \frac{di_{y.r}}{dt} + \frac{\omega_{0.T1}}{\omega_{T.y.r}} L_T \frac{di_n}{dt} \quad (8.13)$$

Voltage  $u_{3a0}$  for the nominal mode equals 25 V.

Overall magnetizing force will be determined from expression

$$F_{MV11/21} = F_{0.y.r1} - F_{0.y.r2} - F_{0.y.r3} \quad (8.14)$$

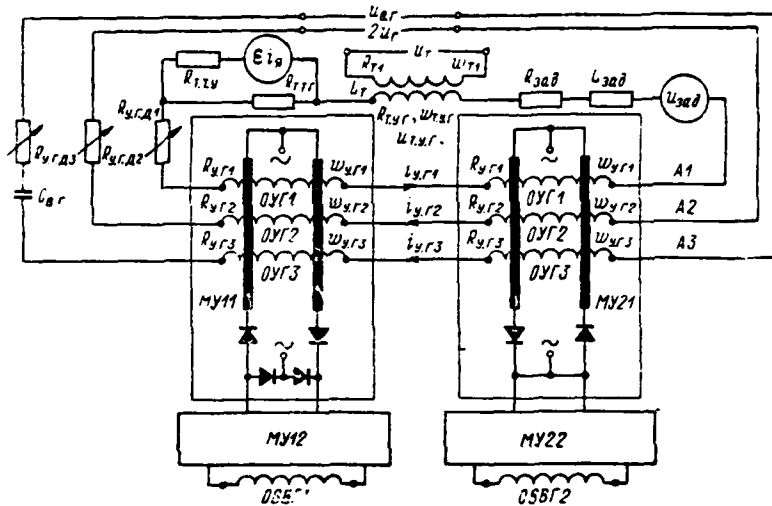


Figure 8.3. Schematic of a Magnetic Amplifier in a Generator Pilot Excitation System (Generator Field Circuit Design Circuit).

Magnetizing force  $F_{MV11/21}$  creates magnetic flux

$$\phi_{MV11/21} = f(F_{MV11/21}) \quad (8.15)$$

One should consider that each MU control winding thus creates in transient processes inductive voltage of the type (considering winding mutual induction)

$$\begin{aligned} u_{MV11/21} &= \omega_{MV11/21} \frac{d\phi_{MV11/21}}{dt} = \omega_{MV11/21} \frac{\partial \phi_{MV11/21}}{\partial F_{MV11/21}} \frac{dF_{MV11/21}}{dt} = \\ &= \omega_{MV11/21} \dot{\phi}_{MV11/21} F_{MV11/21} \end{aligned} \quad (8.16)$$

The following equation is justified for winding OUG1:

$$u_{3A} = \bar{R}_{y,r1} i_{y,r1} + \bar{L}_{y,r1} \frac{di_{y,r1}}{dt} + 2\omega_{y,r1} \frac{\partial \phi_{MY11/21}}{\partial F_{MY11/21}} \frac{dF_{MY11/21}}{dt} + \frac{e}{1+r} i_n + \lambda_r L_r \frac{di_n}{dt}, \quad (8.17)$$

where  $\bar{R}_{y,r1}$  - is circuit UG1 overall resistance:

$$\bar{R}_{y,r1} = R_{3A} + R_{T,y,r} + \frac{R_{T,r,y}}{1+r} + R_{y,r,A1} + 2R_{y,r1}; \quad (8.18)$$

$\bar{L}_{y,r1} = L_{3A} + L_{T,y,r}$  is overall inductivity;  $\lambda_r = \frac{\omega_{r1}}{\omega_{r2}}$  - is a transformation ratio.

The magnitude of transformer secondary winding inductivity  $L_{T,y,r}$  varies during modelling.

In the nominal mode, i. e., for current  $I_{n,ном}$  and voltage  $u_r$ , the UG1 control circuit receives for direct voltage transformer T1 voltage equalling  $e I_{n,ном} V$  and, from the magnetic field switch,  $u_{3A} = 25 V$ , which create field current  $i_{v,r1}$  mA.

The fact that the amount of resistance must be  $R_{v,r,A1}$  ohms stems from this requirement.

The voltage equilibrium equation for control winding OUG2 has the form (if one considers that voltage  $R_{y,r,A2}$  is supplied via resistance  $2u_r$  to winding OUG2):

$$2u_r = (R_{y,r,A2} + 2R_{y,r2}) i_{y,r2} - \omega_{y,r2} \frac{\partial \phi_{MY11/21}}{\partial F_{MY11/21}} \cdot \frac{dF_{MY11/21}}{dt}. \quad (8.19)$$

The second member of the equation's right side equals the induction voltage stipulated by total magnetic flux  $\phi_{MY11/21}$ . In the nominal mode, control current equals  $I_{y,r2}$  mA. It follows from this that at known values  $R_{y,r2}$  and  $2u_r$  additional resistance is determined by value  $R_{v,r,A2}$  kΩ.

The equation for circuit UG3 for control winding OUG3, intended to serve

as voltage unity feedback  $u_{b.r.}$  has the form

$$C_{b.r.} \frac{du_{b.r.}}{dt} = T_{y.r3} \frac{di_{y.r3}}{dt} + \quad (8.20)$$

where

$$+ i_{y.r3} - 2\omega_{y.r3} C_{b.r.} \frac{\partial \phi_{MY11/21}}{\partial F_{MY11/21}} \frac{d^2 F_{MY11/21}}{dt^2},$$

$$T_{y.r3} = C_{b.r.} (R_{y.r.23} + 2R_{y.r3}) = C_{b.r.} \bar{R}_{y.r3}. \quad (8.21)$$

The magnitude of voltage change rate  $u_{b.r.}$  is fed to winding UG3 from exciter VG via capacitor  $C_{b.r.}$  and series-connected resistance  $R_{y.r.23}$ .

Disregarding the values of the second order infinitesimals for overall magnetizing force

$$F_{MY11/21} = \omega_{y.r1} i_{y.r1} - \omega_{y.r2} i_{y.r2} - \omega_{y.r3} i_{y.r3}, \quad (8.22)$$

we will get differential equation

$$T_{MY11/21} \frac{dF_{MY11/21}}{dt} + F_{MY11/21} = \frac{\omega_{y.r1}}{R_{y.r1}} \times \quad /390$$

$$\times \left[ u_{32A} - \frac{ei_n}{1-r} - \lambda_y L_r \frac{di_n}{dt} \right] -$$

$$- \frac{2\omega_{y.r3}}{R_{y.r3}} u_r - \omega_{y.r3} C_{b.r.} \frac{du_{b.r.}}{dt}. \quad (8.23)$$

The MU12 equation will have the form

$$T_{MY12} \frac{du_{b.a.r.}}{dt} + u_{b.a.r.} = u_{MY11/12} (F_{MY11/12}). \quad (8.24)$$

As a result of the voltage from MU12 applied to winding VWG, current  $i_{b.a.r.}$  arises from equation

$$u_{b.a.r.} = R_{b.a.r.} i_{b.a.r.} + L_{b.a.r.} \frac{di_{b.a.r.}}{dt} \quad (8.25)$$

or, following a transform,

$$T_{b.a.r.} \frac{di_{b.a.r.}}{dt} + i_{b.a.r.} = \frac{u_{b.a.r.}}{R_{b.a.r.}} \quad (8.26)$$

Consideration was taken when writing this equation that magnetizing force  $F_{M11/12}$  induces in MU12 and MU22 (Figure 8.3) output voltage  $u_{b, b, r}$ , which is fed to exciter VG field winding in such a way that each winding runs in one direction. For simplification, we assume that  $u_{b, b, r}$  is fed to one winding in positive and negative directions, at the same time disregarding the effect of both field windings.

Generator field winding. Magnetizing force  $F_{b, b, r} = \omega_{b, b, r} i_{b, b, r}$  induces in generator VG voltage  $u_{b, r} = u_{b, r}(F_{b, b, r})$ . In accordance with the exciter VG characteristic, function  $u_{b, r}(F_{b, b, r})$  in the range

$$-1,3 \leq F_{b, b, r} \leq 1,3 \text{ aw}$$

sufficiently accurately is determined by a linear relationship of the type

$$u_{b, r}(F_{b, b, r}) = k_{b, r} F_{b, b, r} \quad (8.27)$$

Then,

$$e_{b, r} = 2L_{b, r, s} \frac{di_{b, r}}{dt} + (R_{b, r} + 2R_{b, r, s}) i_{b, r} + k_r \frac{d\phi_r}{dt}, \quad (8.28)$$

where  $\phi_r$  is one generator's field flux.

In an established mode in which  $I_{n, \text{nom}}$  A,  $2U_{r, \text{nom}}$  V and  $2E_{r, \text{nom}} = 2U_{r, \text{nom}} + 2R_{b, r} I_{n, \text{nom}}$  V, in accordance with the idling characteristic  $I_{b, r, \text{nom}} = \lambda I_{n, \text{nom}}$  A, where  $\lambda = \frac{\omega_{b, r, r}}{\omega_{b, b, r}}$ , corresponds to this value.

Voltage  $U_{b, r, \text{nom}} = I_{b, r, \text{nom}} R_{b, r}$  V corresponds to the set value of field current  $I_{b, r, \text{nom}}$  V. Then,

$$E_{b, r, \text{nom}} = U_{b, r, \text{nom}} + 2R_{b, r, s} I_{b, r, \text{nom}} \text{ a.} \quad (8.29).$$

$F_{b, b, r, \text{nom}}$  aw, or  $I_{b, b, r, \text{nom}} = \frac{F_{b, b, r, \text{nom}}}{\omega_{b, b, r}}$  a, A, or MU12 output voltage  $U_{b, b, r, \text{nom}}$  V /391 corresponds to this emf. Magnetizing force  $F_{b, b, r, \text{nom}}$  and current value  $I_{M11/12}$  mA correspond to voltage value  $U_{b, b, r, \text{nom}}$  in accordance with the characteristic.

Dynamics equations. The initial equilibrium equation for the voltage in the main circuit will be written:

$$2e_r = 2\omega_r \phi_r (i_{n,r} - i_n) = (R_{n,d} + 2R_{n,r}) i_n + (L_{n,d} + 2L_{n,r}) \frac{di_n}{dt} + \phi_d \omega_d. \quad (8.30)$$

Solved for the current derivative, the equation will take the form

$$\frac{di_n}{dt} = \frac{2e_r - \phi_d \omega_d - (R_{n,d} + 2R_{n,r}) i_n}{L_{n,d} + 2L_{n,r}}, \quad (8.31)$$

or, in other form,

$$\frac{di_n}{dt} = \frac{2\omega_r \frac{u_r}{n_r} \frac{3a}{\pi} - \omega_d \frac{2u_d}{n_d} \frac{30}{\pi} - (R_{n,d} + 2R_{n,r}) i_n}{L_{n,d} + 2L_{n,r}}. \quad (8.32)$$

The equation written with numerical factor values is:

$$\frac{di_n}{dt} = a_{11} u_r - a_{12} \omega_d \phi_d - a_{13} i_n. \quad (8.33)$$

The initial equation calculated in relative units (parameter values in the nominal mode are assumed to be the base values) with numerical factor values has the form

$$\frac{d\bar{i}_n}{dt} = a_{11} \bar{e}_r - a_{12} \bar{\phi}_d \bar{\omega}_d - a_{13} \bar{i}_n. \quad (8.34)$$

The initial equation for shafting line torques is

$$\phi_d (i_n) i_n = J_d \frac{d\omega_d}{dt} + m_c.$$

The equation solved for the derivative is:

$$\frac{d\omega_d}{dt} = \frac{\phi_d i_n}{J_d} - \frac{m_c}{J_d}.$$

Taking into account numerical factor values, we have

$$\frac{d\omega_d}{dt} = a_{12} \phi_d i_n - a_{22} m_c.$$

In relative units with numerical factor values, the equation will take the form

$$\frac{d\bar{\omega}_R}{dt} = a_{21}\bar{\phi}_R\bar{i}_R - a_{22}\bar{m}_c. \quad (8.35)$$

The initial equilibrium equation for generator field circuit voltage is /392

$$e_{B,r} = (2R_{B,r,R} + R_{B,r})i_{B,r} + (2L_{B,r,R} + L_{B,r})\frac{di_{B,r}}{dt} + k_r\frac{d\phi_r}{dt}. \quad (8.36)$$

The equation solved for the derivative with calculated numerical factors has the form

$$\frac{di_{B,r}}{dt} = a'_{31}e_{B,r} - a'_{32}i_{B,r} - a'_{33}\frac{d\phi_r}{dt}.$$

We will express it in relative units:

$$\frac{d\bar{i}_{B,r}}{dt} = a_{31}\bar{e}_{B,r} - a_{32}\bar{i}_{B,r} - a_{33}\frac{d\bar{\phi}_r}{dt}. \quad (8.37)$$

The initial equilibrium equation for the generator exciter field circuit voltage is

$$u_{B,B,r} = i_{B,B,r}r_{B,B,r} + L_{B,B,r}\frac{di_{B,B,r}}{dt}.$$

The equation solved for the derivative with numerical factor values:

$$\frac{di_{B,B,r}}{dt} = a'_{41}u_{B,B,r} - a'_{42}i_{B,B,r}.$$

We will write it in relative units:

$$\frac{d\bar{i}_{B,B,r}}{dt} = a_{41}\bar{u}_{B,B,r} - a_{42}\bar{i}_{B,B,r}. \quad (8.38)$$

The initial equation for amplifier MU12 voltages, if we use  $u_{MY 11/12}$  to designate the amplifier input value and  $u_{B,B,r}$  for the output value, has the form

$$T_{MY 12}\frac{du_{B,B,r}}{dt} + u_{B,B,r} = u_{MY 11/12}.$$

The equation solved for the derivative with numerical factor values will take the form

$$\frac{du_{B, B, r}}{dt} = a_{61}' u_{MY 11/12} - a_{62}' u_{B, B, r},$$

and, in relative units,

$$\frac{d\bar{u}_{B, B, r}}{dt} = a_{61} \bar{F}_{MY 11/12} - a_{62} \bar{u}_{B, B, r}. \quad (8.39)$$

Here

$$u_{MY 11/12} = k_{MY 11/12} F_{MY 11/12}$$

The equation for magnetic governor MU11/12 voltages (correspondingly the mmf equilibrium equation), if one disregards induction voltage caused by the /393 magnetic flux, has the form (from the MU11/21 schematic in Figure 8.3)

$$T_{MY 11} \frac{dF_{MY 11}}{dt} + F_{MY 11} = \frac{\omega_{y, r 1}}{R_{y, r 1}} \left( u_{3aA} - \frac{\varepsilon i_n}{1-r} - \lambda_r L_r \frac{di_n}{dt} \right) - \frac{2\omega_{y, r 2}}{R_{y, r 2}} u_r - C_{y, r 3} \omega_{y, r 3} \frac{du_{B, r}}{dt},$$

where

$$T_{MY 11} = T_{y, r 1} + T_{y, r 2} + T_{y, r 3}.$$

The equation solved for the derivative with numerical factor values has the form

$$\begin{aligned} \frac{dF_{MY 11}}{dt} &= a_{61} u_{3aA} - a_{62} i_n - \\ &- a_{63} \frac{di_n}{dt} - a_{64} \frac{du_B}{dt} - \\ &- a_{65} u_r - a_{66} F_{MY 11}, \end{aligned}$$

and, in relative units,

$$\begin{aligned} \frac{d\bar{F}_{MY 11}}{dt} &= a_{61} \bar{u}_{3aA} - a_{62} \bar{i}_n - \\ &- a_{63} \frac{d\bar{i}_n}{dt} - a_{64} \bar{u}_r - a_{65} \frac{d\bar{u}_{B, r}}{dt} - \\ &- a_{66} \bar{F}_{MY 11}. \end{aligned}$$

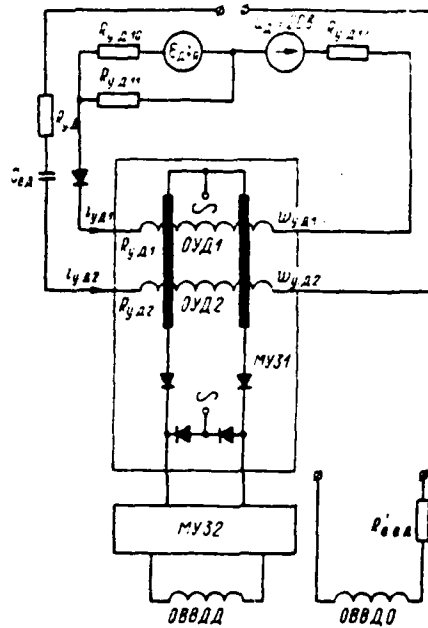


Figure 8.4. Schematic of a Magnetic Amplifier in a Main Propulsion Motor Pilot Excitation System (Main Propulsion Motor Exciter Field Design Circuit).

The MU31 magnetic governor equation in accordance with Figure 8.4 has the form

$$T_{MY31} \frac{dF_{MY31}}{dt} + F_{MY31} = \frac{w_{yA1}}{R_{yA1}} u_{yA1} - C_{yA2} \ddot{w}_{yA2} \frac{de_{eA}}{dt} \quad (8.40)$$

where

$$T_{MY31} = T_{yA2} + T_{yA1} \text{ и } u_{yA1} = \frac{\Delta i_n}{k_{TP}} = \frac{w_{yA1}^2}{R_{yA1}} \cdot \frac{\partial \phi_n}{\partial F_A}$$

The equation solved for the derivative with numerical factor values has the form

$$\frac{dF_{MY31}}{dt} = a_{71} i_n - a_{72} + a_{73} \frac{de_{eA}}{dt} - a_{74} F_{MY31}$$

and, in relative units,

/394

$$\frac{d\bar{F}_{MY31}}{dt} = a_{71} \bar{i}_n - a_{72} + a_{73} \frac{d\bar{e}_{eA}}{dt} - a_{74} \bar{F}_{MY31} \quad (8.41)$$

The equilibrium equation for amplifier MU32 voltages, if the input value is designated by  $u_{MY\ 32} = f(F_{MY\ 31})$  and the output value by  $u_{B.\ B.\ D.\ D}$ , has the form

$$T_{32} \frac{du_{B.\ B.\ D.\ D}}{dt} + u_{B.\ B.\ D.\ D} = u_{MY\ 31}(F_{MY\ 31}).$$

Considering that  $u_{MY\ 31} = k_{MY\ 31} F_{MY\ 31} = 251 F_{MY\ 31}$ , the initial equation solved for the derivative and with numerical factor values has the form

$$\frac{du_{B.\ B.\ D.\ D}}{dt} = a_{81} F_{MY\ 31} - a_{82} u_{B.\ B.\ D.\ D},$$

and, in relative units,

$$\frac{d\bar{u}_{B.\ B.\ D.\ D}}{dt} = a_{81} \bar{F}_{MY\ 31} - a_{82} \bar{u}_{B.\ B.\ D.\ D}.$$

We will write the main propulsion motor exciter field circuit equations. Main winding OVVDO is fed by constant voltage via additional resistance  $R_{B.\ B.\ D.\ O}$  ohms. Considering mutual induction of the windings, where  $\alpha$  is the mutual induction factor, the main winding voltage equilibrium equation has the form

$$u_{B.\ B.\ D.\ O} = (R_{B.\ B.\ D.\ O} + R_{B.\ B.\ D.\ D}) i_{B.\ B.\ D.\ O} + L_{B.\ B.\ D.\ O} \frac{di_{B.\ B.\ D.\ O}}{dt} + \alpha L_{B.\ B.\ D.\ D} \frac{di_{B.\ B.\ D.\ D}}{dt}. \quad (8.42)$$

The winding OVDD equation is:

$$u_{B.\ B.\ D.\ D} = R_{B.\ B.\ D.\ D} i_{B.\ B.\ D.\ D} + L_{B.\ B.\ D.\ D} \frac{di_{B.\ B.\ D.\ D}}{dt} + \alpha L_{B.\ B.\ D.\ O} \frac{di_{B.\ B.\ D.\ O}}{dt}. \quad (8.43)$$

The magnetizing force equation is:

$$F_{B.\ B.\ D.\ D} = w_{B.\ B.\ D.\ D} (i_{B.\ B.\ D.\ O} + i_{B.\ B.\ D.\ D}).$$

Where  $\alpha = 1$  and considering numerical factor values, the exciter VD field circuit equation will take the form

$$\frac{dF_{B.\ B.\ D.\ D}}{dt} = a'_{91} + a'_{92} u_{B.\ B.\ D.\ D} - a'_{93} F_{B.\ B.\ D.\ D}.$$

In relative units, it will be written:

$$\frac{d\bar{F}_{\text{B. B. A. A}}}{dt} = a_{01} + a_{02}\bar{i}_{\text{B. B. A. A}} - a_{03}\bar{F}_{\text{B. B. A. A}} \quad (8.44)$$

The initial equilibrium equation for GED field circuit voltages has the /395 form

$$e_{\text{B. A}} = k_{\text{B. A}} F_{\text{B. B. A. A}} = 0,146 F_{\text{B. B. A. A}} = (R_{\text{B. A. A}} - R_{\text{B. A}}) i_{\text{B. A}} + (L_{\text{B. B. A. A}} + L_{\text{B. A}}) \frac{di_{\text{B. A}}}{dt} \quad (8.45)$$

In relative units, this equation will be written

$$\frac{d\bar{i}_{\text{B. A}}}{dt} = a_{101}\bar{F}_{\text{B. B. A. A}} - a_{102}\bar{i}_{\text{B. A}}$$

Selection of optimal characteristics of GEU dynamics. An electronic modelling set is used for selecting optimal characteristics. Two main modes are investigated here: GEU operation with constant (unregulated) main propulsion motor field flux and a mode in which  $\phi_A = f(i_n)$  when  $i_n > I_{n, \text{nom}}$ .

The propellor-ice interaction mode, i. e., the mode in which additional (ice) moment of resistance is applied to the screw, is simulated by an instantaneously applied rectilinear rotational speed function, while both the value itself and the time of action of the moment will change in a range of values actually obtained during numerous GEU tests in the Arctic.

Characteristics selection occurs stemming from requirements excluding propellor jamming during moment of resistance surges exceeding the moored moment by a factor exceeding 1.5.

For the  $\phi_A = \text{const}$  mode, the system of differential equations written in relative units with numerical factor values (compiled in accordance with Figures 8.2—8.4) has the form:

for the MUII magnetic governor

$$\frac{d\bar{F}_{\text{MVI II}}}{dt} = a_{11}\bar{i}_{\text{MVI II}} - a_{12}\bar{i}_n - a_{13}\frac{di_n}{dt} - a_{14}\bar{e}_r - a_{15}\frac{d\bar{u}_{p, r}}{dt} - a_{16}\bar{F}_{\text{MVI II}} \quad (8.46)$$

(factors  $a_{13}$  and  $a_{15}$  varied);

for the MU12 amplifier circuit

$$\frac{d\bar{u}_{\text{a. b. r}}}{dt} = a_{21}\bar{F}_{\text{MV}11} - a_{22}\bar{u}_{\text{a. b. r}}; \quad (8.47)$$

for the generator exciter field circuit

$$\frac{d\bar{i}_{\text{a. b. r}}}{dt} = a_{31}\bar{u}_{\text{a. b. r}} - a_{32}\bar{i}_{\text{a. b. r}}; \quad (8.48)$$

for the generator field circuit

$$\frac{d\bar{i}_{\text{a. r}}}{dt} = a_{41}\bar{e}_{\text{a. r}} - a_{42}\bar{i}_{\text{a. r}} - a_{43}\frac{d\bar{\phi}_r}{dt}; \quad (8.49)$$

the shafting line torque equilibrium equation is

$$\frac{d\bar{\omega}_x}{dt} = a_{51}\bar{i}_x - a_{52}\bar{m}_{\text{con}}; \quad (8.50)$$

the armature circuit voltage equation

/396

$$\frac{d\bar{i}_x}{dt} = a_{61}\bar{e}_r - a_{62}\bar{\omega}_x - a_{63}\bar{i}_x. \quad (8.51)$$

The computer block diagram considering transient process lag by a factor of 10 is presented in Figure 8.5.

For mode  $\phi_x = f(i_x)$  where  $i_x > I_{x, \text{ном}}$ , the system of differential equations describing the transient process will consider that  $e_x = \phi_x \omega_x$ ,  $m_x = \phi_x i_x$ , as well as the presence of a GED automatic control node with feedbacks.

Equations written in relative units and solved for derivatives have the form:

for the MU11 magnetic governor

$$\frac{d\bar{F}_{\text{MV}11}}{dt} = a_{11}\bar{u}_{\text{ma}} - a_{12}\bar{i}_x - a_{13}\frac{d\bar{i}_x}{dt} - a_{14}\bar{e}_r - a_{15}\frac{d\bar{u}_{\text{a. r}}}{dt} - a_{16}\bar{F}_{\text{MV}11}, \quad (8.52)$$

where  $a_{13}$  and  $a_{15}$  varied;

for an MU12 amplifier

$$\frac{d\bar{u}_{\text{a. b. r}}}{dt} = a_{21}\bar{F}_{\text{MV}11} - a_{22}\bar{u}_{\text{a. b. r}}; \quad (8.53)$$

for the generator exciter field circuit

$$\frac{d\bar{i}_{e. s. r}}{dt} = a_{31}\bar{u}_{e. s. r} - a_{32}\bar{i}_{e. s. r}; \quad (8.54)$$

for the generator field circuit

$$\frac{d\bar{i}_{f. r}}{dt} = a_{41}\bar{e}_{f. r} - a_{42}\bar{i}_{f. r} - a_{43}\frac{d\bar{\phi}_r}{dt}; \quad (8.55)$$

the shafting line equation is

$$\frac{d\bar{\omega}_R}{dt} = a_{51}\bar{i}_n\bar{\phi}_R - a_{52}\bar{m}_{con}; \quad (8.56)$$

the armature circuit voltage equation is

$$\frac{d\bar{i}_n}{dt} = a_{61}\bar{e}_r - a_{62}\bar{\phi}_R\bar{\omega}_R - a_{63}\bar{i}_n; \quad (8.57)$$

the MU31 magnetic governor equation is

$$\frac{d\bar{F}_{MV31}}{dt} = a_{71}\bar{i}_n - a_{72} + a_{73}\frac{d\bar{e}_{e. s. r}}{dt} - a_{74}\bar{F}_{MV31}; \quad (8.58)$$

where  $a_{73}$  varied;

the MU32 magnetic amplifier equation is

$$\frac{d\bar{u}_{e. s. R. R}}{dt} = a_{81}\bar{F}_{MV31} - a_{82}\bar{u}_{e. s. R. R}; \quad (8.59)$$

for the exciter VD field circuit

/399

$$\frac{d\bar{F}_{e. s. R. R}}{dt} = a_{91} + a_{92}\bar{u}_{e. s. R. R} - a_{93}\bar{F}_{e. s. R. R}; \quad (8.60)$$

for the GED field circuit

$$\frac{d\bar{i}_{e. R}}{dt} = a_{101}\bar{F}_{e. s. R. R} - a_{102}\bar{i}_{e. R}; \quad (8.61)$$

A computer block diagram considering transient process lag by a factor of 10 is depicted in Figure 8.6.

Some conclusions on modelling icebreaker GEU dynamics. Investigations /400

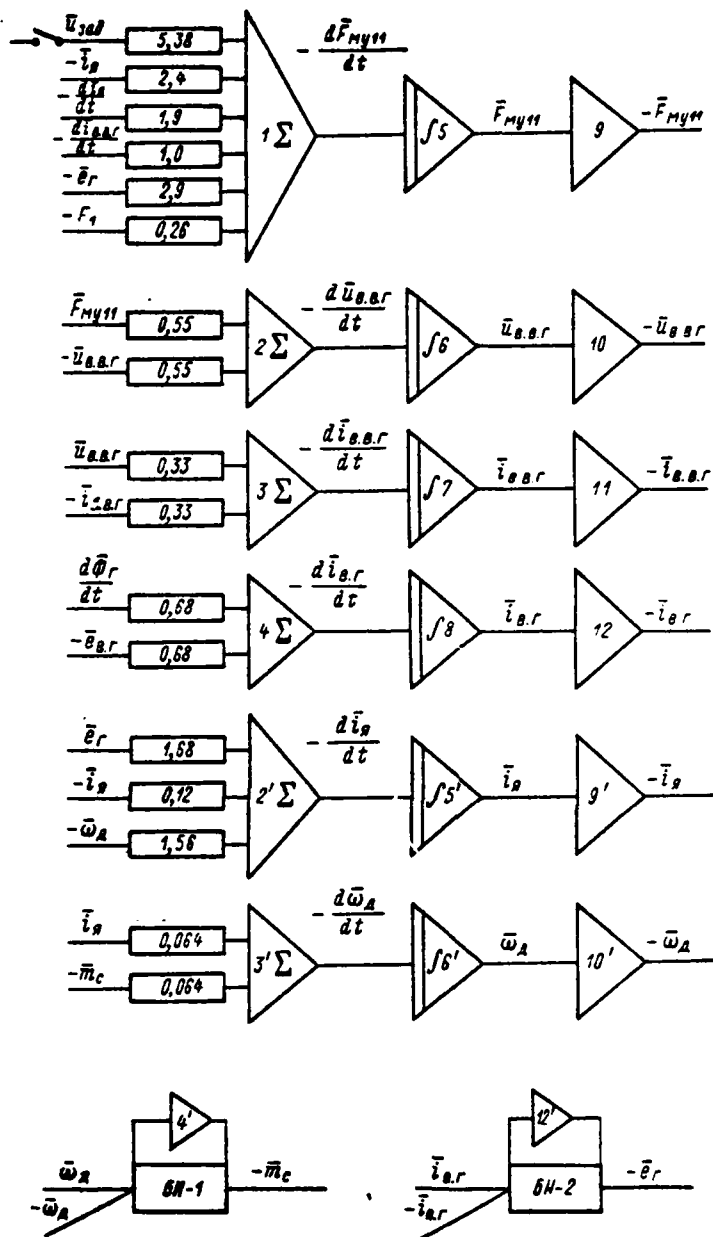


Figure 8.5. GEU Mathematical Modelling Block Diagram Where  $\phi_A = \text{const}$ .

on an electronic model and full-scale tests demonstrated that the GEU aboard the icebreaker "Kiev" compared to other icebreakers better satisfies requirements relative to reliable operation in the propeller-ice interaction mode. So, when ice floes strike a propeller blade in combination with a radical increase in

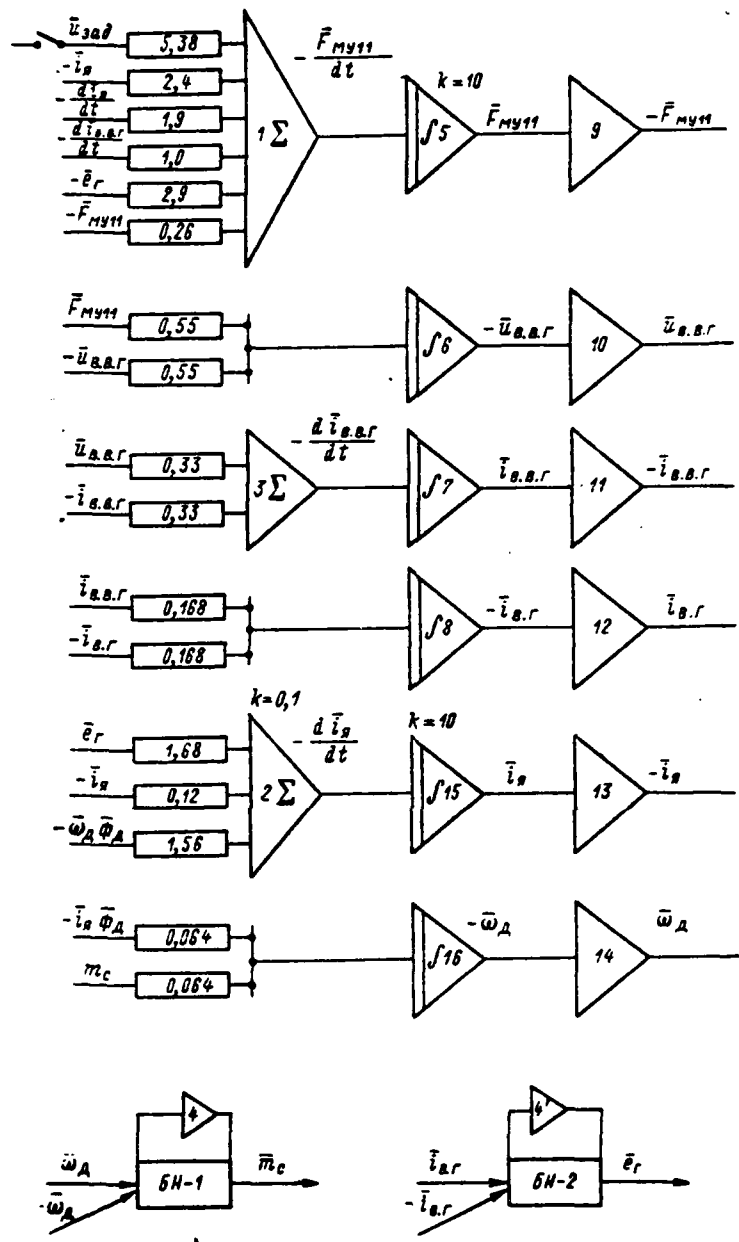


Fig. 8.6.

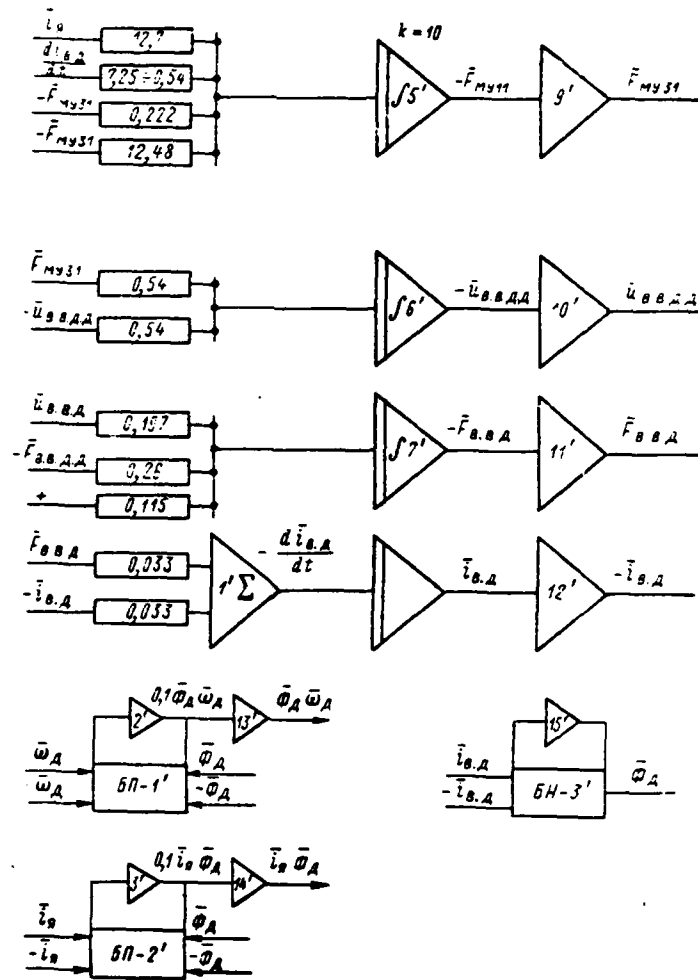


Fig. 8.6. GEU mathematical modelling block diagram where  $\phi_A = I(i_0)$

the moment of resistance, the current in the armature circuit with great speed achieves values close to those exceeding the nominal by a factor of almost 3. A GEU system's regulating capabilities must provide a generator demagnetization rate that eliminates a primary motor power overload. Such a GEU control system reliably protects a primary motor against a so-called "forced reversal." However, presence of field circuit magnetic inertia does not make it possible to obtain the aforementioned demagnetizing rate. Therefore, a diesel power overload /401 (Figure 8.7) of up to 170% occurs within 0.5—0.7 seconds in the first time segment (after the propellor-ice interaction mode begins). True, these overloads, as tests showed, are compensated for by kinetic energy accumulated in the diesel gyrating masses (the diesel generator gyrating masses on the icebreaker "Kiev" have been increased by a factor of 2 compared to the icebreaker "Moskva"). A separate study showed that, during power fluctuations from 30 to 170% of nominal 2 seconds in duration, diesel rotational speed fluctuations comprise +3 to -15%.

Voltage decreases slowly at first, then at a high rate, when there is a large increase in armature circuit current. The more the armature circuit current change is used as a controlling parameter, the greater the voltage drop and the lower the armature circuit current maximum.

A decrease in GED rotational speed automatically is linked with the voltage drop in the generators, since rotational speed to a significant degree is a linear function of voltage. It is possible through corresponding selection of feedback parameters to obtain those GEU characteristics for the icebreaker operating in the ice mode (Figure 8.8), which, given tolerable overshoots, insure that GED rotational speed drop does not go lower than at the zero stop. In such a mode, temporary diesel power overloads occur that do not cause a /402 significant drop in their rotational speed.

Introduction of feedbacks into the control system reduced the maximum power value and overload duration.

A case involving field constant flux was investigated to reveal GEU conduct as an icebreaker navigates in ice. Here, an instantaneous increase in moment of resistance on the propellor due to the additional moment of resistance of

the ice was simulated in the form of a unitary function of rectilinear form given constant values  $\bar{\phi}_A$  equalling

$$\bar{\phi}_{A1} = \bar{\phi}_{A, \text{nom}}; \bar{\phi}_{A2} = 1,2\bar{\phi}_{A, \text{nom}}; \bar{\phi}_{A3} = 1,5\bar{\phi}_{A, \text{nom}}.$$

The modelling demonstrated that when  $\bar{\phi}_{A1} = \bar{\phi}_{A, \text{nom}}$  for a period of 1 second, GED rotational speed decreased to  $0,3\bar{n}_{A, \text{nom}}$ , while when  $\bar{\phi}_{A2} = 1,2\bar{\phi}_{A, \text{nom}}$  considering the additional ice moment of resistance (the so-called "ice torque"), GED rotational speed dropped to  $0,27\bar{n}_{A, \text{nom}}$ . No further GED rotational speed decrease was observed in spite of the continuing action of the increased moment of resistance value (the phenomenon of ice milling was observed).

In the first case, maximum armature circuit current attained value  $2,2I_{A, \text{nom}}$ , reaching  $-2I_{A, \text{nom}}$  in the second instance. Consequently, considering the fact that the rate of magnetic flux increase is small compared to the main circuit current increase, the requisite control effect will be achieved if the GED can develop field flux increased relative to the moored flux and which acts constantly. Here, it is possible to constrain the maximum value of the current and decrease primary motor overload during the initial period of propellor braking. Having assumed the instantaneously-applied ice torque in the form of a unitary function, to a known degree we make the conditions more rigid relative to the actual conditions (the increase in moment of resistance to the maximum during a time frame of 0.2 to 1.2 seconds).

In Figure 8.8, the digit 1 designates the characteristics of the armature circuit current  $\bar{i}_A(t)$ , GED rotational speed  $\bar{n}_A(t)$ , main generator voltage  $\bar{u}_r(t)$ , and GED power  $\bar{p}_A(t)$  where  $\bar{\phi}_A = f(\bar{i}_A)$ ; 2 designates the characteristics of the same variables, but where  $\bar{\phi}_A = \bar{\phi}_{A, \text{nom}} = \text{const}$ ; the digit 3 depicts characteristics of the same variables, but where  $\bar{\phi}_A = 1,2\bar{\phi}_{A, \text{nom}} = \text{const}$ ; the digit 4 designates characteristic  $\bar{\phi}_A = f(\bar{i}_A)$ ; the digit 5 designates  $\bar{\phi}_A = \bar{\phi}_{A, \text{nom}} = \text{const}$ ; the digit 6 designates  $\bar{\phi}_A = 1,2\bar{\phi}_{A, \text{nom}} = \text{const}$ .

Effect of feedback parameters on icebreaker GEU dynamics. The effect of vanishing and unity feedbacks was investigated in a model and their parameters determined whereby transient processes occur with tolerable current, primary motor overload, and propellor rotational speed drop values.

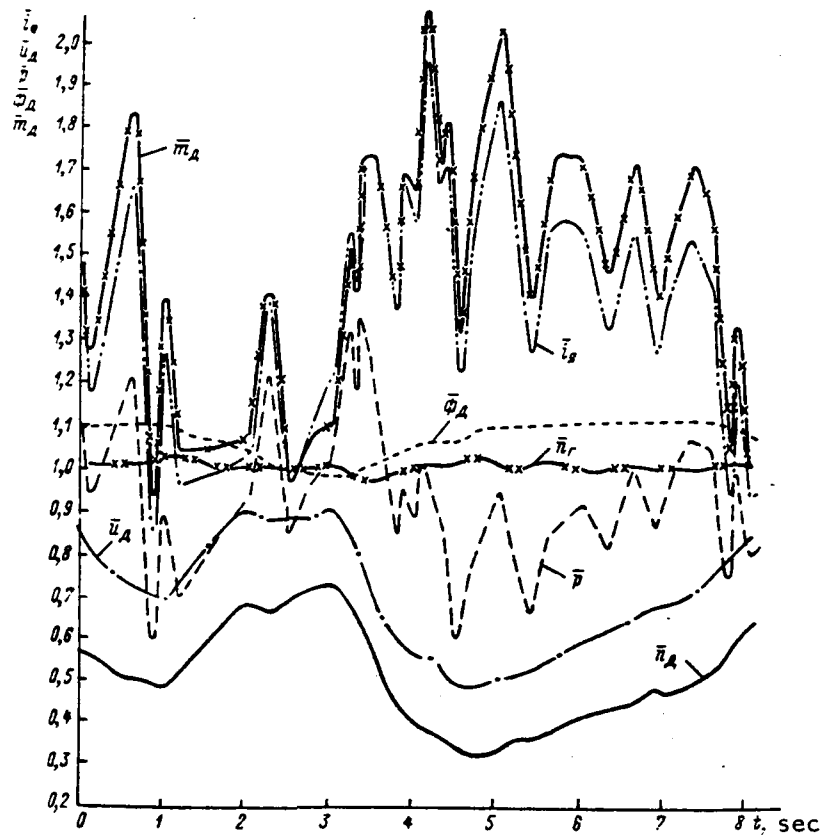


Figure 8.7. Oscillogram of the Propellor-Ice Interaction Mode for a 2+4+2 Circuit (Full-Scale Tests).

So, the time until the screw jams is increased (Figure 8.9) with an intensification of the effect of vanishing negative generator field voltage feedback (achieved by an increase in capacitance in the feedback circuit), /403 given constant GED field flux and given a surge of same based on the numerical value of the "ice torque." The armature circuit current fluctuation radically decreases and, given the greatest factor  $a_{15}$  in expression (8.52), one fluctuation is observed.

The curves of the change of variables in a function of time given varied vanishing generator voltage feedback  $(\frac{d\bar{u}_{g,r}}{dt}) = \text{var}$  values are shown in Figure 8.9. The digits 1, 1', and 1'' designate the curves of the change of variables  $\bar{i}_n(t)$ ,  $\bar{u}_r(t)$  and  $\bar{n}_A(t)$  where the factor of derivative  $\frac{d\bar{u}_{g,r}}{dt}$  equals 30; the digits

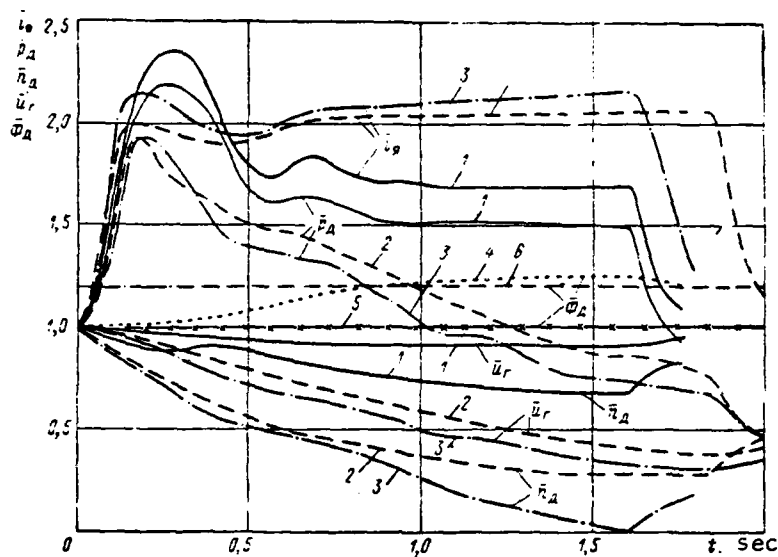


Figure 8.8. Oscillogram of the Propellor-Ice Interaction Mode (Mathematical Modelling).

2, 2', and 2'' do the same where the factor equals 60, and 3, 3', and 3'' do so where the factor equals 100.

It was established that the optimal nature of transient processes occur where the factor equals 60 (i. e., the capacitance in the RC-network must equal  $110 \mu\text{F}$  where other system parameters remain constant); a further increase in the factor where  $\frac{d\bar{u}_{a,r}}{dt}$  has no effect.

The effect of the armature circuit current change rate feedback (Figure 8.9b) exerts considerable influence on the initial current jump and accordingly on the primary motor overload in the first stage of the propellor-ice interaction mode. The curves of the change of the same variables shown in Figure 8.9a are shown in Figure 8.9b, but with different values of armature circuit current vanishing feedback ( $\frac{d\bar{i}_a}{dt} = \text{var}$ ). Meanwhile, curves designated 1, 1', 1'' are constructed where the derivative  $\frac{d\bar{i}_a}{dt}$  factor equals 0; 2, 2', 2'' where it equals 5, and 3, 3', 3'' where it equals 25. So, with a change of the factor where  $\frac{d\bar{i}_a}{dt}$  from 0 to 50, the armature circuit current maximum is decreased from  $3,2 I_{n, \text{nom}}$  to  $2,9 I_{n, \text{nom}}$ . When there is no feedback based on  $\frac{d\bar{i}_a}{dt}$ , a fluctuating



as ice floes strike propellor blades, eliminating its jamming during tolerable primary motor overloads, are determined from the results of the investigation. The method of modelling GEU dynamics in icebreaker operating modes illustrated by the above example is very convenient for analysis and synthesis of automated GEU.

§ 8.3 Methodology of Analog Computer Analysis and Synthesis of the Dynamic Characteristics of GEU with Magnetic Amplifiers in the Excitation System

Differential equations describing GEU transient processes. The system of differential equations for GEU loops is compiled considering the previously-accepted assumptions for the investigated GEU system with magnetic amplifiers as GED exciters and main generator pilot exciters (Figure 8.10).

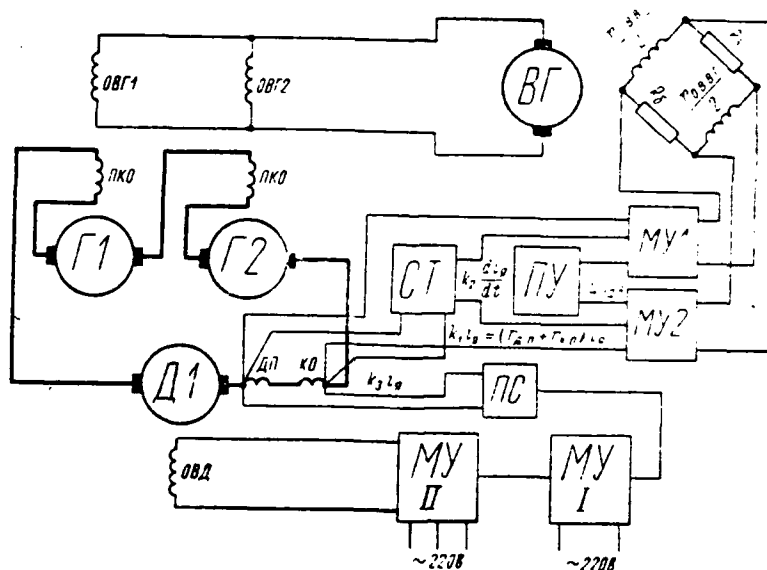


Figure 8.10. Functional Diagram of a GEU with MU as Exciters and Governors. ST--Information sensor on rate of current change in the main circuit;  $R_b$  is ballast resistance in the OVG circuit.

Generator pilot exciter magnetic amplifier equation. The equilibrium equation for the MU—generator pilot exciter loop voltage approximately has the form

$$i_{b.p.r} + (T_{MY} + T_{d.b.p.r}) \frac{di_{b.p.r}}{dt} = \sum \frac{u_k}{r_k} k_i. \quad (8.62)$$



Value  $\sum \frac{u_k}{r_k} k_1$  is made up of the following components:

$$\sum \frac{u_k}{r_k} k_1 = k_1 \left( \frac{u_{3a2} k_{n,y}}{r_{3a2}} - \frac{u_{o.c.T}}{r_{o.c.T}} + i_{RC} \right)$$

where  $u_{3a2}$  is master winding nominal voltage (feed is from PU, see Figure /406 8.10);  $r_{3a2}$  is master winding circuit resistance;  $k_1$  is a proportionality factor;  $u_{o.c.T}$  voltage supplied to the main circuit current feedback winding;  $u_{o.c.T} = (r_{2n} + r_{n.o}) i_n$ ;  $i_{RC}$  is the current in the current vanishing feedback circuit;  $i_{RC} = k_2 \frac{di_n}{dt}$  (see Figure 8.10).

Generator exciter emf equation. The equation linking exciter emf with field n. s. (with field current) given drive motor constant rotational speed is determined by the exciter idling characteristic

$$e_{e.r} = f(i_{e.r}). \quad (8.63)$$

Generator exciter circuit voltage equilibrium equation. The voltage equilibrium equation for the investigated GEU circuit when two series-connected generators run one main propulsion motor has the form

$$e_{e.r} = i_{e.r} r_{e.r} + 2i_{e.r} r_{s.e.r} + L_{e.r} \frac{di_{e.r}}{dt} \quad (8.64)$$

We disregard the inductivity of the exciter armature circuit due to its relative insignificance.

Generator emf equation. This emf is supplied by the idling characteristic as a function of the current of its excitation:

$$e_r = f(i_{e.r}). \quad (8.65)$$

The main circuit voltage equilibrium equation is:

$$2e_r = \sum r_{n.u} i_n + \sum L_{n.u} \frac{di_n}{dt} + e_A, \quad (8.66)$$

where  $e_A = C_{eA} \phi_A n_A$ ;  $\sum r_{n.u}$  is overall armature circuit resistance;

$\sum L_{n.u}$  is overall armature circuit inductivity.

Equilibrium equation for the main propulsion motor—shaft—propellor line torques. This equation has the form

$$m_A = \frac{CD_A^2}{375} \frac{dn_A}{dt} + m_{con}, \quad (8.67)$$

where  $m_A = C_{m,A} i_A \phi_A$  is GED electromagnetic moment;  $m_{con} = m_B + m_A$  is overall icebreaker moment of resistance during movement in ice;  $\phi_A = f(i_{B,A})$  is the GED magnetization curve.

Since control of GED field flux is accomplished through an increase from a certain time constant, motor field voltage approximately can be represented as the sum of two voltages:

$$u_{B,A} = u_{B,A,0} + u_{B,A,A},$$

where  $u_{B,A,0}$  is the main component of overall voltage  $u_{B,A}$ ;  $u_{B,A,A}$  is the additional (variable) portion, which is a function of variable current in the MU control winding.

The following equation is justified for the variable voltage component: /407

$$u_{B,A,A} + T_{MV} \frac{du_{B,A,A}}{dt} = k_{B,A,A} i_y, \quad (8.68)$$

where  $k_{B,A,A} = \frac{\Delta u_{B,A,A}}{\Delta i_y}$  will be found from the two-cascade MU characteristic, while  $i_y = k_A (i_A - I_{A,nom})$ .

GED field winding circuit equation. The GED field circuit voltage equilibrium equation will be written:

$$u_{B,A} = i_{B,A} r_{B,A} + L_{B,A} \frac{di_{B,A}}{dt}$$

The equations of the system solved for derivatives have the form

$$\begin{aligned}
 \frac{di_{n. n. r}}{dt} &= k_1 k_n \cdot \mu_{30} i_n - k_2 i_n - k_3 i_{n. b. r} - k_4 i_{r. c}; \\
 e_{b. r} &= f_1(i_{n. b. r}); \\
 \frac{di_{n. r}}{dt} &= k_5 e_{b. r} - k_6 i_{n. r}; \\
 e_r &= f_2(i_{n. r}); \\
 \frac{di_n}{dt} &= k_7 e_r - k_8 i_n - k_9 \phi_{\Delta} n_{\Delta}; \\
 \phi_{\Delta} &= f_3(i_{n. \Delta}); \\
 \frac{dn_{\Delta}}{dt} &= k_{10} \phi_{\Delta} i_n - k_{11} m_{\text{con}}; \\
 m_{\text{con}} &= f_4(n_{\Delta}); \\
 u_{b. \Delta} &= u_{b. \Delta. 0} + u_{b. \Delta. \Delta}; \\
 \frac{du_{b. \Delta}}{dt} &= k_{12} u_{b. \Delta} + k_{13} i_y; \\
 \frac{di_{n. \Delta}}{dt} &= k_{14} u_{b. \Delta} - k_{15} i_{n. \Delta}.
 \end{aligned} \tag{8.69}$$

Calculation of the parameters and coefficients of the differential equation system. The inductivity of the main generator field winding circuit in the rectilinear portion of the magnetization curve equals

$$L_{b. r1} = 2\rho\sigma\omega_{b. r} \frac{\Delta\phi_{n. r}}{\Delta i_{n. r}} \quad \text{H}$$

Inductivity of characteristics in a range of current change between  $i_{n. b. r. \text{min}}$  and  $i_{n. b. r. \text{max}}$  is determined from an analogous expression.

The generator magnetization characteristic can be determined by means of conversion of the idling characteristic from formula

$$\phi_r = \frac{e_r}{C_{er} n_r} \tag{8.70}$$

where

/408

$$C_{er} = \frac{pN}{a \cdot 60}$$

Main generator field circuit resistance equals

$$r_{b. r. \text{ и } \Delta} = r_{b. r} + r_{b. r. \text{ дон}}$$

Disregarding exciter armature circuit inductivity and resistance, we will find the generator field circuit time constant from formula

$$T_{в.г} = \frac{L_{в.г}}{r_{в.г.ц}} \quad \text{sec.} \quad (8.71)$$

The maximum value of generator field voltage is determined from expression

$$U_{в.г. макс} = \frac{I_{н.г. ном} r_{в.г. ц}}{e^{\delta} - 1} \quad (8.72)$$

where  $\delta = \frac{t_p}{T_{в.г}}$ , where  $t_p$  is generator demagnetization time, which can be assumed as equalling 1 second.

With given value  $U_{в.г. макс}$ , demagnetization time is determined by calculation in inverse order:

$$e^{\delta} = \frac{I_{н.г. ном} r_{в.г. ц} + U_{в.г. макс}}{U_{в.г. макс}} \quad (8.73)$$

and

$$t_p = T_{в.г} \delta \quad \text{sec.}$$

Main generator armature circuit. Armature winding inductivity is determined by the expression

$$L_{н.г} = \frac{k I_{н. ном} \cdot 60}{I_{н. ном} 2\pi n_r} \quad \text{H.} \quad (8.74)$$

where  $k = 0.25$  for compensated high-speed machinery.

Compensating winding inductivity is computed from formula

$$L_{к.о.г} = L_{н.г} \left( \frac{w_{к.о.г}}{w_{н.г}} \right)^2 \quad \text{H.} \quad (8.75)$$

Inductivity of main generator additional poles is:

$$L_{д.г.г} = 0,2 L_{к.о.г} \left( \frac{w_{д.г.г}}{w_{к.о.г}} \right)^2 \quad \text{H.} \quad (8.76)$$

Main propulsion motor field circuit. Inductivity of the operating portion of the magnetization characteristic is calculated from expression

$$L_{в. д. п} = 2\rho w_{в. д} \frac{\Delta\phi_{в. д}}{\Delta i_{в. д}} \text{ H.} \quad (8.77)$$

Inductivity  $L_{в. д. 2}$  of section  $\phi_{д. шв} - \phi_{д. форс}$ , as well as the inductivity of the rectilinear section of GED magnetization characteristic  $L_{в. д. пр}$  is determined from an expression analogous to (8.77).

Main propulsion motor armature circuit. GED armature winding inductivity /409 is calculated from expression

$$L_{я. в. д} = \frac{k \cdot 120 \cdot U_{д. ном}}{I_{я. ном} \cdot 2\rho l_{д. ном}} \text{ H.} \quad (8.78)$$

The inductivities of compensating winding of additional poles are determined from expressions

$$\left. \begin{aligned} L_{к. о. д} &= L_{в. д} \left( \frac{w_{к. о. д}}{w_{в. д}} \right)^2 \text{ H.} \\ L_{к. п. д} &= L_{к. о. д} \left( \frac{w_{д. п. д}}{w_{к. о. д}} \right)^2 \text{ H.} \end{aligned} \right\} \quad (8.79)$$

Calculation of the additional resistances included in a control and bias circuit. The resistance in a generator pilot excitation master winding circuit is determined from assigned catalog values for nominal voltage  $U_{звд. ном}$  and current  $I_{звд. ном}$ . Then,  $r_{звд} = \frac{U_{звд. ном}}{I_{звд. ном}}$ ; here, additional resistance in the master winding circuit will equal

$$r_{звд. дмп} = r_{звд} - 2r_{о. звд}$$

where  $r_{о. звд}$  is resistance of the master winding alone.

We determine resistance in the generator pilot exciter bias winding circuit based on the voltage at the Larionov circuit output:

$$u_{см} = 1,35u_c$$

When feed is from the 220 V ac network

$$u_{cm} = 220 \cdot 1,35 = 295 \text{ V.}$$

Considering bias winding nominal current  $i_{cm}$ , we will find

$$r_{cm} = \frac{u_{cm}}{i_{cm}}$$

and

$$r_{cm \text{ доп}} = r_{cm} - 2r_{o. cm},$$

where  $r_{o. cm}$  is the resistance of the bias winding itself.

First cascade MU control winding resistances  $r_{o. y I}$  and  $r_{o. y II}$  are calculated at a temperature of 75° C.

Given  $u_{cm}$  and  $i_{cm I}$ , first cascade additional bias winding resistance is

$$r_{cm I} = \frac{u_{cm}}{i_{cm I}}$$

and

$$r_{cm I \text{ доп}} = r_{cm I} - r_{o. y I}.$$

Given  $u_{cm}$  and  $i_{cm I} = i_{cm II}$ , output cascade additional bias winding resistance is

$$r_{cm II} = \frac{u_{cm}}{i_{cm II}}$$

and

$$r_{cm II \text{ доп}} = r_{cm II} - r_{o. y II}.$$

Amplifier MU1 and MU2 current winding feed voltage is coupled with main /410 circuit current by relationship

$$u_{o. T} = i_{\pi} (r_{\pi. \text{ птб}} + r_{\pi. \text{ отб}})$$

Calculation of GEU electromagnetic circuit time constants. The time constant of a generator field push-pull magnetic amplifiers MU1 and MU2 is determined as the sum of control winding time constants

$$T_{MV\Sigma} = \sum_{k=1}^n T_{MVk}$$

with use of expression

$$T_{yMV} = \frac{r w_{yMV} (w_{yMV} + \alpha k_1 w_{o.c})}{8f w_{yM}^2 r_y}$$

where  $r = u_{nr} / i_{nr}$  is load circuit resistance;  $w_{yMV}$  is the number of control winding turns;  $\alpha = 1/3$ , since an average current value is during consideration of the effect of feedback;  $k_1$  is a factor determined from the load characteristic;  $w_{o.c} = w_{1\phi}$  (each phase comprises four coils, of which only two operate simultaneously).

The MU time constant from the control circuit (master winding) will be found from expression

$$T_{3\phi R} = \frac{r w'_{3\phi R} (w'_{3\phi R} + \alpha k_1 w_{o.c})}{8f w_{yM}^2 r'_{3\phi R}} \text{ sec,} \quad (8.80)$$

where  $w'_{3\phi R} = 2w_y$  is the number of MU control winding turns when they are connected in series;  $r'_{3\phi R}$  is master circuit impedance.

The following MU time constants are determined by conversion:  
based on the bias winding

$$T_{cm} = T_{3\phi R} \frac{r_{3\phi R}}{r_{cm}} \text{ sec,} \quad (8.81)$$

based on the feedback current winding

$$T_{o.\tau} = T_{3\phi R} \frac{r_{3\phi R}}{r_{o.\tau.R}} \quad (8.82)$$

and based on other MU connected to windings.

The overall MU constant is:

$$T_{MV} = T_{32A} + T_{CM} + T_{0.7} \quad \text{sec.}$$

The generator field circuit time constant is:

$$T_{B.F} = \frac{L_{B.F}}{r_{B.F}} \quad \text{sec.}$$

The GED field circuit time constant is:

$$T_{B.A} = \frac{L_{B.A}}{r_{B.A}} \quad \text{sec.}$$

Considering that windings are connected in series, the generator exciter /411 field circuit time constant is:

$$T_{B.B.F} = \frac{L_{B.B.F}}{2r_{B.B.F}} \quad \text{sec.} \quad (8.83)$$

The armature circuit time constant is:

$$T_{A.U} = \frac{L_{A.U}}{r_{A.U}} \quad \text{sec,}$$

where

$$L_{A.U} = L_{A.1} + L_{A.2} + L_{K.O.A} + 2L_{A.F} + 2L_{A.P.F} + 2L_{K.O.F} \quad \text{H;}$$

$$r_{A.U} = r_{A.1} + r_{A.2} + r_{K.O.A} + 2(r_{A.F} + r_{A.P.F} + r_{K.O.F}) \quad \text{ohms.}$$

The GED field MU time constant is determined as the sum of the control and bias winding time constants:

control winding time constant

$$T_{O.P.A} = \frac{r\omega_p'(\omega_p' + \alpha k_1\omega_{o.c})}{8f\omega_p' r_p'} \quad \text{sec,} \quad (8.84)$$

where  $\omega_p'$  is the number of operating winding turns;  $\omega_{o.c}$  is the number of feedback winding turns;  $\omega_{ac}$  is the number of ac winding turns;  $r = r_{o.B.A} + r_p$  is overall resistance ( $r_p$  is operating winding resistance);  $r_p'$  is output loop control circuit impedance;

MUI--MUII time constant from the MU second cascade bias winding

$$T_{cm II} = T_{o.p. II} \frac{r_p'}{r_{cm}} \quad (8.85)$$

and of the first cascade

$$T_{o.p. I} = T_{kBT} \frac{r_{o.p.}}{r_{o.p.} - r_{d.o.6}} \quad (8.86)$$

where  $T_{kBT}$  is the first cascade MU time constant from the control winding in accordance with catalog data.

The time constant from the first cascade bias winding is:

$$T_{cm I} = T_{o.p. I} \frac{r_{o.p.}}{r_{cm}} \quad (8.87)$$

The overall time constant of a GED field two-cascade circuit is:

$$T_{MVД} = T_{o.p. II} + T_{cm II} + T_{o.p. I} + T_{cm I}$$

The overall time constant of a GED field one-cascade circuit is:

$$T'_{MVД} = T_{o.p.} + T_{cm}$$

where

/412

$$T_{o.p.} = \frac{r_{w_p'} (w_p + ak_1 w_{o.c.})}{8f w_p^2 r_p'} \quad (8.88)$$

and

$$T_{cm} = T_{o.p.} \frac{r_y}{r_{cm}} \quad (8.89)$$

Design formulas for differential equation coefficients. The factors of

the system's differential equations are calculated from ratios

$$\begin{aligned}
 k_1 &= \frac{k_1}{r_{\text{зад}}(T_{\text{МВ}} + T_{\text{в.в.г}})}; & k_2 &= \frac{k_1(r_{\text{д.п.г}} + r_{\text{к.о.г}})}{r_{\text{в.г}}(T_{\text{МВ}} + T_{\text{в.в.г}})}; \\
 k_3 &= \frac{1}{T_{\text{МВ}} + T_{\text{в.в.г}}}; & k_4 &= \frac{k_1}{T_{\text{МВ}} + T_{\text{в.в.г}}}; \\
 k_5 &= \frac{1}{L_{\text{в.г}}}; & k_6 &= \frac{2r_{\text{я}} + r_{\text{п.г}}}{L_{\text{в.г}}}; & k_7 &= \frac{2}{\Sigma L_{\text{я.у}}}; \\
 k_8 &= \frac{\Sigma r_{\text{я.у}}}{\Sigma L_{\text{я.у}}}; & k_9 &= \frac{C_{\text{ед}}}{\Sigma r_{\text{я.у}} T_{\text{я.у}}}; & k_{10} &= \frac{C_{\text{м.д}} 375}{GD_{\text{д}}^2}; \\
 k_{11} &= \frac{375}{GD_{\text{д}}^2}; & k_{12} &= \frac{1}{T_{\text{МВД}}}; \\
 k_{13} &= \frac{k(r_{\text{д.п.д}} + r_{\text{к.о.д}})}{T_{\text{МВ}} \cdot r_{\text{о.г}}}; & k_{14} &= \frac{\Delta u_{\text{в.д}}}{\Delta i_{\text{в.д}}} \quad (\text{based on the idling characteristic}).
 \end{aligned}$$

Reduction of the equation system to machine form. Considering the threshold value of the output voltage of the operational amplifiers of an MPT-9 computer is  $U_{\text{н.р}} = 100\text{V}$ , it is necessary to introduce scale factors into the system (8.69) equations with numerical values of factors  $k_i$ . Scale factor magnitudes are determined from the threshold values of the system's variable magnitudes in the modes studied corrected to the amplifier output voltage. Scale factors are calculated from the following ratios:

for master voltage

$$m_{u_{\text{зад}}} = \frac{U_{\text{зад. макс}}}{50} \quad \text{V/V};$$

for generator field current

$$m_{i_{\text{в.г}}} = \frac{I_{\text{в.г. макс}}}{80} \quad \text{A/V};$$

for exciter field current

$$m_{i_{\text{в.в.г}}} = \frac{I_{\text{в.в.г. макс}}}{80} \quad \text{A/V};$$

for generator field emf

$$m_{e_{\text{в.г}}} = \frac{E_{\text{в.г. макс}}}{80} \quad \text{V/V};$$

for generator emf

$$m_{e_{\text{г}}} = \frac{E_{\text{г. макс}}}{80} \quad \text{V/V};$$

/413

for main circuit current

$$m_{i_{\text{я}}} = \frac{I_{\text{я. макс}}}{80} \text{ A/V};$$

for GED field voltage

$$m_{U_{\text{в. д.}}} = \frac{U_{\text{в. д. макс}}}{80} \text{ V/V};$$

for GED field current

$$m_{i_{\text{в. д.}}} = \frac{I_{\text{в. д. макс}}}{80} \text{ A/V};$$

for magnetic flux

$$m_{\Phi_{\text{д}}} = \frac{\Phi_{\text{д. макс}}}{80} \text{ Wb/V};$$

for moment of resistance

$$m_{M_{\text{в}}} = \frac{M_{\text{в. макс}}}{80} \text{ kg-m/V};$$

for GED rotational speed

$$m_{n_{\text{д}}} = \frac{n_{\text{д. макс}}}{80} \text{ rpm/V};$$

for transient process time (the process lags by a factor of 10)

$$m_t = 0,1.$$

Considering the accepted scales, the initial system solved for derivatives will take the form

$$\begin{aligned}
\frac{m_{i_{B. B. r}}}{m_t} p_{i_{B. B. r}} &= m_{u_{3a\Delta}} k_1 k_{ny} u_{3a\Delta} - m_{i_{\Delta}} k_2 i_{\Delta} - \\
&\quad - m_{i_{B. B. r}} \cdot k_3 i_{B. B. r} + m_{i_{r. c}} k_y i_{r. c}; \\
m_{e_{B. r}} e_{B. r} &= m_{i_{B. B. r}} f_1(i_{B. B. r}); \\
\frac{m_{i_{B. r}}}{m_t} p_{i_{B. r}} &= m_{e_{B. r}} \cdot k_5 e_{B. r} - m_{i_{B. r}} k_6 i_{B. r}; \\
m_{e_r} e_r &= m_{i_{B. r}} f_2(i_{B. r}); \\
\frac{m_{i_{\Delta}}}{m_t} p_{i_{\Delta}} &= m_{e_r} k_7 e_r = m_{i_{\Delta}} k_8 i_{\Delta} - m_{\phi_{\Delta}} m_{n_{\Delta}} k_9 \phi_{\Delta} n_{\Delta}; \\
m_{\phi_{\Delta}} \phi_{\Delta} &= m_{i_{B. \Delta}} f_3(i_{B. \Delta}); \\
\frac{m_{n_{\Delta}}}{m_t} p_{n_{\Delta}} &= m_{\phi_{\Delta}} m_{i_{\Delta}} k_{10} \phi_{\Delta} i_{\Delta} - m_{m_{con}} k_{11} m_{con}; \\
m_{m_{con}} m_{con} &= m_{n_{\Delta}} f_4(n_{\Delta}); \\
m_{u_{B. \Delta}} u_{B. \Delta} &= m_{u_{B. \Delta. o}} u_{B. \Delta. o} + m_{u_{B. \Delta. \Delta}} u_{B. \Delta. \Delta}; \\
\frac{m'_{u_{B. \Delta}}}{m_t} p_{u_{B. \Delta}} &= -m_{u_{B. \Delta}} k_{13} u_{B. \Delta. \Delta} + m_{i_y} k_{13} i_y,
\end{aligned} \tag{8.90}$$

where

$$i_y = (i_{\Delta} - 3600);$$

/414

$$\frac{m_{i_{B. \Delta}}}{m_t} p_{i_{B. \Delta}} = m_{u_{B. \Delta}} k_{14} u_{B. \Delta} - m_{i_{B. \Delta}} k_{15} i_{B. \Delta}.$$

Finally, the machine form for the equations with numerical factor and scale values is:

$$\begin{aligned}
p_{i_{B. B. r}} &= a_{11} k_{ny} u_{3a\Delta} - a_{12} i_{\Delta} - a_{13} i_{B. B. r} + a_{14} i_{r. c}; \\
e_{B. r} &= a_{21} f_1(i_{B. B. r}); \\
p_{i_{B. r}} &= a_{31} e_{B. r} - a_{32} i_{B. r}; \\
e_r &= a_{41} f_2(i_{B. r}); \\
p_{i_{\Delta}} &= a_{51} e_r - a_{52} i_{\Delta} - a_{53} \phi_{\Delta} n_{\Delta}; \\
\phi_{\Delta} &= a_{61} f_3(i_{B. \Delta}); \\
p_{n_{\Delta}} &= a_{71} \phi_{\Delta} i_{\Delta} - a_{72} m_{con}; \\
m_{con} &= a_{81} f_4(n_{\Delta}); \\
u_{B. \Delta} &= a_{91} u_{B. \Delta. o} + a_{92} u_{B. \Delta. \Delta}; \\
p_{u_{B. \Delta}} &= a_{101} u_{B. \Delta} + a_{102} i_y; \\
p_{i_{B. \Delta}} &= a_{111} u_{B. \Delta} - a_{112} i_{B. \Delta}.
\end{aligned} \tag{8.91}$$

Numerical values of the equation factors in system (8.91) are determined from expressions in system

$$\begin{aligned}
a_{11} &= \frac{m_{u_{32}} k_1 m_t}{m_{i_{b,r}}}; & a_{12} &= \frac{m_{i_a} k_2 m_t}{m_{i_{b,r}}}; & a_{13} &= \frac{m_{i_{b,r}} k_3 m_t}{m_{i_{b,r}}}; \\
a_{14} &= \frac{m_{i_{r,c}} k_4 m_t}{m_{i_{b,r}}}; & a_{21} &= \frac{m_{i_{b,r}}}{m_{e_{b,r}}}; & a_{31} &= \frac{m_{i_{b,r}} k_5 m_t}{m_{i_{b,r}}}; \\
a_{32} &= \frac{m_{i_a} k_6 m_t}{m_{i_{b,r}}}; & a_{41} &= \frac{m_{i_{b,r}}}{m_{e_r}}; & a_{51} &= \frac{m_{e_r} k_7 m_t}{m_{i_a}}; \\
a_{52} &= \frac{m_{i_a} k_8 m_t}{m_{i_a}}; & a_{53} &= \frac{m_{\phi_A} m_{n_A} k_9 m_t}{m_{i_a}}; & a_{61} &= \frac{m_{i_{b,r}}}{m_{\phi_A}}; \\
a_{71} &= \frac{m_{\phi_A} m_{i_a} k_{10} m_t}{m_{n_A}}; & a_{72} &= \frac{m_{m_{con}} k_{11} m_t}{m_{n_A}}; & a_{81} &= \frac{m_{n_A}}{m_{m_{con}}}; \\
a_{91} &= \frac{m_{u_{b,d.o}}}{m_{u_{b,d}}}; & a_{92} &= \frac{m_{u_{b,d,d}}}{m_{u_{b,d}}}; & a_{101} &= \frac{m_{u_{b,d}} k_{12} m_t}{m_{u_{b,d}}}; \\
a_{102} &= \frac{m_{i_y} k_{13} m_t}{m_{u_{b,d}}}; & a_{111} &= \frac{m_{u_{b,d}} k_{14} m_t}{m_{i_{b,d}}}; & a_{112} &= \frac{m_{i_{b,d}} k_{15} m_t}{m_{i_{b,d}}}.
\end{aligned} \tag{8.92}$$

Remembering that the values of operational amplifier output voltage are 50 and 80 V, the equation system with numerical values must be rewritten considering the accepted scales.

The following comparative table of variable parameter values for two plant /415 operating modes in actual and machine scales (Table 8.1) is compiled for convenience in circuit selection and equation control.

Having compiled the electronic model and having computed the numerical values of all factors  $a_{ik}$  for a given GEU, it is possible further to investigate and calculate transient processes using any given program, including reversals, startings, propellor jammings, emergency modes, and so on.

Development of the mathematical model's schematic. MPT-9 analog computer units can be used to investigate GEU circuits (Figure 8.10). Electronic model circuits are depicted in Figures 8.11 and 8.12.

#### § 8.4 Selection of the Optimal Dynamic Characteristics of GEU /417 with Thyristor Excitation Systems

Circuit variant for GEU with thyristor pilot exciters. During development of the methodology for mathematical modelling of an icebreaker GEU with thyristor main generator and main propulsion motor pilot exciter systems relative to the

Параметр	(b) Реальный масштаб		(c) Машинный масштаб	
	Режимы			
	(e) швартовный	(f) на свободной воде	(e) швартовный	(f) на свободной воде
$i_{в.в.г.а}$ (g)	$I_{в.в.г.шв}$	$I_{в.в.г.св}$	$\frac{1}{m_{i_{в.в.г.}}} \cdot I_{в.в.г.шв}$	$\frac{1}{m_{i_{в.в.д.}}} \cdot I_{в.в.г.св}$
$i_{в.г.а}$ (g)	$I_{в.г.шв}$	$I_{в.г.св}$	$\frac{1}{m_{i_{в.г.}}} \cdot I_{в.г.шв}$	$\frac{1}{m_{i_{в.д.}}} \cdot I_{в.г.св}$
$e_{в.г.а}$ (h)	$E_{в.г.шв}$	$E_{в.г.св}$	$\frac{1}{m_{e_{в.г.}}} \cdot E_{в.г.шв}$	$\frac{1}{m_{e_{в.г.}}} \cdot E_{в.г.св}$
$e_{г.а}$ (h)	$E_{г.шв}$	$E_{г.св}$	$\frac{1}{m_{e_{г.}}} \cdot E_{г.шв}$	$\frac{1}{m_{e_{г.}}} \cdot E_{г.св}$
$i_{я.а}$ (g)	$I_{я.шв}$	$I_{я.св}$	$\frac{1}{m_{i_{я.}}} \cdot I_{я.шв}$	$\frac{1}{m_{i_{я.}}} \cdot I_{я.св}$
$u_{в.д.а}$ (h)	$U_{в.д.шв}$	$U_{в.д.св}$	$\frac{1}{m_{u_{в.д.}}} \cdot U_{в.д.шв}$	$\frac{1}{m_{u_{в.д.}}} \cdot U_{в.д.св}$
$i_{в.д.а}$ (g)	$I_{в.д.шв}$	$I_{в.д.св}$	$\frac{1}{m_{i_{в.д.}}} \cdot I_{в.д.шв}$	$\frac{1}{m_{i_{в.д.}}} \cdot I_{в.д.св}$
$\phi_{в.д.об}$ (j)	$\Phi_{в.д.шв}$	$\Phi_{в.д.св}$	$\frac{1}{m_{\phi_{д.}}} \cdot \Phi_{в.д.шв}$	$\frac{1}{m_{\phi_{д.}}} \cdot \Phi_{в.д.св}$
$n_{д.об/мин}$ (j)	$n_{д.шв}$	$n_{д.св}$	$\frac{1}{m_{n_{д.}}} \cdot n_{д.шв}$	$\frac{1}{m_{n_{д.}}} \cdot n_{д.св}$
$m_{в.кгм}$ (k)	$M_{в.шв}$	$M_{в.св}$	$\frac{1}{m_{m_{в.}}} \cdot M_{в.шв}$	$\frac{1}{m_{m_{в.}}} \cdot M_{в.св}$

Table 8.1. Scales of Variable Parameter Set Values for Two GEU Operating Modes. a—Parameter; b—Real scale; c—Machine scale; d—Modes; e—Moored; f—In open water; g—A; h—V; i—Wb; j—Rpm; k—kg-m.

schematic presented in Figure 3.56:

- main machinery parameter values obtained by calculation were used;
- the analog model was controlled by full-scale governors;
- modelling was accomplished for main diesel basic rotational speed;
- calculations were performed in real time units.

The methodology was developed for one circuit main loop (center), whose schematic was presented in Figure 3.56. Mathematical modelling methodology for the remaining loops is analogous. The mathematical model of GEU circuit elements is shown in Figure 8.13.

Thyristor bridge and control unit. Figure 8.13a presents a schematic of

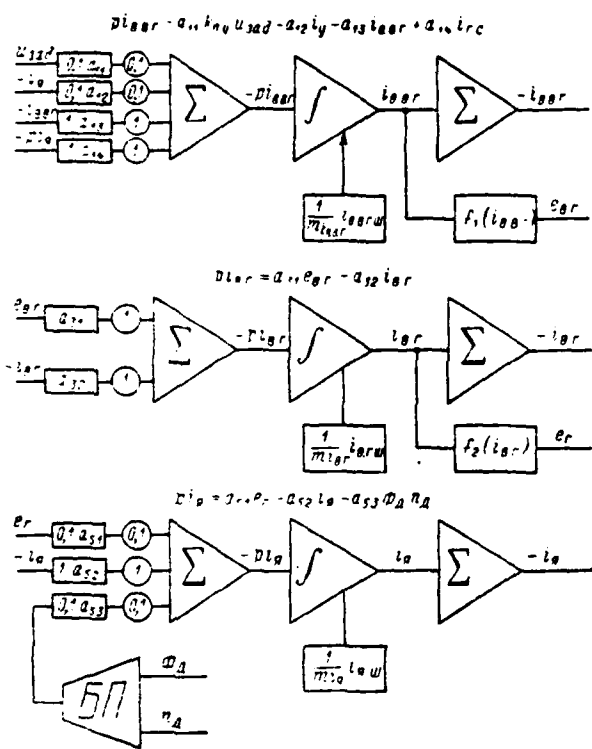


Figure 8.11. Schematic with Main Circuit Current as Output Parameter.

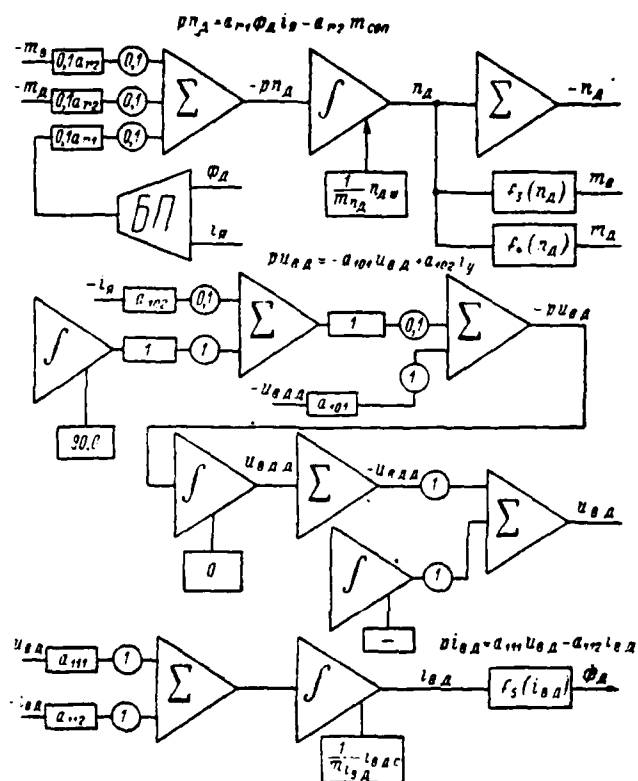


Figure 8.12. Schematic with GED Rotational Speed as Output Parameter.

a thyristor bridge and control unit. A linear relationship of the output value to the input value and its time constant is assumed:

$$T = T_{\text{эл}} - T_{\text{мост}}$$

The analog model is depicted in Figure 8.13a'.

Main generator exciter (field circuit). A schematic of main generator exciters is shown in Figure 8.13b.

We assume that the processes of field voltage increase and reverse flow in accordance with a linear law. Considering  $L_{\text{в.р.г}} \approx 0$  and  $k_{\text{в.р.г}} = \frac{U_{\text{в.р.г}}}{I_{\text{в.р.г}}}$  the

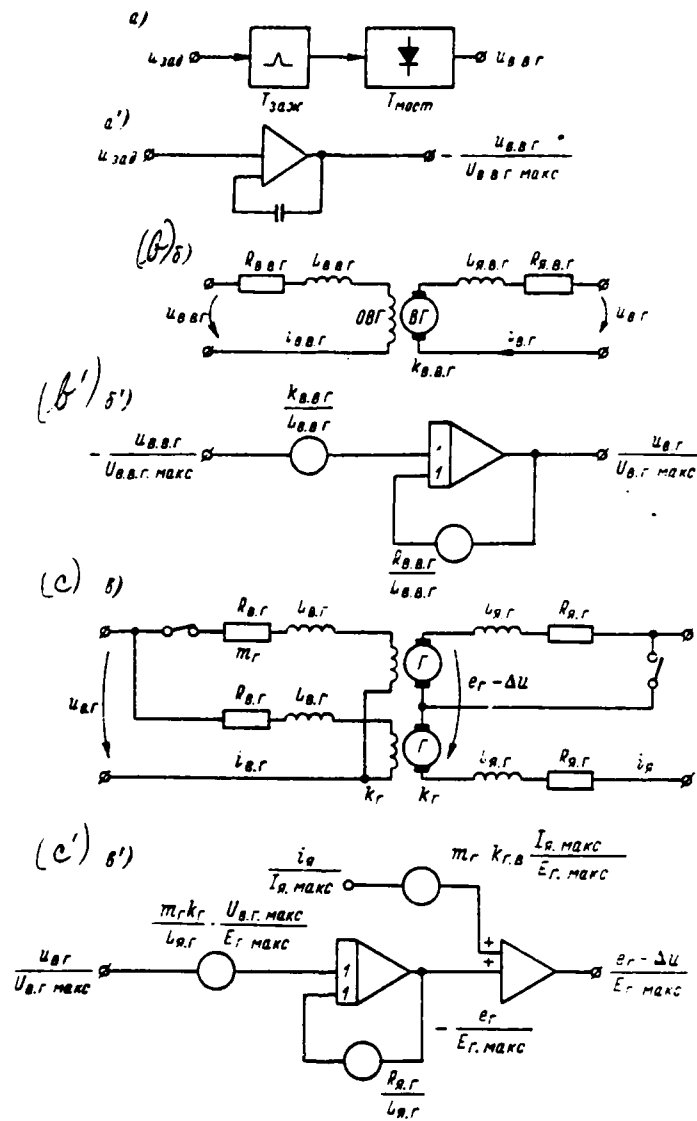


Fig. 3.13.

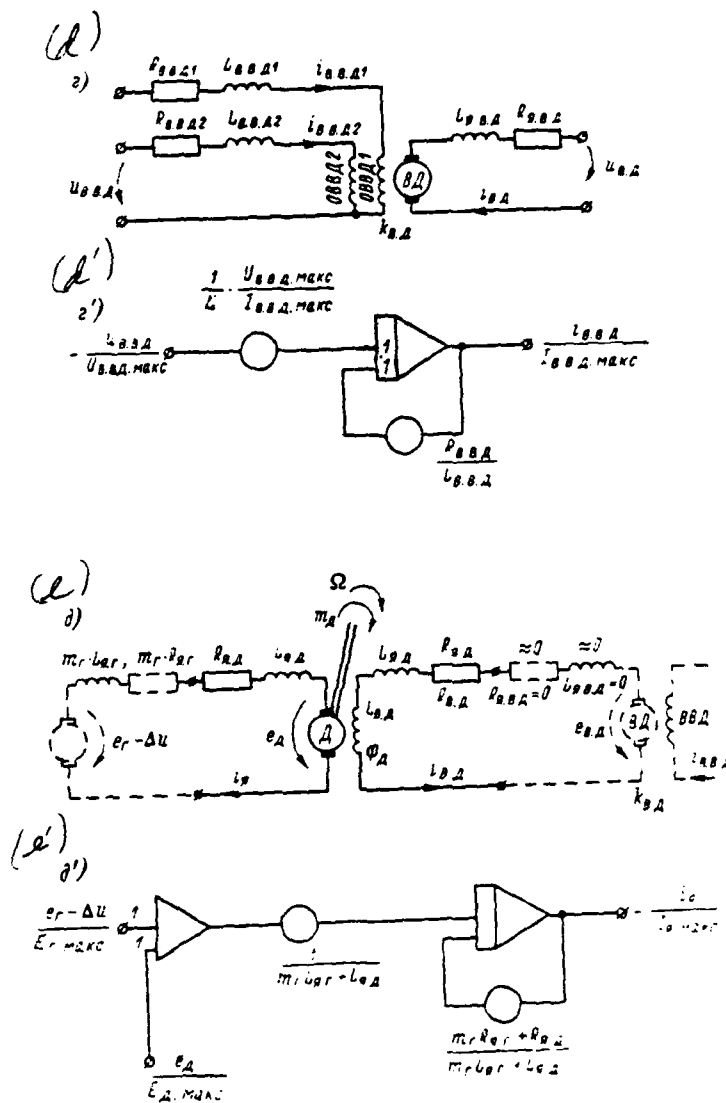


Fig. 8.13. Mathematical model of GEU circuit elements: a - schematic of a thyristor bridge and control unit; a' - analog model of a thyristor bridge; b - schematic of a main generator exciter; b' - analog model of a main generator exciter; c - schematic of main generators; c' - analog model of main generators; d - schematic of a main propulsion motor exciter; d' - analog model of a GED exciter; e - schematic of a main propulsion motor; e' - analog model of a main propulsion motor.

voltage equilibrium equation has the form

$$u_{b, a, r} = i_{b, a, r} R_{b, a, r} - L_{b, a, r} \frac{di_{b, a, r}}{dt} \quad (8.93)$$

where

$$i_{b, a, r} = \frac{1}{k_{b, a, r}} u_{b, a, r}$$

then

$$\frac{du_{b, a, r}}{dt} = \frac{k_{b, a, r}}{L_{b, a, r}} u_{b, a, r} - \frac{R_{b, a, r}}{L_{b, a, r}} u_{b, a, r} \quad (8.94)$$

Value  $k_{b, a, r}$  can be obtained from the main generator exciter's linearized load characteristic.

The analog model compiled from equation (8.94) is shown in Figure 8.13b'.

Main generators (field circuit). Main generator circuitry is shown in /421 Figure 8.13c. Assumptions are:

$$k_r = \frac{E_r}{I_n} = \text{const};$$

$$k_{xsp} = \frac{\Delta u}{I_n} = \text{const}.$$

The number of series-connected generators in one loop is designated  $m_r$ .

The equation determining the transient processes in main generator field circuits has the form

$$u_{b, r} = \frac{1}{m_r} R_{b, r} i_{b, r} - \frac{1}{m_r} L_{b, r} \frac{di_{b, r}}{dt} \quad (8.95)$$

The transformed equation, considering linearized characteristics, is

$$i_{b, r} = \frac{1}{k_r} e_r \text{ and } \Delta u = m_r k_{xsp} i_{b, r}$$

and, solved for generator emf change rate, it will take the form

$$\left. \begin{aligned} \frac{de_r}{dt} &= \frac{m_r k_r}{L_{b, r}} u_{b, r} - \frac{R_{b, r}}{L_{b, r}} e_r; \\ -\Delta u &= m_r k_{xsp} i_{b, r}. \end{aligned} \right\} \quad (8.96)$$

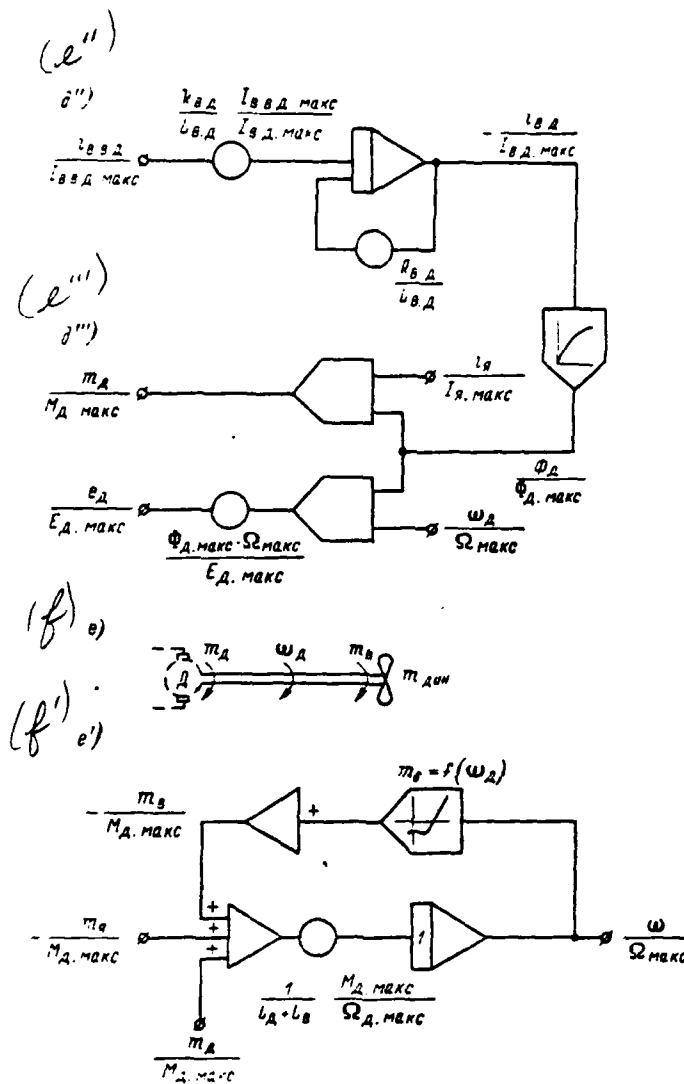


Figure 8.13. Mathematical Model of GEU Circuit Elements.

$e''$ ,  $e'''$ —Analog model of a main propulsion motor;  $f$ —Schematic of the shafting line;  $f'$ —Analog model of the shafting line (shafting line torque equation).

Value  $k_r$  can be obtained from the machinery's linearized field characteristic. Value  $k_{exp}$  is calculated considering the fact that field current  $I_{в. ном}$  corresponds to nominal armature circuit current  $I_{я. ном}$ .

Values  $R_{a,r}$  and  $L_{a,r}$  (armature circuit inductivity and ohmic resistance) consider the corresponding generator and main propulsion motor values.

An analog model of the field circuit is shown in Figure 8.13c'.

Main propulsion motor exciter (field circuit). A schematic of the main propulsion motor field circuit is shown in Figure 8.13d.

Assumptions are:

$$k_{b,d} = u_{b,d} \left( \frac{1}{i_{b,d2}} + \frac{\omega_2}{\omega_1} \frac{1}{i_{b,d1}} \right) = \text{const};$$

$$R_{b,d1} = R_{b,d2};$$

$$L_{b,d} = L_{b,d2} + \left( \frac{\omega_2}{\omega_1} \right)^2 L_{b,d1};$$

Considering the assumptions made, the initial GED field circuit voltage equilibrium equation has the form

$$u_{b,d} = i_{b,d} R_{b,d} + L_{b,d} \frac{di_{b,d}}{dt} \quad (8.97)$$

Equation (8.97), transformed and solved for the rate of current change /422 in the field circuit will have the form

$$\frac{di_{b,d}}{dt} = \frac{1}{L_{b,d}} u_{b,d} - \frac{R_{b,d}}{L_{b,d}} i_{b,d}. \quad (8.98)$$

Value  $k_{b,d}$  is calculated considering main propulsion motor parameters and is determined from the GED exciter linearized load characteristic.

An analog model developed from equation (8.98) is presented in Figure 8.13d'.

Main propulsion motor (main current circuit and field circuit). A schematic for a main propulsion motor with a field circuit is shown in Figure 8.13e.

The main circuit voltage equilibrium equation and the equation of motion have a form identical to that in the previous example.

An analog model of the current circuit developed from the emf equilibrium

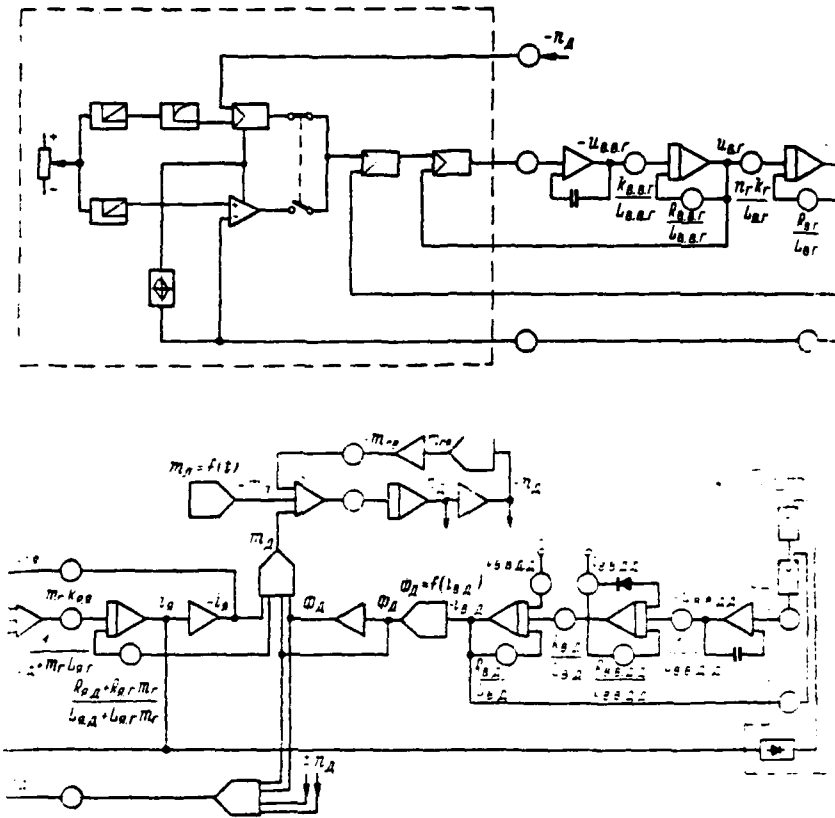


Fig. 8.14. Overall structural diagram of the mathematical modelling of a GEU thyristor pilot excitation system.

equation is presented in Figure 8.13e'. An analog model developed from the GED field circuit emf equilibrium equation is shown in Figure 8.13e" and e'''.

Shafting line. A shafting line schematic is shown in Figure 8.13f. The screw in open water characteristics  $m_s = f(\omega_n)$  and the so-called "ice torque characteristic"  $m_n = f(t)$  are considered to be given. In the characteristics of torques  $m_s$  and  $m_n$  are expressed in kilowatt-seconds,  $\omega_n$  in radians per second, and  $t$  in seconds.

An analog model developed from the shafting line torque equation is depicted in Figure 8.13f.

An overall structural diagram of the analog model for study of transient processes in GEU with a thyristor pilot excitation system is shown in Figure 8.14.

Circuit variant for GEU with a main generator and main propulsion motor /423 thyristor excitation system. A methodology for approximate calculation of transient processes consists of a system of relative units for the functional diagram for the current loop shown in Figure 8.15.

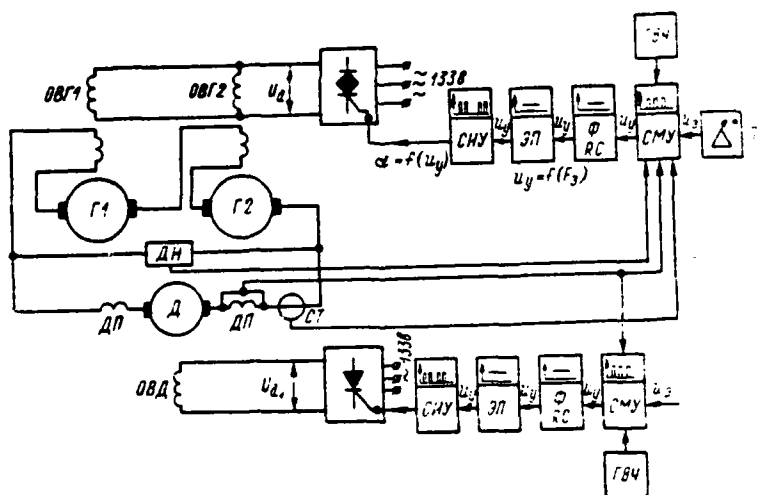


Figure 8.15. Functional Diagram of a GEU with a Thyristor Excitation System. SIU—pulse control system; EP—elementary follower; SMU—adding magnetic amplifier; GVCh—high frequency generator; F—filter.

The initial system of equations was compiled considering the following assumptions: the control system and thyristor unit are looked upon as inertia-free elements; adding magnetic amplifiers also are looked upon as inertia-free /424 links; the effect of winding mutual induction is disregarded; generator and main propulsion motor inductivity values are considered constant.

Remembering that the nominal values of the variables are considered the base values, the equations solved for derivatives can be written:

$$\left. \begin{aligned} \frac{d\bar{\omega}_d}{dt} &= a_1 \bar{\phi}_d \bar{i}_a - a_2 \bar{m}_a; \\ \frac{d\bar{i}_a}{dt} &= a_3 \bar{e}_r - a_4 \bar{i}_a - a_5 \bar{\phi}_d \bar{\omega}_d; \\ \frac{d\bar{F}_{в.г.}}{dt} &= a_6 \bar{\mu}_{зад} - a_7 \bar{i}_a - a_8 \frac{d\bar{i}_a}{dt} - a_9 \bar{\mu}_r - a_{10} \bar{F}_{в.г.}; \\ \frac{d\bar{F}_{в.д.}}{dt} &= A_0 + a_{11} \bar{i}_a - a_{12} \bar{F}_{в.д.} \end{aligned} \right\} \quad (8.99)$$

It is designated in system (8.99):

$$\begin{aligned} a_1 = a_2 &= \frac{1}{T_M} = \frac{C_M \Phi_{д. ном} I_{я. ном}}{J_{д. ном} \omega_{д. ном}}; \\ a_3 &= \frac{2E_{г. ном}}{(\pi r L_{я. г} - L_{я. д}) I_{я. ном}}; \quad a_4 = \frac{\pi r l_{я. г} - l_{я. д}}{\pi r L_{я. г} - L_{я. д}}; \\ a_5 &= \frac{C_e \Phi_{д. ном} \omega_{д. ном}}{(\pi r L_{я. г} - L_{я. д}) I_{я. ном}}; \quad a_6 = \frac{k \mu_{зад}}{R_{в. г} T_{в. г} I_{в. г. ном}}; \\ a_7 &= \frac{k k_1 I_{я. ном}}{R_{в. г} T_{в. г} I_{в. г. ном}}; \quad a_8 = \frac{k k_3 I_{я. ном}}{R_{в. г} T_{в. г} I_{в. г. ном}}; \\ a_9 &= \frac{\omega_{в. г} k k_2 \mu_r}{R_{в. г} I_{о. р}}; \quad a_{10} = \frac{1}{T_{в. г}}; \\ A_0 &= \frac{k F_{const}}{R_{в. д} T_{в. д} I_{в. д. ном}}; \\ a_{11} &= \frac{k k_3 I_{я. ном}}{R_{в. д} T_{в. д} I_{в. д. ном}}; \end{aligned}$$

$a_{12} = \frac{1}{T_{в. д}}$ ;  $k, k_1, k_2, k_3$  are gain for thyristor converter--pulse control system devices, current feedback, main generator voltage feedback, and current negative vanishing feedback, respectively.

A block diagram of the GEU system under study was compiled based on the equations and characteristics  $e_r = f(F_{в.г.})$  and  $m_a = f_1(\omega_d)$ . This makes it possible

to analyze and synthesize transient processes in GEU in the starting, reverse, and propellor jamming modes, as well as to investigate GEU stability in various operating modes.

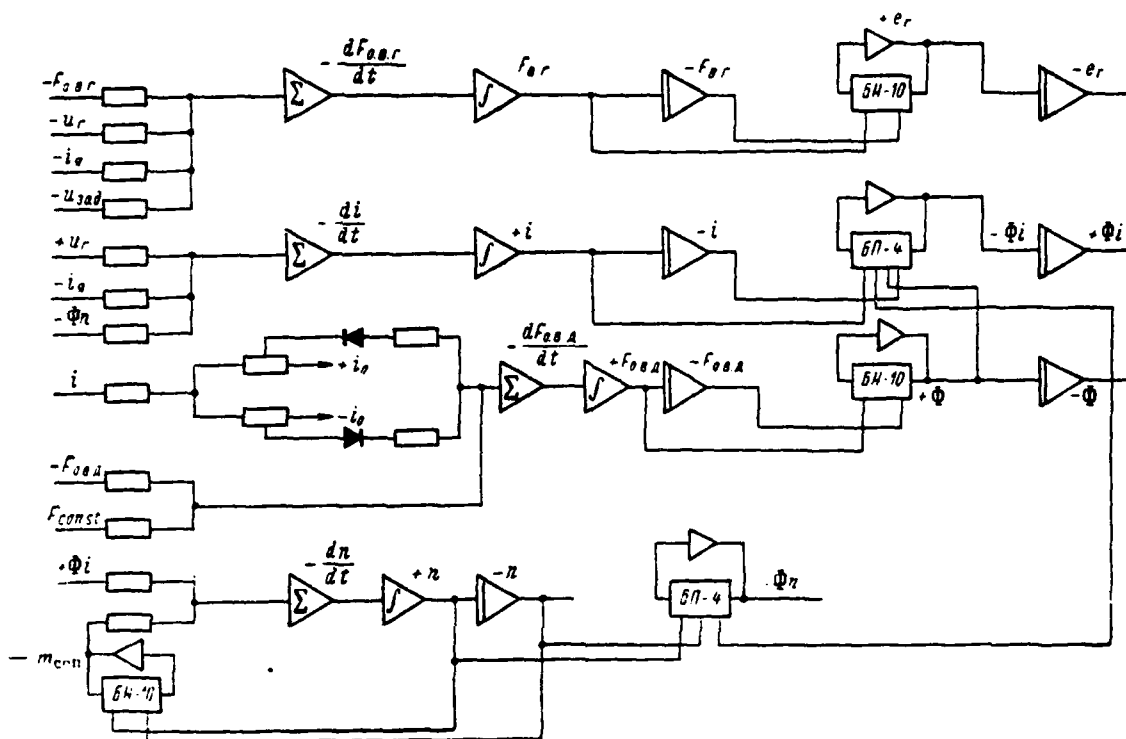


Figure 8.16. Block Diagram of a GEU with a Thyristor Excitation System.

§ 8.5 Calculation and Study of GEU Transient Processes Using an /426 Analog Computer, Taking Primary Motor Dynamics Into Account

Special features of primary motor dynamics and a method for their calculation.

Diesels equipped with an automatic control system are used, as a rule, as primary motors in GEU.

Solution of a system of differential equations describing the dynamic processes of the diesel--governor node makes it possible to obtain the characteristic of the change in controlled parameters over time. If one remembers that a diesel is a primary motor in a GEU system, then the set mode for it is characterized

by the equality of diesel torque  $m_{23}$  and moment of resistance  $m_{\text{con. } 23}$  (or as the sum of generator torque  $m_r$  and friction torque  $m_{r, f}$ ); here, the diesel generator operates at a constant rotational speed. A change in the moment of resistance will lead to acceleration (or deceleration) of motor rotation.

It is known that diesel torque  $m_{23}$  depends on the speed and load operating modes. Here, the speed mode is characterized by the rotational speed of the motor crankshaft, while the load mode is characterized by the torque developed by the motor, which in turn will depend on the amount of fuel supplied per cycle  $\Delta_2$ , and on the effective efficiency  $\eta_e$  of the motor in a given mode. It is assumed in dynamic characteristic calculations that motor torque completely is determined by the position of the control rack and the speed mode, while moment of resistance is determined by the speed mode and the load.

It is possible to represent diesel propelling torque as a function of rotational speed for the section of the motor's speed characteristic given a full fuel supply (the external characteristic):

$$m_{23} = f(n_{23}). \quad (8.100)$$

The relationship for the controlled section of the characteristic has the form

$$m_{23} = f_1(n_{23}, x), \quad (8.101)$$

where  $x$  determines the position of the control rack (fuel supply).

Control over the amount of fuel supplied  $\bar{x}$  will occur through automatic rotational speed control. All-mode direct and indirect governors are used for diesels in GEU systems. A mathematical description is presented below of a control system for D50 and D100 diesels equipped with all-mode indirect rotational speed governors. It is considered in the mathematical description of the /427 dynamics of diesel control that an all-mode governor includes the following basic elements:

a sensing element, which reacts to a change in crankshaft rotational speed (rotational speed deviation sensor);

a hydraulic servomotor, which changes the fuel supply to the cylinders as a result of the action of a signal determined by the sensing element;  
 a feedback device, which insures the stability of the rotational speed stabilization process.

Equations for the governor elements, written in relative deviations of the variables, given that the forces of dry friction are disregarded, have the form

$$\left. \begin{aligned} T_p^2 \frac{d^2 \bar{\eta}}{dt^2} + T_k \frac{d\bar{\eta}}{dt} + \bar{\eta} &= \frac{1}{\delta_0} (\bar{n}_{23} - k_v \bar{\psi}); \\ T_\alpha \frac{d\bar{\sigma}}{dt} &= F(\bar{\beta}); \\ T_i \frac{d\bar{\xi}}{dt} + \bar{\xi} &= \beta_i T_i \frac{d\bar{\sigma}}{dt}; \quad \bar{\beta} = \bar{\eta} - \bar{\xi}; \end{aligned} \right\} \quad (8.102)$$

where  $\bar{\sigma} = \bar{x}$  when  $x < x_{\text{max}}$ ;  $\bar{\sigma} = \bar{x} = 0$  when  $x = x_{\text{max}}$ .

System designations are:  $\bar{\eta}$  - relative deviation of the rotational speed measurement coupling (coupling coordinate  $Z_1$ ). Here, a centrifugal rotational speed meter in this case is the sensing element;  $\bar{\psi}$  is the relative deviation of the coordinates of the all-mode spring cushion, with spring cushions  $Z_2$  the coordinates of the rack;  $\bar{\beta}$  is the deviation of control valve relative to its bushing;  $\bar{\alpha}$  is slide valve coordinate;  $\bar{\sigma}$  is the relative deviation of the servomotor (rod coordinate) equalling the relative deviation of the control rack when it moves to its stop;  $\bar{\xi}$  is the relative deviation of the slide valve bushing (bushing coordinate  $\omega$ ) as a result of the action of the compensator (proportional-plus-integral [PI] feedback);  $T_p$  is rate meter time constant, sec.;  $T_k$  is a time constant stipulated by the viscous friction during rate meter coupling movement;  $T_\alpha$  is a hydraulic servomotor time constant;  $T_i$  is a PI-element time constant.

Time constant and factor values are determined from the following expressions:

$$\begin{aligned}
T_p &= \frac{m' \sigma_{\text{МАКС}}}{2E_0 \sigma_p}; & E_0 &= A_0 \omega_0; & T_0 &= \frac{k_{\text{ТР}} Z_2 \sigma_{\text{МАКС}}}{2L_p} \\
\sigma_0 &= \frac{Z_2 \text{МАКС}}{2E_0} \left( \frac{\partial E_0}{\partial Z} - \omega_0^2 \frac{\partial A}{\partial Z} \right); & k_{\text{В}} &= \frac{\omega_0^2 \sigma_{\text{МАКС}}}{\sigma Z_2} \frac{Z_2 \text{МАКС}}{2L_p} \\
T_{\alpha} &= \frac{\alpha_{\text{П}} c H_{\text{МАКС}}}{\mu_0 U_{\text{М}} \alpha_{\text{О.З}}}; & T_i &= \frac{\alpha_{\text{НЗ}}^2}{ac} + \frac{k_{\text{ТР.НЗ}}}{c}; & \rho &= A \omega^2 \\
\beta_i &= \frac{\alpha_{\text{К.П}} H_{\text{МАКС}}}{\left( \alpha_{\text{НЗ}} + \frac{\alpha k_{\text{ТР.НЗ}}}{\alpha_{\text{НЗ}}} \right) \omega_{\text{МАКС}}}
\end{aligned} \tag{8.103}$$

where  $m$  is corrected meter mass;  $E_0$  is recovery force;  $\sigma_p$  is the degree of /428 irregularity;  $\omega_0$  is the established angular rotational speed;  $k_{\text{ТР}}$  is a hydraulic friction factor;  $\alpha$  is a constant factor characterizing leakage of fluid through PI-element by-pass apertures;  $\alpha_{\text{П.с}}$  is the area of a servomotor piston;  $\mu_0$  is the oil consumption through the slide valve window factor;  $U_{\text{М}}$  is the rate of oil flow through the window;  $\alpha_{\text{О.З}}$  is the area of the slide valve windows;  $\alpha_{\text{М}}$  is the area of the PI-element slave piston;  $c$  is stiffness of the slave piston spring;  $k_{\text{ТР.НЗ}}$  is the PI-element slave piston viscous friction factor;  $\rho$  is the coupling supporting force;  $\alpha_{\text{К.П}}$  is compensating piston area;  $\omega_{\text{МАКС}}$  is the maximum movement of the PI-element slave piston.

The equations examined support the fact that consideration only of the main diesel governor elements will lead to very complicated mathematical expressions of dynamics. However, it is permissible in studying dynamic processes in a GEU system to disregard the time constants of several governor elements in view of their relative insignificance. In particular, introducing equivalent lag time, one can disregard the rate meter time constant. Equivalent time lag is about 0.1 second for D50 and D100 diesels, for example.

For governors installed on Wärtsilä-Sulzer MH 51 diesels (icebreakers "Moskva," "Leningrad," "Kiev," "Murmansk"), an approximate system of equations was determined considering several assumptions, but in such a way that the results of the system's solutions differed little from data obtained from full-scale tests. Here:

a) each diesel's load was determined from diesel power considering its average efficiency  $\eta_r \approx 0.94$ ;

b) all governor nonlinear relationships were considered by one equivalent relationship

$$\bar{m}_i = f(\bar{x}), \quad (8.104)$$

where  $\bar{m}_i$  is full diesel torque, relative units;  $\bar{x}$  is the control rack factor, relative units;

c) the mode selected as nominal is the one based on the characteristic 10% below the intersection point of the external and governor characteristics.

The slope of the governor characteristic determines the diesel rotational speed change when there is a load change within the range of the idling mode to 10% of overload above the nominal.

Given the selected nonlinear relationship  $\bar{m}_i = f(\bar{x})$  for the diesel operating speed mode, the dynamics of the governor's other elements is described by linearized equations.

Considering numerical factor values, the system for a governor has the form

$$\left. \begin{aligned} p\bar{n}_{23} &= 0,156(1,14\bar{m}_i - \bar{m}_i - 0,14\bar{m}_{cr}); \\ p\bar{x} &= 1,12(\bar{y}_1 - \bar{x} + 0,46p\bar{n}_{23}); \quad p\bar{y}_1 = 5,2(\bar{y}_2 - \bar{y}_1); \\ \bar{y}_2 &= \bar{n}_{23}; \quad \bar{m}_i = f(\bar{x}) \end{aligned} \right\} \quad (8.105)$$

(provided graphically)

where  $\bar{y}_1, \bar{y}_2$  are diesel governor intermediate coordinates.

System of equations describing GEU transient processes. The equations /429 for the electromechanical portion of the GEU for a side loop aboard the icebreaker "Moskva" has the form

$$\begin{aligned}
\rho \bar{e}_{B,r} &= a_1 (k_1 \bar{u}_{3,o} - k_2 \bar{e}_{r,r} - k_3 \bar{i}_n - k_4 \bar{i}_{B,r}); \\
\rho \bar{i}_{n,r} &= a_2 (\bar{e}_{B,r} - \bar{i}_{B,r} - \rho \bar{i}_n); \\
\bar{F}_r &= k_5 \bar{i}_{n,r} - k_6 \bar{i}_n; \\
\phi_r &= f_1 (\bar{F}_r); \quad \bar{e}_r = \bar{n}_r \phi_r; \\
\rho \bar{i}_n &= a_3 (k_7 \bar{e}_r - \bar{i}_n - k_8 \bar{n}_2 / \bar{i}_2); \\
\rho \bar{n}_2 &= a_4 (\bar{i}_n \bar{\phi}_2 - \bar{m}_2 - \bar{m}); \\
\rho \bar{i}_{B,d,o} &= a_5 (\bar{u}_{B,d,o} - \bar{i}_{B,d,o} - \rho \bar{i}_{B,d,d}); \\
\rho \bar{i}_{B,d,d} &= a_6 (\bar{e}_{B,d,d} - \bar{i}_{B,d,d} - k_9 \rho \bar{i}_{B,d,o}); \\
\rho \bar{i}_{B,B,d,d} &= a_7 (\bar{u}_{B,B,d,d} - \bar{i}_{B,B,d,d}); \\
\bar{e}_{B,d,d} &= \bar{i}_{B,d,d}; \\
\bar{F}_d &= k_{10} \bar{i}_{B,d,o} - k_{11} \bar{i}_{B,d,d}; \\
\bar{\phi}_2 &= f (\bar{F}_d); \quad \bar{u}_{B,B,d,d} = f (\bar{i}_n); \\
\bar{m}_2 &= j (\bar{n}_2); \quad \bar{m}_3 = j_1 (\bar{n}_2).
\end{aligned}
\tag{8.106}$$

The factors for system (8.106) are calculated in relative magnitudes, with the values of the variables as the icebreaker moves at 3 knots in ice accepted as the base.

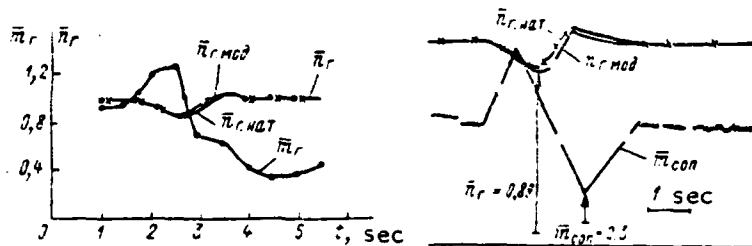


Figure 8.17. Comparative Data on Diesel Rotational Speed Change for the Icebreaker "Moskva."

System (8.106) factors reduced to machine form and considering a lag factor of 5 have the following numerical values:

$$\begin{aligned}
a_1 &= 0.23; \quad a_2 = 0.1; \quad a_3 = 2.4; \quad a_4 = 0.13; \\
a_5 &= 1.27; \quad a_6 = 0.143; \quad a_7 = 0.65; \\
k_1 &= 1.03; \quad k_2 = 0.105; \quad k_3 = 0.725; \quad k_4 = 0.2; \\
k_5 &= 1.15; \quad k_6 = 0.15; \quad k_7 = 13.3; \quad k_8 = 11.3; \\
k_9 &= 0.1; \quad k_{10} = 0.35; \quad k_{11} = 0.65.
\end{aligned}$$

Mathematical modelling of GEU transient processes taking primary motor /430 dynamics into account. A sufficiently-accurate mathematical description of the governor is illustrated in Figure 8.17, in which are presented comparative diesel rotational speed change data for the icebreaker "Moskva" obtained during full-scale tests  $\bar{n}_{r, \text{исп}}$  and by calculations, by the mathematical modelling method  $\bar{n}_{r, \text{мод}}$ , for different moments of resistance  $\bar{m}_i$  in the propellor-ice interaction mode.

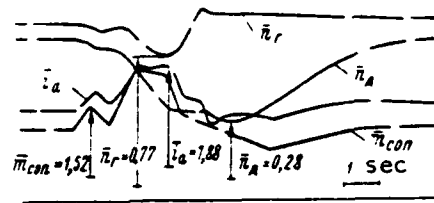


Figure 8.18. GEU Dynamic Characteristics in the Propellor-Ice Interaction Mode (Obtained by Mathematical Modelling).

GEU dynamic characteristics in the propellor-ice interaction mode, obtained by mathematical modelling, are shown in Figure 8.18. Here, the value of the propellor moment of resistance is used based on full-scale test data. A comparative evaluation of full-scale test results and mathematical modelling data demonstrates that deviations do not exceed 10%.

Problems of Alternating Current Electrical Propulsion Plant (GEU) Design  
and Their Prospective Development

§ 9.1 Basic Characteristics and Selection of  
Alternate Current Electrical Propulsion Plant Basic Parameters

Voltage and frequency. Alternating current GEU are built with a voltage up to 6,300 V and with outputs up to 15,000 hp, 3,150 V. In some cases, voltages of 1,05 and 525 V are used. The current frequency determining primary motor and propellor rotational speed usually is 50 or 60 Hz. However, it should be noted that, as opposed to practice on land, the selection of voltage and frequency in an ac GEU is not controlled rigidly. This is evident, for example, from /431 the data in Table 9.1.

Table 9.1

Turboelectric Propulsion Plant (TEU) Basic Characteristics

Ship Name	Plant Output, hp	Voltage, kV	Frequency, Hz
"Normandy"	4 x 40,000	5.5	80
"Kliss Vyver"	1 x 9,000	3.0	57
"Potsdam"	2 x 13,000	6.0	53.3
"Baltika"	2 x 6,000	3.15	52.5

The Rules of the USSR Registry set only the upper limits for voltage. Nominal generator and GED line voltage must not exceed 6,300 V. It is possible to use voltages exceeding this limit only with special permission from the USSR Registry. Selection of ac GED voltage magnitudes is recommended [49] as equating to the permissible threshold current magnitudes in each GED phase. Meanwhile, the current in each phase in low-power plants should be restricted to 1,500-2,000 V and to 2,000-2,500 V in high-power plants. Information on voltages used in foreign-built electric ships is presented in Table 9.2 from statistical materials [49] as a supplement to the Table 9.1 data.

Table 9.2

Voltages Used in Extant TEGU			
Main Propulsion Motor Output, kW	Voltage, kV	Main Propulsion Motor Output, kW	Voltage, kV
500-1,000	0.275-0.500	5,000-10,000	3.0
1,000-2,000	0.500-0.600	7,500-15,000	4.0
1,500-3,000	1.0	10,000-50,000	5.0-6.0
2,500-5,000	2.3		

Although the Rules of the USSR Registry do not legislate the selection of GEU frequencies, it is recommended that the standard frequency of 50 Hz be selected in all cases where this is possible. Thus, it is advisable to use a standard frequency for ac GEU with synchronous GED, which permit power factor control, while it is best to start from the selected nominal value of the power factor for plants with induction GED. Here, the frequency for  $\cos \varphi \leq 0,98$  can be determined from the expression

$$i = \frac{a - \cos \varphi}{60 \frac{b}{n_n} \left( c - d \log \frac{1000N}{n_n} \right)}, \quad (9.1)$$

where  $\varphi$  is the phase shift in the GED stator circuit;  $N$  is GED power, kW;  $/432$   $n_n$  is motor rotational speed, rpm;  $a$ ,  $b$ ,  $c$ ,  $d$  are numerical factors, the values of which average [49]:  $a = 0.985$ ,  $b = 2.8$ ,  $c = 0.008$ ,  $d = 0.001$ ;  $\cos \varphi$  can be assumed to equal: 0.83-0.85 for single squirrel-cage synchronous motors and 0.78-0.80 for double squirrel-cage motors.

Main propulsion motor types. The main propulsion motors used in GEU vary greatly in design. From the electromagnetic point of view, they can be induction, synchronous, and synchronous-induction. Meanwhile, electrical induction motors are built with phase and with double squirrel-cage rotors. From the mechanical point of view, they can be subdivided into low-speed, when connected directly to propellers, and high-speed, when connected via reduction gear to propellers.

Synchronous electric motors are used most widely at the present time in ac electric ships.

Optimal rotational speed selection. One of the most important advantages of GEU, including ac GEU, is the capability to select optimal main propulsion

motor rotational speed and, therefore, propellor rotational speed when it is connected directly to the GED.

The following factors must be considered when selecting the most advantageous GED rotational speed:

- fuel consumption and, consequently, plant total efficiency;
- total plant weight, including fuel;
- initial expenditures for propulsion plant equipment;
- minimum total annual operating costs.

The last two factors involve many competing circumstances and can be provided reliably through direct contact with plant manufacturers, as well as through knowledge of vessel type, its series production, and many other data.

Professor V. I. Polonskiy [49] developed a methodology for calculation of the first two factors. The essence of this methodology is as follows.

If vessel speed remains constant and propellor rotational speed is changed, selecting its parameters based on greatest efficiency, then the amount of power at each propellor shaft  $N_p$  does not remain constant, but will change during the transition from one screw to another. Thus, we will get relationship

$$N_p = f(n_A). \quad (9.2)$$

On the other hand, if one assumes that GED threshold size characteristics correspond to the dimensions of the engine rooms, i. e., that they change during the transition from one screw to another, then GED power  $N_A$  will change with a rotational speed change and, consequently, we will get relationship

$$N_A = \varphi(n_A). \quad (9.3)$$

Striving for minimum fuel consumption, one should select that propeller /433 rotational speed at which the overall plant—screw  $\eta_p$  and GED  $\eta_A$  efficiency will be the highest, i. e.,

$$\eta_y = \eta_p \eta_A. \quad (9.4)$$

It is possible to assume with a sufficiently-close approximation that GED efficiency in the range of possible screw rotational speed variations for each individual case, given identical vessel speed, is constant. Then, to insure maximum  $\eta_v$ , it is possible to constrain achievement of value  $\eta_{p \text{ макс}}$ , which will be obtained at the lowest (of all possible speeds for a given vessel) screw rotational speed. It is evident that lowest GED rotational speed (and, consequently, propellor speed) for a given vessel speed will correspond to condition

$$N_p = N_d \text{ или } f(n_d) - \psi(n_d) = 0. \quad (9.5)$$

Thus, selection of the most advantageous GED rotational speed when it is connected directly with the propellor boils down to compilation and solution of this equation. A simple method is presented in [49] for its graphic solution stemming from the condition of the most advantageous propellor rotational speed in a GEU.

Selection of GED type and number. The selection of the electric motors to drive propellers is, as are other GEU elements, linked with analysis of the specific requirements levied on the vessel and the propulsion plant, as well as of many other technical and economic factors. If one considers only the electrical aspect of this task, then one should begin with comparison of the relative advantages and disadvantages of such electric motor types as induction motors with slip rings, double squirrel-cage induction, synchronous, and synchronous-induction motors. An approach to this selection from the mechanical point of view involves solution of the problem of frame design and method of GED connection to the propellor shaft. In accordance with [49], considerations are presented below in Table 9.3 relative to the most important electric motor indicators for evaluation of the possibilities for their use in the GEU aboard various types of vessels.

Synchronous motors are used most widely in GEU. Usually, GED are either enclosed or open as far as design goes. It is advisable to use an enclosed frame in those instances when the hourly volume of air required to ventilate the GED does not exceed engine room volume by a factor of 30-40. An open GED should be used given higher volume ratios of the air needed to ventilate the GED and the engine room.

Use of high-speed GED connected via various transmissions to propellor shafts can be advisable only given low plant power or given a special engine room layout since use of intermediate transmissions, especially for powerful plants, decreases their reliability and longevity.

Table 9.3

/434

Electric Ship Basic Indicators

GED Characteristics	GED Types			
	Induction with slip rings	Double Squirrel-Cage Induction	Synchronous	Synchronous-Induction
Efficiency	Average	Average	High	High
Power Factor	Average	Low	High	High
Relative Weight	Average	Increased	Slight	Slight
Relative Cost	Average	Increased	Low	Low
Overload Capacity	Average	Great	Average	Slight
Control During Maneuvering	More Complex	Simple	Quite Complex	Complex

In the overwhelming majority of cases, the number of main propulsion motors in an ac GEU corresponds to the number of propellor shafts. However, given sufficiently-high power applied to one propellor shaft and insufficient vessel draft, as well as under the conditions of an extended cruise at low speeds, it becomes advisable to abandon this particular rule and install two GED per propellor shaft.

Threshold power of the ac GED on extant electric ships ranges from 25,000-40,000 hp (for example, "Normandy," "Lexington," "Saratoga").

General information on synchronous GED. Use of synchronous electric motors in modern ac GEU is based on the following advantages:

- for rotational speeds standard for commercial vessels (up to 200 rpm), a synchronous electric motor weighs 10-20% less than an induction motor of equal power (the need for a copper damping cage somewhat decreases this advantage);
- the efficiency of a low-speed synchronous electric motor is about 3-5% higher than that of an induction motor;
- synchronous motor power factor equals 1;
- the large air gap, first, insures simpler shaft design given an identical

flexure factor, reducing the cost of the machinery and decreasing the probability of rotor friction against the stator; second, it creates better operating conditions, considering possible foundation deformations in heavy waves;

- it is possible to remove the poles of a synchronous electric motor without removing the rotor, so stator and rotor windings can be replaced without dismantling the motor;

- there is a possibility on multiscrew vessels to insure even (synchronous) operation of all propellers at absolutely-identical rotational speeds. This advantage occurs because, as is known, a significant part of vessel hull /435 oscillations are caused, in particular, by the operation of both propellers at slightly-different rotational speeds. This results in oscillations of varied amplitude and frequency, causing oscillations in vessel elements.

The following are disadvantages of synchronous machinery:

- inability to switch the number of poles in any ratio other than 2:1;
- a reduction of an electric motor's asynchronous torque with an approximation to synchronous speed, which given the conditions whereby one is operating with increased moment of resistance on the screw can cause difficulties when synchronizing the motor;

- difficulty in combining requisite starting characteristics with operating characteristics;

- rigidity of the external characteristic.

A self-starting synchronous motor is a combination of synchronous and asynchronous machinery. A shorted winding operating when the electric motor is started in the asynchronous mode is installed in the pole shoes: it provides the capability to bring rotor rotational speed up to 95% of the synchronous mode. Then, the field winding is connected to the exciter and the motor rotor is synchronized. When the motor operates at a synchronous speed, its starter winding does not create torque, but operates as a damper, preventing oscillations and rotor wobble. The stator winding has a large number of circuits so, in the event of damage to one of its coils, the entire circuit will not be cut out. Here, the power of the main propulsion motor is in a condition to provide almost full vessel speed.

The motors and generators feeding them are considered to have identical

characteristics for both voltage change and output. This is a requirement so that both generators and the main propulsion motor will be able to operate when  $\cos \phi = 1$  in all power ranges.

The efficiency of a synchronous main propulsion motor is sufficiently high (up to 98%) and will depend on motor power and speed. Its frame is built in the form of welded components, which reduces the weight of the inactive portions almost 40%.

Selection of main generator type, number, and power. Synchronous machinery exclusively was used as generators for GEU: nonsalient-pole machinery in turboelectric propulsion plants (TEGU) and salient-pole in diesel electric propulsion plants. Primary motors, rotating synchronous generators, must have the capability to regulate rotational speed ranging from 25 to 100% of nominal.

Main generators are equipped with a forced ventilation system from individual electric fans built in a closed or open cycle.

Selection of the number of main generators is determined by a desire to provide high plant efficiency, relative simplicity, increased reliability, /436 and low cost. Here, plant efficiency for various long trips must differ little from efficiency at full vessel speed.

Satisfaction of the aforementioned and many other, sometimes contradictory, requirements does not permit identical accomplishment of the assigned task concerning the most advantageous number of main generators. The solution must be accomplished by comparative analysis of compiled variations. Here, for low-power GEU (4,000-5,000 kW), it is preferable to provide a requirement for maximum efficiency and decreased plant cost, which will lead to selection of one main generator per propellor shaft (for a TEGU). It is advisable to use two or more generators for high-power electric ships or passenger ships with several fixed speeds.

Basic main generator and main propulsion motor requirements. Alternating current GEU design practice and operation provide the capability to formulate several basic requirements levied on main generators and synchronous main propulsion motors.

Generators and main propulsion motors must support a current overload without damage. The magnitude and duration of the overload are determined from vessel purpose.

Overloads must not cause a disruption of normal generator operating mode and lead to their premature wear and failure.

Generators and GED are equipped with damper windings to insure stable parallel generator operation during propulsion motor starting and reversal, as well as their reliable synchronization. GED starter windings insure their starting in the asynchronous mode.

Generators must be capable of temporary (20-30 second) field boosting larger by a factor of 2.5-3.5 than the value of the nominal magnitude to insure main propulsion motor starting. Boosting must be accomplished at a decreased current frequency, determined by minimal primary motor rotational speed.

Generators and propulsion motors are capable of a certain field boosting at the nominal frequency and at a frequency 110-115% of the nominal for the purpose of increasing system stability and synchronizing torque during navigation in storms.

Main generator characteristics must satisfy the requirements for extended parallel operations at different frequency values with possible connection of generators operating bus bar auxiliaries using the self-synchronization method.

The following requirements are levied on the motors:

— starting current given nominal frequency must not exceed a value greater by a factor of 6 than nominal current for slip  $s = 2$  and by a factor of 5 when  $s = 1$ ;

— starting torque given nominal frequency and nominal field must be at least one-half of nominal when  $s = 2$  and at least 0.7 when  $s = 1$ ;

— maximum torque given nominal frequency must be at least 1.8 of nominal;

— input moment given nominal frequency and nominal field must comprise 0.8 of nominal when  $s = 0.05$ ;

— input moment given maximum frequency and field boosting by a factor of 3.5 must equal 1.25 of the moment of resistance value when  $s = 0.05$ .

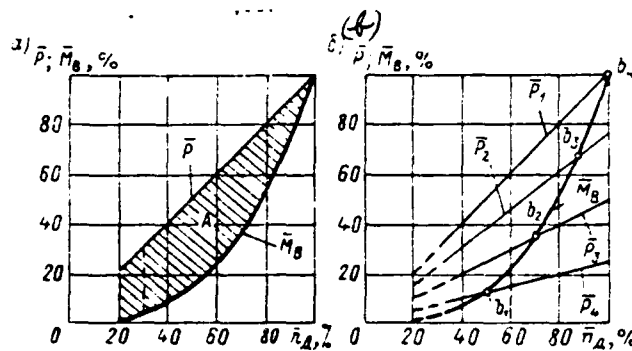


Figure 9.1. Characteristics of the Relationship of Power  $\bar{P}$  and Propellor Resistance  $\bar{M}_B$  to Propellor Rotational Speed  $n_A$ : a—Using full diesel power only in the vessel full speed mode; b—When the same power is supplied to the propellers, but due to parallel operation of four generators. A—Diesel overload range;  $\bar{P}_1, \bar{P}_2, \bar{P}_3, \bar{P}_4$  are power characteristics during operation of four, three, two, and one generator, respectively.

All the aforementioned characteristics must be such that main propulsion motors will be able to operate in the asynchronous mode without overheating for 1-2 minutes when falling out of synchronization (excitation cut out) and again be brought into synchronization (excitation cut in).

#### Regulation of propellor rotational speed and electric ship speed.

Characteristics of the relationship of relative power  $\bar{P}$  and screw moment of resistance  $\bar{M}_B$  to the speed of screw rotation when a diesel is connected directly to a propellor in a range of control from 30-100% of nominal rotational speed are shown in Figure 9.1a. Here, diesel power is used fully only during full vessel speed, i. e., at 100% rotational speed. At all other (intermediate) rotational speeds, the motor is underloaded (the hatched portion of the graph). The same curves are shown in Figure 9.1b, but when the same amount of power is supplied to the propellor due to parallel operation of four generators.

It follows from examination of the graphs that 50% can be achieved (point  $b_1$ ) when one generator is operating, 72% when two are operating (point  $b_2$ ), 87% for three (point  $b_3$ ), and, when four are operating (point  $b_4$ ), 100% of nominal screw rotational speed is achieved. Propellor rotational speed and, therefore, vessel speed in an ac GEU are controlled by a change in frequency in combination

with connection or disconnection of individual generators. For this purpose, primary motors used in ac GEU must have the capability to regulate rotational speed within broad limits: in a 100-25% range for turbines and 100-30% range for diesels. Governors usually are used in the form of all-mode or multimode devices so that faultless diesel generator parallel operation is insured in the entire range of rotational speeds.

## § 9.2 Electrical Propulsion Plant Main Current Circuits

Classification. Alternating current GEU are differentiated: by primary motor type as turboelectric (TEGU), diesel electric (DEGU), and atomic (AGEU); by number of main propulsion motors; by the number of propellor shafts and GED in each of them; by the number of main generators; by total power at propellor shafts; and by several other features.

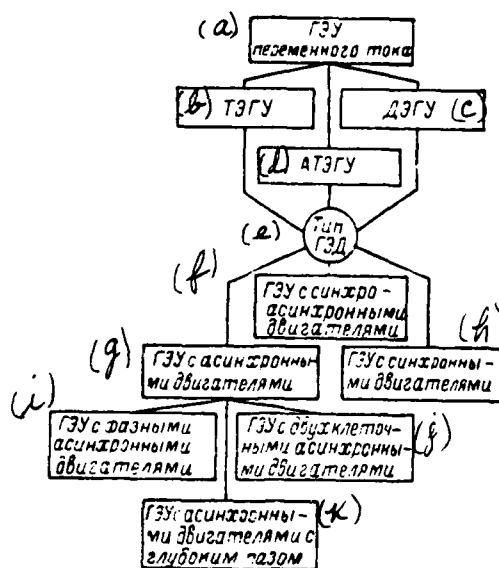


Figure 9.2. Classification of Alternating Current GEU Structure by Primary Motor and Generator Type. a—Alternating current GEU; b—TEGU; c—DEGU; d—ATEGU; e—GED type; f—GEU with synchronous-induction motors; g—GEU with induction motors; h—GEU with synchronous motors; i—GEU with phase induction motors; j—GEU with double squirrel-cage induction motors; k—GEU with induction motors with a deep-bar slot.

Figure 9.2 depicts the classification of ac GEU by primary motor and GED type. The multiplicity of constructed and possible variations of these circuits is linked both by the factors mentioned above and by many others. For example, by plant field, regulation, and control systems used; by protection and monitoring; remote control; synchronization, and so on. However, if one concentrates only on the main current circuit, then all the multiplicity of possible variations is constrained by several types of classified structural circuits, where the operative factors are main propulsion motor type and number of main generators, propellor shafts, and GED.

Turboelectric propulsion plants (TEGU). The number of turbogenerators /439 in a TEGU, as a rule, equals the number of propellor shafts and, accordingly, the power of each generator equals the power consumed by the main propulsion motors. Parallel connection of turbogenerators here usually is not envisioned since this complicates operation and requires a synchronous change in turbine speed as GED rotational speed is regulated. The entire commutating apparatus for the main current circuit calls for accomplishment of the connect and disconnect operation only in a dead circuit, i. e., when generator and GED excitation is removed. Due to the operating principle in which each turbogenerator runs its own propellor shaft, it is possible to construct for a GEU rather simple main current circuits differing only in the number of turbogenerators and main propulsion motors.

A TEGU structural diagram is shown in Figure 9.3. Since in an ac GEU protection elements act not on main circuit switches, but on field circuit disconnect devices, this makes it possible to install only generator isolators  $R_z$  in main circuits. Air switches are installed in place of isolators sometimes in cases of forced switching operations in main circuits, when there is a need to open these circuits prior to the currents in them dying down completely.

Bus-bar isolators  $R_z$  (Figure 9.3e) are installed when there is more than one generator to provide feed for the GED when a particular main generator is in the process of disconnecting. The capability to switch poles in a GED is envisaged to obtain fixed intermediate speeds, with pole switches  $\Pi_n$  installed for this purpose.

Main generator stator winding switches  $\Pi_{0,r}$ , making it possible to switch these windings in three-phase systems from a star to a triangle and in two-phase systems from parallel to series connection.

We will examine typical TEGU circuits using several electric ships as our examples.

The circuit for a TEGU comprising two main turbines 1T and 2T turning generators 1G and 2G is a rather simple but widespread circuit. It is used on the electric passenger vessels "Baltika" and "Abkhaziya", as well as several others (Figure 9.4). In a normal running mode, starboard generator 1G runs its starboard GED 1D, while port generator 2G runs the GED on its side 2D. Parallel operation of the circuit is not envisioned so there is no synchronization system. Reversing switches Pr1 and Pr2 are connected and intersectionalizing switch VS is disconnected. In so-called economic running, both GED can operate either from turbogenerator 1G with isolator Rz1 and intersectionalizing switch VS connected or from turbogenerator 2G with Rz2 and VS connected and Rz1 disconnected. Ship speed equalling about 70% of nominal can be achieved under these conditions.

Use of electromagnetic interlocking between isolators Rz1 and Rz2 and /441 intersectionalizing switch VS eliminates generator parallel operation.

Elements  $C_{r,1}$ ,  $C_{r,2}$  and  $B_{c,1}$ ,  $B_{c,2}$ , shown in the figure designate braking resistances and their switches, respectively.

Other main current circuits also are used. TEGU with two main generators running one propellor and equipped with dynamic braking devices are examples (turboelectric ships "Aurus," "Antilla," "Oruzabu," and others).

Most early turboelectric ships use the simplest circuit where one turbogenerator feeds one main propulsion motor. More than 500 TEGU aboard American Series T2 tankers built from 1940-1945 are equipped in just this way. On these tankers, a 4,200 kW,  $\cos \phi = 1$  at 3,715 rpm, 62 Hz, 2.3 kV turbogenerator runs one 6,000 hp, 90 rpm main propulsion motor. Power takeoff from electric propulsion bus bars (ShED) to station bus bars (ShSN), in particular for powerful cargo pump drive, is envisioned here.

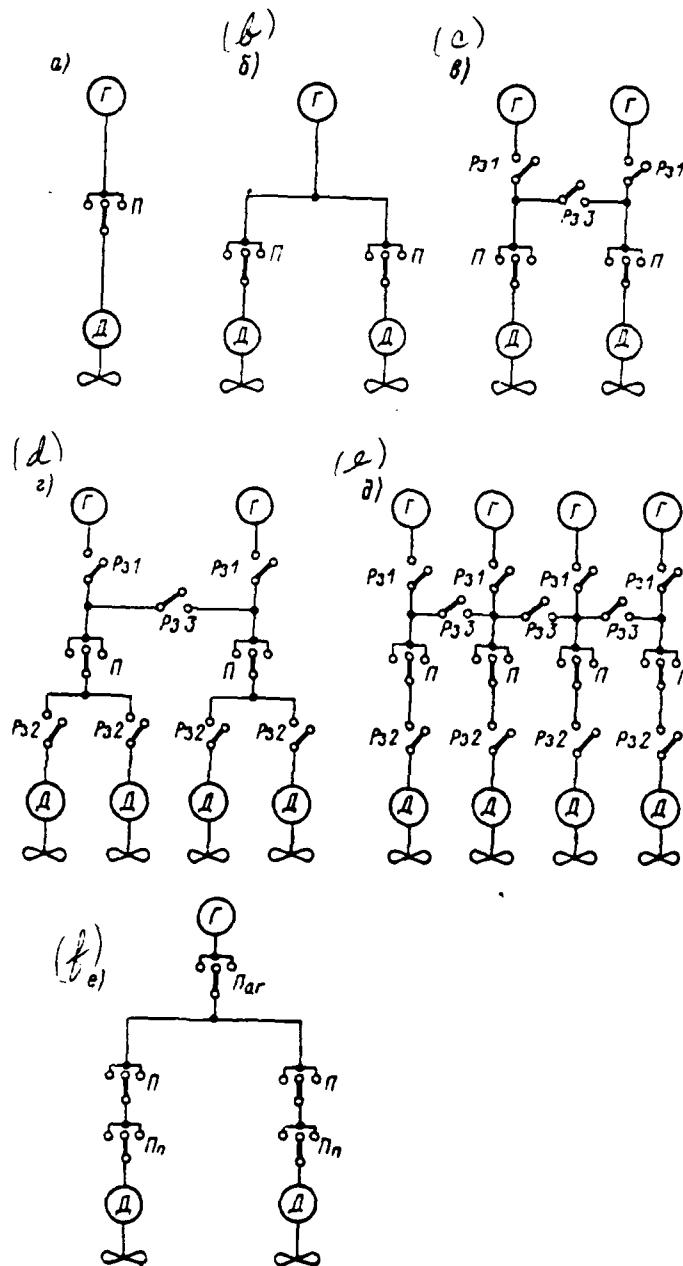


Figure 9.3. TEGU Structural Diagram: a—With one turbogenerator; b—Two-shaft with one turbogenerator; c—Two-shaft with two turbogenerators; d—With two turbogenerators feeding four GED; e—Four-shaft with four turbogenerators; f—Two-shaft with switching of a number of GED poles.

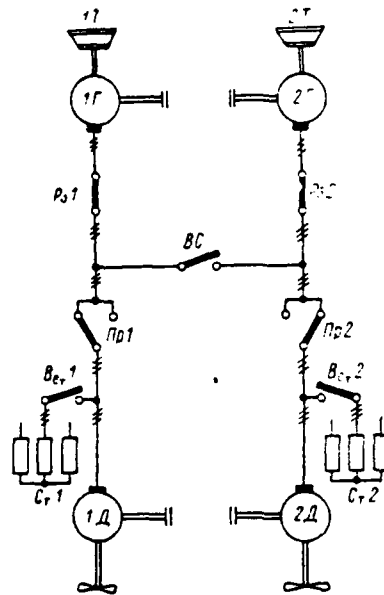


Figure 9.4. Propulsion Plant Circuit for the Turboelectric Ship "Abkhaziya."

A circuit for a TEGU for single-screw vessels with a paired main propulsion motor and with each fed from its own turbogenerator (ac GEU dual-loop circuit) also was used. Here, turbogenerator synchronization is provided via the paired propulsion motor common shaft. One advantage of such a circuit is the capability for main propulsion motor location closer to the vessel's stern thanks to a decrease in their diameter.

The 160,000 propellor shaft hp TEGU in the circuit of the four-screw high-speed "Normandy" comprises four 33,400 hp turbogenerators ( $\cos \phi = 1$  at 2,340 rpm, 6,000 V). Each normally operates its own main propulsion motor at a rotational speed of 243 rpm. The circuit also envisions the capability for one turbogenerator to run two main propulsion motors. A detailed description of the circuit and test materials concerning "Baltika" and "Abkhaziya" is found in [50].

Diesel electric propulsion plants (DEGU). The desire to realize some /442 of the major advantages of DEGU compared to direct diesel drive and the need for transmission of great power to propellor shafts given constrained power of the diesels used will lead to main current circuits in which several diesel

generators run one main propulsion motor. Several structural diagrams of this type of circuit are shown in Figure 9.5. Devices for parallel operation of diesels and remote synchronized control of main diesel rotational speeds are envisaged in DEGU as opposed to TEGU. Salient-pole synchronous generators /443 are used in DEGU due to the low (in relationship to turbines) diesel rotational speeds.

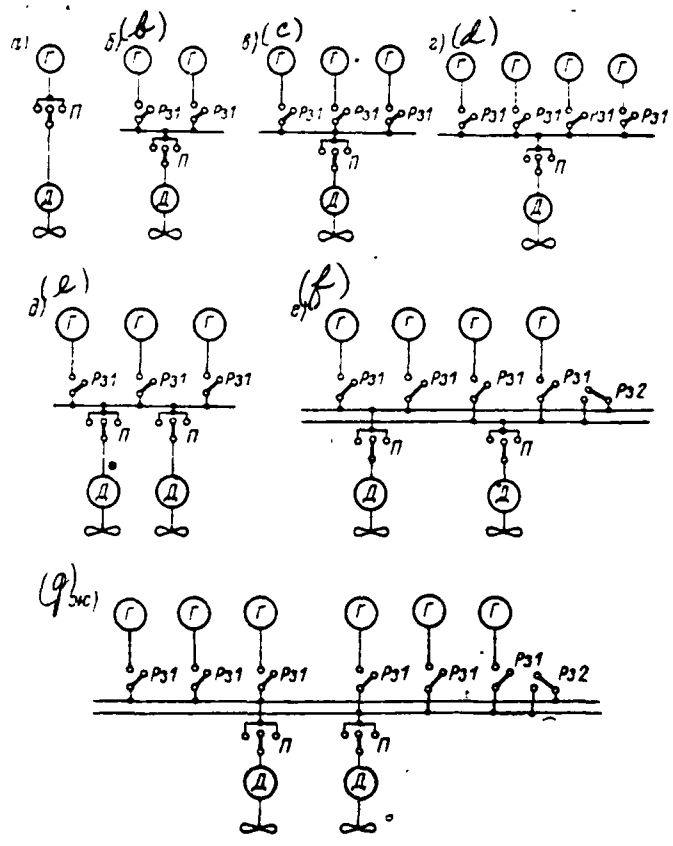


Figure 9.5. DEGU Structural Diagrams: a—Single-shaft with one diesel generator; b—Single-shaft with two diesel generators; c—Single-shaft with three diesel generators; d—Single-shaft with four diesel generators; e—Dual-shaft with an uneven number (three in this case) of diesel generators; f—Dual-shaft with four diesel generators with parallel and separate operation of both side GED; g—Dual-shaft with six generators.

A standard main current circuit of the diesel electric ship "Rossiya" is described in [50]. It envisions six main diesel generators operating two main propulsion motors. In the normal mode, the intersectionalizing switch is disconnected and the first three generators in parallel run the port GED, while the other three generators run the starboard GED.

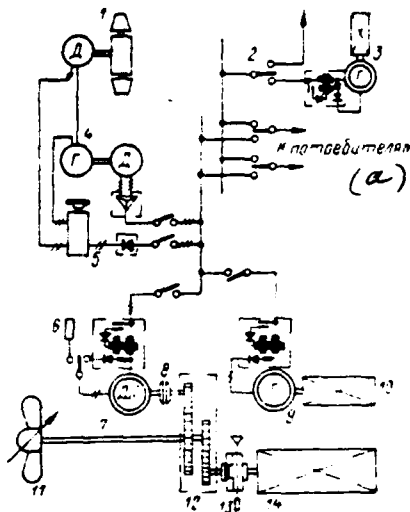


Figure 9.6. Three-Phase Current Additional Propellor Drive Circuit Aboard an "Essen"-Class Trawler. 1—Trawl winch with dc electric motor; 2—Shore-network feed switch; 3—Mooring ac diesel generator; 4—Converter for trawl winch; 5—Field system master controller and semiconductor rectifier; 6—Starting and protective resistances; 7—Compounded three-phase synchronous generator motor; 8—Hydraulic damping coupling; 9—Compounded three-phase synchronous generator with field system; 10—Additional diesel; 11—Controllable-pitch propellor; 12—Reduction gear; 13—Tooth-type coupling, which disengages during a stop; 14—Main diesel; a—To consumers.

Circuit with additional propellor ac electric drive. In many cases, it is advisable to use power from the shipboard electric power station to drive propellers (in special operating modes).

A circuit for a trawler additional ac propellor drive is shown in Figure 9.6. A three-phase alternating current diesel generator (9-10) can provide

consumers 5 with electric power via the shipboard network, as well as converter G—D (4) to drive the trawl winch or feed a synchronous propulsion motor connected to the propellor shaft via a hydraulic (or electromagnetic) coupling. At low vessel speed, the synchronous motor operates as a synchronous shaft generator and supplies the winch drive and shipboard network with electric power. The synchronous machinery is built with a self-excitation system.

### § 9.3 Excitation and Control Systems With Dynamoelectric Automation

Basic assumptions. During development of excitation systems for GEU with synchronous machinery, one should consider the requirement for three- or more fold reexcitation of generators for development of large starting torques. Data on power consumption for excitation on several operating electric ships /444 are presented in Table 9.4.

Generator and GED excitation for electric ships built prior to 1960 was provided by multimachine exciters [50]. At present, achievements in the field of compounding system and thyristor governor development make it possible to use contact-free static field systems in ac GEU.

The limited overload capability of synchronous ac main propulsion motors requires an especially reliable and continuously-operating system of protection against overloads arising during heavy seas, radical transpositions of the rudder blade, vessel circling, and so on. We will examine a schematic with amplidyne (EMU).

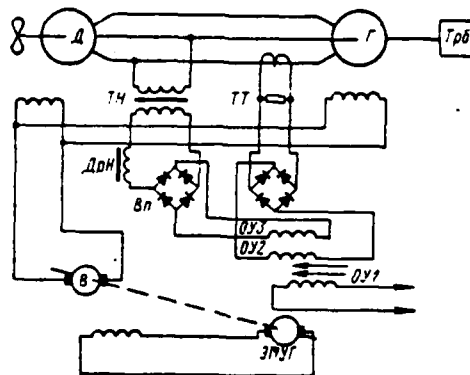


Figure 9.7. Automatic Control Circuit for an AC GEU with an Amplidyne.

In this circuit (Figure 9.7), generator and propulsion motor field windings are fed from one exciter, with a three-stage longitudinal field EMUG used in this role. The winding of amplifier OU1 is a master winding and is fed by an independent dc source. Winding OU3 is connected to voltage transformer TN secondary winding via rectifiers. Saturation choke DrN also is connected to this circuit and its reactance is comparable to the resistance of the winding OU3 circuit. Thanks to such a connection, current in winding OU3 is proportional to the voltage and inversely proportional to the frequency. This winding's mmf is opposite of winding OU1 and OU2 mmf.

Current in winding OU2, which is connected to current transformer TT secondary winding, is proportional to propulsion motor load current. Given a nominal load, winding OU2 and OU3 n. s. compensate one another and, if self-excitation winding resistance exceeds critical resistance, then master winding OU1 provides basic excitation.

An increase in load is accompanied by an increase in main circuit current and a voltage decrease under the influence of generator armature longitudinal reaction, winding OU2 current increases, and winding OU3 current decreases. This will lead to an increase in amplifier field and, consequently, propulsion generator and motor field as well. As a result, the magnitude of the tilting /446 moment increases significantly, which rules out the possibility of their dropping out of synchronization.

When the assigned voltage to frequency ratio is disrupted as a result of a voltage increase or a frequency decrease, the magnitude of current from winding OU3 increases; the increased n. s. of this winding will decrease overall flux created by all three field windings; field voltage will decrease and, accordingly, main circuit voltage also will decrease. This control system is disconnected in transient processes, when it is necessary to obtain boosted excitation.

Results from observing the load on the synchronous main propulsion motors aboard the turboelectric ship "Abkhaziya" in the event the rudder is transposed 30° to port when the vessel is underway at full speed demonstrated that the port turbogenerator current load reached an almost two-fold value ( $I = 523 \text{ A}$ ), resulting in maximum protection tripping. The overloads possible in such

(a) Наименование электроходов	(b) Мощность одного главного генератора, кВт	(c) Возбуждение одного главного генератора						(f) Кратность форсирования по мощности	(g) Мощность одного гребного электродвигателя, кВт	(h) Возбуждение одного гребного электродвигателя		
		(d) нормальное			(e) форсированное					потребляемая мощность		(k) напряжение, В
		(i) кВт	(j) % от мощности генератора	(k) напряжение возбуждения, В	(l) кВт	(m) % от мощности гл. генератора	(n) напряжение, В			(o) кВт	(p) % от мощности ГЭД	
(m) Турбоэлектроход «Абхазия»	3 200	22	6,69	100	137,5	4,34	250	6,25	2 950	75	2,54	230
(n) Турбоэлектроход «Балтика»	4 500	20	0,445	210	83	1,85	210	4,15	4 350	26,6	0,6	220
(o) Дизель-электроход «Россия»	2 160	17,5	0,81	110	75	3,25	300	4,0	5 580	100	1,82	130
(p) Танкер deadweight 13 000 т	5 400	27	0,5	82	108	2,00	164	4,0	4 850	—	—	—
(q) Турбоэлектроход «Нормандия»	33 400	150	0,45	150	660	19,90	330	4,4	33 000	150	0,45	150
(r) Пассажирское судно «Шарнхорст»	1 150	10	0,82	90	60	4,92	230	6,0	4 200	45	0,92	230
(s) Дизель-электроход «Штейрмарк»	2 600	15	0,58	90	110	4,23	255	7,3	4 600	62	1,35	220

Table 9.4. Power Consumed for Excitation in AC GEU Nominal and Transient Modes.

a—Electric ship name; b—Power of one main generator, kW; c—Excitation of one main generator; d—Normal; e—Boosted; f—Power boost factor; g—Power of one main propulsion motor, kW; h—Excitation of one main propulsion motor; i—kW; j—% of generator power; k—Field voltage, V; l—% of GED power; m—Turboelectric ship "Abkhaziya"; n—Turboelectric ship "Baltika"; o—Diesel electric ship "Rossiya"; p—13,000 ton deadweight tanker; q—Turboelectric ship "Normandy"; r—Passenger vessel "Scharnhorst"; s—Diesel electric ship "Steermark".

situations, given this turboelectric ship's extant circuit, made it necessary to constrain the rudder transposition angle, which constrains the vessel's maneuvering qualities to a significant degree.

Two methods of preventing synchronized machinery against going out of synchronization exist at the present time.

The first consists of the fact that machinery is designed for the maximum amount of anticipated overload (usually the torque reserve is accepted as equalling 25% of the nominal value).

The second method involves use of high-speed, highly-sensitive amplidynes instead of conventional exciters or other high-speed systems.

In the circuits of electrical propulsion plants containing automated electrical machinery, excitation of main generators and motors is boosted automatically during instantaneous overloads (when only one machine has regulated excitation, the boosting is doubled) and, in this manner, the requisite torque reserve is created.

The capability for boosting in the event of an overload makes it possible to keep the torque reserve to a minimum. As calculations show, in this event the weight, and consequently, the cost of propulsion generators and motors can be decreased 20-30%.

Automatic torque control. Satisfactory results in controlling a vessel during maneuvering are achieved through automatic control of the generator excitation system, which prevents possible diesel stoppage. Generator field current must be maintained at the maximum level, without the danger of reducing diesel rotational speed below the nominal value. The corresponding GEU control circuit comprising two generators G1 and G2 running main propulsion motor D is depicted in Figure 9.8a.

Small dc controlling generator G with permanent magnets is placed in rotation by three-phase electric induction motor AD fed from main generator G2 via transformer Tr. Generator voltage is proportional to main circuit frequency and, correspondingly, to diesel rotational speed. The same electric induction /447 motor places in rotation controlled standard exciter VVG with shunt and independent field windings.

Resistance in the self-excitation circuit acts so that voltage in generator VG equals zero, when the controlling field equals zero, but radically /448 increases when a slight current flows through the independent field winding.

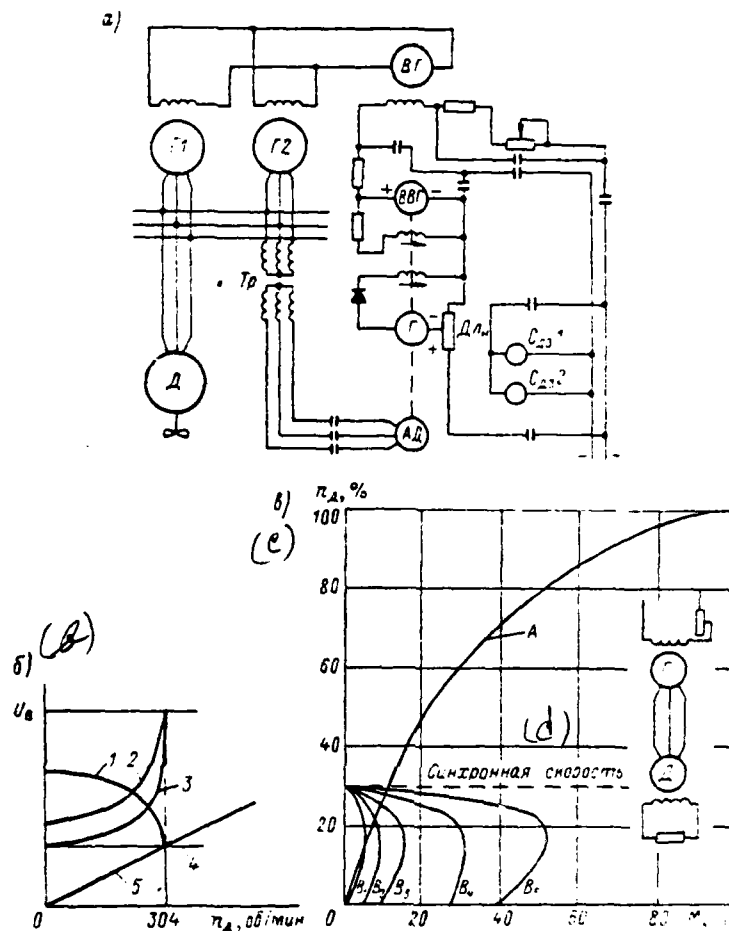


Figure 9.8. GEU Circuit and Characteristics: a—Schematic; b—Automatic control characteristics; c—GED mechanical characteristics at varied generator field values; d—Synchronized speed; 1, 2—Characteristics of the controlled exciter and controlling generator with permanent magnets, respectively; 3-5—Relationships, respectively, of the voltage at the control bus bars, generator field, and exciter field to rotational speed.  $\Delta_{\text{н}}$  is a voltage divider;  $B_1-B_5$  are the mechanical characteristics at varied generator fields; A is the propellor characteristic in the idling mode:  $C_{23}^1, C_{23}^2$  are diesel governor solenoids.

Controlling generator G will close to the portion of the resistance to which standard voltage of opposite polarity is fed. The difference in the voltage of controlling G and standard VVG generators is fed to the controlled generator field.

The drop of voltage in the resistance from an external source is selected as being equal to the voltage of the controlling generator when the magnitude of its speed (and, consequently, diesel speed as well) equals approximately 30% of nominal. With an increase in diesel speed, controlling generator voltage will be greater than the voltage drop in the resistance from a constant source, but current will not flow through the controlled generator's field winding since the rectifier blocks its path. If diesel revolutions drop below 30% of the nominal value as a result of torque surge in excess of the tolerable value, then the voltage drop in the resistance will become greater than the controlling generator's voltage and current will flow through the field winding. The controlling generator's voltage (from an independent source) will increase sharply and its field current and, consequently, that of the main generators will drop. This prevents the diesels from stopping since, in such a circuit, no unsafe torque will be applied to them.

Several curves demonstrating the relative change in field and control voltage during a decrease in diesel rotational speed are shown in Figure 9.8b.

Regulation of the torque is required only when the GED operates as a synchronous motor. Therefore, when the starter leaves the "Underway" position, the governor is disconnected. VVG is disconnected by a separate switch. Diesel governor solenoids  $C_{23}^1$  and  $C_{23}^2$ , which provide for an increase in their torques during maneuvering operations, also are disconnected by their own switch. Here, the governors begin to operate normally after the starter is placed in the underway position.

Operation in hyposynchronous rotational speeds. Minimum screw rotational speed during synchronous operation of a main propulsion motor is constrained by the minimally stable rotational speed of the diesel, equalling approximately 30% of nominal. Aboard a vessel with a nominal speed of 20 knots, the minimum stable speed of a diesel corresponds to a vessel speed of 6 knots. Sometimes, this turns out to be too great for certain classes of ships and the need arises to obtain a less stable speed. This is achieved by running the GED as an induction motor with a starting cage at a speed below synchronous. Its rotational speed changes with a change in generator field below the nominal value, while the GED field winding is connected up to starting (discharging) resistance.

The curves of motor torque for several generator field values are depicted in Figure 9.8c. The points of intersection of these curves with the curve of the propellor torque provide the values of the assigned speeds of movement. /449 The generator field must be considerably lower than the normal magnitude for the underway mode to rule out propulsion motor and generator overheating as a result of great losses. Therefore, operation at speed values ranging from minimal stable synchronous to 70% of its value is impossible. The safe threshold speed must fall in the range of 50% of minimum synchronized speed or 15% of full speed. It is necessary, to provide the capability to operate at such a speed, that the propulsion motor starter have an additional position between "Stop" and "Start" at which the corresponding resistance will be introduced into the generator exciter field circuit. It is sufficient for satisfactory GEU operation in such a mode that 50% of the generators run the movement bus bars.

#### § 9.4 Prospective Alternating Current Electric Propulsion Systems

Review of alternating current GEU control systems. Essentially, all types of ac electric motors are used in ac GEU: induction with a phased rotor; shorted induction with deep-bar slot and double squirrel-cage; induction with switching of the number of pole pairs; synchronous-induction; high-rpm shorted induction running the screw via a step-down reduction gear; and, finally, for the majority of electric ships — synchronous.

Systems with special-use shorted induction motors (deep-bar slot, double squirrel-cage), along with high maneuvering qualities, control simplicity, and great reliability, have the worst economic indicators.

Systems with induction motors with a phased rotor, although they also possess high maneuvering qualities (start, stop, reverse), require a complex control system, are less reliable than systems with shorted motors, and are characterized as not being economical.

Economic multispeed GED with switching of the number of pole pairs also are used in ac GEU. However, rotational speed regulation using this method has several drawbacks. The first is that a staged method of switching does

not provide continuous shipboard GEU regulation. A second drawback of multispeed AD is increased weight and cost compared to conventional induction motors of comparable power.

Systems with synchronous motors have the best economic, weight, and size characteristics. However, their maneuvering qualities are not as good as those of induction systems.

Special methods of regulating main propulsion motor rotational speed are /450 being used at the present time to obtain optimal ship's powerplant indicators, taking the aforementioned special features into consideration.

There are different systems for regulating ac motor rotational speed. They can be divided into two main categories. The first includes controlled drive systems with losses of slip energy (rheostat regulation, drive with a rotating stator, electromagnetic slip clutch, and others). The second includes controlled drive systems in which slip energy is realized (tandem connection of induction motors).

The special features of certain prospective ac controlled propellor electric drive systems are examined in the next section.

#### § 9.5 Electrical Propulsion Plant Rectifier-Cascade Systems

Basic assumptions. A cascade system provides:

- 1) capability of using a fixed-pitch screw, which makes it possible smoothly to regulate vessel speed with installation of a VRSh [controllable-pitch propellor];
- 2) full use of main primary motors running electric propulsion bus bars and power takeoff bus bars thanks to paired generators;
- 3) economic GED rotational speed regulation since, with this system, slip energy is realized.

Slip energy can be realized in two ways when induction motors are connected in tandem: either by direct supply of this energy to the network or by preliminary conversion of this energy to mechanical energy with subsequent transmission to the main motor shaft. Two types of cascade connections, electrical and

electromechanical, are used to differentiate depending on the method of slip energy realization.

Electrical cascades. In electrical cascades, slip power, eliminating losses in intermediate system elements, after appropriate conversion returns to the feed network. The circuit depicted in Figure 9.9 will serve as an example.

Regulation of the rotational speed of induction motor AD in such a system occurs by means of a change in machine MP field current. Cascade torque is determined only by AD torque, while MP emf will depend on field since the MP motor rotates at a fixed speed. Thus, the AD electrical cascade torque is expressed by formula

$$M_{a,x} = \frac{P_{1,2}}{\omega_0} = \frac{m_2 E_{2k,\phi} I_2 \cos \varphi_2}{\omega_0} \approx \frac{\left( E_{d0} - \frac{m X_A}{2\pi} I_d \right) I_d}{\omega_0}, \quad (9.6)$$

where  $P_{1,2}$  is AD power;  $E_{2k,\phi}$  is rotor phase voltage given its open circuit /451 and slip  $s = 1$ ;  $I_d$  is average rectified current;  $X_A$  is AD phase induction resistance supplied to the rotor circuit where  $s = 1$ . The power consumed by machine MP

$$P_{m,n} = \frac{E_{m,n} E_{d0} (s - s_0)}{R_s}. \quad (9.7)$$

Here,  $E_{m,n}$  is MP motor emf;  $E_{d0}$  is average voltage at bridge output where the dc circuit is open ( $s = 1$ );  $s_0$  is AD slip corresponding to the speed of cascade ideal idling;  $R_s$  is equivalent resistance:

$$R_s = \frac{m X_A}{2\pi} s + 2r_A + r_n, \quad (9.8)$$

where  $r_n$  is machine MP armature resistance;  $r_A$  is AD phase active resistance supplied to the rotor circuit where  $s = 1$ .

MP installed capacity is determined by the greatest voltage at the rotor rings supplied to the dc circuit and by the greatest current in the rectified circuit, which will depend on the moment of resistance.

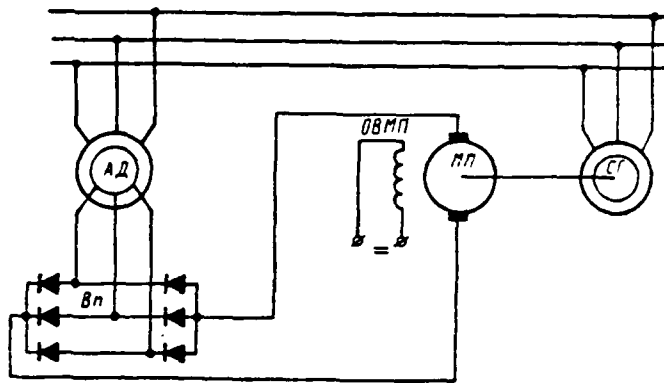


Figure 9.9. Schematic of an Asynchronous Rectifier-Machine Electric Cascade.

Given constant moment of resistance, the lowest AD speed corresponds to the greatest voltage in the rotor circuit and the greatest load current equals the nominal. MP minimum voltage corresponds to the greatest load current for the screw load.

The operating conditions of the elements making up the AD rotor circuit in the event of screw load are much easier than in the case of a fixed load. This circumstance can be used for a decrease in rectifier bridge and machine MP installed capacity given a screw load, which is characterized by a sharp decrease in shaft torque with a decrease in rotational speed. Here, there is a reduction in rectified circuit current and an increase in rectified voltage. And, on the contrary, rectified current increases with a rise in drive speed and voltage decreases.

Thus, there is the capability to use two MP machines rather than one, but at half the power. Here, when an AD develops great torque, both MP machines are connected in parallel; with a decrease in torque and, consequently, speed, a switch is made from parallel to series connection.

We will determine the powers of the elements of this cascade circuit for a regulation range of  $\omega_n - 0,5\omega_n$ .

When one MP machine is used, its installed capacity equals 50% of the power

of the drive since power is determined by production of the greatest voltage (equalling one-half of nominal) to nominal current.

When two MP machines are used, at minimum rotational speed, when the machines are connected in parallel, each receives voltage equalling  $0,25U_{\text{ном}}$  and load current  $0,25I_{\text{ном}}$ .

Upon achieving rotational speed equalling  $0,75\omega_0$ , when the voltage will be  $0,25U_{\text{ном}}$ , switching of the machines from parallel to series connection will occur; the load current for this speed will equal  $\approx 0,56I_{\text{ном}}$ . When speed subsequently is increased, the current in the rectified circuit increases, while voltage decreases. From this, the power of each MP machine equals

$$P_1 = P_2 = 0,56 \cdot 0,25P_{\text{ном}} = 0,14 \cdot P_{\text{ном}}$$

Consequently, two MP machines with a power of  $0,14 P_{\text{ном}}$  each can be used instead of one with a power of  $0,5P_{\text{ном}}$  in the GEU screw drive circuit. Given less MP machine power, two higher-speed MP can be selected. But, an SG also is selected for higher speed. The latter factor noticeably reduces their dimensions.

A shortcoming of this circuit is inclusion in it of additional switching gear, besides the fact that use of a large amount of machinery complicates the entire plant.

The power factor of the AD in a cascade is low and decreases when speed drops. This can be considered by means of a slight increase in SG power and compensate for the reactive component of the power consumed by the AD to the requisite magnitude.

The desire to replace rotating electrical machines, which realize the slip energy, in the rectifier-machine cascade examined above by means of a static converter led to creation of an asynchronous rectifier cascade. An example of such a circuit is shown in Figure 9.10.

An asynchronous rectifier cascade comprises induction motor AD, uncontrolled

converter  $V_p$ , and an inverter consisting of controlled rectifiers  $B_{cr}$  and transformer  $Tr$ .

Converter  $V_p$  is for rectification of rotor current having slip frequency. /453 Rectified current with the aid of the inverter is converted into alternating current with network frequency. Choke  $D_r$  is cut in to smooth it.

The principle of operation of an asynchronous rectified cascade can be represented in the following way. During operation in the motor mode below synchronized speed, AD rotor current is rectified by rectifier  $V_p$ . Additional emf, average rectified inverter voltage (inverter counter emf), is introduced into the rectified current circuit. Rotor rectified current  $E_{dPHS}$  must compensate for inverter counter emf  $E_{di}$ , the voltage drop in the rotor loop active resistances, as well as the voltage drop caused by the rectifier commutation process. Then, one can write

$$E_{dPHS} = E_{di} + \Delta U + I_d R_s \quad (9.9)$$

or

$$I_d = \frac{E_{dPHS} - E_{di} - \Delta U}{R_s}, \quad (9.10)$$

where  $E_{dPHS}$  is rectified voltage at the rings, given an immobile rotor;  $\Delta U$  is voltage drop in the rectifiers;  $I_d$  is rotor rectified current;  $R_s$  is equivalent active resistance of the rotor circuit and rectifier commutation circuit.

Torque developed by an induction motor is proportional to rotor rectified current in accordance with expression

$$M = C\Phi I_2 \cos \psi_s, \quad (9.11)$$

where  $\psi_s$  is the angle between vectors  $I_2$  and rotor  $E_2$  emf;  $\Phi$  is magnetic flux in the motor air gap.

Consequently, regulation of rotor current through changing counter emf magnitudes ( $E_{di}$  in this case) makes it possible to regulate torque and rotational

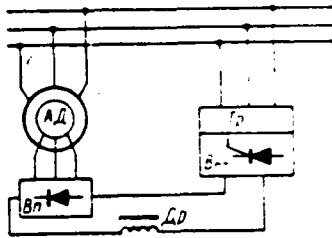


Figure 9.10. Schematic of an Asynchronous Rectified Cascade with Intermediate DC Circuit.

speed magnitude. Inverter counter emf magnitude changes by means of a change in the angle of opening of controlled rectifiers  $B_{cr}$ .

If inverter variable counter emf equals rotor rectified voltage, then the current in the rotor circuit and the torque developed by the motor will equal zero. A decrease in inverter counter emf is accompanied by an increase in the current in the rotor circuit, motor torque increases, and its speed begins to increase. Since an increase in speed is accompanied by a decrease in rotor rectified voltage  $E_{dphs}$ , motor acceleration will occur until such time as there no longer is equality of voltages in the rotor loop. Rotor current and torque increase with an increase in inverter counter emf and motor speed decreases. Rotor rectified voltage increases due to the speed decrease. Rotor current /454 and motor torque increase until the motor torque of the drive equals the static torque of resistance. Here, the motor converts to operation in the established mode with a new speed value, to which equality (9.6) corresponds. Given constancy of the controlling action and a change of load torque to the drive shaft, the transient process flows in a manner analogous to that described.

So, for example, motor speed increases with an increase in motor shaft torque. In this connection, rotor emf increases and, consequently, rectified current and torque increase. Here, the reduction in speed is insignificant and continues until motor torque equals moment of resistance.

The principle of operation of a rectifier-machine electromechanical cascade is analogous to that examined (see Figure 9.9). Here, additional emf is created

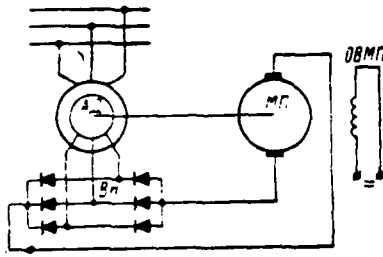


Figure 9.11. Schematic of a Rectifier-Machine Electromechanical Cascade.

by the MP machine, which rotates at a constant speed since SG linked with the feed network is located on its shaft. A change in the magnitude of MP counter emf is accomplished by regulation of its field current.

The equilibrium equation of the voltages in the motor rotor circuit has the form

$$E_{\text{дРHS}} = E_{\text{н}} + \Delta U + I_{\text{а}}R_{\text{с}}, \quad (9.12)$$

where  $E_{\text{н}}$  is MP emf.

Electromechanical cascades. In such cascades, slip energy, eliminating losses, after appropriate conversion returns to the induction motor shaft. An electromechanical cascade (Figure 9.11) comprises induction motor AD with slip-rings and dc machine MP located on the same shaft. The MP armature circuit is fed by induction motor rotor rectified voltage via uncontrolled rectifiers  $V_p$ .

Both machines operate in the motor mode when speed is less than synchronous. Consequently, cascade drive torque  $M_{\text{к}}$  is the sum of the torques developed by the induction motor and dc machine:

$$M_{\text{к}} = M_{\text{а.д}} + M_{\text{м.п.}} \quad (9.13)$$

Torque developed by both machines is proportional to rotor rectified current  $I_{\text{д}}$ , whose regulation is accomplished by a change in the magnitude of dc machine armature counter emf.

AD electromagnetic moment is determined by expression (9.6), while the /455 machine MP electromagnetic moment determined by the ratio

$$M_{m.p.} = C_M' \Phi_{m.p.} = C_M I_d, \quad (9.14)$$

where

$$C_M = C_M' \Phi_{m.p.} = \frac{E_{m.p.}}{\omega_{m.p.}}$$

If one considers that, in an electromechanical cascade

$$\omega_{m.p.} = \omega_0 (1 - s), \quad (9.15)$$

then, having substituted expression (9.6) and (9.14) in (9.13), considering (9.15), we will find

$$M_k = \frac{I_d}{\omega_0} \left[ E_{d0} - C_M \omega_0 - \frac{mN_2}{2\pi} I_d \right]. \quad (9.16)$$

Equality (9.12) applies to an electromechanical cascade, just as it does to an electrical cascade. If counter emf  $E_n$  becomes equal to rotor rectified voltage  $E_{dnhS}$ , then the current in the rotor circuit and drive torques will equal zero, i. e., a specific idling speed  $E_n$  will correspond to each value  $\omega_0$ .

When the load is connected, drive speed begins to drop, rectified voltage to increase, and MP counter emf to decrease. Current in the rotor circuit and the torque of each of the two machines will begin to increase, resulting in motor deceleration occurring until moment of resistance and torque developed by the drive are commensurate. Speed is regulated by changing the current in the machine MP independent field winding.

Drive speed will increase with a decrease in field current. If field current is removed completely, then the additional emf in the rotor circuit will become equal to zero and drive speed will turn out to be close to nominal. In this event, torque is created only by the induction motor. Due to the increase in

field flux, drive speed will decrease, while the moment developed by the dc machine will increase. The induction motor here will be unloaded and consume less power from the network. This determines the basic special feature of an electromechanical cascade, to wit: the power the induction motor consumes from the network (if one disregards losses in the machines) is proportional to drive torque and assigned rotational speed, while, at the same time, this power for all other systems is proportional to the synchronized rotational speed.

As can be seen from analysis of the operation of an electromechanical rectifier-machine cascade, during a very smooth change in propulsion AD rotational speed, the motor's range of regulation does not exceed 2 : 1 and is limited by the dimensions of the MP machine. More intense regulation, in the 10 : 1 range for instance, requires an MP overall power larger by a factor of 9 than propulsion AD power.

The principle of operation of cascade circuits in various modes is easy to explain using energy diagrams, which are determined by drive operating mode /456 and will not depend on the cascade electrical connection circuit.

A diagram of the distribution of power flows (energy) as a rectified cascade operates in the motor mode with a speed below synchronized is shown in Figure 9.12. Characteristic conditions determining this mode are as follows: in the stator circuit, the flow of energy runs from the network to the motor, while it is from the motor to the network in the rotor circuit. Relative to the rectified cascade circuit (see Figure 9.10), rectifiers  $V_p$  operate in the rectified mode (and can be uncontrolled), while rectifiers  $B_{cr}$  operate in the inverter mode.

Power (energy) consumed by a motor from the network,  $P_{dopp}$ , with the exception of stator losses  $\Delta P_{stator}$ , is transmitted to the motor rotor as electromagnetic power  $P_{em}$ .

It is known that, in the motor mode, an induction motor operates simultaneously as a motor and as a transformer. Given an immobile rotor  $s = 1$ , all electromagnetic power is transformed to the rotor in the form of electric power and consumed in the motor's secondary circuit. When the motor operates with minor slips ( $s \ll 1$ ) almost all electromagnetic power is transmitted to the rotor in the

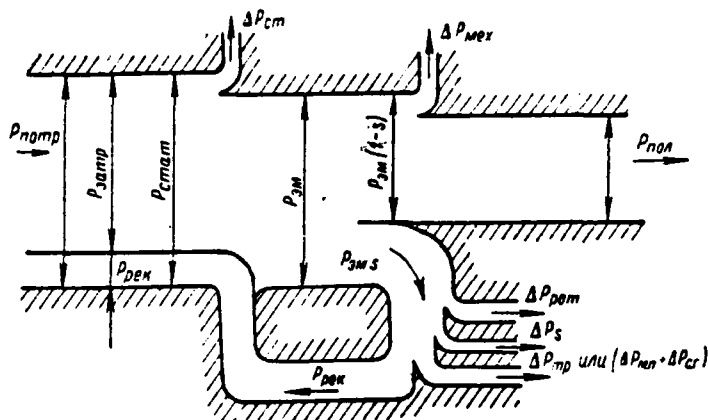


Figure 9.12. Energy Diagram of Asynchronous Rectified and Rectifier-Machine Cascades.

form of mechanical power and is used for useful work. When the motor operates with slip  $0 < s < 1$ , a portion of the power  $P_{зм} s$  (so-called slip power) is transformed to the rotor and consumed in its circuit. Another part  $P_{зм} (1 - s)$  is expended on mechanical work. Considering that an induction motor always consumes from the network power proportional to synchronous rotational speed, and disregarding losses, in the stator and additional losses, it is possible to write

$$P_{нотр} = P_{зм} = M \omega_0. \quad (9.17)$$

The mechanical power to the motor shaft is proportional to drive speed: /457

$$P_{мех} = M \omega. \quad (9.18)$$

The difference between consumed and supplied useful power is the slip power, which must be used up in the rotor circuit:

$$P_s = P_{нотр} - P_{мех} = M (\omega_0 - \omega) = P_{зм} s. \quad (9.19)$$

In the rectified cascade operating mode being examined, slip power, with the exception of losses, in rotor  $\Delta P_{рот}$ , in the rectifiers  $\Delta P_s$ , and in the

transformer  $\Delta P_{TP}$ , is returned to the network (recuperated):

$$P_{pek} = P_{sm} s - (\Delta P_{rot} + \Delta P_u + \Delta P_{TP}). \quad (9.20)$$

Thus, when operating in a rectified cascade circuit, an induction motor consumes from the network more energy than is required to complete useful work  $P_{notp}$ , and the remainder is returned to the network.

Slip energy recuperation occurs in the following way. Rotor ac electrical energy is converted by rectifiers  $V_p$  (see Figure 9.10) into ac energy, which then, with the aid of rectifiers  $B_{cr}$  operating in the inverter mode, is converted into ac energy with a frequency of 50 Hz. This energy via a transformer is returned to the feed network. Power consumed by the drive will be less than that consumed by the AD, by value  $P_{pek}$ , i. e.

$$P_{zstp} = P_{notp} - P_{pek}. \quad (9.21)$$

Thanks to the aforementioned property of a rectified cascade, the efficiency of an asynchronous motor drive during operation at reduced rotational speeds is not reduced materially.

Control of a GEU with an electrical rectified cascade. A main propulsion motor is started by increasing voltage at the stator from 0 to  $U_{low}$ . When magnitude  $U = 0.31U_{nom}$  is reached, the transformer group rectifier control angle increases from 15 to 90° simultaneously with the increase in voltage. Due to GED acceleration, slip power supplied to the network decreases and, finally, at a speed close to synchronous, it suffices only for compensation of losses in the rotor circuit and converters. Its rotor shorts out, the converter is disconnected, and the motor operates in its natural characteristic for the purpose of better use of the motor at low slips.

During a reduction in GED turns, the process repeats itself in reverse order, i. e., the rotor circuit is formed, the jumper shorting out the rotor is removed, and, during a simultaneous voltage and control angle decrease, GED speed decreases with recuperation of slip energy.

A GED is reversed by means of a reduction of voltage at the motor stator to zero (with a simultaneous decrease in control angle), with a subsequent /458 switch of motor phase and, following this, by a repeat of its acceleration but in the opposite direction during a smooth change in voltage and control angle.

The dynamic braking mode is used to stop the GED quickly. This mode involves disconnecting the stator winding from the three-phase ac network and connecting it to a dc source. Direct current passing through stator windings creates magnetic flux immobile in space.

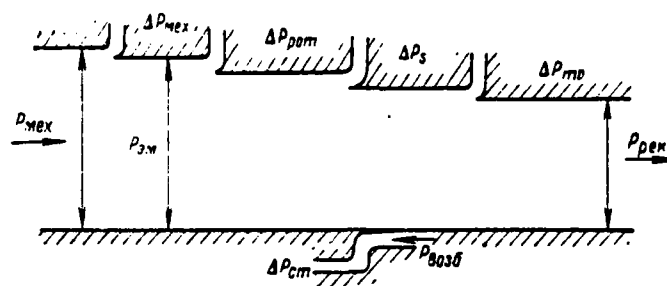


Figure 9.13. Energy Diagram of an Asynchronous Cascade in the Dynamic Braking Mode.

Thus, in this mode, an induction motor operates as a nonsalient-pole synchronous generator excited by direct current. Power  $P_{mex}$ , consumed by the motor (Figure 9.13) from the rotor is transformed by it into ac power  $P_{3\phi}$ , whose frequency will depend on speed. This power then (due to deduction of the power of losses  $\Delta P_{rot}$ ,  $\Delta P_s$ ,  $\Delta P_{rd}$ ) is transformed by the rectifier into power  $P_{pex}$  and supplied to the network. Power consumed for field,  $P_{3\phi}$ , is lost in the stator windings.

Losses of all the braking energy in resistances is a normal shortcoming of induction motor dynamic braking. The rectified cascade circuit eliminates this drawback since here the dynamic braking is recuperative, i. e., all mechanical energy, with the exception of the losses in the cascade, is supplied to the feed network.

## § 9.6 Alternating Current Electrical Propulsion Plants with Static Frequency Converters

General characteristics and prospective development. Use of static frequency converters based on silicon semiconductor instruments makes it possible to free oneself from the shortcomings of dynamoelectric converters and opens wider /459 prospectives for use of frequency control on ships. Therefore, we will dwell in more detail on the overall properties of semiconductor frequency converters and the special features of their use for frequency control of electric propellor drives [7, 8].

Two types of semiconductor frequency converters are used in frequency-controlled electric propellor drives to feed electric induction motors: those with an intermediate dc link and those that have a direct link. Both can be made of completely controlled rectifiers (transistors, technetrons) and of incompletely controlled rectifiers (thyristors). A completely controlled rectifier opens when a control signal is supplied to it and closes when the signal is removed. An incompletely controlled rectifier also opens when a control signal is fed to it, but its closing requires more than just removal of the control signal. It requires that the current passing through the rectifier decrease essentially to zero as well.

The main advantages of static converters in comparison to dynamoelectric converters are:

- greater capabilities for weight and size reductions;
- higher efficiency and lower idling losses through the entire range of loads;
- greater capabilities for noise level reduction;
- essentially instantaneous readiness for operation;
- less lag, greater gains, and precision in automatic or programmed control;
- great capabilities for increased reliability;
- greater convenience in placement, no requirement for attachment on the foundation frame;
- insignificant starting currents, which insure starting of the converters without feed network voltage dips.

It also should be noted that silicon rectifiers also have some disadvantages, the main ones being:

- sensitivity to overloads and increased voltage;
- relationship of several characteristics to temperature;
- distortion in the form of the feed voltage curve;
- significant pulsations of rectified equipment output voltage and the need because of this for ripple filters.

However, proper selection of the cooling system and protection against overcurrents insures highly reliable semiconductor devices. As far as the relationships of some characteristics to the temperature, as well as the their influence on the form of the feed voltage curve, are concerned, these shortcomings can be considered during the design and proper selection of converter circuits.

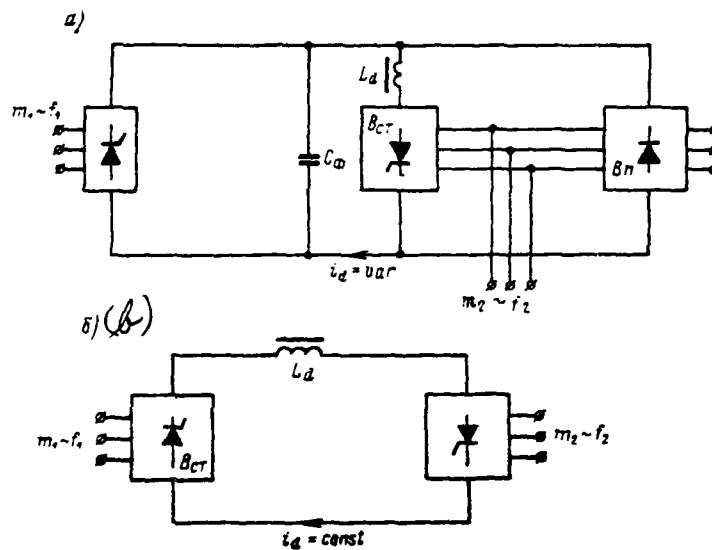


Figure 9.14. Frequency Converter with a DC Link: a—PCH [frequency converter] circuit; b—Inverter schematic;  $m_1$ ,  $m_2$ ,  $f_1$ ,  $f_2$  are number of phases and frequencies at inverter input and output, respectively;  $i_d$  is smoothing input current;  $C_0$  is a capacitor;  $L_d$  is a smoothing choke (reactor).

Frequency converters with a direct current link. Circuits for frequency converters with a dc link (Figure 9.14a) are based upon dual conversion of energy: initially, ac is transformed with the aid of rectifiers into dc, and then the dc is transformed into ac with a controlled frequency by means of an inverter (Figure 9.14b). /460

A rectifier in this type of frequency converter can comprise uncontrolled  $V_p$  or controlled  $B_{cr}$  rectifiers based on one of the known circuits. The one most-often used is a three-phase bridge rectifier, with a more complicated multiphase rectification circuit used for powerful converters. The determinant in these converters are  $B_{cr}$  rectifiers. The following three generalized types are found, depending on the manner in which the inverter commutating capacitors are connected:

- 1) parallel inverter, in which the commutating capacitors are connected parallel to the load (Figure 9.15a);
- 2) series capacitor, with series connection of capacitors (Figure 9.15b);
- 3) series-parallel inverter (Figure 9.15c).

Using circuitry of such invertors operating with fully smoothed input current  $i_d = \text{const}$  will lead to the requirement to connect smoothing choke  $L_d$  with high induction resistance between the rectifier and inverter.

Different variations of thyristor voltage inverters are the most applicable for electric propellor drive frequency control. Several of the many self-excited thyristor inverters are shown in Figure 9.16. It is necessary in induction /461 motor frequency control to regulate voltage at the inverter output simultaneously with a frequency change. The laws of voltage regulation are determined by electric drive requirements and those levied by the operating mechanism.

Methods of regulating voltage at the output to a significant degree determine the inverter circuit and special operating features.

The main ones are:

- regulation at the input;
- latitudinal regulation;
- latitudinal-pulse regulation (it is possible in those cases where the /463

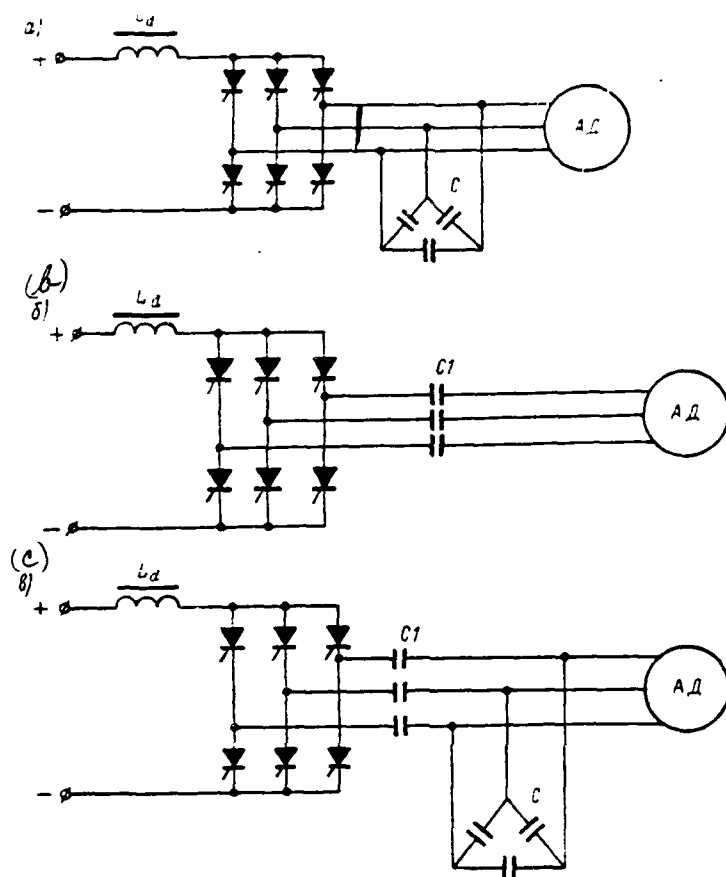


Figure 9.15. Inverter Schematic: a—Parallel; b—Series; c—Series-parallel; C, C1 are capacitors connected in a triangle and a star, respectively.

circuit permits rectifier engage and blanking at any moment in time;

— regulation with the aid of two (or more) inverters with geometrical adding of output voltages.

Several requirements are levied on inverters used in a shipboard ac electric drive frequency-controlled system, to wit:

- operating reliability under given shipboard electric drive conditions;
- provision for the requisite voltage regulation law when frequency changes;
- possible operations when the load power factor changes within wide limits;
- provision for a given motor frequency and rotational speed regulation range;

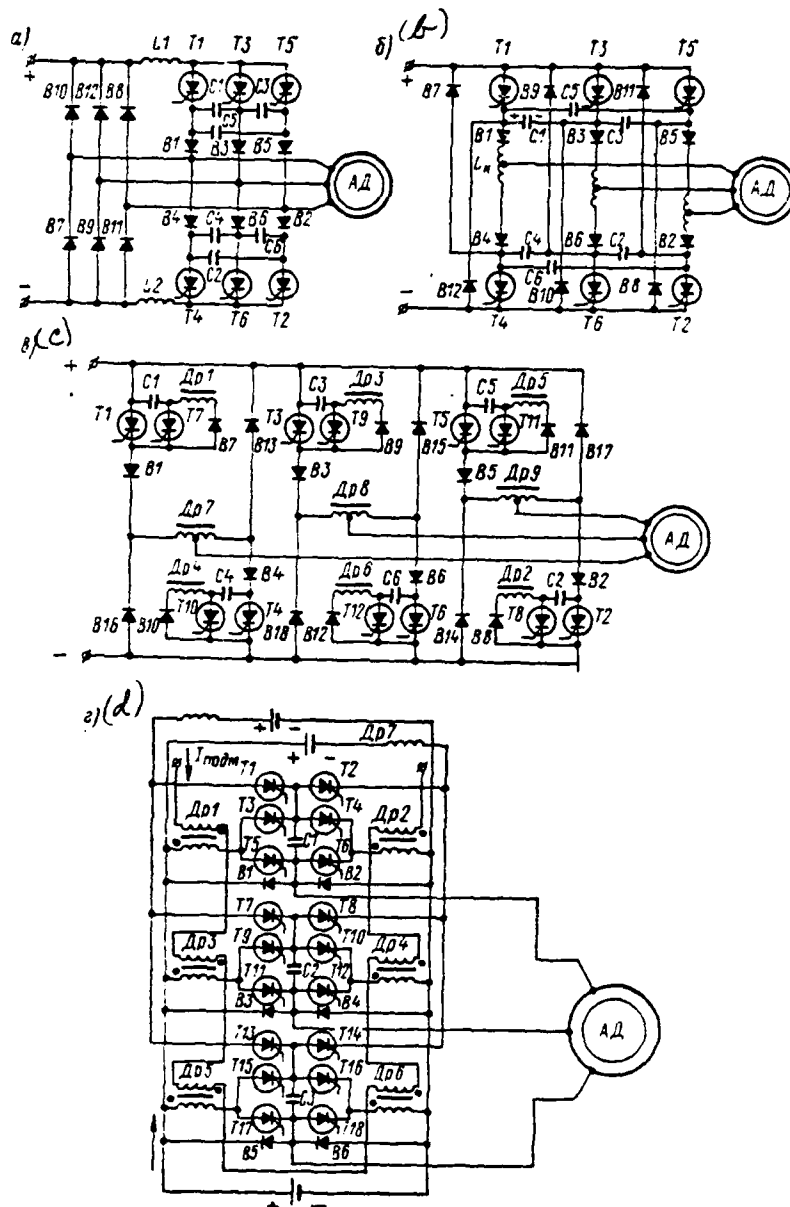


Figure 9.16. Self-Excited Three-Phase Thyristor Inverter Circuits:  
 a—V. F. Shukalov circuit; b—V. Ye. Skorovorov circuit; c—With two-stage  
 commutation; d—With independent commutation.

- provision for requisite precision in regulation of individual values  
 (rotational speed, current, voltage, and so on);
- provision for electric drive braking modes of operation;

- acceptable harmonic composition of voltage and current curves during regulation;
- light weight and small dimensions;
- simplicity in servicing and maintenance, good technical and economic indicators (efficiency,  $\cos \varphi$ , cost).

Thyristor inverter control circuit selection must consider the principles of construction of the inverter power circuit and required electric drive operating modes (availability of reverse, braking, and so forth). Also, control circuits must also satisfy several general requirements, such as:

- provision for a series of rectangular pulses of a given sequence, width, and power;
- capability of regulating control pulse frequency within given limits;
- control pulse amplitude and width independent of frequency;
- sufficient curvature of the output pulse leading edge, especially important when rectifiers work in parallel;
- reliability, simplicity, and economy.

Relative to an electric propellor drive, a control circuit must also provide a change in alternation of inverter output voltage phases.

The following are the main functional elements of an inverter control circuit: master pulse generator, pulse expanders, pulse controlled delay nodes, and output pulse formation nodes. In addition, a control circuit can include several elements insuring that the requisite characteristics and requisite electric drive qualitative operating indicators (tendency to oscillate, overshoot, and so on) are obtained.

An inverter control circuit must provide optimum operation of the electric /464 drive in static and dynamic modes. Concerning static modes, usually it is necessary here during speed regulation to implement the specific law of voltage change depending on frequency and load change. The given operating mode determines current frequency.

Self-excited current or voltage inverters are used in PCh with a dc link as the output power element.

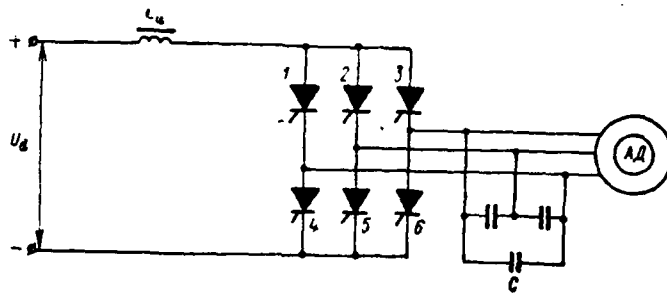


Figure 9.17. Self-Excited Current Inverter Circuit.

Commutation is accomplished with the aid of capacitors  $C$  in thyristor-based current inverters 1-6 (Figure 9.17). Their great installed capacity (especially at low frequencies) restricts the field of use of current inverters with a small regulation range — 1 : 3.

The inverter frequency change range can be increased through a staged change in commutating capacitances.

Circuit simplicity, relatively low rectifier control installed capacity, and non-sensitivity to radical load fluctuations are current inverter advantages. Disadvantages include the capability of the appearance of low-frequency oscillations due to motor capacitor self-excitation. In addition, as already stated, capacitor installed capacity is very great, which greatly changes the form of the output voltage.

Voltage inverters consisting of thyristors 1-6 and of uncontrolled rectifiers 1'-6' (Figure 9.18) differ from current inverters by the amount of inductivity at input. They make it possible to regulate voltage at output in wider ranges (1 : 10) at lower capacitor C1-C6 installed capacity. The threshold for inverter output voltage frequency is 100-150 Hz.

The output frequency control range for the circuits examined is 1 : 20. Maximum output frequency equals 150 Hz; the output voltage control range runs from 1 : 3 to 1 : 10. It is possible to regulate output voltage using a dc link or by the inverter itself; secondary voltage frequency does not depend on feed network frequency.

The disadvantages of self-excited inverters listed above during operation /465 to the motor load determined the overall trend in development of inverters for electric drive — primarily, separation of capacitors from their output. Use of completely controlled silicon rectifiers (technotrons) is the most effective solution to this problem.

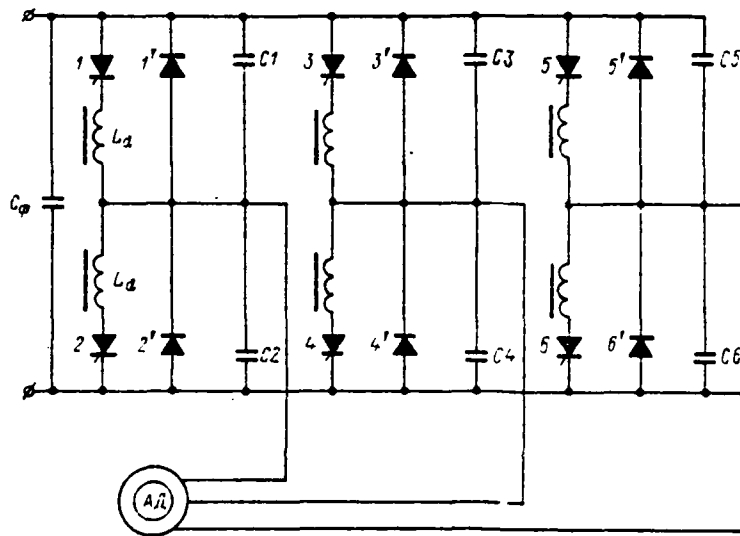


Figure 9.18. Self-Excited Voltage Inverter Circuit.

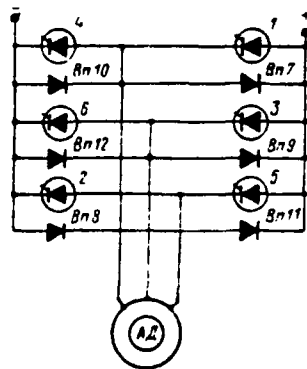


Figure 9.19. Circuit of an Inverter with Completely Controlled Silicon Rectifiers.

An example of such a circuit is shown in Figure 9.19. The inverter comprises technotrons 1-6 and a reverse bridge of uncontrolled rectifiers Vp7-Vp12, intended for return of the reactive power accumulated in the magnetic field to the network.

Besides the aforementioned advantage of frequency converters with intermediate dc coupling, to wit output frequency independent of feed network frequency (which makes it possible to obtain both an increased and a decreased secondary network frequency during a wide range of its change), these PCh also have the following disadvantages:

- requirement for compensation of load reactive power by connection of capacitors and by a change in capacitance value with a change in output frequency;
- requirement to change the capacitance of the capacitors when regulating /466 converter load to provide stable commutation;
- requirement for large capacitance at frequencies below 10-15 Hz;
- presence of a steeply-dropping external characteristic;
- requirement for special measures for smoothing dc pulsations in the intermediate link and rectangular form of the output voltage curve.

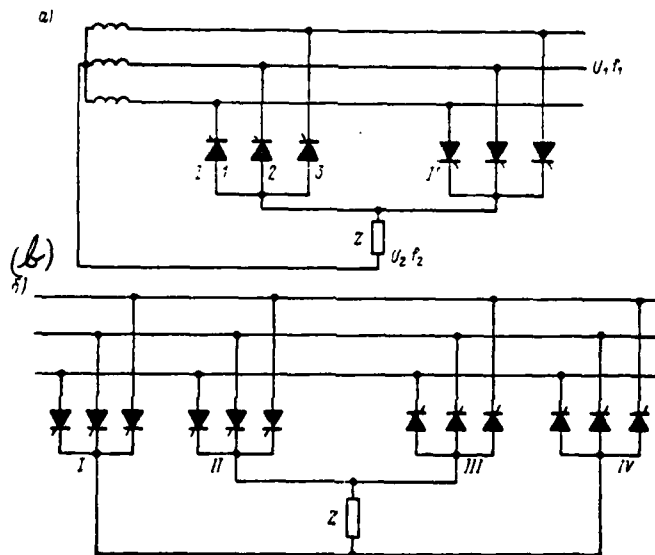


Figure 9.20. Circuit of a Single-Phase Converter with Rectifier Groups I, II (a), and I-IV (b).

Direct frequency converters (NPCh). Frequency converters in which feed network

voltage accomplishes current commutation are called direct frequency converters. These circuits are divided into two basic types, with neutral wire and bridge [7].

Either rectifier groups I, II (Figure 9.20a) or I-IV (Figure 9.20b) can be used in single-phase converters.

Three-, six- and  $m$ -phase rectifiers comprising single-phase rectifiers also are used. The latter's output voltage with the aid of the control system is smoothed to electrical angle  $2\pi m_2$  (where  $m_2$  is the number of consumer phases) and they form a symmetrical system of secondary voltages.

The NPCh principle of operation consists of the following. Each of two matched connected rectifier groups comprising converter phase is intended for the formation of half-waves of output voltage of different polarity. Alternating supply of /467 control pulses to Group I rectifiers, and then to Group II, will lead to a change in the direction of the current flowing in the load. Voltage frequency at PCh output comprises

$$f_2 = \frac{m_1 f_1}{2n - m_1}, \quad (9.22)$$

where  $m_1$  is the number of elementary commutated loops formed during rectification.

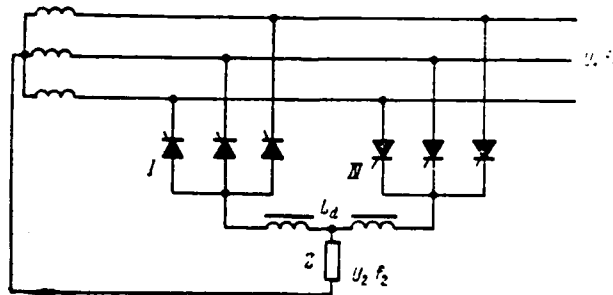


Figure 9.21. Circuit of a Frequency Converter with a Compensating Reactor.

If enabling pulses to the connected group's rectifiers begin to be supplied

after a certain time following cessation of the supply of enabling pulses to the disconnected group, then the voltage frequency at PCh output will equal

$$f_s = \frac{f_1 m_1 \pi}{\pi (2\pi + m_1) + \varphi_n m_1}; \quad n = 0, 1, 2, 3, \dots \quad (9.23)$$

where  $\varphi_n > \left(\frac{\pi}{2} + \frac{\pi}{m}\right)$  is the angle of discontinuity to prevent open burnings, determined from the above expression.

The flow of reactive current caused by energy accumulated in the load magnetic field is provided by rectifier transfer to the inverter operating mode. For this, a portion of the rectifier half-cycle of each group (half-phase) operates in the rectifier mode and a portion of the half-cycle operates in the inverter mode. The ratio between both modes is determined by the ratio between the load's active and reactive component.

A circuit for a PCh with compensating reactor is depicted in Figure 9.21. This type of frequency converter will contain four rectifier groups connected on the bridge principle and operating in pairs (I and IV, II and III) analogously to the PCh shown in Figure 9.20 (for simplicity, only groups I and IV are shown).

The principle of operation of this PCh is as follows. Control pulses are supplied simultaneously to both matched connected rectifier groups. Meanwhile, one of them (I) operates in the rectifier, while the other (IV) in the inverter /468 mode with equal control angles ( $\alpha = \beta$ ). The average amount of rectified voltage via the rectifier group I — compensating reactor ( $L_d$ ) — rectifier group IV loop equals zero.

The magnitude of control angle ( $\alpha$ ) determines voltage in the load loop. Rectifier group IV must be placed in the rectifier mode and group I in the inverter mode in order to change the direction of the current in the load. The compensating reactor's purpose is to constrain compensating currents in the aforementioned loop since instantaneous voltage values can reach great magnitudes when the average value of the voltage in them equals zero.

NPCh advantages include the following:

- simplicity of the circuit's power section;

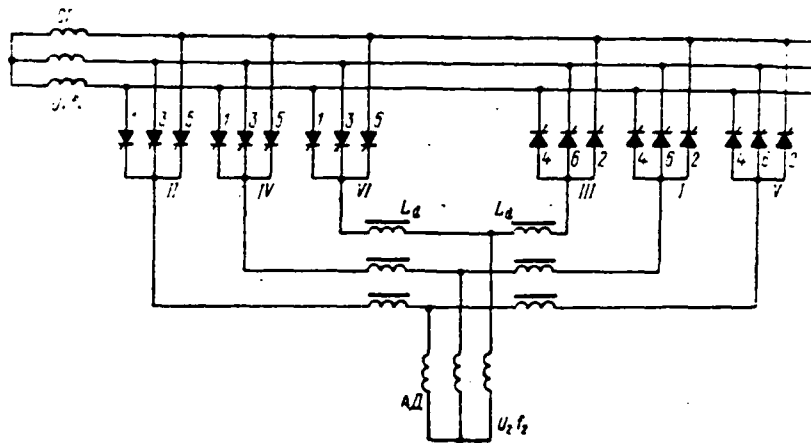


Figure 9.22. Schematic of Three-Phase Full-Wave Bridges Whereby a GED Stator Winding Serves as Load.

- natural current commutation (by means of the feed network), which makes it possible to eliminate commutating capacitors;
- absence of additional elements for passage of reactive current thanks to the fact that rectifiers during a half-cycle of secondary frequency transfer to the inverter operating mode;
- accidental disruptions of the operation of individual rectifiers will not lead to emergencies since the normal mode ends during a half-cycle of network output frequency, which significantly increases converter operating reliability;
- devices to smooth the dc are eliminated.

A disadvantage of such PCh is the maximum output frequency (given its sufficiently smooth regulation and a three-phase feed network) can not exceed 20-40% of feed network frequency.

A three-phase NPCh schematic. A three-phase NPCh comprises 18 control thyristors (Figure 9.22) and is built on a three-phase half-wave rectification principle. /469 Each converter phase consists of two such opposed connection circuits: II-V; IV-I; VI-III. The group consisting of three rectifiers (1, 3, 5) having a common cathode is referred to as "positive" and the group with a common anode (4, 6, 2) is called "negative." The direction of the current in the load will depend on how each operates: "positive" group current passes during one half-cycle of converter output voltage, while "negative" flows during another.

Thanks to current commutation among each group's rectifiers (I-IV), there is a capability to interrupt the current passing through the group. Enabling pulses are supplied alternately to rectifiers initially of one group, then of the other in a specific order, such as to the rectifiers of cathode group II. Within each group, enabling pulses follow the initial frequency via interval  $2\pi/m_1$ .

The magnitude of the secondary frequency assigned by the control circuit determines the duration of a given group's enabling pulse supply interval. Independent of this interval, after a time span of  $2\pi/m_2$  (120 electrical degrees of secondary frequency) enabling pulses begin to reach the rectifiers beyond the cathode (II) group in the order of group operation (this is group IV in the example selected). After another time span of  $2\pi/m_2$ , enabling pulses will begin to reach the third cathode group VI and so on. As is evident, enabling pulses are supplied to the cathode groups of rectifiers with a secondary frequency shift of  $2\pi/m_2$ .

After completion of the enabling pulse supply interval to the rectifiers of cathode group II, enabling pulses begin to be supplied to the rectifiers of anode group V paired with it. If this occurs at the moment of extinction of the last burning rectifier in group II paired with it, then the group's burning time turns out to equal  $\pi$  (one-half of the secondary frequency period). If this occurs a certain period of time after cessation of the supply of enabling pulses to the group II rectifiers, then a discontinuity forms between rectifier group burning ranges. Burning time decreases and control circuit operation must correspond to condition

$$\varphi_n \geq \left( \frac{\pi}{2} + \frac{\pi}{m_1} \right).$$

Within each anode group, enabling pulses reach the rectifiers also after time span  $2\pi/m_1$  of the primary frequency.

Thus, it turns out that cathode group burning ranges shift relative to each other at angle  $2\pi/m_2$  of secondary frequency, while in each pair of groups (II and V, IV and I, VI and III), anode group burning ranges shift one-half of a secondary

frequency period relative to the burning ranges of the cathode groups corresponding to them.

Rectifier group burning time cannot exceed half the second frequency's period. Otherwise, open burnings result, i. e., feed network short circuits. It is impossible to establish a group burning time less than  $2\pi/m_2$ , because, in this event,  $\pi/470$  the rectified current circuit opens.

Burning rectifier groups form three-phase half-wave bridges, whose load is the main propulsion motor stator windings. Six different rectified bridge combinations are formed in accordance with the rectifier group commutation sequence: I-II, II-III, III-IV, IV-V, V-VI, VI-I, and so on (see Figure 9.22), while the current direction in the motor windings changes just as if conventional three-phase voltage with a frequency equalling converter output frequency had been supplied to it.

The basic harmonic components of pulsating alternating current formed in the motor windings create a rotating magnetic field in the air gap. The speed of its rotation will depend on rectifier group burning time, i. e., on the given converter secondary frequency, which is expressed via the feed network frequency in the following way:

given a rectifier group burning time equal to half the output frequency's period ( $\pi$ ),

$$f_s = \frac{m_1 f_1}{m_1 - (n-1)^2}; \quad (9.24)$$

given a rectifier group burning time equal to  $5/6\pi$  (150 electrical degrees of secondary frequency),

$$f_s = \frac{10f_1 m_1}{12[m_1 + 2(n-1)]}; \quad (9.25)$$

given a rectifier group burning time equal to  $2/8\pi$  (120 electrical degrees of secondary frequency),

$$f_s = \frac{2f_1 m_1}{3[m_1 + 6(n-1)]}. \quad (9.26)$$

Overall, given an angle of discontinuity,

$$f_2 = \frac{\pi f_1 m_1}{\pi [m_1 - 2(n-1)] + \varphi_n + m_1}, \quad (9.27)$$

where  $n$  is the number of pulsations interfering during interval  $\frac{T_2}{2}$  ( $T_2$  is the output frequency period).

Three-phase half-wave bridges ( $m = 6$ ) are formed in the PCh examined.

Given a burning time of  $5/12T_2$ , we will get

$$\frac{5}{12} T_2 = \frac{5}{12} 2\pi = \frac{5}{6} \pi = T' = T'_2,$$

where value  $5/12T_2$  is designated by means of  $T'_2$ .

The frequency changes proportionally to the burning time change, i. e.,

$$\frac{f_1}{f_2} = \frac{T'}{T''}; \quad f_2 = f_1 \frac{T''}{T'}; \quad T'' = \frac{10}{12} \pi; \quad \pi = T''.$$

Having substituted these values, we get

/471

$$f_2 = \frac{m_1 f_1}{[m_1 - 2(n-1)]} \cdot \frac{10}{12} \cdot \frac{\pi}{\pi} = \frac{10 m_1 f_1}{12 [m_1 - 2(n-1)]};$$

where  $n = 1$ .

$$f_2 = \frac{10 \cdot 3 \cdot 50}{12 [3 - 2(1-1)]} = 42 \quad \text{Hz.}$$

Given a burning time of  $1/3T_2$  (120 electrical degrees)

$$\frac{f_2}{f_1} = \frac{T'''}{T'}; \quad T''' = \frac{2\pi}{3}; \quad T' = \pi$$

and, for  $n = 1$

$$f_2 = \frac{2 \cdot 3 \cdot 50}{3 [3 - 2(1-1)]} = 33.3 \quad \text{Hz.}$$

Having substituted the various values for  $n$  in formulas (9.24)-(9.27), it is possible to obtain the magnitude of the secondary frequency for various rectifier group burning angles, i. e., given a varied quantity of pulsations accommodated in the interval equalling one-half of output frequency  $f_2$ .

Commutation of the rectifiers within the groups is accomplished by primary network voltage of constant frequency ( $f_1 = \text{const}$ ).

This method is based on the fact that, given low secondary voltage frequency, its period is many times greater than the period of the network frequency. As a result, it is possible within the limits of half-frequency  $f_2$  always to set a whole number of half-periods  $f_1$  and to insure blanking of rectifiers, having picked off control pulses from the blanking group's rectifiers and having simultaneously fed control pulses to the open group of rectifiers. Rectifier blanking will occur here at the moment the current passes through zero.

As pointed out, commutation occurs normally when  $f_2 \ll f_1$ ; a converter is observed to operate most reliably in the 3-25 Hz frequency range.

A special shorted double squirrel-cage motor usually is used.

Frequency converter circuit selection. Power circuit selection is determined by several factors, primary ones being: power and voltage at converter output; ratio of the primary and secondary network frequencies; output voltage curve; thyristor type and nominal data; magnitude and duration of starting and operating overloads; weight and dimensional characteristics; reliability.

The simplest circuits for converters with three-phase outputs fed from the three-phase network will comprise 18 rectifiers (Figure 9.23).

They can be made both with isolation transformers (Figure 9.23a) and without them. However, in the latter case, difficulties arise regarding voltages at the PCh output and loads. This can result in partial use of the voltage converter and, as a result, deterioration in its power indicators. Other disadvantages of such circuits include the requirement for powerful reactors to constrain /473 compensating currents (Figure 9.23b) and maintenance of high harmonics in the

output voltage curve, which may require installation of a smoothing filter at the converter output (Figure 9.23c).

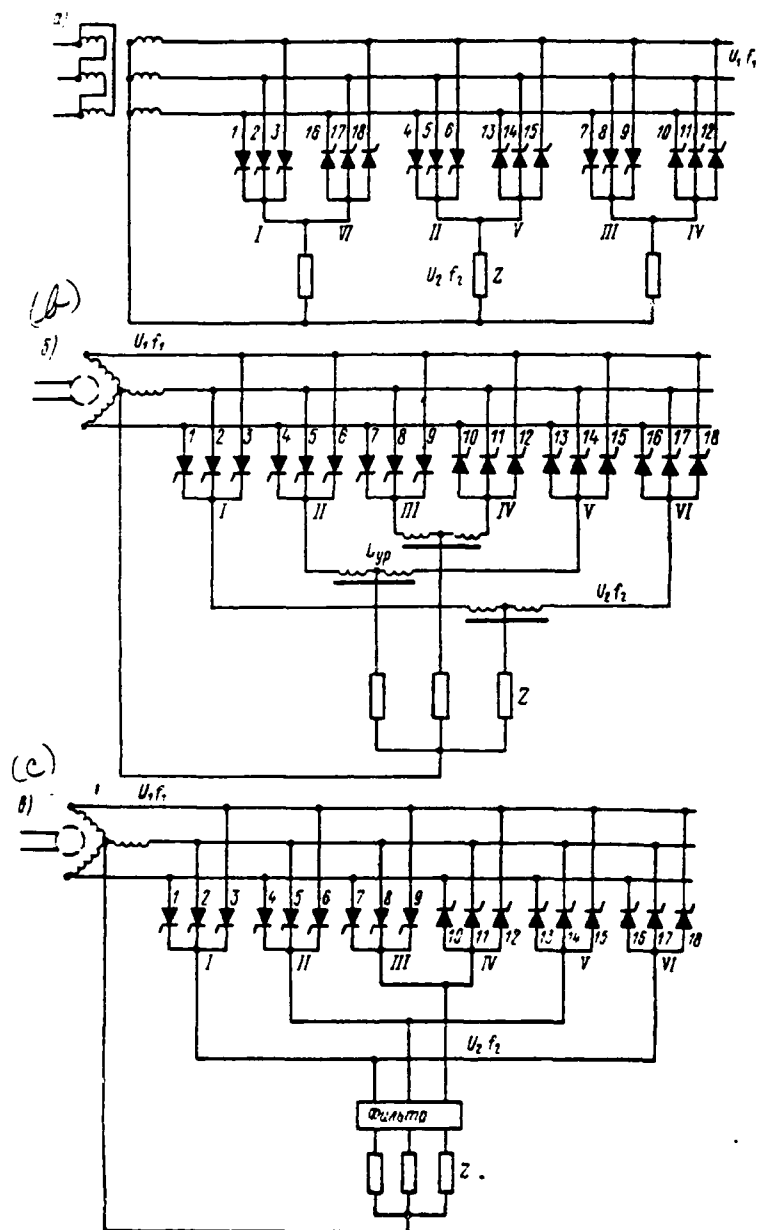


Figure 9.23. Three-Phase Output Frequency Converter Circuits: a—PCh with three-phase rectifiers and with an isolation transformer; b—Independent PCh with compensating reactor  $L_{yp}$ ; c—PCh with smoothing filter.

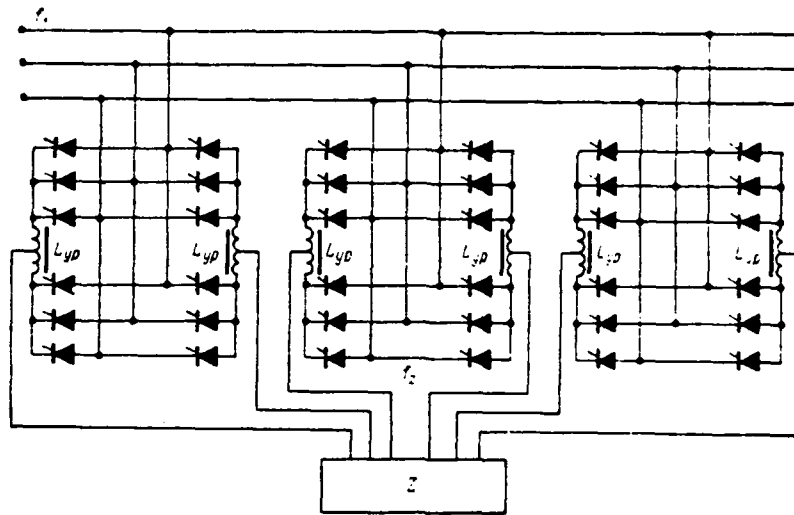


Figure 9.24. Frequency Converter with a Six-Phase (Bridge) Circuit.

A frequency converter made from an equivalent six-phase (bridge) circuit with a three-phase output is depicted in Figure 9.24. The minimum number of thyristors in this circuit is 36.

The advantages of six-phase circuits compared to three-phase include the fact that the amplitude of the pulsations in the output voltage curve here decreases approximately by a factor of 2 during a simultaneous increase by a factor of 2 in pulsation frequency. This makes it possible in a majority of cases to avoid smoothing filters when using an induction motor.

Use of such circuits makes use of an electric drive with a 100-150 kW and larger AD possible and, all other things being equal, to increase the voltage at the converter output by a factor of 2.

Multiphase power circuits significantly improve the form of the curve of the current the PCh consumes from the feed network. Therefore, they are most advisable in those instances where converter and network load power are commensurate.

An increase in converter power is achieved also without changing the power circuit by means of parallel and series connection of thyristors.

Based on everything that has been said, it is possible to formulate the following basic advantages of direct frequency converters:

- current commutation in NPCh rectifiers occurs due to feed network /474 voltage, resulting in no requirement for any special commutators, such as capacitors for example.

- it is possible to make a bilateral power exchange, from the feed network to the load circuit and vice versa. Thanks to this quality, the NPCh operates to load with any power factor without use of special compensators;

- it is possible to provide smooth regulation of the amplitude and frequency of the voltage at output (beginning with zero), which often turns out to be necessary for ac motor frequency control;

- an NPCh is fed directly from the ac network (with or without an isolation transformer), avoiding intermediate rectification, which, in some cases, makes it possible to build power circuits with less rectifiers than converters with dc coupling;

- it is possible and, moreover, quite simple with the aid of a control system to obtain at output current close in form to sinusoidal. This is especially important when operating an average- and high-power propulsion motor.

Along with this, it should be noted that significant NPCh disadvantages do exist. In particular, they require a considerable amount of reactive power from the network. However, use of capacitors to a considerable degree will compensate for this. Another characteristic shortcoming stemming from the very principle of NPCh operation is the constraint on the upper threshold of operating frequencies. But, this also can be overcome to a significant degree by using a higher feed network frequency.

The best prospects for GEU use are frequency converters with direct coupling and natural commutation, making it possible to obtain a frequency at output of from 0 to 16 Hz when fed from a network with a frequency of 50 Hz. It is possible with the aid of these converters to obtain frequencies up to 100 Hz at output, when a shipboard network with a frequency of 400 Hz is available.

Given a feed network frequency of 50 Hz, an output frequency ranging from 20-100 Hz can be obtained by using converters with dc coupling and a parallel-type inverter.

As induction propulsion motors intended for frequency regulation are designed, the following basic factors should be kept in mind:

- feed from voltage with a rectangular form;
- nonstandard feed voltage value;
- forced cooling system;
- reduced stator winding resistance value.

One also should consider that static converters require non-sinusoidal current from the feed network. This, in turn, can lead to distortion of the feed voltage curve, which impacts negatively on feed generators and on individual consumers /475 connected in parallel with the converter. This difficulty can be overcome through connection of resonant filters or through use of multiphase conversion power circuits.

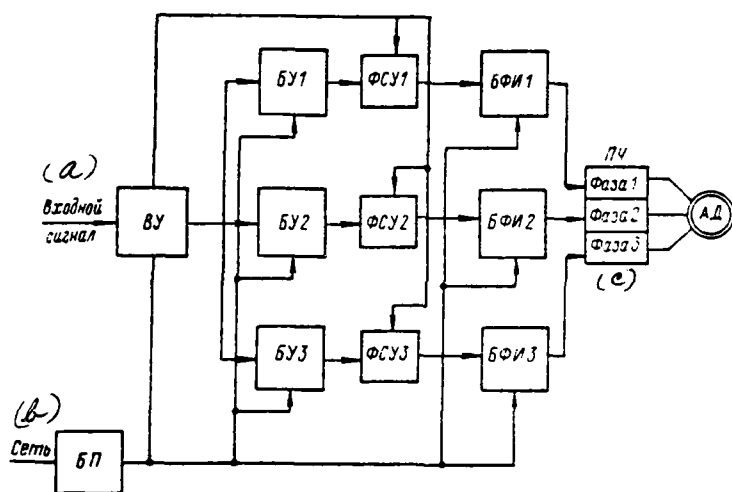


Figure 9.25. Block Diagram of a Frequency Converter Control System.  
a—Input signal; b—Network; c—Phase 1, 2, 3.

Frequency converter control system operating principle. A simplified block diagram of a PCh control system is shown in Figure 9.25. As is evident from the figure, it includes the following basic links.

1. Input device ВУ, which converts the control signal into voltages:
  - three-phase low-frequency, while the frequency and sequence of this voltage's phases are determined by the value and polarity of the control signal, respectively;
  - direct current, the value of which changes in accordance with the given relationship of voltage change at the drive motor terminals to its frequency.

2. Three identical control units BU1, BU2, BU3, each of which provides a duration of operation of both frequency converter half-phases in the rectifier and inverter modes.

3. Three phase shifters FSU1, FSU2, FSU3, which provide the value of the control angles of each PCh phase in the rectifier ( $\alpha$ ) and inverter ( $\beta$ ) modes.

4. Three pulse boosters BFI1, BFI2, BFI3, which control thyristor firing points.

5. Feed unit BP.

Frequency converter circuit operation. A control signal is fed to the /476 input of input device VU, where it is converted into low-frequency three-phase voltage. The frequency of the three-phase output voltage is provided by the value of the control signal, while its polarity provides the alternation of the phases. A change in control signal polarity will lead to AD reverse. At the same time, in the VU the control signal is converted into constant voltage, the value of which determined by the given law for a change in the thyristor control angle depending on the value of the frequency at output.

The low-frequency three-phase voltage goes from the VU output to control unit BU. The voltage curve is formed in it and determines the duration of the operation of each PCh half-phase in the rectifier and inverter modes.

Voltage goes from the BU outputs to phase shifter FSU. Constant voltage from the output device arrives at the same time. Its value is determined by the given law of PCh thyristor control angle change, which provides a constant AD overload capability. Thus, the amplitude of this constant voltage determines the value of control angles  $\alpha$  and  $\beta$  of the operation of each PCh half-phase.

Voltage goes from the FSU output to pulse booster BFI, where formation of control pulses for controlled thyristors occurs.

This examination of the principle of operation of a PCh control system

only covers a general method of obtaining low-frequency three-phase voltage. Therefore, we will turn to the functional and to the time diagrams presented in Figures 9.26 and 9.27, respectively, for a more complete representation of how a control system works.

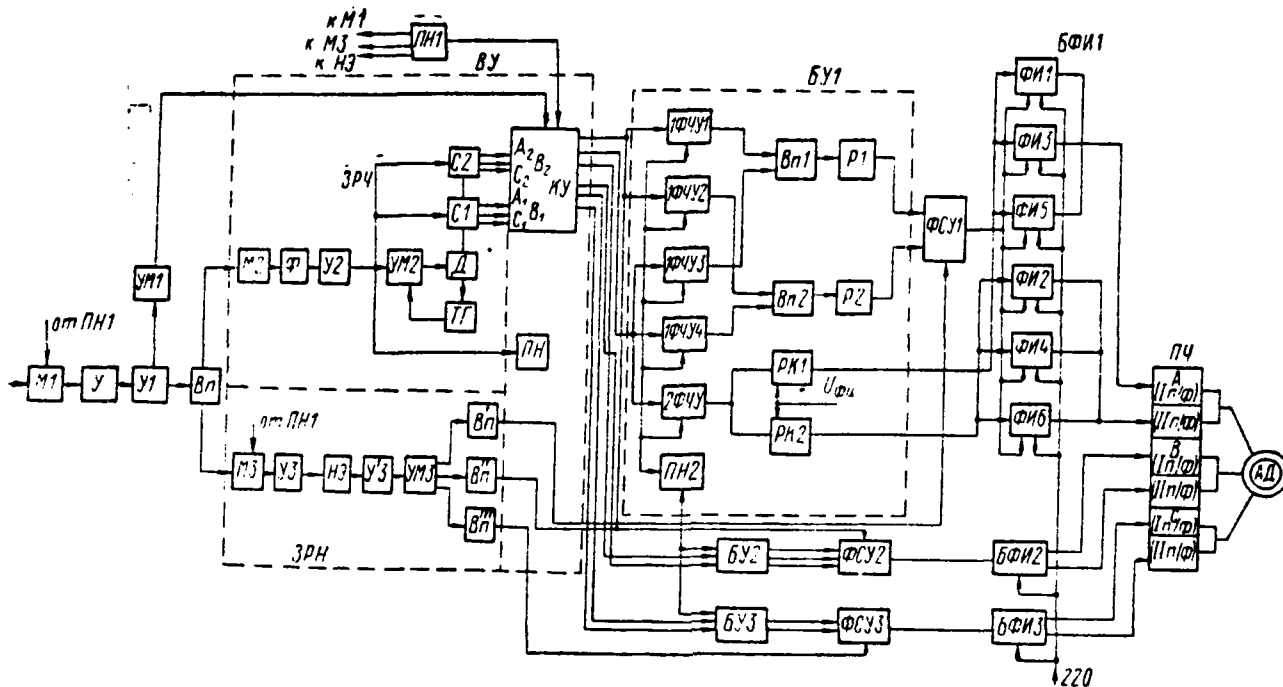


Figure 9.26. Functional Diagram of a Frequency Converter Control System (SUPCh).

The common element in a frequency converter control system (SUPCh) is input device VU, to whose output are connected three identical control units BU1, BU2, BU3 (see Figure 9.26).

A control signal in the form of constant voltage reaches the input device's modulator M1, where it is converted into alternating voltage of rectangular form.

Commutating voltage from voltage converter PN1 is supplied to this same modulator. The modulated voltage is amplified by ac amplifiers U, U1 and then rectified by rectifier Vp.

Simultaneously, the signal goes from amplifier U1 to power amplifier UM1 and then to commutator KU. Voltage at the rectifier Vp output is proportional to the value of the control signal, i. e., it is supplied simultaneously to frequency control link ZRCh and voltage control link ZRN. In the former, the dc signal is supplied to modulator M2. Here, it is converted into an ac signal of rectangular form with a frequency of 50 Hz and is then supplied to filter F, which filters out the basic harmonic of this frequency. From the F output, voltage of /479 sinusoidal form is amplified by amplifiers U2 and UM2 and is supplied to the two-phase motor's control winding, which is linked mechanically with two permanent-magnet-rotor [PMR] synchros S1 and S2 and ac tachogenerator TG.

Motor D rotational speed and, consequently, of the synchros and tachogenerator connected to it, is proportional to the value of the voltage reaching its control winding, i. e., to the value of the control signal.

Speed feedback from tachogenerator TG is introduced into amplifier UM2 to increase the range of motor rotational speed control. Motor D and TG field windings are fed from the ac network, while synchro field windings are fed from voltage converter PN2. The carrier frequency's constant voltage, determined by voltage converter PN modulated in amplitude with a frequency determined by the synchro rotational speed, is transformed in synchro S1 and S2 three-phase windings as the synchros rotate.

The forms of voltage curves  $U_{A1}$  (a) and  $U_{A2}$  (b) at the output of phases  $A_1$  and  $A_2$  of synchros S1 and S2 (see Figure 9.26) are depicted in Figure 9.27a through 9.27f. Alternating voltage  $U_{A1}$  of phase  $A_1$  of synchro S1 and voltage  $U_{A2}$  of phase  $A_2$  of synchro S2 shift relative to each other by angle  $\varphi_n$ , the value of which, which will be clear from what follows, determines the time of operation of each PCh half-phase ( $In\phi$ ,  $IIn\phi$ ) in the inverter mode.

It is possible to change this angle by means of a mutual turn of the synchro stator and thereby to establish the requisite duration ratio of the rectifier and inverter modes.

Three-phase voltage from the output of synchros S1 and S2 via commutator KU, which, during a change in control signal polarity, accomplishes the switching

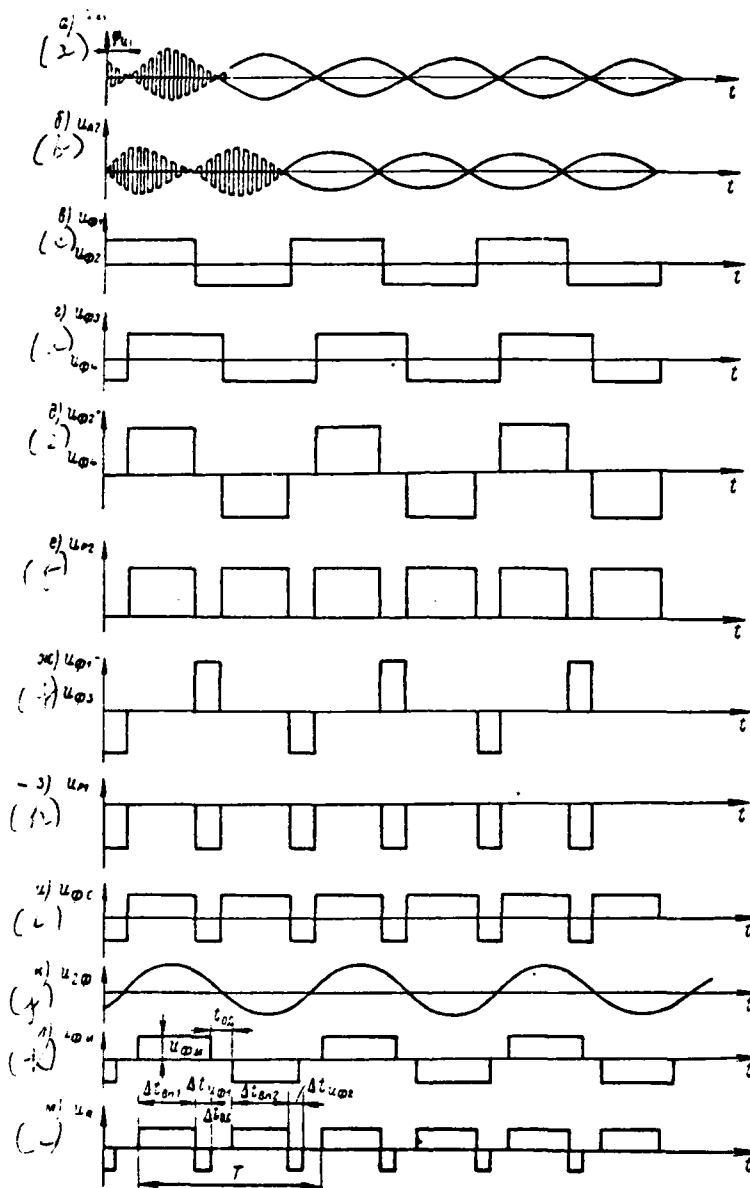


Figure 9.27. Time Diagram for the SUPCh Functional Diagram.

of phase alternation, reaches control unit BU. A signal from amplifier UM1 simultaneously reaches the commutator.

Given positive input signal polarity, synchro voltage at KU output has direct alternation of phases  $A_1B_1C_1$  and  $A_2B_2C_2$ , which corresponds to master motor AD

rotation in one direction. Given negative input signal polarity, the voltage from the synchros at KU output has reverse alternation of phases —  $A_1C_1B_1$  and  $A_2C_2B_2$ , which facilitates reversing the motor.

In the voltage control link ZRN, voltage from the rectifier is supplied to modulator M3, to which commutated voltage is supplied from voltage converter PN1.

Voltage amplified by amplifier U3 is supplied to nonlinear element NE, in which occurs formation of the given law of converter thyristor control angle change depending on the frequency of the voltage applied to motor AD.

Voltage from the NE output is supplied to linear power amplifiers U3 and UM3, then to three rectifiers  $Vp'$ ,  $Vp''$ , and  $Vp'''$  and, from them, to phase shifters FSU1, FSU2, and FSU3.

As pointed out earlier, voltage from the synchro output is supplied via /480 commutator KU to three identical PCh control units. Therefore, it suffices to examine the principle of operation of one unit controlling converter phase A.

Voltage of synchros S1 ( $U_{A1}$ ) and S2 ( $U_{A2}$ ) of phases  $A_1$  and  $A_2$ , respectively (diagrams a and b in Figure 9.27) reaches control unit phase-sensitive amplifiers FChU in the following sequence: from phase  $A_1$  of synchro S1 to 1FChU3, 1FChU4; from phase  $A_2$  of synchro S2 to 1FChU1 and 1FChU2. Voltages at the output of all these FChU operating in the constraint mode (1FChU) and in the amplification mode (2FChU) are depicted in Figure 9.27:  $u_{\phi 1}$  and  $u_{\phi 2}$  (from 1FChU1 and 1FChU2) in diagram c;  $u_{\phi 3}$ ,  $u_{\phi 4}$  (from 1FChU3 and 1FChU4) in diagram d and  $u_{\phi 5}$  (from 2FChU) in diagram j.

Next, voltages from the 1FChU2 and 1FChU4 outputs are plotted (diagram e) and those from the 1FChU1 and 1FChU3 outputs are subtracted (diagram g).

After adding and subtracting, these voltages are supplied to rectifiers  $Vp1$  and  $Vp2$ , then to relays R1 and R2. Voltages of rectangular form  $u_{p1}$  and  $u_{p2}$ , fixed in amplitude (respectively) are received at the latter's output. As can be seen in diagram h, the voltage pulse width at the relay R1 output equals angle  $\varphi_n$ .

Voltages from the aforementioned relays are supplied to phase shifter FSU1, where these voltages are added.

Considering that FSU1 is fed from an input device VU rectifier, the value of the voltage of the negative and positive half-waves at the FSU1 output is proportional to the value of the voltages at the Vp output. The form of the voltage curve at the FSU1 output ( $u_{\phi.c}$ ) is shown in diagram i.

Voltage from the FSU1 output is supplied to pulse generator BF11 comprising six shapers FI1-FI6, with odd shapers controlling the odd group and even shapers controlling the even group of PCh thyristors.

Phase-sensitive amplifier 2FChU operates in the amplification mode and voltage at its output ( $u_{\phi}$ ) has a sinusoidal form (diagram j). Voltage from the 2FChU output is supplied out of phase to the input of two commutating relays RK1 and RK2. The former supplies constant feed voltage  $u_{\phi.n}$  (diagram k) to pulse generators FI1, FI3, FI5, while the latter does so to FI2, FI4, FI6 (diagram l, voltage  $u_R$ ).

Additional bias voltage, which makes it possible to control the potential of their tripping and, thereby, the time of operation of each PCh half-phase, is introduced into both relays.

The tripping potential is selected in such a way that a relay trips after output voltage (from the 2FChU output) has gone through zero, while drop-out occurs at the moment just before output voltage reaches zero. This is illustrated clearly by diagram k, where voltage  $u_{\phi.n}$  is introduced at the output of both relays. The time in which the relay is in the tripped state, i. e., "Switch Closed," is shown in this same diagram and feed is supplied to even and odd FI. As a result, time interval  $\Delta t_{o.c.}$  appears when both relays are in the released state, feed is not supplied to BFI, and control pulses are absent.

A special pulse reaching three thyristors of the PCh half-phase is formed at the moment feed is supplied.

Phase shifter FSU is built in such a way that, when voltage at its output equals zero, the pulse from the FI output is supplied with initial angle  $\alpha = 90^\circ$ .

If the voltage at the FSU does not equal zero and is negative, then the control angle equals  $\alpha$ , with  $|\alpha| = |\beta|$ , since both half-waves of voltage at the FSU1 output are equal in amplitude, which is determined by the voltage at the output of rectifier  $V_p$  of input device VU.

An odd (even) group of thyristors operates during time  $\Delta t_{Bn1}$  ( $\Delta t_{Bn2}$ ) in the rectifier mode with control angle  $\alpha$ , while the odd (even) group operates in the inverter mode with control angle  $\beta$  during time  $\Delta t_{u\phi 1}$  ( $\Delta t_{u\phi 2}$ ).

During time  $\Delta t_{o.c}$ , control pulses are absent in both half-phases. Operation of the remaining converter phases (B and C) occurs in an analogous manner, but with a shift of 120 and 240 electrical degrees of voltage frequency at its output.

The time diagram of the operation of converter phase A is depicted in diagram 1.

Selection of a frequency control system with static converters. Analysis of the operation of an induction motor, given various frequency control laws, will lead to the conclusion that all such control systems boil down to the following four basic groups:

- without correction of feed voltage values relative to frequency;
- correction for load torque;
- with flux constancy maintenance;
- with rotor current constant frequency maintenance.

The first of these is the simplest and lays the foundation for the other three, while the fourth is the most universal.

Frequency control systems without compensators. This system is built from a circuit based on the law of proportional control (Figure 9.28a) and, as noted above, in general does not provide satisfactory indicators regarding either least losses in the motor or its stability characteristics in a broad range of frequency change  $\dot{f}_s$ . However, if a similar system is used to drive mechanisms whose shaft torque changes with the same sign as does speed, then the requisite adjustment can be introduced via the shaft.

Actually, it makes no difference here — do you increase the deviation of the supplied voltage  $\bar{U}$ , from frequency  $\bar{f}_s$  (in relative units) with a decrease in the latter or reduce load torque with a decrease in  $\bar{f}_s$ ? As a result, it is advisable to use such a frequency control system, given drive mechanical /482 characteristics determined by the expression  $\bar{M} = \bar{n}^y$  where  $y \geq 1$ . Fan electric drives, various types of centrifugal pumps, and GED have similar characteristics. Here, it is possible for each converter--motor system to select that load that insures that the difference between critical and nominal torques are positive ( $M_{кр} - M_{ном} > \Delta M$ ) and that this ratio is retained for the entire control range.

In addition, negative voltage feedback  $K_u U_s$  is used in the system being examined. However, this cannot be called a compensating system since it does not create deviation  $\bar{U}$ , from  $\bar{f}_s$ , but, on the contrary, maintains at the motor output a ratio between the control values provided by the control system. In general, this coupling is required since it eliminates the influence of voltage regulator nonlinearity and losses in the converter power unit SBP.

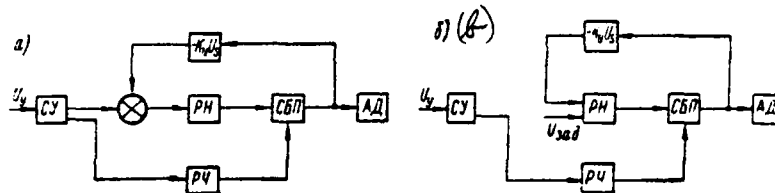


Figure 9.28. Frequency Control Systems Without Compensators: a—For an arbitrary mechanism; b—For speed control of a mechanism with constant power. SU is the control system;  $u_y$  voltage at control system input; RN is voltage regulator; RCh is frequency regulator; SBP is converter power unit;  $K_u U_s$  is voltage feedback.

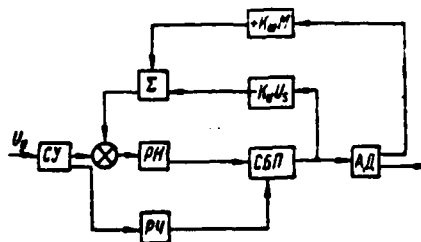


Figure 9.29. Frequency Control Systems with Load Torque Correction.  $K_M M$  is torque feedback.

A similar system also can be used when the mechanism's characteristic is  $\bar{M} = \frac{1}{n_2}$ . But, in this case, a signal is not supplied to voltage regulator RN from the control system. Only stabilization of the voltage supplied to the motor via the feedback channel (Figure 9.28b) occurs.

Frequency control system with correction for load torque. This system is built from a circuit based on the law of frequency control (Figure 9.29) by means of the addition of compensating feedback  $K_M M$  supplied to adder  $\Sigma$  added to the previous system. It is advisable to use similar systems in an automated /483 electric drive where the load torque can deviate from relationship  $\bar{M} = \bar{n}^{\nu}$ , while these deviations will bear either a random character or are caused by the special conditions of mechanism operation, including the GED as well. In this event, the motor operates with smaller losses and provides a rigidity of mechanical characteristics over a larger range than in an uncorrected system. However, here also, with a change in load torque in a sufficiently broad range independent of speed, stable system operation is possible only with constrained limits of the change in frequency of the voltage applied to the stator.

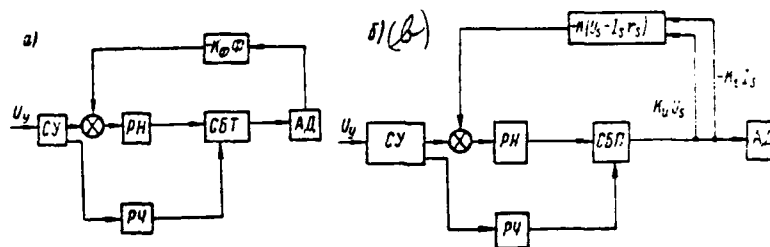


Figure 9.30. Frequency Control Systems with Current Constancy Maintenance: a—With flux ( $-K_\phi\Phi$ ) feedback; b—With emf feedback.

Frequency control system with flux constancy maintenance. This system insures reliable motor operation with any load torque (less than critical torque at nominal frequency) in the selected frequency range  $\bar{f}_s$  of the feed voltage. In this case, it is possible to use a Hall sensor (Figure 9.30a), which makes it possible to measure flux directly, to build compensating flux feedback. However, if you consider that  $E_s = C_f \bar{I}_s \Phi$ , then it is possible to express the condition of flux constancy by ratio  $\frac{E_s}{\bar{f}_s} = \text{const}$ . In other words, providing flux constancy requires that

value  $\bar{E}_s$ , change proportionally to value  $\bar{I}_s$ . This requires use of emf feedback signal  $E_s$  (Figure 9.30b).

It is possible to obtain this signal with the aid of the vector difference of signals based on  $\underline{U}_s$  and  $\underline{I}_s$ , as shown in the figure.

Voltage proportional to the current and coinciding with it in phase is picked off the resistance connected to current transformer secondary windings ( $-K_i I_s$ ).

Using selection of the corresponding transformation factors of the current and voltage transformers, as well as the value of the resistance, it is possible to obtain the sum of the secondary voltages of these transformers, which will be proportional to  $\bar{E}_s (K_u I_s)$ . This system creates unnecessary boosting  $\bar{U}_s$  /484 for the extended motor operation mode at reduced load torque, which will lead to an unjustified increase in losses in the induction motor.

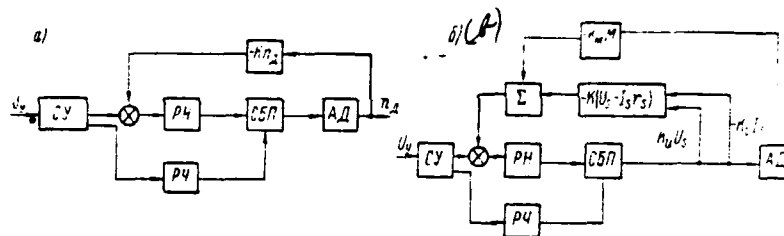


Figure 9.31. Frequency Control Systems With Rotor Current Constant Relative Frequency Maintenance. a—With differential speed feedback; b—With emf and torque feedback.

Frequency control system with rotor current constant relative frequency maintenance. It is most advisable to use this system during a torque change in a broad range independent of speed, in GED in particular. In general, it can insure stable induction motor operation when the losses in the motor are close to minimal. If one considers relationship  $\bar{f}_r = \bar{f}_s - \bar{n}_2$ , then it is possible to build such a system (Figure 9.31a) with the aid of differential speed feedback ( $-Kn_2$ ). Essentially, the characteristics of the control system do not change if compensation  $\bar{U}_s$  for rotor current ( $-K_i I_s$ ) and AD flux (Figure 9.31b) is made. It is advisable to use a second system variant when there are complications in using speed feedback.

Consequently, the following should be considered when selecting a control system:

1. The law of proportional control lies at the foundation of any PCh system, but in such a way that the AD will operate stably and economically over a broad range; but, introduction of compensating couplings is required.

2. Proceeding from point 1, it is possible to categorize all frequency control systems in four classes: without external compensators; with a load torque compensating coupling; with an AD flux compensating coupling; with a rotor current frequency compensating coupling.

3. A frequency control system maintaining  $\bar{i}_r = s_{\text{nom}}$ , providing a constant static overload and economic propulsion motor operation is the most preferable for practical use in ac GEU.

Requirements levied on direct frequency converter control systems. Semiconductor rectifiers are excited by signals supplied to the control electrode and cathode. The power required for control is slight, which makes it possible to use semiconductor instruments and low-power high-speed magnetic amplifiers in such systems. The /485 following requirements are levied on control systems:

— control pulse voltage amplitude must equal 15-20 V for reliable connection of powerful thyristors;

— since the dissimilarity of the thyristor angles of opening will depend on the difference in the characteristics of individual rectifiers and on control pulse curvature, the width of the latter's leading edge must be as small as possible and not exceed the on time of the given rectifier type;

— control pulse width must be greater than the time during which current in the thyristor anode circuit attains the value of the containment current;

— intervals between pulses must correspond to the converter power circuit and be synchronized with it;

— control pulse value and width, the periodicity of their sequence, and their symmetry must remain constant within the broad ranges of change in supplied voltage and environmental temperature;

— the control circuit for added reliability must be simple and have stable, properly-selected thermal and electrical element operating modes.

AD-A114 423

FOREIGN TECHNOLOGY DIV WRIGHT-PATTERSON AFB OH  
FUNDAMENTALS OF ELECTRICAL PROPULSION PLANT DESIGN, (U)  
APR 82 N A KUZNETSOV, P V KUROPATKIN  
FTD-ID(RS)T-1388-80

F/6 21/3

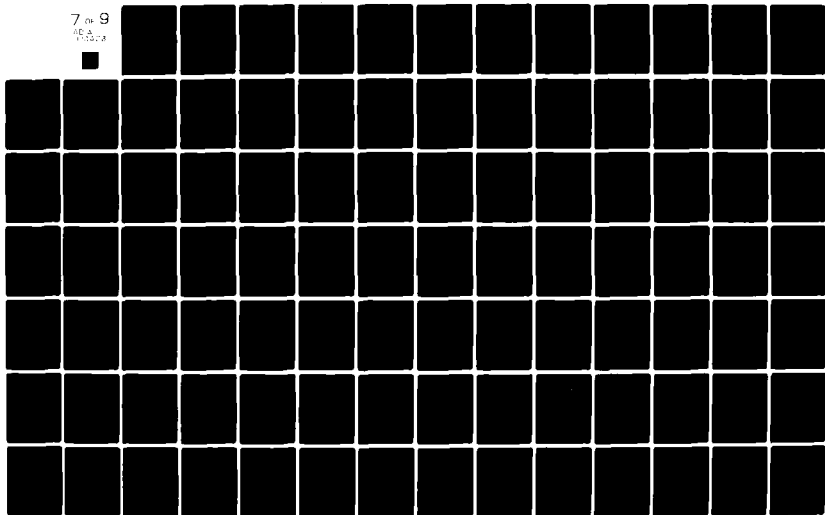
UNCLASSIFIED

NL

7 of 9

NO. 1

1388-80



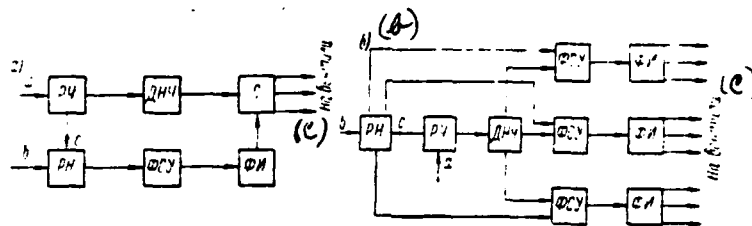


Figure 9.32. Structural Diagrams of Direct Frequency Converter Control Given a Resistive Load: a—With unimproved output voltage curve form; b—With a control angle change; c—To rectifiers.

Besides the aforementioned general requirements, additional requirements stemming from the converter principle of operation are levied on control systems with semiconductor rectifiers.

The structure of an NPC<sub>n</sub> control system will depend on the nature of the load, power circuit layout, and required form of the output voltage curve.

We will examine structural diagrams given resistive-inductive loads. In both cases, they include only units required to provide frequency and voltage and do not consider elements insuring converter operation in the closed control systems of specific drives.

Selection of a direct frequency converter control system given a resistive load. A converter control system with an unimproved form of the output voltage curve is the simplest. Its structural diagram is presented in Figure 9.32a. Low-frequency sensor DNCh generates pulses of the given form, width, and  $\omega$  sequence. These pulses determine converter output frequency, phase sequence, as well as output voltage curve form, since it will depend on low-frequency pulse width.

Low-frequency pulses must be supplied to each rectifier group, i. e., the number of these pulses must equal  $2m_2$  ( $m_2$  is the number of secondary circuit phases). Frequency regulator RCh inputs a signal into the DNCh for frequency control. Voltage regulator RN is an element inputting a signal into the phase shifter for the purpose of changing rectifier control angle  $\alpha$ . Phase shifter FSU insures

the assignment of angle  $\alpha$  by changing the phase of the sinusoidal voltage; this voltage is fed to the high-frequency pulse shaper FI, which shapes from it pulses which trigger the rectifiers. The number of trigger pulses in the converters with natural commutation, besides the systems with double pulses, is usually equal to  $2m_1$  (taking the direct and reverse groups of rectifiers into account). Pulses of the primary frequency enter into the mixer C, which feeds them to groups of rectifiers in the order assigned by the pulse transmitter of the output frequency. As a result, emerging from the mixer in a definite sequence are pulse packets which trigger the rectifiers.

For automation of the operation of the converter from the appropriate transducers, there should be provided inputs a and b into the frequency and voltage regulators and also (when it is necessary to ensure a defined law of the change in voltage from frequency) the coupling of C between them.

To improve the shape of the curve of the output voltage by a change in the control angle  $\alpha$ , the structure when  $m_2 = 3$  is used (Fig. 9.32, b). In this case with the  $m_2$ -phase converter, it is necessary to have  $m_2$  phase-shifting devices, each of which provides the assigned law of the change in the angle of control during the operating time of corresponding groups of rectifiers. Values of  $\alpha$  for groups of rectifiers feeding one phase of the load are assigned by one FSU.

Selection of control systems by direct frequency converters with active-inductive load. The control system by NPCh [direct frequency converter] with active-inductive load should provide the following:

- the cutoff of one of the groups of rectifiers for the time of engagement of the mutually opposing group and for the interrupt time;
- the action of each group of rectifiers in the rectifier and inverter modes with a clear transition from one mode to the other with passage of the reactive current by inversion during the half-period of the output frequency;
- the change in the duration of the rectified and inverted

modes as a function of the nature of the load and requirements for the shape of the output voltage;

- the fulfillment of the assigned laws of the change in angles of control when improvement of the shape of the curve of the output voltage is necessary.

A block diagram of the control of the converter with passage of the reactive current by the inverter without an equalizing reactor and the unimproved shape of the output voltage is given in Fig. 9.33. As was already noted above, such a diagram provides feed of the



Periodic operation of several rectifiers from common control elements (from the FSU, for example) is a special feature of NPCh control systems. In light of this, if each rectifier has its own pulse shaper, it is necessary to provide a small parameter spread for them, which is not always permissible with simple methods. For this reason, it is advisable to control all rectifiers by means of the same control pulses, but supplied in the requisite order to the appropriate rectifiers. In addition, it is desirable for such converters to have rectifiers possessing the best current and control voltage spread characteristics.

## Transient Processes in an Alternating Current Electric Propellor Drive

### § 10.1 Special Features of Main Propulsion Motor Starting and Reversal Calculations

The special feature of the operation of a synchronous or induction electric motor in a GEU system primarily is that motors receive feed not from an external network, with constant frequency and voltage values, as in fixed plants, but from a self-excited generator whose power equals the power of the GED or is commensurate with it. As a result, considerable voltage fluctuations are noted at its terminals when GED loads deviate from the set value.

Voltage drops in the generator as a shorted synchronous or induction propulsion motor is started and reversed cause the need for its significant overexcitation, boosting field current by a factor of 2-3.5 compared to nominal field current and by a factor of 4-5.5 times compared to field current during idling.

For the same reason, as a ship circles or is underway in stormy weather, there is a tendency for slight field boosting of the generator, and sometimes of the motor itself, to increase GED overload capability. For example, as was established during testing of the turboelectric ship "Abkhaziya," during radical transpositions of the rudder blade from side to side, the overload of the inner (relative to circulation trajectory) GED is such that envisaged overload protection trips.

Alternating current GED rotational speed regulation is accomplished almost exclusively by changing generator frequency (primary motor rotational speed).

A propulsion plant with synchronous propulsion motors is started and reversed in an asynchronous mode. Here, the synchronous motor's magnetic system, having a damper winding, acquires the properties of the rotor in a dual squirrel-cage induction motor. This circumstance, in particular, allowed V. I. Kas'yanov to develop a unified method for calculations of ac electric propellor drive starting and reversal. This method is based on the general theory of induction machines.

Starting of the majority of cargo vessel GED with synchronous or induction motors takes several seconds with an essentially stationary vessel since, for /489 such a short time interval, it does not develop any noticeable speed.

Thus, for those cases where vessel mass is incommensurately greater than GED mass, one can calculate that, as the latter is started, the screw operates in the moored characteristic, i. e.,  $m_s = f(n_d)$  where  $v = 0$ . Then, the nominal moment of screw hydraulic resistance will be reached at a speed of its rotation below nominal, usually ranging around  $(0,6-0,8) n_{d, \text{nom}}$ , where  $n_{d, \text{nom}}$  is GED nominal rotational speed, rpm.

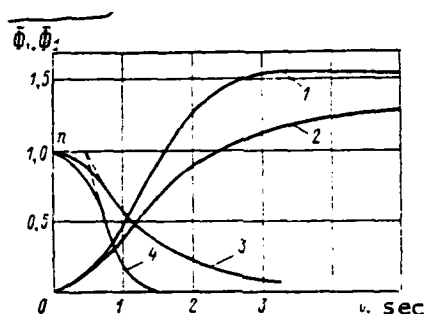


Figure 10.1. Turbogenerator Magnetic Flux Field ( $\bar{\Phi}_1$ ) and Killing ( $\bar{\Phi}_d$ ) Characteristics. 1 and 3—Idling; 2 and 4—When running a braked GED.

A main propulsion motor is started in the following way. An unexcited generator connected to the GED by means of a reversing switch is rotated until the initiation of the start idling; here, the primary motor's automatic governor is set at a speed corresponding to nominal screw moment of resistance from the moored characteristic. Upon receipt of the start instruction, maximum field boosting is applied to the propulsion generator, resulting in its magnetic flux, in about 2 seconds, attaining a sufficient value (Figure 10.1, curve 2). The GED begins to gather rotational speed, overcoming moments of inertia: propellor shafting intrinsic moment, propellor intrinsic moment, and increasing (approximately according to the square law) screw hydraulic moment of resistance.

After several seconds, when the GED starting mode ends and it will begin to rotate at a speed commensurate with nominal screw hydraulic moment of resistance

in the moored characteristic, the screw will develop nominal thrust. Field boosting then is removed from the generator, after which vessel take-off occurs, lasting considerably longer (several minutes) than the starting process itself.

The sequence of starting shorted synchronous and induction main propulsion motors described is the simplest and requires minimum time expended. However, this method of starting was not used widely on electric ships because it occurs during a three- to four-fold overload current, which causes great energy losses and, accordingly, severe heating of shorted synchronous and induction motor starting cells. If a synchronous GED, in addition, also has an insufficient hyposynchronous moment, then it may not go into synchronization at all when such a starting method is used.

In this connection, a simplified starting method at a reduced frequency, /490 which insures a reduction in starting currents and losses, as well as less starting cell heating, is used on most modern electric ships. Also, this provides better conditions for synchronous-type motors to go into synchronization. However, one should consider that starting, given a reduced frequency, requires somewhat more time compared to the starting process previously described.

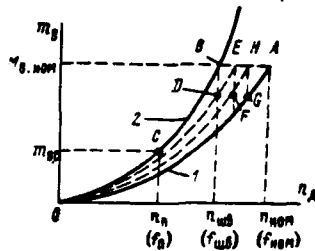


Figure 10.2. Propellor Characteristics  $m_B = f(n_A)$ . 1—When moving in open water; 2—Moored;  $n_n$  ( $f_n$ ),  $n_{шв}$  ( $f_{шв}$ ),  $n_{ном}$  ( $f_{ном}$ ) are GED propellor rotational speeds (frequencies) during starting, in the moored mode, and in the running in open water mode given nominal moment, respectively.

The following is the sequence of starting operations. Just as in the previous case, prior to starting an unexcited generator already connected to the GED by means of a reversing switch idles, but the primary motor governor must be set

to the lowest possible stable rotational speed (equalling 0.2-0.33 of nominal). Generator field boosting (two- to three-fold) is accomplished to increase the asynchronous moment during the entire starting period. As a result, after about 2 seconds its magnetic flux will attain a value sufficient for the motor to move and begin to pick up speed.

When the simplified motor starting mode ends and it begins to rotate at a speed corresponding to reduced generator frequency -- to starting frequency  $f_n$  (Figure 10.2), the propellor will operate in the initial portion of the moored curve (point C), developing rotational speed  $n_n$  and overcoming screw moment of resistance  $m_{s.c}$  corresponding to approximately only 10-20% of nominal. In the case of a synchronous-type GED, when it attains hyposynchronous speed differing from synchronous speed by no more than 5% (for a frequency of 50 Hz -- 2.5 Hz), motor excitation is cut in and, under the effect of the synchronizing torque, it goes into synchronization. Next, over a period of 5-10 seconds, primary motor rotational speed increases gradually and smoothly to a speed corresponding to nominal screw moment of resistance from moored characteristic  $M_{s. nom}$ . Here, GED (synchronous or induction) rotational speed increases smoothly and without kicks in accordance with the increase in generator frequency.

Testing and operational use of ac GEU demonstrated that reliably placing a synchronous motor into synchronization requires that its moment at the end of the period of asynchronous starting, given 5% absolute slip, must exceed screw moment of resistance by 25%. This is referred to as hyposynchronous moment.

At this stage, GED starting ends, the generator reverts from the forced excitation to the nominal mode, and, immediately following, the vessel take-off /491 period begins. It lasts several minutes, with a gradual increase in generator frequency (with an increase in primary motor rotational speed), which corresponds to the screw switching from the moored to the running in open water characteristic (points B, D, E, F, H, G, and A in Figure 10.2).

Thus, almost always the GED (both synchronous as well as induction-synchronous) starting method for an ac GEU involves connecting them to unexcited generators. The sequence of operations is as follows:

- the generator is accelerated by the primary motor to the lowest stable rotational speed;

— given an unexcited generator, main current circuit equipment is connected (high-speed generator circuit breakers and reversing switches); here, the GED turns out to be connected to an unexcited generator;

— excitation is supplied to the generator (or, given a cascade field system, to the generator exciter) with the requisite boosting factor;

— when the GED attains hyposynchronous rotational speed, feed is supplied to its field winding; — after the GED is placed in synchronization, field boosting is removed from the generator.

For GEU with diesel generators in parallel operating electric propulsion bus bars [ShED], after their acceleration an operation is realized to synchronize the generators at a reduced frequency and equalize emf so that there are no compensating currents between generators.

It should be noted that GED starting, beginning with zero frequency, can be used in turboelectric propeller drive, but only in certain instances, since this requires that a preheated turbine be stopped and then again accelerated. As far as diesel electric GEU are concerned, such a purely frequency method of starting encounters rather great difficulties.

During the GED starting process, voltage does not remain constant and does not equal the nominal. In view of this, determination of its moment requires preliminary determination of the value of the voltage at motor stator terminals. Voltage values can be determined by the graphic-analytical method.

## § 10.2 Main Propulsion Motor Reversal

In accordance with what is presented in [49], we will examine reversal diagrams for various GED types.

Reversal diagrams for propulsion plants with induction GED. It follows from propeller mechanical characteristics that the process of their reversal (when the vessel continues to move forward gradually) requires very considerable torques from the motors placing the screws in rotation. Thus, for example, if at the /492 end of the reversal of the propellers a vessel continues to move with a speed close to full speed, then their rotation in the opposite direction with nominal

speed would require torque exceeding the nominal by a factor of 3 or more. This generates a requirement to provide a GED with a large overload capability. However, creation of such large torques can turn out to be insufficient to achieve rapid propellor reversal, which can be explained by GED reversing characteristics (Figure 10.3).

Point A (see Figure 10.3a) characterizes the GED operating mode as the vessel moves forward at nominal speed. This mode corresponds to nominal GED torque and rotational speed values. When the propulsion motor is cut out, the propellor shaft, attracted by the screw, will continue to rotate in the same direction, but at a slightly lower speed equal to approximately 73% of nominal. Point B in the figure characterizes this mode. If  $m-1$  of its phases is switched in the motor for the purpose of its reversal, then the curve of torques  $m_A$  will occupy new position  $m'_A$ . It is evident that, in this case as well, the mode will be characterized by the intersection of this curve and the curve of the screw moment of resistance  $m_s$ , i. e., by point  $B_0$ . The proximity of point  $B_0$  to point B demonstrates that connection of a GED with switched phases will not cause any propellor reversal, but rather does virtually nothing to decrease propellor shaft rotational speed. In such a mode, the motor would have to operate with a slight slip  $s \approx 1,7$ , would slightly brake the propellor shaft, and, thereby, would heat up greatly due to the extraordinarily high currents. This unsatisfactory result obtained is caused, apparently, by insufficient torque values the GED develops in slip zone  $s > 1$ .

In order to evaluate correctly whether or not an unsatisfactory mode has been caused by absence of motor parameter correlation or by its poor use, we will turn to the following expression determining the value of induction motor torque:

$$m_A = \frac{mp\omega_2^2 E_1^2}{2\pi f_1 \omega_1 K_s^2} \cdot \frac{r_2 s}{f_1 [r_2^2 + s^2 (2\pi f_1 L_2)^2]} \quad (10.1)$$

Here,  $K_s = \frac{\Phi_1}{\Phi}$ , where  $\Phi_1$  is total flux created by stator windings;  $\Phi$  is net flux permeating stator and rotor windings;  $L_2$  is a self-induction factor of flux dispersion in the rotor, i. e., of the flux coupling only with rotor current when its value equals 1 ampere.

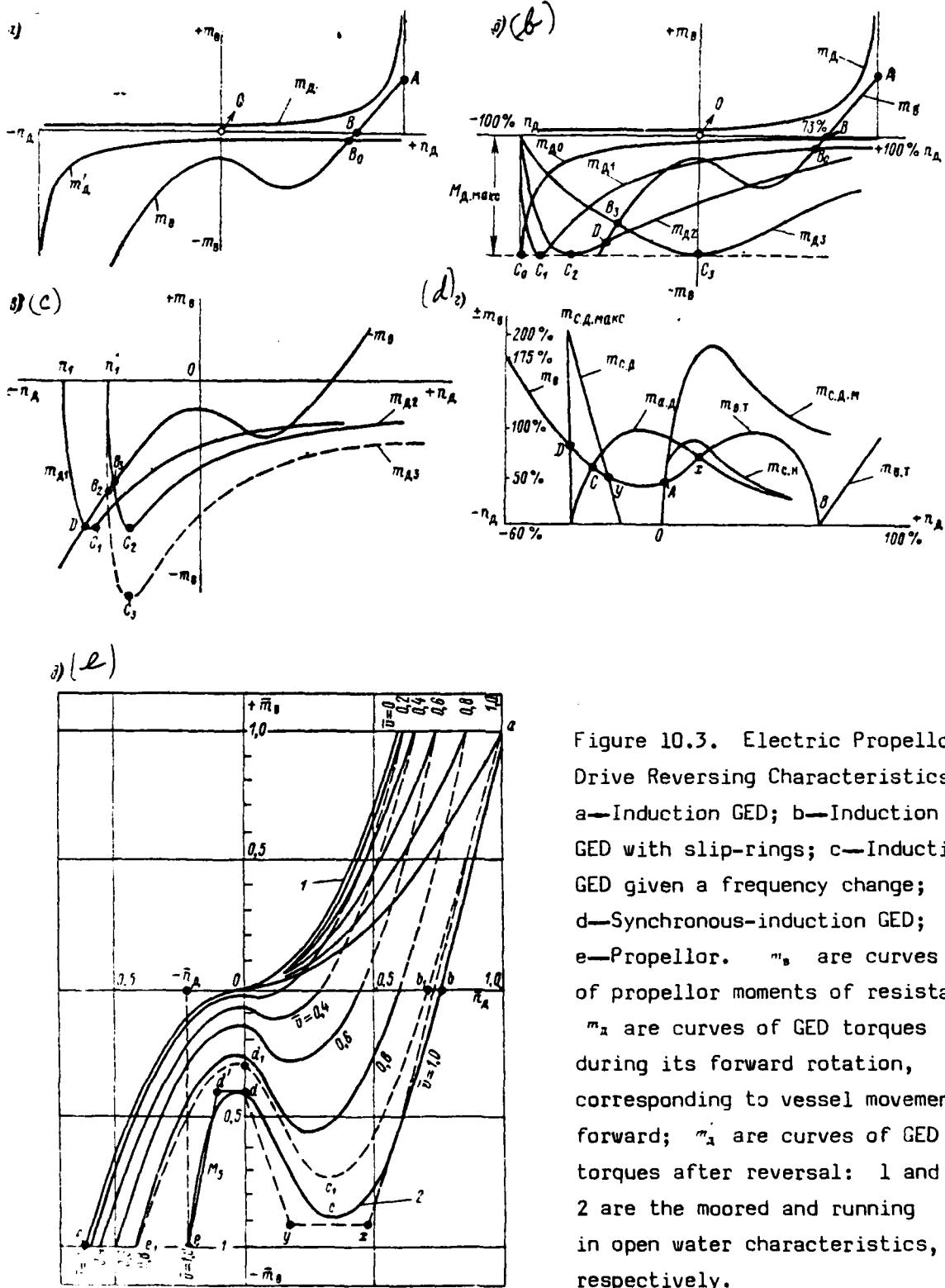


Figure 10.3. Electric Propellor Drive Reversing Characteristics: a—Induction GED; b—Induction GED with slip-rings; c—Induction GED given a frequency change; d—Synchronous-induction GED; e—Propellor.  $m_A$  are curves of propellor moments of resistance;  $m_D$  are curves of GED torques during its forward rotation, corresponding to vessel movement forward;  $m_A'$  are curves of GED torques after reversal: 1 and 2 are the moored and running in open water characteristics, respectively.

Expression (10.1) demonstrates that motor torque  $m_x$  at a specific speed of its rotation will depend only on values  $E_1$ ,  $r_2$ , and  $f_1$ , i. e.,

$$m_x = \psi(E_1, r_2, f_1).$$

Given induction motors with slip-rings, it is possible to regulate the /493 torque value at a given rotational speed by a change in rotor circuit resistance. Here, as is known, the numerical value of critical moment  $m_k$  remains unchanged. Actually, if we take the derivative from the expression for  $m_x$  (10.1), compare it to zero, and solve the resultant equation for  $s$ , then we will get

$$s = \frac{r_2}{2\pi f_1 L_2}; \quad (10.2)$$

$$m_k = \frac{mp\omega_1^2 E_1^2}{8\pi f_1 \omega_1^2 K_1^2 L_2}. \quad (10.3)$$

The absence in expression (10.3) of resistance  $r_2$  confirms independence of its value  $m_k$ .

It is possible to illustrate the process of reversing an induction propulsion motor with slip-rings by the characteristic shown in Figure 10.3b. Here, curve  $m_x$ , determines torques developed by GED where rheostat resistance in the rotor circuit  $R = 0$ . Changing this resistance by sequential connection of its sections  $R_1, R_2, R_3$ , and so on, we will get, respectively, torque curves  $m_{x1}, m_{x2}, m_{x3}$  and so forth. Their peaks  $C_1, C_2, C_3$ , corresponding to critical moments  $m_k$ , lie on straight line  $C_0C_3$  parallel to the X-axis and, by virtue of an increase in values  $R$ , the peaks of curves  $m_{xi}$  will shift to the right, i. e., towards an increase in slips.

The characteristic examined demonstrates that, given a sufficient magnitude of resistance connected to the GED rotor circuit, the form of the curve of torques  $m_{xi}$  will insure a transition to a mode in which the propellor shaft turns in the opposite direction. Thus, for example, given magnitude of resistance in the rotor external circuit  $R_3$ , the torque curve will occupy position  $m_{x3}$  and point  $B_3$  lying in the quadrant of negative values  $n_x$  already will characterize the set mode.

When, during the reversing process, the propellor shaft begins to rotate in the opposite direction, then in many cases it is useful, on the other hand, to reduce resistance  $R$ , to value  $R_2$  for example, to achieve a more significant effect. Then, the set mode (with joint operation of the propellor shaft and GED reversing characteristic) can be shifted from point  $B_3$  to point  $D$ , further from the origin of coordinates in the negative direction.

If there is a need to boost the reversal even further, one then must change not only values  $r_2$ , but  $E_1$  as well, changing voltage  $U$  applied to the GED stator.

It is possible to increase voltage  $U$  by increasing (boosting) main generator field current. This requires the presence either of an exciter with a large field current regulation factor (on the order of at least 4) or so-called boosters. The armatures of the latter are connected in series to the exciter armatures /496 in the main generator field winding circuit. Boosters can provide a 20-30% increase in main generator voltage compared to nominal.

However, one should keep in mind that essentially it is advisable to increase voltage applied to a GED only in those zones where motor torques are close to the motor's critical value, i. e., in the zone of relatively slight slips. In the slip zone where  $s = 1-2$ , this measure turns out to be insufficient as a result of low motor torque values at nominal voltage. This also can lead only to overheating of the motor's stator and rotor windings and its steel.

If the conditions required for a significant voltage increase are absent during reversal, then in this instance one must use a change in the frequency of the feed current by decreasing main generator rotational speed. Two variations are possible here. In the first variation, field current remains as before during a decrease in frequency and then, as is evident from expression (10.3), the maximum value of motor torque will remain practically unchanged since ratio  $\frac{E_1}{f_1} = \text{const}$ . However, thanks to a shift in the position of the peak of curve  $m_{A1}$  from point  $C_1$  to point  $C_2$ , it is possible to improve the mode significantly (see Figure 10.3b).

In another variation, when a decrease in frequency is accompanied by an increase in field at the main generators and, consequently, of net magnetic flux, ratio  $E_1/f_1$  increases slightly. Since, in accordance with expression (10.3), the maximum

magnitude of torques is proportional (all other conditions being equal) to the square of this ratio, then, as a result, a more efficient reversal is provided. The dotted line in Figure 10.3c characterizes this variant.

The recommendation is gradually to shift from the decreased frequency to the nominal to further increase propellor rotational speed in the opposite direction after the mode denoted by points  $B_2$  or  $B_3$  in the figure has been attained. It is possible also to reduce field current to the nominal value to avoid extraordinary overheating of main generators. Here, the GED operating mode will shift to point D.

Reversal diagrams for propulsion plants with synchronous and synchronous-induction GED. The propellor reversal process in GEU with synchronous motors is complicated by the fact that the motors need to be transferred to asynchronous operation. In addition, it is advisable in the intermediate stage of reversal to use GED dynamic braking to accelerate propellor shaft retardation. Synchronous propulsion motors need to be equipped with powerful damper windings playing /497 the role of induction windings during the reversal to provide sufficient reversal process efficiency when such motors operate asynchronously. Thanks to the circumstance that the motor is envisioned for both synchronous and asynchronous operation, the reversal process for synchronous-induction GEU flows more effectively, but the sequence of both stages of operation, in the main, remains analogous.

A synchronous-induction GED is reversed in the following sequence:

- the speed governor for the main diesels or main turbogenerators will be set to a position equating approximately to 25-30% of full speed;
- switching of GED phases will occur, having first cut out their field and that of the main generators;
- field is connected in the GED, if required, then boosting, and they are forced to shift to operation as generators. Here, propellers rotated by the GED are retarded until almost a complete stop;
- field is connected to the main generators and is cut out from the GED, which then shift from the generator mode to operation as induction motors at a frequency of 25% of nominal;
- after the main propulsion motors develop speed approximating 25% of nominal in the opposite direction, they are supplied maximum field and transfer to the synchronous mode. After the motors go into synchronization, field is reduced to the minimum;

— main generator rotational speed gradually increases and, consequently, GED rotational speed simultaneously does the same, bringing the speed smoothly up to the assigned value.

The reversing characteristic of GEU with synchronous-induction motors is shown in Figure 10.3d. Curve  $m_{a,\tau}$  is the curve of the screw braking torques. For greater characteristic compactness, quadrants with negative torques are rotated  $180^\circ$  around the X-axis and combined with the positive quadrants. Curve  $m_{c,d,max}$  corresponds to the mode in which a GED operates as a synchronous generator with maximum field and of main generators with field cut out and operating as induction motors. When the propellor turns out to be retarded sufficiently and the mode approaches point A, it is possible to decrease the degree of GED field to the nominal value. As a result, curve  $m_{c,u}$  will characterize torques developed by the motor. It should be noted that it is impossible to achieve complete stopping of the screw during braking in the aforementioned manner or during any dynamic braking. However, point A essentially characterizes the mode usually close to complete screw stoppage.

The very reverse of the propellor itself is the next stage. The curve of torques  $m_{a,d}$  characterizes the first zone of this reverse, corresponding to GED asynchronous operation at a frequency of about 25% of nominal. Point C /498 will determine the dynamic equilibrium mode. Maximum field, which corresponds to transfer in the characteristic from point C to point D, is transmitted to it for GED transition to synchronous operation, while the curve itself acquires new form  $m_{c,d}$ . It is possible after the GED goes into synchronization to begin to increase main generator rotational speed to the nominal value.

One must pay attention in the mode change process to adherence to the following conditions: during the transition from curve  $m_{c,u}$  to  $m_{a,d}$ , point x of the intersection of the curves of the motor torque  $m_{a,d}$  and of the screw  $m_{b,\tau}$  must lie to the right of point A since only then will the process continue in the direction of reversal. Next, during transition from the curve of torques  $m_{a,d}$  and  $m_{c,d}$ , point y of intersection of curve  $m_{c,d}$  with curve  $m_{b,\tau}$  also must lie to the right of point C. In addition, condition  $m_{a,d} > m_{b,\tau}$  must be observed at points x and y.

Stages of GED reversal and methodology of their calculation. The process of ac GED reversal and vessel braking can be divided into the following three stages.

1. GED disconnect from electric propulsion bus bars and its preparation for the braking and reversal process. Motor self-braking from curve ab to propellor rotational speed value  $Ob$  (see Figure 10.3e, curve  $\bar{v} = 1$ ) as these operations are being accomplished; here, screw moment of resistance is assumed to be zero.

2. GED braking by means of plugging (countercurrent flow) from the speed determined by the same segment  $Ob$  until the motor stops completely. Here, the propellor, flowing as the vessel moves due to inertia of the oncoming water current, places it in rotation, i. e., operates in the water turbine mode, developing negative (propelling) moment. Early in this stage (and sometimes even early in the first stage), generator rotational speed and, consequently, its frequency as well, are reduced to a value equalling 0.2-0.4 of nominal.

3. GED reverse occurs after it stops, i. e., starting in the opposite direction of rotation to rotational speed equalling approximately  $(0.2-0.3) \bar{n}_{d. nom}$  at which the screw develops nominal moment of resistance. Next comes intensive vessel braking using the frequency method, i. e., with a slow, over a period of several minutes, increase in frequency by increasing primary motor rotational speed.

Attention should be placed on the fact that reversal of an ac GED is more prolonged than for a dc drive. Therefore, vessel translational velocity during the reversal process is decreased more vigorously. This can be envisaged ahead of time, having assumed as the computational characteristic reversing characteristic  $a, b_1, c_1, d_1, e_1$  (see Figure 10.3e) — the average among the characteristics where vessel speeds  $\bar{v} = 1$  and  $\bar{v} = 0.8$  (dotted).

We will dwell in more detail on all three stages of GED reversal in order /499 to explain several special features of this process.

In the first stage of reversal, following receipt of the appropriate command, primary motor rotational speed is decreased to the minimum stable speed comprising 0.2-0.33 of nominal. Depending on diesel or turbine special design features,

this stage will last from several to dozens of seconds; field is removed from the generator and the GED (if a synchronous-type motor) and the generator magnetic field killing circuit is cut in (and, given a synchronous motor, its magnetic field killing circuit also is cut in).

These operations in several plant types are accomplished in the following manner: the primary motor automatic speed governor is transferred to the minimal stable rotational speed (0.2-0.3 of nominal), as a result of which after several seconds it opens the access of steam to the turbine or fuel to the diesel. Simultaneously, the generator and GED (if it is synchronous) magnetic field killing circuit is cut in. As a result, the turbogenerator or diesel generator due to mechanical and ventilation losses begins to lose its rotational speed.

The propellor, deprived of torque from the GED, also reduces rotational speed, expending intrinsic kinetic energy and motor rotor energy to operate the hydrodynamic forces creating screw thrust. Thus, due to the decrease in moment of hydraulic resistance from curve ab (see Figure 10.3e), screw rotational speed attains value  $0b$ ; here, torque will equal zero. Generator magnetic flux will be killed in about 2 seconds (see Figure 10.1), with closing off of steam or the fuel supply continuing also about 2 seconds.

Everything stated makes it possible to introduce several assumptions considerably simplifying calculation, to wit: one can assume that screw self-braking from curve ab begins only at the moment when the generator simultaneously loses both voltage and primary motor propelling moment. This assumption thus somewhat extends the duration of the first stage of reversal.

If it is a synchronous GED, the moment arrives during the killing of its and the generator's magnetic fields when the motor drops out of synchronization. This is accompanied by current and torque kicks, although they are insignificant in magnitude and temporary, as is evident from the curvature of curve 4 in Figure 10.1. One can obtain a representation of the numerical values of such current and torque kicks from oscillograms of the reversal of the turboelectric ship "Abkhaziya" [50].

2-5 %

When the generator magnetic flux reaches about ~~2%~~ of nominal, GED rotating field reversal is accomplished by switching two of its phases. If the aforementioned

conditions are accomplished, then the reversing switch breaks generator residual current (1-1.5% of nominal).

It should be noted that there is a special position, "Hold," between the /500 zero and first positions on the control wheel aboard in-service electric ships operating on alternating current (for example, the diesel electric ship "Rossiya"), where reversal is accomplished in much the same way as described above. As the GED is stopped and reversed, operating personnel hold the wheel in that position until the moment currents in the main circuit as magnetic fields are being killed reaches values about 1-1.5% of nominal. Overall, the reversing switch is designed to break the circuit when current is absent in it. After phase switching, maximum boosted field is supplied to the generator, resulting in the motor transferring to the braking mode by means of countercurrent flow [50].

The duration of the reversal's first stage is determined by adding the time segments watch personnel require to accomplish the enumerated operations. If one keeps in mind remote control (from the station) by the primary motor governor, reversing switch, and generator field regulator, then the duration of the operation will be 5-8 seconds, given that the time for reduction of primary motor rotational speed (from nominal to minimum stable speed) does not exceed 3 seconds.

It is possible more precisely to determine the period of the reversal's first stage if one calculates the time expended on screw self-braking from the formula

$$\Delta t = \frac{GD_{\text{д. ном}}^2 \Delta n_{\text{д}}}{375 M_{\text{в. ном}} (m_{\text{д. ср}} - m_{\text{в. ср}})} \quad (10.4)$$

The second stage of a reversal begins at the moment countercurrent flow braking mode is established in the GED, i. e., from the moment of origin of a rotating magnetic field in the motor in a direction opposed to rotor rotation. The GED stator winding in this mode is fed from an overexcited generator, while the rotor turns in the direction opposite to the stator pole with slip  $s \geq 1$ . Next, the rotor gradually loses its speed and, in its starting cells, energy absorption occurs (in the form of heat emission), formed from:

— the kinetic energy reserve of the gyrating masses of the rotor, propellor shaft, and propellor, reducing to zero the speed of its rotation, beginning with the value corresponding to segment 0b (see Figure 10.3e);

— the propellor's kinetic energy, which, given a decrease in rotational speed from the value of the same segment 0b to zero, operates in the hydraulic turbine mode and supplies mechanical energy to the GED rotor;

— the turbogenerator (or diesel generator), whose rotational speed is reduced to 0.2-0.33 of nominal.

Countercurrent flow braking ends at the moment of equilibrium of torques is achieved: of propellor torque equal to segment 0d and of GED electromagnetic moment created by the stator rotating magnetic field where  $s = 1$ . The motor /501 loses its rotational speed and will stop at the instant equilibrium of the aforementioned torques is established. In essence, the second reversal stage ends at this point, followed by starting of the GED in the opposite direction of rotation.

Special emphasis needs to be placed on the fact that vessel braking, following the reversal and lasting several minutes, is possible with frequency control of motor rotational speed with a slow increase in generator frequency from 0.3-0.4 up to 0.6-0.7 of its nominal value. At nominal frequency, it is impossible to brake a vessel as a result of too large slip losses in rotor starting cells and losses in generator and GED stator windings. Thus, reversal of a shorted synchronous and induction GED and subsequent braking of a vessel moving forward at full speed can be accomplished using the aforementioned method only with conservation of safe generator and motor overheating.

Calculation of a reversal's second stage using the approximation by iteration method is done in the following sequence (relative only to TEGU).

Initially, turbogenerator rotational speed losses in the first stage of reversal are determined, given simultaneous reduction of turbine rotational speed and generator and GED (synchronous) magnetic field killing. Here, one must consider that its greatest losses in the rotation process without an influx of steam comprise turbine ventilation losses, whose moment of resistance  $m_{T.vent}$  is proportional to the square of the rotational speed. Consequently, if one uses  $M_{T.vent}$  to designate the moment of ventilation losses at turbine nominal rotational speed  $n_{r,ном}$ , then for the time segment corresponding to average turbine rotational speed  $n_{r,ср} = n_{r1} + \frac{\Delta n_{r1}}{2}$ , the moment of ventilation (mechanical losses)  $m_{T.vent}$  (disregarding

terms of second order infinitesimal) can be computed from the following expression (in relative units):

$$\begin{aligned} \bar{m}_{\tau, \text{VENT}} &= \bar{M}_{\tau, \text{VENT}} \bar{n}_{r, \text{CP}}^2 \approx \bar{M}_{\tau, \text{VENT}} \left( \bar{n}_{r1} + \frac{\Delta \bar{n}_{r1}}{2} \right)^2 \approx \\ &\approx \bar{M}_{\tau, \text{VENT}} (\bar{n}_{r1}^2 + \bar{n}_{r1} \cdot \Delta \bar{n}_{r1}), \end{aligned} \quad (10.5)$$

where  $\bar{M}_{\tau, \text{VENT}}$  is the relative value of the moment of ventilation losses (relative to nominal primary motor torque);  $\bar{n}_{r1}$  is the relative value of turbogenerator rotational speed at the initial moment in time;  $\Delta \bar{n}_r$  is the rotational speed increment for the examined time segment.

Having substituted the value of the moment of ventilation losses based on (10.5) in the torque equilibrium equation (6.1a) and having solved it for rotational speed increment  $\Delta \bar{n}_r$ , we will get

$$\Delta \bar{n}_r = \frac{-\bar{M}_{\tau, \text{VENT}} \bar{n}_{r1}^2 - \bar{m}_{r, \text{CP}}}{\frac{GD_{\text{ДГ}}^2}{375} \cdot \frac{\bar{n}_{r, \text{НОМ}}}{M_{\text{ДЗ, НОМ}} \Delta t} + \bar{M}_{\tau, \text{VENT}} \bar{n}_{r1}} \quad (10.6)$$

where  $\bar{m}_{r, \text{CP}}$  is the average generator torque value expressed in relative units;  $GD_{\text{ДГ}}^2$  is the turbogenerator or diesel generator moment of gyration.

One can assume that the moment of resistance in diesel generators is constant and equals  $(0,2-0,25) M_{r, \text{НОМ}}$ , while rotational speed losses can be computed from formula

$$\begin{aligned} \Delta \bar{n}_r &= \frac{375 \bar{M}_{r, \text{НОМ}} (-\bar{M}_{\tau, \text{VENT}} - \bar{m}_{r, \text{CP}}) \Delta t}{GD_{\text{ДГ}}^2 \bar{n}_{r, \text{НОМ}}} = \\ &= T_M (-\bar{M}_{\tau, \text{VENT}} - \bar{m}_{r, \text{CP}}) \Delta t. \end{aligned} \quad (10.7)$$

Designation  $\Delta t$  infers the overall duration of operations equalling 4-6 seconds, given determination of generator speed losses in the first stage of reversal from formulas (10.6) and (10.7). Average generator torque values occurring during these operations can be assumed to equal, respectively

$$\frac{1+0}{2} = 0,5 \quad \text{and} \quad \frac{0+1}{2} = 0,5.$$

Hence, the average value of the resultant torque during all three operations included in the aforementioned formulas can be assumed to equal

$$m_{r, \text{cp}} \approx \frac{2 \cdot 0,5 + 1,0 + 2 \cdot 0,5}{2 + 1 + 1} = 0,6.$$

Using formula (10.4) and disregarding friction torque in the propellor shafting line, we will substitute in it the motor rotational speed value in segment Ob (see Figure 10.3e) instead of  $\Delta \bar{n}_x$  and, instead of  $\bar{m}_{x, \text{cp}}$ , the average ordinate of area Ob, c, d, 0 and  $\bar{m}_{x, \text{cp}} = 0,5 (\bar{m}_{x1} + \bar{m}_{x2})$ , where  $\bar{m}_{x1}$  and  $\bar{m}_{x2}$  are GED torques at the beginning and the end of braking, approximately determining duration  $\Delta t_2$  in the second stage of reversal.

From formulas (10.6) and (10.7), we will find generator rotational speed losses, in these formulas substituting, in place of  $\Delta t$ , second stage duration  $\Delta t_2$  and value  $\bar{m}_{r, \text{cp}} = 0,5 (\bar{m}_{r1} + \bar{m}_{r2})$ , where  $\bar{m}_{r1}$  and  $\bar{m}_{r2}$  are generator torques at the beginning and at the end of braking. For diesel GeU, where a diesel generator quite rapidly loses its rotational speed, one should make a determination of the generator speed loss in two or in three stages.

In view of the fact that, in practice, relationship  $\bar{n}_r = f(\bar{n}_x)$  is almost linear, one can introduce certain refinements into the calculations, such as: the section of the GED rotational speed change curve from point b to point d, where  $n_x = 0$  (see Figure 10.3e), is divided into several segments and, for resultant values  $\bar{n}_x$ , GED braking torques are computed, as pointed out above, for time segment  $\Delta t$  — from formula (10.4) and refined values  $\Delta \bar{n}_r$  — from formulas (10.5) and (10.7). Slight discrepancies among relationship  $\bar{n}_r = f(\bar{n}_x)$ , values assumed at the outset and obtained from the calculation in this case are of little significance since motor braking torques change little, in the frequency change range by 10%.

The third stage does not differ from the starting process examined for a synchronous or induction electric motor in the first two stages, but is accomplished in reverse and at a constant frequency. The methodology of calculating such starting involves the following.

After a synchronous GED is placed in synchronization or an induction motor attains normal slip, a further increase in propeller rotational speed to brake the vessel is accomplished by means of frequency regulation, i. e., by a smooth increase in generator (primary motor) rotational speed. Primary motor overload during calculations of reversal and starting can be determined by computation of generator torque from formula

$$m_r = \delta_n^2 \cos \psi \left[ (X_n + X_{aq}) \sin \psi + \frac{(r_n + r_1) \cos \psi}{f} \right], \quad (10.7a)$$

where  $\delta_n = \frac{1}{\cos \varphi - f}$ ;  $r_1$ ;  $X_n$ ;  $X_{aq}$  are generator parameters. Here, it should be considered that a safe torque overload comprises for turbines is  $0.4M_{r, \text{nom}}$ , for diesels is  $0.1M_{r, \text{nom}}$ , and for temporary overloads lasting 2-3 seconds is  $(1.5 \div 2.5) M_{r, \text{nom}}$ . Instantaneous rotational speed "gaps" will correspond to these overloads, while, for turbogenerators, they are restored independent of their values, while, for diesel generators, only in those cases where the gap does not attain the lower range of the stable rotational speed value (from 0.1 to 0.33 of nominal). It is possible to compute the value of the gap, given absence of access of steam to the turbine or fuel to the diesel from formulas (10.6) and (10.7), while, given influx of steam or fuel, by the formula written in the form of finite increments:

$$\Delta \bar{n}_r = \frac{M_{\text{дв. ном}} 375 (\bar{m}_{\text{дв. ср}} - \bar{m}_{r, \text{ср}}) \Delta t}{GD^2 \bar{n}_{r, \text{ном}}} \quad (10.8)$$

In expression (10.8),  $\bar{m}_{r, \text{ср}}$  is the average value of the overload torque for time segment  $\Delta t$ , found from formula (10.7a) or from the  $\bar{m}_r = f(t)$  graph.

#### Measures to improve alternating current starting and braking characteristics.

Insufficient starting and braking torques a main propulsion motor develops during reversals will lead to the fact that reversal of a shipboard GED encounters great difficulties when the vessel is moving at full speed. Consideration must be made for the time of vessel speed drop to a value where maximum moment of propeller hydraulic resistance according to the reversing characteristic becomes less than the GED braking torque. Maneuvering characteristics can be improved through adoption of the following measures:

- by use of automatic transient process regulation and control systems insuring

accomplishment of the latter based on optimal characteristics;

— by an increase in generator field boosting during a simultaneous transition to a lower frequency for the purpose of increasing GED torque;

— by use of an automatic generator field boosting regulating system insuring even boosting at initiation of braking and maximum boosting during the transition through the maximum propellor moment of resistance;

— by using GED with more favorable torque overload characteristics;

— by use of GD dynamic braking, with subsequent transition to countercurrent flow braking.

### § 10.3 Calculation of Generator Excitation Characteristics

Initial calculation data. The duration of generator or synchronous GED voltage (magnetic flux) build-up and blanking processes is commensurate with the duration of electric propellor drive starting and reversing processes. Therefore, the nature and duration of change of these voltages must be determined beforehand and considered in calculations.

Coupling between magnetic flux  $\Phi$  (or emf  $E_r$ ) and field current  $I_{ar}$  during an idling generator's magnetic flux build-up and blanking is determined by the idling characteristic (Figure 10.4). Generator energy supplied by the exciter during excitation is confined in the magnetic flux and, during blanking, it is absorbed by discharging resistance or returns to the exciter, depending on the blanking system used.

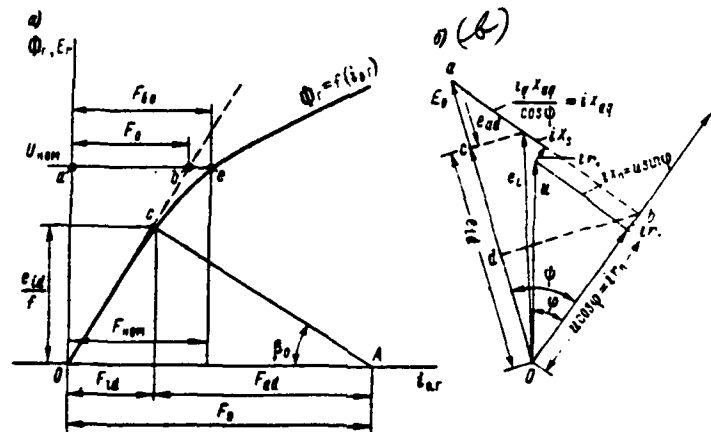


Figure 10.4. Generator Idling Characteristics (a) and Its Vector Diagrams (b).

The stator reaction exerts material influence on the process of generator magnetic flux excitation or blanking process when the generator is running a rotating or braked electric motor. Here, coupling between resultant generator magnetic flux (along the longitudinal axis) and field current is expressed by magnetization curves  $\Phi_r = f(i_{a,r})$ .

When calculating GED starting and reversing processes, one must have available: the idling generator and synchronous motor magnetic flux field and blanking characteristic as the upper threshold, with the lower being the magnetic flux /505 field and blanking characteristic of a generator connected to a stationary shorted motor. In addition, one must determine the values of applied active  $r_n$  and inductive  $X_n$  resistance, where slip  $s = 1$  and frequency  $\bar{T}_n = 1$ .

Calculation methodology. We will examine construction of so-called "threshold characteristics," i. e., curves of an idling generator's magnetic flux field and blanking and when it runs a stationary or slowly rotating shorted electric motor (change curves  $\Phi_r = f(t)$ ). Here, one should keep in mind that, for normal operating conditions, the generator idling mode generally has no practical significance, while for ac GED (both synchronous and induction), it even is impracticable since, in all operating modes, it remains connected to the generator (with the exception of a very short period when two phases are switched prior to reversal).

A GED is started and reversed by means of boosted field of an already rotating generator, with transition to normal field occurring only upon the conclusion of starting and reversing transient processes. How a GED is taken out of operation (stopped) depends on the type of motor: this occurs for an induction motor by removing field from the generator (by cutting out field current) and, for a synchronous motor, by simultaneously removing or slightly shifting over time field removed both from the generator and from the GED.

Thus, calculation of electric propellor drive starting and reversing processes requires having two threshold characteristics available: the idling synchronous motor and generator magnetic flux field and blanking characteristic as the upper threshold and the generator (connected to a stationary shorted motor) magnetic /506 flux field and blanking curve as the lower threshold. For this, characteristic  $\Phi_r = f(t)$  will be constructed, with this done in the following manner.

We will find the values of parameters  $r_n$  and  $X_n$  where slip  $s = 1$  and frequency  $f_{\text{NOM}} = 1$ . Then we determine  $\text{tg } \beta_0$  (Figure 10.4a).

In light of the approximate nature of the transient process calculations made (stipulated by insufficient validity of propellor reversing characteristics in the negative torque area), it is possible when calculating field characteristics to disregard the delaying effect of eddy currents in the magnetic circuit, also considering the short duration of the transient processes in the stator winding. In addition, one can assume for consideration of exciter intrinsic time that the rise and fall of its voltage does not occur instantaneously, but with a lag on the order of 0.5 seconds.

The emf electrical equilibrium circuit for a generator or synchronous motor field circuit has the form

$$u_{b,r} = i_{b,r}(r_{b,r} + r_{b,r,A}) + \frac{2p_r w_{b,r} K_w (0,2 + 0,8\sigma_b) d\Phi_r}{dt}, \quad (10.9)$$

where  $u_{b,r}$  is exciter voltage;  $i_{b,r}$ ;  $r_{b,r}$  are generator field current and field winding resistance, respectively;  $r_{b,r,A}$  is additional or discharging resistance in the field winding circuit;  $2p_r$  is the number of generator poles;  $w_{b,r}$  is the number of field winding turns per pole;  $K_w$  is the winding factor of the field winding, equalling 0.8 for turbogenerators and 1.0 for salient-pole machinery;  $\sigma_b$  is the dispersion coefficient which can be assumed to equal on the average 1.35 for salient-pole machinery and 1.2 for turbogenerators;  $(0,2 + 0,8\sigma_b)$  is a hypothetical dispersion factor of magnetic flux coupled with the complete number of field winding turns;  $\Phi_r$  is the generator magnetic flux to a pole pair.

We will assume as our base values: nominal values of flux at the pole  $\Phi_{r,\text{NOM}}$ , nominal field current  $I_{b,r,\text{NOM}}$ , and nominal voltage at the exciter  $U_{b,r,\text{NOM}}$  corresponding to generator or GD idling at nominal stator voltage and frequency values.

Equation (10.9) in relative units will have the form

$$\frac{\bar{u}_{B,r}}{U_{B,r,NOM}} U_{B,r,NOM} = \frac{i_{B,r}}{I_{B,r,NOM}} (r_{B,r} + r_{B,r,d}) I_{B,r,NOM} + \frac{2\rho_r \omega_{B,r} K_w (0,2 - 0,8\sigma_B) \Phi_{r,NOM} d}{dt} \frac{\Phi_r}{\Phi_{r,NOM}}$$

Having divided all terms by  $U_{B,r,NOM}$ , we will get the emf equilibrium equation in relative units:

$$\bar{u}_{B,r} = \bar{i}_{B,r} \frac{I_{B,r,NOM} (r_{B,r} + r_{B,r,d})}{U_{B,r,NOM}} + \frac{2\rho_r \omega_{B,r} K_w (0,2 - 0,8\sigma_B) \Phi_{r,NOM}}{U_{B,r,NOM}} \cdot \frac{d\bar{\Phi}_r}{dt} \quad (10.10)$$

Converting to finite increments, expression (10.10) can be rewritten: /507

$$\bar{u}_{B,r} = \bar{i}_{B,r} \frac{I_{B,r,NOM} (r_{B,r} + r_{B,r,d})}{U_{B,r,NOM}} + \frac{2\rho_r \omega_{B,r} K_w (0,2 - 0,8\sigma_B) \Phi_{r,NOM}}{U_{B,r,NOM}} \cdot \frac{\Delta\bar{\Phi}_r}{\Delta t}$$

and, solving it for  $\Delta t$ , we will get

$$\Delta t = \frac{2\rho_r \omega_{B,r} K_w (0,2 - 0,8\sigma_B) \Phi_{r,NOM}}{U_{B,r,NOM} \left[ \bar{u}_{B,r} - \bar{i}_{B,r} \frac{I_{B,r,NOM} (r_{B,r} + r_{B,r,d})}{U_{B,r,NOM}} \right]} \Delta\bar{\Phi}_r \quad (10.10a)$$

Since

$$\bar{i}'_{B,r,CP} = \bar{i}_{B,r} + \frac{\Delta i'_{B,r}}{2} = \frac{\bar{i}'_{B,r} + \bar{i}_{B,r}}{2}$$

and

$$\bar{u}'_{B,r,CP} = \bar{u}_{B,r} + \frac{\Delta \bar{u}'_{B,r}}{2} = \frac{\bar{u}'_{B,r} + \bar{u}_{B,r}}{2}$$

(where  $\bar{u}'_{B,r}$  and  $\bar{i}'_{B,r}$  are values of the aforementioned magnitudes at the beginning of time segment  $\Delta t$ , while  $\bar{u}_{B,r}$  and  $\bar{i}_{B,r}$  are values of the same magnitudes at the

end of the same time segment), then, substituting values  $\bar{i}_{\text{в.г.ср}}$  and  $\bar{u}_{\text{в.г.В}}$  in (10.10a), we will get standard working formulas of the type

$$\Delta t = \frac{2\rho_r w_{\text{в.г.}} K_w (0,2 - 0,8\sigma_B) \Phi_{\text{г. ном}} \Delta \bar{\Phi}_r}{U_{\text{в.г. ном}} \left[ \left( \frac{\bar{u}_{\text{в.г.}} + \bar{u}_{\text{в.г.}}}{2} \right) - \left( \frac{\bar{i}'_{\text{в.г.}} - \bar{i}_{\text{в.г.}}}{2} \right) \frac{I_{\text{в.г. ном}} (r_{\text{в.г.}} - r_{\text{в.г.д}})}{U_{\text{в.г. ном}}} \right]}$$

Assuming that  $\bar{u}_{\text{в.г.}}$  is a constant value, we get final standard working formula

$$\Delta t = \frac{2\rho_r w_{\text{в.г.}} K_w (0,2 - 0,8\sigma_B) \Phi_{\text{г. ном}} \Delta \bar{\Phi}_r}{U_{\text{в.г. ном}} \left[ \bar{u}_{\text{в.г.}} - \left( \frac{\bar{i}'_{\text{в.г.}} + \bar{i}_{\text{в.г.}}}{2} \right) \frac{I_{\text{в.г. ном}} (r_{\text{в.г.}} - r_{\text{в.г.д}})}{2U_{\text{в.г. ном}}} \right]} \quad (10.11)$$

#### § 10.4 Calculation of the Starting and Reversal Process for an Electric Propellor Drive with Synchronous Machinery

Assumptions made. Starting and reversing synchronous or induction GED will occur at a reduced frequency and changing generator voltage. Based upon the general theory of induction machinery given varying frequency and on methods of determining the voltage of a synchronous generator with a changing load, Professor V. T. Kas'yanov developed a method of starting and reversing a main propulsion motor [20]. The assumption was made here that transient and supertransient processes are absent during starting and reversing, while the generator voltage change will depend /508 on the established armature reaction value, i. e., on reactive resistance  $X_d$ . This assumption is fully justified since the GED acceleration and braking time is incommensurably greater than the generator transient and supertransient process time, while the current consumed by the motor during the period of an electro-mechanical transient process changes relatively little. The result is that transient current values are insignificant and can be disregarded.

Calculation based on generator static characteristics, i. e., based on parameters  $X_d$  and  $T_d$ , are linked with the most difficult GED operating conditions since the voltage gap in the static mode always is greater than the voltage gap in the dynamic mode ( $X_d \geq X'_d$ ). Therefore, if the calculation given the aforementioned conditions shows that starting and reversing flow reliably and provide conditions sufficient for placing the motor into synchronization, then, under actual conditions (considering transient current values), GED torque as it is cut in apparently will be greater, while the acceleration or braking time will be reduced.

Calculation methodology given GED reversal with plugging. Calculation of the transient process consists of three stages for GED in which plugging is used for the starting and reversing processes:

- 1) determination of resolved (equivalent) GED (induction or synchronous) parameters  $r_n$  and  $X_n$  and its mechanical characteristic;
- 2) calculation of mechanical transient processes;
- 3) determination of motor frequency acceleration time.

First stage: determination of resolved (equivalent) GED (synchronous or induction) parameters  $r_n$  and  $X_n$  depending on the rotor frequency and calculation of the GED mechanical characteristic. Asynchronous starting of a synchronous GED is possible given the presence of a damper cage, whose rod lies in the pole piece slots. During starting and reversing, this type GED operates in the induction mode with alternating frequency and changing voltage. Therefore, in the methodology proposed by V. I. Kas'yanov [20], calculation of transient processes is based upon replacement of the synchronous motor's salient-pole rotor equipped with a starting cage by the equivalent cylindrical shorted rotor. Thus, use of both induction machinery design formulas turns out to be possible for calculation of a synchronous motor's starting and reversing characteristics.

The parameters of a cylindrical shorted rotor equivalent to a synchronous motor's salient-pole rotor are determined in the sequence presented below.

The parameters of a synchronous electric motor are provided in relative units and are designated as follows:

- $r_1$  — stator winding resistance;
- $X_1$  — stator dispersion reactivity;
- $X_{ad}$  — armature reaction longitudinal reactivity;
- $X_{aq}$  — armature reaction transverse reactivity; /509
- $r_b$  — field winding resistance;
- $X_b$  — field winding dispersion reactivity;
- $r_{kd}$  — starting cage resistance along the longitudinal axis;
- $X_{kd}$  — starting cage dispersion longitudinal reactivity;
- $r_{kq}$  — starting cage resistance along the transverse axis;
- $X_{kq}$  — starting cage dispersion transverse reactivity;
- $n_{д. ном}$  — nominal rotational speed;

$\cos \varphi_{\text{НОМ}}$  — nominal power factor;

$k_{\text{НОМ}}$  — ratio of generator nominal current to GED nominal current;

$\frac{GD_2^2}{M_{\text{д.НОМ}}}$  — ratio of propellor shaft moment of gyration to GED nominal torque.

Next, we examine a salient-pole rotor rotating in a stator magnetic field with relative slip  $s = \frac{f_2}{f}$ , where  $f$  is the frequency of the current in the stator and  $f_2$  is the frequency of the current in the rotor in fractions of nominal frequency.

Two electrical circuits parallel relative to magnetic flux are located on the poles' longitudinal axis: starting cage circuit, which given  $s$ , i.e., given frequency  $f_2$ , has resistance  $Z_{kd} = r_{kd} + jf_2 X_{kd}$  and field winding circuit, which, given the same conditions, has resistance  $Z_{fs} = r_f K - jf_2 X_f$ , where  $K$  is the field circuit resistance factor equalling  $K = \frac{r_b + r_{\text{доп}}}{r_b}$ , with  $r_{\text{доп}}$  being additional external resistance to which the field winding is closed during rotor starting and braking.

The resultant rotor resistance along the longitudinal axis, given absolute slip  $f_2$ , is determined from formula

$$Z_{2ds} = \frac{1}{\frac{1}{r_b + jf_2 X_b} + \frac{1}{r_{kd} - jf_2 X_{kd}}} = r_{2d} + jX_{2ds}$$

This same resistance, recomputed from frequency  $f_2$  to the nominal (50 Hz), in a system of relative units will be determined from expression

$$Z_{2d} = r_{2d} + jX_{2ds} \frac{I_{\text{НОМ}}}{f_2} = r_{2d} + jX_{2d} \quad (10.12)$$

Expression (10.12) can be transformed from symbolic into scalar form, which, in a specific instance where  $f_2 = 0$ , has the form:

$$r_{2d0} = \frac{r_b r_{kd}}{r_b + r_{kd}}; \quad X_{2d0} = \frac{r_b^2 X_{kd} + r_{kd}^2 X_b}{(r_b + r_{kd})^2} \quad (10.13)$$

Resultant impedance  $Z_2$  of a nonsalient-pole rotor at frequency  $f_2$ , recomputed

to nominal frequency, can be assumed to equal the half-sum of its resistances /510 along the longitudinal and transverse axes [20].

$$Z_2 = \frac{r_{kd} + r_{kq}}{2} + j \frac{X_{kd} + X_{kq}}{2} = r_2 + jX_2. \quad (10.14)$$

Considering that there are two electrical circuits with different parameters along the rotor's longitudinal axis, it becomes possible, as will be seen next, to look upon the salient-pole rotor of synchronous machinery as the rotor of a double squirrel-cage motor, with its corresponding properties, to wit: resultant resistance  $r_2$  and resultant impedance  $X_2$  determined from formula (10.14) change with a change in frequency  $f_2$ . Relationships  $r_2 = \varphi(f_2)$  and  $X_2 = \varphi_1(f_2)$  can be expressed in the form

$$r_2 = r_{20}K_r \text{ и } X_2 = X_{20}K_x, \quad (10.15)$$

where  $r_{20}$  and  $X_{20}$  are the values of parameters  $r_2$  and  $X_2$  in the limiting case of rotor zero frequency determined from expressions (10.13) and (10.14). Value  $K_r$ , which changes depending on frequency  $f_2$  is referred to as the rotor resistance increase factor, while value  $K_x$  is the rotor reactivity decrease factor. These factors, being individual synchronous motor characteristics, can be constructed with the help of (10.15): first, we will find values  $r_{20}$  and  $X_{20}$  from expressions (10.13) and (10.14), followed by computation of their actual values ( $r_2$  and  $X_2$ ).

With the help of curves  $K_r = \varphi_1(f_2)$  and  $K_x = \varphi_2(f_2)$ , it is possible to compute all characteristics of a synchronous machine operating in an asynchronous mode from the general formulas for an induction machine, substituting in them the actual values of parameters  $r_2$  and  $X_2$  from formula (10.15).

The synchronous motor equivalent parameters obtained ( $X_1, r_1, r_2, X_2$ ) are substituted in the formulas for an induction motor.

The current, torque, and power factor of a GED operated at frequency  $f$  and slip  $s$  by a generator with the given parameters and field current, in accordance with the aforementioned methodology, are determined in the following sequence.

Formulas for the motor's mechanical characteristic are used for calculation of the influence of the voltage and frequency change:

$$\bar{m}_a = \frac{\delta u_1^2 r_2'}{f \left( \alpha s + \beta + \frac{\gamma}{s} \right)} \quad (10.16)$$

The factors entering into formula (10.16) can be obtained from the following expressions:

$$\delta = \frac{1}{\cos \varphi_{\text{ном}} - r_1}; \quad (10.17)$$

$$\alpha = [C_2 r_1]^2 + f^2 [X_1 + C_1 X_2']^2; \quad (10.18)$$

$$\beta = 2r_1 r_2'; \quad (10.19)$$

$$\gamma = \left[ \frac{r_1 r_2 b}{f} \right]^2 + [C_1 r_2']^2. \quad (10.20)$$

Here,  $r_1$  and  $X_1$  are stator resistance and inductive impedance;  $r_2$  and  $X_2$  are rotor resolved resistance and inductive impedance.

$$b = \frac{1}{X_m}; \quad (10.21)$$

$$C_1 = 1 + \frac{X_1}{X_m}; \quad (10.22)$$

$$C_2 = 1 + \frac{X_2'}{X_m}, \quad (10.23)$$

where  $X_m$  is mutual induction resistance.

Maximum torque is determined from expression

$$\bar{m}_{a, \text{maxc}} = \frac{\delta u_1^2 r_2'}{f (\beta \pm 2 V \alpha \gamma)} \quad (10.23a)$$

(the minus sign corresponds to the generator mode).

In order to determine slip given maximum torque (critical slip  $s_{kp}$ ), we compare the derivative from expression (10.16)  $\left(\frac{d\bar{m}_n}{ds} = 0\right)$  to zero, hence

$$s_{kp} = \pm \sqrt{\frac{Y}{\alpha}}. \quad (10.24)$$

Stator current will be found from expression

$$\bar{i}_1 = \bar{u}\bar{Y}_n = \bar{u}(g_n - jb_n), \quad (10.25)$$

where

$$g_n = \frac{r_1 C_2^2 s + r_2' + \left[ r_1 + \frac{r_{n2}'^2 b^2}{f^2 s} \right]}{\alpha s - \beta - \frac{Y}{s}}; \quad (10.26)$$

$$b_n = \frac{C_2 (X_1 + C_1 X_2') / s \left[ \frac{C_1 r_{n2}'^2 b}{f s} \right]}{\alpha s - \beta - \frac{Y}{s}}. \quad (10.27)$$

One can disregard the expressions in the square brackets in formulas (10.26) and (10.27) due to their relative insignificance.

Equivalent resistance and its active and reactive components are determined from the following expressions

$$Z_n = \frac{1}{Y_n} = r_n + jX_n, \quad (10.27a)$$

where

$$\left. \begin{aligned} r_n &= \frac{\sigma_n g_n}{g_n^2 + b_n^2}; \\ X_n &= \frac{\sigma_n b_n}{g_n^2 + b_n^2}; \end{aligned} \right\} \quad (10.28)$$

$$\sigma_n = \frac{I_{r, \text{ном}}}{I_{\Delta, \text{ном}}}; \quad (10.28a)$$

$g_n, b_n$  are GED conductance and susceptance, respectively.

Stator current is determined from formula

$$\bar{i}_1 = \frac{u_1}{\sqrt{r_n^2 + X_n^2}}, \quad (10.29)$$

and the power factor from formula

$$\cos \varphi = \frac{1}{\sqrt{1 + \operatorname{tg}^2 \varphi}}, \quad (10.30)$$

where

$$\operatorname{tg} \varphi = \frac{b_n}{g_n} = \frac{X_n}{r_n}. \quad (10.31)$$

Using expressions (10.12), (10.25), and (10.26), it is possible to calculate the values of stator current torque and GED power factor given any frequency and voltage values.

Generator voltage during the GED starting process is determined with the help of a vector diagram for a salient-pole synchronous machine (Figure 10.4b), given known values of external circuit resistance, field current, and nominal frequency, as well as the generator idling characteristic.

Voltage vector  $u$  can be divided into two components:  $ir_n = u \cos \varphi$  and  $iX_n = u \sin \varphi$ . Side  $Ob = i(r_n + r_1)$ ; side  $ab = u \sin \varphi + i(X_s + X_{ad}) = i(X_n + X_d)$ . Given alternating frequency, equivalent inductive impedances are proportional to frequency. The internal emf longitudinal component is

$$e_{id} = Od + dc = i(r_n + r_1) \cos \psi + i(X_n + X_s) f \sin \psi. \quad (10.31a)$$

This emf in the idling characteristic (see Figure 10.4a) corresponds to n. s.  $F_{id}$ . Complete n. s. equals

$$F_n = F_{id} + F_{ad}. \quad (10.32)$$

It follows from triangle OAc:

$$\operatorname{tg} \beta_0 = \frac{e_{id}}{iF_{ad}}, \quad (10.33)$$

and, from expressions (10.31a) and (10.33):

$$\operatorname{tg} \beta = \frac{(r_n + r) \cos \psi + (X_n + X_s) f \sin \psi}{f(X_d - X_s) \sin \psi}. \quad (10.34)$$

Obtaining angle  $\beta$  in geometric degrees requires introduction of scale /513 factor  $K_d = \frac{m_F}{m_e}$ , where  $m_F$  is the n. s. scale in A/cm or relative units/cm;  $m_e$  is the emf scale in V/cm or relative units/cm.

When constructing the idling characteristic, the nominal n. s. value  $F_{\text{nom}} = F_{60}$  (for the idling mode) is used as the n. s. unit, while inductive impedances  $X_{ad}$  and  $X_{aq}$  are determined from the idling rectified characteristic. Here, it is necessary to multiply term  $(X_d - X_s) = X_{ad}$  (see Figure 10.4b) in expressions (10.31) and (10.34) by expression (see Figure 10.4a):

$$C_0 = \frac{F_0}{F_{60}} \approx \frac{ab}{ae}, \quad (10.34a)$$

and replace factor  $K_d$  with factor

$$K = \frac{K_d}{C_0} = \frac{m_F}{m_e C_0}.$$

Then

$$\operatorname{tg} \beta_0 = \frac{K}{X_d - X_s} \left[ X_n + X_s + \frac{(r_n + r) \cos \psi}{f \sin \psi} \right], \quad (10.35)$$

generator current

$$\tilde{i}_n = \frac{\tilde{F}_{ad}}{C_0 \sin \varphi (X_d - X_s)} \quad (10.36)$$

and GED current

$$\tilde{i} = \sigma \tilde{i}_n. \quad (10.37)$$

Generator voltage equalling GED voltage is determined from formula

$$\bar{U} = \bar{i}_n \sqrt{r_n^2 + (fX_n)^2}, \quad (10.38)$$

while values  $\cos \psi$  and  $\sin \psi$  by expressions

$$\cos \psi = \frac{r_n + r_1}{\sqrt{(r_n + r_1)^2 + [f(X_n - X_d)]^2}}; \quad (10.39)$$

$$\sin \psi = \frac{(X_n - X_d) f}{\sqrt{(r_n + r_1)^2 + [f(X_n - X_d)]^2}}. \quad (10.40)$$

Second stage. calculation of GED transient processes. This calculation uses torque equilibrium equation (10.4). Base values used are nominal torque  $M_{д. ном}$  and rotational speed  $n_{д. ном}$  values. We previously obtained the standard working formula in relative units (10.4) in the form of finite increments. In light of generator rotational speed change during transient processes, there also is a requirement to consider the deviation from the accepted standard working frequency in this formula. For the stated purpose, we will use the generator /514 set torque equation in relative units:

$$\frac{m_r}{M_{д. ном}} = 0,95 \left[ \frac{m_{дз}}{M_{дз. ном}} - \frac{GD_{дз.г}^2}{375} \cdot \frac{n_{г. ном}}{M_{дз. ном}} \cdot \frac{d \left( \frac{n_r}{n_{г. ном}} \right)}{dt} \right], \quad (10.41)$$

where  $m_r$  - is generator torque;  $m_{дз}$ ,  $M_{дз. ном}$  are primary motor actual and nominal torques;  $GD_{дз.г}^2$  is generator and primary motor moment of gyration;  $n_r$ ,  $n_{г. ном}$  - are generator (primary motor) actual and nominal rotational speed.

It is possible from expression (10.41) to get the standard working formula in finite increments and in relative units:

$$\Delta t = \frac{0,95}{375 (0,95 \bar{m}_{дз. cp} - \bar{m}_r. cp)} \times \frac{GD_{дз.г}^2 \bar{n}_{г. ном} \Delta \bar{n}_r}{M_{дз. ном}} = \frac{0,957 M \Delta \bar{n}_r}{0,95 \bar{m}_{дз. cp} - \bar{m}_r. cp}. \quad (10.42)$$

Third stage. determination of GED frequency acceleration time. After the GED has gone into synchronization, its further acceleration is achieved by increasing frequency, i. e., by increasing primary motor rotational speed.

Determination of motor acceleration time under these conditions requires compilation of the equation of motion of the entire system: primary motor — generator — main propulsion motor — propellor, considering associated masses of water. Solving this equation, we obtain the expression determining transient process duration from the moment of the initiation of the frequency increase until its set value is reached. The aforementioned system equation of motion, being at the same time the equilibrium equation of the torques applied to the shaft of the main primary motor, can be written in the following form:

$$m_{\text{ms}} = \frac{GD_{\text{cncr}}^2 dn}{375 dt} + m'_{\text{rs}}, \quad (10.43)$$

where  $m_{\text{ms}}$  is primary motor torque;  $GD_{\text{cncr}}^2$  is moment of gyration of the system's rotating parts (primary motor — generator — GED — propellor shaft — screw, with associated masses of water) applied to the primary motor shaft;  $m'_{\text{rs}}$  is propellor moment of resistance against the primary motor shaft ( $m'_{\text{rs}} = \frac{m_{\text{p}} K}{\eta_{\text{p}} \eta_{\text{d}} \eta_{\text{r}}}$ ;  $\eta_{\text{p}}$ ,  $\eta_{\text{d}}$ ,  $\eta_{\text{r}}$  are propellor shaft, GED, and main generator efficiency, respectively).

Moment of gyration  $GD_{\text{cncr}}^2$  is determined by expression

$$GD_{\text{cncr}}^2 = GD_{\text{ms}}^2 + GD_{\text{r}}^2 + (GD_{\text{g}}^2 + GD_{\text{p}}^2) K^2,$$

where  $GD_{\text{ms}}^2$ ,  $GD_{\text{r}}^2$ ,  $GD_{\text{g}}^2$ ,  $GD_{\text{p}}^2$  are the moments of gyration of the rotating parts of the primary motor, main generator, GED, and propellor with propellor shaft /515 and associated masses of water, respectively;  $K$  is the transmission factor from the GED shaft to the primary motor shaft:

$$K = \frac{n_{\text{g. nom}}}{n_{\text{r. nom}}}.$$

Solving equation (10.43) for  $dt$ , i. e., synchronous starting process time, we will find

$$dt = \frac{GD_{\text{cncr}}^2 dn_{\text{r}}}{375 (m_{\text{ms}} - m'_{\text{rs}})}.$$

Considering the nonlinear nature of torques entering into this expression, it is advisable to do the calculation using the approximation by iteration method.

Then, the standard working formula in relative units and in finite increments will have the form:

$$\Delta t = \frac{GD_{\text{снст}}^2 (\bar{n}_r - \bar{n}_r')}{375 \left[ \left( \frac{\bar{m}_{\text{дз}} + \bar{m}_{\text{дз}}'}{2} \right) - \left( \frac{\bar{m}_p - \bar{m}_n}{2} \right) \right]} = \frac{GD_{\text{снст}}^2 \Delta \bar{n}_r \cdot \text{ном}}{375 M_{\text{дз. ном}} (\bar{m}_{\text{дз. ср}} - \bar{m}_{1\text{в. ср}})} = T_M \frac{\Delta \bar{n}_r}{(\bar{m}_{\text{дз. ср}} - \bar{m}_{1\text{в. ср}})} \quad (10.44)$$

It is convenient to reduce the calculations to tabular form:

$\bar{n}_r$	$\Delta \bar{n}_r$	Средние значения моментов сопротивления (a)				$\Delta t_{\text{сск}}$	$t_{\text{сск}}$	$T_{\text{сск}}$
		$\bar{m}_{\text{дз}}$	$\bar{m}_p$	$\bar{m}_{1\text{в}}$	$\bar{m}_{\text{дз. ср}} - \bar{m}_{1\text{в. ср}}$			

Key: a—Average values of moments of resistance; b--Seconds.

Data for filling in the third column will be taken from the primary motor torque curves in the given characteristic  $\bar{m}_{\text{дз}} = f(n)$ . The fourth column is filled in from the propellor characteristic in the moored mode. The eighth column shows synchronous starting time, while the ninth shows overall time, i. e., asynchronous and synchronous time.

### § 10.5 Synchronous Main Propulsion Motor Dynamic Braking

**Braking process.** At times, reversal of a synchronous GED while a vessel is moving forward at full speed turns out to be impossible or occurs with great difficulty as a result of unsatisfactory induction braking characteristics. In these cases, the braking mode in the second stage of reversal is possible by /516 resorting to dynamic braking. However, this requires additional equipment: loading devices (metallic or liquid rheostats) with the corresponding control devices, mechanical brakes on the propellor shaft (with remote control), capable of developing sufficient braking torque (approximately 50% of nominal).

Dynamic braking relative to ac GEU is accomplished in the following manner. After field is removed from the GED (in the first stage of reversal) and it is

disconnected from the generator by means of the reversing switch, the motor simultaneously is connected to a loading rheostat and field (less than nominal) again is fed to it. As a result of these operations, in the second stage of reversal, the GED rotated by the propellor operates like a generator to the loading rheostat with alternating frequency, which decreases in a range of 0.7-0.05 of nominal. Here, the kinetic energy of the propellor and GED rotor, as well as the kinetic energy of vessel motion supplied to the propellor (operating in this mode as a hydraulic turbine) turns into heat. When screw rotational speed attains a value approximately 0.05 of nominal, field is removed from the motor, it is disconnected from the loading rheostat (braking resistance), and is connected to the electric propulsion bus bars (to a generator). Boosted field is supplied to the generators, resulting in the motor finally losing its speed. Then, it begins to rotate in the opposite direction. Thus, the third stage of the reversal process begins — the reversal itself.

Braking resistance can be uncontrolled (one-stage) or controlled (multistage). During uncontrolled dynamic braking, control has a simpler arrangement but occurs in approximately two fold jumps of current in the stator, while in regulated resistance stator current does not exceed a 1- to ~~3~~<sup>1.2</sup>-fold jump. But, since in the first instance the process naturally accelerates, in a majority of electric ships with dynamic braking, a one-stage loading rheostat is used.

The transition from dynamic to countercurrent flow braking, i. e., switching the GED from braking resistance to a generator, requires from 3 to 7 seconds (based upon "Abkhaziya" test data); the duration of the remaining stages is shown in Table 10.1, compiled from averaged data from the testing of several electric ships. The duration of the operation to transfer a GED from dynamic to countercurrent flow braking (given vessel initial speeds from 16 to 5 knots) also is shown in that table. The nature of GED dynamic braking is explained in Figure 10.5.

In the absence of brakes on the GED shaft, during the time the GED is switched from dynamic to countercurrent flow braking, propellor rotational speed can be increased to the initial value (point  $b_1$  in Figure 10.5) due to the action of the oncoming stream of water while a ship is moving due to inertia. /517

Table 10.1.

Operations	Duration (Based on 10 Tests), seconds	
	Maximum and Minimum	Average
From the moment field is removed from the GED until the reversing switch is cut in (magnetic field killing process)	0.7-4.6	1.8
Switching the GED from the loading rheostat to a generator	0.5-2.3	1.4
Generator field process	1.2-3.0	1.8
Average		5

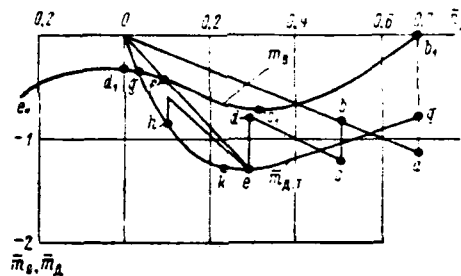


Figure 10.5. GED Braking Torque Characteristics.

A satisfactory result is attained during dynamic braking if the propellor is not allowed to increase the speed of its rotation, for this purpose having braked the propellor shaft during the motor switching process. It is possible to reduce the duration of operations involving switching and subsequent generator field boosting by automating this process.

When a mechanical brake is available, the reversing sequence is as follows. After propellor rotational speed has been brought to 0.05 of  $\bar{n}_{2, nom}$  it is stopped finally by the brake on the GED shaft. Then field is removed from the motor, it is disconnected from the loading rheostat (braking resistance), and it is connected

to an unexcited generator to which boosted field is supplied, simultaneously releasing the brake. As a result, the motor stops and begins to rotate in the opposite direction.

In the absence of a mechanical brake, GED magnetic field boosted killing must be accomplished after screw rotational speed is brought down to 0.05 of  $\bar{n}_{A, \text{НОМ}}$ , with subsequent GED connection to a previously-overexcited generator by means of an oil switch. This will reduce the transfer from dynamic braking to countercurrent flow braking to 1.5-2 seconds. However, such devices still /518 are absent from vessels active in the maritime fleet. Therefore, one must strive towards full automation of the aforementioned processes.

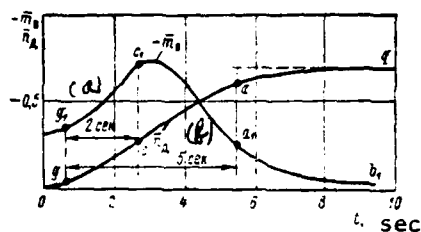


Figure 10.6. Propellor Acceleration Characteristics Given the Action of Vessel Motion. a—2 seconds; b—5 seconds.

Calculation of the propellor acceleration rate given the action of vessel motion due to inertia must precede calculation of the dynamic braking mode. Curves are constructed for that purpose (Figure 10.6).

Their construction presupposes that the propellor is stopped and is located at point  $d_1$  of reversing characteristic  $b_1, c_1, d_1, e_1$  (see Figure 10.5), and then is released and left alone. Then, under the influence of negative torque  $0d_1$ , propellor rotational speed will increase in accordance with torque equilibrium equation

$$\bar{m}_A = -\frac{GD_A^2 d\bar{n}_A}{375 dt} + \bar{m}_y.$$

Consequently, it is possible to calculate the acceleration of a preliminarily-stopped screw under the influence of vessel motion from the overall torque equilibrium equation, assuming in it that propelling torque  $\bar{m}_A$  equals zero.

Effective dynamic braking of a synchronous GED requires that its braking torque be 25-30% greater than propellor torque in the entire rotational speed range (from  $0,7\bar{n}_{d, nom}$  to  $\approx 0,1\bar{n}_{d, nom}$ ). The established braking condition is determined by point g of intersection of reversing characteristic  $b_1, c_1, d_1, e_1$  with the braking torque characteristic  $\bar{m}_{x, \tau}$  (see Figure 10.5). The value of initial motor braking torque (b, q) must not, where possible, exceed its nominal value  $M_{d, nom}$ , since, otherwise, a severe shock transmitted to the vessel hull occurs in the motor. This shock is ameliorated considerably if the duration of GED magnetic field increase is less than 1.5-2.5 seconds.

Motor braking torque curve  $\bar{m}_{x, \tau} = f(n_d)$  during one-stage braking is reminiscent of an induction motor torque curve. Its character and the position of point K of maximum torque (see Figure 10.5) will depend on the magnitude of braking resistance  $r_\tau$  (loading rheostat), with point k shifting to the left when it decreases.

It is clear from an examination of Figure 10.6 that, if one assumes the operation to switch dynamic braking to countercurrent flow braking takes 5 seconds, then GED dynamic braking is impracticable since, during this time, the propellor increases rotational speed almost to the initial state, from point g to point  $b_1$ . Repeat braking will not provide the necessary effect. A rapid transition from dynamic to countercurrent flow braking, lasting approximately 2 seconds, also will not bring about the desired results since the propellor during this time increases its speed to a magnitude characterized by the segment from point g to point  $c_1$ , in which its torque equals  $0,7\bar{m}_{d, nom}$  and cannot under all conditions be brought into equilibrium by asynchronous braking torque. In this event, only one possibility remains: to keep the propellor at point g in the braked state during the entire aforementioned switching period.

Calculation methodology. During the dynamic braking process, the motor operates in the mode of a synchronous generator loaded to resistance  $Z_n = \sqrt{Z_n^2 + (fX_n)^2}$ . Since it is possible here to assume that  $X_n = 0$ , then  $Z_n$  will equal  $r_n$ .

The moment of resistance of a GED operating in the generator mode is determined by a generator torque equation, which can be written in the form

$$\bar{m}_{x, \tau} = \frac{\delta_n^2 \cos \psi [(X_n + X_q) f \sin \psi - (r_n + r_1) \cos \psi]}{f}. \quad (10.45)$$

Using expressions

$$r_n + r_1 = \cos \psi \sqrt{(r_n + r_1)^2 + [f(X_n + X_q)]^2}$$

and

$$f(X_n + X_q) = \sin \psi \sqrt{(r_n + r_1)^2 + [f(X_n + X_q)]^2}$$

and, substituting them in torque equation (10.45), we will get

$$\begin{aligned} \bar{m}_{x, \tau} &= \frac{\delta_n^2 \cos \psi}{f} [\sqrt{(r_n + r_1)^2 + [f(X_n + X_q)]^2} (\cos^2 \psi + \sin^2 \psi)] = \\ &= \frac{\delta_n^2 \cos \psi}{f} \sqrt{(r_n + r_1)^2 + [f(X_n + X_q)]^2}. \end{aligned} \quad (10.46)$$

Considering that  $X_n = 0$ , we will get the following formula for computation of torques in the mode examined:

$$\bar{m}_{x, \tau} = \frac{\delta_n^2 \cos \psi}{f} (r_n + r_1). \quad (10.47)$$

In the absence of a curve of the relationship of the thrust of the motive force developed by the propellor to screw rotational speed at various vessel speeds,  $P = f(\bar{n}_s)$ , one can assume approximately, in relative units, that  $\bar{P} = \bar{m}_s$ .

Proceeding from the vessel equation of motion during braking

$$Km_s \frac{dv}{dt} = P + R_c, \quad (10.47a)$$

where  $R_c$  is vessel total resistance to motion.

We assume that the greatest braking effect will occur at the greatest value of propellor thrust but, since we assumed above that  $\bar{P} = \bar{m}_s$ , then relative

to a vessel with screw reversing curves (Figure 10.7), given braking at rate  $\bar{v} = 1.0$ , the greatest screw thrust will be in rotational speed  $n_x = (0.53 \div 0.2) n_{x, \text{nom}}$ . Consequently, in order to use propellor braking thrust more fully, braking must be accomplished as rapidly as possible since a decrease in vessel speed is accompanied by a decrease in its thrust as well.

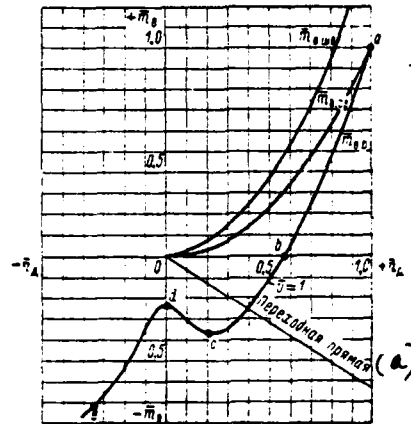


Figure 10.7. Propellor Hydrodynamic Characteristics.  $m_{x, \text{moored}}$ ,  $m_{x, \text{open water}}$ ,  $m_{x, \text{reversing}}$  are the characteristics when moored, in open water, and reversing, respectively, where  $v = 1$ . a—Translational straight line.

Most effective dynamic braking requires determination of the magnitude of the resistance of the loading rheostat and GED field in the generator mode of GED operation. It is possible to provide a propulsion motor boosted field  $i_{b, x} = 1.2-1.5$  and, in so doing, insure receipt of the greatest braking torque, but this does not allow attainment of the assigned task of braking the vessel itself to a value at which reversal can be accomplished. Thus, attainment of effective braking coincides with the requirement for the most complete use of screw thrust. Having been given the magnitude of GED field and resistance  $r_n$ , it is possible through use of resolved standard working formulas for various frequency values to find the magnitude of torque  $\bar{m}_{x, r}$ . Converting to determination of the relative value of dynamic braking resistance  $r_r$  and GED field  $i_{b, x}$  during dynamic braking, it should be noted that, in view of the complex mutual coupling of these parameters with torque  $\bar{m}_x$ , it is more convenient to obtain them using the trial and error method. For this purpose, several values for  $r_r$  and  $i_{b, x}$  are substituted in

the family of curves  $\bar{m}_x = f(\bar{n}_x)$  and then those values corresponding to optimum braking torques are used.

A family of propellor reversing characteristics in speed range  $v = 1.0-0.4$  is shown in Figure 10.8. The curve of the braking torque calculated where  $r_T = 0.4$  and  $i_{x,x} = 0.6$  are plotted here (dotted line).

The results of the calculation are reduced to tabular form:

$\Delta \bar{n}_D$	$\bar{n}_D$	$f$	$\cos \psi$	$\sin \psi$	$\operatorname{tg} \beta_0$	$\beta_0$	$F_{ad}$	$i_{\Pi}$	$\bar{m}_{D,T}$	$\Delta t, \text{сек}$	$t, \text{сек}$
										(a)	(a)

Key: a—Seconds.

Braking time can be found from formula

/521

$$\Delta t = \frac{GD_D^2 \bar{n}_{D, \text{ном}}}{375 \bar{M}_{D, \text{ном}}} \cdot \frac{\Delta \bar{n}_D}{(\bar{m}_{D, \text{cp}} - \bar{m}_{B, \text{cp}})} = T_M \frac{\Delta \bar{n}_D}{(\bar{m}_{D, \text{cp}} - \bar{m}_{B, \text{cp}})} \quad (10.48)$$

where  $T_M = \frac{GD_D^2 \bar{n}_{D, \text{ном}}}{375 \bar{M}_{D, \text{ном}}}$  is the propellor drive electromechanical time constant;

$\bar{m}_{D, \text{cp}}$  is the average motor torque value in relative units in section  $gq$ ;  $\bar{m}_{B, \text{cp}}$  is the average propellor moment of resistance in section  $gb_1$  (see Figure 10.6).

The calculations are reduced to tabular form:

$\Delta \bar{n}_D$	$\bar{n}_D$	$\bar{m}_{B, \text{cp}}$	$\bar{m}_{D, \text{cp}}$	$\Delta t, \text{сек}$	$t, \text{сек}$	$\Delta \bar{v}$	$\bar{v}$
				(a)	(a)		

Key: a—Seconds.

It should be kept in mind that it is possible to take the screw resistance value from the reversing curve for actual vessel speed, the change in which determined from the vessel equation of motion (10.47a).

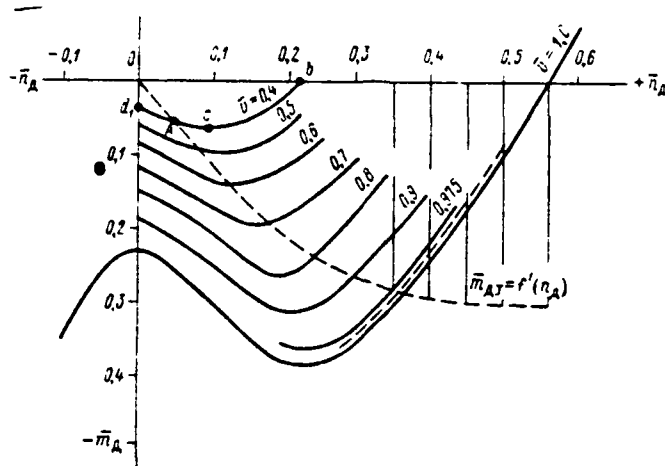


Figure 10.8. Family of Propellor Reversing Characteristics and GED Braking Torque.

Calculation of maximum braking torque. The frequency, or propellor rotational speed, at which maximum braking torque is achieved can be determined from expression (10.45). We have from the emf vector diagram (see Figure 10.4b):

$$e_{id} = E_0 - \bar{e}_{ad} \text{ и } \bar{e}_{ad} = i \sin \psi f X_{ad}$$

or

/522

$$\bar{E}_0 = \bar{i}_n [(r_n + r_1) \cos \psi + f(X_n + X_s + X_{aq}) \sin \psi].$$

Then

$$\bar{i}_n = \frac{\bar{E}_0}{(r_n + r_1) \cos \psi + f(X_n + X_s + X_{aq}) \sin \psi}. \quad (10.49)$$

But, since  $X_n = 0$  and  $X_s + X_{aq} = X_{ad}$ , then

$$\bar{i}_n = \frac{\bar{E}_0}{(r_n + r_1) \cos \psi + f X_{ad} \sin \psi}. \quad (10.49a)$$

Substituting obtained expression (10.49a) in torque equation (10.47), we will find

$$\bar{m}_{a, \tau} = \frac{\delta_n \bar{E}_0^2}{f} (r_n + r_1) = \frac{\delta_n (r_n + r_1) \bar{E}_0^2}{f [(r_n + r_1) \cos \psi + f (X_d \sin \psi)]^2}. \quad (10.50)$$

The latter is solved with the aid of expressions (10.39) and (10.40).

Having substituted values  $\cos \psi$  and  $\sin \psi$  in torque formula (10.50), where  $X_n = 0$ , we will get

$$\bar{m}_{a, \tau} = \frac{\delta_n (r_n + r_1) \bar{E}_0^2 [(r_n + r_1)^2 + f^2 X_d^2]}{f [(r_n + r_1)^2 + f^2 X_d X_q]^2}. \quad (10.51)$$

We will introduce designations:

$$r_n + r_1 = R; \quad X_d X_q = C; \quad (10.52)$$

$$\bar{E}_0 = \bar{E}_{(50)} f, \quad (10.53)$$

where  $\bar{E}_{(50)}$  is voltage at 50 Hz. Then equation (10.51) can be rewritten as:

$$\bar{m}_{a, \tau} = \frac{\delta_n \bar{E}_{(50)}^2 f R (R^2 + f^2 X_q^2)}{(R^2 + f^2 C)^2}. \quad (10.54)$$

For determination of the frequency at which maximum torque occurs, one must take its frequency derivative and find the value of the latter, reducing the derivative to zero, using expression (10.54):

$$\begin{aligned} \frac{d\bar{m}_{a, \tau}}{df} &= \delta_n \bar{E}_{(50)}^2 R \frac{(R^2 + f^2 C)(R^2 + 3f^2 X_q^2) - 4f^2 (R^2 + f^2 X_q^2)}{(R^2 + f^2 C)^3} = \\ &= \delta_n \bar{E}_{(50)}^2 R \frac{R^4 + 3f^2 X_q^2 R^2 + f^2 C R^2 + 3f^4 C X_q^2 - 4f^2 C R^2 - 4f^4 C X_q^2}{(R^2 + f^2 C)^3} = \\ &= \delta_n \bar{E}_{(50)}^2 R \frac{R^4 - 3f^2 X_q^2 R^2 - 3f^2 C R^2 - f^4 C X_q^2}{(R^2 + f^2 C)^3}. \end{aligned}$$

From condition

$$\frac{d\bar{m}_{a, \tau}}{df} = 0$$

we have

/523

$$\delta_n \bar{E}_{(50)} R [R^4 + 3f^2 X_q^2 R^2 - 3f^2 C R^2 - f^4 C X_q^2] = 0$$

and, finally

$$f^4 C X_q^2 - 3f^2 R^2 (X_q^2 - C) - R^4 = 0.$$

Solving this equation for frequency  $f$ , we will find

$$\begin{aligned} f &= \pm \sqrt{\frac{3R^2(X_q^2 - C) \pm \sqrt{9R^4(X_q^2 - C)^2 - 4X_q^2 C R^4}}{2X_q^2 C}} = \\ &= \pm R \sqrt{\frac{3(X_q^2 - C) \pm \sqrt{9(X_q^2 - C)^2 - 4X_q^2 C}}{2X_q^2 C}}. \end{aligned}$$

Having substituted corresponding values  $R$  and  $C$ , we will get the final expression determining the frequency at which braking torque has the maximum value:

$$f_{\tau}^2 = \pm (r_n \pm r_1) \frac{3X_q(X_q - X_d) \pm \sqrt{9(X_q - X_d)^2 X_q^2 - 4X_q^3 X_d}}{2X_q^2 X_d}. \quad (10.55)$$

When computing magnitude  $f_{\tau}$ , it is necessary to use correction factor  $C_o$ , with parameter  $X_{ad}$  multiplied by this factor. One should also consider value  $X_{ad}$  given saturation for a precise determination of  $f_{\tau}$ .

Thus, the braking torque peak will depend on the magnitude of the braking resistance of the loading rheostat and GED parameters. Consequently, value  $m_{\text{br. max}}$  can be regulated with the aid of braking resistance. The braking characteristic is constructed from equation (10.54), followed by determination of the value of the frequency at which braking torque achieves maximum value in accordance with equation (10.55). The magnitude of the braking moment peak next is used for location of the requisite GED field in the dynamic braking mode from formula

$$\bar{m}_{\text{br. } \tau} = f_{\tau} \frac{\bar{E}_{(50)}^2 R (R^2 - f_{\tau}^2 X_q^2)}{(R^2 - f_{\tau}^2 C^2)}. \quad (10.56)$$

hence

$$\bar{E}_{(50)}^2 = \frac{\bar{m}_{a,r} (R^2 - f_r^2 C^2)}{f_r R (R^2 + f_r^2 X_d^2)} \quad (10.57)$$

Motor field current is determined from its idling characteristic. Knowing the approximate value of the braking resistance and field current, it already is possible to carry out a sufficiently precise calculation using the method examined.

#### § 10.6 Methodology for Transient Process Calculation During Main Propulsion Motor Starting

Initial data. The values of the following parameters must be known to calculate transient processes:

##### For the generator

- $P_{r, \text{HOM}}$ , kVA — nominal power;
- $U_{1л}$ , V — line voltage;
- $I_{r, \text{HOM}}$ , A — nominal current;
- $\cos \varphi_r$  — power factor;
- $n_{r, \text{HOM}}$ , rpm — nominal rotational speed;
- $f_{1 \text{HOM}}$ , Hz — nominal frequency;

For the stator:

Winding connection — star;

- $r_1$ , ohms — resistance;
- $X_s$ , r. u. — inductive dispersion impedance; [r. u. -- relative units]
- $X_d$ , r. u. — inductive impedance synchronized along the longitudinal axis;
- $X_q$ , r. u. — inductive impedance synchronized along the transverse axis;

For the rotor:

- $r_f$ , ohms — field winding resistance;



$i_{s, 2}$ , r. u. — field current;  
 $GD_A$ ,  $\text{kg-m}^2$  — moment of gyration;

Idling characteristic:

For the Propellor and Shafting Line

$GD_{A_1}^2$ ,  $\text{kg-m}^2$  — moment of gyration of the propellor shaft, propeller, and water it attracts;

$\bar{m}_{20}$  r. u. — moment of resistance of GED take-off;

$\bar{m}_{s, m_s} = f(\bar{n}_2)$  — propellor moored characteristic for the given pitch ratio.

Calculation sequence. The following is the sequence of the calculation of transient processes during GED starting.

1. Value  $\bar{m}_s$  for various values  $\bar{n}_2$  is determined for a given propellor moored characteristic. Next, GED slip values are found: relative — from the expression  $\bar{s} = \frac{f \mp n_2}{f}$  r. u.; absolute — from the expression  $s_s = f \pm n_2$  r. u.

2. Relationship  $K_r = f(f_2)$  and  $K_X = \underline{f}(f_2)$  are calculated: they are set by the values of frequency  $f_2$  in relative units in a range of 0.03 of nominal to double the nominal and, for each of these values, conductance is computed from expressions

$$Y_f = g_f - jb_f = \frac{r_f - jf_2 X_f}{r_f^2 - (f_2 X_f)^2};$$

$$Y_{kd} = g_{kd} - jb_{kd} = \frac{r_{kd} - jf_2 X_{kd}}{r_{kd}^2 - (f_2 X_{kd})^2};$$

$$Y_{2ds} = g_{2ds} - jb_{2ds} = (g_f - g_{kd}) - (b_f - b_{kd});$$

$$Z_{2ds} = \frac{1}{Y_{2ds}} = r_{2ds} + jX_{2ds};$$

$$Z_{kd} = r_{2ds} + jX_{2ds} \left( \frac{f_0}{f_2} \right); \quad Z_{2g} = r_{kd} + jX_{kd}.$$

Impedance will be found with the aid of expressions (10.17)--(10.23) and (10.26)--(10.28), set by slip values  $s$  from 0.05 to 1.

3. Values of  $\cos \psi$  and  $\sin \psi$  are determined from formulas (10.39) and (10.40), then  $\text{tg} \beta_0$  is determined from expressions (10.35).

4. The values of generator and GED currents in relative units are calculated from formulas (10.36) and (10.37). Here, the magnitude of  $\bar{F}_{ad}$  in formula (10.36)

is determined from the generator idling characteristic (see Figure 10.4a) in the following manner: for the field boosting selected, at point A in this case, path AC at angle  $\beta_0$  is constructed and the value of the component of magnetization force  $F_{ad}$  is found. This parameter also can be computed from the formula

$$F_{ad} = C I_{r. nom} X_{ad} \sin \psi, \quad \text{where magnitude } C \text{ is assumed as equalling } 0.9.$$

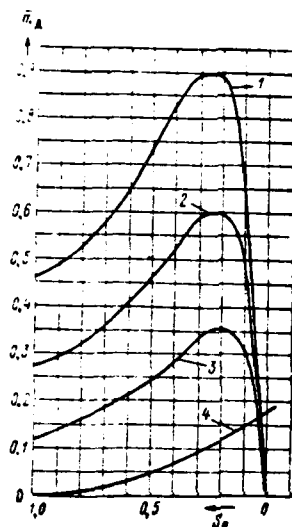


Figure 10.9. GED Torque Characteristics as a Function of Slip:  $\bar{m}_A = f(s_a)$ . 1—4 are starting from four, three, two, and one generator, respectively.

5. GED voltage during GED starting is calculated from formula (10.38).

6. GED torque during starting is determined by conversion of the initial formula for torque (10.16) to form

$$m_A = \frac{\delta u^2 r_{20} K_r}{f Z_n^2}, \quad (10.58)$$

where  $\delta$  will be found from expression (10.17), while voltage  $u$  from expression (10.38). The GED torque change characteristic depending on slip  $\bar{m}_A = f(s_a)$  is shown in Figure 10.9.

7. Calculation of the time of GED asynchronous starting will occur proceeding from the condition of equilibrium of torques, which, in relative magnitudes and finite increments, has the form

$$\bar{m}_d = \frac{GD_d^2}{375} \cdot \frac{n_{d, \text{НОМ}}}{M_{d, \text{НОМ}}} \cdot \frac{\Delta \bar{n}_d}{\Delta t} + \bar{m}_B \quad (10.58a)$$

Having solved this equation for time increment  $\Delta t$ , we will get the following standard working formula:

$$\begin{aligned} \Delta t &= \frac{GD_d^2 n_{d, \text{НОМ}} (\bar{n}_1 - \bar{n}_2)}{375 M_{d, \text{НОМ}} \left[ \frac{(\bar{m}_1 - \bar{m}_2)}{2} - \frac{(\bar{m}_B - \bar{m}_B)}{2} \right]} \\ &= \frac{GD_d^2 n_{d, \text{НОМ}}}{375 M_{d, \text{НОМ}}} \cdot \frac{\Delta \bar{n}_d}{(\bar{m}_d, \text{cp} - \bar{m}_B, \text{cp})} = T_M \frac{\Delta \bar{n}_d}{\bar{m}_d, \text{cp} - \bar{m}_B, \text{cp}} \end{aligned} \quad (10.59)$$

Here,  $\Delta \bar{n}_d = \bar{n}_1 - \bar{n}_2$  is an increment of GED rotational speed equalling the /527 difference in rotational speeds at the end and at the beginning of time segment

$\Delta t$ ;  $\bar{m}_d, \text{cp} = \frac{\bar{m}_1 + \bar{m}_2}{2}$  is the average GED torque value in the calculated section;

$\bar{m}_B, \text{cp} = \frac{\bar{m}_B - \bar{m}_B}{2}$  is the average value of propellor moment of resistance in calculated section  $\Delta \bar{n}_d$  (from the moored characteristic);  $\frac{GD_d^2 n_{d, \text{НОМ}}}{375 M_{d, \text{НОМ}}}$  is a propellor shaft line electromechanical time constant.

Consequently, introducing the average value of propellor rotating moment of resistance corresponding to the given rotational speed into the standard working formula, we will find from formula (10.59) the unknown value of time  $\Delta t$  for the section being examined. The calculations will be reduced to tabular form:

s	$\bar{n}_d$	$\bar{m}_d$	$\bar{m}_B$	$\Delta t, \text{сек}$ (a)	$\Delta t, \text{сек}$ (a)

Key: a—Seconds.

Slip s ranges from 1 to 0.05.

Calculation of the GED mechanical characteristic during starting  $\bar{m}_A = f(\bar{n}_A)$  provides the basis for construction of the curve of the relationship of GED torque  $\bar{m}_A$  to absolute slip  $s_d = f_2$ , while relative slip for each rotational speed value  $\bar{n}_A$  is calculated from expression

$$s = \frac{f_2}{f} = \frac{f - \bar{n}_A}{f} = 1 - \frac{\bar{n}_A}{f} = 1 - \frac{\bar{n}_A}{0,333} \quad (10.60)$$

while absolute slip from expression

$$s_a = f_2 = f - \bar{n}_A = 0,333 - \bar{n}_A \quad (10.61)$$

The calculation is reduced to tabular form:

$\bar{n}_A$	$\bar{m}_B = K_n \bar{n}_A^2$			

GED torque characteristics as a function of absolute slip during starting by one, two, three, and four diesel generators are shown in Figure 10.9.

It is convenient to reduce the entire calculation of the duration of asynchronous starting of a GED to combined tabular form:

$\bar{n}_A$	$\bar{m}_B$	$s$	$s_a$	$K_r$	$K_X$	$\alpha$	$\beta$	$\gamma$	$Z^2$	$\xi_n$	$b_n$	$\gamma^2$	$r_n$
$X_n$	$\cos \psi$	$\sin \psi$	$\operatorname{tg} \beta$	$F_{ad}$	$\bar{i}_r$	$\bar{i}_A$	$\bar{u}$	$\bar{m}_A$	$\Delta t$	$t$			

The characteristic of the relationship of GED torque to absolute slip  $s_a$  (see Figure 10.9) is constructed based upon such a summarized calculation table.

## § 10.7 Calculation of Transient Processes During Main Propulsion Motor Reversal

Initial data. The initial data on main generators, GED, shaft, and propellor required for the calculation are identical to those needed for starting (see Figure 10.6), but the reversing characteristic must be used in place of the moored characteristic.

Reversing stages given absence of dynamic braking. GED reversing can occur while a stationary vessel is moored and while it is moving at a particular speed. The first case differs from the starting maneuver only in that the motor is started in the opposite direction. Therefore, the processes flows with different numerical ratios between screw moment of resistance and the speed of its rotation.

Otherwise, the essence of the process remains the same. Therefore, calculation methodology does not differ from that examined for starting an electric motor.

We now will examine the most complicated GED reversal variant, when a vessel is moving forward at full speed. In this event, the reversal process can be divided into the following stages (given the absence of dynamic braking):

First stage — braking the propellor with a synchronously-operating GED in a rotational speed range from full to approximately  $0,8n_{d. \text{HOM}}$ ;

Second stage — propellor self-braking when the GED is cut out of the circuit in a rotational speed range of approximately  $0,8n_{d. \text{HOM}}$  to  $0,67n_{d. \text{HOM}}$  whereby screw moment of resistance will become equal to zero;

Third stage — GED braking in the asynchronous mode using the plugging /529 method in a rotational speed range from  $0,67n_{d. \text{HOM}}$  to  $n_x = 0$  (given the absence of GED dynamic braking devices);

Fourth stage — GED acceleration in the opposite direction: from zero rotational speed to hyposynchronous, corresponding approximately to  $0,36n_{d. \text{HOM}}$ ;

Fifth stage — increasing the rotational speed of primary motors (as well as that of generators connected rigidly with them) and GED from  $0,36n_{d. \text{HOM}}$  to a speed corresponding to complete vessel stop;

Sixth stage — further increase in main generator frequency, which will occur simultaneously with vessel acceleration in the astern direction.

The methodology for reversal calculation for the enumerated stages is presented below.

Braking of a propellor with a synchronously-operating GED. Examination of the process of propellor braking in the first stage of reversal is based on analysis of the equilibrium equations of the torques of the diesel generator (or turbo-generator) and propellor shafting line. The initial torque equation for a diesel generator can be written in the form

$$K_{дз} \left[ m_{дз} - \frac{GD_{дг}^2}{375} \cdot \frac{dn_r}{dt} \right] = m_r, \quad (10.62)$$

where  $K_{дз}$  is a factor used in calculations equal to 0.95;  $m_{дз}$  is diesel torque;  $m_r$  is braking (for the motor) torque created by the generator;  $GD_{дг}^2$  is the diesel generator moment of gyration.

Written in relative units and in finite increments, the torque equilibrium equation will have the following form:

$$0,95 \left( \bar{m}_{дз} - \frac{GD_{дг}^2 \cdot n_{г. ном} \Delta \bar{n}_r}{375 M_{дз. ном} \Delta t} \right) = \bar{m}_r = \bar{m}_д \frac{n_{г. ном}}{n_{д. ном}} = K \bar{m}_д. \quad (10.63)$$

We will use equation (10.1), we will solve it jointly with equation (10.63), and we will present both equations in differential form and in a system of relative units. Then we will get

$$0,95 \left[ \bar{m}_{дз. ср} - \frac{GD_{дг}^2 \cdot n_{г. ном} \Delta \bar{n}_r}{375 M_{дз. ном} \Delta t} \right] = \frac{KGD_{дг}^2 \cdot n_{д. ном} \Delta \bar{n}_д}{375 M_{дз. ном} \Delta t} + K \bar{m}_{в. ср}. \quad (10.64)$$

Assuming diesel torque average value  $\bar{m}_{дз. ср} = 0$  and having solved equation (10.64) for time  $\Delta t$ , we will get the standard working formula for determination of the duration of the first stage of reversal:

$$\Delta t = A \frac{\Delta \bar{n}_д}{\bar{m}_{в. ср}}, \quad (10.65)$$

where A is a constant component.

Calculation of propellor self-braking time (GED and propellor run-out). /530

Self-braking, or propellor run-out, begins at the moment when a GED reduces its rotational speed as a result of a cessation of the steam supply to a turbine or fuel to a diesel. From Figure 10.7, this case corresponds to screw reversing characteristic ab (for  $\bar{u} = 1$ ) in a range of rotational speed values  $\bar{n}_x = 1.0-0.56$ , in which  $m_{sp} = 0$ . Calculation accuracy can be improved if several linear sections approximate nonlinear section ab of the reversing characteristic and the time for each of them is computed. Self-braking time is determined from the initial torque equation during run-out

$$0 = \frac{GD_x^2}{375} \frac{dn_x}{dt} - m_{sp}$$

After appropriate conversions of this equation, solving it for the time increment and in relative units for various values, we will get final standard working formula

$$\Delta t = \frac{GD_x^2 n_{x, \text{ном}}}{375 M_{x, \text{ном}}} \cdot \frac{\Delta \bar{n}_x}{\bar{m}_{sp, \text{cp}}} = T_x \frac{\Delta \bar{n}_x}{\bar{m}_{sp, \text{cp}}} \quad (10.66)$$

It is convenient to reduce the results of calculations using formula (10.66) to tabular form:

$\bar{n}_x$	$\bar{m}_{sp, \text{cp}}$	$\Delta \bar{n}_x$	$\bar{m}_{sp}$	$\Delta t, \text{сек}$ (a)	$t, \text{сек}$ (a)

Key: a—Seconds.

The values of screw moments of resistance corresponding to selected values  $\bar{m}_{sp}$  in section  $\bar{n}_x$  of the reversing curve (see Figure 10.8) are entered in the second column of the standard working table.

Calculation of braking by plugging. This is done by bringing screw rotational speed down to zero ( $n_x = 0$ ) where vessel speed is  $v = 0.4$ . The countercurrent flow braking process is accomplished at reduced generator rotational speed,  $f = 0.333$  (which is about 18 Hz at a nominal frequency of 50 Hz).

The following is the calculation sequence:

- 1) GED relative slip is determined from expression

$$s = \frac{f - \bar{n}_A}{f} = 1 + \frac{\bar{n}_A}{f} = 1 + \frac{\bar{n}_A}{0,333}; \quad (10.67)$$

- 2) rotor current frequency (absolute slip) will be found from expression

$$s_a = f + \bar{n}_A = 0,333 + \bar{n}_A; \quad (10.68)$$

- 3) values of the moments of resistance  $\bar{m}_b$  from the propellor reversing /531 characteristic constructed for vessel speed  $v = 0.4$  in a range of  $\bar{n}_A$  values from 0.2 to 0.4 are determined.

Computational results are reduced to tabular form:

$\bar{n}_A$	$\bar{m}_b$	$s$	$s_a$

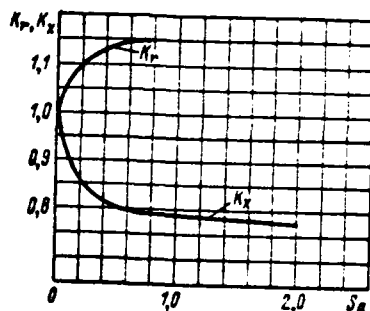


Figure 10.10. Characteristics for Calculation of Parameters  $K_r$  and  $K_x$ .

- 4) Parameters  $\alpha$ ,  $\beta$ ,  $\gamma$ ,  $Z^2$ ,  $b_n$ ,  $g_n$ ,  $Y^2$ ,  $r_n$ ,  $X_n$  are determined for various slip values (from 1 to 1.2) in a manner analogous to that used in GED starting

calculations. Factor  $K_r$  and  $K_x$  values will be taken from the graph in Figure 10.10 and results are reduced to tabular form:

s	$\alpha$	$\beta$	$\gamma$	$\frac{\gamma}{s}$	$\sin \alpha$	$Z'$	$\varepsilon_n$	$b_n$	$Y'$	$X_n$	$r_n$

5)  $\operatorname{tg} \beta_0$  will be found from the aforementioned values  $s = 1-1.2$  and from expression (10.35). Values  $\sin \psi$  and  $\cos \psi$  are computed from formulas (10.39) and (10.40). Calculations are reduced to tabular form:

s	$\sin \psi$	$\cos \psi$	$\operatorname{tg} \beta_0$

6) the following values are determined: a) generator starting current  $i_n$  from expression (10.36), with factor  $C_0$  found from expression (10.34a), while armature reaction n. s.  $F_{ad}$  found just as in GED starting (see Figure 10.4a); b) GED current from expression (10.37); c) generator voltage equal to voltage at the GED armature terminals from expression (10.38).

Calculations are reduced to tabular form:

s	$F_{ad}$	$i_n$	$i$	$U$

7) values of GED electromagnetic torque will be found with the aid of /532 formula (10.58) based on the given values of relative slip  $s$ .

Calculations are reduced to tabular form:

s	$\bar{m}_A$

8) plugging braking time is determined from the given values of  $s$  using standard working formula

$$\Delta t = \frac{GD_{\Sigma}^2}{375} \frac{n_{\text{д. ном}}}{M_{\text{д. ном}}} \frac{\Delta \bar{n}_{\text{д}}}{\frac{m_{\text{д}} + m_{\text{д}}}{2} \frac{m_{\text{в}} + m_{\text{д}}}{2}}$$

$$= T_{\text{м}} \frac{\Delta \bar{n}_{\text{д}}}{m_{\text{д. ср}} - m_{\text{в. ср}}}$$

Calculations are reduced to tabular form:

$s$	$\bar{n}_{\text{д}}$	$\bar{m}_{\text{д}}$	$\bar{m}_{\text{в}}$	$\bar{m}_{\text{д. ср}}$	$\bar{m}_{\text{в. ср}}$	$T_{\text{м}}$	$\Delta t, \text{сек}$	$t, \text{сек}$

Key: a—Seconds.

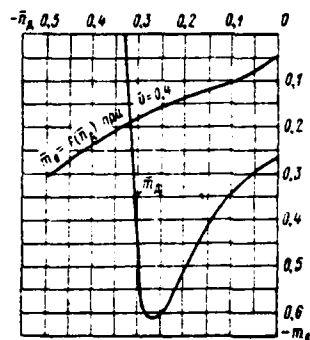


Figure 10.11. GED Acceleration Characteristics in the Asynchronous Mode.

GED acceleration in the asynchronous mode. This operation is determined by GED starting time in the opposite direction of rotation at frequency  $f = 18 \text{ Hz}$ , for which the following curves are constructed: a) propelling torque curve (calculated for a case of starting "forward"); b) propellor moment of resistance curve for vessel speed  $v = 0.4$  (Figure 10.11). One can consider the change in generator rotational speed by using formula (10.42). Calculation of the second stage of synchronous GED reversal concludes here.

Calculation of the duration of a frequency synchronized GED. Calculation

of the third stage of reversal involves determination of GED acceleration time in the synchronized mode, which ends with GED reversal, and is accomplished from formula (10.44). It is convenient to calculate motor acceleration considering the vessel equation of motion [20, 70] in tabular form:

$\bar{n}_A$	$\Delta \bar{n}_A$	$\bar{n}_{A, cp}$	$\bar{m}_{A, cp}$	$\bar{m}_A$	$\frac{\Delta t_{cek}}{(\bar{A})}$	$t_{cek}$ ( $\bar{A}$ )	$\bar{n}_T$	$\Delta \bar{v}$	$\bar{v}$	$\Delta \bar{z}$	$\bar{z}$

Key: a—Seconds.

It is possible to increase GED rotational speed by reducing the speed of /533 a vessel continuing to move forward. However, this must be done so that no primary motor torque overload occurs.

## Geometrical and Weight Characteristics of Electrical Propulsion Plant Main Machinery

### § 11.1 General Considerations

Initial data. The GED and generators in electrical propulsion plants operate in various modes. Therefore, determination of electrical parameters and design of switch gear require consideration of all possible types of operation, selecting for calculation the most complex, i. e., proceeding from maximum torque and highest rotational speed or greatest current and voltage. Consequently, electrical machinery rated capacity can differ from actual capacity. This circumstance must be considered especially often when dealing with GEU aboard tugs, icebreakers, and Arctic navigation vessels, and sometimes even in emergency or economic running modes. These conditions can occur also in other types of vessels.

Rated capacity equals the nominal for dc GEU with a flat mechanical characteristic. In a majority of cases, machinery rated capacity is higher than the nominal in systems with a countersequential winding or electromechanical automation, which must be kept in mind during design.

It is necessary when determining dc electrical machinery size and weight characteristics:

- to select the configuration;
- to know their electrical power;
- to establish their length and diameters thresholds, proceeding from the ship's hull or guided by threshold dimensions acceptable for machinery transportation.

Machinery configuration. Electrical machinery can have the following configurations (Figure 11.1):

- on two bearings, single-armature, with flanged shaft (Figure 11.1a);
- on one bearing, single-armature, used mainly for propulsion plant generators (Figure 11.1b);
- on two bearings, dual-armature, with flanged shaft (Figure 11.1c);
- on two bearings, dual-armature, with flanged shaft for connection between

armatures by means of a sleeve coupling seated on the shaft line side (Figure 11.1d).

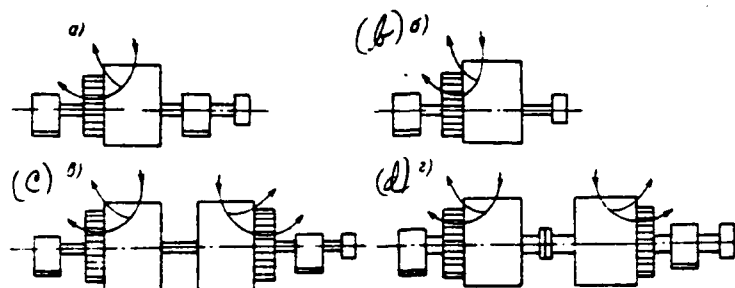


Figure 11.1. Direct Current GEU Electrical Machinery Configurations.

The latter two configurations are used mainly for GED, while the second allows one to have only one armature in reserve.

Electrical machinery shafts are designed for maximum operating torque. Where required, their section is reinforced for generators taking torsional vibrations into account, while for GED taking into consideration frequent starts, reverses, and operating conditions in which propeller jamming is possible.

The following configurations exist, depending on how air is supplied for cooling:

- normally open;
- with external air supply;
- blown.

In the latter case, air is collected either from the engine room with its return to the room or by forced ventilation in a closed cycle.

Methods of preliminary determination of direct current machinery size characteristics. Two methods are used for this purpose. In the first, the value of "machine constant"  $C$  is determined ahead of time and it is used to find the magnitude of basic electrical machinery parameters; in the second, one is guided

by the fixed initial diameters and other factory series electrical machinery data. We will examine the special features of approximate calculation of machine constant C. This methodology, proposed by V. T. Kas'yanov and N. F. Malyshev [21], involves the following.

One must keep in mind two conditions when projecting the placement of electrical machinery of given capacity and rotational speed in a ship's hull:

1. Common series-produced ac turbogenerators, from the design standpoint, /535 are long and have a relatively small diameter, which allows them to be placed conveniently in a relatively narrow ship's hull.

2. Synchronous machines and dc machines of average and high power (800 kW and above), especially with a low rotational speed, in their normal configuration often do not satisfy the requirements for installation aboard ship due to large external diameter with comparatively short overall length. The problem arising in this case is determination of rough overall dimensions and weight of GEU electrical machinery proceeding from given capacity and rotational speed, with simultaneous satisfaction of the requirement for a reduction in outer diameter.

This methodology for approximate calculation of weight and size characteristics is applicable to salient-pole synchronous machinery with a frequency of 40-70 Hz and to average- and high-power shipboard-use dc machinery with a rotor or armature diameter of 1 meter and more, given peripheral velocity from 13 to 55 meters/second. Results obtained here are a bit inflated due to an approximate 10% increase in machine constant C values compared with its actual value for contemporary machinery. These values are inflated because this methodology is based on machinery which has slightly higher weight.

Determination of electrical machinery approximate overall dimensions involves use of machine constant  $C_A$  determined from formula

$$C_A = \frac{D^n l n}{P}, \quad (11.1)$$

where D and l are diameter and length, respectively, of the machine rotor's active portion, meters; n is rotational speed, rpm; P is motor or generator net capacity, kW.

Considering that, for approximate calculation of a machine, the magnitude of the air gap between rotor and stator does not play a material role, one can assume the value of the outer diameter of the rotor equals the inner diameter of the stator.

Having written expression (11.1) in the form

$$C_A = \frac{\frac{\pi}{4} D^2 l}{\frac{\pi}{4} \cdot \frac{P}{n}}, \quad (11.2)$$

one can see that magnitude  $C_A$  is the volume of the machine's rotor in cubic meters per (considering a slight factor) unit of torque. Since the machine constant changes within significant limits depending on machine torque, it most often is called the "machine volumetric use factor" and the  $C_A$  values usually are set /537 between two boundary curves.

Graphs for determination of  $C_A$  values as a function of ratio  $P/n$  are presented in Figure 11.2.

§ 11.2 Methodology for Approximate Calculation of Basic Dimensions  
and Weight of a GEU Salient-Pole Synchronous Machine  
(Using Volumetric Use Factor  $C_A$ )

Initial formulas. When planning the installation aboard a vessel of synchronous propulsion GED or a synchronous diesel generator with given capacity  $P$ , kW, and given rotational speed  $n$ , rpm, if the ratios of the overall dimensions of the selected machine (found in technical reference books) do not satisfy requirements for its installation aboard ship, several variations of the basic dimensions are calculated with the aid of the methodology being examined. The optimum variant then is selected. Recommendations presented make it possible to reduce the number of "test" calculational variants.

As is known, the following ratios apply to a synchronous machine:

$$f = \frac{2pn}{120} \text{ Hz} \quad (11.3)$$

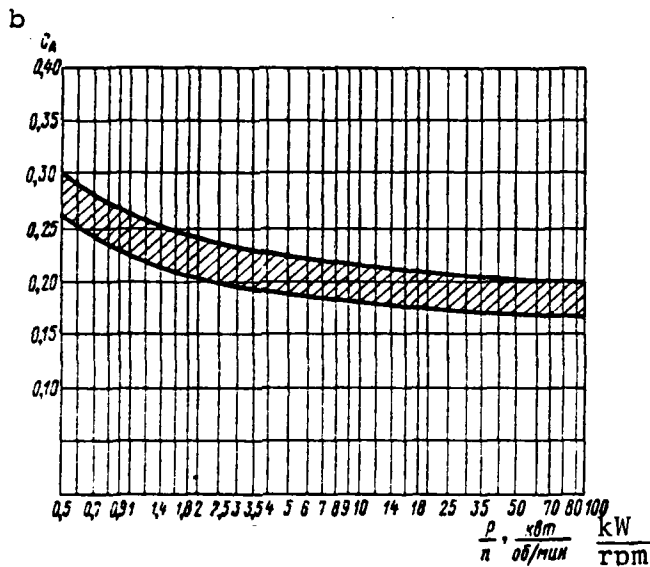
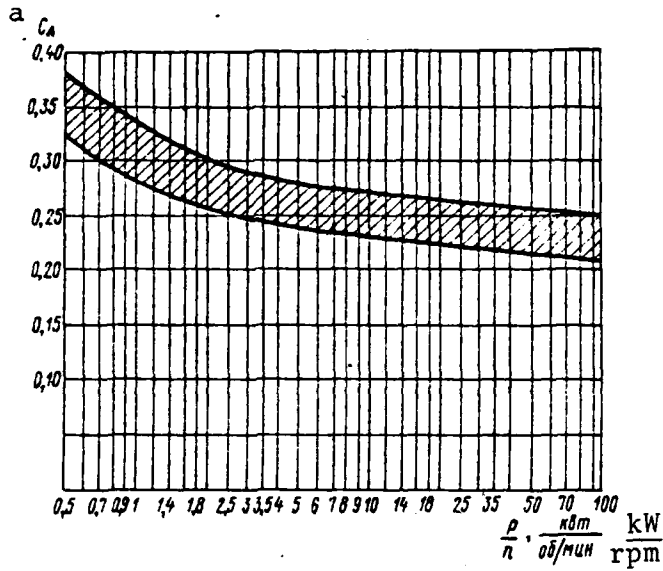


Figure 11.2. Graphs for Determination of the Machine Constant (Volumetric Use Factor)  $C_A$  for Shipboard Salient-Pole Machinery Where  $\cos \varphi = 1$  (a) and for Shipboard DC Machinery (b).

$$\tau = \frac{\pi D}{2p} \text{ м.} \quad (11.4)$$

where  $f$  is current frequency, Hz (usually  $f = 50-60$  Hz for GEU);  $2p$  is the number of poles;  $D$  is stator inner diameter, meters;  $\tau$  is pole pitch, meters.

Rotor peripheral velocity is determined from formula

$$v = \frac{\pi D n}{60} \text{ m/sec.} \quad (11.5)$$

With the aid of formulas (11.3) and (11.4), we will find

$$D = \frac{120 \tau f}{\pi n} \text{ m.} \quad (11.6)$$

and, from formula (11.5), finally we have

$$D = \frac{60v}{\pi n} \text{ m.} \quad (11.7)$$

For low-speed synchronous GED proceeding from the conditions of starting cage placement and obtaining satisfactory characteristics, pole pitch  $\tau$  must be at least 0.15 meters. It is advisable from consideration of the electrical /538 calculation for a given GED type to assume that  $\tau = 0.20\text{--}0.25$  meters.

Having substituted these values for  $\tau$  in formula (11.6), we will get smallest acceptable stator diameter

$$D_{\text{min}} \geq \frac{120f(0.13 \div 0.15)}{\pi n} \text{ m.} \quad (11.8)$$

Sequence for calculation of basic machinery dimensions. This calculation occurs in the following sequence:

1. We determine stator inner diameter:.

$$D_0 \geq \frac{120 \cdot f \cdot 0.25}{\pi n} \quad (11.9)$$

Since the greatest peripheral velocity for high-speed diesel generators must not exceed 60 meters/second, then, substituting this value in formula (11.7), we will get the standard working expression for largest acceptable stator diameter

$$D_{\text{max}} = \frac{3600}{\pi n} \text{ m.} \quad (11.10)$$

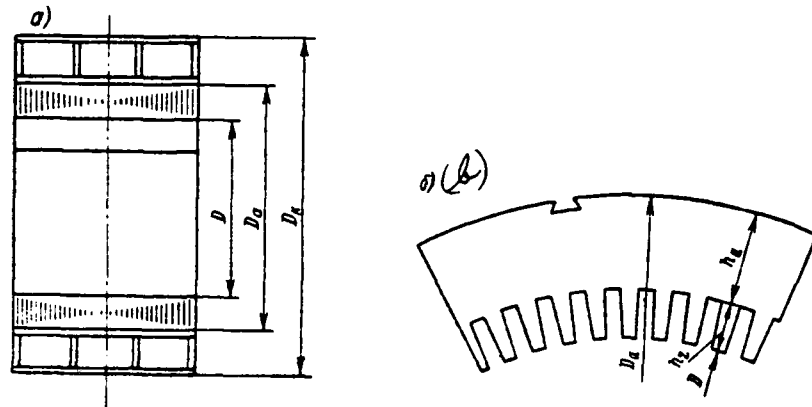


Figure 11.3. Stator Dimension Designations: a--Core and housing; b--Core only.

2. We determine stator core diameter  $D_a$  equal to the sum of inner diameter  $D$ , double the height of toothed zone  $2h_z$  and double the height of back edge  $2h_a$ .

Designations for stator core and housing dimensions are shown in Figure 11.3a, with core dimensions only shown in Figure 11.3b.

Given normal values for induction in the stator gap and back edge, slot depth, and thickness of dovetail wedges holding the stator core, the following expression can be used to calculate stator core external diameter:

$$D_a = D + 2h_z + 2h_a + 0,03 = D \left( 1 + \frac{0,015\pi}{f} \right) + 0,17 \text{ м.} \quad (11.11)$$

3. We determine stator housing exterior diameter  $D_k$  (see Figure 11.3a) and housing width at the feed  $B_k$  (Figure 11.4), using polyempirical formulas /539 obtained after analysis of objective laws in many synchronous machinery configurations in use:

$$D_k = 1,14D_a + 0,4 \text{ м;} \quad (11.12)$$

$$B_k = 1,12D_k \text{ м.} \quad (11.13)$$

The diameter of stators in domestically-produced synchronous machinery are shown in Table 11.1.

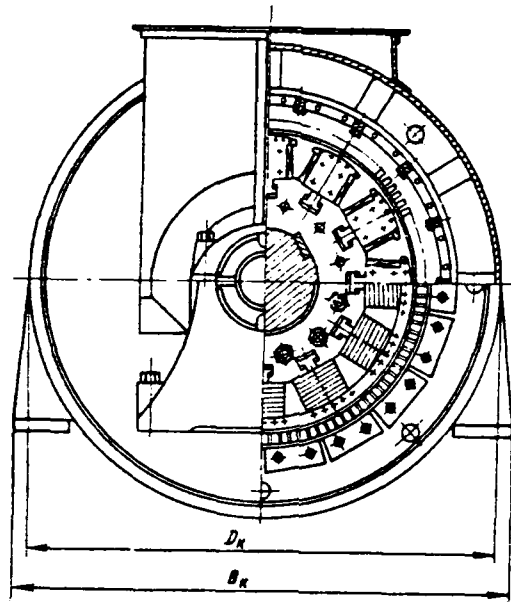


Figure 11.4. Synchronous Machine Cross Section.

If dimensions obtained from standard working formulas (11.9) and (11.11)--(11.13) are applicable from the point of view of overall dimensions (i. e., proceeding from the largest acceptable machine housing diameter based on the conditions of its installation aboard ship), then calculations continue. Otherwise, we will find the smallest possible machine housing diameter from formulas (11.8) and (11.11)--(11.13). Then, after several tests, a certain intermediate diameter falling fully within the required established clearance is selected. If it turns out that the smallest dimension of all those selected also does not correspond to the given overall dimension, then one must examine the possibility of using a lower frequency, for diesel generator plants in particular.

4. We determine stator length, proceeding from machine total length  $L$  between the outer edges of labyrinth packings (Figure 11.5) equal to the sum of the following terms:

-- length of stator active iron (core)  $l$ ;

(a) Диаметры статора				
(b) наружный $D_a$ , м	(c) внутренние D, м			
	1,16	0,8	0,86	0,92
1,40	1,04	1,10	1,16	—
1,70	1,34	1,39	1,45	—
2,13	1,75	1,71	1,83	1,88
2,60	2,17	2,22	2,30	—
2,90	2,44	2,50	2,57	2,64
3,25	2,75	2,82	2,90	2,95
3,45	3,45	—	—	—
4,25	3,55	3,75	3,80	4,0
5,5	4,85	4,90	4,96	5,0
5,5	5,05	5,10	—	—
6,55	5,86	5,88	5,95	6,0
6,55	6,05	6,10	—	—

Table 11.1. Synchronous Machinery Design Dimensions. a--Stator diameters; b--Exterior  $D_a$ , meters; c--Interior D, meters.

-- doubled full overhang of stator winding end-connectors  $l_s$  (including /540 the distance between the stator winding heads and panel end wall, which is determined by dielectric stability and cooling air supply conditions;

-- lengths of the slip-rings and brush device ;

-- two lengths of bearing pedestals C and C' ;

-- doubled gap  $\delta$  between the panel and bearing labyrinth packings /541 required for convenient panel disassembly;

-- calculation error allowance equalling 0.16 meters:

$$L = l + 2l_s + l_k + C + C' + 2\delta + 0,16 \text{ м.} \quad (11.14)$$

Using formulas (11.14) and (11.1), we find desired stator length

$$l = \frac{C_A P}{D^2 n} \text{ м.} \quad (11.15)$$

where  $C_A$  is taken as the upper threshold curve in Figure 11.2a and D is selected stator interior diameter.

We can assume for contemporary synchronous machinery with shortened winding pitch and voltage up to 6,000 V

$$l_s \approx 0,20 + \frac{0,012 D n}{f} \text{ м.} \quad (11.16)$$

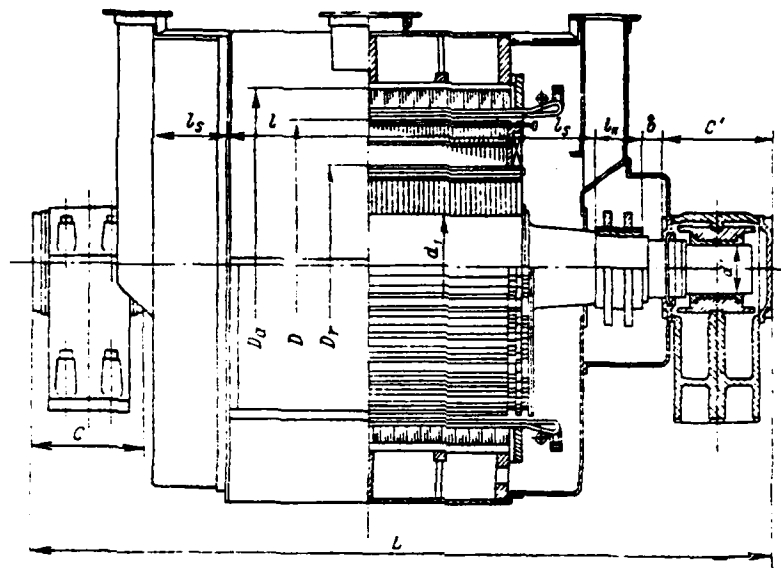


Figure 11.5. Longitudinal Section of a Synchronous Machine.

Slip-ring length  $l_k$  will be found from formula

$$l_k = 0,14 + \frac{P}{60\,000} \text{ м.} \quad (11.17)$$

In order to determine the axial length of bearings C and C', one initially must find the diameter of the shaft journal transmitting full torque, using formula

$$d = 0,16 \sqrt[3]{\frac{P}{n}} \text{ м.} \quad (11.18)$$

The second shaft journal, if it does not transmit torque, can have a diameter equalling

$$d' \approx 0,75d \text{ м.} \quad (11.19)$$

Having calculated the diameters of shaft journals  $d$  and  $d'$  and having rounded off their values relative to Table 11.2 (considering the height from the base to the center of the shaft as equalling 0.6 meters), we select applicable bearings from that table and we will find their dimensions C and C'. Bearing dimension designations are presented in Table 11.6.

Having substituted in formula (11.14) values  $l_s$  and  $l_k$  from expressions (11.16) and (11.17) and having added the constant values, we will find total machine length (see Figure 11.5).

$$L \approx l + \frac{0.024Dn}{f} + \frac{P}{60000} + C + C' + 0,7 \text{ м.} \quad (11.20)$$

5. We will find air duct dimensions, proceeding from the amount of cooling air determined from formula

$$Q = \frac{(0,04 + 0,05) P}{1,15 \Delta\theta} \text{ м}^3/\text{sec}, \quad (11.21)$$

where  $P$  is machine rated capacity, kW; 0.04--0.05 is a factor considering losses carried away by the air (in fractions of nominal power);  $\Delta\theta$  is cooling air temperature increase when passing over the machine (18-20° C).

From formula (11.21) we have /542

$$Q \approx (0,0018 + 0,0022) P \text{ м}^3/\text{sec}. \quad (11.22)$$

The first factor applies to high-speed and the second to low-speed machinery.

Having determined the amount of cooling air and having established the /543 velocity of its movement in inlet and outlet ducts (on the order of 12-18 meters/second), one can find the desired air duct dimensions.

6. Proceeding from the selection and calculation of electrical parameters, rotor mechanical stability, and ventilation conditions, the practicability of machine placement is checked based on adherence to the following conditions:

$$\left. \begin{aligned} \tau &= \frac{\pi D}{2p} = \frac{\pi D n}{120f} > (0,13 + 0,15) \text{ м;} \\ v &= \frac{\pi D n}{60} \leq 60 \text{ м/sec; } l < (1,8 + 2) \text{ м.} \end{aligned} \right\} \quad (11.23)$$

Диаметр шейки вала $d$ , м (б)	(а) Размеры подшипника (см. рис. 11.6)			Вес, т (в)
	A	B	C	
0,1	0,8	0,225	0,33	0,22
0,11	0,8	0,225	0,33	0,22
0,12	0,85	0,235	0,34	0,24
0,13	0,85	0,235	0,34	0,24
0,14	0,9	0,245	0,35	0,295
0,15	0,9	0,245	0,35	0,295
0,16	0,95	0,285	0,4	0,415
0,18	0,95	0,285	0,4	0,425
0,20	1,00	0,325	0,44	0,495
0,22	1,00	0,325	0,44	0,51
0,25	1,1	0,365	0,48	0,72
0,28	1,2	0,43	0,56	0,92
0,30	1,2	0,43	0,56	0,92
0,35	1,35	0,49	0,62	1,43
0,40	1,45	0,54	0,67	1,72
0,45	1,7	0,6	0,75	2,54
0,50	1,8	0,65	0,80	3,1
0,55	1,9	0,72	0,87	3,6
0,60	2,0	0,75	0,92	4,1
0,65	2,08	0,78	0,97	4,6
0,7	2,15	0,82	1,00	5,2
0,75	2,2	0,85	1,05	5,6

Table 11.2. Bearing Dimensions and Weight. a--Bearing dimensions (See Figure 11.6); b--Shaft journal diameter  $d$ , meters; c--Weight, tons;

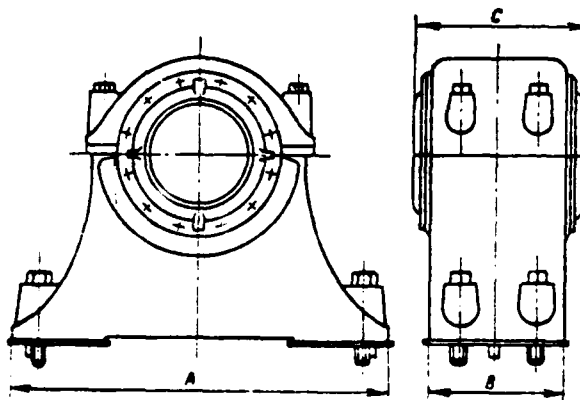


Figure 11.6. Bearing Dimension Designations.

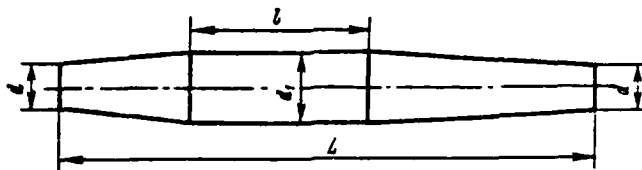


Figure 11.7. Designations for Dimensions of a Simplified Shaft Design.

In the event even one of these three conditions is not adhered to, the projected variant, if of special interest, needs to be reexamined.

Weight calculation of individual machinery parts. The weights of individual machinery parts can be determined from the following formulas in which numerical coefficients have been obtained through analysis of several operating machines.

1. Weight of a welded housing with feet (see Figure 11.4):

$$G_{\kappa} \approx 1,2 (D_{\kappa}^2 - D_a^2) l \text{ t.} \quad (11.24)$$

2. Weight of stator core with winding, terminal plates, and pins:

$$G_s \approx 4,7 (D_s^2 - D) (l + 0,15) \text{ t.} \quad (11.25)$$

3. In order to determine the weight of a shaft, we will simplify its form, as shown in Figure 11.7. Here, value  $d$  is taken from formula (11.18), while the diameter of the center portion of the shaft  $d_1$  comes from formula

$$d_1 = 1,05d \sqrt[3]{\sqrt{1,1 + \left(\frac{Ln}{3,20}\right)^2}} \text{ m.} \quad (11.26)$$

Shaft weight without flanges:

$$G_s \approx 2,1d^2 \left[ \left(\frac{d_1}{d}\right)^2 (L + 2l) + \left(\frac{d_1}{d} + 1\right) (L - l) \right] \text{ t.} \quad (11.27)$$

4. Rotor weight is determined from the following conditions. The body of the rotor to which the poles are fastened is designed either in the form of /544 a continuous drum made of thick bolted iron sheets seated directly on the shaft (Figure 11.8a) or, given large diameters, in the form of a poured or welded design consisting of a rim, spider (discs), and sleeve (Figure 11.8b). The rotor drum's exterior diameter  $D_r$  or of its rim can be determined from formula

$$D_r = D - \frac{Df(0,63 \cdot 2p)}{1,15Df + 8,2 \cdot 2p} \text{ m.} \quad (11.28)$$

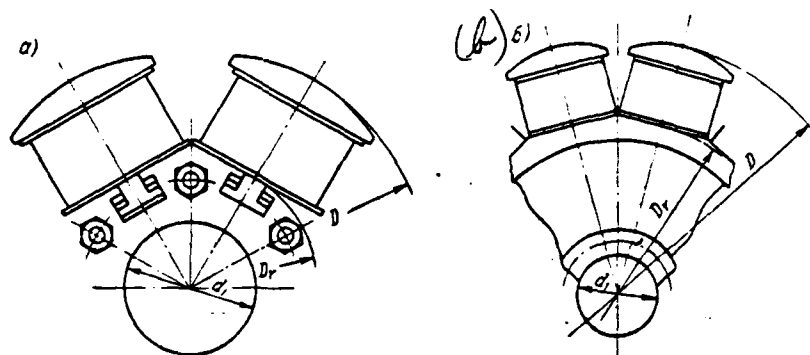


Figure 11.8. Rotor Sketch: a--With a solid core; b--With a rim, disks, and sleeve.

A rotor in the form of a solid drum (see Figure 11.8a) is used given relatively small diameters, when

$$\frac{800(D_r - d_1)}{\pi} < 1, \quad (11.29)$$

where  $d_1$  is determined from formula (11.26).

In other instances, the design shown in Figure 11.8b is more preferable. The weight of the body of a rotor consisting of a solid drum:

$$G_r = 6,2 (D_r^2 - d_1^2) (l + 0,2) \text{ t.} \quad (11.30)$$

The weight of the rotor rim, disk, and sleeve

$$G_r = \left[ \frac{0,02DnD_r}{f} + 0,08D_r^2 + d_1^2 \right] 1,7,8 \text{ t.} \quad (11.31)$$

5. We determine the weight of the poles of a rotor with a winding and starting (damper) cell from formula

$$G_m \approx 4,7 (D^2 - D_r^2) (l + 0,1) \text{ t.} \quad (11.32)$$

6. We determine the weight of bearings  $G_p$  and  $G'_p$  from Table 11.2.

7. The weight of the panels with ducts where the wall is 3 mm thick, taking elbows into account:

$$G_s = 0,037 (D_k - 0,1) (4l_s + 2l_k + D_k - 0,1) \text{ t.} \quad (11.33)$$

8. Total machine weight; /545

$$G_0 = 1,05 (G_k + G_a + G_s + G_r + G_m + G_s + G_p + G'_p) \text{ t.} \quad (11.34)$$

9. Rotor moment of gyration:

$$GD^2 = G_m \left( \frac{D + D_r}{2} \right)^2 + \left[ \frac{0,02 D n D_r^3}{f} + 0,04 D_r^4 + 1,6 d_1^4 \right] 1,7,8 \text{ t} \times \text{m}^2. \quad (11.35)$$

All dimensions for the remaining values are given in meters in the formulas presented for determination of the weights of individual machinery parts.

Calculation of fan drive motor power. The power of the fan drive motor (or motors) is determined from formula

$$P_o \approx \frac{Qh}{102\eta_o}, \quad (11.36)$$

where  $Q$  is amount of cooling air in cubic meters/second;  $h$  is pressure, mm water column (100-120 mm);  $\eta_o$  is fan efficiency (0.5--0.6).

§ 11.3 Methodology for Approximate Calculation of Basic  
Direct Current GEU Machinery Dimensions and Weight  
(Using Armature Volumetric Use Factor  $C_A$ )

Initial formulas. Just as for synchronous machinery (see § 11.2), if ratios of the overall dimensions of a domestically-produced series motor or dc generator of a given power are unsuitable for a projected GEU, then the required ratios of machinery dimensions are determined by means of test calculations using the semi-empirical formulas presented below. They also are the result of analysis of the objective laws of the corresponding types of machinery in use.

From formula (11.1) determining the ratio between armature diameter  $D$  and its length  $l$ , we have

$$l = \frac{C_A P}{D^2 n} \text{ m.} \quad (11.37)$$

where  $P$  is motor or generator net capacity, kW;  $n$  is rotational speed, rpm;  $C_A$  is armature volumetric use factor determined from the graph (value  $D$  and  $l$  dimensions in meters).

Sequence for calculation of machinery dimensions. The calculation is made in the following sequence.

1. We determine the dimensions of the armature, using for the first test /546 variant  $D = l$ . Then, from formula (11.37), we will find

$$D = l = \sqrt[3]{C_A \frac{P}{n}}, \quad (11.38)$$

where value  $C_A$  is taken from the upper threshold curve in Figure 11.2b.

2. We calculate the exterior dimensions of the machine in cross section, i. e., its interior and exterior diameters and the width of the main frame at

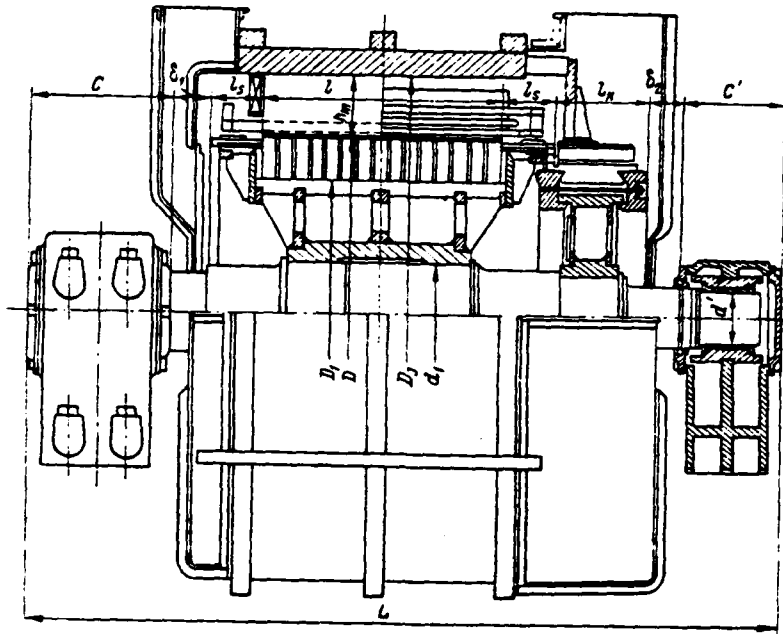


Figure 11. 9. Longitudinal Section of an AC Machine.

the feet (overall dimension designations are shown in Figures 11.9 and 11.10) from formulas:

interior diameter

$$D_j \approx 1,05D + 0,40 \text{ m}; \quad (11.39)$$

exterior diameter

$$D_k = 1,10D_j + 0,20 \text{ m}; \quad (11.40)$$

frame width at the feet

$$B_k = 1,12D_k \text{ m}; \quad (11.41)$$

We will find the length of active iron from expression (11.37).

3. The practicability of machine placement is checked based on adherence /547 to the following conditions and proceeding from empirical and mechanical calculations:

$$\frac{P}{D} \leq 2500; \quad (11.42)$$

$$Dln < 550; \quad (11.43)$$

$$v = \frac{\pi D n}{60} < (55 \div 60) \text{ m/sec.} \quad (11.44)$$

If all three conditions are met, then the machine can be manufactured with the armature dimensions found. If it turns out that the required overall dimensions (acceptable threshold dimensions based on placement conditions on the vessel) cannot be used, then one must increase the diameter of the armature and again do the calculations in formulas (11.39)--(11.41), adding full use of the installed machine's overall dimensions. If, on the other hand, it does not fall within the requisite clearance limits, then the armature diameter must be decreased accordingly.

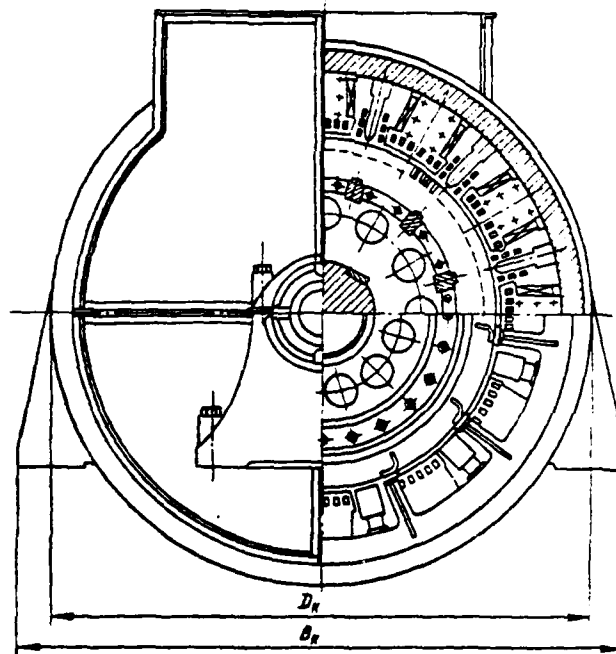


Figure 11.10. Direct Current Machine Cross Section.

4. We determine commutator diameter and length. Here, one should consider that, for shipboard machinery, it is advantageous to use commutators with the largest possible diameter to reduce their overall length. But, the value is /548

constrained by several design considerations and safe peripheral velocity. This will lead to the following requirements:

$$d_k \leq D - 0,4(0,2) \text{ m}, \quad (11.45)$$

or

$$d_k = (0,7 \div 0,8) D \text{ m}, \quad (11.45a)$$

or

$$d_k \leq \frac{670}{n} \text{ m}. \quad (11.46)$$

The commutator's total length is determined by formula

$$l_k = 0,08 + \frac{0,14P}{U d_k} \text{ m}, \quad (11.47)$$

where P is machine capacity, kW; U is voltage at the commutator.

5. We determine the number of poles. For compensated machinery, the normal number of poles equals (rounded off to the nearest whole number)

$$2p \approx 6,5D. \quad (11.48)$$

On the other hand, proceeding from acceptable commutator bar thickness, it is necessary to insure the condition:

$$2p \leq \frac{10000d_k}{U}. \quad (11.49)$$

Armature dimensions and number of poles for compensated dc machinery produced domestically are presented in Table 11.3.

$\frac{D, \text{ m}}{2p}$	0,99	1,12	1,4	1,6	1,83	2,10	2,56	2,85	3,10	3,40	3,81	4,1	4,5
	6	8	8-10	10	12	14	16	18	20	22	24	26	28

Table 11.3. Compensated DC Machinery Design Data.

6. We determine bearing dimensions. The diameter of a shaft journal which is transmitting machine torque equals

$$d \approx 0,16 \sqrt[3]{\frac{P}{n}} \text{ m.} \quad (11.50)$$

The diameter of the second shaft journal, if it does not transmit torque, can be assumed to equal

$$d' \approx 0,75d \text{ m.} \quad (11.51)$$

We round off the values of journal diameters to the high side from Table 11.2 and, from it, we will find axial diameters of bearings C and C' (see Figure 11.9).

7. We determine total machine length. Doubled armature winding end-connector overhang, in accordance with 11.9, equals

$$2l_1 = \frac{2,5D}{2p} + 0,08 \text{ m.} \quad (11.52)$$

Specific gaps must be available to insure reliable machine operation, supply of cooling air, and convenient disassembly: between the panel inner end wall and armature winding rear end-connectors; between the commutator and panel wall; between panel full-scale walls and bearing labyrinth packings (see Figure 11.9). The total of these gaps is determined by expression

$$\sum \delta = 0,02D + 0,13 \text{ m.} \quad (11.53)$$

Total machine length between the exterior surfaces of the bearing labyrinth packings equals

$$L = l + l_k + 2l_i + \sum \delta + C + C' \text{ m.} \quad (11.54)$$

Substituting in this expression values of the magnitudes from formula (11.47), (11.52), and (11.53) and having rounded off the results to the high side, we will get

$$L = l + \frac{0,14P}{Ud_k} + \frac{2,5P}{2\rho} + C + C' - 0,30 \text{ m.} \quad (11.55)$$

8. The amount of cooling air is calculated from expression

$$Q = \frac{(0,05 + 0,065) P}{1,15 \Delta t} \text{ m}^3/\text{sec}, \quad (11.56)$$

where P is machine net capacity, kW; a numerical factor (0.05--0.065) considers losses carried away by the air (in fractions of net capacity);  $\Delta t$  is the increase in cooling air temperature (equalling 18° C).

Having substituted these values in expression (11.56), we will get final standard working formula

$$Q = (0,0024 + 0,0031) P \text{ m}^3/\text{sec}. \quad (11.57)$$

Here, the first factor applies to high-speed and the second to low-speed machinery.

8. [sic] Having determined the amount of cooling air and having assumed that the speed of its movement in the ducts (12--15) in meters/second, we will find duct section and dimensions.

The power of the fan motor (or motors) is computed

$$P_v = \frac{Qh}{102\eta_v}, \quad (11.58)$$

where value  $Q$  is taken from formula (11.56);  $h$  is air pressure, mm water column (110--125);  $\eta_v$  is fan efficiency (0.5--0.6).

9. Having determined the amount of cooling air and duct dimensions, overall dimensional drawings are compiled. A judgement is made as to the suitability /550 of the given variant and the requirement for any changes and corrections.

Weight calculation of individual machinery parts. The calculation is carried out in the following sequence.

1. Preliminarily, we will find the internal diameter of armature iron  $D_i$ , internal frame diameter  $D_j$ , and frame cross section  $B_j$  from formulas

$$D_i = D \left( 1 + \frac{2}{2p} \right) - 0,10 \text{ m}; \quad (11.59)$$

$$D_j = 1,05D + 0,40 \text{ m}; \quad (11.60)$$

$$B_j = 1,1 \frac{Dl}{2p} \text{ m}. \quad (11.61)$$

2. The weight of the frame (including feet) is determined from standard working expression

$$G_k = 28(1,25D_k - 0,4)S_j \text{ t}. \quad (11.62)$$

3. The weight of the main and additional poles with their windings (including the compensating winding):

$$G_m = 5(D_i^2 - D^2)l \text{ t}. \quad (11.63)$$

4. The weight of the armature active iron with a winding, compensating connections, and winding holders:

$$G_a = 5(D^2 - D_i^2)(l + 0,15) \text{ t}. \quad (11.64)$$

for small machinery, value  $d_1$  should be substituted for  $D_i$  in expression (11.64).

5. The full weight of the commutator (sleeve and commutator bars):

$$G_{\text{ком}} = 4,7 (d_k - 0,13) l_k \quad \text{t}, \quad (11.65)$$

where  $d_k$  and  $l_k$  are determined from formulas (11.45) and (11.47).

6. Shaft weight:

$$G_s = 2,1 d^2 \left[ \left( \frac{d_1}{d} \right)^2 (L + 2l) + \left( \frac{d_1}{d} + 1 \right) (L - l) \right] \quad \text{t}. \quad (11.66)$$

In formula (11.66), shaft diameter beneath the armature sleeve (see Figures 11.9 and 11.10) is determined by expression

$$d_1 = 1,05 d \sqrt[3]{1,1 + \left( \frac{L_n}{320} \right)^2}. \quad (11.67)$$

7. Armature sleeve and star weight:

$$G_3 = 4,5 [0,1 D_i (D_i - 1,5) + d_i^2] (l + 0,1) \quad \text{t}. \quad (11.68)$$

8. The weight of both panels with ducts (given iron 3 mm thick):

$$G_4 = 0,037 (D_j + 0,2) (4l_s + 2l_k + D_j + 0,2) \quad \text{t}. \quad (11.69)$$

9. Weight of a crossbeam with brackets and brushes:

$$G_n = 0,37 (0,1 l_k \cdot 2p + d_k + 0,6) \quad \text{t}. \quad (11.70)$$

10. The weight of bearings  $G_p$  and  $G'_p$  is determined from Table 11.2. /551

11. The total weight of the machine comprises:

$$G = 1,05 (G_k + G_m + G_a + G_{\text{ком}} + G_n + G_3 + \\ + G_r + G_n + G_p + G'_p) \quad \text{t}. \quad (11.71)$$

Calculation of armature moment of gyration. Armature moment of gyration (for machinery with diameter  $D > 1$  meter) is determined from expression

$$GD^2 = 1,6l(D + D_i)^3(D - D_i) + 0,4D^4 + 3,5d_k^2 l_k t \times m^2 \quad (11.72)$$

This methodology makes it possible with sufficient accuracy to calculate overall dimensions and weights of GEU electrical machinery while the project still is in the draft stage.

## Dual-Current Electrical Propulsion Plants

§ 12.1 Dual-Current Electrical Propulsion Plant Special Features  
and Developmental Prospects

Overall advantages. The level of technology achieved in converting alternating current into direct current makes it possible now to create electrical propulsion plants essentially of any power while retaining their advantages both in alternating and in direct current. GEU in which synchronous generators place primary motors into rotation at a constant speed and propellers with dc motors being fed by these generators via semiconductor rectifiers are called "dual-current GEU."

Use of this type of plant improves the quality of the entire shipboard electric power plant, reduces its weight and size, and increases technical and economic indicators. In addition, the most favorable conditions are created for effective introduction of automation with optimum quality of static and dynamic characteristics.

Dual-current systems have favorable capabilities for:

- use of highly-economical high-speed high-power primary motors (steam /552 and gas turbine);
- direct connection of high-speed ac generators to primary motors without reduction gear. Here, use of generators of increased frequency is presupposed, which makes it possible to reduce the overall dimensions of the machinery and rectified voltage pulsation;
- provision of great GEU circuit reliability and an increase in its efficiency thanks to use of ac generators (convenient maintenance and repair also should be considered);
- independence of propeller rotational speed and its regulation from primary motor rotational speed;
- operating the GED armature with any number of primary motors and generators;
- automatic GED torque change over a wide range, given fixed values for primary motor rotational speed and power;
- power take-off from electric propulsion bus bars to auxiliary bus bars.

Thus, combination of these advantages of alternating and direct current in a given type GEU circuitry makes this very promising. But, know-how in creation of dual-current GEU still is lacking in foreign and domestic shipbuilding practice. Therefore, when designing such systems, one must consider several of their special features as well as surmount many technical difficulties, which require further study.

Design difficulties mainly are determined by the commensurability (and sometimes even equilibrium) of electric power source and consumer capacities, i. e., by the entire combination of conditions involving a synchronous ac generator in stationary and transient modes running, via a rectified bridge, a dc GED that is commensurate in capacity.

It should be noted that practice in use of dual-current systems in industry has the following special features compared with such systems in a GEU:

-- a dc transmission line is connected to an industrial power system in which powerful synchronous generators are operating, while the rectified load and converter power are commensurate. However, the nature of the load itself -- in the form of a line with distributed parameters -- differs to a considerable degree from a GEU system load;

-- a dc electric motor in an industrial network is fed from an ac transmission line, whose capacity essentially can be considered infinitely high compared to rectifier drive power.

In a GEU, GED power is commensurate with SG power.

The field windings of powerful generators in an industrial network are fed via a rectifier from special exciters--SG. Here, the rectified load is /553 commensurate in power with the feed source. In a GEU, field feed comes from the shipboard network: its influence on electric power quality needs to be considered.

Conversion systems. Rectified converters are used for operation in direct current in a GEU main circuit. Such GEU circuits can be in two modifications:

-- synchronous generator--uncontrolled rectifier--direct current GED (SG--V--GED);

-- synchronous generator--controlled rectifier--direct current GED (SG--VU--GED).

A particular modification is selected considering the advantages and disadvantages of controlled and uncontrolled rectifiers, the level of assimilation and know-how in their use, and technical and economic indicators.

In spite of the insufficient number of tests and absence of know-how in design and operation of dual-current GEU with controlled rectifiers in a main circuit, the work done in this area to date makes it possible to point out several clear advantages of such GEU with thyristor converters:

- high mechanical stability and reliability of the elements and of the system as a whole;

- very high speed since feedbacks "will be directed" to an inertia-free control system, bypassing field system links;

- capability of a broad range of regulation and accomplishment of GED reversal by an effect in the control system;

- very slight power required for control;

- relatively high efficiency;

- broad prospects for creation of a single shipboard electric power plant with simultaneous feed of GED and auxiliary consumers.

An example of calculations of a GEU for a three-shaft vessel with provision for independent rotational speed and reversal control for each propeller, given any number of operating primary motors, can represent some of the special features of using one of the two aforementioned dual-current GEU system variants.

The need for two turbines in the role of primary motors when the first variant with an uncontrolled rectifier unit is used requires installation of six (three per turbine) main generators running three two-armature GED. Here, regulation of the voltage supplied to the main propulsion motor and, correspondingly, the speed of its rotation, is accomplished through a change in synchronous generator field.

In the second variation, with a controlled rectifier, the number of main generators equals the number of primary motors, turbines in this case, and /554 GED rotational speed regulation is accomplished by a change in the controlled rectifier's control angle. Voltage at the synchronous generator terminals remains constant here.

A serious drawback to the first system variant is the turbine-driven set's long shafting line, which will lead to a reduction in its reliability and to an increase in engine room dimensions. As far as the GEU system variant with controlled rectifiers is concerned, it, on the contrary, has several major advantages, making it more prospective. These advantages are:

-- voltage constancy at synchronous generator terminals; this permits optimal solution of the problem of power take-off from electric propulsion bus bars all the way to creation of a single shipboard electric power plant (GED and shipboard electric power plant for auxiliaries);

-- absence of tight coupling among main generators and GED, which creates the capability for their autonomous control as well as selection of a number of main generators equalling the number of primary motors. GEU economic indicators rise here.

Even though at present the overall dimensions and cost of controlled rectifiers is higher and their reliability compared to uncontrolled rectifiers is lower, nonetheless a dual-current GEU system with controlled rectifiers should be considered the most promising. This assertion is illustrated in Table 12.1, where several comparative results from calculations are presented: for the turbine-driven set for the first variant where each generator is rated at 4,000 kW and for a turbine-driven set for the second variant where each generator is rated at 16,000 kW (turbine-driven set rotational speed in both variants is 3,000 rpm).

Table 12.1

Several Technical and Economic Indicators of Dual-Current GEU Systems With Uncontrolled (Variant 1) and Controlled (Variant 2) Rectifiers

Parameter Designation	Turbine-Driven Set	
	With Three 4,000 kW Synchronous Generator (Variant 1)	With a 16,000 kW Synchronous Generator (Variant 2)
Turbine-driven set length less turbine, mm	9,040	4,200
Turbine-driven set weight less turbine, t	3 x 10.0	27.0
Synchronous generator efficiency, %	96.5	97.5
Synchronous generator diameter, mm	990	1,280

Research and design tasks. Primary tasks concerning creation of dual- /555 current GEU systems, both with controlled and uncontrolled rectifiers, include:

- 1) selection of optimum parameters for generators, GED, and rectifier circuits;
- 2) selection of optimal control and automatic regulation circuits;
- 3) study of the effect of motor load on synchronous generator operation given commensurate or equal generator and GED capacities;
- 4) determination of the spectrum of the harmonic components of current and voltage for alternating and direct current, given commensurate generator and GED capacities, and development of a methodology for their calculation;
- 5) study of the possibility of feeding auxiliary bus bars from electric propulsion bus bars;
- 6) study of the influence of rectified voltage and current pulsations on dc GED operation, its characteristics, and commutation;
- 7) development of a methodology for calculation of dynamic and static characteristics;
- 8) consideration of additional losses and certain special features of GED reversal in these systems.

It is known that one must change the direction of the current in the armature winding or in the motor field winding to reverse a dc motor. In this connection, all reversing drive circuits with controlled rectifiers must be divided into two classes:

- a) those with a change in current direction in the armature winding;
- b) those with a change in current direction in the field winding.

Since it is possible to change current direction in a system with controlled rectifiers by use either of a reversing rectification circuit or a reversing switch, the following basic types of reversing drives are accomplished here:

- with two rectifiers in the armature circuit;
- with one rectifier and a reversing switch in the armature circuit;
- with one rectifier in the armature circuit and two rectifiers in the motor field circuit;
- with one rectifier in the armature circuit and with one rectifier and a reversing switch in the field circuit.

The type with two rectifiers in the armature circuit is the most convenient

and reliable. However, here the number of rectifiers is double, which significantly increases rectifier unit cost. Also, additional devices to eliminate compensating currents between rectifiers and two sets of control devices are required.

Rectifier unit cost is reduced considerably when a circuit with one rectifier and a reversing switch is used in the armature circuit (since a switch is /556 cheaper than a set of rectifiers). In addition, a powerful switch is needed here and it is impossible to brake with recuperation. However, in spite of these drawbacks, this circuit is sufficiently reliable since a propulsion plant is characterized by an insignificant number of reversals per hour. It also is faster than the circuit in which GED reversing is accomplished by a change in current direction in the field circuit.

As can be seen from this abbreviated listing of research and practical tasks involving dual-current GED development, effective solution requires joint efforts on the part of scientific and engineer-technical personnel.

#### § 12.2 Special Features of Electrical Machinery Operation in a Dual-Current GEU System with Uncontrolled Rectifiers

##### Diagram of the mmf of a synchronous generator running a rectified load.

A special feature of a synchronous generator in a dual-current GEU is that its normal steady-state mode is asymmetrical, which to a considerable degree will depend upon the magnitude and nature of the load, as well as on the rectifier circuit used. It is possible to differentiate two modes relative to a three-phase bridge circuit in accordance with converter operating conditions:

- conductance mode when current flows in two generator phases;
- commutation mode when current flows in three generator phases.

Thus, the normal mode is a quasi-steady state SG operating mode with periodicity  $m$  determined by rectifier circuit.

Three-dimensional diagrams of generator mmf are presented in Figure 12.1 to illustrate the aforementioned processes occurring in an SG; here, the locus of the vector tips is constructed: armature reaction mmf  $F_a$ , exciting basic field mmf  $F_o$ , and resultant mmf  $F$  where  $I_d = \text{const.}$

In the conductance mode (Figure 12.1), given a time reading from the axis passing through the origin of phase A emf:

$$-\left(\frac{\pi}{6} - \gamma\right) \leq t \leq \frac{\pi}{6}$$

(where  $\gamma$  is the commutation angle), current flows in phases B and C. The mmf vectors of these phases (b and c) and resultant armature reaction mmf vector  $F_o$  are stationary in space when  $I_d = \text{const}$  and are constant in magnitude. The exciting field mmf vector  $F_o$  is constant in magnitude, rotates at rotor speed  $\omega_p$ , and its tip during time of conductance describes arc  $d_1b_1$ . Arc  $ab$  is the locus of the tip of resultant mmf vector  $F$ . Consequently, the resultant mmf vector changes in magnitude and displaces in space with average angular velocity  $\omega_1$  differing from  $\omega_p$ .

For the period of commutation of phases C and A  $\left(\frac{\pi}{6} \leq t \leq \frac{\pi}{6} - \gamma\right)$ , considering it as being rectilinear, straight line  $b_2c_2$  will be the locus of the tip of armature reaction mmf vector  $F_a$ , while straight line  $bc$  will be the locus of the tip of resultant mmf vector  $F$ . The displacement in space of vector  $F_a$  essentially will depend on machine load, i. e., on the angle of commutation. The average angular velocity of vector  $F_a$  is determined by expression  $\omega_2 = \frac{\pi}{3\gamma} \omega_p$ , while  $\omega_2 > \omega_p$ ; given angle of commutation  $\gamma = \frac{\pi}{3}$ , values  $\omega_2$  and  $\omega_p$  will become equal.

It can be seen from the constructed diagrams that the tip of resultant mmf vector  $F$  describes complex curve  $kabcd$  having periodicity  $m$ . The velocity of displacement in space and magnitude of vector  $F$  and, consequently, of resultant machine flux, periodically change, as a result of which additional emf of varied frequencies are induced in stator and rotor windings.

The locus of the tip of mmf vector  $F$  will change with an increase in load and will be characterized by curve  $ka'bc'd$ . Given a load corresponding to angle of commutation  $\gamma = \frac{\pi}{3}$ , the locus takes on the form of a circle passing through point  $kbd$ .

Replacement of the actual generator by a source with a sinusoidal equivalent emf with amplitude  $E_m$  and equivalent resistance  $X_r$  will lead to replacement of the loci of the tips of the mmf vectors  $F_a$  and  $F$  determined by straight line

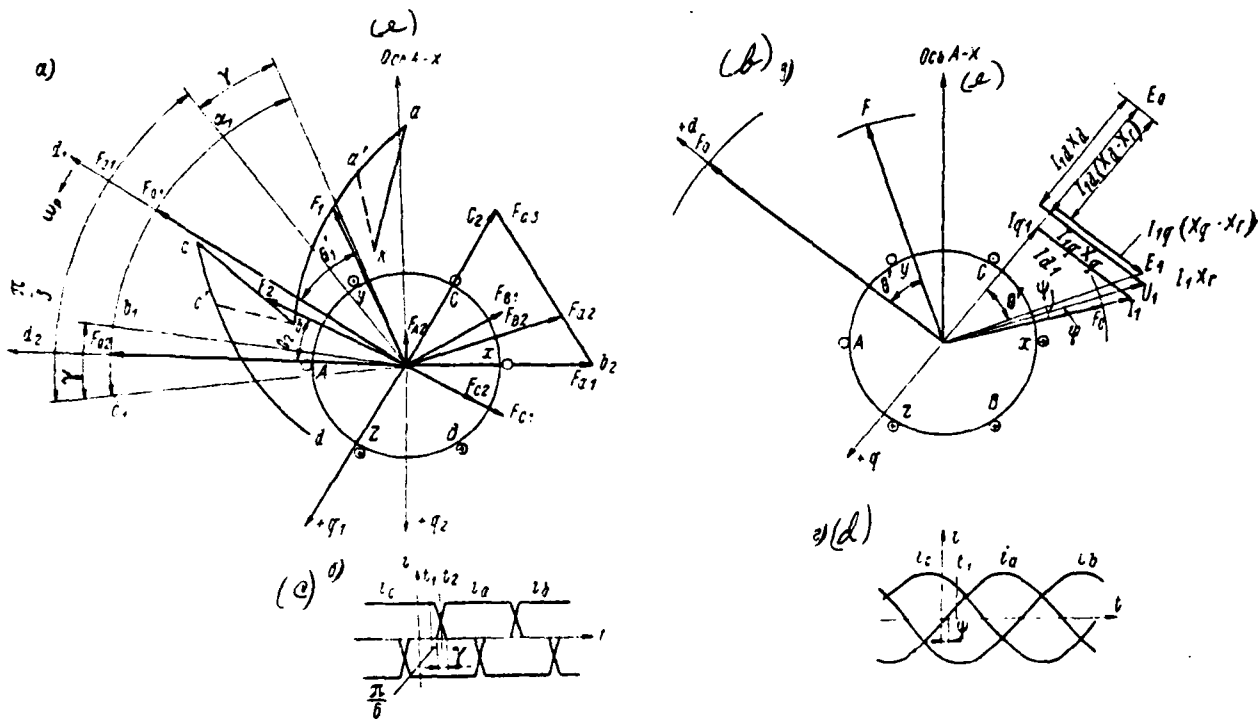


Figure 12.1. Three-Dimensional Diagrams of Generator Magnetomotive Forces: in the conductance mode (a); of converter currents (b); of actual emf, voltage, and current values (c); of phase currents (d); e--Axis A-X.

$b_2c_2$  and by curve  $kabcd$  by several circles. Sinusoidal phase currents correspond to the locus of armature reaction mmf vector in the form of a circle. Consequently, one must expand the actual phase currents in a Fourier series and extract their first harmonics in order to find  $E_m$  values.

A time diagram of converter currents is presented in Figure 12.1b.

A vector diagram for an SG operating a rectified load for actual emf, voltage, and current values is shown in Figure 12.1c. Since only the first harmonic components of the phase currents are considered, armature reaction flux and, consequently, resultant flux as well, rotate in synchronization with the rotor. Emf  $E_1$ , which corresponds to resultant flux and is used as basic design emf, can be determined with the aid of this diagram. In actuality, the form of the generator phase current

is not sinusoidal. Therefore, phase voltage is not sinusoidal either. However, distortions will be identical in each phase. The first harmonics of phase /559 voltages form a symmetrical direct sequence system and differ from emf  $E_1$  by the magnitude of the voltage drop at resistance  $X_r$ . A phase current diagram is presented in Figure 12.1d.

Electrical machinery operating modes. Use of electrical machinery in dual-current GEU is determined by the quality of the electric power consumed by the rectifier unit and at the converter output.

There is a requirement to try to reduce rectified voltage and current pulsations to insure normal commutation conditions and the condition of GED insulation. However, until the present time, substantiated acceptable pulsation norms for GED, considering the special features of their operation, still are lacking. Tests on a 1,250 kW machine [30] run from a dc generator and from a pulsating current source demonstrated that, in the case of the second source and given current pulsations more than 2%, the width of the arcless commutation zone decreased more than 10% compared to feed from the first source.

Having in mind that a main propulsion motor must satisfy the requirement for prolonged operation in difficult operating modes (frequent reverses, torque surge and discharge, vibrations), prior to development of substantiated norms, rectified voltage pulsations should be constrained to a magnitude of 1-2% (usually it is determined by the ratio of the amplitude of the fundamental rectified current harmonic to its average value). It should be noted that rectified current pulsations cause increased heating of the electric motor and its vibration due to oscillations of electromagnetic power. However, as research showed [84, 30], these factors are of secondary importance.

Rectified voltage pulsations degrade the condition of GED insulation. So, given voltages ranging from 1,000--1,2000 V, exceeding the instantaneous rectified voltage value by 10--15% can require that insulation be reinforced, causing an increase in GED overall dimensions and weight.

Two factors should be considered when evaluating a synchronous generator

running a rectified load:

1) the ratio of the true power of rectified current to required SG installed capacity:

$$\kappa = \frac{P_d}{S} = \frac{U_d I_d}{m U_\phi I_\phi},$$

where  $U_d$ ,  $I_d$  are average values of rectified voltage and current, respectively;

$U_\phi$ ,  $I_\phi$  are actual values of phase voltage and current, respectively;

2) the presence in the stator current curve of higher harmonic components which are the source of additional losses. One should consider here that, for /560 these higher harmonics, stator winding resistances increase due to the phenomenon of surface leakage. One also must keep in mind that higher harmonic stator currents create fields rotating asynchronously with the rotor. They exert an especially harmful influence on turbogenerators with a large solid rotor having high loop resistances. The safe load must be reduced in order to retain normal synchronous generator operating conditions. Therefore, improved generator use requires that such conditions be created so that, on the one hand, minimum additional losses would be insured. On the other hand, value  $\kappa$  would approximate 1.

The rectifier requirement for nonsinusoidal current is accompanied by voltage distortion at SG terminals. This can be discernible interference when solving the problem of power take-off from electric propulsion bus bars for auxiliaries since the operating conditions for electric power consumers -- induction motors -- are degraded, the losses in them increase, and the power factor decreases. An SG operating a rectified load also is accompanied by electromagnetic moment pulsations, which, given certain circumstances, can cause vibrations.

All the aforementioned special features must be kept in mind during the design of a converter and comparative evaluation of different conversion circuits.

### § 12.3 Selection of Dual-Current Electrical Propulsion Plant Rectifier Unit Circuits

General assumptions. Circuits in 6- and 12-phase rectification modes were examined in [34]. Use in dual-current GEU of similar conversion circuits with m-phase SG operating in m-phase modes of rectification (half-wave conversion)

is not advantageous due to the low value of  $\ast$ . This is explained by the fact that, given half-wave conversion for stator windings, constant and current components flow along with the higher harmonics.

In view of the aforementioned circumstances, now we examine bridge conversion circuits, primarily conventional three-phase (single-bridge converter) circuits. Such a circuit operating in a six-phase mode must be distinguished by high use of active SG materials ( $\alpha = 0$ ,  $\ast = 0.955$ ). Calculations show, however, that, in several cases, given a single-bridge converter, the magnitudes of rectified voltage and current pulsations exceed the acceptable value. This creates the requirement for a smoothing reactor in the power circuit. A decrease in pulsations can be achieved also by transition to a 12-phase rectification mode created /561 by feeding the rectifier bridges from a three-phase SG via a three-winding transformer, one secondary winding of which is connected to a star and the other to a triangle.

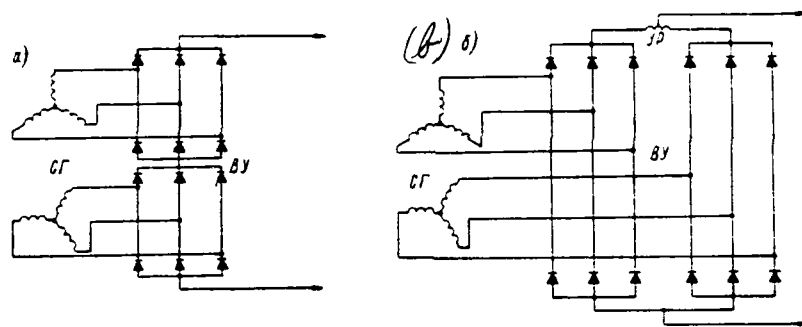


Figure 12.2. 12-Phase Conversion Circuits with Series (a) and Parallel (b) Rectifier Bridge Connection.

This method found wide use in powerful rectifier drives and provides high-quality rectified voltage and current. In addition, a reduction is achieved here in additional losses in the SG from higher harmonic components since, in the stator current, there are no harmonics, whose series is determined by the ratio  $\nu = 12m \pm 5$ ,  $m = 0, 1, 2, \dots$ . However, it should be noted that the presence of a transformer increases converter unit overall dimensions and weight and reduces its efficiency.

In autonomous plants, including GEU, a 12-phase rectification mode without



an additional transformer can be obtained through use of SG with two opposed three-phase windings (dual-bridge converter), as shown in Figure 12.2. Such generators were called 6-phase 12-zone ac generators.

Bridges on the rectified voltage side can be connected in series (Figure 12.2a) and parallel (Figure 12.2b). The type of connection should be selected after consideration of the relationship of rectifier operation and SG design capabilities to the magnitude of its voltage.

So-called circuits with joint windings (Figure 12.3) developed under the direction of Ye. L. Ettinger [83] also are of interest for dual-current GEU. Here, given a constraint on compensating currents, with the aid of compensating reactors UR1 and UR2 characteristics will approximate those of a three-phase bridge conversion circuit. Using an SG with two three-phase windings shifted 30 electrical degrees, it is possible to obtain a 12-phase mode (see Figure 12.2). The advantage of such circuits [83, 84] is their increased reliability, while a disadvantage is the increase in weight and size indicators due to the need for installation /562 of compensating reactors and poor use of rectifiers. Along with the advantages of the circuit operation itself, 12-phase conversion systems also have the advantages of 6-phase 12-zone SG compared to 3-phase 6-zone SG. Basic advantages are:

- 1) increase in the value of winding factors due to a decrease, by a factor of 2, in the width of the phase zone and, consequently, also an increase in the use of active materials of the same overall dimensions (by about 5--6%);
- 2) reduction in additional losses on the rotor surface caused both by higher stator current harmonics and by the first harmonic.

Calculation of rectifier unit basic characteristics. The relative /563 magnitude of rectified current harmonics can be determined approximately from formula [83]

$$\frac{I_{mv}}{I_d} = \frac{1}{\bar{u}_a} \frac{1}{\omega_r T_a} \frac{U_{mv}}{U_d}, \quad (12.1)$$

where  $T_a = \frac{L_a}{r_a}$  is an armature circuit time constant;  $\bar{u}_a = \frac{I_c R}{U_d}$  is relative voltage drop in the armature circuit;  $\frac{U_{mv}}{U_d}$  is relative magnitude of rectified voltage harmonics;  $\omega_r = 2\pi v f$ ;  $f$  is SG frequency.

Armature circuit inductance can be determined from empirical formula

$$L_a = \frac{(3 + 5)}{2pn_{d, \text{НОМ}}} \cdot \frac{U_{d \text{ НОМ}}}{I_{d \text{ НОМ}}}, \quad (12.2)$$

where factor 3 corresponds to compensated and factor 5 to uncompensated machinery;  $U_{d \text{ НОМ}}$ ,  $I_{d \text{ НОМ}}$ ,  $n_{d, \text{НОМ}}$  are nominal values of armature voltage and current and machine rotational speed.

Current pulsations when working with nominal parameters are calculated from formula

$$\frac{I_{mv}}{I_d} = 2pn_{d, \text{НОМ}} \frac{1}{(3 + 5)\omega_r} \frac{U_{mv}}{U_d}, \quad (12.3)$$

obtained by substituting values  $\bar{u}_r$ ,  $T_a$  and  $L_a$  in expression (12.1).

Magnitude  $2pn_{d, \text{НОМ}}$  for projected and operating domestically-produced GED will fall in the 1,500--3,000 range, while its greatest values correspond to machinery of greatest power.

The relative magnitude of rectified voltage harmonics is a function of the regulation and commutation angles. Ratio  $U_{mv}/U_d$  in plants with uncontrolled rectifiers will depend only on the commutation angle, which is determined by commutating reactive resistances. The methodology for calculation of these characteristics will be examined separately.

Rectifier unit comparative evaluation. Considerations from analysis of the basic indicators of single- and dual-bridge converters are presented below.

Relationships  $U_{vm}/U_d$  and  $U_{im}/U_d$  for both aforementioned converter types are shown in Figure 12.4. The dual-bridge converter curves correspond to the two values of factor A, which characterizes the degree of mutual influence of one three-phase winding on the other. Considering that commutating reactive resistances  $x$  of ac generators in use (expressed in relative units) will range from 0.12--0.3 for three-phase SG and 0.2--0.5 for six-phase SG, with the aid of the curves in Figure 12.4 and formula (12.3), it is possible to conclude [34]

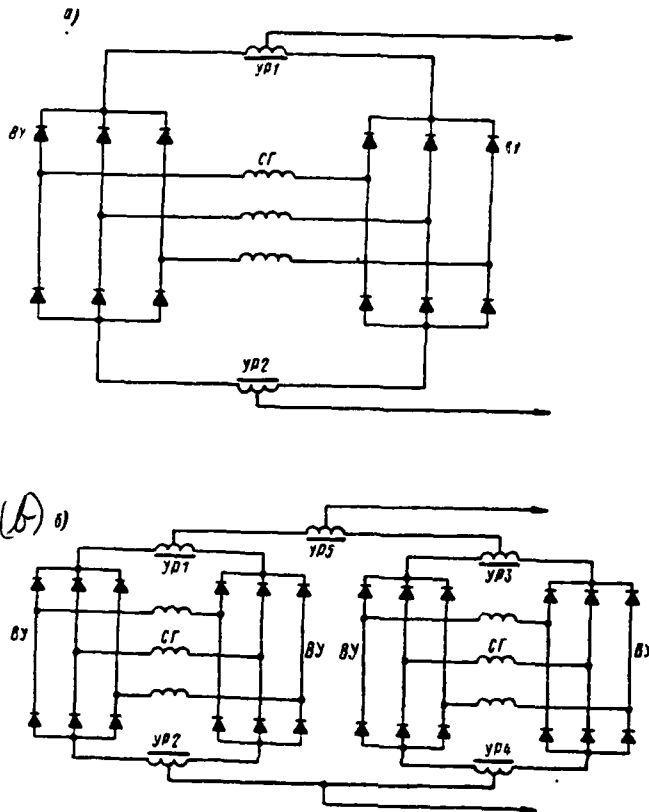


Figure 12.3. Conversion Circuits With Joint Windings For 6-Phase (a) and 12-Phase (b) Circuits.

that rectified current pulsations in a dual-bridge converter are several times less than in a single-bridge converter. Calculations in this same work [34] /564 demonstrated that a three-phase bridge circuit also responds in many instances to the requirement to constrain rectified current pulsations to 2% in plants with uncontrolled rectifiers. In particular, this is accomplished in average-power dual-current GEU and in GEU with a synchronous generator of increased frequency. From the point of view of reducing the amplitude of rectified voltage, proceeding from the characteristics provided, preference also should be given to dual-bridge converters.

Comparison of the conversion circuits examined based on the influence of higher stator current harmonics on SG operation is of interest. A synchronous

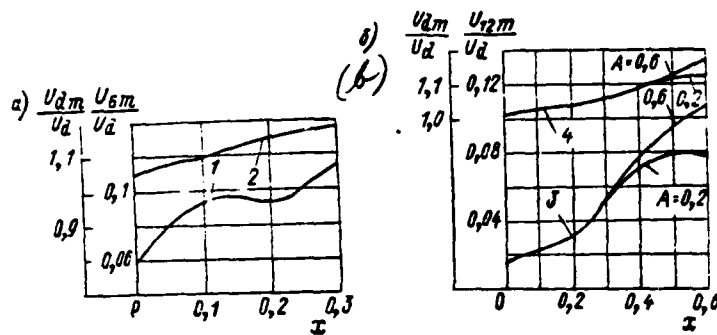


Figure 12.4. Converter Characteristics: a--Single-bridge; b--Dual-Bridge.

$$1 - \frac{U_{dm}}{U_d} = f(x); \quad 2 - \frac{U_{6m}}{U_d} = f(x); \quad 3 - \frac{U_{12m}}{U_d} = f(x); \quad 4 - \frac{U_{dm}}{U_d} = f(x).$$

generator's safe load can be determined from formulas proposed by R. A. Lyuter [37].

The power reduction factor for the stator current's first harmonic component, in accordance with the conditions of the invariability of the heating of its winding, will be found from expression

$$\xi_{scr} = \sqrt{\frac{K_f}{K_f - \sum \bar{I}_v^2 - (K_f - 1) \sum (\bar{I}_v U)^2}}, \quad (12.4)$$

where  $K_f$  is the Field coefficient for the stator current's first harmonic;  $\bar{I}_v$  is the value of the  $v$ -th harmonic of the current in relative units (in relation to the first harmonic of the current).

The power reduction factor for the rotor current's first harmonic component, in accordance with the conditions of the invariability of the heating of its winding, is calculated from the formula

$$\xi_{por} = \sqrt{\frac{Q_{por}}{Q_{por} + R_2 \sum \bar{I}_v^2 V(v \neq 1)}}, \quad (12.5)$$

where  $Q_{por}$  are rotor losses as an SG operates a purely sinusoidal load with /565 a power equalling the power of the first harmonic;  $R_2$  is rotor circuit referred resistance.

Formulas (12.4) and (12.5) do not consider specific design data. Therefore, they are approximate. In addition, they are compiled in the assumption that additional losses from stator current higher harmonics must not lead to an increase in temperature above the safe level for a given class of insulation or material in any single portion of the SG rotor and stator. In spite of this, these formulas do permit one to make a sufficiently accurate evaluation of the influence of the conversion circuit on generator operation.

A 12-phase converter with a 6-phase SG has the following important advantages. As [30] shows, fields of both three-phase windings from the higher harmonics of the current and stator, the sequence of which determined by expression (12.1), are mutually compensated; thanks to this, the degree of additional losses in rotor windings is reduced in such a conversion circuit. The following example illustrates this situation.

Let  $v = 5$ . Then the expression for the fifth harmonic of the stator winding current has the form

$$i_{n(5)} = I_{m(5)} \sin 5(\omega t - \varphi_n).$$

Here, index  $n$  denotes the phase number ( $n = 1, 2, 3, 4, 5, 6$ ), with 1, 2, 3 being the phases of one three-phase system and 4, 5, 6 being the phases of the other. We select the zero time reference so that phase shift angle  $\varphi_1 = 0$ . Consequently,  $\varphi_2 = 120^\circ$ ,  $\varphi_3 = 240^\circ$ ,  $\varphi_4 = 30^\circ$ ,  $\varphi_5 = 150^\circ$ , and  $\varphi_6 = 270^\circ$ .

Distribution of the mmf first spatial harmonic along the stator circle from the fifth current harmonic will be written this way:

$$F_{n(5)} = F_{m(5)} \cos\left(\frac{\pi}{\tau} x - \beta_n\right) \sin 5(\omega t - \varphi_n). \quad (12.6)$$

This expression is the pulsating field equation and can be expanded into the sum of two equations characterizing rotating fields:

$$F_s = \frac{F_{m(5)}}{2} \sin\left[\left(5\omega t + \frac{\pi}{\tau} x\right) - (5\varphi_n + \beta_n)\right] + \frac{F_{m(5)}}{2} \sin\left[\left(5\omega t - \frac{\pi}{\tau} x\right) - (5\varphi_n - \beta_n)\right]. \quad (12.7)$$

In expressions (12.6) and (12.7),  $F_{m(s)}$  is the amplitude of the mmf first spatial harmonic;  $\beta_n$  is the angle between the winding axis and axis of the ordinates;  $\tau$  is pole pitch;  $x$  is a space coordinate. We join the axis of the ordinates with the axis of phase 1; then  $\beta_1 = 0$ ,  $\beta_2 = 120^\circ$ ,  $\beta_3 = 240^\circ$ ,  $\beta_4 = 30^\circ$ ,  $\beta_5 = 150^\circ$ , and  $\beta_6 = 270^\circ$ .

After certain transforms, we will get the following expressions for the /566 resultant mmf of each three-phase winding:

$$F_{1(s)} = \frac{3}{2} F_{m(s)} \sin \left( 5\omega t + \frac{\pi}{\tau} x \right);$$

$$F_{11(s)} = \frac{3}{2} F_{m(s)} \sin \left( 5\omega t + \frac{\pi}{\tau} x - \pi \right).$$

From which follows confirmation of the property of a 12-phase converter with a 6-phase SG presented above, that the mmf first space harmonic from the fifth harmonic of the current of one three-phase winding  $F_{1(s)}$  compensates the corresponding mmf of the other three-phase winding  $F_{11(s)}$ . It is easy to demonstrate in a similar way that resultant mmf from current harmonics, the sequence of which is determined by expression (12.1), equals zero.

Consequently, based upon the above, one can assume that, for  $v = 12m \pm 5$ ,  $I_v = 0$  when determining the magnitude of  $E_{pot}$  in a conversion circuit with a six-phase SG.

From the safe load point of view, calculations showed that, during transition to a conversion circuit with a six-phase SG, the safe rectified load can be increased 10-15%.

#### § 12.4 Elements of the Theory and Calculation of the Characteristics of Dual-Current Electrical Propulsion Plants With Uncontrolled Rectifiers

##### Calculation of synchronous generator current and voltage harmonic components.

The presence of a converter unit in dual-current GEU circuits will lead to the appearance of higher of SG phase current and voltage harmonics.

First harmonics determine the transmission of energy from a generator to

a receiver. A converter with an ac motor is a generator of higher harmonics. Therefore, the power of the fundamental wave supplied to a receiver can be divided into two components:

- useful power consumed in the receiver;
- power used to cover the magnitude of higher harmonic losses in the feed system.

Consequently, for the plant being examined, the main propulsion motor is the receiver of fundamental wave power, while the feed system is the receiver of the power of the higher harmonics. Relative to the feed system, a converter with a GED will serve as a generator of reactive power.

There is a requirement to consider the appearance of the aforementioned higher harmonic components caused by an SG running a rectified load for:

- calculation of losses in copper in stator and rotor windings, losses /567 in steel and in damper windings (calculation methods for the extant spectrum of phase current harmonics are shown in the bibliography);

- explanation of the capabilities to feed an auxiliary station and analysis of the operation of the main shipboard consumers and control circuits given distorted voltage;

- determination of the harmonic components in rectified voltage.

Extant methods of calculating higher harmonics proceed from the condition that  $I_d = \text{const}$ , which is not substantiated sufficiently where GEU circuits are concerned.

Yu. K. Timofeyev's research into higher harmonics for dual-current GEU circuits made it possible to establish the following [64].

The magnitude of the higher harmonics in SG phase voltages and currents in such circuits and the shift angles of their phases relative to equivalent emf will depend greatly on the ratio of reactive resistances  $\epsilon$  on the direct and alternating current side.

The greatest influence of parameter  $\epsilon$  is observed for the 5-th and 7-th harmonics at commutation angles up to 40 electrical degrees.

The magnitude of the first harmonic of phase current and voltage with less than 2% error can be determined from condition  $\epsilon = \infty$ .

To avoid a large error, the phase shift angles of the first harmonics of phase currents and voltages should be determined considering finite value  $\epsilon$ .

Actual current and voltage values with error not exceeding 10% for current and 1.5% for voltage can be determined from condition  $\epsilon = \infty$ .

The average rectified voltage value essentially does not depend on parameter  $\epsilon$ .

Finite value  $\epsilon$  must be considered when determining the average rectified current value.

The condition  $I_d = \text{const}$  indicated above, which lies at the foundation of harmonic component calculations can be assumed for plants that have a power feed source significantly greater (and, in a majority of cases, incomparably greater) than the power of the converter. In these instances,  $X_r \ll X_{\text{nom}}$ , i. e.,

$$\epsilon = \frac{X_{\text{nom}}}{X_r} \approx \infty.$$

where  $X_{\text{nom}} = 2\pi f_1 L_{\text{nom}}$  is nominal load resistance given a frequency of feed source fundamental harmonic  $f_1$  and  $X_r$  is the commutation resistance of a synchronous generator used as the feed source.

Magnitude  $X_r$  is calculated from formula

$$X_r = \frac{X_d'' - X_2}{2} = \frac{X_d'' - \sqrt{X_d'' X_q''}}{2}, \quad (12.8)$$

where  $X_d''$  and  $X_q''$  are supertransient resistances along the longitudinal and transverse axes, respectively;  $X_2$  is reverse sequence resistance.

The value of parameter  $\epsilon$  can be found in the  $0.5 < \epsilon < 10$  range for electrical propulsion plants (since GED and feed source power are commensurate or equal).

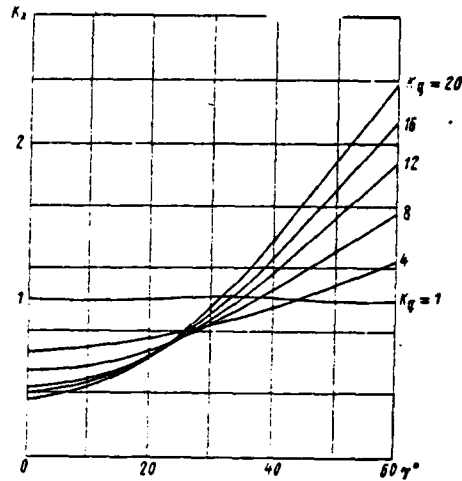


Figure 12.5. Characteristics of Factor  $K_x = f(\gamma, K_g)$ .

It should be noted that use of a methodology for calculation of higher harmonics for dual-current GEU circuits based on the assumption  $\epsilon = \infty, \infty$  will lead to significant errors. Consideration of parameter  $\epsilon$  introduces an appreciable correction into this calculation methodology corresponding to GEU specifics.

One other assumption is used in extant calculation methods. It assumes the invariability of generator phase commutation resistance:  $X_c = \text{const}$ . In actuality, generator phase resistances will depend on rotor angular position. Since the generator operations in a quasi-steady state mode, this relationship also is distributed to the commutation resistance, with the relationship determined by expression

$$X_r(t) = \frac{X_q'' + X_d''}{2} - \frac{X_q'' - X_d''}{2} \cos 2t, \quad (12.9)$$

where  $t$  is time in radians.

The average value of resistance  $X_{r, \text{cp}}$  for commutation period  $\gamma$  equals

$$X_{r, \text{cp}} = \frac{1}{\gamma} \int_{\alpha}^{\alpha+\gamma} X_r(t) dt = \frac{X_q'' + X_d''}{2} - \frac{X_q'' - X_d''}{2} \frac{\sin \gamma}{\gamma} (2\alpha + \gamma), \quad (12.10)$$

where  $\alpha$  (or  $\alpha_0$ ) is the control angle given controlled rectifiers (or forced regulation angle given uncontrolled rectifiers).

The simultaneous conductance of three rectifiers mode occurs for a three-phase bridge converter upon attainment of commutation angle  $\gamma = 60$  electrical degrees. Forced control angle  $\gamma$  occurs with a further increase in load, while the magnitude of angle  $\gamma$  remains unchanged (60 electrical degrees). Simultaneous conductance of three rectifiers continues until  $\alpha_0 = 30$  electrical degrees, followed by /569 onset of the alternating conductance of three and four rectifiers mode.

It is possible with the aid of expression (12.10) to determine  $X_{r, cp}$  given the aforementioned bridge converter operating modes.

The characteristics of coefficient  $K_X = f(\gamma, K_q)$  given  $\alpha_0 = 0$ , where  $K_q = \frac{X_q}{X_d}$ , are constructed in Figure 12.5. This factor considers a change in generator resistance given its varied parameters ( $1 < K_q < 20$ ) and is considered from expression

$$K_X = \frac{X_{r, cp}}{X_r} = \frac{K_q + 1}{1 + K_q} - \frac{K_q - 1}{1 - K_q} \cdot \frac{\sin \gamma}{\gamma} \cos(2\alpha_0 + \gamma), \quad (12.11)$$

while magnitude  $X_{r, cp}$  is determined from formula (12.10) and  $X_r$  from formula (12.8).

The equation of the phase current curve of a synchronous generator for half a period in the basic mode lies at the foundation of the method of calculating dual-current GEU harmonic components described in [64]. This equation, which consists of equations of phase current by sections [16], is obtained for an overall case -- presence of a controlled rectifier bridge. For a frequent instance when the basic mode of uncontrolled rectifiers is being examined, one should place  $\alpha = 0$  in the aforementioned equations. Then, in accordance with [65], the following is the assumed sequence of higher harmonic calculation.

1. A graph of auxiliary function  $\xi_{dX} = f_6(\gamma, \epsilon)$ , whose calculation is reduced conveniently to the following form, will be constructed for specific value  $K_q$ :

$\gamma^\circ$	0	5	10	...	$\gamma_i$	...	60	Задано (a)
$K_X$	$K_{X1}$	$K_{X2}$	$K_{X3}$	...	$K_{Xi}$	...	...	по рис. 12.5 для дан. значения $K_q$ (b)
$\epsilon$	$\epsilon_1$	$\epsilon_2$	$\epsilon_3$	...	$\epsilon_i$	...	...	$\epsilon = \frac{X_{ном}}{X_r K_X}$
$\xi_d$	$\xi_{d1}$	$\xi_{d2}$	$\xi_{d3}$	...	$\xi_{di}$	...	...	по рис. 12.6 (c)
$\xi_{dX}$	$\xi_{dX1}$	$\xi_{dX2}$	$\xi_{dX3}$	...	$\xi_{dXi}$	...	...	$\xi_{dX} = \xi_d K_X$

Key: a--Given; b--From Figure 12.5 for given value  $K_q$ ; c--From Figure 12.6

2. Function  $\xi_{dX}$  for the given mode is determined from formula

$$\xi_{dX} = \frac{\pi U_d}{3I_d X_r}, \quad (12.12)$$

where generator commutation resistance  $X_r$  is found from expression (12.8). It is possible also to obtain this function graphically, using ratio

$$\xi_{dX} = K_X \xi_d = f_6(\gamma; \epsilon)$$

and known relationships:

/570

$$\xi_d = f_6(\gamma; \epsilon); \quad K_X = f(\gamma; K_d).$$

while intermediate function

$$\xi_d = \frac{\pi U_d}{3I_d X_{r, cp}} = \frac{\pi U_d}{3I_d X_r K_X} = f_6(\alpha, \gamma, \epsilon). \quad (12.13)$$

This expression is obtained as the quotient of magnitude

$$U_d = \frac{\sqrt{3} E_m \left[ \cos \frac{\gamma}{2} + \sqrt{3} \sin \frac{\gamma}{2} \left( \frac{A_1}{A_2} - 1 \right) \right]}{\frac{\pi}{3} + \gamma \left( \frac{A_1}{A_2} - 1 \right)} \cos \left( \alpha + \frac{\gamma}{2} \right) \quad (12.14)$$

divided by

$$I_d = \frac{E_m}{X_{r, cp}} \left\{ \sqrt{3} \sin \left( \alpha + \frac{\gamma}{2} \right) \sin \frac{\gamma}{2} + \frac{9}{\pi A_2} \sin \left( \alpha + \frac{\gamma}{2} \right) \right. \\ \times \left[ \sin \frac{\gamma}{2} - \frac{\gamma}{2} \cos \frac{\gamma}{2} \right] + \frac{6\sqrt{3}}{\pi A_1} \left[ \sin \left( \frac{\pi}{6} - \frac{\gamma}{2} \right) - \right. \\ \left. \left. - \left( \frac{\pi}{6} - \gamma \right) \cos \left( \frac{\pi}{6} - \frac{\gamma}{2} \right) \right] \sin \left( \alpha + \frac{\pi}{2} \right) \right\}. \quad (12.15)$$

The expression for commutation angle  $\gamma$  from formulas (12.14) and (12.15) can be obtained in explicit form, for which intermediate function  $\xi_d$  from expression (12.13) will be introduced.

This function, depending on angle  $\gamma$ , has been constructed in two scales (I and II) in Figure 12.6 for a case where  $\alpha = 0$ . As follows from the figure, its value changes from 500 to 3. Scale I corresponds to commutation angles up to 20 electrical degrees, while scale II from 20 up to 60 electrical degrees.

One must know the magnitude of factor  $K_\chi$  to determine, from expression (12.13), the value of function  $\xi_d$ , corresponding to a given mode. This function, in turn, will depend on commutation angle  $\gamma$ . Therefore, it is necessary to reconstruct curves  $\xi_d = f_\xi(\gamma, \epsilon)$ , considering factor  $K_\chi$  for a specific synchronous generator, determining the value of  $K_\chi$  from the curves in Figure 12.5 and the values of  $K_q$  from known generator parameters.

3. Based on curves  $\xi_{dX} = f_\xi(\gamma, \epsilon)$  and  $i_d = f_i(\gamma, \epsilon)$  (see Figure 12.6), we will find angle  $\underline{\gamma}$  and the relative value of rectified current  $I_d$  (short-circuit current  $I_0 = \frac{E_m}{X_{r, cp}}$ ) is assumed as its base value). It also is possible to obtain the magnitude of  $I_d$  from expression (12.15).

Presented in Figure 12.6 are the curves of relationship

$$I_d = f_i(\gamma, \epsilon) \quad \text{where } \alpha = 0.$$

We will find the magnitude of the first harmonic of phase current  $I_1 = K_{i1} I_d$  from the graph presented in Figure 12.7.

The phase current equation for half a period is determined from formula

$$i_a(t) = i_1(t) + i_2(t) + i_3(t) + i_4(t) + i_5(t).$$

(12.16)

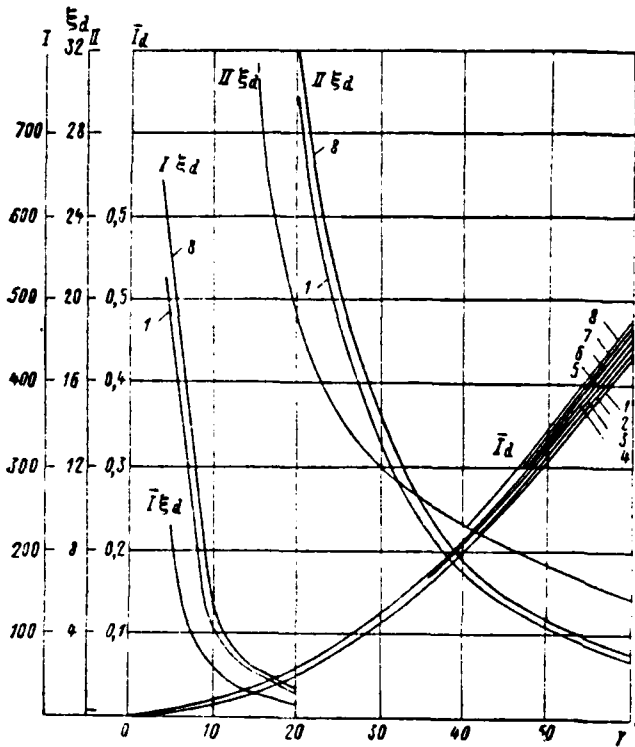


Figure 12.6 Characteristics of Auxiliary Function  $\xi_d$  and Rectified Current  $I_d$  Relative Values.

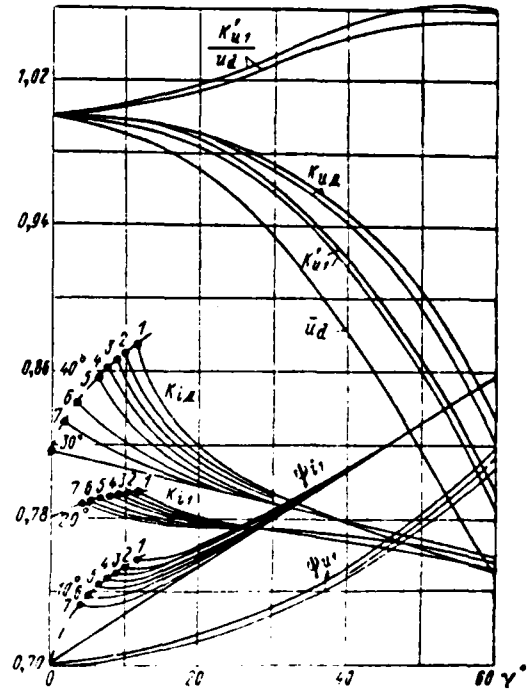


Figure 12.7. Harmonic Parameters Depending on Angle  $\gamma$ .

Since the phase current curve is symmetrical relative to the X-axis, it will contain only odd components when expanded into a Fourier series. The amplitudes of these sine and cosine current harmonics accordingly will be found from expressions

$$\left. \begin{aligned} a_{in} &= \frac{2}{\pi} \int_{\alpha - \frac{\pi}{3}}^{\alpha + \frac{2\pi}{3}} i_a(t) \cos nt \, dt, \\ b_{in} &= \frac{2}{\pi} \int_{\alpha - \frac{\pi}{3}}^{\alpha + \frac{2\pi}{3}} i_a(t) \sin nt \, dt. \end{aligned} \right\} \quad (12.17)$$

In addition, relationships presented in Figure 12.7 are

$$K_{i1} = \frac{I_1}{I_d} = f_1(\gamma, \epsilon) \quad \text{and} \quad \psi_{i1} = f_2(\gamma, \epsilon).$$

where  $I_1 = \frac{\sqrt{a_{i1}^2 + b_{i1}^2}}{\sqrt{2}}$  is the actual value of the first harmonic of phase current;  
 $\psi_{i1} = \arctg \frac{b_{i1}}{a_{i1}}$  is the angle between the first current harmonic and emf  $E_m$ ;  $I_d$   
 is the average value of the rectified current determined from formula (12.15).

Integration of formula (12.17) for  $n > 1$  will lead to unwieldy expressions difficult to use in engineering calculations. Coefficients  $a_{in}$  and  $b_{in}$  were computed on a "Minsk-22" electronic computer by the author of [64] to simplify them and, based on these data, in Figure 12.8 curves were constructed of the change in phase current harmonics on the order of  $n = 5, 7, 11, \text{ and } 13$  (where  $\alpha = 0$ ) depending on load

$$\frac{I_n}{I_1} = f_3(\bar{I}_d, e),$$

where  $I_n = \frac{\sqrt{a_{in}^2 + b_{in}^2}}{\sqrt{2}}$  is the actual value of the n-order harmonics;  $\bar{I}_d$  is the relative rectified current value.

5. The relative content of the higher harmonics in the phase current curve for a given mode will be found from the curves in Figure 12.8.

Based on the calculations made, presented in Figure 12.7 is the relationship of actual phase current value  $I$  on parameter  $e$  and commutation angle  $\gamma$ :

$$K_{i\alpha} = f_7(\gamma, e).$$

where

$$K_{i\alpha} = \frac{I}{I_d}; \quad I = \sqrt{\sum_{n=1}^{\infty} I_n^2}.$$

Calculation of phase voltage harmonic components considering finite value  $\frac{1}{574}$   $\epsilon$  and generator commutation resistance change  $X_c$  can be accomplished from the known phase current harmonic component value.

Keeping in mind that n-order (where  $n > 1$ ) current and voltage harmonics

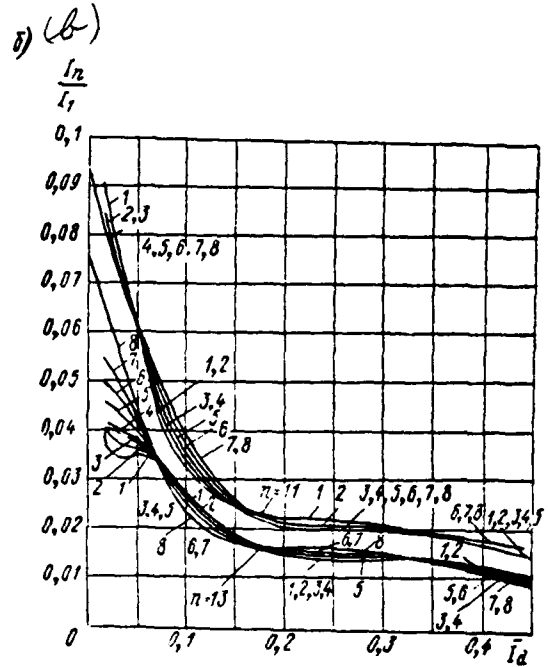
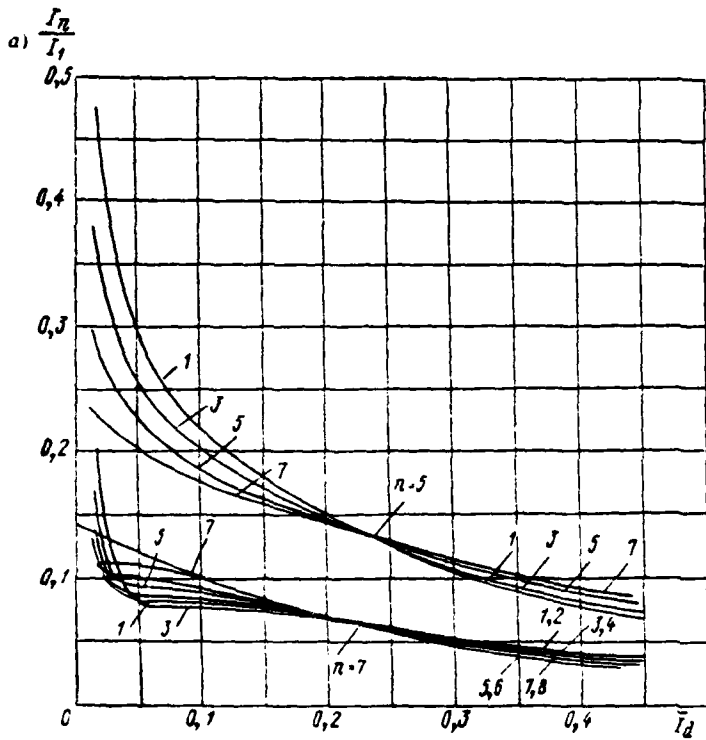


Figure 12.8. Characteristics  $\frac{I_n}{I_1}(\bar{I}_d, \nu)$ : a For a 0--0.5 scale; b--For a 0--0.1 scale.

are shifted  $\frac{\pi}{2}$  in phase, it is possible to write the ratios

$$\begin{cases} a_{un} = b_{in}nX_r, \\ b_{un} = -a_{in}nX_r, \end{cases} \quad (12.18)$$

where  $a_{un}$ ,  $b_{un}$  are the cosine and sine voltage harmonic components, respectively.

Here

$$K_{u1} = \frac{U_1}{E} = \frac{\sqrt{(E_m - a_{u1})^2 + b_{u1}^2}}{E_m} = f_0(\gamma, \nu),$$

where  $U_1$  is the phase voltage first harmonic,  $E$  is an emf calculated value, while the phase shift angle between them will have the form

$$\psi_{u1} = \arctg \frac{b_{u1}}{E_m - a_{u1}} = f_0(\gamma, \nu).$$

The coupling between rectified voltage and calculated emf can be obtained from expression (12.14):

$$\bar{U}_d = \frac{U_d \pi}{E 3 \sqrt{6}} = f_{10}(\gamma, \epsilon),$$

where  $\bar{U}_d$  is the relative rectified voltage value (idling rectified voltage  $U_{d_{x,x}} = \frac{3\sqrt{6}E}{\pi}$ ) is assumed as the base value).

Relationships  $f_8(\gamma, \epsilon)$ ;  $f_9(\gamma, \epsilon)$ ;  $f_{10}(\gamma, \epsilon)$  where  $\alpha \neq 0$  are shown in Figure 12.7.

The actual generator phase voltage value based on the known calculated emf value will be found from expression

$$U = \sqrt{\sum_{n=1}^{\infty} U_n^2}.$$

Also presented in Figure 12.7 is relationship

$$K_{u_n} = f_{11}(\gamma, \epsilon),$$

where

$$K_{u_n} = \frac{U_n}{E}.$$

Considering ratio (12.18), it is possible to find the n-order relative voltage harmonic value (relative to the first harmonic) from known value  $\frac{I_n}{I_1}$ , which is /575 determined with the aid of the Figure 12.8 curves:

$$\frac{U_n}{U_1} = \frac{n X_r K_X I_n}{U_1} = n C_X \frac{I_n}{I_1},$$

where

$$C_X = \frac{\sqrt{2} K_{11}}{K_{u1}} \bar{I}_d = \frac{I_1}{U_1} X_r K_X = \frac{X_r K_X}{Z_1}.$$

$Z_1 = \frac{U_1}{I_1}$  is the entire GEU circuit's equivalent resistance supplied by the first harmonics to the SG.

It should be noted that the value of the ratio of first harmonic voltage  $U_1$  to the average rectified voltage  $U_d$  value will depend little on commutation angle  $\gamma$ .

Also presented in Figure 12.7 are the curves of relationship

$$K_{u1} \frac{\pi}{3\sqrt{6}} = \frac{K_{u1}'}{U_d} = f_{12}(\gamma, \epsilon),$$

where  $K_{u1}' = \frac{U_1}{U_d}$ .

Calculations made and Figure 12.7 curves demonstrate that the first harmonics of phase voltage  $U_1$ , phase current  $I_1$ , and actual value  $U$  will depend little on parameter  $\epsilon$  and their values can be determined from condition ( $\epsilon = \infty$ ) ( $I_d = \text{const}$ ). Here, acceptable error is determined from expression

$$\delta = 1 - \frac{K_{\epsilon}}{K_{\infty}}, \quad (12.19)$$

where  $K_{\epsilon}$  and  $K_{\infty}$  are the factors for given values  $\epsilon$  and  $\epsilon = \infty$ .

The largest error values calculated from expression (12.19) do not exceed the following:

- for the first voltage harmonic  $\delta_{u1 \text{ макс}} = 1^{\circ}$ ;
- for the first current harmonic  $\delta_{i1 \text{ макс}} = 2^{\circ}$ ;
- for the actual voltage value  $\delta_{u2 \text{ макс}} = 1.5^{\circ}$ ;

One should consider given value  $\epsilon$  when determining actual current value  $I$ . If  $I$  is determined from the curves for  $\epsilon = \infty$ , then error  $\delta_{i \text{ макс}}$  can reach values of 7--9%.

It follows from examination of Figure 12.7 curves that, when determining phase shift angles  $\psi_{u1}$  and  $\psi_{i1}$  between first voltage harmonics  $U_1$  and  $I_1$  and undistorted emf  $E$ , one also must consider given value  $\epsilon$ . If  $U_1$ ,  $I_1$ , and  $\varphi$  are determined for construction of synchronous generator load characteristics,

then it is possible to take the values of phase shift angle  $\varphi = \psi_{u1} - \psi_{i1}$  from curves  $\varepsilon = \infty$ , since the angle error has little effect on the accuracy of load characteristic construction.

Numerical example of calculation of higher harmonics for GED\*. It is /576 necessary to determine parameter  $\varepsilon$  and commutation angle  $\gamma$ : to do the calculation following the proposed methodology:

$$\varepsilon = \frac{X_n}{X_r} = \frac{2\pi f L_n}{X_r} = \frac{2\pi f K U_{\text{ном}} 60}{X_r I_{\text{ном}} 2\pi p n_n} \text{ H,}$$

where  $p = 18$  -- the number of pole pairs;  $n_n = 130$  rpm -- nominal GED rotational speed;  $K = 0.25$  -- factor for machinery with a compensated winding;  $U_{\text{ном}} = 1,100$  V -- nominal voltage;  $I_{\text{ном}} = 8,500$  A -- nominal current;  $f = 100$  Hz -- SG frequency.

Hence

$$L_n = 0,25 \frac{1100}{8500} \frac{60}{2 \cdot 18 \cdot 3,14 \cdot 130} = 0,000132 \text{ H;}$$

$$X_n = 2\pi f \cdot L_n = 2 \cdot 3,14 \cdot 100 \cdot 0,000132 = 0,083 \text{ ohms.}$$

When a synchronous generator feeds a rectifier for a commutation mode, using the symmetrical component method, an expression was obtained for generator equivalent commutation resistance  $X_r$

$$X_r = \frac{X_d^{\circ} + X_2}{2},$$

where

$$X_2 = \sqrt{X_q^{\circ} X_d^{\circ}}.$$

If you assume  $X_d^{\circ} \approx X_d^{\prime}$ , then we will get value

$$X_r = \frac{X_d^{\circ} + X_d^{\circ}}{2} = X_d^{\circ}; \quad (X_d^{\circ} \approx 13,4\% \text{ or } 0.016 \text{ ohms}),$$

---

\*Calculation done by Engineer M. D. Sverdlov.

hence

$$e = \frac{0,083}{0,016} = 5,2.$$

In the case where average rectified voltage  $U_d$  and current  $I_d$  values are known, the commutation angle can be determined from them. Since it is impossible to obtain commutation angle  $\gamma$  in explicit form, additional function  $\xi_d$ , is introduced into the examination. It is determined by the formula

$$\xi_d = \frac{\pi U_d}{3 I_d X_r \text{ cp}} = \frac{\pi U_d}{3 I_d X_r K_X}.$$

We are given the value of the load current for every mode for determination of current  $I_d$  in all GED load modes. We will assume a mode corresponding to values  $I_d = 85,00$  A and  $U_d = 1,100$  V as nominal.

We will find the voltage  $U_d$  values for remaining modes from the condition of GED power constancy in the range of its operation in characteristics from running in open water to moored.

We will assume for the moored mode that the load on the motor will increase /577 5% compared to nominal and will comprise  $I_{d \text{ moored}} = 8925$  A where  $U_d = 1,050$  V; correspondingly,  $I_{d \text{ ca}} = 7650$  A where  $U_d = 1,220$  V for the "running in open water" mode. Then

$$\xi_{d \text{ nom}} = \frac{3,14 \cdot 1100}{3 \cdot 8500 \cdot 0,016 \cdot 1} = 8,5 \quad (\text{nominal mode});$$

$$\xi_{d \text{ moored}} = \frac{3,14 \cdot 1050}{3 \cdot 8925 \cdot 0,016 \cdot 1} = 7,8 \quad (\text{moored mode});$$

$$\xi_{d \text{ ca}} = \frac{3,14 \cdot 1220}{3 \cdot 7650 \cdot 0,016 \cdot 1} = 10,4 \quad (\text{running in open water mode}).$$

Based on  $\xi_{di}$  values found, we will find angle  $\gamma$  with the aid of Figure 12.6:  $\gamma_{\text{nom}} = 38^\circ$  (nominal mode);  $\gamma_{\text{moored}} = 43^\circ$  (moored mode);  $\gamma_{\text{ca}} = 35^\circ$  (running in open water mode).

Next, based on these commutation angle values and parameter  $e$ , we will

find in this same figure magnitude  $\bar{I}_d = \frac{\bar{I}_d}{I_n}$ , where  $\bar{I}_d$  is the rectified current value;  $I_0 = I_m = \frac{E_m}{X_r}$  is the base current value;  $\bar{I}_{d \text{ ном}} = 0,18$  (nominal mode);  $\bar{I}_{d \text{ шв}} = 0,25$  (moored mode);  $\bar{I}_{d \text{ св}} = 0,17$  (running in open water mode).

Then, based on these values of  $I_d$ , using the Figure 12.8 curves, we will find, for  $n = 5, 7, 11, \text{ and } 13$ , corresponding values  $\frac{I_5}{I_1}; \frac{I_7}{I_1}; \frac{I_{11}}{I_1}; \frac{I_{13}}{I_1}$ , and, with the aid of Figure 12.9 curves, corresponding values  $\frac{U_{dm13}}{U_{d0}}$  and  $\frac{U_{dm24}}{U_{d0}}$ .

Data from the calculations are reduced to the following tabular form:

Параметры (б)	Режимы (а)		
	номинальный (с)	швартовый (д)	ход в свободной воде (е)
$I_5/I_1$	0,15	0,13	0,16
$I_7/I_1$	0,076	0,052	0,083
$I_{11}/I_1$	0,019	0,018	0,022
$I_{13}/I_1$	0,016	0,015	0,017
$U_{dm13}/U_{d0}$	0,045	0,062	0,047
$U_{dm24}/U_{d0}$	0,021	0,023	0,022

Key: a--Modes; b--Parameters; c--Nominal; d--Moored; e--Running in open water.

Calculation of converter control characteristics. The special features of calculating converter control characteristics in a dual-current GEU system are presented below based on [30].

Converter control characteristics are taken to mean the relationship of SG field current  $I_s$  to converter load current  $I_d$ , given constant voltage  $U_d$  at /578 its output:  $I_s = f(I_d)$  where  $U_d = \text{const}$ .

The vector diagram method was used widely during calculation of these characteristics for synchronous generators feeding a conventional "sinusoidal" load. In the case of the rectified load examined, instead of a diagram based on Gorev-Park equations (Figure 12.10a), a simplified vector diagram (Figure 12.10b) is used, for which the following ratios are justified:

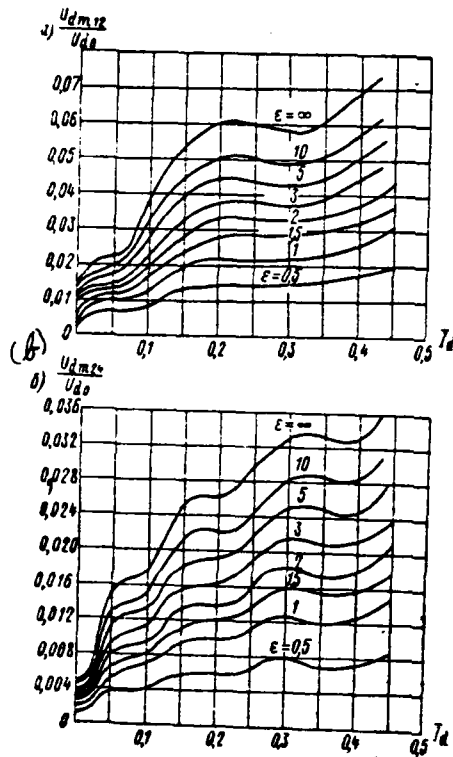


Figure 12.9. Characteristics  $\frac{U_{dm12}}{U_{d0}}$  (a)(a) and  $\frac{U_{dm12}}{U_{d0}}$  (b) Depending on  $\bar{I}_d$ ,  $\epsilon$  Where  $\alpha = 0$ .

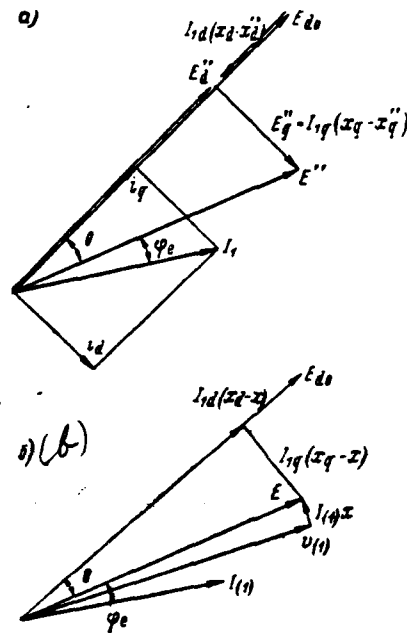


Figure 12.10. Vector Diagram of Voltages of an SG Operating a Rectified Load: a--Based on Gorev-Park equations; b--Simplified.

$$E_q = \sqrt{E^2 + I_{(1)}^2 X_{aq}^2 + 2EI_{(1)} X_{aq} \sin \varphi_e}; \quad (12.20)$$

$$\cos \psi = \frac{E \cos \varphi_e}{E_q}; \quad (12.21)$$

$$\sin \theta = \frac{I_{(1)} X_{aq} \cos \varphi_e}{E_q}. \quad (12.22)$$

Since, for an SG with a massive rotor or with a rotor having a complete /579 damper system, undistorted emf essentially coincides with the emf in the air gap, SG field current will be determined as the sum of currents

$$I_s = I_s' + I_s''.$$

where  $I_a$  is field current required for creation of the emf longitudinal component in the air gap  $E_d = E \cos \theta$  and determined from the idling characteristic;  $I_a'$  is field current compensating for the voltage drop along the longitudinal axis and determined from the rectified idling characteristic.

Such an approach was proposed for the first time in [80] and developed in [14]. It was demonstrated in [32] that resultant mmf from each three-phase winding or (during construction of a voltage vector diagram) current considering the effect of the stator reaction equals

$$I_{(1)} = I_{(1)1} + I_{(1)2},$$

where  $I_{(1)1}$  and  $I_{(1)2}$  are currents considering the effect of the stator reaction of the first and second three-phase systems, respectively.

Consequently, the vector diagram presented in Figure 12.10b and ratios (12.1)--(12.3) are justified also for a 6-phase 12-zone SG.

The following ratios required for construction of a vector diagram were obtained in [30].

The relationship of the actual value of the stator current first harmonic to converter rectified current in a general case is determined from expression

$$I_{(1)} = K(\alpha, \gamma) I_d, \quad (12.23)$$

where  $K(\alpha, \gamma)$  -- a function depending on forced firing angle  $\alpha$  and commutation angle  $\gamma$ , considers a change of current  $I_{(1)}$  during a change in the form of the stator current curve.

If a converter operates at commutation angles  $\gamma < \pi/3$ , then with accuracy sufficient for practical calculations it is possible to use simplified relationship

$$K(\gamma) = \frac{\sqrt{6}}{\pi} \left( 1 - \frac{\gamma^2}{24} \right), \quad (12.23a)$$

where angle  $\gamma$  is in radians.

In modes approximating a converter short circuit, when  $\gamma > \pi/3$ , it is possible to consider that

$$K(\gamma) = K\left(\frac{\pi}{3}\right).$$

A relatively simple expression for magnitude  $\cos \varphi_e$  in formulas (12.21) and (12.22) is presented in [15] proceeding from the following considerations.

Since emf  $E$  is not distorted by commutating processes and will contain /580 only the first harmonic, active power  $P_a$ , consumed by the converter at the point of application of this emf, is determined from expression

$$P_a = 3EI_{(1)} \cos \varphi_e. \quad (12.24)$$

Active power supplied to a dc motor, given completely smoothed rectified current, equals

$$P_a = U_d I_d. \quad (12.25)$$

Disregarding SG stator winding resistances, we have

$$P_a = P_d \frac{\partial n}{\partial I} 3EI_{(1)} \cos \varphi_e = U_d I_d. \quad (12.26)$$

Then substituting expression (12.23) in this formula instead of  $I_{(1)}$ , after transforms we will get

$$\cos \varphi_e = \frac{U_d}{3K(\gamma)E}. \quad (12.27)$$

Given commutation angles  $\gamma \leq 30^\circ$ ,

$$\cos \varphi_e = \frac{\pi}{3\sqrt{6}} \frac{U_d}{E}. \quad (12.28)$$

Ratios obtained make it possible, in accordance with [30], to recommend the following control characteristic calculation sequence:

- 1) the converter operating mode is determined from the magnitude of ratio  $\frac{xI_d}{U_d}$  ;
- 2) the magnitude of undistorted emf, commutation angle  $\gamma$  , and forced firing angle  $\alpha$ ; are determined from the appropriate formulas presented in [32];
- 3) from formula

$$I_{(1)} = \frac{\sqrt{6}}{\pi} \left(1 - \frac{\gamma^2}{24}\right) I_d$$

the actual value of the stator current's first harmonic will be found;

- 4)  $\cos \varphi_{sc}$  is determined from formula (12.27);
- 5) emf  $E_q$  will be found from expression (12.20);
- 6)  $\cos \psi$  and  $\sin \theta$ ; are determined from formulas (12.21) and (12.22);
- 7) the emf longitudinal component in the air gap will be found:  
 $E_d = E$  and, based on the SG idling characteristic, field current  $I_s$ ;
- 8) the voltage drop along the longitudinal axis is determined:  
 $I_{(1)} X_{ad} \sin \psi$  and, based on the rectified idling characteristic, magnitude  $I_s$ ;
- 9) overall field current is computed from the condition

$$I_s = I_s + I_s$$

Having the family of complete control characteristics obtained in the /581 described, it is simple to construct the converter's external characteristics, given SG field constant current.

Using this calculation methodology, SG saturation is considered only along the longitudinal axis, which is generally assumed in the theory of synchronous machinery.

Special features of calculating static characteristics. Calculation of dual-current GEU static characteristics is distinguished by several special features caused by the following:

- the mode in which a synchronous generator runs a dc main propulsion motor via a rectifier is nonsymmetrical;
- during construction of load characteristic  $U_d = f(I)_{I_s, I_d = \text{const}}$  must consider the aforementioned specified SG operating mode;

-- as an SG operates a rectified load commensurate (or equal) in power, generator commutating resistance  $X_r$  will depend on commutation angle  $\gamma$ .

-- harmonic components on the alternating and direct current side, as well as the integral characteristics of the rectifier circuit, will depend on parameter  $\epsilon$ .

In connection with these special features, there is a requirement to determine the influence of a change in resistance  $X_r$  and finite value of parameter  $\epsilon$  on synchronous generator load characteristics.

Having completed construction of a family of load characteristics  $U_d = f(I_d, r)$  considering the conditions noted, it is thus possible to replace the synchronous generator with an equivalent dc generator. Further construction of dual-current GEU static characteristics is accomplished using conventional methods for calculation of a dc GEU. Here, the following data must be known in order to construct load characteristics: SG idling characteristic; three-phase short circuit characteristic; Potier active resistance  $X_p$  and generator resistance  $r$ .

If resistance  $X_p$  is unknown, then it is possible to assume that it is equal approximately to stator inductive dispersion reactance  $X_s$ .

Synchronous generator magnitudes  $U_1$ ,  $I_1$ , and  $\varphi_1$  required for load characteristic construction, are found in this sequence.

A series of rectified voltage  $U_d$  values is given for a specific rectified current  $I_d$  value. Here, these ratios are considered

$$\gamma = \arccos \frac{\xi_d - 1}{\xi_d + 1} \quad (12.29)$$

and

$$\alpha_s = \arctg \frac{2 - \xi_d}{\sqrt{3}(1 + \xi_d)}, \quad (12.30)$$

where  $\gamma$  is commutation angle;  $\alpha_s$  is forced control angle;  $\xi_d = \frac{\pi U_d}{3 I_d X_r}$  is /582 an auxiliary function.

Next, based on computed value  $\xi_d$  and with the aid of Figure 12.6 [64, 65], angle  $\gamma$  or  $\alpha_n$  is determined and, based on them and Figure 12.7, corresponding values of magnitudes  $K_{u_i}$ ,  $K_{i_i}$  and  $\psi_i$ . Then, using Figure 12.6, we will find magnitude

$$\bar{I}_d = \frac{I_d}{I_0}, \quad (12.31)$$

where  $I_0 = \frac{E_m}{X_r}$  is base current value.

The methodology described for construction of load characteristics is justified for rectifier operation at  $\gamma$  angles up to 60 electrical degrees and  $\alpha_n$  angles up to 30 electrical degrees, i. e., to values  $\xi_d \geq 1$ . Where  $\xi_d < 1$ , the mode in which three and four rectifiers operate alternately occurs, which corresponds to a mode approximating a synchronous generator short circuit.

In this mode, the load characteristic has a steeply-dipping nature. Therefore, it is sufficient to determine field current  $I_{a,r}$  for  $U_d = 0$  and given value  $I_d$ . The desired magnitude  $\bar{I}_{a,r}$  will be found for the SG three-phase short circuit characteristic.

Static characteristics are calculated using the graphic-analytical method in relative units.

Comparing these static characteristics with similar characteristics for dc GEU, one should note their variety, explained by the corresponding variety of load and, consequently, of external characteristics of a synchronous generator and of a dc generator.

Relative to a synchronous generator, a dc GED with a rectifier is a resistive-inductive load. Therefore, the external characteristic, due to the strong influence of armature reaction, has a steeply-dipping character, which is a factor favorable for creation of dual-current GEU circuits (armature reaction in dc machinery is a negative phenomenon due to poor commutation conditions). Consequently, SG armature reaction plays the role of internal generator current feedback. A dual-current circuit (synchronous generator--rectifier--GED complex)

as far as static characteristics are concerned is analogous to the circuitry of a dc GD with a generator three-winding exciter.

Thus, having examined the special features and methodology of calculating dual-current GEU static characteristics, we come to the following conclusions:

1. It is possible, with accuracy sufficient for engineering practice, to calculate static characteristics from the condition

$$e = \infty \quad \text{and} \quad X_r = \text{const.}$$

2. The natural characteristics of a dual-current GEU are analogous to identical characteristics in the circuitry of a DC GEU with negative feedbacks at generator exciter input (or at pilot exciter input).

3. A synchronous generator's armature reaction plays the role of internal current feedback.

4. Functional couplings in dual-current GEU control circuits make it possible to obtain the requisite main propulsion motor characteristics.

#### § 12.5 Elements of the Theory and Calculation of the Characteristics of Dual-Current Electrical Propulsion Plants With Controlled Rectifiers

Power characteristics. As a synchronous generator runs a dc GED via controlled (thyristor) rectifier units, voltage distortions can be observed in the form of the current and voltage curves both in the ac and in the dc stator. In addition, appearance of higher harmonic components of this or that order along both sides from the converter unit is unavoidable.

In this connection, it is necessary for design and operating purposes to determine the nature of the aforementioned distortions and percent composition of higher harmonics depending on load current and at different control angles supplied by the thyristor control system.

Results obtained to a known degree make it possible to judge the capability

of power take-off for GEU bus bars to auxiliary bus bars, as well the power conditions of GED operation.

Form of the current and voltage curves on the alternating current side.

As is known, conversion of electrical power is accompanied by distortion of the current and voltage curves and a phase shift between their fundamental harmonics in converter ac circuits. It follows from examination of established symmetrical modes of a three-phase bridge converter that the process recurrence interval comprises 60 electrical degrees (7.3). Using at separate intervals in all three phases equations of alternating currents and voltages with consideration of their symmetry, it is possible to construct the curves of the currents and voltages in any of the phases for the entire alternating current period.

Operation of the rectifiers in twos and in threes is the basic mode in the fields of nominal converter loads. Therefore, it is sufficient to analyze the form of the current and voltage curves only for this mode. Based on ratios describing its electromagnetic processes, standard working formulas for current and voltage for phase A in the case of a single-bridge converter for the duration of half a period of alternating current are presented in Table 12.2.

The following designations are introduced in the table: /584

$\bar{X}_s = \bar{X}_r = \frac{\bar{X}_d' - \bar{X}_2}{2}$  is generator commutating resistance;

$$\bar{I}_{d \text{ NOM}} = \frac{2I_d X_s}{\sqrt{3} E_m} = \frac{2I_d X_s U_n}{\sqrt{3} I_{\text{NOM}} E_m}, \quad (12.31a)$$

where  $I_d$  is main loop current;  $X_s = \frac{\bar{X}_s U_{\text{NOM}}}{I_{\text{NOM}}}$ ;  $U_{\text{NOM}} = \frac{U_n}{\sqrt{3}}$  is nominal phase voltage;  
 $I_{\text{NOM}}$  is nominal phase current;

$$\gamma = \arccos(\cos \alpha - \bar{I}_d) - \alpha. \quad (12.32)$$

Calculations were made for a number of plant modes considering that its automatic control system works out the problem of maintaining nominal current in the main circuit when there is a change in the moment of resistance in the screw above a safe value (screw jamming), i. e., for one of the GEU's most difficult modes.

(a) Интервал		Номера проводящих вентилей (d)	$d(t)$	$U_d(t)$
(b) начало	(c) конец			
$\alpha - \gamma - \frac{\pi}{6}$	$\alpha - \frac{\pi}{6}$	6, 1	0	$\bar{E}_m \sin t$
$\alpha - \frac{\pi}{6}$	$\alpha - \gamma - \frac{\pi}{6}$	6, 1, 2	$\frac{\cos \alpha - \cos(t - \frac{\pi}{6})}{\cos \alpha - \cos(\alpha + \gamma)} I_d$	$\frac{\bar{E}_m \sin t - \sin(t - \frac{\pi}{6})}{\cos \alpha - \cos(\alpha - \gamma)} \bar{I}_d \bar{X}_s$
$\alpha - \gamma - \frac{\pi}{6}$	$\alpha - \frac{\pi}{2}$	1, 2	$\bar{I}_d$	$\bar{E}_m \sin t$
$\alpha - \frac{\pi}{2}$	$\alpha - \gamma + \frac{\pi}{2}$	1, 2, 3	$\bar{I}_d$	$\bar{E}_m \sin t$
$\alpha - \gamma - \frac{\pi}{2}$	$\alpha - \frac{5\pi}{6}$	2, 3	$\bar{I}_d$	$\bar{E}_m \sin t$
$\alpha - \frac{5\pi}{6}$	$\alpha - \gamma + \frac{5\pi}{6}$	2, 3, 4	$\frac{\cos(t - \frac{5\pi}{6}) - \cos(\alpha + \gamma)}{\cos \alpha - \cos(\alpha + \gamma)} \bar{I}_d$	$\frac{\bar{E}_m \sin t - \sin(t - \frac{5\pi}{6})}{\cos \alpha - \cos(\alpha + \gamma)} \bar{I}_d \bar{X}_s$

Table 12.2 Standard Working Formulas for Phase Current and Voltage. a--Interval; b--Begin; c--End; d--Numbers of conducting rectifiers.

Characteristics  $\bar{U}_a(t)$  and  $\bar{I}_a(t)$ , where the values of parameter  $t$  are expressed in electrical degrees, are shown in Figure 12.11.

Calculation of generator phase current harmonics. We will expand the phase A current curve into harmonic components. Due to symmetry relative to the  $X/585$  axis, the current curve in the converter three-phase circuit will have odd harmonics only. Therefore, when determining the Fourier series coefficient, integration will occur in half of an alternating current period. Amplitudes of the cosine  $a_k$  and sine  $b_k$  of the field component harmonics will be found from expressions:

$$a_k = \frac{2}{\pi} \int_{\alpha - \gamma - \frac{\pi}{6}}^{\alpha - \gamma - \frac{\pi}{6}} i_a(t) \cos kt dt \quad (12.33)$$

$$b_k = \frac{2}{\pi} \int_{\alpha - \gamma - \frac{\pi}{6}}^{\alpha - \gamma - \frac{\pi}{6}} i_a(t) \sin kt dt \quad (12.34)$$

After integration and conversion, we will get

$$a_{ik} = \frac{4 \sin K \frac{\pi}{3} \sin K \frac{\pi}{2} I_d}{\pi n (n^2 - 1) [\cos \alpha - \cos (\alpha - \gamma)]} [K \sin (\alpha - \gamma) \cos K (\alpha - \gamma) - K \sin \alpha \cos K \alpha + \sin K \alpha \cos \alpha - \sin K (\alpha + \gamma) \cos (\alpha + \gamma)] \quad (12.35)$$

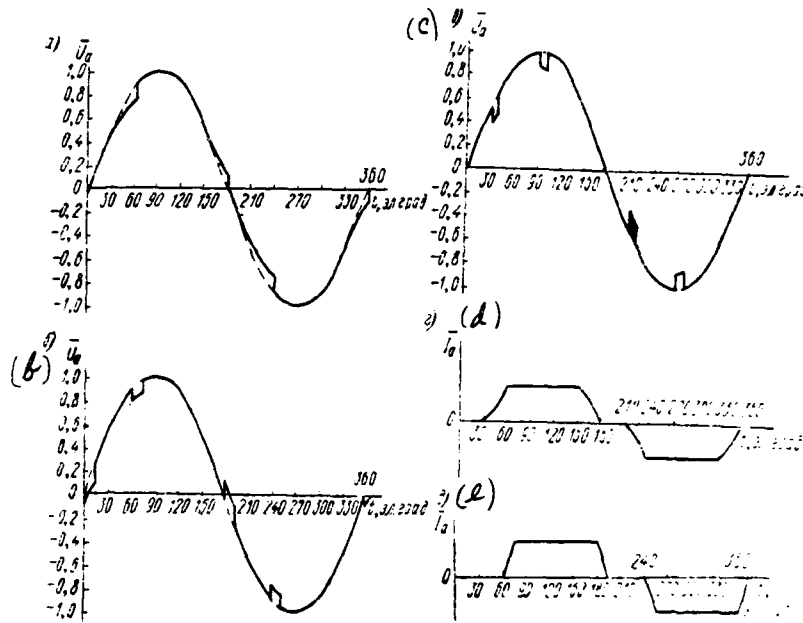


Figure 12.11. Characteristics  $\bar{U}_a(t)$  and  $\bar{I}_a(t)$  where  $\bar{I}_d = \bar{I}_{nom}$ : a-- $\bar{U}_a(t)$  where  $\alpha = 0$  and  $\gamma = 30^\circ$ ; b--Same, where  $\alpha = 30^\circ$  and  $\gamma = 13^\circ$ ; c--Same, where  $\alpha = 60^\circ$  and  $\gamma = 8^\circ$ ; d-- $\bar{I}_a(t)$  where  $\alpha = 0$  and  $\gamma = 30^\circ$ ; e--Same, where  $\alpha = 30^\circ$  and  $\gamma = 13^\circ$ .

/586

$$b_{ik} = \frac{4 \sin K \frac{\pi}{3} \sin K \frac{\pi}{2} I_d}{\pi K (K^2 - 1) [\cos \alpha - \cos (\alpha + \gamma)]} [K \sin (\alpha + \gamma) \sin K (\alpha + \gamma) - K \sin \alpha \sin K \alpha + \cos (\alpha + \gamma) \cos K (\alpha + \gamma) - \cos \alpha \cos K \alpha] \quad (12.36)$$

where  $K = (mk \pm 1)$   $k = 0, 1, 2, 3, \dots$

For a three-phase bridge circuit  $m = 6$ . Consequently, phase current will contain harmonic components on the order of 1, 5, 7, 13, 17, ...

The values of the harmonic amplitudes and their shift angles relative to the Y axis (relative to undistorted emf in this case) are determined by expressions

$$I_{mk} = \sqrt{b_{ik}^2 + a_{ik}^2} = C_{ik}; \quad \text{tg } \psi_{ik} = \frac{a_{ik}}{b_{ik}}. \quad (12.37)$$

In accordance with (12.35) and (12.36), for the first harmonic component we have:

$$a_{ik} = \frac{2\sqrt{3}I_d}{4\pi[\cos\alpha - \cos(\alpha + \gamma)]} [2\gamma + \sin 2\alpha - \sin 2(\alpha + \gamma)]; \quad (12.38)$$

$$b_{ik} = \frac{\sqrt{3}}{\pi} [\cos\alpha - \cos(\alpha + \gamma)] I_d. \quad (12.39)$$

Based on expressions (12.35)--(12.39), harmonic amplitudes and their shift angles are calculated for harmonic components on the order of  $k = 1, 5, 7, 11, 13$  given control angle  $\alpha$  change in the range  $0, 15, 30, 45, 60, 75, \text{ and } 90^\circ$  and commutation angle  $\gamma$  in the range of  $15, 30, 45, \text{ and } 60^\circ$ . Based on the data obtained, the curves of the relative values of the higher harmonics  $\left(\frac{I_5}{I_1}; \frac{I_7}{I_1}; \frac{I_{11}}{I_1}; \frac{I_{13}}{I_1}\right)$  can be constructed as a function of load current expressed in relative units for varied values of angle  $\alpha$ .

It follows from examination of these curves that, in the area of nominal loads ( $I_d = 0.1\text{--}0.3$ ), the fifth harmonic comprises 18--20%, the seventh 12--14%, the eleventh 7--9%, and the thirteenth 4--6% of the fundamental harmonic. A control angle  $\alpha$  increase means that the percent ratio will increase.

Phase voltage harmonics can be found from ratios

$$\left. \begin{aligned} a_{uk} &= -b_{ik}X_sK; \\ b_{uk} &= a_{ik}X_sK; \\ U_{mk} &= \sqrt{b_{uk}^2 + a_{uk}^2} = X_sK I_{mk}. \end{aligned} \right\} \quad (12.40)$$

while the actual current and voltage values can be found from ratios

$$\left. \begin{aligned} I &= \sqrt{\frac{1}{2} (I_{m1}^2 + I_{m5}^2 + I_{m7}^2 + I_{m11}^2 + \dots)}; \\ U &= \sqrt{\frac{1}{2} (U_{m1}^2 + U_{m5}^2 + U_{m7}^2 + U_{m11}^2 + \dots)}. \end{aligned} \right\} \quad (12.41)$$

Calculation of rectified voltage harmonics. As is known, conversion of /587 synchronous generator alternating voltage into constant voltage is accompanied by rectified voltage pulsations, which will depend upon the rectification circuit and load.

We will examine the optimal circuit -- a dual-bridge circuit with pulsation periodicity  $m = 12$ . But, first we will look at a three-phase single-bridge circuit having pulsation periodicity  $m = 6$ . Then, turning to the dual-bridge circuit, we will show the advantages of its use.

The average rectified voltage value is determined from expression

$$\begin{aligned} U_{d\alpha} &= \frac{6}{2\pi} \int_{-\frac{\pi}{6} + \alpha}^{\frac{\pi}{6} + \alpha} \sqrt{3} E_m \cos t \, dt = \frac{\sqrt{3} \cdot 6}{\pi} E_m \sin \frac{\pi}{6} \cos \alpha = 1,65 E_m \cos \alpha \\ &= 2,33 E_\phi \cos \alpha = 1,35 E_n \cos \alpha = U_{d0} \cos \alpha. \end{aligned} \quad (12.42)$$

The character of the rectified voltage curve changes with an increase in converter load. Expressions for the rectified voltage of a single-bridge converter in two intervals are presented in Table 12.3.

(a) Интервал		Номера проводящих вентилей (d)	$\bar{U}_d$
начало (b)	конец (c)		
$\alpha + \gamma + \frac{\pi}{6}$	$\alpha + \frac{\pi}{2}$	1, 2	$\sqrt{3} E_m \sin \left( t - \frac{\pi}{6} \right)$
$\alpha + \frac{\pi}{2}$	$\alpha - \gamma - \frac{\pi}{2}$	1, 2, 3	$\frac{3}{2} E_m \sin t$

Table 12.3. Standard Working Formulas For Single-Bridge Converter Rectified Voltage. a--Interval; b--Begin; c--End; d--Number of conducting rectifiers.

We will construct rectified voltage characteristics based on calculations made for modes corresponding to the form of the curve of voltages and currents on the alternating current side (Figure 12.12).

In addition, for the  $[I_{d \text{ NOM}}, \alpha = 30^\circ]$  mode, we will construct a curve analogous to the basic curve, but shifted in time 30 electrical degrees. It corresponds to a dual-bridge converter fed three-phase voltage.

Considering that, in this case,  $\bar{U}_d = U_{d1} - U_{d2}$ , it is possible, combining the curves obtained, to construct the rectified voltage characteristic for a dual-bridge converter. Here, distortions are decreased considerably, which is its strong point.

The amplitudes of the cosine and sine components of rectified voltage /589 harmonics for a dual-bridge circuit are determined by expressions:

$$a_n = \frac{6}{\pi} \int_{\alpha + \gamma - \frac{\pi}{2}}^{\alpha + \gamma + \frac{\pi}{2}} U_d(t) \cos nt \, dt; \quad (12.43)$$

$$b_n = \frac{6}{\pi} \int_{\alpha + \gamma - \frac{\pi}{2}}^{\alpha + \gamma + \frac{\pi}{2}} U_d(t) \sin nt \, dt. \quad (12.44)$$

After integration and transformation, we will get the following expressions:

$$a_n = \frac{U_{d0}}{2} \left[ \frac{\sin(n-1)(\alpha - \gamma) + \sin(n-1)\alpha}{n+1} - \frac{\sin(n-1)(\alpha + \gamma) + \sin(n-1)\alpha}{n-1} \right]; \quad (12.45)$$

$$b_n = \frac{U_{d0}}{2} \left[ \frac{\cos(n-1)(\alpha - \gamma) - \cos(n-1)\alpha}{n+1} - \frac{\cos(n-1)(\alpha + \gamma) - \cos(n-1)\alpha}{n-1} \right], \quad (12.46)$$

where  $n = km$  ( $k = 1, 2, 3, \dots$ ).

Consequently, the rectified voltage in a single-bridge converter will comprise

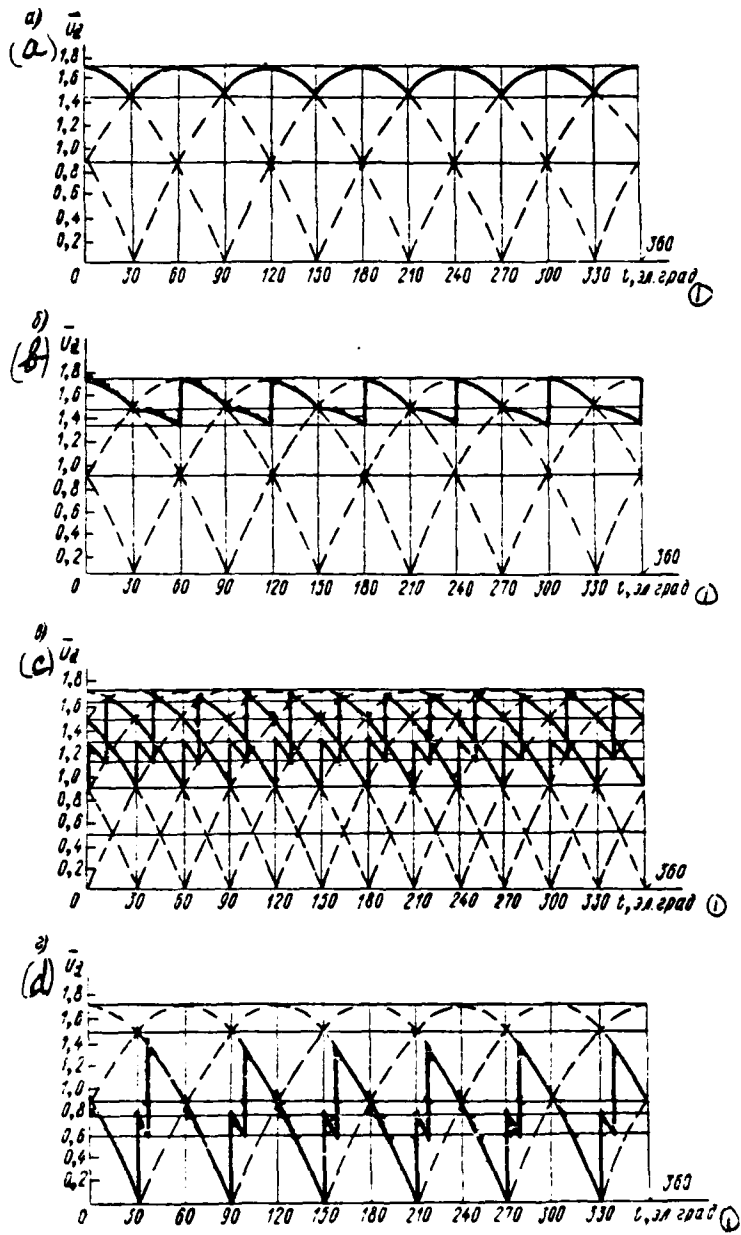


Fig. 12.12.

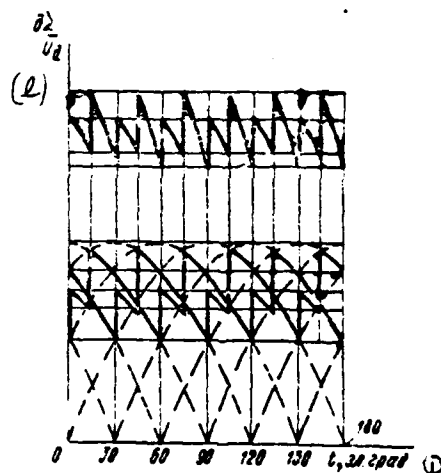


Figure 12.12. Characteristics of Rectified Voltage  $\bar{U}_d = f(t)$ : a--Where  $\alpha = 0^\circ$ ,  $I_d = 0$ ,  $\gamma = 0^\circ$  (idling mode); b--Where  $\bar{I}_d = I_d$ ,  $\alpha = 0.0^\circ$ ,  $\gamma = 30^\circ$ ; c--Where  $\bar{I}_d = I_d$ ,  $\alpha = 30^\circ$ ,  $\gamma = 13^\circ$ ; d--Where  $\bar{I}_d = I_d$ ,  $\alpha = 60^\circ$ ,  $\gamma = 8^\circ 30'$ ; e--Given a static winding shift of 30 electrical degrees.

1 - el-degree  
 harmonics on the order of 6, 12, 18, 24, . . . , while in a dual-bridge circuit -- only 12, 24, 36. . . .

The amplitude of rectified voltage harmonics equals

/590

$$U_{dmk} = \sqrt{b_n^2 + a_n^2} = \frac{U_{d0}}{2} C_n. \quad (12.47)$$

Based on formulas (12.46) and (12.47), calculation will be made of harmonics on the order of 12, 24, 36 given a change in control angle  $\alpha$  (0, 20, 40, 90°) and commutation angle  $\gamma$  (15, 30, 45, 60°).

Based on the data obtained, it is possible to construct the curves of the amplitudes of voltage harmonics  $\left(\frac{U_{d12}}{U_{d0}}, \frac{U_{d24}}{U_{d0}}, \frac{U_{d36}}{U_{d0}}\right)$  depending on load current expressed in relative units and for various control angles  $\alpha$ . Here, in the range of nominal loads, the amplitude of harmonics on the order of  $n = 12$  comprise 8-9%, those on the order  $n = 24$  (given large control angles) about 7%, and those at  $n = 36$  about 3% of the average rectified voltage value when idling.

If you consider that the percent content of harmonics will increase with a decrease in their order, then, given rectified voltage in a single-bridge converter, the percent content in rectified voltage of harmonics increases (due to the presence of harmonics on the order of  $n = 6, 18, \dots$ ) compared to a dual-bridge circuit.

#### § 12.6 Problems Using the Analytical Method in Calculation of Transient Processes in Dual-Current Electrical Propulsion Plants

General assumptions. Calculations of dual-current GEU characteristics, just as during the design of dc and ac GEU, requires solution of the following problems:

- a) selection of the control system structure which provides stable operation and optimal flow of transient processes in all operating modes;
- b) determination of the influence of system structure and parameters on the nature of transient process flow;
- c) determination of the mathematical relationships describing the conduct of GEU elements in steady-state and transient processes.

Having in mind that regulation in the SG--V--D (synchronous generator--rectifier--dc GED) system is accomplished by an effect on SG and GED field windings, this system, from the automatic control point of view, does not differ in principle

from the G--D system in direct current. Consequently, the methodology for calculation of dual-current GEU transient processes primarily involves mathematical description of the SG--V system and, in particular, obtaining the relationship of converter /591 rectified voltage as a function of SG field current and rectified current.

Next, the importance of the determination of other characteristics required for converter equipment design should be underscored. In other words, one should be able in transient modes to calculate the magnitude of the amplitude of rectified voltage, maximum magnitude of reverse voltage in the rectifiers, average value of current across the rectifiers, and so forth.

Calculation of transient processes for GEU of the type being examined encounters considerable difficulties, primarily because dynamic processes in such plants are described by a very complex system of nonlinear differential equations.

In this connection, the modelling method of research into the transient processes in modern dual-current GEU became widespread. In several practical instances (usually for predesign evaluations), a simplified method developed relative to powerful converter units [83, 53] merits attention.

At the present time, investigations are underway into use of the principles of combined modelling of dual-current GEU dynamic processes and a description is provided of an extant modelling unit using analog computers, research done with this unit, and devices which simulate special GEU load characteristics. Use of a similar combined modelling method, which makes it possible to conduct quite complete and comprehensive research into transient processes with a great degree of accuracy, however, does not rule out the usefulness of mathematical modelling and simplified analytical methods.

The special feature of the simplified analytical method is that it permits an approximation of the converter systems, which are circuits with discrete links -- continuous links. In accordance with this method, the static converter is replaced by an equivalent dc generator whose parameters will depend on the conversion circuit, its operating modes, and corresponding parameters.

This method was developed in [14] relative to an SG--V circuit. Its use

for a GEU two three-phase windings shifted 30 electrical degrees on the SG stator is described in [30]. Its author obtained the parameters of the equivalent generator replacing the SG--V--D system's 12-phase circuit and compiled the equations for determination of undistorted emf in a transient mode.

Analytical method for an approximate calculation. Basic assumptions for calculation of transient processes using this method are founded on the assumption that replacement of the controlled SG--uncontrolled rectifier system with an equivalent uncompensated dc generator is possible.

An equivalent circuit for the synchronous generator--rectifier--GED /592 (SG--V--D) system is shown in Figure 12.13 and the following ratio can be written for it:

$$U_d = E_r - R_r I_d - X_r \frac{dI_d}{d\gamma} \quad (12.48)$$

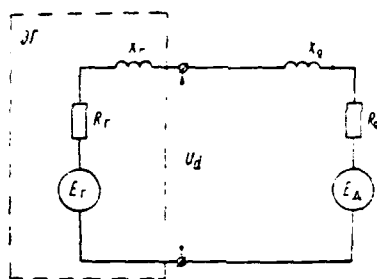


Figure 12.13. SG--V--D System Equivalent Circuit.  $E_r$  -- equivalent generator EG emf;  $R_r$ ,  $X_r$  -- equivalent generator resistance and inductive reactance, respectively, supplied to the dc circuit;  $U_d$  -- generator rectified voltage;  $E_d$  -- GED equivalent voltage;  $R_d$ ,  $X_d$  -- equivalent dc armature circuit resistance and inductive reactance, respectively.

Equivalent generator parameters  $E_r$ ,  $R_r$  and  $X_r$  need to be determined. Expression (12.48) written for a converter transient mode will be justified also for a steady-state mode.

Then, given  $\frac{dI_d}{d\gamma} = 0$ ,

$$U_d = E_r - R_r I_d \quad (12.49)$$

In addition, generalized expressions are known for a converter's external characteristic given a fixed magnitude of undistorted emf:

-- the relationship of average rectified voltage value to firing and commutation angles

$$U_d = U_0 [\cos(\alpha - \psi_0) - \cos(\alpha - \gamma - \psi_0)]; \quad (12.50)$$

-- the relationship of the average rectified current value to firing and commutation angles

$$I_d = I_k [\cos(\alpha - \psi_0) - \cos(\alpha - \gamma - \psi_0)]. \quad (12.51)$$

Assumed as base expressions here are:

for circuits with series-connected bridges

$$U_0 = 1.6 E; \quad I_0 = \sqrt{\frac{3}{2}} \frac{E}{X};$$

for circuits with parallel-connected bridges

$$U_0 = \sqrt{\frac{3}{2}} E; \quad I_0 = 1.6 \frac{L}{X}.$$

The different values of magnitudes  $U_0$ ,  $I_k$ , and  $\psi_0$  corresponding to different converter operating modes are shown in Table 12.4.

The following expression is used for determination of reactive resistance  $X$  [30]:

$$X = X_m - 2X_B - \frac{X_{ad}'' - X_{ad}'}{2}$$

and

$$A = \frac{X_m - \frac{X_{ad}'' - X_{ad}'}{2}}{X_m - 2X_B - \frac{X_{ad}'' - X_{ad}'}{2}}$$

(a) Режимы горения вентилей	$U_d$	$I_d$	$\alpha$
4-5	$\frac{3}{\pi}$	$I$	$\alpha$
5-6	$\frac{3}{\pi} \frac{\sqrt{4-6A-3A^2}}{2-\sqrt{3}A}$	$\frac{\sqrt{4-6A-3A^2}}{2-\sqrt{3}A}$	$\alpha$
6-7	$\frac{3}{\pi} \sqrt{3}(1-A) \frac{\sqrt{4-6A-3A^2}}{2-\sqrt{3}A}$	$\frac{\sqrt{4-6A-3A^2}}{\sqrt{3}(1-A)(2-\sqrt{3}A)}$	$\alpha$
7-8	$\frac{3\sqrt{3}}{\pi} (1-A)$	$\frac{1}{\sqrt{3}(1-A)}$	$\alpha$
Примечание. (b)			
$\operatorname{tg} \alpha_{4-5} = \frac{1-3A}{4-3A}$ $\operatorname{tg} \alpha_{6-7} = \frac{1-3A}{\sqrt{3}(1-A)}$			

Table 12.4. Converter Parameters Given Different Operating Modes. a--Rectifier burning modes; b--Note.

Undistorted or calculated emf, which can be determined from the simplified /593 vector diagram, must be used as emf E.

Excluding commutating angles  $\gamma$  from formulas (12.49) and (12.50), it is possible to obtain the expressions for converter external characteristics, given calculated emf constancy.

Knowledge of relationships  $U_d = f(E, I_d, X, A)$ , solved for emf E turns out in a number of cases to be required. In addition, since parameters  $U_d$  and  $I_d$  are given for a dual-current GEU, for the purpose of speeding up the calculation, it is convenient to express the formulas for commutation angles  $\gamma$  and firing forced angle  $\alpha$  via these parameters.

These parameters are shown in Table 12.4 for a circuit with series and parallel bridge connection. The value of equivalent generator emf  $E_r$  and its resistance for any mode are determined from a kh. kh. [idling] and k. z. [short circuit] /594 test:

$$E_r = U_d \quad \text{where } I_d = 0;$$

$$R_r = \frac{E_r}{I_d} \quad \text{where } U_d = 0.$$

Values  $E_r$  and  $R_r$  for various equivalent generator operating modes are presented in Table 12.5.

(a) Режимы горения вентилей	$E_r$	$R_r$
4-5	$\frac{3\sqrt{6}}{\pi} E$	$\frac{3}{2\pi} x$
5-6	$\frac{3\sqrt{6}}{\pi} \cdot \frac{\sqrt{4-6A-3A^2}}{2-\sqrt{3}A} E$	$\frac{3}{2\pi} \cdot \frac{2-\sqrt{3}A}{2-\sqrt{3}A} x$
6-7	$\frac{9\sqrt{2}}{\pi} (1-A) \frac{\sqrt{4-6A-3A^2}}{2-\sqrt{3}A} E$	$\frac{9}{2\pi} (1-A^2) \frac{2-\sqrt{3}A}{2-\sqrt{3}A} x$
7-8	$\frac{9\sqrt{2}}{\pi} (1-A) E$	$\frac{9}{2\pi} (1-A^2) x$

Table 12.5. Standard Working Formulas For Equivalent Generator Parameters.  
a--Rectifier burning modes.

For the five and six rectifier constant burning mode, the converter's external characteristic, given a constant magnitude of undistorted emf, will be expressed by an ellipse equation: the values of equivalent emf  $E_r$  and internal resistance  $R_r$  will depend on converter load.

It is possible in the aforementioned modes to obtain parameters  $E_r$  and  $R_r$  for a point's certain specific value from an equation applicable to this desired point.

The magnitude of "active" resistance  $R_r$  will be determined as a derivative of expression (12.48) where  $X_r = \frac{dI_d}{d\gamma} = 0$ , but with the opposite sign:

$$R_r = -\frac{dU_d}{dI_d},$$

while equivalent emf will be determined from the expression

$$E_r = U_d + \left(-\frac{dU_d}{dI_d}\right) I_d.$$

Finally, the formulas for  $E_r$  and  $R_r$  will have the form: /595  
for a 5-rectifier mode

$$E_r = \frac{3}{\pi} \sqrt{6E^2 \cos^2 \frac{\pi}{12} - \frac{1}{4} \operatorname{ctg}^2 \frac{\pi}{12} (X I_d)^2} - \frac{1.5 \operatorname{ctg} \frac{\pi}{12} X I_d}{\sqrt{1.5 \sin^2 \frac{\pi}{12} \left(\frac{E}{X I_d}\right)^2 - 1}}; \quad (12.52)$$

$$R_r = 1.5 \operatorname{ctg} \frac{\pi}{2} \frac{X}{\sqrt{1.5 \sin^2 \frac{\pi}{12} \left(\frac{E}{X I_d}\right)^2 - 1}}; \quad (12.53)$$

for a 6-rectifier mode

$$E_r = \frac{3}{\pi} \frac{(1-A)}{(2-\sqrt{3}A)} \sqrt{18E^2 - \frac{3}{4}(2-\sqrt{3}A)^2 (X I_d)^2} - \frac{3\sqrt{3}}{2\pi} (1-A) \frac{2-\sqrt{3}A}{2-\sqrt{3}A} \frac{X I_d}{\sqrt{\frac{24}{2-\sqrt{3}A} \left(\frac{E}{X I_d}\right)^2 - 1}}; \quad (12.54)$$

$$R_r = \frac{3\sqrt{3}}{2\pi} (1-A) \frac{2-\sqrt{3}A}{2-\sqrt{3}A} \frac{X}{\sqrt{\frac{24}{2-\sqrt{3}A} \left(\frac{E}{X I_d}\right)^2 - 1}}; \quad (12.55)$$

Based on the proof presented in [53], equivalent converter inductive reactance  $X_r$ , given the burning of  $n$  rectifiers, equals the resistance of the feed source to direct current, given the burning of an identical number of rectifiers. Then, in a mode of alternate burning of  $n$  and  $(n+1)$  rectifiers, magnitude  $X_r$  will be determined as the average between values  $X_{r(n)}$  and  $X_{r(n+1)}$ :

$$X_r = \frac{X_{r(n)} \tau_1 + X_{r(n+1)} \left(\frac{\pi}{6} - \tau_1\right)}{\frac{\pi}{6}}, \quad (12.56)$$

where  $\tau_1$  is the burning time of  $n$  rectifiers.

Hence, for a 4-5 rectifier mode, we will get

$$X_{4-5} = X \left[ \frac{2 - \sqrt{3}A}{2} - \frac{2 - \sqrt{3}A}{7 - 4\sqrt{3}A} \cdot \frac{3\gamma}{\pi} \right]. \quad (12.57)$$

Expression for undistorted emf in a transient mode. An equivalent generator fully characterizes the SG--V system in systems where a rectifier is fed from an infinite power network via a matching transformer (while the magnitude of undistorted emf E remains constant when load current changes).

In GEU, a change in GED armature current due to the demagnetizing action /596 of stator reaction causes a change in emf E, i. e., the SG--V system is an uncompensated dc generator.

As already noted, the complexity of investigating transient processes of SG operating a rectified load is caused by the sinusoidal form of the stator current curve. Therefore, we assume for calculation simplicity that stator reaction is determined only by the first harmonic modulated in amplitude by the average value of the changing GED current.

This makes it possible to determine emf E for a three-phase SG from known Gorenv-Park equations. Considering a damper system with two damping loops and keeping in mind that the magnitude of the emf beyond the commutating reactance essentially coincides with its value in the air gap, we will get a system of equations

$$\left. \begin{aligned} -e_d &= X_{ad} p i_d - X_{aq} i_q + X_{ad} p i_f + X_{ad} p i_{kd} - X_{aq} i_{kq} \\ -e_q &= X_{ad} i_d + X_{aq} p i_q + X_{ad} i_f + X_{ad} i_{kd} + X_{aq} p i_{kq} \\ u_f &= X_{ad} p i_d + r_f i_f + X_f p i_f + X_{ad} p i_{kd} \\ 0 &= X_{ad} p i_d + X_{ad} p i_f + (r_{kd} + X_{kd} p) i_{kd} \\ 0 &= X_{aq} p i_q + (r_{kq} + X_{kq} p) i_{kq} \end{aligned} \right\} \quad (12.58)$$

Here

$$\left. \begin{aligned} i_d &= \frac{2}{3} [i_a \cos \theta + i_b \cos(\theta - 120^\circ) + i_c \cos(\theta + 120^\circ)]; \\ i_q &= -\frac{2}{3} [i_a \sin \theta + i_b \sin(\theta - 120^\circ) + i_c \sin(\theta + 120^\circ)]. \end{aligned} \right\} \quad (12.59)$$

where  $e_d, e_q$  are projections of the emf  $E$  vector on the  $d$  and  $q$  axis, respectively;  $i_d, i_q$  are projections of the imaginary vector of the current on the axis tightly coupled with the rotor;  $\theta$  - is the angle between the axes of phases  $a$  and  $d$ .

It is possible in an approximate investigation of electromechanical transient processes to disregard transformer emf in stator windings and processes in damper loops. Here, expression (12.58) is simplified and has the form

$$\left. \begin{aligned} -e_d &= -X_{aq}i_q \\ -e_q &= X_{ad}i_d - X_{ad}i_q \\ u_i &= X_{ad}p i_d + (r_l + X_l p)i_l \end{aligned} \right\} \quad (12.60)$$

The first two equations in equation system (12.60) are the equations of the balance of stator circuit voltages in a steady-state mode. They can be obtained from the simplified vector diagram, from which we have the following relationships:

$$\left. \begin{aligned} e_d &= E \cos \theta; & e_q &= E \sin \theta; \\ i_d &= I_1 \sin(\theta + \varphi_1); & i_q &= I_1 \cos(\theta + \varphi_1). \end{aligned} \right\} \quad (12.61)$$

If you exclude field currents, then the aforementioned two equations in /597 system (12.60) considering the (12.61) equations will contain four unknowns:  $E, I_{(1)}, \theta$  and  $\varphi$ . It is possible to use the following expression for a steady-state mode [32] as the missing two equations, considering that they remain justified for transient modes as well:

$$\begin{aligned} I_{(1)} &= K(\alpha, \gamma) I_j; \\ \cos \varphi_e &= \frac{U_d}{3K(\gamma) E}. \end{aligned}$$

During some research, during analysis of stability in particular, it is convenient to use the basic equations of transient processes in the SG--V--D system, written in the form

$$I_d(p) = \frac{K_1}{T_1 p - 1} [E_r(p) - E_2(p)]; \quad (12.62)$$

$$E_r(p) = \frac{K}{T_2 p - 1} U_1(p). \quad (12.63)$$

Equation (12.62) can be obtained from the equivalent circuit (see Figure 12.13), here

$$K_1 = \frac{1}{R_r - R_n} \text{ и } T_1 = \frac{L_r - L_n}{R_r - R_n},$$

while equation (12.63) can be obtained from the (12.60) system, here

$$K_2 = K_n \frac{\sqrt{(r^2 - X^2) [r^2 - (X - X_d)^2]}}{r^2 - (X - X_d)(X - X_d)}; \quad (12.64)$$

$$T_2 = \frac{r^2 + (X - X_d)(X - X_d')}{r^2 - (X - X_d)(X - X_d)} T_{20}, \quad (12.65)$$

where  $K_n$  - is the coefficient of proportionality of equivalent generator  $E_1$  and undistorted emf  $E$ ;  $r$ ,  $x$  are the parameters of the equivalent ac load:

$$r = \frac{E}{I_{(1)}} \cos \varphi_e \text{ и } X = \frac{E}{I_{(1)}} \sin \varphi_e.$$

The simplified methodology described for calculation of transient processes in the SG--V--D system's main circuit makes it possible:

a) to replace the controlled synchronous generator--uncontrolled rectifier system with an equivalent uncompensated dc generator;

b) to consider the interaction of stator and rotor circuits only from the stator current's first harmonic, modulated in amplitude by the average rectified current value;

c) to use ratios coupling alternating and direct current circuit currents and voltages obtained for the converter's steady-state operating mode.

Here, it is acceptable to disregard several factors accompanying the /598 transient process flow. In particular, no attention is paid to the aperiodic component in the stator current or the periodic component in the rectified current when an equivalent generator replaces an SG--D system.

General assumptions. Difficulties in the study and calculation of transient processes in dual-current GEU also include a limited capability for sufficiently-accurate mathematical description of such processes. Use of standard electronic computers (EVM) for these purposes requires one to make several assumptions idealizing to a certain degree the nature of the transient processes occurring in a system. Know-how accumulated to date will lead to the conclusion that the most valid information on dynamic processes in dual-current GEU comes from a combined method using analog computers and GEU elements in the form of physical models (based on the laws of physical modelling). A mathematical modelling method using individual computers without costly and complex physical modelling devices is very effective for obtaining approximate transient process characteristics at an early project planning stage. These approximations are very important for several project planning decisions.

Such a methodology is presented below for approximate calculation of transient processes described by nonlinear differential equations using an LMU-1 standard structural-sectional modelling unit along with a KNB nonlinear unit set and NBN-1 nonlinear units.

Initial modelling data. We will examine a block diagram of the main loop of a double-armature GED system (Figure 12.14). Its rectification circuit is shown in Figure 12.14a, where SG has two three-phase windings shifted 30 electrical degrees relative to each other. Each winding is connected in a star and, as the GED operates, is cut in via its own three-phase rectifier bridge (made of uncontrolled rectifiers). Both rectifier bridges are connected in series. The main current block diagram for one loop of one side of the examined system is shown in Figure 12.14b.

A variation of a main current loop and field system block diagram studied for modelling is shown in Figure 12.15. The modelling methodology here applies to a circuit with an equivalent single-armature GED (D), equivalent exciters VG and VD (for the SG and D, respectively), as well as to an equivalent regulation /599 system. Stoppage torque and ice scarifying torque are provided by SG and rectifier

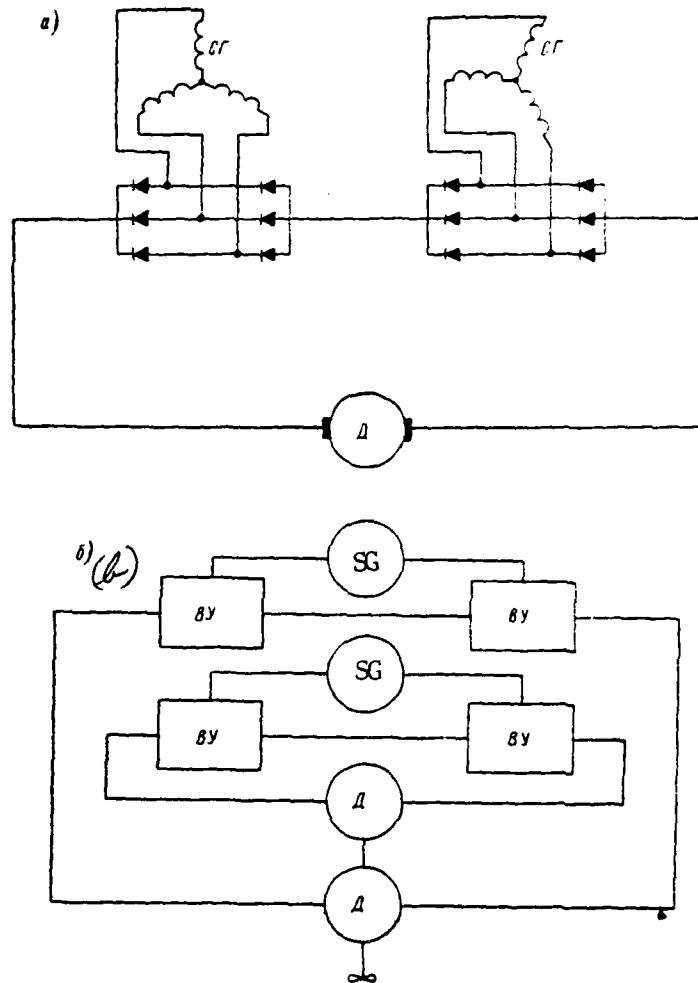


Figure 12.14. Main Loop Block Diagram: a--Rectification circuit; b--Block diagram of one side's main current.

unit VU external characteristics, as well as by main circuit current unity feedback (from sensor DT) acting upon SG field. Voltage at the MU output, whose control winding is bypassed by main circuit current, is used as a signal proportional to SG current.

The power constancy mode in a sufficiently-broad range of screw characteristic changes automatically is provided by the actions of two feedbacks: main /600 circuit current negative unity  $K_{3i_n}$ , acting upon SG voltage and voltage unity feedback (from voltage sensor DN)  $K_{1(u - U_{\pi})}$ , acting upon GED magnetic flux. GED

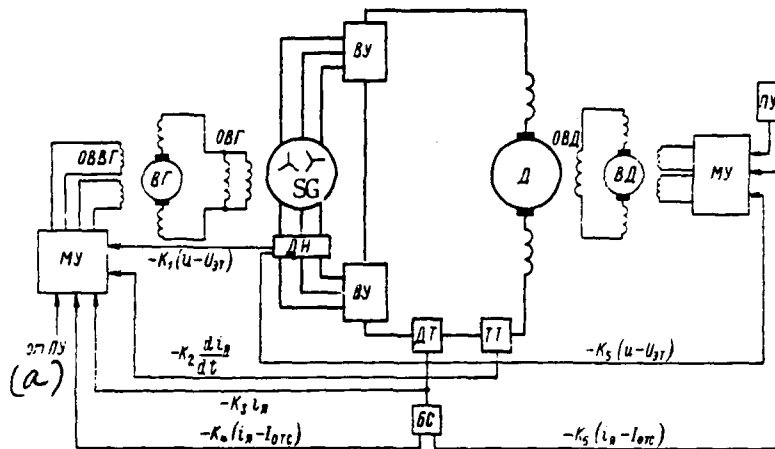


Figure 12.15. Schematic of One Loop's Main Current and Field. SG--equivalent synchronous generator equal in power to two SG in Figure 12.14; D--one side's equivalent main propulsion motor; TT--main circuit current change rate sensor;  $U_{гр}$ --reference voltage;  $I_{огр}$ --cutoff current; a--From PU.

(D) magnetic flux is regulated by a demagnetizing winding connected to the difference in synchronous generator voltage and the voltage reference value --  $K_5 (u - U_{гр})$ .

The GED is reversed by a change in the polarity of its field system. Braking during reversal occurs in the plugging mode. Here, current in the main circuit is restricted with the aid of negative current feedback (from sensor DT and comparator BS) with cut-off --  $K_6 (i_g - I_{огр})$ . Feedback action, when a safe current value in the main circuit is exceeded, weakens the magnetic flux of the GED, which operates here in the generator mode.

The system under examination also envisions connection of main circuit current change rate (from sensor TT)  $(-K_2 \frac{di_g}{dt})$  and main circuit current constraint  $[-K_4 (i_g - I_{огр})]$  feedbacks. These couplings via the MU act upon SG field.

Synchronous generator electronic model. It is possible to obtain the initial system of equations used for mathematical modelling of an SG from the following considerations.

The equivalent SG includes four loops: three phase loops and a field loop.

We will designate the potentials of the phase loop points of connection to the neutral  $e_a$ ,  $e_b$ , and  $e_c$ , respectively, and the potential at the field loop terminals  $e_r$ . We will consider the positive direction of the currents in the phases -- /60° from the neutral point of the windings to the SG terminals and positive direction of field current -- as that at which the magnetic field it creates is directed in the positive direction of the rotor axis.

Positive directions of the emf induced in stator phases coincide with the positive directions of the currents in them; we will assume the opposite directions as positive directions of external applied emf. The positive direction of external emf applied to the field loop coincides with the positive direction of the field current.

SG equations written in a stationary system of coordinates linked with phase axes, following a series of transforms, can be obtained in the form

$$\left. \begin{aligned} (r + p \frac{1}{\omega_p} X_0) i_0 &= -e_0; \\ (r + p \frac{1}{\omega_p} X_d) i_d - \gamma \frac{1}{\omega_p} X_q i_q - p M_{dr} i_r &= -e_d; \\ -\gamma \frac{1}{\omega_p} X_d i_d - (r + p \frac{1}{\omega_p} X_q) i_q - \gamma \frac{1}{\omega_p} X_{rd} i_r &= -e_q; \\ p \frac{1}{\omega_p} X_{rd} i_d - (r_r + p \frac{1}{\omega_p} X_r) i_r &= e_r, \end{aligned} \right\} \quad (12.66)$$

where

$$X_0 = \omega_p L_0; \quad X_d = \omega_p L_d; \quad X_q = \omega_p L_q; \quad X_r = \omega_p L_r; \quad X_{rd} = \omega_p M_{dr};$$

$\omega_p$  is synchronous rotational speed.

The first equation in the above system is not dependent on the others. As a result, the presence of the zero component of current in the stator phases has absolutely no effect on rotor movement in transient modes. This makes it possible to disregard this component when examining transient processes in SG. Then system (12.66), written in relative units, will have the form

$$\left. \begin{aligned} -\bar{e}_d &= \left( r + \frac{1}{\omega_p} \rho X_d \right) \bar{i}_d + \gamma \frac{1}{\omega_p} X_q \bar{i}_q + \frac{1}{\omega_p} \rho X_{rd} \bar{i}_r; \\ -\bar{e}_q &= -\gamma \frac{1}{\omega_p} X_d \bar{i}_d + \left( r + \frac{1}{\omega_p} \rho X_q \right) \bar{i}_q - \gamma \frac{1}{\omega_p} X_{rd} \bar{i}_r; \\ \bar{e}_r &= \rho X_{rd} \bar{i}_d \frac{1}{\omega_n} + \left( r + \frac{1}{\omega_n} \rho X_r \right) \bar{i}_r. \end{aligned} \right\} \quad (12.67)$$

The steady-state values of parameters of variable magnitudes, in this case in the moored mode, are taken as the base magnitudes. In this event:

$$\begin{aligned} U_6 &= 2 \sqrt{2} U_{\text{НОМ}}, & U & \text{ is nominal amplitude phase voltage;} \\ I_6 &= \sqrt{2} I_{\text{НОМ}}, & I & \text{ is phase current amplitude value;} \\ S_{\text{НОМ}} &= \frac{3}{2} 2 \sqrt{2} U_{\text{НОМ}} \sqrt{2} I_{\text{НОМ}} = 6 U_{\text{НОМ}} I_{\text{НОМ}}, & \text{kVA is nominal apparent power;} & /602 \\ \omega_6 &= \omega_{\text{НОМ}} = 2\pi f_{\text{НОМ}}, & \frac{1}{\omega_6} & \text{ is nominal synchronous angular rotational speed;} \\ Z_6 &= \frac{U_6}{I_6}, & \text{ohm is impedance;} \\ \Psi_6 &= L_6 I_6 = \frac{Z_6}{\omega_6} I_6 = \frac{U_6}{\omega_6}, & \text{Wb is flux linkage;} \\ M_6 &= M_{\text{НОМ}} = \frac{P_{\text{НОМ}}}{9.81 \omega_6}, & \text{kg-m is torque corresponding to active power } S_{\text{НОМ}} = P_{\text{НОМ}}, & \\ & & \text{given synchronous speed.} & \end{aligned}$$

Further transformations of system (12.67) and its reduction to a form suitable for mathematical modelling occur proceeding from the following considerations:

1. In accordance with an SG vector diagram, if a load has an inductive or active-inductive nature [58], vectors  $i_d$  and  $i_r$  are opposites.

Then

$$\psi_d = M_d i_r - L_d i_d \quad \text{и} \quad \psi_r = L_r i_r - M_d i_d.$$

Having substituted argument  $\psi$  in place of  $X$  in system (12.67), we will get

$$\left. \begin{aligned} -e_d &= \dot{i}_d r + \rho \dot{\psi}_d + \gamma \dot{\psi}_q; \\ -e_q &= -\gamma \dot{\psi}_d + r \dot{i}_q + \rho \dot{\psi}_q; \\ e_r &= i_r r + \rho \dot{\psi}_r. \end{aligned} \right\} \quad (12.68)$$

2. We will introduce internal emf values.

$$\left. \begin{aligned} \bar{e}_{dq} &= -X_{rd} \bar{i}_d + X_{rd} \bar{i}_r; \\ \bar{e}_{da} &= -X_{rd} \bar{i}_q. \end{aligned} \right\} \quad (12.69)$$

3. Combination of equations (12.68) and (12.69) makes it possible to compile a system of equations which describe electromagnetic transient processes in an SG:

$$\left. \begin{aligned} p\psi_r &= e_r - r_r i_r; \\ e_{\delta q} &= \omega_s \psi_r - X_{rs} i_r; \\ \omega_s \psi_d &= e_{\delta q} - X_{sd} i_d; \\ \omega_s \psi_q &= -e_d; \\ i_r &= \frac{e_{\delta q}}{X_{rd}} + i_d. \end{aligned} \right\} \quad (12.70)$$

We will introduce a new flux linkage measurement unit to simplify writing

$$\bar{\psi} = \omega_s \psi = \omega_s L i = X i.$$

Having designated  $e_d = u_d$ ,  $e_r = u_r$ ,  $e_{\delta q} = e$ , also, we will rewrite equation /603 (12.70) in the form

$$\left. \begin{aligned} p\bar{\psi}_r &= \omega_s (\bar{u}_r - r_r \bar{i}_r); \\ \bar{e} &= \bar{\psi}_r - X_{rs} \bar{i}_r; \\ \bar{\psi}_d &= \bar{e} - X_{sd} \bar{i}_d; \\ \bar{\psi}_q &= \bar{u}_d; \\ \bar{i}_r &= \frac{\bar{e}}{X_{rd}} - \bar{i}_d. \end{aligned} \right\} \quad (12.71)$$

The next mathematical modelling stage concerns reduction of SG initial equation system (12.71) to a form suitable for computer processing ("machine form"), with transformation of variables accomplished by means of formula

$$X_{o.e} = m_\chi \bar{X}_{m.e.},$$

where  $X_{o.e}$  is magnitude in relative units (r. e.);  $m_\chi$  is scale conversion factor;  $\bar{X}_{m.e.}$  is magnitude in machine units (m. e.).

Considering that  $\psi_q = X_q i_q$  and having replaced the last system (12.71) equation with equation

$$\bar{i}_r = \frac{1}{X_{rd}} (\bar{e} - \bar{i}_d),$$

it is possible finally to write a machine system of SG equations, considering scales  $m_i$ , in this way:

$$\left. \begin{aligned} p\bar{\psi}_r &= K_{11}\bar{u}_r - K_{12}\bar{i}_r; \\ \bar{e} &= K_{21}\bar{\psi}_r - K_{22}\bar{i}_r; \\ \bar{\psi}_d &= K_{31}\bar{e} - K_{32}\bar{i}_d; \\ \bar{\psi}_q &= K_{41}\bar{i}_q; \\ \bar{i}_r &= K_{51}\bar{e} - K_{52}\bar{i}_d; \\ \bar{u}_d &= K_{61}\bar{\psi}_q; \\ \bar{u}_q &= K_{71}\bar{\psi}_d. \end{aligned} \right\} \quad (12.72)$$

Designations are introduced here:

$$\begin{aligned} K_{11} &= \frac{m_i \omega_s m_u}{m_\psi}; & K_{12} &= \frac{m_i m_i \omega_s r_r}{m_\psi}; \\ K_{21} &= \frac{m_\psi}{m_u} = 1; & K_{22} &= \frac{m_i X_{rs}}{m_u}; & K_{31} &= \frac{m_u}{m_\psi} = 1; \\ K_{32} &= \frac{m_i X_s}{m_\psi}; & K_{41} &= \frac{m_i X_q}{m_\psi}; & K_{51} &= \frac{m_u}{m_i X_{rd}}; \\ K_{52} &= \frac{m_{ir}}{m_{id}}; & K_{61} &= \frac{\omega_s m \bar{\psi}_d}{m_{iq}}; & K_{71} &= \frac{\omega_s m u_{\psi}}{m \bar{\psi}_d}, \end{aligned}$$

where  $m_i$  is the values of the corresponding modelling scales.

/604

Reduction of rotor winding resistance to stator winding resistance can be accomplished by the circuit described in [36]:

$$r_{np} = K_{\text{в.с}} r,$$

where  $r_{np}$ ,  $r$  are reduced and unreduced resistances, respectively;

$$r = r_{r(75)} = r_{r(15)} K_i; \quad (12.73)$$

$K_{\text{в.с}}$  is reduction factor:

$$K_{\text{в.с}} = \frac{2m}{\pi^2} \cdot \frac{\omega_s^2 K_{\text{обм}}^2}{p \omega^2} K_{ad}^2; \quad (12.74)$$

$m$  is the number of phases;  $\omega_s$  is the number of windings per stator winding phase;

$\omega_r$  is the number of rotor windings per pole;  $K_{00m}$  is the resultant winding factor for the fundamental harmonic;  $p$  is the number of pole pairs;  $K_{ad}$  is the longitudinal reaction factor.

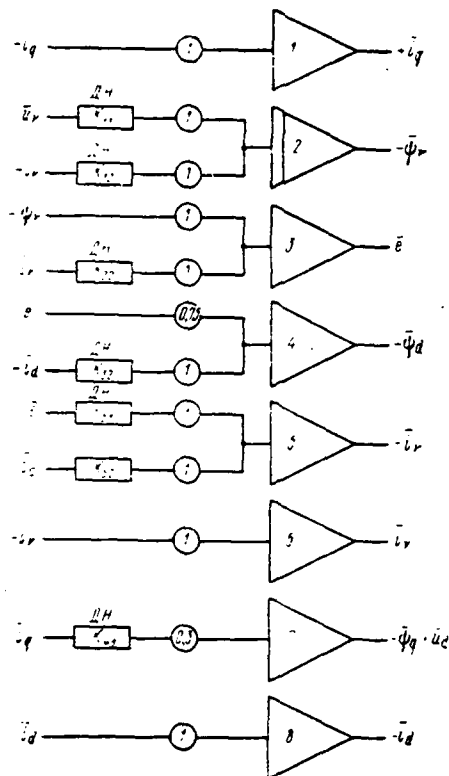


Figure 12.16. SG Electronic Model Block Diagram.

A block diagram of an SG model corresponding to equation system (12.72) is shown in Figure 12.16.

Electronic model of a GED and its exciter. Transient processes in a dc GED with independent excitation are described by equations

$$\left. \begin{aligned} u_A &= C_e n_A \Phi_A + r_A i_A + L_A \frac{di_A}{dt}; \\ C_M i_A \Phi_A &= m_n + \frac{GD^2}{375} \cdot \frac{dn_A}{dt}. \end{aligned} \right\} \quad (12.74)$$

The following assumptions are made here:

-- voltage drop under the brushes  $\Delta U_m$ ; is not considered;

-- GED armature circuit inductance is assumed to be constant and no consideration is given to the inductance of compensating winding additional poles and GED exciter (VD) armature circuit.

The GED and VD are considered to be saturated machinery.

Initial equations, given that GED electromagnetic moment is  $m_a = C_M i_a \Phi_a$ , its counter emf is  $e_a = C_e n_a \Phi_a$ , and dynamic moment of resistance is /605

$m_{a, \text{дин}} = \frac{GD_a^2}{375} \frac{dn_a}{dt}$ , can be written in a form solved for derivatives:

$$\frac{di_a}{dt} = \frac{1}{L_a} u_a - \frac{r_a}{L_a} i_a - \frac{1}{L_a} C_M n_a \Phi_a \quad (12.75)$$

$$\frac{dn_a}{dt} = \frac{375}{GD_a^2} C_M i_a \Phi_a - \frac{375}{GD_a^2} m_a \quad (12.76)$$

$$\frac{di_{v, a}}{dt} = \frac{1}{L_{v, a}} e_{v, a} - \frac{r_{v, a}}{L_{v, a}} i_{v, a} \quad (12.77)$$

Then equations (12.75), (12.76), and (12.77) in relative units will have the form

$$\left. \begin{aligned} \frac{d\bar{i}_a}{dt} &= K_{81} \bar{u}_a - K_{82} \bar{n}_a \bar{i}_{v, a} - K_{83} \bar{i}_a \\ \frac{d\bar{n}_a}{dt} &= K_{91} \bar{i}_a \bar{i}_{v, a} - K_{92} \bar{m}_a \\ \frac{d\bar{i}_{v, a}}{dt} &= K_{101} \bar{e}_{v, a} - K_{102} \bar{i}_{v, a} \end{aligned} \right\} \quad (12.78)$$

The following designations are introduced here:

$$K'_{21} = \frac{U_6}{L_a I_{a, 6}}; \quad K'_{22} = \frac{C_M n_{a, 6} K_{v, a} I_{v, a, 6}}{L_a I_{a, 6}};$$

$$K'_{23} = \frac{r_a}{I_a} = \frac{1}{T_a};$$

$$K'_{91} = \frac{375 C_M K_{v, a} I_{v, a, 6} I_{a, 6}}{GD_a^2 n_{a, 6}} = \frac{375}{GD_a^2} \cdot \frac{M_{2, 6}}{n_{a, 6}};$$

$$K'_{92} = K'_{91};$$

$$K'_{101} = \frac{u_{v, a, 6}}{L_{v, a} I_{v, a, 6}} = \frac{r_{v, a, 6}}{L_{v, a, 6}};$$

$$K'_{102} = \frac{r_{v, a}}{L_{v, a}} = \frac{1}{T_{v, a}};$$

where index «6», just as before, applies to base values.

System (12.78) reduced to machine form will be written:

$$\left. \begin{aligned} \frac{d\bar{i}_a}{dt} &= K_{81}\bar{u}_a - K_{82}\bar{i}_{a, a} - K_{83}\bar{i}_a; \\ \frac{d\bar{n}_a}{dt} &= K_{91}\bar{i}_{a, a} - K_{92}\bar{n}_a; \\ \frac{d\bar{i}_{a, a}}{dt} &= K_{101}\bar{e}_{a, a} - K_{102}\bar{i}_{a, a} \end{aligned} \right\} \quad (12.79)$$

where

$$\begin{aligned} K_{81} &= \frac{m_i m_a}{m_i} K'_{81}; & K_{82} &= \frac{m_i m_i m_n}{m_i} K'_{82}; & K_{83} &= \frac{m_i m_i}{m_i} K'_{83}; \\ K_{91} &= \frac{m_i m_i m_i}{m_n} K'_{91}; & K_{92} &= \frac{m_i m_a}{m_n} K'_{92}; \\ K_{101} &= \frac{m_i m_a}{m_i} K'_{101}; & K_{102} &= \frac{m_i m_i}{m_i} K'_{102}. \end{aligned}$$

/606

Examination of the special features of GED operation from a rectifier unit.

The special features of running a GED from a rectifier unit (VU) are considered for the following two modes:

1) screw exposure mode, when GED emf can exceed the value of the rectified voltage  $u_a$ , applied to the armature. These ratios are justified for this mode

$$\left. \begin{aligned} i_a &> 0 \quad \text{where } u_a > e_a > 0; \\ i_a &= 0 \quad \text{where } u_a < e_a > 0; \end{aligned} \right\} \quad (12.80)$$

2) GED reversal mode, when it operates in the braking mode, where additional current developed by GED emf acting in this mode in accordance with applied voltage  $u_a$  flows through the armature circuit. Then, current in the armature circuit will comprise two components -- SG voltage and GED emf. Current on the ac side equals the difference between its overall value in the armature circuit and the value of the current from GED emf. These ratios are justified for this mode

$$\left. \begin{aligned} i_{\Sigma a} &= i_a \quad \text{where } e_a > 0; \\ i_{\Sigma a} &= i_a - \left| \frac{e_a}{r_a} \right| \quad \text{where } e_a < 0. \end{aligned} \right\} \quad (12.80a)$$

Equations (12.80a) reduced to machine form in relative units will be written as:

$$\left. \begin{aligned} \bar{i}_{\Sigma R} &= \bar{i}_R; \\ \bar{i}_{\Sigma R} &= \bar{i}_R - K_{112} \bar{n}_{R' B, R} \end{aligned} \right\} \quad (12.81)$$

where

$$K_{112} = \frac{C_e K_{B, R} n_{R, B} I_{B, R, B}}{r_{B, R, B}} m_{n, R}$$

Block diagrams of a GED and VD electronic model based on systems (12.79) and (12.81) are presented in Figure 12.17.

Electronic model of coupling between an SG and GED. In a real dual-current GEU, SG input signals are primary motor torque and the voltage applied to the field winding. The signal at output is ac voltage.

SG input signals in the electronic model are currents  $\bar{i}_d$  and  $\bar{i}_q$  and field /608 voltage  $\bar{u}_r$ . It is possible to obtain input signals  $\bar{i}_d$  and  $\bar{i}_q$  by dividing current  $\bar{i}$  in the converter by these components. Rectified voltage  $\bar{u}$  supplied to the GED armature is obtained, having allowed the voltage of its components  $\bar{u}_d$  and  $\bar{u}$  through the converter, as SG output signals.

Current converter electronic model. It is possible to express the coupling between currents  $i$ ,  $\bar{i}_d$ , and  $\bar{i}_q$  in the following way:

$$\left. \begin{aligned} \bar{i}_q &= \bar{i} \cos \theta, \quad \text{where} \quad \cos \theta = \frac{\bar{u}_q}{\bar{u}}; \\ \bar{i}_d &= \bar{i} \sin \theta, \quad \text{where} \quad \sin \theta = \frac{\bar{u}_d}{\bar{u}}. \end{aligned} \right\} \quad (12.82)$$

These relationships are realized in an analog model in two ways:

- 1) values  $\cos \theta$  and  $\sin \theta$  are obtained in dividers and are supplied to multipliers along with value  $\bar{i}$  or
- 2) values  $\cos \theta$  and  $\sin \theta$  are obtained at integrator output (where a multiplier is connected to the feedback circuit) and then are supplied to multipliers.

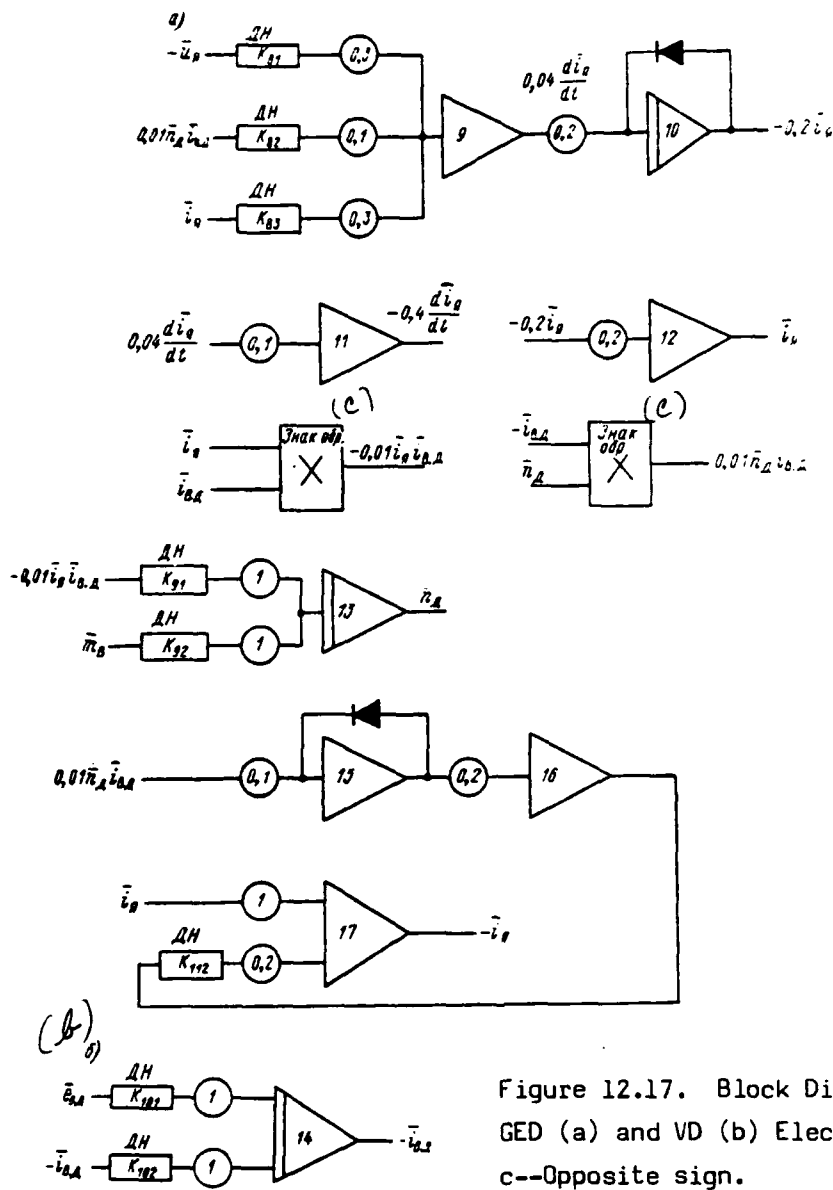


Figure 12.17. Block Diagram of a GED (a) and VD (b) Electronic Model. c--Opposite sign.

The second method usually is used since the first is characterized by unstable divider operation.

A current converter block diagram is presented in Figure 12.18a.

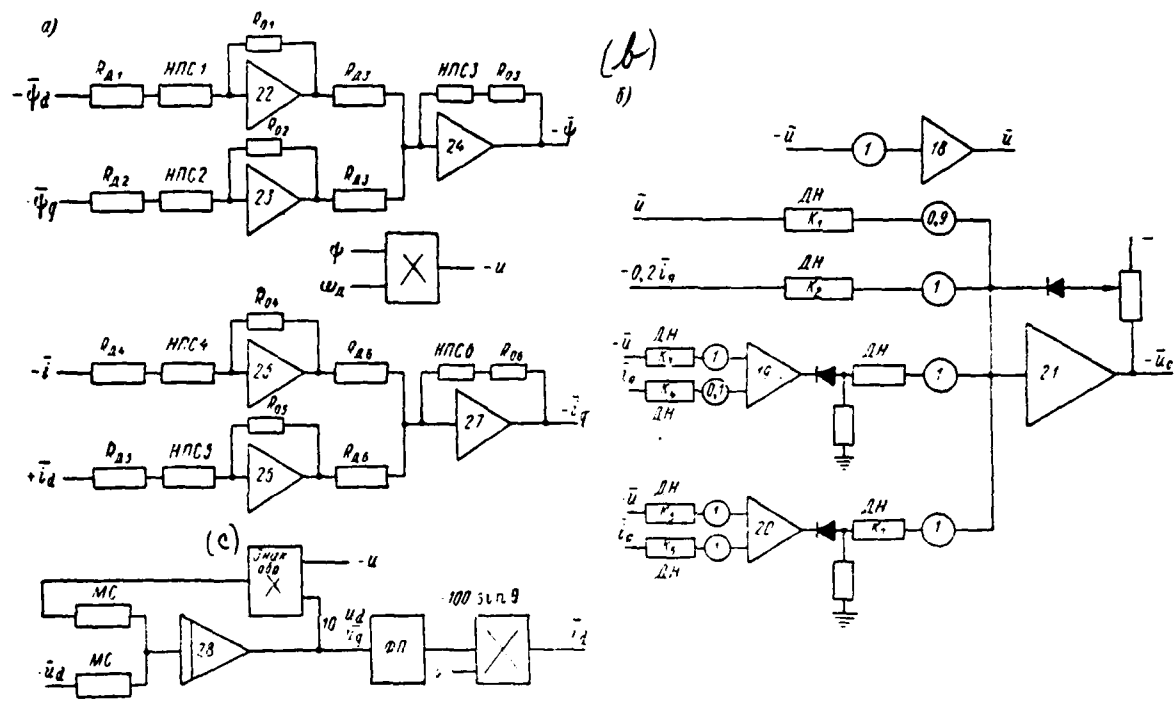


Figure 12.18. Block Diagram for SG Current Coordinate (a) and Voltage (b) Conversion. c--Opposite sign.

Voltage converter electronic model. Magnitudes  $\bar{u}$ ,  $\bar{u}_d$ , and  $\bar{u}_q$  are coupled by the following ratio

$$\bar{u} = \sqrt{\bar{u}_d^2 + \bar{u}_q^2} = \omega \sqrt{\bar{\psi}_d^2 + \bar{\psi}_q^2} \tag{12.83}$$

Voltages  $\bar{u}_d$  and  $\bar{u}_q$  are obtained as output signals from the SG. With the aid of nonlinear semiconductor resistances (NPS) connected to inverter inputs and, given appropriate selection of resistances  $R_A$  and  $R_O$ , raising to the square of the input magnitude is accomplished. Extraction of a root occurs in a circuit where an NPS is connected to the inverter feedback circuit. The voltage conversion circuit is depicted in Figure 12.18b. Resultant voltage  $\bar{u}$  is a GED input signal (see Figure 12.18a).

Examination of a rectifier unit. A commutated drop in voltage in the rectifier

bridge is accomplished by introduction of the rectifier's external characteristic [66].

Assumed base magnitudes are:

$$U_0 = \sqrt{3} E_m; \quad I_0 = \frac{\sqrt{3} E_m}{2X_R},$$

where  $E_m$  is equivalent emf acting upon resistance  $X_R$ ;  $X_R$  is commutation loop reactive resistance.

Magnitude  $X_R$  can be calculated from formula (12.8) when a self-excited /610 generator runs the rectifier. The external characteristic is approximated with three sectors and a block diagram of it is shown in Figure 12.18b.

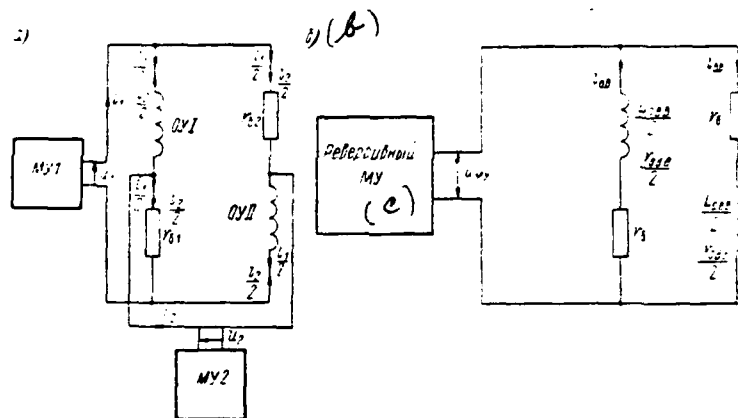


Figure 12.19. Exciter Field System Schematic (a) and Equivalent Circuit (b). c--Reversing MU.

Excitation system modelling considering feedbacks. A schematic of an SG and GED exciter field is depicted in Figure 12.19a.

The MU operate separately: this makes it possible in the equivalent circuit (Figure 12.19b) to examine the connection of only one MU, while it is assumed that the polarity of its output voltage will depend on the direction of the control signal. The ballast resistance value is determined by the expression  $r_0 = \frac{r_{0.в.в.}}{2}$ .

The equation of electromagnetic equilibrium in the exciter field circuit for the equivalent circuit (see Figure 12.19b), written in relative units and solved for the derivative, has the form

$$\frac{d\bar{i}_{\text{в.в.}}}{dt} = \frac{2}{T_{\text{в.в.}}} \bar{u}_{\text{МУ}} - \frac{2}{T_{\text{в.в.}}} \bar{i}_{\text{в.в.}} \quad (12.84)$$

We will introduce designations:  $U_{\text{МУ} \sigma} = U_{\text{МУ} \text{НОМ}}$ ;  $I_{\text{в.в.}\sigma} = I_{\text{в.в.}\text{НОМ}}$ ;  $r_{\text{о.в.в.}} = r_{\text{о.в.в.}\text{НОМ}} = r_{\text{о.в.в.}\sigma}$ ;  $\frac{L_{\text{о.в.в.}}}{r_{\text{о.в.в.}}} = T_{\text{в.в.}}$  is a time constant, which, for the generator ( $T_{\text{в.в.}\Gamma}$ ) and for the motor ( $T_{\text{в.в.}\Delta}$ ), is determined, respectively by the expressions:

$$T_{\text{в.в.}\Gamma} = \frac{2\rho\omega_{\text{в.в.}\Gamma}^2}{r_{\text{в.в.}\Gamma}} + \frac{\Delta\Phi_{\text{в.в.}\Gamma}}{\Delta i_{\text{в.в.}\Gamma}\omega_{\text{в.в.}\Gamma}};$$

$$T_{\text{в.в.}\Delta} = \frac{2\rho\omega_{\text{в.в.}\Delta}^2}{r_{\text{в.в.}\Delta}} + \frac{\Delta\Phi_{\text{в.в.}\Delta}}{\Delta i_{\text{в.в.}\Delta}\omega_{\text{в.в.}\Delta}}.$$

The values of nominal fluxes  $\Phi_{\text{в.в.}\Gamma\text{НОМ}}$  and  $\Phi_{\text{в.в.}\Delta\text{НОМ}}$ , as well as of currents  $I_{\text{в.в.}\Gamma\text{НОМ}}$  and  $I_{\text{в.в.}\Delta\text{НОМ}}$ , will be found from smoothed magnetization characteristics ( $\bar{u}_{\text{в.в.}} \approx \bar{i}_{\text{в.в.}}$ ).

The following input signals (see Figure 12.15) are supplied to MU input:

- master signal from PU;
- signal proportional to main circuit current on the GED (D) side from DT;
- main circuit current rate change unity feedback signal (current transformer TT output);

- signal from the voltage cut-off unit (DN) supplied in the event SG voltage exceeds the nominal  $U_{\text{НОМ}}$ ;

- signal from the current cut-off unit (BS) supplied in the event main circuit current (on the GED side) exceeds specific given current magnitude  $I_{\text{н.НОМ}}$ .

Voltage from MU output is supplied to OVVG. A block diagram of the SG field system is depicted in Figure 12.20a. Disregarding MU control winding inductance, it is possible to write:

$$u_{\text{в.в.}\Gamma} = u_{\text{п.у}} - K_{121}i_{\text{я}} - K_{122}\frac{di_{\text{я}}}{dt} - K_{123}(u - U_{\text{зт}}) - K_{124}(i_{\text{я}} - I_{\text{отс}});$$

$$u > U_{\text{зт}} = 1,2U_{\text{НОМ}}; \quad i_{\text{я}} > I_{\text{отс}} = 1,7I_{\text{я.НОМ}} \quad (12.85)$$

For the GED field system

$$\begin{aligned} u_{\text{в.в.д}} &= u_{\text{п.у}} + K_{131}(i_{\text{я}} - I_{\text{отс}}) - K_{132}(u - U_{\text{ст}}); \\ i_{\text{я}} > I_{\text{отс}} &= 1,7 I_{\text{д.ном}} \quad u > U_{\text{ст}} = 1,2 U_{\text{ном}}, \end{aligned} \quad (12.86)$$

where  $u_{\text{п.у}}$  is the master signal from PU;  $K_{131}(i_{\text{я}} - I_{\text{отс}})$  is the signal from the current cut-off unit (in Figure 12.15,  $K_{131}$  is designated  $K_6$ );  $K_{132}(u - U_{\text{ст}})$  is the signal from the voltage cut-off unit (in Figure 12.15a,  $K_{132}$  is designated  $K_5$ ).

At the  $M_{\text{в.д}}$  output, we get voltage, which is supplied to the OVVD.

Consequently, considering that exciters are saturated machinery, it is possible to describe an SG field system by means of equations (12.85), (12.86), and

$e_{\text{в.г}} = K_{\text{в.г}} i_{\text{в.г}}$ , while the GED system can be described by means of equations (12.85), (12.86), and  $e_{\text{в.д}} = K_{\text{в.д}} i_{\text{в.д}}$ .

Initial equations for SG and GED field systems, converted into machine form and expressed in relative units, will be written in the following manner.

#### 1. For the SG exciter field system

$$\left. \begin{aligned} \bar{u}_{\text{в.г}} &= \bar{u}_{\text{п.у}} - K'_{121} \bar{i}_{\text{я}} - K'_{122} \frac{d\bar{i}_{\text{я}}}{dt} - \\ &- K'_{123} (\bar{u} - \bar{u}_{\text{ст}}) - K'_{124} (\bar{i}_{\text{я}} - \bar{I}_{\text{отс}}); \\ \frac{d\bar{i}_{\text{в.г}}}{dt} &= K'_{131} \bar{u}_{\text{в.г}} - K'_{132} \bar{i}_{\text{в.г}}; \\ \bar{e}_{\text{в.г}} &= \bar{i}_{\text{в.г}} \end{aligned} \right\} \quad (12.87)$$

where

/612

$$\begin{aligned} K'_{121} &= \frac{K_1 I_{\text{отс}}}{U_{\text{в.г}} m_{\text{в.г}}}; & K'_{122} &= \frac{K_2 I_{\text{отс}}}{m_{\text{в.г}} U_{\text{в.г}}}; & K'_{123} &= \frac{K_3 U_{\text{ст}}}{U_{\text{в.г}} m_{\text{в.г}}}; \\ K'_{124} &= \frac{K_4 I_{\text{отс}}}{U_{\text{в.г}} m_{\text{в.г}}}; & K'_{131} &= \frac{2 U_{\text{в.г}}}{T_{\text{в.г}} I_{\text{в.г}}}; & K'_{132} &= \frac{2 m_{\text{в.г}}}{T_{\text{в.г}} m_{\text{в.г}}}. \end{aligned}$$

An SG exciter field system electronic model, compiled from the system (12.87) equations, is shown in Figure 12.20b.

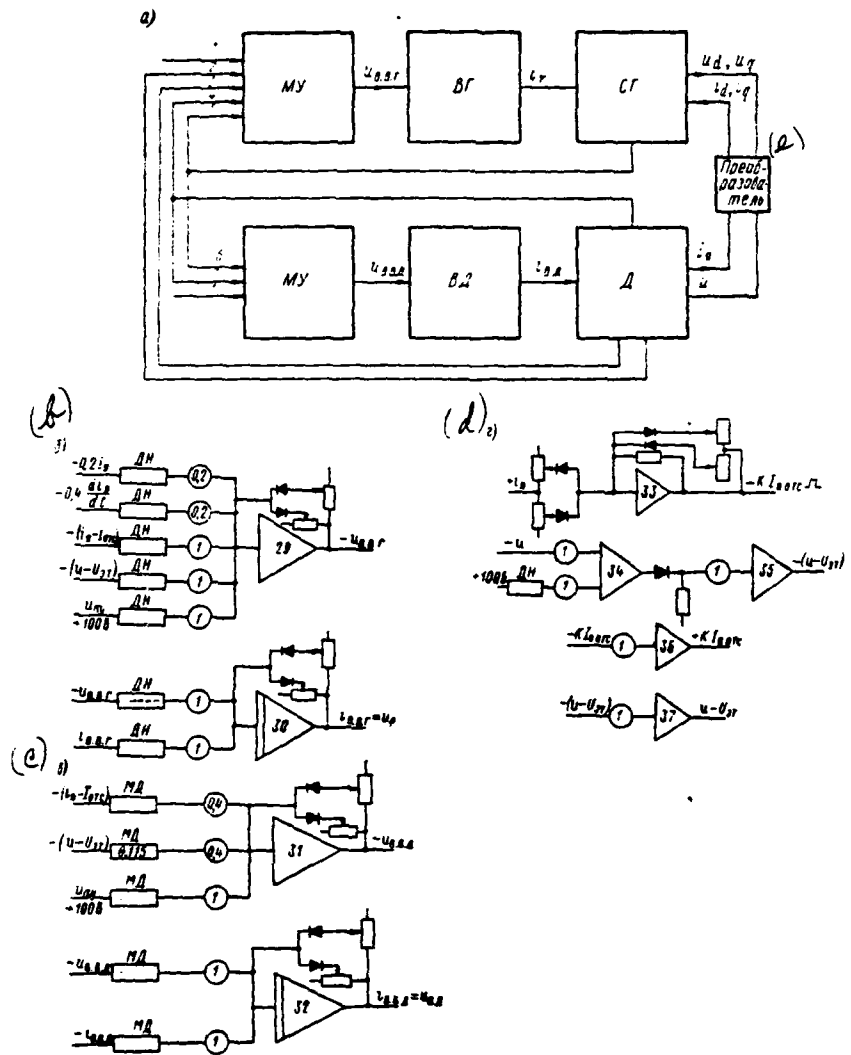


Figure 12.20. Block Diagrams of Field System Electronic Models: a--Field circuit; b--SG; c--GED; d--Feedbacks; e--Converter; 1--From PU; 2--Current feedback  $K_2 i_n$ ; 3--Armature circuit current rate change feedback  $K_3 \frac{di_n}{dt}$ ; 4--Main circuit voltage cut-off feedback  $K_4 (u - U_{gr})$ ; 5--Main circuit current cut-off feedback  $K_5 (i_n - I_{gr})$ ; 6--Current cut-off feedback  $K_6 (i_n - I_{gr})$ ; 7--Main circuit voltage cut-off feedback  $K_7 (u - U_{gr})$ .

$$\left. \begin{aligned} \bar{u}_{\text{в. в. д}} &= \bar{u}_{\text{н. у}} + K'_{141} (\bar{i}_{\text{н}} - \bar{I}_{\text{орс}}) + K'_{142} (\bar{u} - U_{\text{эв}}); \\ \frac{di_{\text{в. в. д}}}{dt} &= K'_{151} \bar{u}_{\text{в. в. д}} - K'_{152} \bar{i}_{\text{в. в. д}}; \quad \bar{e}_{\text{в. в. д}} = \bar{i}_{\text{в. в. д}} \end{aligned} \right\} \quad (12.88)$$

where

$$\begin{aligned} K'_{141} &= \frac{K_7 I_{\text{с}} m_i}{U_{\text{в. в. д. с}} m_i}; & K'_{142} &= \frac{K_8 U_{\text{с}}}{U_{\text{в. в. д. с}}}; \\ K'_{151} &= \frac{m_i U_{\text{в. в. д. с}}}{T_{\text{в. в. д. с}} m_i}; & K'_{152} &= \frac{2 m_i m_i}{T_{\text{в. в. д. с}} m_i}. \end{aligned}$$

A block diagram of a GED exciter field system electronic model compiled from system (12.88) equations is depicted in Figure 12.20c, while that of feedbacks is shown in Figure 12.20d.

Transient process electronic modelling. The electronic model obtained for investigation of transient processes realizes a system of equations which will approximately describe these processes in a dual-current GEU. It makes it possible to obtain the corresponding characteristics during GED starting and reversal, during radical changes in the moment of resistance on the propellor, and in emergency situations. It also makes it possible to investigate the influence of feedback parameters and to determine their values for optimum transient process flow in different operating modes.

Research and computer-assisted calculations provide the capability to solve complex problems of GEU element synthesis and structure.

Propellor moored and reversing characteristics are composed in units of nonlinearities after their preliminary representation in the form of a piecewise-linear approximation.

Transfer function modelling. Achievement of considerable simplification during preliminary calculations of transient processes using the mathematical modelling method is possible by using the following transfer functions as the initial equations [68].

Since the condition  $\omega L_{\text{н}} \gg R_{\text{н}}$ , where  $\omega$  is the converter commutational cycle

frequency and  $L_s$  and  $R_s$  are the GED armature self-inductance and resistance, respectively, usually are used for GEU, transient processes in a GEU significantly are longer than the synchronous generator--rectifier (SG--Vp) converter commutational cycle. Here, SG dynamic properties reflect transfer functions sufficiently:

for field voltage

$$K_1(p) = \frac{R}{T_{do}p + 1}, \quad (12.89)$$

where  $K_1 = \frac{X_{af}}{r_f \cos \delta}$  is generator voltage amplification factor;  $X_{af} = \frac{U_\phi}{I_f}$  is the reactivity of the mutual induction between stator and rotor;  $U_\phi$  is generator /614 phase voltage;  $I_f$ ,  $r_f$  are field winding current and resistance, respectively;  $\delta$  is the angle between the generator voltage vector and the direction of axis q:

$$\delta = \arctg \frac{I_d (X_q \cos \varphi - r \sin \varphi)}{U - I_d (r \cos \varphi - X_q \sin \varphi)};$$

$X_q$  is stator synchronous reactance along the transverse axis;  $r$  is stator resistance;  $T_{do}$  is a rotor time constant, given an open stator;  $I_d$  is generator load current;  $U$  is generator voltage;

for current considering armature reaction

(12.90)

where

$$K_2(p) = \beta_1 \frac{K_c T_{do} p + 1}{T_{do} p - 1},$$

$$\beta_1 = \frac{X'_d \sin \psi - r \cos \psi}{\cos \delta}; \quad K_c = \frac{X'_d \sin \psi - r \cos \psi}{X_d \sin \psi - r \cos \psi};$$

$$\psi = \varphi - \delta,$$

$X'_d$ ,  $X_d$  are stator synchronous resistance and synchronous transient resistance, respectively, along the longitudinal axis.

The SG transfer functions presented do not consider the influence of damper windings and the aperiodic component of stator current. Factors  $\beta_1$  and  $K_c$  are the nonlinear functions of load current  $I_d$ .

The SG current transfer function can be represented in the following form:

$$K_2(p) = \frac{\beta_1}{T_{d0}p + 1} + \beta_1 K_c T_{d0} p \frac{1}{T_{d0}p + 1}. \quad (12.91)$$

The first equation (12.91) term is a transfer function of an aperiodic link with time constant  $T_{d0}$ ; factor  $\beta_1$  here determines the SG static external characteristic in the entire load current change range.

This equation's second term is the transfer function of the inertial differential link with amplification factor  $\beta_1 K_c T_{d0}$  and inertial delay time constant  $T_{d0}$ . It is possible to consider factor  $\beta_1$  as a nonlinear external characteristic during mathematical modelling of an SG--Vp system. The differential inertial link's amplification factor also is a nonlinear load current function. This link is modelled rather simply with the help of an operational element, in which an RC network is used as amplifier feedback resistance.

During piecewise-linear approximation of the external characteristic of an SG--Vp system, with three linear sections for example, the equation for its mathematical modelling will have the form

$$U_d = U_{d0} - K_1 I_d + K_2 \text{sign}(K_3 U_{d0} - K_4 I_d) + K_5 \text{sign}(K_6 U_{d0} - K_7 I_d).$$

Factors  $K_1$ -- $K_7$  are determined from ratios:

/615

$$K_1 = \frac{U_{d0} - U_{d1}}{I_{d1}} \frac{mU_d}{mI_d}; \quad K_3 = \frac{U_{d1}}{U_{d0}}; \quad K_4 = \frac{U_{d1}}{I_{d1}} \frac{mU_d}{mI_d};$$

$$K_2 K_4 - K_1 = \frac{U_{d1} - U_{d2}}{I_{d2} - I_{d1}} \frac{mU_d}{mI_d};$$

$$K_5 = \frac{U_{d2}}{U_{d0}}; \quad K_7 = \frac{U_{d0}}{I_{d2}} \frac{mU_d}{mI_d};$$

$$K_5 K_7 + K_3 K_5 + K_2 = \frac{U_{d2}}{I_{d3} - I_{d2}} \frac{mU_d}{mI_d}.$$

where  $U_d$ ,  $I_d$  are voltage and current at the SG--Vp system output;  $mU_d$ ,  $mI_d$  are voltage and current scale factors.

A diagram of the external characteristic's model is shown in Figure 12.21a. D7Zh rectifiers Vp1 and Vp2 are used to separate voltage negative in sign. Resistors R1, R2 insure that rectifiers Vp1 and Vp2 operate in the linear portion of the volt-ampere characteristic. Rectifier Vp3 constrains the output voltage sign. A change in voltage  $U_{d0}$  is accompanied by an equivalent change in displacement of the SG--Vp system's external characteristic.

The system of equations for GED modelling is analogous to system (12.78) and can be written in the following form:

$$\left. \begin{aligned} \frac{di_a}{dt} &= K_{11}u_a - K_{12}n_d\Phi_{в.д} - K_{13}i_a; \\ \frac{dn_d}{dt} &= K_{21}i_a\Phi_{в.д} - K_{22}m_b; \\ \frac{di_{в.д}}{dt} &= K_{31}u_{в.д} - K_{32}i_{в.д}, \end{aligned} \right\} \quad (12.92)$$

where

$$\begin{aligned} K_{11} &= \frac{m_{i_a}}{m_{n_d} m_{\Phi_{в.д}}} \frac{U_{я.ном}}{I_{я.ном} L_{я.}}; \\ K_{12} &= \frac{m_{i_a}}{m_{n_d} m_{\Phi_{в.д}} m_t} \frac{E_{д.ном}}{L_{я} I_{я.ном}}; \\ K_{13} &= \frac{1}{m_t} \frac{r_{я}}{L_{я}}; \\ K_{21} &= \frac{m_{n_d}}{m_{i_a} m_{\Phi_{в.д}} m_t} \cdot \frac{375}{GD^2} \frac{M_{д.ном}}{n_{д.ном}}; \\ K_{22} &= \frac{m_{n_d}}{m_{m_b} m_t} \frac{375}{GD^2} \frac{M_{д.ном}}{n_{д.ном}}; \\ K_{31} &= \frac{m_{i_{в.д}}}{m_{u_{в.д}} m_t} \frac{r_{в.д}}{L_{в.д}}; \quad K_{32} = \frac{1}{m_t} \frac{r_{в.д}}{L_{в.д}}. \end{aligned}$$

A diagram of this model, which differs little from that shown in Figure /616 12.17, is presented in 12.21b. Voltage  $U_d$  from the SG--Vp system model directly is fed to the GED model, while current  $i_a$  from the GED model is supplied to the SG-Vp model in the form of current  $I_d$ . Additionally, condition  $i_a \geq 0$  must be accomplished for all modes for the SG--Vp--D model.

## § 12.8 Dual-Current System Main Circuit Circuitry

Circuit selection. Selection of the main current circuit for electric ships with dual-current systems is determined, first, by vessel type and purpose, navigating area, special requirements -- based on use of primary motor full power in all

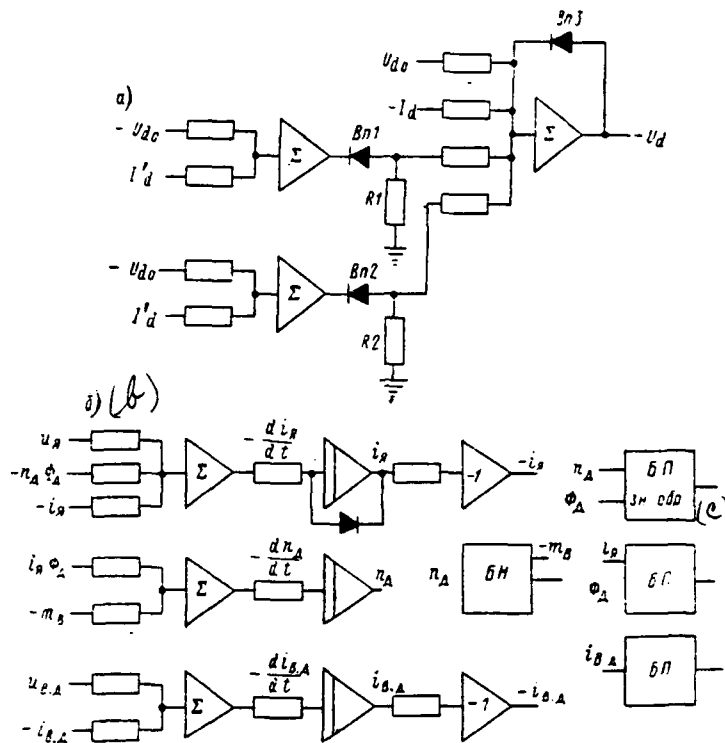


Figure 12.21. SG-VU--D System Mathematic Model: a--Model of the Rectifier Unit (SG--VU) External Characteristic; b--GED model; c--Opposite sign.

operating modes, by power take-off from electric propulsion bus bars for /617 auxiliaries and for plant viability, and, second, by requirements relative to GED control range and speed and its reversing. Here, requirements levied for electric power quality on the alternating and direct current side also are taken into consideration.

Dual-current GEU can consist either of steam and gas turbines or diesels where primary motors are concerned. An important feature for classification of the GEU type being examined is the nature of the main current rectification circuit used: with uncontrolled or with controlled rectifiers. Synchronous generator voltage and frequency are regulated in the first type of rectifier unit (VU), while voltage and frequency remain constant in the second VU type.

Circuits for VU consisting of uncontrolled rectifiers. The main current circuit in such plants will comprise a synchronous generator (one or several),

whose voltage can be controlled from the nominal value to zero, which provides a broad range of dc GED rotational speed control. Here, current frequency can be either constant or it will change (for diesel generators) at slow vessel speeds to increase the service life of the diesels. The GED is reversed by changing the direction of the GED field current.

Turbine-driven set circuit variants. Main current circuits relative to line icebreaker GEU requirements are examined below. The most important of these requirements are: identical power of all three aft GED (propellor power distribution ratio 1 : 1 : 1); capability to run three GED (aft and forward) with the generators of the same primary motor; capability to run two armatures of a double-armature GED with two generators of different sides; self-sufficiency of the field system (each of two) of double-armature GED machinery.

The schematic presented in Figure 12.22 satisfies the enumerated requirements, very necessary to insure reliable and trouble-free icebreaker GEU operation. Here, three paired GED feed electric power to four turbine-driven sets. The latter comprise turbines 1--4, on the shaft of which are mounted three synchronous ac generators each. Each of them, along with rectifier unit VU, are a single unit, whose output voltage is regulated by SG field. Each GED armature is fed from two generators of varied turbine-driven sets located in different engine rooms (one forward and another aft). Two of them (located accordingly in the aforementioned engine rooms) feed the forward -- port, amidships, and starboard armatures of three GED ( $I_{a. n.}, I_{c. n.}, I_{n. n.}$ ), while the other two feed the aft armatures ( $I_{a. k.}, I_{c. k.}, I_{n. k.}$ ).

The fore and aft GED armatures are not connected electrically and have autonomous field systems. Each armature, along with generator--rectifier units, form a loop. There are six such loops.

The circuit under examination insures high reliability and viability, /618 essentially eliminating the probability of a complete disappearance of torque in the GED, which, to a known degree, is protection against damage to propellor blades and shaft. Operation of the GEU aboard the icebreaker "Lenin" confirms the advantages of similar two-loop circuits.

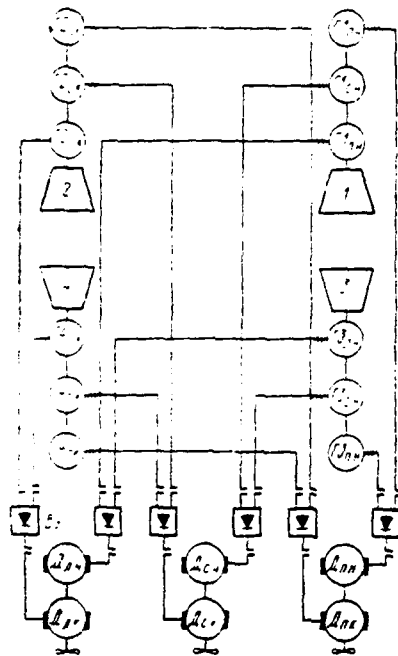


Figure 12.22. Schematic of a Turboelectric Propulsion Plant (TEGU). 1-4--Main turbines; Γ<sub>л.к</sub>, Γ<sub>с.к</sub>, Γ<sub>п.к</sub> --Main machinery of the port, amidships, and starboard GED aft armature loops; Γ<sub>л.л</sub>, Γ<sub>с.л</sub>, Γ<sub>п.л</sub> --Main machinery of the port, amidships, and starboard GED forward armature loops.

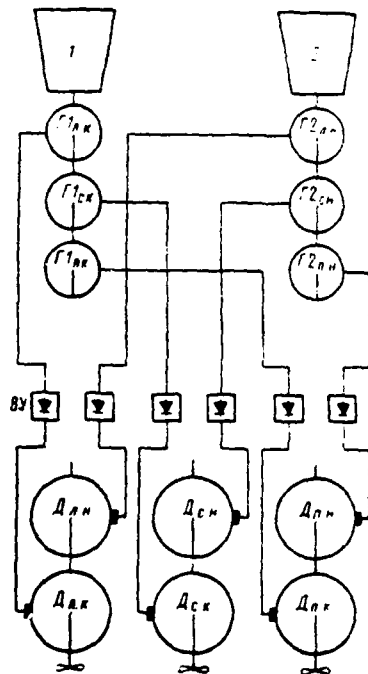


Figure 12.23. Schematic of a TEGU With Two Main Turbines.

A main current circuit comprising two turbine-driven sets operating three paired GED (Figure 12.23) satisfies identical requirements. Here, each of the two turbines is connected to three synchronous generators.

Circuits with diesel generators. When developing main current circuits with uncontrolled rectifiers, one must consider the capability of feeding the GED from two or more diesel generators. Examples are presented below of several conceptual solutions for such circuits.

When GED are fed from two or more generators, converters are connected in series on the direct current side. Connecting them in any manner on the ac /619 side is not recommended to avoid short circuits across the rectifiers.

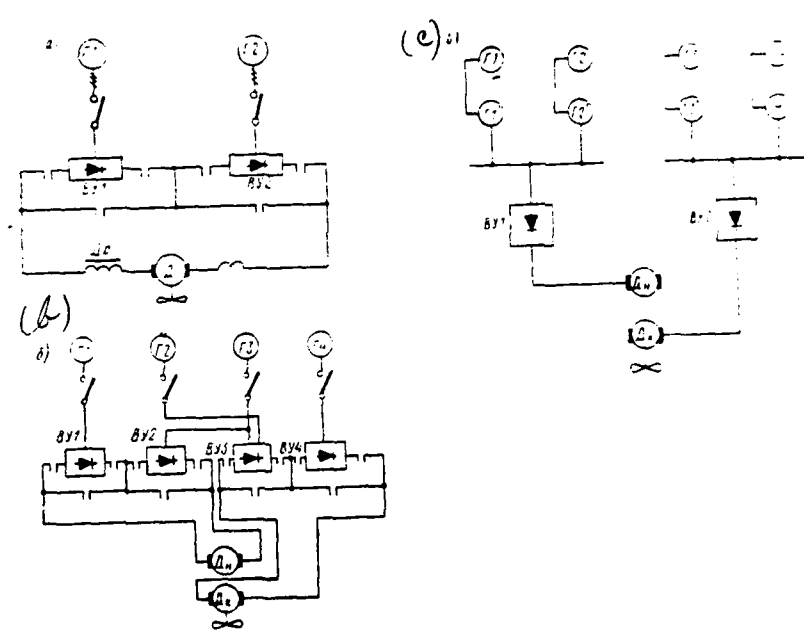


Figure 12.24. Diesel Electric Propulsion Plant Circuits With Uncontrolled Rectifiers. a--Circuit with series-connected VU to feed one GED (D) armature; b--Circuit with series-connected VU for feeding a double-armature GED; c--Circuit with paired main generators.

A main current circuit in which rectifiers (VU1, VU2) are connected in series to feed one GED (D) armature is depicted in Figure 12.24a; a variant in which four main generators 1--4 feed a double-armature GED (D) in a two-loop system is shown in Figure 12.24b, while a single-wire circuit with paired main generators

is presented in Figure 12.24c. Other main current circuit types using uncontrolled rectifiers, those with series-connected GED armatures in particular, also can be used.

GED voltage selection is based on the following considerations.

Given voltage of 1,100 V at the GED armature, the line voltage  $U_{r.l}$  of each of two series-connected main generators G1 and G2 (see Figure 12.24a and 12.24b) equals

$$U_{r.l} = \frac{1100}{2 \cdot 1.2} = 458 \text{ V,}$$

where 1.2 is the voltage rectification factor under load.

Considering the voltage drop in the rectifiers and network, this voltage will be somewhat greater, but not more than 550 V. Thus, a disadvantage of this circuit is the limited capability of voltage selection for SG. This drawback has special significance, given high generator capacities, due to difficulties with placement of windings rated for high currents in the machine stator slots.

Circuits for GEU with controlled rectifiers in the main circuit. We will /620 examine a schematic of a GEU which uses controlled rectifiers in the main circuit.

Circuit variant with reversal in the main current circuit. Such a circuit (Figure 12.25) comprises four ac diesel generators G1--G4, four rectifier units VU1--VU4, and three GED (D), with the amidships one being a double-armature GED. Each GED armature is fed from its own generator via the appropriate VU. Consequently, there are four independent loops. This circuit insures maximum GEU viability and operating reliability, making the following operating modes possible:

Mode I -- each generator runs its own GED armature: G1 to D1, G2 to  $D2_1$ ; /621  
G3 to  $D2_2$ , G4 to D3;

Mode II -- three generators run three GED armatures: G1 to D1, G2 to на  $D2_1$ ,  
or G3 to  $D2_2$ , G4 to D4;

Mode III -- two generators run two armatures: G1 to D1, G4 to D4 or G2 to  
 $D2_1$ , G3 to  $D2_2$ ;

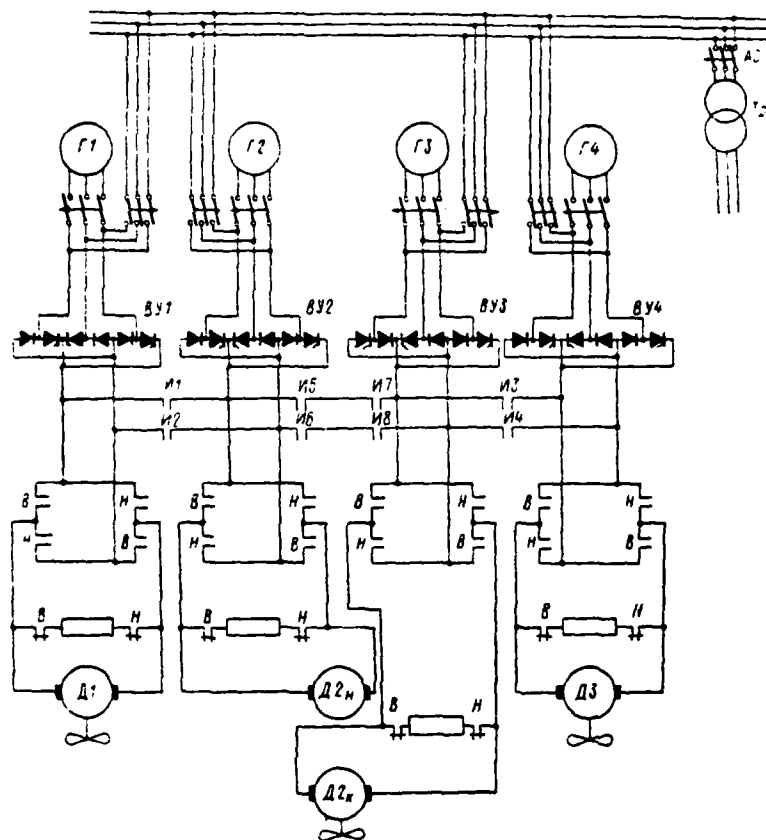


Figure 12.25. Diesel Electric Propulsion Plant With Reversal in the Main Current Circuit. ВУ--Rectifier units with controlled rectifiers; N, V [Reverse, Forward]--Reversing switch contacts.

Mode IV -- one generator runs one amidships GED armature: G2 to  $\Delta 2_n$  or G3 to  $\Delta 2_k$  ;

Mode V -- four generators run three GED armatures and thruster electric motor: G1 to D1, G4 to D4, G2 to  $\Delta 2_n$  ; G3 to PU or G3 to  $\Delta 2_k$  ; G2 to PU.

Generators G3 and G4 running the outboard GED and generators G1 and G4 running the amidships GED also is envisioned.

Circuit selection occurs with selector switch IP only when generator field is removed. Generators are connected by means of generator switches, which are mutually interlocked with the selector switches. This provides the capability for power take-off to auxiliary bus bars from each main generator. Power take-off

from two generators suffices for all vessel operating modes. Therefore, in the underway mode, power to the auxiliary station is picked either off the two generators running outboard GED or the two running the amidships GED.

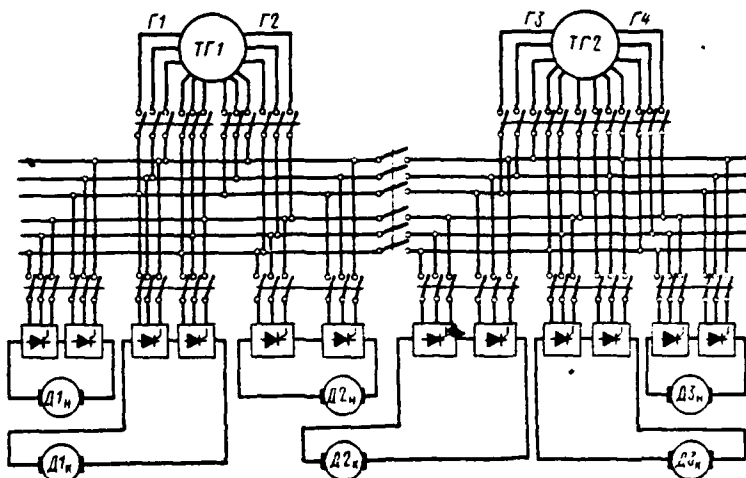


Figure 12.26. GEU Variant With Two Turbine-Driven Sets and Thyristor Converters in the Main Circuit.

GEU circuit for an icebreaker with two turbine-driven sets and three propellers.

We will examine a variant of a GEU with two turbine-driven sets comprising two generators each connected to each turbine. All three GED are the double-armature /622 type.

Each GED armature is fed by its own converter unit, with the converters fed from the port and starboard GRShch [main distribution board] ac collecting buses. Fixed voltage is maintained in the buses. The main current circuit set-up (Figure 12.26) is accomplished on the ac side with six-pole switches: both sides' GRShch buses are connected by an intersectionalizing switch.

The circuit allows the plant to operate in the following basic modes:

Mode I -- all GED armatures are fed from all four turbine-driven sets. Power at the screws is distributed in the ratio 1 : 2 : 1;

Mode II -- generator G2 and GED Д2. Power distribution at the screws is 1 : 1 : 1 (25% : 25% : 25%);

Mode III -- generators G1 and G2 and GED  $I_{1..}$   $I_{2..}$  are connected. Power distribution at the screws is 1 : 0 : 1 (25% : 0 : 25%);

Mode IV -- generators G3 and G4 are cut in and GED D1,  $I_{2..}$ , and D6 are operating. Power distribution is 1 : 2 : 1 (12.5% : 25% : 12.5%);

Mode V -- generators G1 and G2 are connected and GED  $I_{1..}$   $I_{1..}$   $I_{3..}$   $I_{3..}$  are operating. Power distribution is 1 : 0 : 1 (25% : 0 : 25%).

### § 12.9 Dual-Current Electrical Propulsion Plant Excitation Systems

Excitation system special features. This type GEU, where uncontrolled rectifiers are used, is regulated mainly by a change in synchronous generator field. Therefore, they are required to provide stability and reliability as SG voltage is regulated over a sufficiently large range.

Given these conditions, the nature of the transient processes in GEU mainly involve the field system's speed of response. This is one reason for wide use of thyristor field systems. They can be set up in one of the following circuits: separate field, self-excitation, or field from the network.

Separate field with the exciter on the main set's shaft usually is not used due to design shortcomings. A self-excitation system also is rather unwieldy, considering the requirement for a significant range of SG modes and difficulties with initial excitation. Therefore, thanks to the presence of a powerful shipboard station, a system with excitation from the shipboard electric power station is more preferable. However, if you remember that GEU generator field will serve as a considerable additional load for the shipboard electric power station and is of a recuperative nature, then a combined system -- one with parallel current compound excitation (TK) -- should be preferable to a field system from the network.

Excitation system with parallel current compound excitation. An advantage of this system is the capability of significant discharge of the shipboard electric power station since the compound excitation channel provides the greater portion of field power. Here, generators must not operate in modes approximating idling. In addition, the compound excitation channel accepts all overloads involving large stator currents. A field system with parallel TK is examined in more detail in

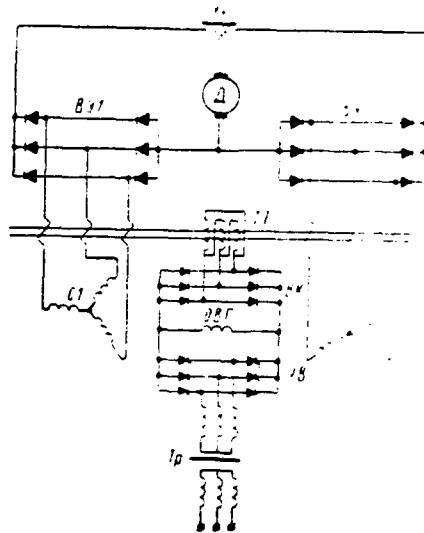


Figure 12.27. Schematic of a Field System With Parallel Current Compound Excitation.

[35] relative to GEU circuits using SG with two three-phase windings on the stator connected in a star and shifted 30 electrical degrees (Figure 12.27).

Each of two stator windings S1 and S2 feeds its own rectifier bridge VU1 and VU2, which on the dc side are connected in parallel via balancing reactor UR. Generator field winding OVG is fed from these bridges via controlled rectifiers UV (fed from the shipboard ac network via matching transformer Ir) and from uncontrolled rectifier VK (fed from current transformer TT). The current transformer has two three-phase sets of primary windings (connected to two generator stator windings); its secondary windings can be connected in a star or triangle.

A special feature of using such a GEU synchronous generator field system is the requirement that the compound excitation channel be set up so that generator controllability is not degraded.

Controlled rectifier UV will not convert to the inverter mode when the load

is shunted by uncontrolled rectifier VK. However, this shortcoming has no real significance since, in normal operation, the inverter mode essentially is not used: the capability to protect the power rectifier by rapid killing of the generator field using the inverter mode, given a low field voltage ratio, is not sufficiently effective.

The absence of a need for an inverter mode, in turn, determines the advisability of using a variable-control circuit. This provides a higher power factor as voltage is regulated and also is simpler since only one of the groups -- anode or cathode -- will comprise controlled diodes [14].

The source feeding the variable-control circuit operates with four current harmonics. It is possible for circuitry for GEU with double-armature GED, each armature fed from a separate generator, to build variable-control circuits so that one SG will have a controlled anode group and the other a controlled cathode group. It is possible to suppress the even harmonics in the source current characteristic in this manner.

Controlled rectifier UV compiled as a three-phase circuit with control angles exceeding  $10^\circ$ , when connected in parallel to compound excitation rectifier VK, operates in the intermittent current mode. In the intervals when the UV is closed, all field winding current passes through the VK, all rectifiers of which are usually open (the six rectifier mode).

If the maximum value of the compound excitation current (TK) is less than field current, then an UV mode change when the compound excitation source (IK) is cut in will lead mainly to a change in UV current magnitude and form. Given parallel operation with the compound excitation source, UV current equal to the difference of the field winding and IK currents will contain the significant variable component corresponding to the form of VK current. Here, field voltage as usual is determined by the control angle and essentially changes with a change in stator current. The process described also insures that SG controllability is maintained.

At control angles greater than  $60^\circ$ , the maximum value of compound excitation current equals field current. Nonetheless, in this event, field determines UV, although its control characteristic changes somewhat when IK is cut in. If the

maximum TK value is unacceptable from the point of view of maintaining controllability, field mainly will be determined by IK and the UV mode will change materially. In such a mode, to be called the "controllability loss mode," UV has little influence. It occurs, in particular, during SG self-excitation as a result of residual magnetization. In this event, field is determined by IK, while UV is closed for almost the entire period.

It is accepted for dual-current GEU that the action of the armature reaction is stipulated by the first harmonic component of stator current  $I_1$ . Its relationship to maximum compound excitation current  $I_{к. макс}$  determines the so-called compound /625 excitation factor (KK) [14]:

$$KK = \frac{I_1}{I_{к. макс}}$$

The armature reaction of a generator running a rectifier has an inductive character. Here, one should consider a steady-state short circuit as the most difficult steady-state mode from the controllability maintenance point of view. If generator controllability is retained here, then this means that it also is retained in all other steady-state modes as well. This condition constrains the KK value.

For a nonsalient-pole SG, in accordance with [35],

$$KK \geq \frac{I_{1 ном}}{I_{в. ном}} \sqrt{\frac{1 + (X_d - X)^2 - 2(X_d - X) \sin \varphi_{ном}}{X_d}},$$

where  $I_{1 ном}$ ,  $I_{в. ном}$  - are the first harmonic component of stator current and field current, respectively, in the nominal mode;  $X_d$ ,  $X$  are commutating resistance and inductive reactance expressed in relative units ( $I_{1 ном}$  are assumed base values and emf is assumed for commutating resistance).

Maintenance of SG controllability (for steady-state short circuit) is sufficient if stator current has only a transient component and has no hypotransient component. It also is sufficient for GEU generator operative transient processes, which flow

relatively slowly, with consideration for the influence of shafting line gyrating masses, armature circuit inductance, and so forth.

One condition to be met for normal system operation is that the VK will be open for any UV voltage. Otherwise, IK will cut out and UV will overload. This condition is met if IK saturation voltage is at least equal to maximum UV voltage which, in turn, determines the magnitude of compound excitation transformer KT (Tr) calculated voltage.

Consequently, a KT needs to be set up in such a way that:

-- in all modes, the maximum compound excitation current value will be less than field current (or so that at UV control angles above 60°, TK will equal field current);

-- IK saturation voltage is greater than UV maximum voltage.

Then, in accordance with [35], generator field is determined by UV (just as when compound excitation is absent), and rotor current distribution between sources will depend on stator current.

System of GED excitation from controlled rectifiers. Thyristor exciters found use in GEU circuitry during GED reversal by means of field current direction change.

Firing angle  $\alpha_\phi$  is established to increase the field current which might be required as an electric motor operates. It can stipulate higher exciter /626 voltage than is necessary to obtain the field current required in the steady-state mode, which creates boosting of the field process. The field current  $i_s$  increase is characterized by the equation

$$E_{d0} \cos \alpha_\phi = i_s r_s + e_s,$$

where  $\alpha_\phi$  is firing angle during field boosting;  $i_s$  and  $r_s$  are field current and field winding resistance, respectively;  $e_s$  is field winding self-induction emf.

The increase in magnitude  $i_s$  will occur (where  $\alpha_\phi = \text{const}$ ) according to

exponential law. When the requisite field current value is attained, the automatic control system increases the control angle, reducing thyristor exciter voltage and the rise in current  $i_a$  ceases. Occurring in the steady-state mode is ratio

$$E_{a0} \cos \alpha_y = I_{a,y} r_a,$$

where  $\alpha_y$  and  $I_{a,y}$  are firing angle and field current, respectively, in the steady-state mode.

Thus, the field current growth process when a rectified exciter is used can occur with boosting subordinating itself to the conventional laws of boosted field, while the thyristor exciter operates in the rectification mode.

A decrease in field current is required in the event motor speed increases above the basic speed (for any mode). This process can occur depending on operating mode, both with and without boosting.

Initially, we will examine the process flow without boosting. We will assume that, when a thyristor exciter operates in the steady-state mode, control angle  $\alpha = 90^\circ$  was established for the purpose of killing field. Exciter voltage will become equal to zero and field current begins to decrease; self-induction emf supporting the passage of current through a rectifier (i. e., emf direction coincides with current direction through the rectifier). Field current change is subordinate to the law:

$$0 = i_a r_a + e_a.$$

Consequently, field current decreases to zero and, as was stipulated, this process flows without boosting.

Now, we will propose that a control angle exceeding  $90^\circ$  has been established, i. e., the thyristor exciter has been transformed to the inverter mode, to decrease field current. Then, thyristor converter negative voltage, which will boost the field current decrease, will turn out to have been introduced into the field winding circuit. This, in turn, will elicit the appearance of great self-induction emf supporting the current through the rectifier, in spite of the opposing converter voltage.

Thus, the thyristor voltage will invert the current, which does not require switchings in the anode--cathode circuit or use of two rectifier sets, as in main current circuits, since self-induction emf, creating positive voltage at the /627 anode, automatically receives the direction required for inversion.

In absolute magnitude, self-induction emf is greater than thyristor exciter emf in the inverter mode. Therefore, it creates at the anodes positive potential relative to the cathode. It follows from this that, given thyristor excitation, transient processes flow more rapidly than in an electrodynamic excitation system, while it is possible to obtain a boosted decrease in field current only by using the exciter inversion mode.

Since a thyristor exciter must suppress feed to a GED field winding with voltage alternating both in magnitude and in sign, two rectifier sets usually are used in a GED field circuit (use for this purpose of switches that can provide current reversal in a field winding will lead to an increase in transient process duration and to a reduction in reliability). The connection of the rectifier sets is antiparallel, with each set connected in a three-phase zero circuit. Such a circuit, selected to decrease the number of rectifier cells in the converter control system (which provides a known economic effect), operates in the following manner.

Each rectifier set has three control cells, just like the ones for main power circuits. The control system is tuned in such a way that, given one field current direction, controlling electrodes receive pulses for one rectifier set given positive half-waves of transformer voltage, and, for the other set, given negative half-waves. Thus, the first set operates in the rectified mode, providing the requisite field current change right up until inversion during a boosted drop in field current, while the second set operates in the inverter mode, which, given the corresponding selection of firing angles, constrains balancing currents. The assumption usually is  $\alpha_1 \geq \beta_1$ , where  $\beta_2 = 180^\circ - \alpha_2$ . To change field current, one set, having operated in the rectified mode, will convert to the inverter mode, while the other will convert to the rectified mode. Then, the second set accomplishes all voltage and field current change modes. Here, maintenance of inequality  $\alpha_2 \geq \beta_1$  is mandatory.

The drawbacks of this rectifier connection circuit include: significant reverse voltage ( $U_{\text{обp}} = 2,44U_{\text{с}}$ ), which requires installation of high-quality rectifiers; pulsation factor is higher than in a Larionov circuit (single-bridge  $\beta = 0.25$ , three-phase bridge  $\beta = 0.057$ ). The second drawback has no real significance for a field circuit, by the way.

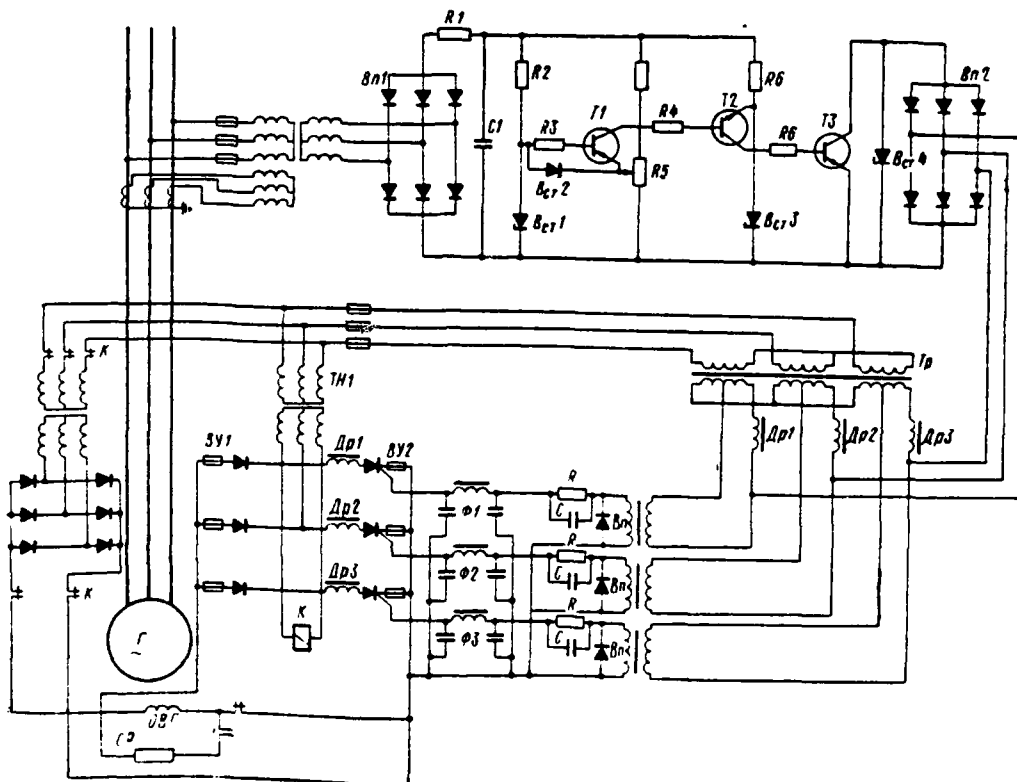


Figure 12.28. Thyristor Excitation System for a Self-Regulated Synchronous Generator.

GEU excitation system during reversal in the main current circuit. We will examine briefly such a field circuit relative to the main current system /628 presented above (see Figure 12.25). Excitation of synchronous generators with self-regulation and use of controlled rectifiers is envisioned in the circuit. From a design standpoint, it will comprise two nodes: initial self-excitation and self-regulation (Figure 12.28).

The initial self-excitation node will comprise rectifier unit VU1 consisting

of uncontrolled rectifiers and voltage transformer TN1. The uncontrolled rectifiers operate for a short time parallel to rectifier unit VU2 consisting of controlled rectifiers. When generator G attains a voltage close to nominal, contactor K trips and VU1 cuts out. The automatic voltage control unit discerns a generator voltage deviation, amplifies it, and changes the control voltage phase in accordance with the deviation. Generator voltage is transformed into constant current voltage, which is used as the base transistor amplifier and is applied to a bridge circuit comprising a stabilitron  $B_{\sigma 1}$  of resistances R2, R4, and R5.

The voltage deviation detected by comparison with stabilitron  $B_{\sigma 1}$  voltage is amplified by the transistors. If the generator voltage increases for any reason, then this causes a decrease in the currents of the base -- initially of transistor T1, then of transistor T2 of the second cascade; the intrinsic resistance of phase-shift transistor T3 increases, which will lead to a rotation of the phase-shift circuit's vector to the lag side. As a result, firing of the controlled rectifiers is delayed, field current decreases, causing a reduction in generator voltage to the assigned value.

A stabilitron with an almost zero temperature factor is used as the standard in the regulator and this insures minimum change in the voltage setting during temperature oscillations. Phase-shift circuit output voltage is supplied via a series resistance to the control electrode.

A rectifier is connected in parallel to the control electrode to eliminate negative voltage in this electrode. A stabilitron is placed between the phase-shift transistor T3 emitter and collector to protect it against surges. The controlled rectifier is three-phase, with thyristors connected only to one arm of the bridge. This makes it possible to decrease the number of thyristors by a factor of 2 and somewhat simplify the control device, both due to the decrease in the number of thyristors and to the elimination of the requirement for a specific width of the negative pulse.

Chokes Dr1--Dr3 are connected between the transformer's secondary winding and the semiconductor rectifiers to decrease the rate of current rise across the transistors. Otherwise, given a high rate exceeding  $(3 - 10) \times 10^6$  A/sec, an overload of sections of the silicon wafer located near the control electrode can



in each rectifier's circuit by high-speed fuses. Overall, this field circuit provides high stable generator voltage, especially important for power take-off to auxiliary bus bars.

GED field is separate from the ac network via a rectifier (Figure 12.29) and, just like a synchronous generator, from the three-phase bridge circuit, with rectifier unit VU1 consisting of controlled rectifiers installed in one arm of the bridge and, in the other arm, VU2 consisting of uncontrolled rectifiers. A system with half-wave magnetic amplifiers is used for thyristor control. This GED field circuit's operating principle consists of the fact that formation of a control pulse and regulation of its phase are accomplished in one element -- a saturable reactor, the magnetic circuit of which is made of material with hysteresis loops close to rectangular. The reactor's moment of saturation determines pulse phase and will depend on the core's magnetic state. Half-wave amplifiers here also accomplish the function of adder.

Saturable reactors DN1--DN3 have one operating winding (OP) and four control windings: master (OZ), bias (OSm), main circuit current feedback (OTd), and motor field current feedback (OTv). Maintenance of fixed GED field current is achieved in this manner during ac network voltage oscillations and main circuit current constraint.

§ 12.10 Dual-Current Electrical Propulsion Plant  
With Single Electrical Power Plant  
(With Power Take-Off for Shipboard Network Consumers)

General assumptions. Several very simple circuitry solutions using both controlled and uncontrolled rectifiers are proposed to provide simultaneous electric power feed to GEU and shipboard network consumers. Here, there is a requirement to envisage a capability for a broad range of voltage regulation at the GED armature, while voltage at the shipboard ac network bus bars must remain unchanged.

We will examine several circuits for such GEU, which are of practical interest in project planning of electric ships with power take-off from electrical propulsion bus bars (ShED) for shipboard network consumers.

Circuit with power take-off from ShED for a three-shaft propulsion plant.

A variant of such a circuit where the main current circuit comprises three loops is depicted in Figure 12.30.

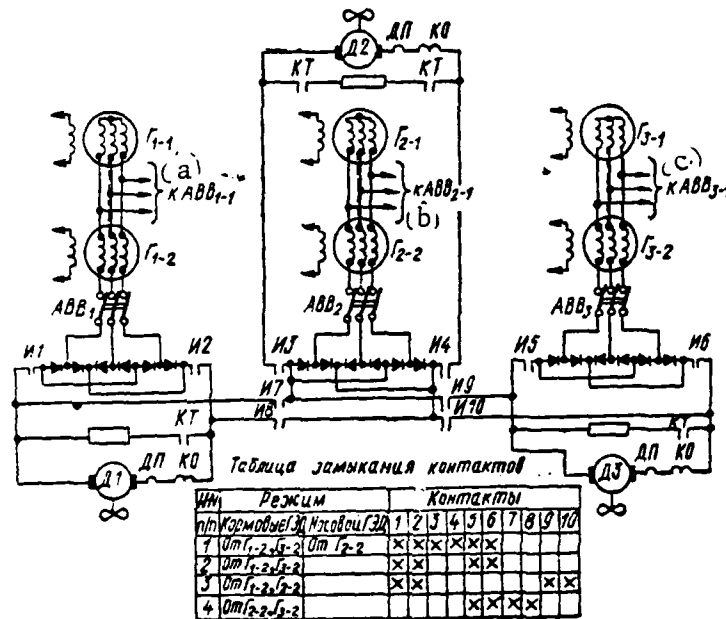


Figure 12.30. Circuit for a Dual-Current GEU With Paired Synchronous Generators. a--To AVV<sub>1-1</sub>; b--To AVV<sub>2-1</sub>; c--To AVV<sub>3-1</sub>.

Contact Closing Table

No.	Mode		Contacts									
	Aft GED	Fore GED	1	2	3	4	5	6	7	8	9	10
1	From G <sub>1-2</sub> , G <sub>3-2</sub>	From G <sub>2-2</sub>	х	х	х	х	х	х				
2	From G <sub>1-2</sub> , G <sub>3-2</sub>						х	х				
3	From G <sub>1-2</sub> , G <sub>2-2</sub>		х	х							х	х
4	From G <sub>2-2</sub> , G <sub>3-2</sub>						х	х	х	х		

Main current circuit basic modes.

I. Normal (maneuvering-towing) mode -- six generators run three GED (two generators per GED):

$$G_{1-1} + G_{1-2} \text{ to D1; } G_{2-1} + G_{2-2} \text{ to D2; } G_{3-1} + G_{3-2} \text{ to D3}$$

II. Emergency-rescue mode (two generators run each aft GED):

$$G_{1-1} + G_{1-2} \text{ to D1; } G_{3-1} + G_{3-2} \text{ to D3}$$

Here, the power of generators  $G_{2-1}$ ,  $G_{2-2}$  is used for electric drive /632 (direct and alternating current) of special and rescue devices (pump and monitor units, fire and loading pumps, and so on).

III. Emergency mode:

(a)  $G_{1-1} + G_{1-2}$  to D1;  $G_{2-1} + G_{2-2}$  to D3

(b)  $G_{2-1} + G_{2-2}$  to D1;  $G_{3-1} + G_{3-2}$  to D3

GED braking and reversing. We will examine GED reversal and braking for an automatic control system variant (Figure 12.31) with a transverse field EMU analogous to the circuit used on "Lenin"-class electric ships [50].

As the control station PU lever is moved from forward to reverse, generator voltage is reduced and GED counter emf begins to exceed generator (rectifier unit) voltage. In addition, rectifiers hinder the passage of current in the opposite direction and, for a short time, current in the main circuit will equal zero. When the potentiometric rheostat lever PUI occupies the position in which the contactor KT1 coil circuit closes, its N. O. main contact in braking resistance  $R_r$  circuit and the N. O. blocking contact in the contactor KT2 coil circuit trip and close. The latter, tripping with a slight time delay, closes its N. O. /633 main contact and shunts a portion of  $R_r$ .

Current will begin to flow anew at the moment resistance  $R_r$  is connected

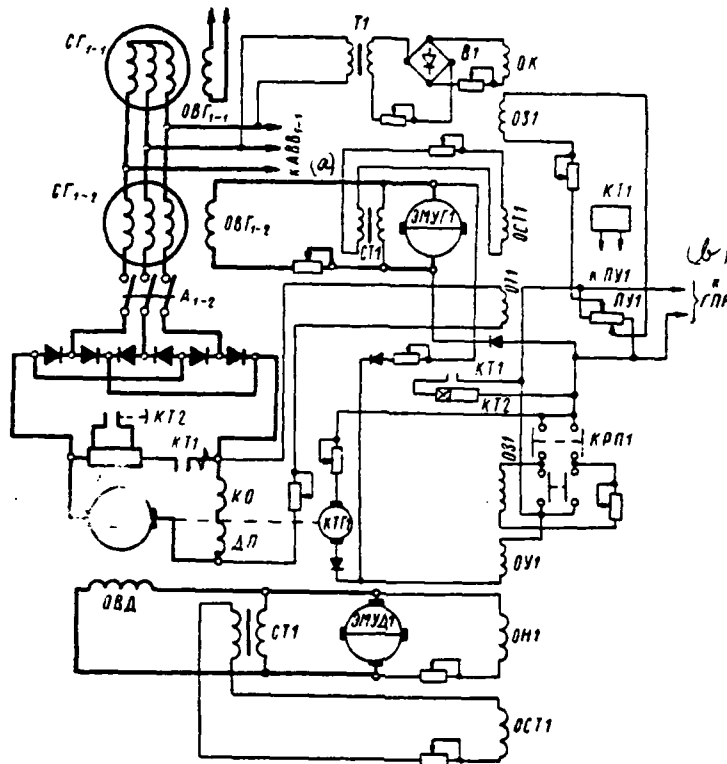


Figure 12.31. Braking and Reversing Circuit With a Transverse Field EMU.  
 a--To AVV<sub>1-1</sub>; b--To GPN.

in the main circuit, but it is of the opposite direction and the GED will convert to the dynamic braking mode. When KT2 trips and a portion of resistance  $R_r$  is shunted, GED braking is established higher than the lower threshold when resistance  $R_r$  is connected fully. During the entire dynamic braking period, current in winding OUI will not flow since a rectifier impedes it. If it is absent, GED braking would not be feasible since, given a change in the direction of the current in the main circuit and absence of master winding OZ1 EMUG1 magnetic flux, winding OT1 would create magnetic flux, decreasing winding OK EMUG1 ampere-turns, as a result of which the generator again would begin to feed the GED.

When the control station PUI lever passes through the zero point, the /634 direction of current in winding OZ1 EMUG1 is changed by means of the reversing switch. Here, the direction of the main circuit current changes again. Recuperative braking would correspond to such a position. However, the rectifier unit does

not permit passage of power (GED/Ya) to the current generator. Therefore, final GED stoppage will occur during countercurrent flow braking. At the initial moment, main circuit current and counter emf coincide in direction. However, the GED already has braked itself partially and its counter emf has decreased, as a result of which the current inrush must not be great.

A rise in winding magnetic flux due to an increase in main circuit current will occur with a simultaneous rise in winding OZ1 EMUG1 magnetic flux as the PU1 lever is transposed to the "reverse" position. And, since these winding OZ1 and OT1 magnetic fluxes are opposites, synchronous generator voltage will not be great and, in a special case, when magnetic fluxes are equal, it will equal zero. Due to the slight resistance in the main circuit, the current in it all the same will be of sufficient magnitude so that the GED finally will brake itself and then will begin to rotate in the opposite direction. If GED speed was unable to decrease materially during dynamic braking (for example, during a too rapid transposition of the PU lever from the "full ahead" to "full astern" position), then the current inrush will turn out to be considerable. However, in this event, the automatic control system (SAR) will strive to maintain the current magnitude within safe limits.

During the countercurrent flow braking period, EMUG1 direction mainly is determined by winding OZ1 and OT1 magnetic fluxes, while the winding OT1 magnetic flux increases significantly, exceeding that of winding OZ1, amplifying winding OK1 magnetic flux and reducing the output voltage of the synchronous generators (in the rectifier unit) and, consequently, main circuit current as well.

Thus, in the dual-current circuit examined (with synchronous generators connected in series), GEU remote control occurs during starting, braking, and reversal, with primary motor (PD) constant rotational speed and without GED deviation from the generator. Main synchronous generator PD starting requires that exciter sets be started initially in order to place winding OK EMUG1 in operation.

GED reversal occurs during a small time interval, while in an ac GEU, it is a rather lengthy process since it includes time for receipt of commands via the engine room telegraph, PD speed regulation, a delay in the "Wait" position until current decay in the main circuit, and so on.

The circuit also will comprise GED protection against runaway with use of monitoring tachogenerator KTG1.

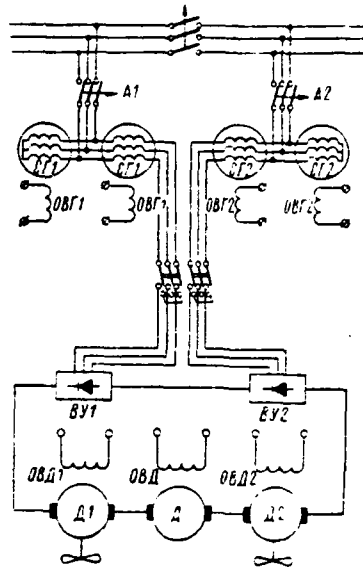


Figure 12.32. Fixed Current GEU System With Rectifier Units in the Main Circuit.

Circuit variant with power take-off for a fixed current system. Systems with power take-off also can be built on the fixed current principle (Figure 12.32), when production-type electric motors D (soil pumps and steering devices on /635 dredgers, fire pumps, electric motors for trawl and deep-water pumps, and the like) are connected to the main current loop along with GED (D1, D2).

Use of such systems for dredgers, hydrographic vessels, rescue craft, fireboats, trawlers, and so on can be very promising. The capability for recuperative electric motor braking in them is ruled out, which, on the one hand, extends the time transient processes occur (and vessel maneuvering modes are drawn out accordingly) and, on the other, does protect primary motors against runaway during reversals.

Special features of a power take-off and automatic control given a two-loop GEU circuit. We will examine a variant of a GEU for a dual-current system with uncontrolled rectifiers and connection of double-armature GED in a two-loop circuit in the basic mode [69]. Rectification circuit selection will occur following

consideration of best generator and rectifier use, as well as receipt of the appropriate constant current quality.

In such a circuit, 12-phase rectification is accomplished in the following way. Each paired generator, comprising two stators and two rotors, has a separate three-phase winding in the stator and a separate field winding. The rotors of both halves of the generator are located on one shaft with a 30 electrical degree shift. Each stator winding is connected to its own three-phase rectifier bridge and both bridges on the ac side are connected in series.

The main current schematic for one side's loop is shown in Figure 12.33a. As follows from the figure, circuit breakers A1 and A2 are cut in and A3 and A4 cut out in modes where only the GED are operated. The circuit insures addition of two voltages having sextuple pulsations and shifted 30 electrical degrees relative to each other. Rectified voltage, given VU1 and VU2 series connection, corresponds to a 12-phase rectification circuit. The voltage pulsation factor of the 12th harmonic  $(K_U = \frac{U_{\text{max}12}}{U_d})$  equals 4% at commutation angles up to 40°. Here, the 1/637 current pulsation factor  $(K_I = \frac{I_{\text{max}12}}{I_d})$  considering full armature circuit impedance equals 1% [69].

In low speed modes when GED voltage and rotational speed are less than nominal (which considerably facilitates commutation), the circuit makes it possible to convert to six-phase rectification from one stator, with the second stator disconnected from the GED feed circuit for operation of the shipboard network. Here, circuit breakers A1 and A3 are cut in while A2 and A4 are cut out (see Figure 12.33a). The field windings of the stator running auxiliaries is fed from a separate self-excitation system. Given 400 V shipboard network voltage, the magnitude of the voltage in the GED armature (without considering commutational voltage drop and voltage drop in the cable path) will be 1,080 V. This voltage ratio makes it possible to use full generator power both when operating a GED and the shipboard network.

The circuit we are examining is distinguished by several advantages compared, for example, with circuits using a generator with 3-phase windings in the stator placed with a 30 electrical degree shift with 12-phase rectification. Since both

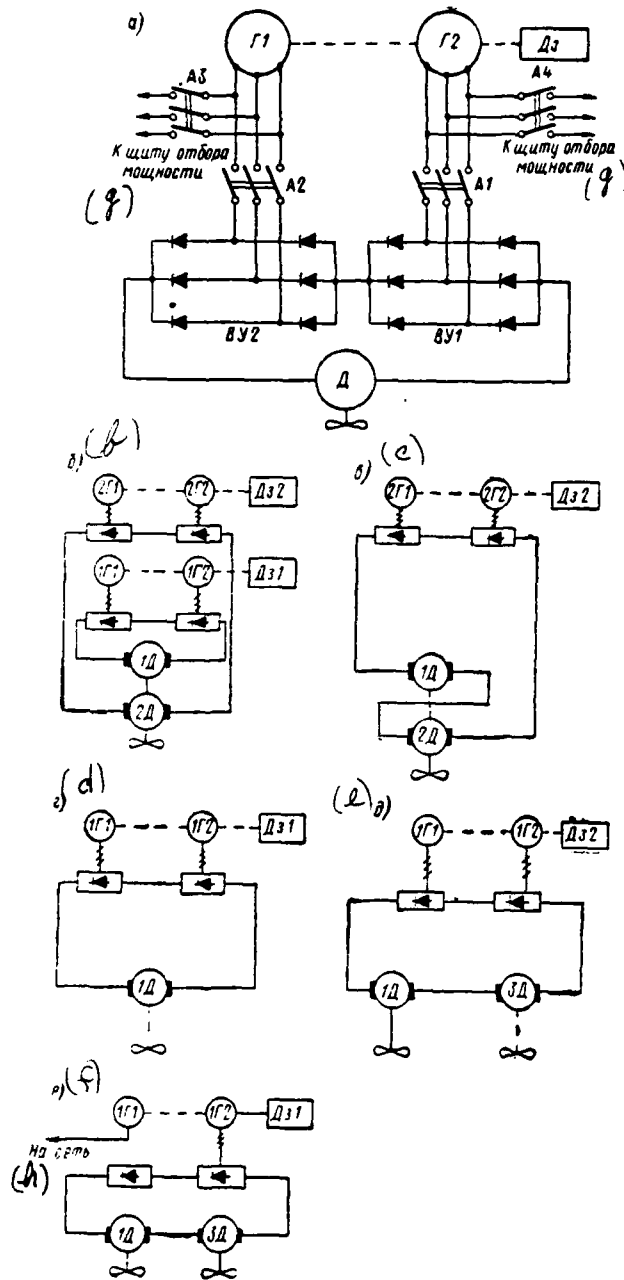


Figure 12.33. Circuits of One Side of a Double-Loop Circuit for a Dual-Current GEU With Power Take-Off: a--One loop's main current circuit; b--Circuit for one side's GEU basic mode; c, d--One generator's operating modes to two armatures of its own side's GED and to its own GED's armature, respectively; e--Circuit for the operating mode where one generator runs two GED armatures of different sides; f--Circuit for running two GED armatures of different sides; g--To the power take-off panel; h--To the network.

stators here have a common field winding, this precludes power take-off for shipboard consumers. The circuit with paired synchronous generators depicted in Figure 12.29 provides the capability to provide simultaneous GED and shipboard consumer feed. But, its shortcomings should be pointed out:

1. Since a circuit with paired generators provides six-phase rectification, then high-power GED require connection of a smoothing choke on the dc side;
2. Voltage distortions arising as a result of a generator running a rectified bridge affect the shipboard network. There may be a requirement to use powerful filters for high capacities;
3. The electrical propulsion circuit and the shipboard network are connected electrically and all transient processes in one system influence the operation of the other, which greatly complicates the regulation and protection process.

Based on the analysis done, it is possible to come to a conclusion as to advisability of using systems with paired synchronous generators, especially evident for GEU, which are tasked to operate in many modes for a long period of time.

Main current circuit operating modes. Three-pole circuit breakers for protection against short circuits and connection of generators either to a rectifier unit (when operating the GED) or to the power take-off panel (when operating the network and large consumers) are envisioned on the ac side. Operation of the shipboard network (with one or two stators) is possible both jointly with GED feed (at low speeds) or independently from any generator that is not feeding GED bus bars, except the circuit's basic operating mode (Figure 12.33b), which corresponds to nominal power. In this mode, each diesel generator (paired generator) runs /638 its own double-armature GED armature.

This circuit also is capable of other operating modes. A circuit in which one generator runs two armatures of a GED on its side connected in series is depicted in Figure 12.32c, while a circuit in which one generator runs its own GED armature (the second armature is cut out here) is shown in Figure 12.32d. A circuit where one generator runs two armatures of series-connected GED of different sides is presented in Figure 12.32e. The mode in which one generator stator runs two armatures of series-connected GED of different sides (Figure 12.32f) also is of interest. Here, the generator's second stator runs the power take-off, while the rectifier bridge of the generator's nonoperating stator is not cut out, but operates in the "transition mode."

Another possibility is an approach in which one stator, via rectifiers, feeds dc consumers with voltage regulation, while a second stator feeds dc consumers. Such a circuit comprises cam selector switches (GIP), which will cut power circuit and field circuit switches in and out. Each side has its own GIP. GED starting, stopping, reversing, and rotational speed regulation are accomplished from a control station. Diesel rotational speed regulation is envisaged in a range of 1 : 2 in four stages. In this case, the change in GED field flux also will occur in four stages at the identical control station positions used for diesel rotational speed change.

In this GEU circuit, power constancy at diesel underway rotational speed is maintained at different settings corresponding to safe diesel power for a given speed. Settings are provided from the control station.

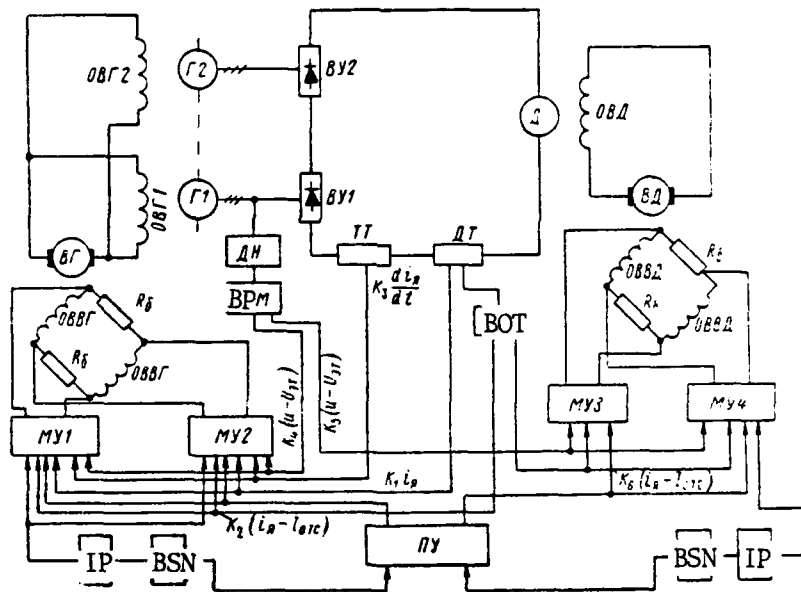


Figure 12.34. Functional Schematic of Dual-Current GEU Automatic Control. BPM--Power maintenance unit; БОТ--Current constraint unit; BSN--Voltage stabilization unit; IP--Feed source.

We will examine a field system variant for a GEU with rotating exciters and magnetic amplifiers as pilot exciters. Separate field windings of both stators OVG1 and OVG2 are connected in parallel and are fed from one exciter VG (Figure

12.34). The GED exterior armature's field winding (OVD) is fed by its own exciter VD. Electromagnetic exciter units comprising three series-produced machines (electric induction drive motor and dc machines (motor exciter (VD) and generator exciter (VG)) are used as exciters. Each loop has its own exciter unit. The GED is reversed by a change in the polarity of its field flux, which is accomplished by a generator pilot exciter reversing circuit, also built as reversible. This makes it possible to accomplish generator field deboosting and thereby provide protection against current bumps in the main circuit and diesel overloads in the propeller-ice interaction mode. This is a reserve measure since relatively high-speed generator demagnetization can occur due to the strong action of synchronous generator armature reaction.

Generator and GED pilot excitation systems (see Figure 12.34) are built /639 from a reversible bridge circuit in which exciter field windings (OVVG and OVVD) will be divided into two half-windings connected to opposing bridge arms; ballast resistances ( $R_0$ ) are connected to the other two bridge arms. The winding OVVG bridge is fed by two three-phase magnetic amplifiers MU1 and MU2 and, correspondingly, winding OVVD bridge by MU3 and MU4.

The following are advantages of this bridge circuit variant: reduction in overall dimensions, weight, and expenditure of exciter copper due to elimination of one field winding; a decrease in the time constant and improvement in dynamic characteristics in connection with the absence of the effect of field winding self-induction.

System for automatic regulation of one side (see Figure 12.34) insures: maintenance of GEU power constancy when vessel operating conditions change -- from the moored to the running in open water modes; restriction on moment of stoppage when the propeller jams; creation of the requisite torque on the propeller in the "ice scarifying" mode; protection of the GEU against extraordinary rotational speed during propeller blade exposure or shear; protection of GEU elements against overloads; satisfactory flow of dynamic processes during GED starts and /640 reversals. In this connection, information on system parameter values is provided:

-- master signals from the control station PU;

-- by a signal proportional to GED current  $K_1 i_n$ , with voltage at current sensor DT output playing this role.

The sensor is an elementary magnetic amplifier; a main current bus bar will serve as its control winding. It provides at output a signal of sufficient power and galvanic isolation of control system elements and the main current circuit, which is under a high potential;

-- by a signal from synchronous generator voltage  $K_4(u-U_{gr})$ . A three-phase transformer, which is connected to the control circuit via a rectifier bridge and ripple filter, is used as the sensor of this voltage (DN);

-- by a signal for the current rate change in the main circuit  $K_3 \frac{di_a}{dt}$ . Transformer  $\Pi$  is used to provide this circuit's current unity feedback.

Power constancy is maintained by means of automatic regulation of GED magnetic flux. Powerful generator armature reaction and GED current feedback ( $K_1 i_a$ ), acting on its field provide a steeply-dipping external characteristic. A decrease in load is accompanied by an increase in generator voltage and coupling  $K_5(u - U_{gr})$  weakens GED magnetic flux. Current during reversal in the dynamic braking mode is constrained by main circuit current coupling with cut-off  $K_6(i_a - I_{ore})$ , which weakens GED magnetic flux. A coupling proportional to main circuit current change rate  $K_8 \frac{di_a}{dt}$  and main circuit current coupling with cut-off  $K_2(i_a - I_{ore})$  affecting the generator and deboosting its field are used to reduce current bumps in the GEU. Signal  $K_4(u - U_{gr})$  and constraint on the effect of coupling  $K_5(u - U_{gr})$ , which also weakens the GED magnetic flux, provide protection against GED runaway during propellor exposure or shear.

All automatic control system feedbacks are added in magnetic amplifiers MU1 and MU2 of the generator pilot excitation system and MU3, MU4 in the GED pilot excitation system (see Figure 12.34).

#### § 12.11 Foreign Know-How in Building Dual-Current Electrical Propulsion Plants

Several publications covering project planning developments and patents describing operational electric ships using dual-current systems have appeared in the foreign press in the last several years.

Thus, "Clermont," the first experimental pusher tug with a gas /641 turboelectric alternating-direct current GEU, was built in 1965 in the USA. This

AD-A114 423

FOREIGN TECHNOLOGY DIV WRIGHT-PATTERSON AFB OH  
FUNDAMENTALS OF ELECTRICAL PROPULSION PLANT DESIGN. (U)  
APR 82 N A KUZNETSOV, P V KUROPATKIN  
FTD-ID(RS)T-1388-80

F/G 21/3

UNCLASSIFIED

NL

9 of 9  
004  
0004



END  
DATE  
FILMED  
6-82  
DTIC

choice was dictated by the vessel's small dimensions since the tug was intended for transporting barges with missiles on the canal system and the Mississippi River, as well as serving as a fireboat. Its basic dimensions (in meters) are: length 20, beam 6, depth 3, and draft 2.1 [86].

This GEU is a two-shaft plant comprising a 1,000 hp gas turbine placing series-connected 334 kW, 445 V synchronous generators and two dc GED into rotation at 1,800 rpm. Each GED, via 5.15 : 1 step-down reduction gears, runs its own screw, produces 424 hp at 600 V, 1,200 rpm, and is connected with the generators via two 334 kW, 445/600 V silicon rectifier units in one rack. A 7,500 l/min fire pump can be connected with the aid of an electromagnetic clutch to the main turbogenerator. The plant is controlled from the pilot house. The plant is fully automated and can be operated without maintenance.

Various system types can be obtained in the alternating-direct current GEU, using control principles identical to those used for a dc GEU: conventional generator--motor systems, power constancy systems, and fixed current.

Since primary motor rotational speed in such systems is constant, it is possible to use mounted ac generators in the shipboard network, which makes it possible to create a single power system.

Among other experimental developments, a patent for a fixed current set (England) is noteworthy. It will comprise an ac diesel generator, rectifier units, propulsion and other actuating dc electric motors connected in series in a common loop, and shipboard network synchronous generators (mounted on the diesel generator sets).

Experiments with the use of controlled rectifier units comprising thyristors also are worthy of mention. Such systems make it possible to use the power of the generators both for vessel movement and to feed shipboard consumers.

The GEU circuit with thyristor control of the dc GED aboard the new West German trawler "Tiko-1" is shown in Figure 12.35. Two 1,000 kW controlled power units are connected to the bus bars of a single shipboard ac electric power station. The thyristors operate as a three-phase bridge circuit with seven parallel branches in each phase.

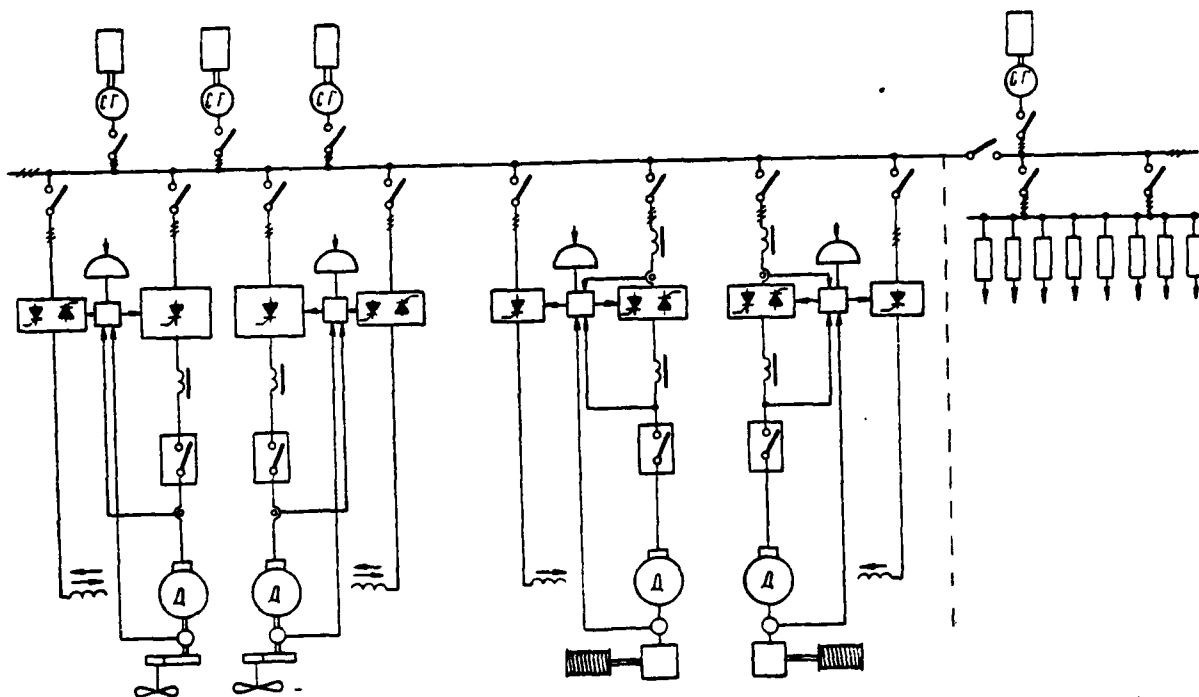


Figure 12.35. GEU Circuit Aboard the West German-Built Trawler "Tiko-1."

The control and regulation circuit also comprises thyristors. It constrains armature current, weakens magnetic flux, changes rotational speed, and constrains recuperative power, i. e., it functions both as a power unit, changing the magnitude of output voltage, and as a GED field circuit.

The GED is reversed with a contact-free field polarity switch with the /644 aid of two anticonnected thyristor bridges. During the reversal process, the rectifier unit turns out to be in the countercurrent flow mode for a short period of time since armature current direction does not change. Recuperation power is constrained by weakening GED magnetic flux.

Power unit thyristor load current is decreased by a factor of 2 automatically if a thyristor or fuse breaks down or if there is a rise in cooling air temperature. A high-speed current switch is used to protect the constant current circuit. As tests showed, no mutual GED influence was observed.



1. Agafonov N. A. "Design of the Electrical Propulsion of the Icebreaker 'Lenin' (with an atomic power plant)". Trudy NTO Sudproma, 1959, Vol. 8, Issue 6.
2. Alekseyev A. Ye. Iyagovyye elektricheskiye mashiny i preobrazovateli ("Electric Traction Machines and Transformers"). Leningrad, Energiya, 1967.
3. Anko A. Matematika dlya elektro- i radioinzhenerov ("Mathematics for Electrical and Radio Engineers"). Moscow, Nauka, 1965.
4. Antonov S. I., Itskovich Yu. L. Dizel'-elektrokhody ("Diesel-Electric Powered Ships"). Moscow, Transport, 1964.
5. Basharin A. V., Golubev F. N., Kepperman V. G. Primery raschetov avtomatizirovannogo elektroprivoda ("Examples of Computations of an Automated Electric Drive"). Leningrad, Energiya, 1964.
6. Basharin A. V. Raschet dinamiki i sintez nelineynykh sistem upravleniya ("Computation of the Dynamic and Synthesis of Non-linear Control Systems"). Moscow-Leningrad, Gosenergoizdat, 1960.
7. Bernshteyn I. Ya. Tiristornyye preobrazovateli chastoty bez zvena postoyannogo toka ("Thyristor Frequency Converters Without a Direct Current Link"). Moscow, Energiya, 1968.
8. Bulgakov A. A. Chastotnoe upravleniye asinkhronnymi elektrodvigatelyami ("Frequency Control of Electric Induction Engines"). Moscow, Nauka, 1966.
9. Vavilov A. A. Chastotnyye metody rascheta nelineynykh sistem ("Frequency Methods for Computation of Non-linear Systems"). Leningrad, Energiya, 1970.
10. Vasil'yev D. V., Mikhaylov V. A., Nornevskiy B. I. Avtomatizatsiya sudovykh ustanovok ("Automation of Shipboard Plants"). Leningrad, Sudostroyeniye, 1965.
11. Venikov V. A. Primeneniye teorii podobiya i fizicheskogo modelirovaniya v elektrotekhnike ("Use of the Similarity Theory and Physical Modelling in Electrical Engineering"). Moscow-Leningrad, Gosenergoizdat, 1949.
12. Veretennikov L. P., Potapkin A. I., Raimov. Modelirovaniye, vychislitel'naya tekhnika i perekhodnyye protsessy v sudovykh elektroenergeticheskikh sistemakh ("Modelling, Computers, and Transient Processes in Shipboard Electrical Power Systems"). Leningrad, Sudostroyeniye, 1964.
13. Voronov A. A. Osnova upravleniya ("Foundation of Control"). Moscow, Energiya, 1965.

14. Glebov I. A. Sistemy vozbuzhdeniya sinkhronnykh generatorov s upravlyayemyimi preobrazovatelyami ("Excitation Systems for Synchronous Generators with Control Converters"). Moscow-Leningrad, Izd-vo AN SSSR, 1960.
15. Glinternik S. R. Elektromagnitnyye protsessy i rezhimy raboty moshchnykh staticheskikh preobrazovateley ("Electromagnetic Processes and Operating Modes of Powerful Static Converters"). Moscow, Nauka, 1968.
16. Yemel'yanov V. I. "Three-Phase Bridge Circuit". Izvestiya NIPI, 1961, No. 8.
17. Yermolin N. P. Perekhodnyye protsessy v mashinakh postoyannogo toka ("Transient Processes in Direct Current Machinery"). Moscow-Leningrad, Gosenergoizdat, 1951.
18. Kazovskiy Ye. Ya. Perekhodnyye protsessy v elektricheskikh mashinakh peremennogo toka ("Transient Processes in Alternating Current Electric Machinery"). Moscow-Leningrad, Izd-vo AN SSSR, 1962.
19. Kas'yanov V. T. "Computation of Processes for Regulation of Electrical Machinery Magnetic Fields". Vestnik elektropromyshlennosti, 1964, No. 3-5.
20. Kas'yanov V. T. Raschety manevrennykh kharakteristik sudov s elektricheskim grebnym privodom ("Computations of the Maneuvering Characteristics of Ships with Electric Propellor Drive"). Leningrad, Sudopromgiz, 1949 (Trudy TsNII imeni A. N. Krylov, Issue 52).
21. Kas'yanov V. T., Malyshev I. F. "Determination of the Dimensions [646] and Weight of Electrical Machinery for Propellor Drives". Sudostroyeniye, 1951, No. 6.
22. Kogan B. Ya. Elektronnyye modeliruyushchiye ustroystva i ikh primeneniye dlya issledovaniya sistem avtomaticheskogo regulirovaniya ("Electronic Modelling Devices and Their Use in Studying Automatic Control Systems"). Fizmatgiz, 1959.
23. Kostenko M. P. Elektricheskiye mashiny. Spetsial'naya chast' ("Electrical Machinery. Special Part"). Moscow-Leningrad, Gosenergoizdat, 1949.
24. Kostenko M. P. "Electrodynamic Model for Studying Stability". Elektrichestvo, 1950, No. 9.
25. Kostenko M. P. Elektricheskiye mashiny, ch. 1-2 ("Electrical Machinery, Parts 1-2"). Moscow, Energiya, 1964-1965.
26. Kuznetsov N. A. "Electric Propulsion on Rescue Vessels". Trudy NTO Sudproma, 1959, Vol. 8, Issue 5.
27. Kuropatkin P. V. Avtomatizatsiya grebnykh elektricheskikh ustanovok ("Automation of Electrical Propulsion Plants"). Moscow, Transport, 1964.

28. Kuropatkin P. V. Kompleksnoye regulirovaniye grebnykh ustanovok postoyannogo toka ("Integrated Control of Direct Current Electrical Propulsion Plants"). Leningrad, Sudostroyeniye, 1971.

29. Lebedev A. N. Primeneniye analogovykh vychislitel'nykh ustroystv v sudovykh sistemakh avtomaticheskogo upravleniya ("Use of Analog Computers in Shipboard Automatic Control Systems"). Leningrad, Sudostroyeniye, 1970.

30. Levin A. M. Issledovaniye 12-faznogo preobrazovatelya glavnoy tsepi grebnoy elektricheskoy ustanovki ledokola ("Study of a 12-Phase Converter in an Icebreaker Electrical Propulsion Plant Main Circuit"). Author's Summary of his dissertation for the Candidate of Technical Sciences degree. Leningrad, 1970 (LVIMU imeni S. O. Makarov).

31. Levin A. M., Leykin V. S. Raschetnaya skhema dlya elektromagnitnykh protsessov v 12-faznoy skheme preobrazovaniya avtonomnogo istochnika pitaniya ("Design Circuit for the Electromagnetic Processes in a 12-Phase Automatic Feed Source Converter Circuit"). In the collection Voprosy avtomatizatsii i nadezhnosti elektroenergeticheskikh i elektrogrebnykh sudovykh ustanovok ("Problems of Automation and the Reliability of Shipboard Electrical Power and Propulsion Plants"). Leningrad, Sudostroyeniye, 1967 (GTO Sudproma. Materialy po obmenu opytom, Issue 95).

32. Levin A. M., Leykin V. S. "Problems in Computation of the Control Characteristics of Converters in SG--V--D Systems". Trudy NOT Sudproma, 1968, Issue 114.

33. Levin M. I. Avtomatizatsiya sudovykh dizel'nykh ustanovok ("Automation of Shipboard Diesel Plants"). Leningrad, Sudostroyeniye, 1969.

34. Leykin V. S., Levin A. M., Rodshteyn L. A. "Relative Analysis of Converters in Alternating-Direct Current Electrical Propulsion Plants". Sudostroyeniye, 1969, No. 9.

35. Leykin V. S., Semenov M. A. Sistemy возбуждениya sinkhronnogo generatora grebnoy elektricheskoy ustanovki po skheme sinkhronnyy generator-vypryamitel'-dvigatel' postoyannogo toka ("Excitation Systems of an Electrical Propulsion Plant Synchronous Generator Based on a Synchronous Generator-Rectifier-Direct Current Motor"). In the collection Voprosy avtomatiki i nadezhnosti elektroenergeticheskikh i elektrogrebnykh sudovykh ustanovok ("Problems of Automation and Reliability of Electrical Power and Propulsion Plants"). Leningrad, Sudostroyeniye, 1967 (NTO Sudproma. Materialy po obmenu opytom, Issue 95).

36. Lyuter R. A. "Turning Moments of a Synchronous Machine in an Asynchronous Mode". Vestnik elektropromyshlennosti, 1948, No. 10.

37. Lyuter R. A. "Consideration of the Influence of Higher Harmonics and the Current Curve on Operation of Synchronous Generators Feeding Mercury Rectifiers". Elektrosila, 1948, No. 5.

38. Malishevskiy V. Ye. "Special Features of the Operation of Icebreaker Electrical Propulsion Plants as the Propellor Strikes the Ice During Jams". Sudostroyeniye, 1961, No. 5.

39. Meyerov M. V. Sistemy mnogosvyaznogo regulirovaniya ("Multiconnection Control Systems"). Moscow, Nauka, 1965.

40. Mezin Ye. K. Sudovyye elektricheskiye mashiny ("Shipboard Electrical Machinery"). Moscow-Leningrad, Transport, 1964.

41. Meleshkin G. A. Sudovyye sinkhronnyye generatory ("Shipboard Synchronous Generators"). Leningrad, Sudpromgiz, 1962.

42. Merriem [Merriam] K. Teoriya optimizatsii i raschet sistem upravleniya s obratnoy svyaz'yu ("Optimization Theory and Computation of Control Systems with Feedback"). Moscow, Mir, 1967.

43. Miniovich I. Ya. "Approximate Formulas for Determination of the Maximum Values of Torque and Braking Thrust of a Propellor in Reverse". Sudostroyeniye, 1947, No. 3.

44. Mikhaylov V. A., Rukavishnikov S. B., Freydzon I. R. Elektrodvizheniye sudov i elektroprivod sudovykh mekhanizmov ("Electric Propulsion of Ships and Electric Drive of Shipboard Mechanisms"). Leningrad, Sudostroyeniye, 1965.

45. Morozov D. P., Boytsov Yu. A. "Generalized Methodology for Study [647] of Transient Processes in Electric Drive Circuits". Sudostroyeniye, 1957, No. 7.

46. Novosel'tsev Ya. V., Lebedev A. N. Schetno-reshayushchiye ustroystva ("Computers"). Moscow, Mashgiz, 1954.

47. Osnovy avtomaticheskogo regulirovaniya ("Fundamentals of Automatic Control"). Vol. 2. Edited by V. V. Solodovnikov. Moscow, Mashgiz, 1959.

48. Polonskiy V. I. "Electrical Propulsion Plants". Leningrad, Morskoy transport, 1958.

49. Polonskiy V. I. Grebnyye elektricheskiye ustanovki morskikh sudov ("Maritime Vessel Electrical Propulsion Plants"). Moscow, Transport, 1968.

50. Polonskiy V. I., Khaykin A. B. Elektrohody i perspektivy ikh razvitiya ("Electric Ships and Perspectives for Their Development"). Leningrad, Sudpromgiz, 1960.

51. Poluprovodnikovyye vypryamiteli ("Semiconductor Rectifiers"). Edited by F. I. Kovalev and G. P. Mostkovoy. Moscow, Energiya, 1967.

52. Popov Ye. P., Pal'tov I. P. Priblizhennyye metody issledovaniya nelineynykh avtomaticheskikh sistem ("Approximate Methods of Studying Non-linear Automated Systems"). Moscow, Fizmatgiz, 1960.

53. Posse A. V. "Substantiation for Replacement of a Rectifier with the Equivalent Generator for Computation of Transient Processes". Izvestiya AN SSSR Energetika i transport, 1965, <sup>8th</sup> No. 4.

54. Ravinskiy P. A., Tikan V. A. Ventil'nyye preobrazovateli chastoty bez zvena postoyannogo toka ("Frequency Converters Without the Direct Current Section"). Moscow, Nauka, 1965.

55. Rozenblat M. A. Magnitnyye elementy avtomatiki i vychislitel'noy tekhniki ("Automation and Computer Magnetic Elements"). Moscow, Nauka, 1966.

56. Rukavishnikov S. B. Avtomatizirovannyye grebnyye elektricheskkiye ustanovki ("Automated Electrical Propulsion Plants"). Leningrad, Sudostroyeniye, 1968.

57. Ryudenberg. Perekhodnyye protsessy v elektroenergeticheskikh sistemakh ("Transient Processes in Electrical Power Systems"). Moscow, IL, 1955.

58. Saburov F. F. Issledovanie zamknutykh sistem avtomaticheskogo regulirovaniya dvigatel'-generatornoy ustanovki lokomotiva ("Study of Closed Automated Control Systems for a Locomotive Diesel Generator Plant"). Author's dissertation summary (LIIZhT), 1961.

59. Sidorov M. N., Yagodkin V. Ya. "Requirements Levied on Modern Electrical Propulsion Plant Circuits in Icebreakers and Vessels Active in Ice Navigation". Trudy NTO Sudproma, 1959, Vol. 8, Issue 5.

60. Skott [Scott] N. R. Tekhnika analogovykh i tsifrovyykh vychislitel'nykh mashin ("Analog and Digital Computer Technology"). Moscow, IL, 1963.

61. Solodovnikov V. V. Statisticheskaya dinamika lineynykh sistem avtomaticheskogo regulirovaniya ("Statistical Dynamics of Linear Automatic Control Systems"). Fizmatgiz, 1960.

62. Spetsial'nyye voprosy avtomatizirovannogo elektroprivoda ("Special Problems of Automated Electric Drive"). Edited by D. A. Zavalishin and V. V. Rudakov. Moscow-Leningrad, Izd-vo AN SSSR, 1961.

63. Syromyatnikov I. A. Rezhimy raboty asinkhronnykh i sinkhronnykh elektrodvigateley ("Induction and Synchronous Electric Motor Operating Modes"). Moscow, Gosenergoizdat, 1963.

64. Timofeyev Yu. K. Issledovaniye vysshikh garmonicheskikh napryazheniya i toka v grebnoy elektricheskoy ustanovke dvoynogo roda toka ("Study of Higher Harmonics of Voltage and Current in a Dual-Current Electrical Propulsion Plant"). Author's Summary of his Candidate Dissertation. (LVIMU imeni S. O. Makarov).

65. Timofeyev Yu. K. Computation of the Higher Harmonics on the Alternating Current Side in Dual-Current Electrical Propulsion Plant Circuits". Trudy TsNIIMF, 1967, Issue 87.
66. Tipikin A. P. "Mathematical Modelling of the External Characteristics of a Control Rectifier". Elektromekhanika, 1966, No. 10.
67. Ushakov V. B. "On Continuous-Operation Mathematical Machines". Priborostroyeniye, 1967, No. 11.
68. Freydzon I. R. Matematicheskoye modelirovaniye sudovykh sistem avtomaticheskogo upravleniya ("Mathematical Modelling of Shipboard Automatic Control Systems"). Leningrad, Sudostroyeniye, 1964.
69. Khavinson Ye. G. et al. Skhema GEU dvoynogo roda toka s otborom moshchnosti ("Circuit of a Dual-Current Electrical Propulsion Plant with Take-off"). In the collection Voprosy teorii i proyektirovaniya elektrodvizeniya sudov ("Problems of the Theory and Design of Ship's Electric Propulsion"), Issue 163. Sudostroyeniye, 1971.
70. Khaykin A. B. Dinamika grebnykh elektricheskikh ustanovok ("Electrical Propulsion Plant Dynamics"). Leningrad, Morskoy transport, 1962.
71. Khaykin A. B. "Dynamics of Propellor Interaction With Ice". Sudostroyeniye, 1963, No. 9.
72. Khaykin A. B. Avtomatizirovannyye grebnyye elektricheskiye ustanovki [648] ("Automated Electrical Propulsion Plants"). Moscow, Transport, 1968.
73. Khaykin A. B. Optimizatsiya i matematicheskoye modelirovaniye rezhimov avtonomnykh elektroenergeticheskikh sistem metodami passivnogo i aktivnogo eksperimenta ("Optimization and Mathematical Modelling of the Modes of Autonomous Electrical Power Systems Using the Methods of a Passive and Active Experiment"). In the collection Voprosy avtomatizatsii i nadezhnosti elektroenergeticheskikh i elektrogrebnykh ustanovok ("Problems of Automation and Reliability of Electrical Power and Propulsion Plants"). Leningrad, Sudostroyeniye, 1967 (NTO Sudproma. Materialy po obmenu opytom, Issue 95).
74. Khaykin A. B. Sovremennyye i perspektivnyye elektrokhody ("Modern and Future Electric Vessels"). Leningrad, Sudostroyeniye, 1969.
75. Khaykin A. B., Libin L. M. "Electrical Propulsion Plants With Electrochemical Current Generators". Sudovye silovyye ustanovki, Scientific and Technical Collection, 1967, No. 6.
76. Khaykin A. B., Timofeyev Yu. K. "Electrical Propulsion Plants With Power Rectifier Blocks". Morskoy flot, 1964, No. 5.

77. Khaykin A. B., Yagodkin V. Ya. "Operation of an Icebreaker's Electrical Propulsion Plant in the Ice Destruction Mode Using Propeller Blades". Morskoy flot, 1966, No. 8.

78. Khaykin A. B., Yagodkin V. Ya. "Computation of the Steady-State Characteristics of Icebreaker Electrical Propulsion Plants". Sudostroyeniye, 1966, No. 1.

79. Khomyakov N. M., Denisov V. V. Elektrooborudovaniye i elektrodvizhenie sudov ("Vessel Electrical Equipment and Electric Propulsion"). Leningrad, Sudostroyeniye, 1969.

80. Shekhtman M. G. "Operation of a Generator to a Rectified Load". Trudy LPI, 1940, No. 3.

81. Shekhtman M. G. "Electromagnetic Power of a Synchronous Machine When It Operates to a Rectifier". Izvestiya NIIPI, 1958, No. 3.

82. Eterman I. I. Matematicheskiye mashiny nepreryvnogo deystviya ("Continuous-Operation Mathematical Machines"). Moscow, Mashgiz, 1957.

83. Ettinger Ye. L. "Perspectives for Development of a High-Power Ion Electric Drive". Vestnik elektropromyshlennosti, 1962, No. 10.

84. Ettinger Ye. L. "External Characteristics of Multiphase Rectifiers". Trudy VNIIEP, 1963, Vol. 1.

85. Ahshaya. Der erste diselektrische Hafen-Schlepper fur Bombay. "The First Diesel-Electric Harbor Tug for Bombay". Schiff und Hafen, 1961, No. 3.

86. "'Claremont'. Gas turbine-powered tug handles space vehicles". Shipbuilding and Shipping Record, 1965, No. 24.

87. Dunaiski R. M. "The effect of rectifier power Supply on large d-c motors". Power Apparatus and Systems, 1960, No. 48.

88. "Diesel-electric [sic] Installations in chain Ferris". Motor Ship, 1961, vol. 41, No. 488.

89. "The diesel-electric [sic] Installation for propulsion and Cargo Handling of the Bulk Cement Carrier 'John Wilson'". Motor Ship, 1961, vol. 42, No. 496.